

Aspects of Confinement  
in a Functional Approach to  
Coulomb Gauge QCD

Klaus Lichtenegger

thesis in order to obtain the degree of  
*doctor rerum naturalium*  
at the Karl-Franzens Universität Graz

2010



## Abstract

The topic of this thesis are several aspects of the confinement phenomenon in Coulomb gauge Quantum Chromodynamics. In particular we have dealt with the quark propagator and with properties of Yang-Mills theory at finite temperature. The tools employed are mostly functional methods, though some general topics are also considered from the lattice point of view.

The introductory part consists of a brief synopsis of some basic quantum field theory, a pedagogic treatment of several current topics in Non-Abelian quantum gauge theories (with a particular focus on confinement scenarios) and an introduction to the Green function formalism as well as the use of Dyson-Schwinger equations. This is followed by a discussion of different approaches to the Coulomb gauge and an overview over the advantages and peculiarities of this gauge.

The first major research topic was the quark gap equation with an infrared-divergent Coulomb gluon propagator  $D_{00}$ . As an extension to studies performed so far, some forms of an infrared-divergent spatial quark-gluon vertex have been tested, but the results remain inconclusive. There is, however, considerable evidence that some infrared dressing is required in order to obtain quantitatively reliable results. The numerical studies performed in this thesis indicate that neither the vertex form derived from the approximate Abelian Ward-Takahashi identity nor a globally divergent vertex is fit for this purpose.

The second major research topic of this thesis, finite-temperature studies of pure gauge theory, again consists of two separate strands:

First, following a recent proposal of Zwanziger, the Gribov-Zwanziger approach has been extended to the “deconfined” phase of Yang-Mills theory. The resulting gap equation has been solved numerically, which yields the Gribov mass. From this, the free energy, the anomaly (the interaction measure) and the bulk viscosity have been determined.

Second, the asymptotic infrared behaviour of bare-vertex truncated Dyson-Schwinger equations of first-order Coulomb gauge SU(3) theory have been analyzed. They yield a more than linearly rising potential for three spatial dimensions – a result which has yet to be understood.

Apart from the two main topics, this thesis contains several smaller conjectures and findings: They include a proposal to systematize the set of gauges by introduction of an appropriate metric, a discussion of the role of interpolating gauges, a justification for the use of to non-integrable potentials by means of analytic continuation and a general expression for the number of components in the tensor decomposition of arbitrary Green functions.

## Zusammenfassung

Das Thema dieser Dissertation sind verschiedene Aspekte des Einschlussmechanismus der Quantenchromodynamik in Coulomb-Eichung. Insbesondere wurden der Quark-Propagator und die Eigenschaften von Yang-Mills Theorie bei endlicher Temperatur untersucht. Die Werkzeuge, die dabei zum Einsatz kamen, waren in erster Linie funktionale Methoden, einige allgemeine Fragen wurden auch aus der Sicht der Gitterdiskretisierung erörtert.

Die Einleitung besteht aus einer kurzen Übersicht über Grundlagen der Quantenfeldtheorie, einer pädagogischen Behandlung einiger aktueller Fragestellungen zu Nicht-Abel'schen Eichtheorien (mit besonderem Augenmerk auf Szenarien für den Einschlussmechanismus) und einer Einführung in den Formalismus der Greensfunktionen und der Dyson-Schwinger Gleichungen. Dem folgt eine Diskussion der verschiedenen Zugänge zur Coulomb-Eichung und ein Überblick über Vorteile und Besonderheiten dieser Eichung.

Das erste Hauptforschungsthema war die Quark-*Gap*-Gleichung mit einem infrarot-divergenten Coulomb-Gluon-Propagator  $D_{00}$ . Als Erweiterungen zu früheren Untersuchungen wurden einige Formen eines infrarot-divergenten räumlichen Quark-Gluon Vertex getestet; die Resultate sind allerdings wenig aussagekräftig. Auf jeden Fall gibt es beträchtliche Evidenz dafür, dass ein gewisses Ausmaß an Infrarot-*Dressing* notwendig ist, um quantitativ verlässliche Resultate zu erhalten. Die numerischen Studien, die in dieser Arbeit durchgeführt wurden, deuten an, dass weder die Vertexform, die sich aus der näherungsweise gültigen Abel'schen Ward-Takahashi-Identität herleiten lässt noch ein global infrarot-divergenter Vertex für diese Zwecke ausreichen.

Das zweite Hauptforschungsthema dieser Arbeit, Studien reiner Eichtheorie bei endlicher Temperatur, besteht selbst wieder aus zwei Strängen:

Erstes wurde, einer Anregung von Zwanziger folgend, der Gribov-Zwanziger Zugang auf die „nicht-ingeschlossene“ Phase der Yang-Mills-Theorie ausgedehnt. Die resultierende *Gap*-Gleichung wurde numerisch gelöst, was die Gribov-Masse liefert. Aus dieser konnten die freie Energie, die Anomalie (das Wechselwirkungsmaß) und die Volumenviskosität bestimmt werden.

Zweitens wurde das asymptotische Infrarot-Verhalten der Dyson-Schwinger Gleichungen für SU(3) Theorie in Coulomb-Eichung im erste-Ordnung Formalismus in der Trunkierung nackter Vertices untersucht. Die Gleichungen liefern für drei Raumdimensionen ein stärker als linear ansteigendes Potential – ein Resultat, das erst noch verstanden werden muss.

Abgesehen von diesen zwei Hauptthemen enthält diese Arbeit verschiedene kleinere Anregungen und Ergebnisse: Diese beinhalten einen Vorschlag, die Menge der Eichungen durch Einführung einer geeigneten Metrik zu systematisieren, eine Diskussion der Rolle interpolierender Eichungen, eine Rechtfertigung für die Verwendung nicht-integrabler Potentiale mittels analytischer Fortsetzung und einen allgemeinen Ausdruck für die Zahl der Komponenten der Tensorzerlegung von Greensfunktionen.

# Contents

<b>Prologue</b>	<b>1</b>
The Puzzle of Confinement . . . . .	1
Some Remarks on this Thesis . . . . .	2
Acknowledgements . . . . .	4
<b>1 QCD, Confinement and All That</b>	<b>5</b>
1.1 Portrait of a Gauge Theory . . . . .	5
1.1.1 The Gluon Sector . . . . .	6
1.1.2 The Quark Sector and Chiral Symmetry . . . . .	8
1.1.3 Renormalization . . . . .	10
1.1.4 Approaches to QCD . . . . .	10
1.2 The Idea of Gauge-Fixing and Some Consequences . . . . .	11
1.2.1 The Procedure of Gauge-Fixing . . . . .	11
1.2.2 BRST-Symmetry . . . . .	14
1.2.3 The Gribov Problem . . . . .	15
1.2.4 Gauge-Fixing by Functional Minimization . . . . .	16
1.2.5 The Fundamental Modular Region . . . . .	17
1.2.6 Convexity of the Gribov Region and the FMR . . . . .	17
1.2.7 Further Properties of $\Omega$ and $\Lambda$ . . . . .	19
1.2.8 The Zwanziger Conjecture . . . . .	20
1.2.9 Remarks on Nonperturbative Gauge-Fixing . . . . .	21
1.3 The Problem of Confinement . . . . .	22
1.3.1 On the Definition of Confinement . . . . .	22
1.3.2 The Gribov-Zwanziger Scenario . . . . .	25
1.3.3 Some Other Scenarios . . . . .	27
1.4 Standard and Nonstandard Gauges . . . . .	29
1.4.1 Linear Covariant Gauges . . . . .	29
1.4.2 Coulomb Gauge and Weyl Gauge . . . . .	30
1.4.3 Lightcone, Axial and Planar Gauges . . . . .	30
1.4.4 Color Symmetry-Breaking Gauges . . . . .	31
1.4.5 Gauges Breaking Translational Invariance . . . . .	31
1.4.6 Interpolating Gauges . . . . .	32
1.4.7 Gauge Overfixing . . . . .	32
1.5 Comments on a Possible Metric Structure of Gauge Space . . . . .	33
1.5.1 More Thoughts on Gauge Fixing . . . . .	33
1.5.2 The Metric Space of Unique Gauges . . . . .	34
1.5.3 The Distance between General Gauges . . . . .	36
1.5.4 Metric Considerations regarding Topologically Nontrivial Spaces . . . . .	38
1.5.5 Further Comments on the Distance between Gauges . . . . .	40
1.5.6 $\mathbb{Z}_2$ Gauge-like Theory on One Plaquette . . . . .	41

<b>2</b>	<b>The Dyson-Schwinger Approach</b>	<b>43</b>
2.1	The Green Function Formalism . . . . .	44
2.1.1	Full Green Functions and the Generating Functional . . . . .	44
2.1.2	Connected Green Functions . . . . .	45
2.1.3	Proper (1PI) Green Functions . . . . .	46
2.1.4	A Note on Fermionic Fields . . . . .	48
2.1.5	The Role of the Vacuum . . . . .	48
2.2	The Dyson-Schwinger Equations . . . . .	49
2.2.1	From the Action to Equations of Motion . . . . .	49
2.2.2	The Formal Derivation of DSEs . . . . .	52
2.3	DSEs for Finite-Temperature Coulomb-Gauge YM Theory . . . . .	54
2.3.1	Action and Fields . . . . .	54
2.3.2	The Generating Equation . . . . .	55
2.3.3	DSE for a Two-Point Function (in Position Space) . . . . .	56
2.3.4	Truncated DSE (in position space) . . . . .	57
2.3.5	Truncated DSE in momentum space . . . . .	59
2.4	Ward-Takahashi and Slavnov-Taylor Identities . . . . .	61
2.4.1	Restrictions on Propagators and Vertices . . . . .	61
2.5	Infrared Exponents . . . . .	62
<b>3</b>	<b>QCD in the Coulomb Gauge</b>	<b>63</b>
3.1	Some Fundamental Issues . . . . .	64
3.1.1	Coulomb-Gauge Propagators . . . . .	64
3.1.2	Coulomb-Gauge Vertices . . . . .	64
3.1.3	Further Notes on Propagators and 1PI Functions . . . . .	65
3.1.4	Energy Divergences . . . . .	67
3.1.5	The First-Order Formalism . . . . .	68
3.1.6	Renormalization of the Coulomb Gauge . . . . .	69
3.2	Why Coulomb Gauge is Special . . . . .	70
3.2.1	The Remnant Symmetry . . . . .	70
3.2.2	The Physical State Space . . . . .	71
3.2.3	The Color-Coulomb Potential . . . . .	72
3.2.4	Causality in the Coulomb gauge . . . . .	73
3.2.5	Further Notes on the Remnant Symmetry . . . . .	73
3.3	Hamiltonian Formulation of Coulomb Gauge QCD . . . . .	76
3.3.1	Gauß' Law . . . . .	76
3.3.2	The Operator Ordering Problem . . . . .	77
3.3.3	Connection between Hamiltonian and Functional Formalism . . . . .	77
3.3.4	$(1 + 1)$ -dimensional Coulomb Gauge . . . . .	78
3.4	Selected Results on the Coulomb Gauge . . . . .	79
3.4.1	On the Lattice: Propagators and the Coulomb String Tension . . . . .	79
3.4.2	The Transverse Gluon Energy and Gribov's Formula . . . . .	79
3.4.3	Perturbative Expansion and Dyson-Schwinger Equations . . . . .	80
3.4.4	Infrared Exponents in the Coulomb Gauge . . . . .	80
3.4.5	The Gluon Chain Model . . . . .	80
3.5	Interpolating Gauges and their Limits . . . . .	81
3.5.1	Tree-Level Propagators . . . . .	81
3.5.2	Access to the Physical Coulomb Gauge? . . . . .	81
3.5.3	Rescaling of Momenta and Further Hints at Discontinuities . . . . .	83
3.5.4	Interpolating Gauges on the Lattice . . . . .	84
3.5.5	A Picture of the Interpolation Process . . . . .	85
3.5.6	Proposal of a New Type of Interpolating Gauge . . . . .	88

<b>4</b>	<b>The Coulomb-Gauge Gap Equation</b>	<b>89</b>
4.1	Gap Equation and Propagators . . . . .	89
4.1.1	Structure of the Quark Propagator . . . . .	89
4.1.2	Parameterization of the Gluon Propagator . . . . .	90
4.1.3	The Resulting Gap Equation . . . . .	92
4.1.4	Applications of the Quark Propagator: the Mass Function . . . . .	93
4.2	The Quark-Gluon Vertex . . . . .	95
4.2.1	Naive Decomposition . . . . .	95
4.2.2	The Ball-Chiu and the Curtis-Pennington Vertex . . . . .	95
4.2.3	Restrictions from Ward Identities . . . . .	96
4.2.4	Perturbative Investigation of the Vertex . . . . .	97
4.2.5	Other Forms for the Quark-Gluon Vertex . . . . .	97
4.2.6	Considerations on an Infrared-divergent Vertex $\Gamma_i$ . . . . .	98
4.3	Truncation Schemes and Numerical Results . . . . .	100
4.3.1	The Instantaneous Approximation . . . . .	100
4.3.2	Inclusion of Transverse Gluons and Retardation . . . . .	100
4.3.3	Explorative Study of an Infrared Divergent Vertex $\Gamma_i$ . . . . .	102
4.3.4	Some Notes on the Numerical Challenges . . . . .	106
4.3.5	Conclusions . . . . .	107
4.4	A Note on Mesons . . . . .	108
<b>5</b>	<b>Finite Temperature Theory</b>	<b>109</b>
5.1	General Remarks on Finite Temperature QCD . . . . .	110
5.1.1	Rise and Fall of the Quark-Gluon Plasma . . . . .	110
5.1.2	How to Study High Temperatures . . . . .	110
5.1.3	The Perturbative Problem in the Infrared . . . . .	111
5.1.4	Direct Perturbative Approach . . . . .	111
5.1.5	Effective Field Theory . . . . .	112
5.1.6	Functional Approaches . . . . .	114
5.1.7	Lattice Gauge Theory . . . . .	115
5.1.8	Other Approaches . . . . .	115
5.1.9	Comparison of Results . . . . .	116
5.2	Pure Gauge Theory with an Extended Action . . . . .	117
5.2.1	Equation of State from a Local Action . . . . .	117
5.2.2	The Gap Equation . . . . .	118
5.2.3	Choice of the Renormalization Scale . . . . .	118
5.2.4	Calculational Methods . . . . .	119
5.2.5	Results . . . . .	120
5.2.6	Discussion and Outlook . . . . .	123
5.3	Coulomb-Gauge Infrared Exponents at Finite Temperature . . . . .	125
5.3.1	Local action . . . . .	125
5.3.2	Definition of propagators and proper 2-point functions . . . . .	126
5.3.3	Truncated Dyson-Schwinger equations . . . . .	127
5.3.4	Definition of infrared critical exponents . . . . .	128
5.3.5	Infrared asymptotic DS equations . . . . .	128
5.3.6	Determination of infrared critical exponents . . . . .	131
5.3.7	Relations among the $b$ -coefficients . . . . .	137
5.3.8	Range of Validity . . . . .	139
5.3.9	Discussion of the Infrared Exponents . . . . .	139
5.4	Quarks at Finite Temperature – a Brief Remark . . . . .	141
	<b>Epilogue</b>	<b>143</b>

<b>A</b>	<b>The Quark Gap Equation: Remarks and Details</b>	<b>145</b>
A.1	Conventions . . . . .	145
A.1.1	Natural Units . . . . .	145
A.1.2	Indices . . . . .	145
A.2	The Quark Gap Equation with a Bare Vertex . . . . .	146
A.2.1	Inversion of the Quark Propagator . . . . .	146
A.2.2	Expansion of the Gap Equation . . . . .	146
A.2.3	Projection onto Basis Elements . . . . .	147
A.2.4	Symmetry and Wick-Rotation . . . . .	149
A.2.5	Introduction of Spherical Coordinates . . . . .	150
A.2.6	Some Important Dirac Traces . . . . .	153
A.3	Renormalization of the Quark Gap Equation . . . . .	154
A.4	The Mixed Gluon Propagator in Coulomb Gauge . . . . .	155
A.5	Complete Decomposition of the Quark Gap Equation . . . . .	156
<b>B</b>	<b>Elements of Tensor Decomposition</b>	<b>165</b>
B.1	Covariant Tensor Decomposition . . . . .	166
B.1.1	General Considerations . . . . .	166
B.1.2	Extended Lorentz Structure . . . . .	168
B.1.3	Inclusion of Fermions . . . . .	169
B.1.4	The Number of Covariant Tensors . . . . .	170
B.2	Limits of Tensor Decomposition . . . . .	172
B.3	Non-Covariant Tensor Decomposition . . . . .	173
B.3.1	The Fermion-Photon Vertex with Broken Lorentz Invariance . . . . .	173
B.3.2	The Number of Non-Covariant Tensors . . . . .	177
<b>C</b>	<b>Bits and Pieces</b>	<b>179</b>
C.1	The Negative Dimensional Integration Method . . . . .	179
C.1.1	Hypergeometric Functions . . . . .	180
C.1.2	Application to Coulomb Gauge Problems . . . . .	181
C.2	Fourier Transform of Rising Potentials . . . . .	182
C.2.1	A Further Comment on Infrared Divergences in DSEs . . . . .	186
C.3	Notes on a General Asymptotic Expansion . . . . .	188
C.4	Finite Temperature Calculations . . . . .	190
C.4.1	The Anomaly from an Analytic Derivative . . . . .	190
C.4.2	Evaluation of Power-Law Integrals . . . . .	192



# Prologue

## The Puzzle of Confinement

Quantum Chromodynamics (QCD) is generally accepted as the best theory of strong interaction, i.e. of the forces responsible for stabilizing atomic nuclei (which would otherwise immediately desintegrate due to electrostatic repulsion and Pauli pressure).

While providing an accurate description of nuclear physics, QCD is formulated in terms quite different from those experimental physicists would use. Instead of referring to particles like protons, neutrons, pions or kaons, etc., employs fields called quarks and gluons which carry a certain kind of charge termed *color*.

Quarks and gluons have never been observed as isolated particles. The phenomenon that it is seemingly impossible to break up a “white” object (color singlet) into its colored constituents is called *confinement* and up to now only partially explained.

In quantum electrodynamics (QED), *perturbation theory* provides a calculational scheme, which allows to determine most observables to almost arbitray precision.<sup>1</sup> The situation is completely different in QCD. Perturbation theory only works for small values of the coupling constant, which is true for QCD at large momentum transfer, but not at small momenta – the region which defines the properties of hadrons.

Thus, while perturbative QCD is useful to describe high-energy scattering processes, it fails when certain other fundamental issues are considered. This is especially true for three main questions:

- **Confinement:** Why is it impossible to break apart white objects into their colored constituents (or separate color charges)? Are there any circumstances where this is possible (deconfinement)?
- **Chiral Symmetry Breaking:** The most “down-to-earth” hadrons, the proton and the neutron are at least 50 times heavier than the three quarks they are made of (in the most simple picture). How does this work?
- **The Mass Gap:** If we consider physical (white) objects that are made solely from gluons (so-called *glueballs*), why are even the lightest of them so heavy?

The last question, packaged together with the proof that quantum Yang-Mills theory (roughly speaking the gluonic part of QCD) is well-defined at all, has been chosen as one of the seven millenium problems, [52]. While no one can expect to “just find” a solution to even one of these three questions, an increasing number of concepts and approaches hopefully fosters our general understanding. In many respects the situation is similar to a huge jigsaw puzzle: The more parts are available (and put roughly to the correct place or at least in the correct relation), the greater are the chances to recognize the underlying picture.

---

<sup>1</sup>Of course the more mathematically inclined reader may regard it as slightly unsettling that this scheme involves expanding quantities of a presumably ill-defined theory in a divergent series and keeping only the first few terms of the expansion. Still, by doing so, one obtains some of the most accurate results currently available in science.

Like in a jigsaw puzzle, the border is the easiest piece to assemble. The borders of a theory are typically certain limits in which it is easier to handle. The weak coupling limit (approached for large momentum transfers), which is accessible by perturbative expansion, has been studied in great detail, but, as already mentioned, cannot answer some of the most fundamental questions.

For other borders, like the infrared (i.e. low momentum) limit, investigations are still pursued only by few researchers. Still the infrared regime is presumably the best place to look at, if one wants to gain deeper understanding of confinement and chiral symmetry breaking. In last few years lattice-based methods began to have access to the deep infrared, but still the field is dominated by functional approaches, based on Green functions and equations which relate them to each other.

This is also the approach we will use in this thesis (though at some points we employ lattice arguments as well) in order to investigate the infrared properties of quarks and gluons in a quite particular setting – the *Coulomb gauge*.

## Some Remarks on this Thesis

*Where is the wisdom we have lost in knowledge?*

*Where is the knowledge we have lost in information?*

T.S. Eliot, Choruses from *The Rock*

The availability of scientific information is constantly improving, mainly due to the web and other electronic media. This is particularly true for the members of those organizations which can afford to subscribe to all relevant journals. But also for those not so lucky, the arXiv, [www.arxiv.org](http://www.arxiv.org), and other open platforms provide a vast amount (though not necessarily complete) of up-to-date research information.

The mastering of scientific *knowledge*<sup>2</sup>, on the other hand, is becoming an increasingly difficult task. In particular for beginners in a field the situation can be extremely frustrating. (For more information on the various obstacles one might have to face in order to obtain a PhD, consult [47].)

The gap between what is covered by well-written textbooks and what is required to understand current research articles is widening. The amount of scientific information generated per year steadily increases and the average number of sources required to understand the average article increases as well. Older articles contain information which is – sometimes even concerning content, more often concerning notation and other aspects of presentation – not up-to-date. Nevertheless, having read these articles is still necessary for understanding current work. Topical reviews which should provide a remedy for this, too often fail on this objective.

Sooner or later this situation will require qualitatively new approaches to the handling and dissemination of knowledge, while up to now we mainly employ (though in a sometimes refined and extended version) concepts which have essentially stayed the same since the next-to-last century. This will require a deep analysis of concepts of knowledge, which will presumably integrate findings of linguistics, didactics, pedagogics, information sciences, neurosciences and artificial intelligence.

At the moment, however, the best the present author can hope to do is to embed his own work as good as possible in a broader context, not to state facts (which might appear as self-evident for accomplished experts, but not for beginners) without any source or explanation – in short, to keep with those rules of presentation which seem to be accepted on general grounds, but typically violated in everyday work.

---

<sup>2</sup>In this context, knowledge could be loosely described as the ability to judge the relevance and consistency of given information, the ability to classify and integrate pieces of information and to establish links and connections between them.

With this in mind, this thesis has been written in order to be accessible also for readers which possess only basic knowledge of quantum field theory (as covered for example by [158] or by [3, 4]), but may be unfamiliar with advanced functional methods or the peculiarities of non-Abelian gauge theories (in particular in the context of non-covariant gauge fixing). At the same time, the thesis includes a number of research results, some already published, some yet unpublished. As a consequence, different chapters of this thesis have a very different status, a situation which is briefly summarized in the following list:

1. Chapter 1 is intended as a brief introduction to the peculiarities of Non-Abelian gauge theories. The focus lies on gauge-fixing and its consequences, in particular gauge-dependent confinement scenarios. While we point out certain features that are not yet textbook knowledge, sections 1.1 to 1.4 contain no new results or insights. Section 1.5, however, has a very different status: It is devoted to the discussion of an additional mathematical structure hidden in gauge theories, which, to the knowledge of the present author, has not been discussed so far in the literature.
  2. Chapter 2 is an introduction to the Green function formalism and the quantum equations of motion, which relate them, the *Dyson-Schwinger equations* (DSEs). This chapter will mostly contain no new results, but instead focus on pedagogic aspects. As a concrete example, in section 2.3 we derive DSEs for Coulomb gauge Yang-Mills theory in the infinite-temperature limit, which will be used in section 5.3 and in [132].
  3. Chapter 3 gives a synopsis of what is known about the formulation of QCD in a particularly interesting (and often difficult) gauge, the Coulomb gauge. Most of this chapter summarizes known results, except for sec. 3.5.5 and sec. 3.5.6 which discuss new aspects of certain interpolating gauges. Sec. 3.3.4, adjusted to finite temperature, appears as appendix B of [132].
  4. Chapter 4 discusses the quark gap equation in Coulomb gauge, continuing on the project initiated by [6] and picked up again in [11, 121, 124]. We summarize some old findings and give certain new results, including general statements about the quark-gluon vertex and some numerical results for the quark propagator, obtained by solving the gap equation with different vertex ansätze. A publication on this topic (together with R. Alkofer, G. Lassnig and R. Krenn), which might contain also parts of chapter 3 as an introduction, is in preparation.
  5. Chapter 5 discusses Yang-Mills theory at finite temperature along the lines of [231]. In this chapter we analyze the equation of state by incorporating the Gribov-Zwanziger confinement scenario and discuss infrared exponents in the infinite-temperature limit. The first part of this work, which has been done together with Daniel Zwanziger, has been published as [131], the second part is available as [132].
- A. Appendix A fixes some of the notation and contains a more detailed discussion and some calculations regarding the quark gap equation. This includes the full tensor decomposition of the equation in Coulomb as well as a Landau-Coulomb interpolating gauge.
  - B. Appendix B discusses the tensor decomposition of Green functions, which is a key ingredient in making Dyson-Schwinger equations numerically tractable. While most of this is standard, we derive general formulae for the number of tensor components, which have (to the knowledge of the present author) never been given explicitly anywhere else.
  - C. Appendix C contains several small discussions and calculations, including the Fourier transform of linearly and general rising potentials, a comment on hypergeometric functions and the Negative-Dimensional Integration Method (NDIM) and an example for the evaluation of power-law integrals. All of this is (advanced) standard and just given for completeness.

## Acknowledgements

During this project the author was supported by the Doktoratskolleg *Hadronen im Vakuum, in Kernen und Sternen* (FWF DK W1203-N08) and by the *Graz Advanced School of Science* (NAWI-GASS). He would like to express his thanks for the hospitality of New York University (NYU), where he spent a semester on a research stay and where most of the work presented in chapter 5 has been done.

He expresses his gratitude to his advisor Reinhard Alkofer who first confronted him with Dyson-Schwinger equations and with the Coulomb gauge in the context of non-Abelian gauge theories, and to Daniel Zwanziger from whom he has learned about many of the particularities of this approach. He also thanks his co-advisors Enrico Arrigoni and Christof Gattringer, as well as Bernd-Jochen Schaefer for critically reading the first version of this thesis.

In addition he recalls with pleasure stimulating discussions with Peter Arnold, Martina Blank, Huan Chen, David Dudal, Gernot Eichmann, Christian S. Fischer, Jeff Greensite, Tina Herbst, Markus Q. Huber, Markus Kloker, Andreas Krassnigg, Roland Krenn, Christian B. Lang, Gernot Lassnig, Markus Leder, Felipe Llanes Estrada, Axel Maas, Veronika Macher, Mario Mitter, Diana Nicmorus, Markus Pak, Willibald Plessas, Anton Rebhan, Hugo Reinhardt, Craig Roberts, Andreas Rüdinger, Wolfgang Schleifenbaum, York Schröder, Wolfgang Schweiger, Kai Schwenzer, Martin Schwinzerl, Nan Su, Peter Tandy, Nele Vandersickel, Selim Vilalba Chavez, Robert Wagenbrunn, Peter Watson and others which have contributed to his understanding of science in general, quantum field theory, non-Abelian gauge theories and the strategies how to approach them.

# Chapter 1

## QCD, Confinement and All That

*If the Lord Almighty had consulted me before embarking upon Creation,  
I should have recommended something simpler.*

Alfonso X (the Wise) of Castille and León, on  
having the Ptolemaic system of epicycles ex-  
plained to him, [216]

In this chapter we first briefly discuss the gauge principle and the QCD Lagrangian, mostly to fix the notation. Then we dive into the issue of gauge-fixing, where we summarize general considerations (including the Gribov problem and properties of the Gribov region) and give a short synopsis of some important gauges.

After this, we discuss some aspects of confinement, in particular the Gribov-Zwanziger scenario and its relation to other approaches. Finally, in the last section we present some new ideas how to define the set of *gauges* (in contrast to the set of gauge transformations) and how to possibly endow this set with some additional structure.

### 1.1 Portrait of a Gauge Theory

To present day knowledge, nature is described on the most fundamental level in terms of *gauge theories*. Gauge symmetry made (historically) and makes (in the typical physics curriculum) its first appearance in electrodynamics, where the physical fields  $\mathbf{E}$  and  $\mathbf{B}$  can be determined from a scalar potential  $\phi$  and a vector potential  $\mathbf{A}$  as

$$\mathbf{E} = -\text{grad } \phi - \frac{\partial \mathbf{A}}{\partial t}, \quad \mathbf{B} = \text{rot } \mathbf{A}. \quad (1.1)$$

These potentials are not unique; in particular one can add the gradient of any function  $\chi \in C^2$  to  $\mathbf{A}$  without changing  $\mathbf{E}$  or  $\mathbf{B}$ . In the relativistic formulation (using, as always in this thesis  $c = 1$ ), it makes sense to combine those two potentials into one four-vector  $A^\mu = (\phi, A^i)$ ,  $\mu \in \{0, 1, 2, 3, 4\}$ . In this formalism, gauge transformations are given by  $A^\mu \rightarrow A^\mu + \partial^\mu \chi$  with some function  $\chi$ .<sup>1</sup>

When moving on to quantum electrodynamics (QED), these *gauge transformations* have to be accompanied by a phase change of the fields  $\psi$ . The QED Lagrangian reads

$$\mathcal{L}_{\text{QED}} = \bar{\psi}(i\not{D} - m)\psi + F_{\mu\nu}F^{\mu\nu} \quad (1.2)$$

with  $\not{D} \equiv \gamma^\mu D_\mu$ , the covariant derivative  $D_\mu = \partial_\mu + ie A_\mu$  and the field strength tensor  $F_{\mu\nu} = \partial_\mu A_\nu - \partial_\nu A_\mu$ . One notes that  $\mathcal{L}_{\text{QED}}$  (and thus the whole theory) is not only gauge invariant,

---

<sup>1</sup>Usually one chooses  $\chi \in C^2(\mathbb{R}^4)$ . As discussed for example in [149], using functions  $\chi$  which are not twice continuously differentiable can give surprising effects – for example it allows the construction of monopoles.

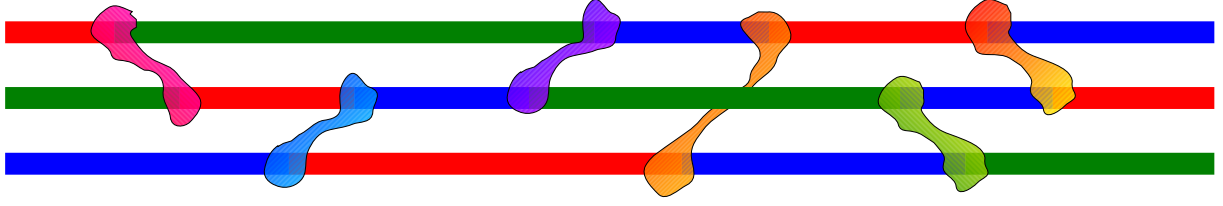


Figure 1.1: In a naive picture, one can imagine fields in the fundamental representation having one color (red, green or blue) and fields in the adjoint representation one color and one anticolor (green-antiblue, red-antigreen, ...). The binding force between colored particles (here quarks) is mediated by exchange of adjoint fields (gluons).

but can actually be *derived* from demanding invariance under local  $U(1)$  transformations. While gauge invariance may be regarded as an oddity (and sometimes even a nuisance) in the case of QED, matters are different when turning to the electroweak theory or QCD.

Since these theories are not realized in nature on classical level, invoking the correspondence principle is not possible. The only construction mechanism available is demanding invariance under local symmetry transformations, which are all contained in a Lie group  $\mathbb{G}$  (with corresponding Lie algebra  $\mathfrak{g}$ ).<sup>2</sup>

For QCD, one has  $\mathbb{G} = \text{SU}(N_c)$  and  $\mathfrak{g} = \mathfrak{su}(N_c)$ , where  $N_c = 3$  has been determined experimentally. Demanding invariance under  $\text{SU}(N_c)$  transformations, insisting on renormalizability and discarding the  $CP$ -violating  $\Theta$ -term [215, 214], one obtains the QCD Lagrangian

$$\mathcal{L}_{\text{QCD}} = \bar{\psi} (i \not{D} - m) \psi - \frac{1}{4} F_{\mu\nu}^a F^{a,\mu\nu}, \quad (1.3)$$

with quark fields  $\psi$  and gluon fields  $A_\mu^a$ ,  $a = 1, \dots, N_c^2 - 1$ , which are contained in the covariant derivative  $D_\mu = \partial_\mu + ig \frac{\lambda^a}{2} A_\mu^a$  and in the field strength tensor

$$F_{\mu\nu}^a = \partial_\mu A_\nu^a - \partial_\nu A_\mu^a + g f^{abc} A_\mu^b A_\nu^c. \quad (1.4)$$

Here  $f^{abc}$  denotes the antisymmetric structure constants of the Lie algebra. The contraction  $F_{\mu\nu}^a F^{a,\mu\nu}$  not only gives a kinetic term, but also describes gluon-gluon interaction (see also figure 1.4). Thus, the Yang-Mills Lagrangian  $\mathcal{L}_{\text{YM}} = -\frac{1}{4} F_{\mu\nu}^a F^{a,\mu\nu}$  alone already describes an interesting theory.

### 1.1.1 The Gluon Sector

The gluon fields in  $\text{SU}(N_c)$  gauge theory are described by  $(N_c^2 - 1)$ -tuples of vector fields  $A_\mu^a(x)$ ,  $\mu = 0, \dots, 3$ ,  $a = 1, \dots, N_c^2 - 1$ , which are typically combined with the group generators  $t^a \in \mathfrak{su}(N_c)$  to

$$A_\mu(x) := t^a A_\mu^a(x). \quad (1.5)$$

In very dense notation we will sometimes denote the collection  $(A_\mu^a(x))_{\mu=0,\dots,3}^{a=1,\dots,N_c^2-1}$  simply as  $A$ . The set of all gauge field configurations  $A$  (being sufficiently regular<sup>3</sup> and compatible with the

<sup>2</sup>For a short introduction to Lie groups and algebras see section 15.4 of [158], for a more comprehensive text see for example [86]. The most important concepts of Lie group theory needed here are generators, structure constants and Casimir operators. We will typically consider the fundamental and the adjoint representation of the group, which corresponds to quarks and gluons/ghosts. Color indices always belong to the adjoint representation. A naive picture of fundamental and adjoint representation is given in figure 1.1.

<sup>3</sup>Since in the standard treatment there are derivatives up to second order acting on the gauge fields and one demands the fields and their (weak) derivatives up to second order to be square-integrable, the Sobolev space  $H^2(\mathbb{R}^4) \equiv W^{2,2}(\mathbb{R}^4)$  is natural candidate to define the gauge fields. At least one can expect  $H^2(\mathbb{R}^4)$  to be a dense subset of the space of gauge configurations.

boundary conditions) is denoted by  $\mathcal{A}$ . Employing the scalar product

$$\langle A_{(1)}, A_{(2)} \rangle = -\text{tr} \int_{\mathbb{R}^4} d^4x A_{(1),\mu}^a(x) t^a A_{(2)}^{\mu,b}(x) t^b \quad (1.6)$$

$\mathcal{A}$  becomes a unitary space; the induced norm is given as usual by

$$\|A\| := \sqrt{\langle A, A \rangle}. \quad (1.7)$$

Completing  $\mathcal{A}$  with respect to this norm one obtains a Hilbert space. For some purposes it can be convenient to use other norms, as we will see in subsection 1.2.4. We typically call  $A \in \mathcal{A}$  a *configuration* or a *point* of this space.

A local gauge transformation is characterized by an element of  $\mathbb{G}$  located at each point of space-time. In order to have a symbol at hand, we will denote the set of all local gauge transformations (which inherit their group structure from  $\mathbb{G}$ ) by  $\mathbb{G}_{(\mathbb{R}^4)}$  or simply by  $\mathbb{G}_{(X)}$  if the domain  $X$  has not been fixed yet.

Local gauge transformations take the form (see section 15.1 of [158].)

$$\psi \rightarrow U\psi, \quad \bar{\psi} \rightarrow \bar{\psi}U^\dagger, \quad A_\mu^a \rightarrow U A_\mu^a U^\dagger + \frac{i}{g} U \partial_\mu U^\dagger \quad (1.8)$$

with  $U \in \mathbb{G}_{(\mathbb{R}^4)}$ . Their infinitesimal version is given by

$$\psi \rightarrow (1 + i\alpha^a t^a)\psi, \quad \bar{\psi} \rightarrow \bar{\psi}(1 - i\alpha^a t^a), \quad A_\mu^a \rightarrow A_\mu^a + \frac{1}{g} \partial_\mu \alpha^a + f^{abc} A_\mu^b \alpha^c \quad (1.9)$$

with functions  $\alpha^a \in C^1(\mathbb{R}^4)$  and the generators  $t^a \in \mathfrak{g}$ .

A *gauge orbit*  $\mathcal{O}$  is an equivalence class of field configurations connected by local gauge transformations and thus corresponding to the same physical state,

$$\mathcal{O}[A_O] := \mathbb{G}_{(X)} A_O = \{A \in \mathcal{A} \mid \exists U \in \mathbb{G}_{(\mathbb{R}^4)} \text{ such that } A = U A_O\}. \quad (1.10)$$

We denote the set of all gauge orbits by  $\mathcal{O}$  and note that since all configurations on one orbit describe the same physical situation,  $\mathcal{O}$  is expected to be – up to zero norm states and global color rotations – isomorphic to the space of physical states  $\mathcal{P}$ ,

$$\mathcal{O} = \mathcal{A}/\mathbb{G}_{(X)} \simeq \mathcal{P}. \quad (1.11)$$

While gauge orbits are infinite-dimensional objects, it is sometimes useful to sketch them as curves, connecting equivalent configurations (represented as points). This is used for example in figure 1.2.

### Chromoelectric and Chromomagnetic Fields

For several purposes it is useful to formulate QCD a way very similar to standard electrodynamics. To do so, one introduces *chromoelectric* and *chromomagnetic* fields as

$$E_i^a = F_{0i}^a \quad \text{and} \quad F_{ij}^a = \varepsilon_{ijk} B_k^a. \quad (1.12)$$

In an appropriate gauge (the Weyl gauge,  $A_0 = 0$ , see also subsections 1.4.2 and 3.3), one can then express the Yang-Mills Lagrangian and Hamiltonian as

$$\mathcal{L}_{\text{YM}} = \frac{1}{2} (\mathbf{E}^a \cdot \mathbf{E}^a - \mathbf{B}^a \cdot \mathbf{B}^a) \quad \text{and} \quad \mathcal{H}_{\text{YM}} = \frac{1}{2} (\mathbf{E}^a \cdot \mathbf{E}^a + \mathbf{B}^a \cdot \mathbf{B}^a). \quad (1.13)$$

Choosing  $A_0 = 0$  leads to the loss of one equation of motion, which now has to be imposed as an additional constraint on the wave functional. This equation turns out to be Gauß' law, which reads in the absense of all non-gluonic color charges

$$\mathcal{D}_\mu^{ab} F^{b,\mu 0} = (\mathbf{D} \cdot \mathbf{E})^a = 0. \quad (1.14)$$

As dicussed in chapter 3, this condition can be included directly by employing the Coulomb gauge.



### 1.1.2 The Quark Sector and Chiral Symmetry

When considering  $N_f$  different quark flavors, the Lagrangian takes the form

$$\mathcal{L}_{\text{QCD}} = i \sum_{j=1}^{N_f} \bar{\psi}_j \not{D} \psi_j - \sum_{j,k=1}^{N_f} \bar{\psi}_j M_{jk} \psi_k - \frac{1}{4} F_{\mu\nu}^a F^{a,\mu\nu} \quad (1.15)$$

with the *quark mass matrix*  $M = \text{diag}(m_1, m_2, \dots, m_{N_f})$ .

#### Vector and Axialvector Currents

For massless (and in an approximate sense also for very light) quarks, QCD exhibits an additional symmetry in addition to gauge invariance. Our starting point is the quark part of the QCD Lagrangian, including three different flavors  $u$ ,  $d$  and  $s$  of quarks,

$$\mathcal{L}_{\text{quark}} = \bar{u} (i \not{D} - m_u) u + \bar{d} (i \not{D} - m_d) d + \bar{s} (i \not{D} - m_s) s \quad (1.16)$$

In the case  $m_u = m_d = m_s$ , this Lagrangian is invariant under transformations

$$q(x) = \begin{pmatrix} u(x) \\ d(x) \\ s(x) \end{pmatrix} \rightarrow q'(x) = \mathbf{U} \begin{pmatrix} u(x) \\ d(x) \\ s(x) \end{pmatrix} = e^{i\theta^a \frac{\lambda^a}{2}} \begin{pmatrix} u(x) \\ d(x) \\ s(x) \end{pmatrix} \quad (1.17)$$

with  $\mathbf{U} \in SU(3)$ . According to Noether's theorem this symmetry leads to conserved currents, the *vector currents*

$$V_\mu^a(x) = \bar{q}(x) \frac{\lambda^a}{2} \gamma_\mu q(x), \quad a = 1, \dots, 8. \quad (1.18)$$

In the case  $m_u \neq m_d \neq m_s$ , as realized in nature, the  $SU(3)$  symmetry is not exact. The vector currents can still be defined, but they are not conserved. For example, the current that changes a down to an up quark is  $V_+^\mu = V_1^\mu + iV_2^\mu$ , and one finds  $\partial_\mu V_+^\mu = i(m_u - m_d)\bar{u}d$ .

In the *chiral limit*  $m_u = m_d = m_s = 0$  also the symmetry transformation

$$q(x) = \begin{pmatrix} u(x) \\ d(x) \\ s(x) \end{pmatrix} \rightarrow q'(x) = e^{i\theta^a \frac{\lambda^a}{2} \gamma_5} \begin{pmatrix} u(x) \\ d(x) \\ s(x) \end{pmatrix} \quad (1.19)$$

leaves the Lagrangian invariant. This leads to the *axialvector currents*

$$A_\mu^a(x) = \bar{q}(x) \frac{\lambda^a}{2} \gamma_\mu \gamma_5 q(x), \quad a = 1, \dots, 8. \quad (1.20)$$

In analogy to the vector case, the axialvector currents can still be defined for nonvanishing quark masses, but they are no longer conserved. For example, for  $A_+^\mu = A_1^\mu + iA_2^\mu$  one has  $\partial_\mu A_+^\mu = i(m_u + m_d)\bar{u}\gamma_5 d$ .

The sources of the axialvector currents are closely related to the pseudoscalar mesons. These particles are comparatively light, so the *PCAC* (partially conserved axial current) hypothesis states that the axialvector current is almost conserved.

#### The Current Algebra

From vector and axial vector currents, charges can be derived the usual way,

$$Q^a(t) = \int d^3x V_0^a(x), \quad Q^{5a}(t) = \int d^3x A_0^a(x). \quad (1.21)$$



They have the commutation relations

$$\begin{aligned} [Q^a(t), Q^b(t)] &= if^{abc}Q^c(t), & [Q^{5a}(t), Q^{5b}(t)] &= if^{abc}Q^c(t), \\ [Q^a(t), Q^{5b}(t)] &= if^{abc}Q^{5c}(t). \end{aligned} \quad (1.22)$$

This defines the chiral  $SU(3)_V \times SU(3)_A$  algebra. While the vector charges  $Q^a(t)$  form a subalgebra, the axialvector charges  $Q^{5a}(t)$  do not. The commutation relations remain valid even in the case  $m_u \neq m_d \neq m_s \neq 0$ .

### The Chiral $SU(3)_L \times SU(3)_R$ Algebra

When projecting out left- and right-handed fermions,  $\psi_L = P_L\psi = \frac{1-\gamma^5}{2}\psi$ ,  $\psi_R = P_R\psi = \frac{1+\gamma^5}{2}\psi$ , they mix only via the mass term,

$$\mathcal{L}_{\text{fermion}} = \bar{\psi}_L (\not{D} - m) \psi_L + \bar{\psi}_R (\not{D} - m) \psi_R - m (\bar{\psi}_L \psi_R + \bar{\psi}_R \psi_L). \quad (1.23)$$

In the chiral limit  $m = 0$ , left- and right-handed fermions decouple. When again considering three types of quarks in this limit, the Lagrangian is invariant under the two independent transformations  $q_L \rightarrow e^{i\theta_L^a \frac{\lambda^a}{2}} q_L$  and  $q_R \rightarrow e^{i\theta_R^a \frac{\lambda^a}{2}} q_R$ , i.e. under the group  $U(3) \times U(3)$ . When factoring out  $U_V(1)$  (responsible for baryon number conservation) and  $U_A(1)$  (responsible for the axial anomaly, related to the puzzle of the  $\eta'$  mass [213, 8]) one obtains invariance under  $SU(3)_L \times SU(3)_R$ . This symmetry gives rise to 16 Noether currents

$$j_R^{\mu,a} = \bar{q}_R \gamma^\mu \frac{\lambda^a}{2} q_R, \quad j_L^{\mu,a} = \bar{q}_L \gamma^\mu \frac{\lambda^a}{2} q_L, \quad a = 1, \dots, 8. \quad (1.24)$$

These currents are linked to vector and axialvector current via

$$V^{\mu,a} = j_R^{\mu,a} + j_L^{\mu,a}, \quad A^{\mu,a} = j_R^{\mu,a} - j_L^{\mu,a}. \quad (1.25)$$

Again, charges can be constructed as spatial integrals; they fulfill  $Q^a = Q_R^a + Q_L^a$ ,  $Q^{5a} = Q_R^a - Q_L^a$  and the commutation relations

$$[Q_L^a(t), Q_L^b(t)] = if^{abc}Q_L^c, \quad [Q_R^a(t), Q_R^b(t)] = if^{abc}Q_R^c, \quad [Q_L^a(t), Q_R^b(t)] = 0. \quad (1.26)$$

These define the chiral  $SU(3)_L \times SU(3)_R$  algebra, which is isomorphic to  $SU(3)_V \times SU(3)_A$ .

### Spontaneous Breaking of Chiral Symmetry

The ground state of QCD has not the full chiral symmetry of the Lagrangian. (Else there were parity doublets, which are clearly absent from the physical particle spectrum.) So the  $SU(3)_L \times SU(3)_R$  symmetry is reduced to  $SU(3)_V = SU(3)_{L+R}$ .

$SU(3)_A$  is broken, and, according to Goldstone's Theorem, for each broken global symmetry, there exists a massless boson. In the case of  $SU(3)_A$  these particles are the pseudoscalar mesons  $\pi^\pm$ ,  $\pi^0$ ,  $K^\pm$ ,  $K^0$ ,  $\bar{K}^0$  and  $\eta$ . Since chiral symmetry is also explicitly broken, these mesons are not massless, but still lighter than all other hadrons.

The breaking of chiral symmetry is accompanied by a “re-sorting” of the ground state; the vacuum is filled with scalar quark-antiquark pairs. These pair constitute the *chiral condensate*,

$$\langle \bar{\psi}\psi \rangle = \langle 0 | \bar{u}u | 0 \rangle + \langle 0 | \bar{d}d | 0 \rangle + \langle 0 | \bar{s}s | 0 \rangle, \quad (1.27)$$

from which hadrons draw most of their mass. For the pion, which were massless in the chiral limit, the *Gell-Mann–Oakes–Renner relation* gives

$$m_\pi^2 \sim (m_u + m_d) \langle \bar{u}u + \bar{d}d \rangle + \mathcal{O}(m_{u,d}^2). \quad (1.28)$$

### 1.1.3 Renormalization

The theory described so far contains bare parameters and leads to divergent expressions, thus it has to be regularized and renormalized. There are different procedures available to do so, and some are intimately related to certain calculational methods. Typically we will either use dimensional regularization and the modified minimal subtraction ( $\overline{\text{MS}}$ ) scheme or employ a hard momentum cutoff (MOM or related schemes).

### 1.1.4 Approaches to QCD

The ultimate goal of QCD is to provide a description of physical particles and processes in terms of quarks, gluons and the symmetries which induce them. There exist several methods to extract physics from a quantum field theory, which all have their merits and shortcomings:

**Perturbation theory** is a versatile and successful instrument for many problems, and therefore treated in almost all textbooks on quantum field theory. Unfortunately, most problems which occur in QCD are not tractable perturbatively. Perturbative methods are typically limited to the case of interactions being “small”, which is not the case for QCD at low momenta.<sup>4</sup> One can show, for example, that initially massless QCD stays massless in each order of perturbation theory – in contrast to mass generation via dynamical chiral symmetry breaking. Still, perturbative results are extremely valuable in order to connect to the large-momentum region.

**Lattice regularization** is based on the idea of Wick-rotating the Minkowski theory to the Euclidean regime and, by discretizing  $\mathbb{R}^4$ , to replace infinite dimensional functional integrals like

$$\begin{aligned} \langle O \rangle &= \frac{1}{Z} \int \mathcal{D}[A, \bar{\psi}, \psi] O[A, \bar{\psi}, \psi] e^{-\int_{\mathbb{R}^4} d^4x \mathcal{L}_{\text{QCD}}} \\ \text{with } Z &= \int \mathcal{D}[A, \bar{\psi}, \psi] e^{-\int_{\mathbb{R}^4} d^4x \mathcal{L}_{\text{QCD}}} \end{aligned} \quad (1.29)$$

by very high-, but finite-dimensional ones. Originally this was meant to provide a rigorous mathematical foundation of gauge theories. While this goal has not been fully achieved<sup>5</sup>, lattice methods offer the possibility to evaluate various observables via Monte-Carlo integration.

A very short introduction to the lattice is given in [53]. A classical introduction (also for lattice methods applied to spin systems) can be found in [122], for a more recent reference, one may consult [170] or [64]. Since the finite size of a lattice corresponds to an infrared cutoff in momentum space, extremely huge lattices are required to study the infrared asymptotics of quantities, and there is still an ongoing debate about systematic errors, [56, 206].

**Functional methods** aim at extracting information from equations relating the Greens functions of the theory. A quantum field theory is solved when all Greens functions are known – which is of course out of reach in all realistic cases. Still it is possible to obtain valuable information on important Greens functions (in particular propagators and vertices). This is usually done either employing (exact) renormalization group equations or Dyson-Schwinger equations (DSEs). In most of this thesis we will study DSEs, which are discussed in chapter 2.

---

<sup>4</sup>Note however that even in case of small couplings, perturbative series are typically at best asymptotic, but by no means convergent [151]. In addition, since the set of operators with purely discrete spectrum is dense in the set of self-adjoint operators [42], already in ordinary quantum mechanics one can construct examples where arbitrarily small perturbations turn a continuous spectrum into a discrete one, thus dramatically changing the characteristics of a system.

<sup>5</sup>Lattice regularization is very useful for various considerations, and often it is most convenient to formulate an idea first on the lattice before translating it to the continuum. Unfortunately, there are still problems connected with the thermodynamic limit (number of degrees of freedom, i.e. physical volume  $\rightarrow \infty$ ), the continuum limit (lattice spacing  $\rightarrow 0$ ) and possible remnants of the initial hypercubic symmetry, so when applying mathematical standards, this approach cannot be considered as fully rigorous.

## 1.2 The Idea of Gauge-Fixing and Some Consequences

Gauge freedom is the main construction principle of QCD. The fact that one physical state is represented not by one, but by an uncountable infinity of field configurations is typically not an obstacle in the lattice approach. However, one faces a completely different situation both in perturbation theory and when applying functional methods.

### 1.2.1 The Procedure of Gauge-Fixing

*Herr und Meister! Hör mich rufen! –  
Ach, da kommt der Meister!  
Herr, die Not ist groß!  
Die ich rief, die Geister  
werd ich nun nicht los.*

J.W. von Goethe,  
*Der Zauberlehrling*

For perturbative calculations or those based on Greens functions it is necessary to *fix the gauge*, i.e. to impose conditions which single out some configurations (in the best case precisely one) on each gauge orbit. Typically this is done by imposing a condition  $F[A] = 0$  on the gauge fields by inserting a delta functional. In a more general form this reads

$$\mathbb{1} = \int_{\mathbb{G}(x)} \mathcal{D}U J_F[U A] \delta(F[U A] - \omega), \quad (1.30)$$

where one makes use of the invariance of the measure,  $\mathcal{D}[A] = \mathcal{D}[U A]$ , and of the action,  $S[A] = S[U A]$ . The technical details of the procedure are described in any textbook on (non-Abelian) gauge theories, for example in sections 9.4 (Abelian case) and 16.2 (non-Abelian case) of [158].<sup>6</sup> Such a gauge condition corresponds to introduction of a curved surface, as illustrated in figure 1.2.c. The curvature is described by the Jacobian  $J_F = \det \frac{\delta F[U A]}{\delta U}$  which has to be introduced to balance the delta functional.<sup>7</sup> A simple geometric picture is given in figure 1.3.a.

For linear functionals  $F$ , like  $F[A] = n_\mu A^\mu$  or  $F[A] = \partial_i A^i$ , the Jacobian is independent of  $g$ , and the complete  $g$ -integration can be factored out. In the Abelian case,  $J_F$  is even independent of  $A$  and can be completely pulled out of the functional integral, to be absorbed in the normalization. In non-Abelian theories the last step is no longer possible.

Since calculations on curved spaces (i.e. manifolds) tend to be cumbersome, one usually follows Faddeev and Popov [77] in expressing the determinant  $J_F$  as a Gaussian integral over Grassmann-valued (i.e. fermionic) scalar ghost fields  $c$  and  $\bar{c}$ ,

$$\det(\mathcal{M}) = \int \mathcal{D}[\bar{c}, c] e^{\bar{c} \mathcal{M} c}. \quad (1.31)$$

These fields now encode information about the curvature of the gauge-fixing surface. The delta functional is rewritten by functional integration over  $\omega(x)$  in (1.30) with a Gaussian measure centered at  $\omega = 0$  with width  $\xi$ , which describes to what extent field fluctuations around the surface defined by  $F[A] = 0$  are allowed.

$$\int_{-\infty}^{\infty} e^{-\frac{\omega^2}{2\xi}} \delta(F[A] - \omega) d\omega = e^{-\frac{F[A]^2}{2\xi}} \quad (1.32)$$

<sup>6</sup>Note that the standard derivation employs *infinitesimal* gauge transformations, so it is only valid perturbatively. As discussed in sec. 1.2.9, the Faddeev-Popov method has to be modified in the full non-perturbative context.

<sup>7</sup>For a function  $\mathbb{R} \rightarrow \mathbb{R}$  with one simple root  $x_0$  we find  $\delta(f(x)) = \frac{\delta(x-x_0)}{|f'(x_0)|}$ . Thus one has  $1 = \int |f'(x_0)| \delta(f(x)) dx$ . All such equations are of course meant in distributional sense, i.e. they are valid only “under an integral”.

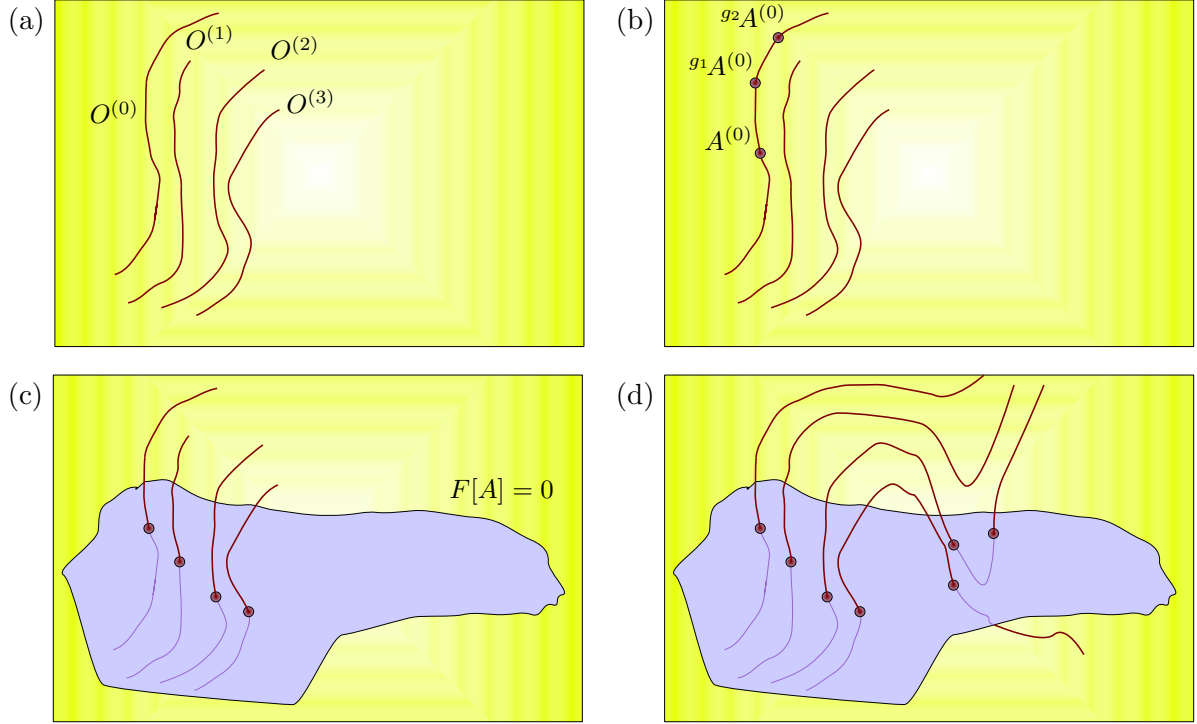


Figure 1.2: The process of gauge-fixing, which we try to illustrate by giving a cartoon of the space  $\mathcal{A}$  of all gauge configurations. (a) All configurations on one gauge orbit  $O^{(k)}$  describe the same physical state. (b) For example there exist gauge transformations  $g_1$  and  $g_2$  which transform the field configuration  $A_1$  to  $g_1 A_1$  and  $g_2 A_1$  while not altering any physical observable. (c) Gauge fixing corresponds to introducing a hypersurface in the space  $\mathcal{A}$  which is typically done by imposing a condition  $F[A] = 0$ . In a (very hypothetically) ideal world this surface would intersect each gauge orbit exactly once. (d) As discussed in section 1.2.3, in non-Abelian gauge theories there are typically gauge-equivalent configurations which fulfill the same gauge condition (Gribov copies). This means the gauge-fixing surface intersects each orbit not only once, but several times.

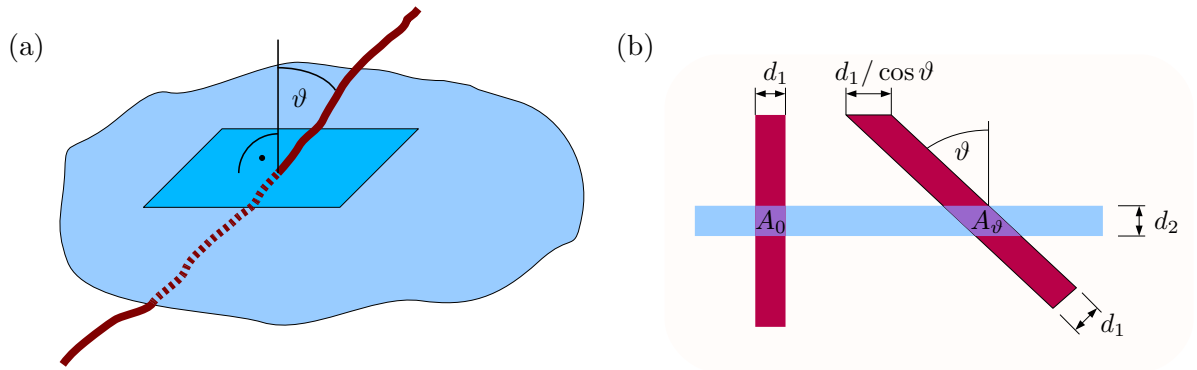


Figure 1.3: (a) The Jacobian  $J_F$  introduced in (1.30) can be interpreted as a factor analogous to  $\cos \vartheta$ , which eliminates the angle dependence in the non-orthogonal intersection of a surface. (b) For non-orthogonal intersection, the area  $A_\vartheta = \frac{d_1 d_2}{\cos \vartheta}$  is larger than the area  $A_0 = d_1 d_2$  obtained by orthogonal intersection. In order to put equal weight to both intersections,  $A_\vartheta$  has to be multiplied by a factor  $\cos \vartheta$ . Analogous reasoning is true also in the higher (and even infinite-)dimensional case, where the Jacobian  $J_F$  replaces  $\cos \vartheta$ .

$$\begin{aligned}
\mathcal{L}_{\text{FP}} = & \bar{\psi} (i \not{D} - m) \psi & \text{---} \xrightarrow{\quad} \text{---}^{-1} \\
& + \frac{1}{2} (\partial_\mu A_\nu^a - \partial_\nu A_\mu^a) (\partial^\mu A^{a,\nu} - \partial^\nu A^{a,\mu}) & \text{---} \text{---} \text{---} \text{---} \text{---} \text{---} \text{---} \text{---} \text{---}^{-1} \\
& + \frac{1}{2\xi} (\partial^\mu A_\mu^a) (\partial^\nu A_\nu^a) & \text{---} \text{---} \text{---} \text{---} \text{---} \text{---} \text{---} \text{---} \text{---}^{-1} \\
& + (\partial^\mu \bar{c}^a) (\partial_\mu c^a) & \text{---} \text{---} \text{---} \text{---} \text{---} \text{---} \text{---} \text{---} \text{---}^{-1} \\
& - g \bar{\psi} \frac{\lambda^a}{2} A_\mu^a \gamma^\mu \psi & \text{---} \text{---} \text{---} \text{---} \text{---} \text{---} \text{---} \text{---} \text{---}^{-1} \\
& + g f^{abc} (\partial_\mu \bar{c}^a) c^b A^{c,\mu} & \text{---} \text{---} \text{---} \text{---} \text{---} \text{---} \text{---} \text{---} \text{---}^{-1} \\
& + g f^{abc} (\partial_\mu A_\nu^a) A^{b,\mu} A^{c,\nu} & \text{---} \text{---} \text{---} \text{---} \text{---} \text{---} \text{---} \text{---} \text{---}^{-1} \\
& + \frac{g^2}{4} f^{abc} f^{ade} A^{b,\mu} A^{c,\nu} A_\mu^d A_\nu^e & \text{---} \text{---} \text{---} \text{---} \text{---} \text{---} \text{---} \text{---} \text{---}^{-1}
\end{aligned}$$

Figure 1.4: Disentangling the Fadeev-Popov Lagrangian (in linear covariant gauge): Each term is supplemented by a graphical representation. Note that the terms quadratic in the fields correspond to the *inverse* propagators, which is indicated by  $^{-1}$ .

This allows to include all factors in the exponent, i.e. to define a modified Lagrangian and cast the generating functional in the form

$$Z = \int \mathcal{D}[A, \bar{\psi}, \psi, \bar{c}, c] e^{i \int d^4x \left( \mathcal{L}_{\text{QCD}} - \frac{1}{2\xi} F^2[A] - \bar{c}^a \mathcal{M}^{ab} c^b \right)}, \quad (1.33)$$

where the the Faddeev-Popov operator  $\mathcal{M}^{ab} = \mathcal{M}^{ab}[A]$  depends on the type of gauge-fixing condition, as for example

$$\mathcal{M}^{ab} = -\partial^\mu D_\mu^{ab}[A] = -\partial^\mu \left( \partial_\mu \delta^{ab} + g f^{acb} A_\mu^c \right) \quad (1.34)$$

for the linear covariant gauges,  $F[A] = \partial_\mu A^\mu$ , or

$$\mathcal{M}^{ab} = -\partial^i D_i^{ab}[A] = -\partial^i \left( \partial_i \delta^{ab} + g f^{acb} A_i^c \right) \quad (1.35)$$

for the Coulomb gauge,  $F[A] = \partial_i A^i$ . The full Lagrangian together with a graphical representation is displayed in figure 1.4. An overview over different prescriptions for gauge-fixing is given in section 1.4.

### Nakanishi-Lautrup Fields

A convenient way to implement gauge-fixing, in particular in the formally singular case  $\xi = 0$ , is by using *Nakanishi-Lautrup fields*  $b$ , which act as Lagrange multipliers, imposing the gauge condition. For Coulomb gauge, this gives a gauge-fixing term  $i(\partial_i b) A_i$  in the action and an additional integration over the auxiliary  $b$ -field,

$$Z = \int \mathcal{D}[A, \bar{\psi}, \psi, \bar{c}, c, b] e^{i \int d^4x \left( \mathcal{L}_{\text{QCD}} + i(\partial_i b^a) A_i^a - \bar{c}^a \mathcal{M}^{ab} c^b \right)}. \quad (1.36)$$

Since  $b$  has no real dynamics (no kinetic term in the action) it can be integrated out by completing the square and performing a Gaussian integral. For many purposes, however, it is useful to include the  $b$ -field in the calculations and integrate it out (thus impose the gauge condition) only in the very last step.

### 1.2.2 BRST-Symmetry

Gauge-fixing inevitably removes gauge-invariance. We can now ask if actually *all* of the symmetries we have gained from the gauge principle have vanished again in this procedure, and the answer is no. There is still a considerable amount of the gauge symmetry left, even though disguised in a way in which it is not immediately recognizable.

As discovered by Becchi, Rouet and Stora [34] and, independently, by Tyutin [196], there exists a certain nontrivial symmetry operator (carrying itself nonzero ghost number), usually denoted by  $s$ , for which we have<sup>8</sup>

$$s\mathcal{L} = s\mathcal{L}_{\text{YM}} + s\mathcal{L}_{\text{gaugefix}} = 0. \quad (1.37)$$

Observables are required to be  $s$ -invariant – in the gauge-fixed theory this substitutes for the gauge invariance present in the initial theory. The BRST operator  $s$  acts analogously to a derivative operator, in particular it is linear and fulfills the product rule,

$$s(\alpha + \beta\gamma) = s\alpha + (s\beta)\gamma + \beta(s\gamma). \quad (1.38)$$

Thus only the action of  $s$  on the elementary fields has to be stated in order to define the operator,

$$\begin{aligned} sA_\mu^a &= D_\mu^{ab}c^b, & sc^a &= -\frac{g}{2}f^{abc}c^bc^c, \\ s\bar{c}^a &= ib^a, & sb^a &= 0. \end{aligned} \quad (1.39)$$

The BRST-operator fulfills  $s\mathcal{L}_{\text{YM}} = 0$  (which is straightforward to check) and it raises the ghost number of any expression by one. Thus the action of  $s$  can be interpreted as *ghost-valued* gauge transformation.

The BRST operator is *nilpotent*, i.e. it fulfills  $s^2\omega = 0$  for any expression  $\omega$ . So we can add any term  $\mathcal{L}_{\text{add}}$  with  $s\mathcal{L}_{\text{add}} = 0$  to the Lagrangian and still preserve the symmetry  $s\mathcal{L} = 0$ . Due to nilpotency, an easy way to obtain such a term is take it of the form  $\mathcal{L}_{\text{add}} = s\mathcal{L}_{\text{something}}$  with arbitrary  $\mathcal{L}_{\text{something}}$ . Such a term does not change the expectation value of physical observables.

Therefore, the easiest way to implement gauge fixing in the BRST formulation is to choose  $\mathcal{L}_{\text{gaugefix}} = s\gamma$ , where the choice of  $\gamma$  is the choice of gauge [231]. Physics is independent of  $\gamma$ , provided that it gives a well-defined calculational scheme. The Coulomb gauge, for example, is defined by the choice  $\gamma_{\text{coul}} = (\partial_i\bar{c}^a)A_i^a$ , which gives

$$\mathcal{L}_{\text{coul}} = s\gamma_{\text{coul}} = s(\partial_i\bar{c}^a)A_i^a = i(\partial_ib^a)A_i^a - (\partial_i\bar{c}^a)D_i^{ab}c^b. \quad (1.40)$$

### The Cohomology of $s$

The nilpotency<sup>9</sup> of the BRST operator  $s$  is actually the key to a very powerful mathematical structure – cohomology. In the following we study an arbitrary nilpotent operator  $s$  that acts on expressions  $\alpha, \beta, \dots$  which we call *forms*. We call a form  $\beta$  *closed*, if  $s\beta = 0$  and call it *exact*, if we can write  $\beta = s\alpha$  with some form  $\alpha$ .

Obviously, each exact expression is closed. We can now ask whether the converse is true as well – if every closed form  $\beta$  is also exact. Interestingly the answer depends on the space on

<sup>8</sup>In this section we will only employ the Yang-Mills Lagrangian, inclusion of quarks is straightforward.

<sup>9</sup>A very important nilpotent operator, which can serve as an excellent example for many concepts, is the exterior derivative  $d$  of modern differential geometry. The apparently simple equation  $d^2 = 0$  contains the relations  $\text{curl grad} = 0$  and  $\text{div curl} = 0$  as well as their generalizations to higher dimensions [149]

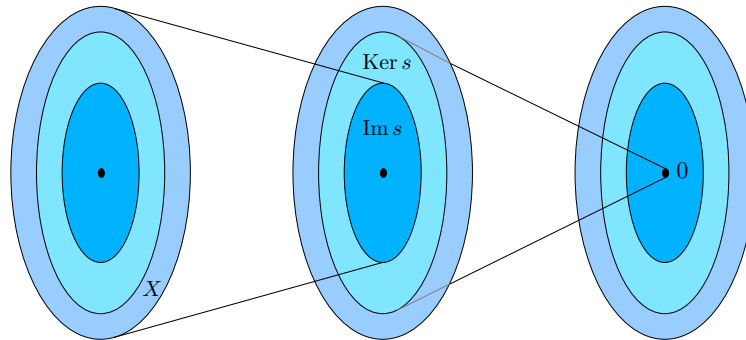


Figure 1.5: For a nilpotent operator  $s: X \rightarrow X$ , it is obvious that  $\text{Im } s \subseteq \text{Ker } s$ . For spaces  $X$  with nontrivial topology,  $\text{Im } s$  can be a proper subset of  $\text{Ker } s$ .

which the forms are defined. There are spaces in which indeed each closed form is exact. In some sense, these spaces are, however, quite boring – their topology is trivial.

For spaces with nontrivial topology, the set of closed forms is in general “larger” than the one of exact ones, so the quotient space  $H_s = \text{Ker } s / \text{Im } s$  can be used to classify the topology of the underlying space.<sup>10</sup> This ratio is called the *cohomology* of the operator  $s$ , see also figure 1.5.

In gauge theories, with  $s$  being the BRST operator, adding  $s$ -exact terms to the action does not change any physical quantity. So one can “factor out” changes by  $s$ -exact terms, and what remains is the cohomology  $H_s$  – which is assumed to contain the set of physical observables.

### Importance of BRST Symmetry

Using BRST symmetry, one can derive several identities for the Greens functions of the theory (usually called Zinn-Justin equations, Ward-Takahashi-identities or Slavnov-Taylor-identities). This is discussed in section 2.4 and plays a key role in proving renormalizability of a quantum field theory.

The Kugo-Ojima confinement scenario, briefly discussed in subsection 1.3, is based on BRST symmetry. The best way of ensuring that additional auxiliary fields do not affect physics is to derive them from an  $s$ -exact term in the action. Nevertheless sometimes also theories with broken BRST symmetry are studied [71, 70] and we will use a related approach in chapter 5.

### 1.2.3 The Gribov Problem

The original goal of imposing a gauge condition was to single out one representative of each orbit. As Gribov has shown [95] the usual gauge conditions do not achieve this in non-Abelian gauge theories.<sup>11</sup> Gauge-equivalent configurations which fulfill the same gauge condition are called *Gribov copies*, see figures 1.2.d and 1.6.

<sup>10</sup>Here  $\text{Ker}$  denotes the kernel and  $\text{Im}$  the image of a mapping. If one recalls that  $\text{Ker}$  contains all elements which are mapped to zero and  $\text{Im}$  all possible image elements of the mapping, it is clear that we can describe  $s$ -closed and  $s$ -exact forms this way.  $\text{Ker } s$  is obviously of the same size or larger than  $\text{Im } s$ , so one can at least hope that such a set-theoretical quotient makes sense – and indeed it does.

<sup>11</sup>In Abelian gauges, it is actually easy to show that the Coulomb gauge condition  $\partial_i A^i = 0$  uniquely fixes the gauge (up to purely time-dependent gauge transformations). Assume that there were two gauge-equivalent configurations  $A_{(1)}^\mu$  and  $A_{(2)}^\mu$  which satisfy  $\partial_i A_{(1)}^i = \partial_i A_{(2)}^i = 0$ . Since one has  $A_{(2)}^i = A_{(1)}^i + \partial^i \chi$  one finds the condition  $\partial_i \partial^i \chi = -\Delta \chi = 0$  and since one is restricted to fields which vanish at infinity,  $\chi$  has to vanish at infinity as well. The maximum principle for harmonic functions now implies  $\chi(x) \equiv 0$ , i.e.  $A_{(1)}^i = A_{(2)}^i$ . This reasoning does no longer hold in non-Abelian gauge theories, since the gauge transformation is done inhomogeneously (according to (1.8)) and the gluon fields at spatial infinity only have to approach a *pure gauge*, i.e. a configuration which is gauge-equivalent to  $A^\mu = 0$ .

In [95] the issue was discussed for Coulomb gauge, but in [181] the emergence of gauge-equivalent configurations fulfilling the same gauge condition was shown to be a general problem of all continuous gauges.



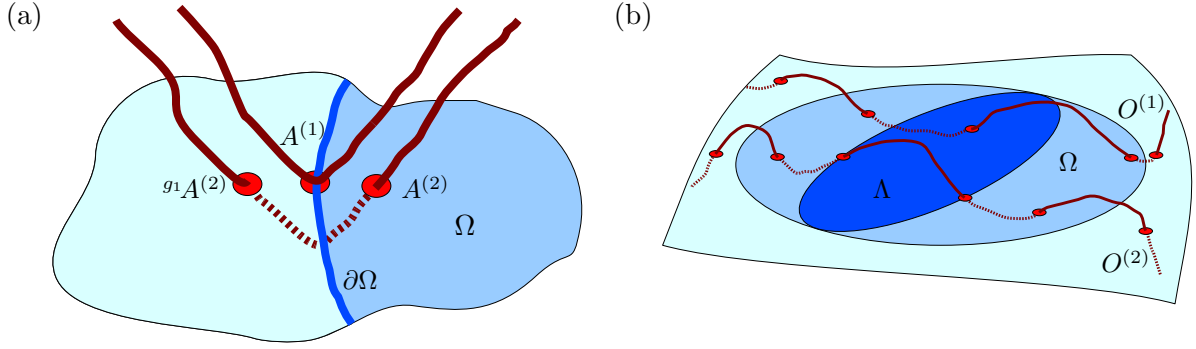


Figure 1.6: (a) For a configuration  $A^{(1)}$  on the Gribov horizon  $\partial\Omega$  we have  $J_F = 0$ , i.e. the orbit touches the gauge-fixing surface. As discussed already in [95], to each configuration  $A^{(1)}$  inside the Gribov region  $\Omega$  and close to the horizon, there exists a gauge-equivalent configuration  $g_1 A^{(2)}$  also close to the horizon, but outside of  $\Omega$ .

(b)  $\Omega$  and the Fundamental Modular Region  $\Lambda$  are both bounded, convex and contain the configuration  $A = 0$ ; they also have some boundary points in common. While orbit  $O^{(1)}$  has a precisely one representative belonging to  $\Lambda$ , the orbit  $O^{(2)}$  has two representatives on the boundary  $\partial\Lambda$ , which have to be identified. Note that while two-dimensional cartoons of infinite-dimensional objects always are somehow misleading, this is aggravated here by the fact that boundary points of  $\Lambda$  have to be identified. Strictly speaking, as soon as this identification has been performed,  $\Omega$  and  $\Lambda$  are no longer subsets of the same space and thus it's particularly dangerous to put both in the same picture.

Originally Gribov had hoped that restriction to the region where the Faddeev-Popov operator  $\mathcal{M}^{ab}$  is positive, the Gribov region  $\Omega$ , would be sufficient to obtain uniqueness while at the same time not missing any gauge orbits. It has been shown [67, 197] that the Gribov region is *overcomplete*. It indeed contains configurations from each orbit – but typically more than once. Thus there are Gribov copies within  $\Omega$ , and an additional condition is necessary to achieve uniqueness, see below.

#### 1.2.4 Gauge-Fixing by Functional Minimization

As first suggested by 't Hooft [192] one can view gauge-fixing also as the process of minimizing the square of a certain norm  $\|A\|_F$ , related to a suitable functional  $F$ . In particular [176, 220] choosing  $\|\cdot\|_F$  as the Hilbert norm (1.7), the stationarity condition  $\delta\|A\|^2 = 0$  yields the transversality condition  $\partial_\mu A^\mu = 0$ . In order to certainly obtain a minimum, one requires the second variation to be positive,  $\delta^2\|A\|_F^2 > 0$ . For  $\|\cdot\|_F = \|\cdot\|$  this condition reads  $(-\partial^2 - A \times \partial) > 0$ , which is positivity of the Faddeev-Popov operator.

Therefore minimization of  $\|\cdot\|$  leads to the Gribov region. The re-interpretation of gauge-fixing as a minimization procedure is important for gauge-fixed lattice calculations and also the starting point for the proof that indeed every gauge orbit intersects the Gribov region, [65].

In general, for a reasonable choice of  $F$ , the first variation yields the gauge-fixing condition and the second variation gives a stability condition which involves a Faddeev-Popov-like operator. In particular, choosing

$$\|A\|_F^2 = \int d^3x \sum_{a,i} |A_i^a|^2 = - \int d^3x \operatorname{tr} \left[ t^a A_i^a t^b A_i^b \right] \quad (1.41)$$

one obtains the Coulomb gauge.



### 1.2.5 The Fundamental Modular Region

We have seen that the Gribov region can be interpreted as the set of all *local* minima of a gauge-fixing functional  $\|A\|_F$ . Uniqueness can be now obtained by specializing to the *global* minimum, identifying degenerate minima. In the metric space induced by  $\|A\|_F$  this corresponds to choosing on each orbit the point(s) closest to the origin  $A = 0$ .

This process gives the *Fundamental Modular Region* (FMR), usually denoted by  $\Lambda$ . While providing unique gauge-fixing,  $\Lambda$  has certain disadvantages as compared to  $\Omega$ :

- Since one invokes a global condition, no local procedure is at hand to implement a restriction to the FMR (and for certain setups it is indeed impossible to find such a local condition, [181]).
- Degenerate minima of  $\|A\|_F^2$  have to be identified. Such degenerate minima only occur on the boundary  $\partial\Lambda$ , but this still gives rise to a complicated topology of  $\Lambda$ , which is difficult to handle.

One can prove some quite general properties of  $\Omega$  and  $\Lambda$ : One finds  $\Lambda \subset \Omega$ , both regions are convex and they have some boundary points in common,  $\partial\Omega \cap \partial\Lambda \neq \emptyset$ . This is depicted (with all caveats that apply for such illustrations) in figure 1.6.b.

In the following we summarize some results, give some proofs (which are typically surprisingly simple) and discuss the question whether it is valid to replace  $\Lambda$  by  $\Omega$  in practical calculations.

### 1.2.6 Convexity of the Gribov Region and the FMR

We are interested in the region where the Faddeev-Popov operator is positive (semi)definite,

$$\mathcal{M}[A] := -\partial^2 - A \times \partial \geq 0. \quad (1.42)$$

For  $A = 0$  this is certainly true, since in this case  $\mathcal{M}$  reduces to the negative Laplacian, which is known to be positive definite.<sup>12</sup>

#### Convexity of $\Omega$

We consider two configurations  $A_1$  and  $A_2$  which both belong to the interior of the Gribov region, so we have  $\mathcal{M}[A_1] > 0$  and  $\mathcal{M}[A_2] > 0$ . One immediately sees that  $M$  is positive for any convex combination of  $A_1$  and  $A_2$  as well, since for  $\alpha_1 > 0$  and  $\alpha_2 > 0$  with  $\alpha_1 + \alpha_2 = 1$  we immediately find due to affine linearity

$$\begin{aligned} \mathcal{M}[\alpha_1 A_1 + \alpha_2 A_2] &= -\partial^2 - (\alpha_1 A_1 + \alpha_2 A_2) \times \partial \\ &= -(\alpha_1 + \alpha_2) \partial^2 - (\alpha_1 A_1 + \alpha_2 A_2) \times \partial \\ &= \alpha_1 (-\partial^2 - A_1 \times \partial) + \alpha_2 (-\partial^2 - A_2 \times \partial) \\ &= \alpha_1 \mathcal{M}[A_1] + \alpha_2 \mathcal{M}[A_2] > 0. \end{aligned} \quad (1.43)$$

Since this result holds for arbitrary  $A_1 \in \Omega$  and  $A_2 \in \Omega$ , we conclude that  $\Omega$  is convex.

With the same argument we can deduce some interesting other properties of  $\mathcal{M}$ . We see for example that outside of  $\Omega$  there exist no points where  $\mathcal{M}[A]$  is positive definite. Else the same would be true for all points on the line segment connecting this point and any point in the Gribov region. (The situation is sketched in figure 1.7.) Such a line segment would inevitably contain a point on the Gribov horizon, where  $M$  is known to be not positive definite.

<sup>12</sup>The minus sign is indeed required to make the operator positive. An intuitive argument for that is that we have  $\frac{d^2}{dx^2} \sin(kx) = -k^2 \sin(kx)$  and  $\frac{d^2}{dx^2} \cos(kx) = -k^2 \cos(kx)$ , so for these functions  $f$  an additional minus sign is required to give  $f''$  the same sign as  $f$ . Since any “reasonable” function can be expressed as Fourier series or Fourier transform, this argument holds for a large class of function.

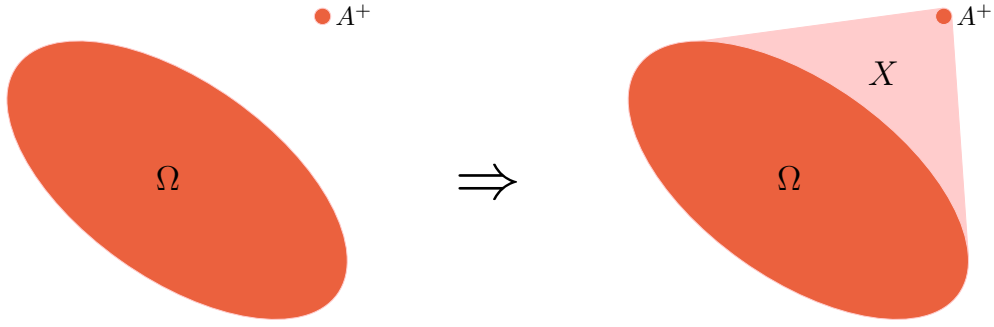


Figure 1.7: The Faddeev operator  $\mathcal{M}$  cannot be positive definite outside of the Gribov region  $\Omega$ . If it was positive in one point  $A^+ \notin \Omega$ , then, due to the convexity argument given in subsection 1.2.6, it would have to be positive also in the whole region  $X$  which consists of all line segments connecting  $A^+$  and points  $A \in \Omega$  and thus also contains a part of the Gribov horizon where  $M$  is known to have zero eigenvalues.

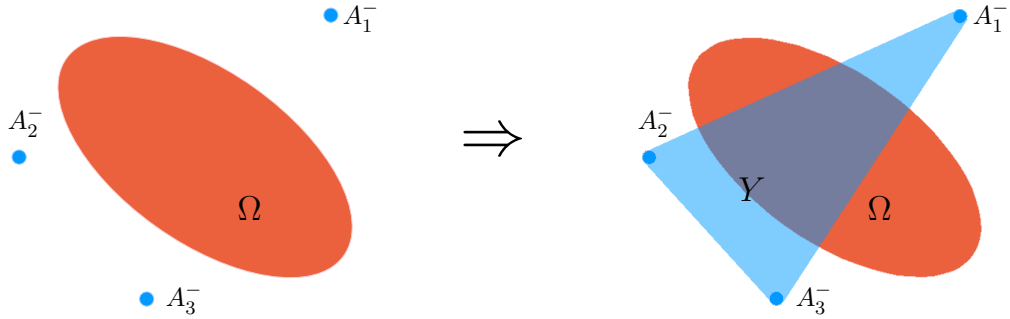


Figure 1.8: If the Faddeev operator  $M$  is negative (semi)definite at some points  $A_i^-$ , then it has to be so also in the convex  $Y$  hull of these points. If such points were to lie “on opposite sides” of  $\Omega$ , this would be in conflict with the positivity of  $M$  inside of the Gribov region.

On the other hand, while the lowest eigenvalue of  $\mathcal{M}$  turns negative when crossing the Gribov horizon, this does by no means imply that  $\mathcal{M}$  becomes negative definite. Rather on the contrary, while we cannot exclude that there is a region for which  $\mathcal{M}[A]$  becomes negative (semi)definite, the range of possibilities for this is extremely restricted.

First, as the gauge field would have to be constructed in a way such that it compensates the positive contribution from  $-\partial^2$  for *all* directions, which, in momentum space, would imply  $|A(k)| \sim k^\alpha$  with  $\alpha \geq 1$ , which is does not look like a particularly well-defined gauge configuration. Since it contains a non-integrable singularity at  $k = \infty$  respectively  $x = 0$  it is no element of  $W^{2,2}(\mathbb{R}^4)$ .

Second, as soon as  $\mathcal{M}$  is negative (semi)definite for a set  $\{A_1^-, A_2^-, \dots\}$  of configurations, this has to be true also for their convex hull. So, for example, a situation as sketched in figure 1.8 is not possible since it contradicts the positivity of  $M$  inside the Gribov region.

### Convexity of $\Lambda$

It is only slightly more involved to show that the FMR is convex as well. We assume that  $A_1$  and  $A_2$  both belong to  $\Lambda$ , i.e.  $\|A_1\|^2 \leq \|U A_1\|^2$  and  $\|A_2\|^2 \leq \|U A_2\|^2$  for all gauge transformations  $U$ . To show that  $A = \alpha_1 A_1 + \alpha_2 A_2$  is an element of  $\Lambda$  as well, we must prove that  $\|A\|^2 \leq \|U A\|^2$  for all gauge transformations  $U$  as well. Employing

$$\|U A\|^2 = \|U^{-1} \partial U + U^{-1} A U\|^2 \stackrel{\text{unitary transf.}}{=} \|(\partial U) U^{-1} + A\| \quad (1.44)$$

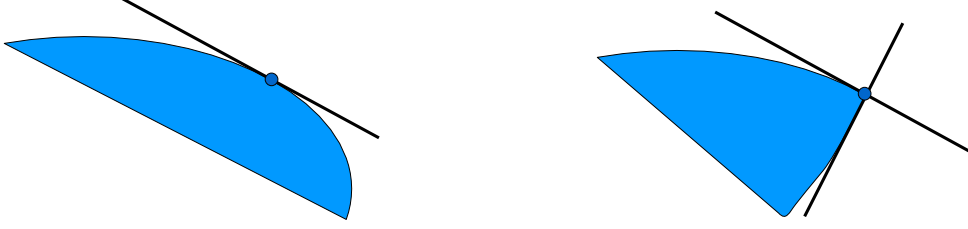


Figure 1.9: For a configuration on the Gribov horizon there is at least one zero-mode direction, tangent to the horizon. There can be (and indeed there are) configurations which have more than one such zero-mode direction and which thus correspond to conical or wedge singularities of the horizon.

we find (with “c.s.” denoting the completion of a square and “u.t.” a unitary transformation)

$$\begin{aligned}
 \|U A\|^2 - \|A\|^2 &= \|U^{-1} \partial U + U^{-1} A U\|^2 - \|A\|^2 = \|(\partial U) U^{-1}\|^2 + 2((\partial U) U^{-1}, A) \\
 &= (\alpha_1 + \alpha_2) \|(\partial U) U^{-1}\|^2 + 2((\partial U) U^{-1}, \alpha_1 A_1 + \alpha_2 A_2) \\
 &= \alpha_1 \left( \|(\partial U) U^{-1}\|^2 + 2((\partial U) U^{-1}, A_1) \right) + \alpha_2 \left( \|(\partial U) U^{-1}\|^2 + 2((\partial U) U^{-1}, A_2) \right) \\
 &\stackrel{\text{c.s.}}{=} \alpha_1 \left( \|(\partial U) U^{-1} + A_1\|^2 - \|A_1\|^2 \right) + \alpha_2 \left( \|(\partial U) U^{-1} + A_2\|^2 - \|A_2\|^2 \right) \\
 &\stackrel{\text{u.t.}}{=} \alpha_1 \left( \|U^{-1} \partial U + U^{-1} A_1 U\|^2 - \|A_1\|^2 \right) + \alpha_2 \left( \|U^{-1} \partial U + U^{-1} A_2 U\|^2 - \|A_2\|^2 \right) \\
 &= \alpha_1 \left( \|U A_1\|^2 - \|A_1\|^2 \right) + \alpha_2 \left( \|U A_2\|^2 - \|A_2\|^2 \right) > 0. \tag{1.45}
 \end{aligned}$$

Thus one sees that also the convex combination  $A = \alpha_1 A_1 + \alpha_2 A_2$  is a global minimum and thus belongs to the Fundamental Modular Region, which is convex as well.

### 1.2.7 Further Properties of $\Omega$ and $\Lambda$

As shown in [66], the Gribov region is contained within a certain ellipsoid and thus bounded.<sup>13</sup> One also knows [67] that the Gribov region is (overcomplete) in the sense that indeed every gauge orbit has a configuration contained in  $\Omega$ .

With the property of convexity in mind, one is tempted to imagine  $\partial\Omega$  as a smooth hypersurface – a picture which is further strengthened by the sketches usually drawn (admittedly also in this thesis.) But convexity does not imply smoothness, as seen for example in the case of regular polygons, and indeed, the naive picture does not really capture the true situation. On the contrary, the Gribov horizon is known to have conical or wedge singularities.

If a configuration belongs to  $\partial\Omega$  this means that there is at least one zero-mode direction, which is, roughly speaking, tangent to the horizon. But there are also configurations which have two or more such directions which are (partially) tangent to the horizon, and, as sketched in figure 1.9 these can be interpreted as “corners” or “tips”.

As shown in [94], one obtains such “tips” – at least in lattice gauge theory – as gauge transforms of special topological configurations called *center vortices* which are believed to play an important role for confinement. Since there are many such center vortex configurations, there are also many “tips” – thus the Gribov region auf lattice gauge theory has been described as similar to a “very high-dimensional pineapple”.

<sup>13</sup>So one knows that  $\Omega = \Omega^0 \cup \partial\Omega$  is both closed and bounded. However since the configuration space  $\mathcal{A}$  is infinite-dimensional, this does not imply that  $\Omega$  is compact.

### 1.2.8 The Zwanziger Conjecture

We have seen that the Gribov region can be described in an local way, while the definition of the FMR requires nonlocal conditions which are much harder to handle. The FMR posses a complicated topology and since on each orbit there are many almost-degenerate minima of  $\|\cdot\|_F^2$ , the problem of finding the absolute minimum is hard – computationally equivalent to finding the ground state of a spin-glass.

Therefore it is convenient to choose  $\Omega$  as the domain of functional integration, even though one should employ  $\Lambda$  instead. It is, however, not entirely clear if this procedure produces valid results. If one knew, for example, that the Gribov region contained  $N_{\text{cop}}$  gauge configurations on each orbit<sup>14</sup> (up to possibly a set of zero measure), integration over  $\Omega$  would yield perfectly valid results, since the gauge orbits were still equally sampled. If, however, for example half of the orbits contained  $N_{\text{cop},1}$  and the other half  $N_{\text{cop},2}$  configurations in the Gribov region, for  $N_{\text{cop},1} \neq N_{\text{cop},2}$ , choosing  $\Omega$  as domain of integration would result in a systematic bias.

This bias could not be circumvented by choosing configurations from  $\Omega$  and transforming them to the FMR, because such a procedure would still inherit the bias contained in  $\Omega$ . It is the process of choosing orbits which determines whether one obtains the correct functional integrals – shifting probability density along the orbit does not influence physics.

Still there are strong arguments [229] that integrating over  $\Omega$  instead of  $\Lambda$  is indeed a valid operation at least for low moments, i.e. for expectation values of products of a few fields. These arguments are based on stochastic quantization and on the relationship between volume and radius in high- and infinite-dimensional spaces.

As it is well-known, the power-dependence of the volume element in  $n$  dimensions,

$$dV_n = r^{n-1} dr d\Omega_n, \quad (1.46)$$

leads to the fact that for large  $n$  almost all of the volume of a sphere is concentrated in a region close to the surface (the “entropy argument”, which is also a main ingredient in the Gribov-Zwanziger confinement scenario, to be discussed in section 1.3.2).

So one can have two sequences of regions  $(\mathcal{R}_1^{(n)})_{n=1}^\infty$  and  $(\mathcal{R}_2^{(n)})_{n=1}^\infty$  in  $\mathbb{R}^n$  with radii  $R_1^{(n)}$  respectively  $R_2^{(n)}$  and  $n$ -volumes  $V_1^{(n)}$  respectively  $V_2^{(n)}$ , which fulfill

$$\lim_{n \rightarrow \infty} \frac{R_1^{(n)}}{R_2^{(n)}} = 1 \quad \text{and} \quad \lim_{n \rightarrow \infty} \frac{V_1^{(n)}}{V_2^{(n)}} = 0 \quad (1.47)$$

at the same time. In fact such a situation is expected to be the case for the FMR and the Gribov region on a sequence of lattices approaching the continuum.

On the one hand, due to vanishing ratio of volumes one would suspect that integrals over both regions give different values. On the other hand, for low moments of the fields it is not the volume which counts. Since each instance of a field contributes a factor roughly proportional to the radius of the domain of integration, one finds for product of  $\nu$  fields

$$\frac{\langle A_{x_1} \dots A_{x_\nu} \rangle_1}{\langle A_{x_1} \dots A_{x_\nu} \rangle_2} \sim \left( \frac{R_1}{R_2} \right)^\nu. \quad (1.48)$$

Thus for  $\nu \ll n$ , the ratio of the radii, not the ratio of the volumes determines the ratio of the expectation values. For small  $\nu$  and  $\frac{R_1}{R_2} \approx 1$ , this ratio is close to one, so it shouldn't matter whether an expectation value is calculated in region  $\mathcal{R}_1^{(n)}$  or  $\mathcal{R}_2^{(n)}$ .

Thus gluon propagators or vertices should not feel the difference between  $\Omega$  and  $\Lambda$ . Unfortunately (or not) the situation is different for the ghost, since  $\langle \mathcal{M}^{-1}[A] \rangle$  contains moments of all orders – so the Faddeev-Popov operator and thus the ghost propagator is expected to be sensitive to the domain of integration.

---

<sup>14</sup>To simplify the presentation we only regard the case of a finite number of Gribov copies within the Gribov region.

### 1.2.9 Remarks on Nonperturbative Gauge-Fixing

The perturbative (i.e. weak coupling) expansion is an expansion of the action around the Gaussian minimum ( $A_\mu = 0$  in Lie algebra respectively  $U_\ell = \mathbb{1}$  in Lie group language). Such an expansion yields quadratic terms in some directions, but there are also flat directions where variation does not change the value of the action. Such flat directions correspond to gauge transformations, which would introduce the volume of the gauge group and which are eliminated by gauge-fixing.

In sec. 1.2.1 we have outlined the procedure required to implement such gauge-fixing in the perturbative setup. However, the straightforward Faddeev-Popov procedure, making use of (1.30), does only work if the condition  $F[A] = 0$  provides unique gauge-fixing.

While this is true perturbatively, the existence of Gribov copies obscures the issue in full non-perturbative treatment, and accordingly, the Faddeev-Popov procedure has to be modified [220]. A comprehensive summary of various approaches has been given in the introduction to [102]:

One suggestion [152] was that all Gribov copies, weighted with the Faddeev-Popov determinant, should contribute to the functional integral. This is equivalent to insertion of a topological invariant [29, 30] into the partition functions. Unfortunately, this invariant, the Euler characteristic of  $SU(N_C)$ , turns out to be zero due to cancellations between positive and negative contributions, so in this approach all observables are indefinite quantities of the form  $\frac{0}{0}$ . This is the famous *Neuberger problem*.

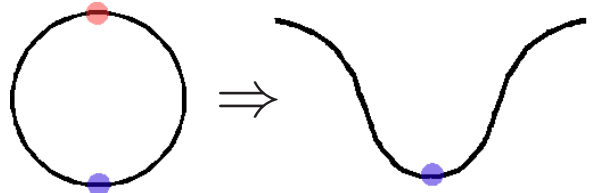
For Dyson-Schwinger equations, to be discussed in chapter 2, the situation is fortunately clearer. Using stochastic quantization to bypass the Gribov problem, Zwanziger showed [229] that the system of Dyson-Schwinger equations is unchanged, but supplemented by additional constraints which reflect that gauge configurations are restricted to the Gribov region.

In fact, many manipulations of functional integrals (“partial integration”) require boundary terms to vanish. This can be achieved by imposing suitable boundary conditions at infinity (in function space), but also by cutting off the functional integral at a nodal surface like the Gribov horizon. This guarantees that boundary terms vanish, and therefore functional integrals restricted to  $\Omega$  may have a more sound mathematical foundation than those defined on the whole space  $\mathcal{A}$ .

On the lattice, a procedure based on stochastic quantization has been proposed [102] in order to find a way around the Gribov problem and to determine – for Coulomb gauge in a certain limit – the FMR configuration without having to solve a spin-glass problem.

There are also proposals to directly circumvent the Neuberger problem. In [206] it was suggested that stereographic projection could yield a solution. The main idea can be illustrated best when using  $\mathbb{G} = SU(2)$ , which is geometrically a 3-sphere. The sphere has two critical point, the north pole and the south pole, which correspond to opposite signs and thus give zero when combined additively.

When projecting one of the critical points to infinity, the corresponding contribution is removed and quantities with support on the critical points no longer vanish by construction, but may acquire a finite value. When performed correctly, such a projection does not change the continuum limit, the same way the replacement of  $\sin \psi$  by  $\tan \psi$  or  $\ln(1 + \psi)$  does not change the  $\mathcal{O}(\psi)$  part in a neighbourhood of  $\psi = 0$ .



## 1.3 The Problem of Confinement

One of the hardest – and most fascinating – topics of QCD is the issue of *confinement*. Unfortunately already the mere question how to properly define this term is tough. For a good introduction to the topic see [9].

### 1.3.1 On the Definition of Confinement

Since gauge theories are constructed by demanding gauge invariance, it is obvious that a closed system described by such a theory has to be gauge invariant as well. This is not necessarily true if one considers smaller subsystems. One could imagine a colorless object, composed of a red quark in Graz, a green quark in New York and a blue quark behind the moon – so the single colored objects could be studied almost independently.<sup>15</sup> This is not what is observed in nature – color charges are always confined to much smaller length scales of about  $\frac{1}{\Lambda_{\text{QCD}}} \approx 1 \text{ fm}$ .

There is no color analogue to ionization in electrodynamics – the attempt to kick out a colored particle always results in the production of new colorless objects. This can be understood the following way: When trying to separate, for example, the quark and antiquark of a meson, the energy of the system is at some point large enough to create a quark-antiquark pair which splits up and color-neutralizes both constituents. So instead of a quark and an antiquark, one has obtained two mesons.

The main requirement for this picture is that indeed enough energy is stored in the quark-antiquark system, i.e. that the force does not fall off, at least not too rapidly (as the  $\frac{1}{r}$ -potential of electrodynamics does, which permits ionization).

### Asymptotic Space of Colorless States

One possible way to impose confinement is to demand that colorless asymptotic states are exclusively scattered into colorless asymptotic states by all possible processes. If colorless initial conditions are imposed, this guarantees confinement.

Unfortunately this definition is plagued with severe difficulties. Typically one identifies asymptotic states with states of the free (non-interacting) theory and the interaction is switched on and off adiabatically. While such a procedure makes sense to all orders in perturbation theory (by the Gell-Mann–Low theorem), it is in conflict with Haag’s theorem which states that theories with different interaction strength are unitarily inequivalent. This is in particular true for the free and any interacting theory – the Fock spaces are just different and there is no unitary mapping between them.<sup>16</sup> (However parts of this problem can be circumvented; see [99] for a rigorous discussion.) In some sense *all* gauge theories are either confining (or strictly speaking ill-defined, as it is the case for QED<sup>17</sup>). For example the physical electron is a bound state of a (massless) naked electron and the Higgs field which neutralizes the weak charge.

---

<sup>15</sup>Actually, an appropriate rotation in color space could transform a red quark into a green or a blue one, so it makes little sense to speak of color itself as if it was a genuine physical property. However, any device designed to measure the color of an object would be affected as well, so a single color charge could nevertheless be considered as a reasonable physical object.

<sup>16</sup>This can be understood already intuitively. For the free theory, the eigenstates of the Hamiltonian are the eigenstates of the momentum operator, i.e. plane waves. A plane wave  $e^{ikx}$  extends over all of spacetime, so what is a plane wave will stay a plane wave forever. Conversely, if an interaction affects a particle at any time, it can’t have been a plane wave in the first place.

<sup>17</sup>QED has no mass gap, i.e. it permits states of arbitrarily small mass (photons of arbitrarily small energy). Any possible detector has a certain minimum energy threshold, thus for any given detection device there are infinitely many states which are indistinguishable since they only differ by soft photons with energies below the detection threshold. [Note that chiral QCD contains massless pions and thus suffers from a similar problem!]

Far worse, QED presumably has a *Landau pole*  $\Lambda_{\text{QED}}$  at extremely large momenta which might render the whole theory ill-defined for any non-vanishing interaction strength. This is a sign that in spite of its tremendous success, QED has to be embedded in a more complete theory, which modifies or cuts off this momentum region. The Landau pole indeed lies beyond the Planck scale, where quantum gravity is expected to set in.



### BRST Quartets and the Kugo-Ojima Picture

In QED, the Gupta-Bleuler prescription guarantees that unphysical longitudinal and scalar (timelike) photons cancel in Feynman amplitudes and thus in physical observables. In QCD this issue is complicated by the self-interaction of the gluons. A consistent quantization is possible in the BRST formalism (see subsection 1.2.2), where longitudinal and timelike gluons form a *metric quartet* with ghosts and antighosts.

It has been conjectured that global BRST symmetry is unbroken. If this is the case, by virtue of Noether's theorem there exists a BRST-charge, which has to be regarded as “unphysical”. Such a charge is carried by all members of such BRST quartet, while physical states are precisely those with vanishing BRST charge. In this picture confinement can be set in correspondence with the existence of such a BRST charge – this is the basis of the *Kugo-Ojima* confinement scenario: Since longitudinal and timelike gluons form metric quartets with ghosts, they are “unphysical”, i.e. do not appear in the space of asymptotic states. If transverse gluons carry BRST charge as well, they are removed from the physical spectrum as well.

### Positivity Violation

From asymptotic scattering theory (see e.g. section 5.1 in [109]) one can deduce that asymptotic fields (i.e. those with excitations which can be regarded as “real” particles) and their combinations can be expressed in terms of nonnegative spectral functions  $\sigma$  which vanishes outside of the forward light-cone,

$$\sigma(p) = \sigma(p^2) \Theta(p_0) \quad \text{with} \quad \sigma(p^2) = 0 \quad \text{if} \quad p^2 < 0. \quad (1.49)$$

For the time-ordered product of two scalar fields (a two-point Green function, see section 2.1), for example, this *Källen-Lehmann representation* has the form

$$\begin{aligned} G(x, y) &\equiv \langle 0 | \mathcal{T} \varphi(x) \varphi(y) | 0 \rangle \\ &= i \int_0^\infty d\mu^2 \sigma(\mu^2) \int \frac{d^4 k}{(2\pi)^4} \frac{1}{k^2 - \mu^2 + i\epsilon} e^{-i k \cdot (x-y)}. \end{aligned} \quad (1.50)$$

The existence of a nonnegative spectral function translates to the condition that the wavefunction of an (potentially) asymptotic particle can be expressed as a nonnegative function. In the typical sloppy speech of physics this nonnegativity condition is frequently referred to as *positivity*. We note that wave functions which extend to spatial infinity have to fulfill the momentum-space condition  $\tilde{\psi}(0) \neq 0$ . From the Fourier integral representation

$$\tilde{\psi}(k) = \int_{\mathbb{R}^d} d^d x e^{-i k \cdot x} \psi(x) \quad (1.51)$$

we obtain for confined fields (which vanish at infinity) at  $k = 0$

$$\tilde{\psi}(0) = \int_{\mathbb{R}^d} d^d x \psi(x) \stackrel{!}{=} 0. \quad (1.52)$$

This can only be possible (in the nontrivial case  $\psi \not\equiv 0$ ) if contributions with different phases cancel. If  $\psi$  is chosen real, this means that one finds open regions  $X_1 \in \mathbb{R}^d$  and  $X_2 \in \mathbb{R}^d$  with  $\psi(x_1) > 0$  for all  $x_1 \in X_1$  and  $\psi(x_2) < 0$  for all  $x_2 \in X_2$ . Thus positivity is violated.

### The Linearly Rising Potential

In quenched lattice gauge theory one can show [23] that the physical potential between two static fundamental charges (which may be interpreted as infinitely heavy quarks) the inequalities

$$-\frac{dV(r)}{dr} < 0 \quad \text{and} \quad \frac{d^2V(r)}{dr^2} \leq 0 \quad (1.53)$$

hold. The second inequality is precisely saturated by a linearly rising potential and lattice data (see e.g. [24]) indicates that the static potential between fundamental charges is indeed linearly rising (or at least very close to a linearly rising) for larger distances.<sup>18</sup>

For this reason one sometimes (in particular in lattice gauge theory) *identifies* confinement with the existence of an asymptotically linearly rising potential<sup>19</sup>. In this sense even full QCD is not confining, only screening, since one observes *string breaking* and the potential (if one even dares to define one) flattens out. Still even in full QCD the (presumably) linearly rising potential governs the behaviour at intermediate distances and provides the energy for pair creation.

We note that the linearly rising static potential

$$V(\mathbf{x}, t) = \sigma |\mathbf{x}| \delta(x_0) \quad (1.54)$$

with constant string tension  $\sigma$  can – with some caveats<sup>20</sup> – be transformed to momentum space. For this transformation one obtains (with  $k := \|\mathbf{k}\|$ )

$$\begin{aligned} V(\mathbf{k}^2, k_0) &= \int_{\mathbb{R}^4} d^4x e^{-i(k_0 x_0 - \mathbf{k} \cdot \mathbf{x})} \sigma |\mathbf{x}| \delta(x_0) = \sigma \int_{\mathbb{R}^3} d^3x e^{i\mathbf{k} \cdot \mathbf{x}} |\mathbf{x}|^{1+\alpha} \\ &= 2\pi\sigma \int_0^\infty dr \int_{-1}^1 d(\cos \vartheta) e^{ikr \cos \vartheta} r^3 = \frac{4\pi\sigma}{k} \int_0^\infty dr r^2 \sin(kr) \\ &= \frac{4\pi\sigma}{k^4} \int_0^\infty d(kr) (kr)^2 \sin(kr) = \frac{4\pi\sigma}{k^4} \int_0^\infty t^2 \sin t dt. \end{aligned} \quad (1.55)$$

This dimensionless integral does not exist in the immediate Lebesgue sense, but the straightforward  $e^{-\varepsilon t^2}$  regularization yields the value  $(-2)$ , thus one obtains

$$V(\mathbf{k}, k_0) = -\frac{8\pi\sigma}{k^4}. \quad (1.56)$$

The details of this calculation (and its generalizations, see below) are given in appendix C.2. A modified version of this potential (changed in order to reproduce the correct UV behaviour) is an important input for the calculations performed in chapter 4.

One can generalize these considerations to potentials of the form

$$V(\mathbf{x}, x_0) = \sigma |\mathbf{x}|^{1+\alpha} \delta(x_0) \quad (1.57)$$

with  $-1 < \alpha < 1$ , for which one obtains

$$V(\mathbf{k}, k_0) = \frac{2^{2+\alpha} \sqrt{\pi} \Gamma(2 + \frac{\alpha}{2})}{\Gamma(-\frac{1}{2} - \frac{\alpha}{2})} \frac{4\pi\sigma}{k^{4+\alpha}}. \quad (1.58)$$

<sup>18</sup>The quantities actually studied are rectangular *Wilson loops*. If the expectation value of a Wilson loop is proportional to its area (*area law*), this corresponds to a linearly rising potential. In contrast, a *perimeter law* would indicate deconfinement.

<sup>19</sup>This condition is very strict and motivated mostly by phenomenology. In principle any monotonically rising unbounded potential is sufficient for the effect of confinement.

<sup>20</sup>Neither the linear rising function nor the  $\frac{1}{k^4}$ -potential that's obtained by Fourier transform belong to  $\mathcal{L}^1$ , the space of Lebesgue-integrable functions. Thus a regularization procedure is necessary to define the Fourier-transform of such a linearly rising potential.



### 1.3.2 The Gribov-Zwanziger Scenario

In [95] Gribov has not only shown that there are typically many gauge copies which fulfill the same gauge condition, but he has also pointed out a possible explanation for confinement (originally proposed in Coulomb gauge). He roughly estimated that configurations close to the Gribov horizon contribute to a  $1/k^4$ -potential for color charges and thus to confinement.

As already briefly mentioned in sec. 1.2.8, most of the volume of a high-dimensional convex object is contained in the region close to its surface. The volume of a ball  $B_r$  with radius  $r$  in  $D$  dimensions is proportional to  $r^D$ , more accurately we have

$$V(B_r) = \frac{2\pi^{D/2}}{\Gamma(D/2)} \frac{r^D}{D} =: \frac{A_D r^D}{D}. \quad (1.59)$$

Accordingly, the volume of a spherical shell  $S_{r_1, r_2}$  with  $r_1 > r_2$  is given by  $V(S_{r_1, r_2}) = \frac{A_D}{D}(r_1^D - r_2^D)$ . For the ratio of this volume to the one of a ball of radius  $r_1$ , we obtain

$$\frac{V(S_{r_1, r_2})}{V(B_{r_1})} = \frac{r_1^D - r_2^D}{r_1^D} = 1 - \left(\frac{r_2}{r_1}\right)^D \xrightarrow{D \rightarrow \infty} 1. \quad (1.60)$$

Thus even if  $r_2$  is very close to  $r_1$ , for sufficiently high dimensions still an arbitrarily large fraction of the total volume is contained in such a thin shell. That's an even stronger statement in the infinite-dimensional case, where the surface may contain *all* of the volume.<sup>21</sup>

Thus configurations close to the Gribov horizon  $\partial\Omega$  are expected to dominate a functional integral restricted to the Gribov region  $\Omega$ . If a sufficient fraction of configurations on  $\partial\Omega$  could be shown to be confining, one could deduce that the whole theory defined by the functional integral was confining as well.

This scenario has been elaborated by Zwanziger [221, 222] who succeeded in incorporating the influence of the Gribov horizon into a local action. This is achieved by introducing a cutoff function (horizon function)

$$H = -\frac{1}{2C_A} \int d^d x d^d y \left\{ D_\mu^a(x) \mathcal{M}^{-1}[A]^{ab}(x, y) D^{\mu, b}(y) - d(N_C^2 - 1) \right\} \quad (1.61)$$

at the Gribov horizon and localizing it by integration over a quartet  $(\varphi, \bar{\varphi}, \omega, \bar{\omega})$  of auxiliary ghost fields,

$$Z = \int \mathcal{D}(A, c, \bar{c}, b, \varphi, \bar{\varphi}, \omega, \bar{\omega}) e^{i \int d^d x (\mathcal{L}_{\text{YM}}[A] + \mathcal{L}_{\text{gf}}[A, c, \bar{c}, b] + \mathcal{L}_{\text{GZ}}[A, \varphi, \bar{\varphi}, \omega, \bar{\omega}])} \quad (1.62)$$

$$\mathcal{L}_{\text{gf}} = i(\partial^\mu b^a) A_\mu^a + \bar{c}^a \mathcal{M}^{ab} c^b \quad (1.63)$$

$$\mathcal{L}_{\text{GZ}} = \bar{\varphi}^{\mu, ab} \mathcal{M}^{bc} \varphi_\mu^{ca} + \bar{\omega}^{\mu, ab} \mathcal{M}^{bc} \omega_\mu^{ca} + \gamma^{1/2} C_A^{-1/2} f^{abc} \varphi^{\mu, ac} A_\mu^b \quad (1.64)$$

with a thermodynamic parameter  $\gamma$  to be fixed by a stationarity condition. Consequently the term *Gribov-Zwanziger scenario* is typically used for this approach to confinement.

---

<sup>21</sup>This argument is essential in statistical physics. In the microcanonical ensemble (where the energy  $H(p, q)$  of a system takes a fixed value  $E$ ), it doesn't matter whether one looks at all configurations with  $H(p, q) = E$  or  $H(p, q) \leq E$ , thus one can write in a sloppy, but basically correct way

$$\delta(E - H(p, q)) = \Theta(E - H(p, q)),$$

as long as the integral is taken over the whole configuration space. In the transition to the canonical ensemble, one can remain basically correct by performing the replacement

$$\delta(E - H(p, q)) \rightarrow e^{-\beta H(p, q)}$$

where the inverse temperature  $\beta \equiv \frac{1}{k_B T}$  is chosen such that  $\langle H(p, q) \rangle = E$ .

Configurations close to  $\partial\Omega$  have at least one near-zero mode in the Faddeev-Popov operator  $\mathcal{M}^{ab}[A]$  and thus the ghost propagator (which is essentially the inverse of  $\mathcal{M}^{ab}[A]$ ) blows up. For this effect the term *ghost dominance* has been coined. Ghost dominance has the potential to solve a puzzle which has accompanied confinement for a long time – the question of *confining* vs. *confined gluons* (see also the discussion in [13]):

On the one hand one would expect the gluon propagator to *vanish* for small momenta  $k$  (i.e. long distances) since gluons should not appear as asymptotic states – confined gluons. On the other hand one expects gluons to mediate the confining force, i.e. the propagator should *diverge* or at least remain finite for small momenta – confining gluons.<sup>22</sup> In the ghost dominance scenario the gluon propagator can safely vanish for small  $k$  since confinement is mediated by the (already a priori unphysical) ghost.

In Landau gauge the connection between an infrared-enhanced ghost and an infrared-vanishing gluon is most easily understood by analyzing the gluon Dyson-Schwinger equation [13, 204, 205].

$$\text{Gluon loop}^{-1} = \dots + \text{Gluon self-energy} + \text{Ghost loop} + \dots \quad (1.65)$$

The ghost loop on the right-hand side is infrared enhanced and thus the gluon propagator is accordingly suppressed – the gluon cannot propagate over long distances. (For details on such equations, in particular in the deep infrared, see chapter 2.)

While this scenario is regarded as well-established in functional Landau-gauge, the translation to other gauges (including the Coulomb gauge) turned out to be significantly more involved. In Coulomb gauge the picture is additionally modified by the fact that a piece of the gluon propagator, namely  $D_{00}(k)$ , indeed diverges for  $k \rightarrow 0$ . This issue is discussed in more detail in chapter 3.

For a while, gauge-fixed lattice data seemed to support the picture of an infrared-diverging ghost and an infrared-vanishing gluon very well. Recent publications, however, which use huge lattices, have cast a shadow of doubt on this scenario [56]. At the moment it is heavily discussed how to interpret results which point towards a finite ghost and a massive gluon (the “massive solution” as opposed to the “scaling solution” required for Gribov-Zwanziger) [82, 57]. In addition there is still an ongoing debate about systematic errors introduced by gauge-fixing on the lattice [206].

Another possible point of criticism is the gauge-dependence of the scenario – the Gribov region and the Gribov horizon look different in different gauges, so different configurations are made responsible for confinement. In some sense, however, the scenario incorporates certain gauge-invariant features [233]:

Consider  $\omega$  from the Lie algebra, which transforms covariantly, i.e. which fulfills  $D_\mu[A]\omega = 0$ . This means that one has

$$\partial_\mu \omega + A_\mu \times \omega = 0. \quad (1.66)$$

This equation is gauge-invariant in the sense that for any gauge transformation  $g$  the transformed equation  $D_\mu({}^g A){}^g \omega = 0$  holds as well.<sup>23</sup>

Equation (1.66) implies (since it is required to hold as an identity for all  $x \in \mathbb{R}^d$ ) also  $\partial^\mu D_\mu[A]\omega = 0$ , i.e. the (Landau gauge) Gribov horizon condition which consequently survives gauge transformations as well. So in this case gauge transformations don’t act freely, but we have found a gauge-invariant condition which selects a special class of orbits.

<sup>22</sup>This picture has been called *infrared slavery* as opposed to asymptotic freedom.

<sup>23</sup>Note that for a transformation  $g = 1 + \omega$  we have  ${}^g A_\mu = A_\mu + D_\mu[A]\omega = A_\mu$ .

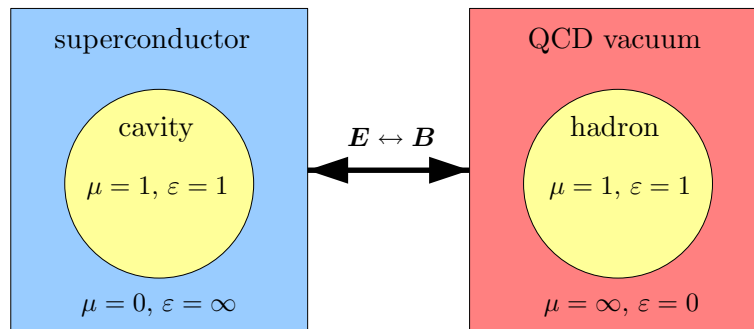


Figure 1.10: The dual Meissner effect and the bag model

### 1.3.3 Some Other Scenarios

There are several other confinement scenarios which are discussed in the literature, and sometimes it is hard to locate the border between true explanations and mere descriptions of the effect. We have mentioned the Kugo-Ojima scenario on page 23 and discussed the Gribov-Zwanziger scenario in sec. 1.3.2. Now we will briefly review some other scenarios and point out certain connections to the Gribov-Zwanziger picture.

#### Dual Meissner Effect

Older explanations are often given in the language of chromoelectric and chromomagnetic fields as well as corresponding quantities. For example one can define a chromoelectric permittivity  $\varepsilon = \varepsilon_{\text{chr}}$  and a chromomagnetic permeability  $\mu = \mu_{\text{chr}}$ . Since gluons, which are interpreted as quantized chromoelectromagnetic waves, propagate with the speed of light  $c$ , one still has

$$\varepsilon \mu = 1 = c^2. \quad (1.67)$$

In (electromagnetic) superconductors the magnetic field is collimated to a flux tube – similar to what is expected from the chromoelectric field in QCD. Since the role of (chromo)electric and magnetic fields is interchanged as compared to superconductivity, the scenario is called the *dual Meissner Effect*.

As illustrated in figure 1.10 a hadron is seen as analogously to a cavity in a superconductor. Within the hadron, the quarks and gluons behave as free particles, but they cannot penetrate the QCD vacuum, characterized by  $\mu = \infty$ .

Since the hadrons can be interpreted as “bags” of perturbative vacuum, embedded in the “true” nonperturbative vacuum, this picture is also known as the (MIT) *bag model*. The energy difference between perturbative and nonperturbative vacuum is characterized by the bag constant  $B$ .

#### Supercritical Charges

In [96, 97] it has been speculated that the confinement of light quarks is based on the supercriticality of color charge, combined with properties of the pion cloud (Gribov’s Picture of Confinement, not to be confused with the Gribov-Zwanziger scenario).

The appealing basic idea is that in contrast to QED where one needs  $Z > 137$  in order to have supercriticality, in QCD with its large coupling constant even a single color charge may be supercritical and thus generate new color charges from the vacuum in order to screen itself.

One problem of this picture is that gluons (living in the adjoint representation of  $SU(3)$ ) cannot screen quarks (carrying fundamental charge), and recent investigations [83] have found no evidence for the picture of supercriticality.

### Topological Objects: Instantons, Monopoles, Center Vortices

In the path integral picture, it may be possible to make certain configurations responsible for confinement.<sup>24</sup> Typically one is particularly interested in configurations which can be characterized by nontrivial topology (“topological defects”).

These defects can be zero-dimensional (e.g. instantons), one-dimensional (e.g. monopoles) or two-dimensional (e.g. vortices). Instantons<sup>25</sup>, representing solutions of the classical field equations and characterizable (via the Atiyah-Singer index theorem [21, 22]) by

$$\frac{g^2}{32\pi^2} \int d^4x F_{\mu\nu}^a \tilde{F}^{a,\mu\nu} \quad \text{with} \quad \tilde{F}^{a,\mu\nu} = \epsilon^{\mu\nu\rho\sigma} F_{\rho\sigma}^a \quad (1.68)$$

have been intensively studied in the past, but by now the general consensus is that instantons alone are not confining (in four dimensions). Matters are different for monopoles and in particular (center) vortices which are repeatedly held responsible for confinement (see also sec. 1.4.4).

Topologically nontrivial configurations cannot be reached by small perturbations, consequently they are inaccessible in perturbation theory. This manifests itself in the fact that instanton contributions to the action have the form  $\exp(\frac{\dots}{g^2})$ , i.e. they have an essential singularity in the coupling.

### Abelian Dominance

While SU(3) Yang-Mills theory is genuinely non-Abelian, it has been postulated that nevertheless Abelian configurations (i.e. those diagonal in color space,  $A_\mu = A_\mu^3 \frac{\lambda^3}{2} + A_\mu^8 \frac{\lambda^8}{2}$ ) are responsible for confinement. This issue is best discussed in the Maximum Abelian gauge (MAG), see sec. 1.4.4.

### Connections to the Gribov-Zwanziger Scenario

Several of the scenarios mentioned in this section are related to the Gribov-Zwanziger approach: After introducing the Gribov-Zwanziger term in the QCD Lagrangian, stationarity of the effective action defines a new vacuum which has different energy from the original (perturbative) one. This energy shift and the value of the constant  $\gamma$  could be set in direct correspondence with the bag constant  $B$ . The “true” nonperturbative vacuum is influenced by the additional term which is invisible in the perturbative approach.

Both the Abelian dominance and the center vortex scenario are related to Gribov-Zwanziger as well: When transformed to the Coulomb gauge, most Abelian configurations end up on the Gribov horizon. As shown in [94], when transforming a (thin) center vortex configuration to Coulomb gauge, it ends up on the Gribov horizon, where it constitute conical or wedge singularities (i.e. a point where the Faddeev-Popov operator has more than one zero eigenvalue).

**Further Notes** There seems to be a close connection between confinement and chiral symmetry breaking; at least for massless quarks chiral symmetry breaking is expected to be a necessary condition for confinement [46].<sup>26</sup> On the other hand it is heavily disputed whether confinement is also necessary for chiral symmetry breaking or if one could find a phase where confinement is absent, but chiral symmetry is still broken.

<sup>24</sup>On the lattice it is easy to check the influence of certain configurations by simply removing them from the ensemble. One should, however, be cautious when drawing direct conclusions from this procedure.

<sup>25</sup>It is also possible to separate one instanton into  $N_C$  dyons. At finite temperature calorons take the place of instantons; calorons with nontrivial holonomy (Kraan-van Baal calorons) have particularly peculiar properties.

<sup>26</sup>This argument by Casher has roughly the following form: Imagine a chiral quark and a corresponding anti-quark flying away from each other in opposite directions. A confining force between them has to pull them back at some point, which means it has to flip helicity. This helicity flip, however, is only possible if the quarks have nonzero mass, i.e. if they have acquired mass via dynamical chiral symmetry breaking. This argument is widely believed to be correct, but see also [89].

## 1.4 Standard and Nonstandard Gauges

*People played the old game of  
“My gauge is better than yours”.*

Peter Arnold at the 46<sup>th</sup>  
Schladming winter school

While all physical processes and quantities are unaffected by the choice of gauge, this is usually not true for objects which are not directly observable – for example Greens functions, to be discussed in chapter 2. The same physical effect can be generated by completely different “mechanisms”, depending on the gauge.

In the gauge-dependent sector one can discover fields which violate the spin-statistics theorem (for example the Faddeev-Popov ghosts, which happen to be scalar fermions), instantaneous interactions (which would clearly violate locality and thus causality if they were also present in the physical sector) and so on.

Various gauges have completely different advantages and disadvantages, thus it is no surprise that a large number of them has been employed over the years to study various aspects of QCD. We will shortly review some of the most popular ones.

### 1.4.1 Linear Covariant Gauges

Linear covariant gauges are probably the most popular choice for gauge fixing. They are defined by the condition

$$\partial_\mu A^\mu = 0, \quad (1.69)$$

with fluctuations around zero described by the gauge parameter  $\xi$  (as discussed in subsection 1.2.1). One typically chooses the Feynman-t’Hooft gauge  $\xi = 1$  for perturbative calculations and the Landau gauge  $\xi \rightarrow 0$  in the functional approach. This is motivated by the fact that the gluon propagator takes the most simple form for  $\xi = 1$ , while  $\xi = 0$  is a fixed point under renormalization. Sometimes other values of  $\xi$  are employed as well, and several calculations can be done for general  $\xi$ .

In momentum space, the gauge condition takes the form  $k_\mu A^\mu(k) = 0$ , so it is obviously a four-dimensional transversality condition. Note that if we demand  $\partial_\mu A^\mu = 0$  we find for the gluon propagator

$$D_{\mu\nu}(x) = \langle A_\mu(x) A_\nu(0) \rangle \quad (1.70)$$

the same transversality condition,

$$\partial^\mu D_{\mu\nu}(x) = \langle \partial^\mu A_\mu(x) A_\nu(0) \rangle = \langle 0 \cdot A_\nu(0) \rangle = 0. \quad (1.71)$$

This four-dimensional transversality condition has the advantage of being manifestly covariant, which simplifies most considerations (especially in the high-energy regime). A propagator  $D_{\mu\nu}(k)$  depends only on one momentum scale  $k^2 = k \cdot k$ , while in non-covariant settings, certain components have to be treated independently.

The disadvantage of this condition is that the physical interpretation is often less clear. For photons, only the two degrees of freedom singled out by the three-dimensional transversality condition  $\mathbf{k} \cdot \mathbf{A} = 0$  describe physical particles, while the longitudinally polarized and the time-like photon cancel each other for all physical processes. The linear covariant gauge now mixes physical and unphysical parts of the photon.

While in contrast to photons, there are no freely propagating gluons, still three-dimensionally transverse gluons are considered “more physical” than three-dimensionally longitudinal or time-like ones. So one encounters a mixing of would-be physical and unphysical components, which is sometimes hard to disentangle.

### 1.4.2 Coulomb Gauge and Weyl Gauge

One can circumvent the problem of this “unphysical” mixing by demanding the Coulomb gauge condition

$$F[A] = \partial_i A_i = 0, \quad (1.72)$$

i.e. three-dimensional instead of four-dimensional transversality. This is imposed by the gauge-fixing functional  $\mathcal{L}_{\text{gf, Coul}} = \frac{1}{2\xi}(\partial_i A_i^a)^2$  with  $\xi \rightarrow 0$ .<sup>27</sup> This simplifies the physical interpretation and brings other benefits, but introduces also severe problems. They are closely related to the fact that the Coulomb gauge condition is left invariant by purely time-dependent gauge transformations. The Coulomb gauge is discussed in detail in chapter 3.

To some extent the benefits of the Coulomb gauge stem from the fact that time is singled out and treated on different footing than the spatial dimensions. Such separation of space and time can also be achieved by other gauges, for example the Weyl (or temporal) gauge which is typically formulated as  $A_0 = 0$ . Choosing the Weyl gauge eliminated problems in the canonical formulation of the theory; thus it is a appropriate starting point for the Hamiltonian formalism, to be discussed in section 3.3.

When employing periodic boundary conditions in time, the condition  $A_0 = 0$  fixes the value of time-like Wilson loops to one, which is unacceptable since Wilson loops are gauge-invariant objects. Therefore in periodic setups the weaker condition  $\partial_0 A_0 = 0$  is used. This version of the Weyl gauge is obviously left invariant by purely space-dependent gauge transformations  $g(\mathbf{x})$ .

### 1.4.3 Lightcone, Axial and Planar Gauges

Abandoning transversality conditions altogether, one can define various other gauges. So one can choose a fixed null vector  $n \in \mathbb{R}^4$ ,  $n^2 \equiv n_0^2 - \mathbf{n}^2 = 0$  and demand

$$n^\mu A_\mu = 0, \quad \text{i.e. minimize} \quad \mathcal{L}_{\text{gf, LC}} := \frac{1}{2\xi} (n^\mu A_\mu^a)^2 \quad \text{with} \quad \xi \rightarrow 0. \quad (1.73)$$

The choice of  $n$  (e.g.  $n = (1, 0, 0, 1)$ ) picks out a preferred axis in spacetime, thus manifest covariance is broken. Since for  $n^2 = 0$  the vector  $n$  lies on the light cone, this gauge is called *light-cone gauge*.

Very popular types of gauges are obtained if the vector  $n$  is chosen as spacelike instead of null,  $n^2 < 0$ .<sup>28</sup> In the *pure axial gauge* one demands  $n^\mu A_\mu^a(x) = 0$ , in the *inhomogeneous axial gauge* one has  $n^\mu A_\mu^a(x) = \omega^a(x)$  with an arbitrary field  $\omega$  (which can be integrated over, c.f. (1.32)). The gauge-fixing is implemented by

$$\mathcal{L}_{\text{gf, axial}} = \frac{1}{2\xi} (n^\mu A_\mu^a)^2 \quad (1.74)$$

with  $\xi \rightarrow 0$  for the pure and  $\xi = 1$  for the inhomogeneous axial gauge. A special version of the axial gauge is the *planar gauge* with gauge-fixing functional

$$\mathcal{L}_{\text{gf, planar}} = -\frac{1}{2} n \cdot A^a \frac{\partial^2}{n^2} n \cdot A^a. \quad (1.75)$$

Axial gauges are particularly popular for theoretical considerations (but far less for actual calculations). While the Faddeev-Popov determinant decouples from the gauge field integration (and thus can be absorbed in the normalization), in special cases ghost contributions can still be important [140, 49, 48, 85], see also section 4.4 of [129]. On the lattice a complete axial gauge has been presented in [156].

<sup>27</sup>Note that this functional can be written in a formally covariant way as  $\mathcal{L}_{\text{gf, Coul}} = \frac{1}{2\xi} [(n^\mu \partial^\mu - n_\nu \partial^\nu n^\mu) A_\mu^a]^2$  where covariance is broken by the explicit choice  $n^\mu = (1, 0, 0, 0)$ .

<sup>28</sup>For  $n^2 > 0$  one can always find a proper Lorentz transformations which changes  $n^\mu$  to  $n^\mu = (n, 0, 0, 0)$ , so one basically recovers the Weyl gauge.



### 1.4.4 Color Symmetry-Breaking Gauges

#### Maximum Abelian Gauge

Abelian configurations are believed to play a special role for confinement (Abelian dominance scenario). The diagonal generators of a Lie algebra define the Cartan subalgebra, which is Abelian (since diagonal matrices commute). In the Maximum Abelian Gauge (MAG) one aims at minimizing the coefficients of the non-diagonal generators.

For  $\mathbb{G} = \text{SU}(2)$  the gauge field can be written as

$$A_\mu = A_\mu^1 \frac{\tau_1}{2} + A_\mu^2 \frac{\tau_2}{2} + A_\mu^3 \frac{\tau_3}{2} \quad (1.76)$$

with the Pauli matrices  $\tau_i$ . In the usual representation the generator  $\tau_3$  is diagonal while  $\tau_1$  and  $\tau_2$  are not. Correspondingly one tries to employ gauge transformations to make  $A^1$  and  $A^2$  as small as possible, i.e. one wants to minimize the functional  $\|A^1\|^2 + \|A^2\|^2$ .

For  $\mathbb{G} = \text{SU}(3)$  the generators  $t_3 = \frac{\lambda_3}{2}$  and  $t_8 = \frac{\lambda_8}{2}$  are diagonal; correspondingly one tries to minimize the norm of the coefficients  $A^1$ ,  $A^2$  and  $A^4$  to  $A^7$ . The MAG breaks isotropy of color space; one has to distinguish “diagonal” and “off-diagonal” gluons which may exhibit dramatically different behaviour.

In contrast to their counterparts in linear covariant gauges, the MAG ghosts can interact with each other. The gauge-fixed Lagrangian includes a  $cc\bar{c}\bar{c}$ -vertex which is the source of various formal complications. It shares this vertex with general ghost-antighost symmetric gauges, the *Curci-Ferrari gauges*.

#### Maximum Center Gauge

For  $\mathbb{G} = \text{SU}(2)$  the center of the group consists of the elements  $\mathbb{1}$  and  $-\mathbb{1}$ , for  $\mathbb{G} = \text{SU}(3)$  one finds the center

$$C = \{\mathbb{1}, e^{2i\pi/3}\mathbb{1}, e^{-2i\pi/3}\mathbb{1}\}. \quad (1.77)$$

In the lattice Maximum Center Gauge (MCG) one employs gauge transformations to choose all (group-valued) link variables as close as possible to a center element.<sup>29</sup>

### 1.4.5 Gauges Breaking Translational Invariance

A real-space analogon to transversality conditions are the Poincaré gauge and the Fock-Schwinger gauge, where values are prescribed for the functional

$$\begin{aligned} F_{\text{Poinc.}}[A] &= x^\mu A_\mu, \\ F_{\text{Fock-Schw.}}[A] &= (x^\mu - z^\mu) A_\mu \end{aligned}$$

with a “gauge parameter”  $z$ . Other choices (partly more useful in the electroweak or even supergravity context than in QCD) encompass the Dirac gauge, Flow gauges, the ’t Hooft-Veltmann gauge, the Wess-Zumino gauge, Contour gauges, the Laplace gauge [201, 198], certain nonlinear gauges and others. For a comprehensive list of popular gauges with useful references see tables 1 to 3 (on p. 4 to 6) of [129].

---

<sup>29</sup>It is believed that strong statements about confinement can be made already by studying only the projection to the center (center vortex scenario). For  $\text{SU}(2)$  the group can be visualized as a sphere with the center elements as north and south pole. In the center projection elements on the northern hemisphere are replaced by  $\mathbb{1}$  (the north pole) and all elements on the southern hemisphere by  $-\mathbb{1}$ . It is widely believed that one can tell from such a  $\mathbb{Z}_2$  configuration whether or not the original configuration contributes to the string tension (see subsection 1.3.1) and thus is important for confinement.

### 1.4.6 Interpolating Gauges

Given two gauges, defined by  $\mathcal{L}_{\text{gf},A}$  and  $\mathcal{L}_{\text{gf},B}$ , one can always define an *interpolating gauge*, i.e. a gauge condition  $\mathcal{L}_{\text{gf}}(\lambda)$  with a parameter  $\lambda$ , which fulfills

$$\mathcal{L}_{\text{gf}}(0) = \mathcal{L}_{\text{gf},A} \quad \text{and} \quad \mathcal{L}_{\text{gf}}(1) = \mathcal{L}_{\text{gf},B}. \quad (1.78)$$

Sometimes it is useful to employ a vector-valued instead of a scalar interpolation parameter and in certain cases it can be helpful to introduce more than one interpolation parameter.

The hope when using such interpolating gauges is to be able to solve a problem for general  $\lambda$  and having access to both gauges  $A$  and  $B$  by performing the limits  $\lambda \rightarrow 0$  and  $\lambda \rightarrow 1$ . In addition one could see how a mechanism associated with gauge  $A$  gradually translates to another one, associated with gauge  $B$ . Interpolating gauges have been discussed for example in [31, 44].

Unfortunately it is typically not clear if both limits are continuous (provided they exist at all), so unfortunately up to now interpolating gauges have a very limited range of applicability. The special case of a Landau-Coulomb interpolating gauge is discussed in sec. 3.5.

### 1.4.7 Gauge Overfixing

The main requirement for any gauge is that (up to possible set of measure zero) *all orbits* are represented *with equal weight*. If one demands conditions which restrict configuration space too much, one does not obtain a valid gauge any more – the gauge is *overfixed*.

Also if the gauge is fixed in an unbalanced way, giving unequal weight to different orbits, the partition sum and thus observables get distorted. To see an example for an overfixed gauge, we try to impose simultaneously Coulomb and Weyl gauge on the functional integral.<sup>30</sup> This would mean to demand

$$\partial_i A_i = 0 \quad \text{and} \quad A_0 = 0. \quad (1.79)$$

Taking a time derivative of the second condition yields  $\partial_0 A_0 = 0$ , a condition which has to be fulfilled as well and which already has been identified as a weaker version of the Weyl gauge. From

$$\partial_i A_i = 0 \quad \text{and} \quad \partial_0 A_0 = 0 \quad (1.80)$$

we see that the covariant condition

$$\partial_\mu A^\mu = \partial_0 A_0 - \partial_i A_i = 0 \quad (1.81)$$

is fulfilled as well. However, most configurations which satisfy (1.81) will do this because one finds

$$\partial_0 A_0(x) = \partial_i A_i(x) = u(x) \quad (1.82)$$

with a function  $u(x) = u(\mathbf{x}, t)$  which is in general not identically zero. Configurations which fulfill  $u \equiv 0$  almost everywhere (as demanded by (1.80)) constitute only a very small subset of these configurations.

So if (1.80) were indeed a valid gauge-fixing condition, the Landau gauge would be tremendously overcomplete – which is contradicted by most results known about this gauge. Accordingly it is not possible to impose (1.80) on the lattice, [134].

A remedy to gauge overfixing is to implement gauge fixing by a sequence of functionals which are consecutively minimized. In the Landau-Coulomb example one could for example first minimize  $F_{\text{Coul}}[A] = (\partial_i A_i)^2$  (where the minimum  $F_{\text{Coul}}[A] = 0$  can be achieved on each orbit) and then minimize with respect to the remaining degrees of freedom the functional  $F_{\text{Weyl}}[A] = (\partial_0 A_0)^2$ . Only on certain orbits the minimum is again found at  $F_{\text{Weyl}}[A] = 0$ .

---

<sup>30</sup>It is possible to employ Coulomb and Weyl gauge together in the Hamiltonian formalism, discussed in section 3.3. In this case, the Weyl condition is only imposed on one initial timeslice and not fulfilled identically for all times.



## 1.5 Comments on a Possible Metric Structure of Gauge Space

*No one exceeds their potential. If they did, it would mean we did not accurately gauge their potential in the first place.*

Director Josef in *Gattaca*

When discussing questions of gauge-fixing and gauge-depended mechanisms, one sometimes loosely speaks of gauges which are “more or less similar”, which are “close to each other” or not. Such a notion of distance implicitly assumes that a metric is given in the space of *gauge conditions*.

In the following, we give a proposal how a space of gauges could be defined and which metric properties it can be expected to have. This section, though being relatively sketchy, deals with a property of gauges theories which – to the author’s best knowledge – has not been discussed in the literature so far.

### 1.5.1 More Thoughts on Gauge Fixing

As outlined in section 1.2, gauge-fixing corresponds to a restriction of functional integration, which is typically achieved by demanding a condition  $G[A] = 0$ . But one can also approach matters from a different direction. Instead of imposing an analytic condition one can base the very definition of a gauge on set and measure theoretical foundations.

Imposing a condition  $G[A] = 0$  achieves two things: It picks out a subset  $G^A$  of the configuration space  $\mathcal{A}$  and it induces a measure  $\mathcal{D}_G A = J_G[A] \mathcal{D}A$  on this subset. In order to have a valid gauge, one has to demand (in the Euclidean formulation)

$$\frac{1}{Z} \int_{\mathcal{A}} \mathcal{D}A X[A] e^{-S[A]} = \frac{1}{Z_G} \int_{G^A} \mathcal{D}_G A X[A] e^{-S[A]} \quad (1.83)$$

for all observables  $X$ , with

$$Z = \int_{\mathcal{A}} \mathcal{D}A e^{-S[A]} \quad \text{and} \quad Z_G = \int_{G^A} \mathcal{D}_G A e^{-S[A]}. \quad (1.84)$$

However there may be subsets  $G^A \subset \mathcal{A}$  with corresponding measures  $\mathcal{D}_G A$  which fulfill (1.83) but cannot be characterized by imposing a functional condition. Still such a pair  $(G^A, \mathcal{D}_G A)$  should count as a valid gauge (even though may be hard to access for practical calculations). Since we are exclusively interested in *integrated* quantities we dismiss all differences which are only present on a set of measure zero. In addition constant factors in the measure are removed by normalization. This gives rise to the following definition:

*A gauge  $G$  is an equivalence class of pairs  $(G^A, \mathcal{D}_G A)$  which satisfy (1.83), where equivalent pairs  $(G_1^A, \mathcal{D}_{G_1} A)$  and  $(G_2^A, \mathcal{D}_{G_2} A)$  fulfill, up to a set of measure zero,  $G_1^A = G_2^A$  and for which there exists a constant  $c \neq 0$  such that, again up to a set of measure zero, on  $G_1^A$  the relation  $\mathcal{D}_{G_1} A = c \mathcal{D}_{G_2} A$  holds.*

A sufficient condition to have a gauge is that a representative of each orbit is contained in  $G^A$  and that the measure  $\mathcal{D}_G A$  attributes equal weight to each orbit.<sup>31</sup> Up to a set of zero measure this condition is also necessary.

Since for all practical purposes a gauge can be characterized by one representative, we will just call  $(G^A, \mathcal{D}_G A)$  a gauge, we also often omit the characterization “up to a set of zero measure”.

<sup>31</sup>The following simple scenario, for example, would be perfectly valid:

There are two families of gauge orbits,  $O^{(s,1)}$ ,  $s \in S$  and  $O^{(t,2)}$ ,  $t \in T$  with appropriate index sets  $S$  and  $T$ . A gauge-fixing surface  $G^A$  intersects all orbits  $O^{(s,1)}$  once and all orbits  $O^{(t,2)}$  twice, with  $\mathcal{D}_G A^{(s,1)} = \mathcal{D}_G A_a^{(t,2)} + \mathcal{D}_G A_b^{(t,1)}$  for almost all  $(s, t) \in S \times T$ , where  $A^{(t,1)} = G^A \cap O^{(t,1)}$  and  $\{A_a^{(t,2)}, A_b^{(t,2)}\} = G^A \cap O^{(t,2)}$ .

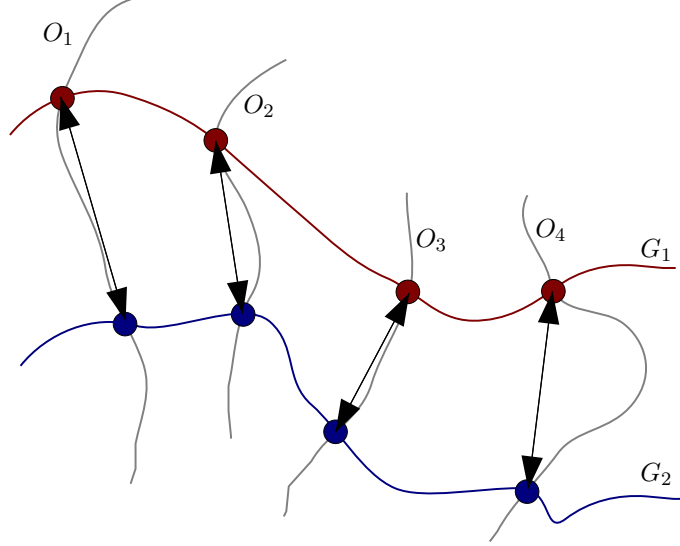


Figure 1.11: The distance between two (unique) gauges  $G_1$  and  $G_2$  is based on the distance between configurations in  $A_1 \in G_1^A$  and  $A_2 \in G_2$  that lie on the same gauge orbit  $O_\alpha$ .

### 1.5.2 The Metric Space of Unique Gauges

The basic idea underlying the definition of a distance between gauges is illustrated in figure 1.11. We start by considering the distance  $\|A_1^k - A_2^k\|$  between configurations which belong to two different gauges  $G_1$  and  $G_2$  and lie on the same gauge orbit  $O_k$ . All such distances are integrated over the set which characterizes  $G_1$  respectively  $G_2$ .

This rough concept has of course to be formalized. Since incomplete gauge-fixing and Gribov copies complicate matters, we will focus here on *unique* gauges. A unique gauge  $G$  is characterized by the condition that all elements of  $G^A$  are pairwise gauge-inequivalent, i.e. for arbitrary  $A_1 \in G^A$  and  $A_2 \in G^A$  there exists no gauge transformation  $g$  such that  $A_2 = gA_1$ . As outlined in section 1.2, unique gauges are hard to construct, but here this can be regarded as a merely technical obstacle which does not affect the following considerations. We denote the set of all unique gauges with  $\mathcal{G}_U$  and demonstrate in the following that this set can be promoted to a metric space in a relatively straightforward way.

To formalize the idea sketched in figure 1.11 we define a map  $d: \mathcal{G}_U \times \mathcal{G}_U \rightarrow \mathbb{R}_0^+$ ,

$$d(G_1, G_2) := \frac{1}{Z_{G_1}} \int_{G_1^A} \mathcal{D}_{G_1} A_1 e^{-S_{\text{YM}}[A_1]} \|A_1 - g_{12} A_1\| \quad (1.85)$$

where  $g_{12}$  denotes the uniquely defined gauge transformation necessary to transport  $A_1 \in G_1^A$  to  $g_{12} A_1 = A_2 \in G_2^A$ . Before proving that  $(\mathcal{G}_U, d)$  is a metric space, we first point out, that  $d$  as defined in (1.85) is well defined at all. Apart from a set of measure zero, for each configuration  $A^1 \in |G_1|$ , there exists per construction an equivalent configuration  $A_2 = g_{12} A_1 \in G_2^A$ . So for any  $A_1 \in G_1^A$ , the quantity  $\|A_1 - g_{12} A_1\|$  is well defined, and due to the weight  $e^{-S_{\text{YM}}[A_1]}$ , the functional integral is supposed to converge. Thus we can safely check the axioms of a general metric space:

- (M1) **Definiteness:** The integrand in (1.85) is positive definite, so also  $d$  is non-negative. It is zero only if  $\|A_1 - g_{12} A_1\|$  is zero for all configurations  $A_1$  except possibly a set of zero measure, i.e. if

$$A_1 = g_{12} A_1 =: A_2$$

almost everywhere. Since such gauges have already been identified in the first place, we have  $d(G_1, G_2) = 0$  if and only if  $G_1 = G_2$ .

(M2) **Symmetry:** We have to check

$$\begin{aligned} d(G_2, G_1) &= \frac{1}{Z_{G_2}} \int_{G_2^A} \mathcal{D}_{G_2} A_2 e^{-S_{\text{YM}}[A_2]} \|A_2 - g^{21} A_2\| \\ &\stackrel{?}{=} \frac{1}{Z_{G_1}} \int_{G_1^A} \mathcal{D}_{G_1} A_1 e^{-S_{\text{YM}}[A_1]} \|A_1 - g^{12} A_1\| = d(G_1, G_2) \end{aligned} \quad (1.86)$$

Since we only consider unique gauges, the element  $A_1 = g^{21} A_2$  is uniquely determined for each  $A_2 \in G_2^A$ . Thus each pair  $(A_1, A_2) \subset \mathcal{A}^2$  is unique and appears precisely once in each of the two integrals,

$$\|A_2 - g^{21} A_2\| = \|A_2 - A_1\| = \|A_1 - A_2\| = \|A_1 - g^{12} A_1\| \quad (1.87)$$

with  $g_{21} = (g_{12})^{-1}$ . Since a valid gauge puts equal weight to equivalent configurations one has

$$\left. \frac{\mathcal{D}_{G_1} A_1}{Z_{G_1}} \right|_{A_1 \in G_1^A} = \left. \frac{\mathcal{D}_{G_2} A_2}{Z_{G_2}} \right|_{A_2 \in G_2^A} \quad (1.88)$$

for equivalent configurations  $A_1$  and  $A_2$ . The Yang-Mills action is gauge-invariant, thus one can replace  $e^{-S_{\text{YM}}[A_2]}$  by  $e^{-S_{\text{YM}}[A_1]}$  at any instance. From invariance of the measure, invariance of the action and invariance of the integrand we see that (1.86) indeed holds.

(M3) **Triangle Inequality:** The triangle inequality holds in  $\mathcal{A}$ , i.e. we have

$$\|A_1 - A_3\| + \|A_3 - A_2\| - \|A_1 - A_2\| \geq 0 \quad (1.89)$$

for arbitrary  $(A_1, A_2, A_3) \in \mathcal{A}^3$ . Now we specify this to  $A_1, A_2$  and  $A_3$  being gauge-equivalent configurations belonging to  $G_1^A, G_2^A$  and  $G_3^A$ . Then we can rewrite (1.89) using the gauge transformations  $g_{12}$  and  $g_{13}$  as

$$\|A_1 - g^{13} A_1\| + \|g^{13} A_1 - g^{12} A_1\| - \|A_1 - g^{12} A_1\| \geq 0 \quad (1.90)$$

All quantities are well-defined for any given  $A_1 \in G_1^A$ . The inequality remains valid also when multiplied with the positive definite function  $e^{-S_{\text{YM}}[A_1]}$  and integrated over  $G_1^A$  with the measure  $\mathcal{D}_{G_1} A_1$  and the weight  $\frac{1}{Z_{G_1}}$ ,

$$\frac{1}{Z_{G_1}} \int_{G_1^A} \mathcal{D} A_1 e^{-S_{\text{YM}}[A_1]} \left( \|A_1 - g^{13} A_1\| + \|g^{13} A_1 - g^{12} A_1\| - \|A_1 - g^{12} A_1\| \right) \geq 0. \quad (1.91)$$

Due to linearity, the integration can split up, and due to equivalence of the measure and invariance of the action,

$$\left. \frac{\mathcal{D} A_1}{Z_{G_1}} e^{-S_{\text{YM}}[A_1]} \right|_{A_1 \in G_1^A} = \left. \frac{\mathcal{D} A_3}{Z_{G_3}} e^{-S_{\text{YM}}[A_3]} \right|_{A_3 \in G_3^A},$$

the second resulting integral can be rewritten as one over  $G_3$ ,

$$\begin{aligned} &\frac{1}{Z_{G_1}} \int_{G_1^A} \mathcal{D} A_1 e^{-S_{\text{YM}}[A_1]} \|A_1 - g^{13} A_1\| + \frac{1}{Z_{G_3}} \int_{G_3^A} \mathcal{D} A_3 e^{-S_{\text{YM}}[A_3]} \|A_3 - g^{32} A_3\| \\ &\quad - \frac{1}{Z_{G_1}} \int_{G_1^A} \mathcal{D} A_1 e^{-S_{\text{YM}}[A_1]} \|A_1 - g^{12} A_1\| \geq 0. \end{aligned} \quad (1.92)$$

Each functional integral defines a distance  $d$  in  $\mathcal{G}_U$ , so we end up with a triangle inequality

$$d(G_1, G_2) \leq d(G_1, G_3) + d(G_3, G_2)$$

which completes the proof that  $(\mathcal{G}_U, d)$  is a metric space.  $\square$

We note that  $\mathcal{G}_U$  also inherits completeness from  $\mathcal{A}$ , so for every Cauchy sequence of unique gauges the limit is a unique gauge as well. Due to continuity of the metric, any metric space can be embedded in a Banach algebra (see for example A 159.6 in [103]); thus one could also proceed with studying algebraic properties of  $\mathcal{G}_U$ .

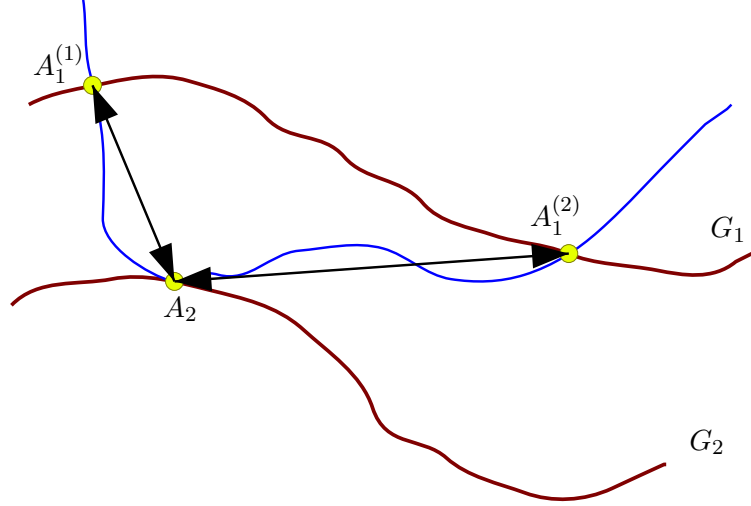


Figure 1.12: A Problem with definition (1.94): When integrating over the set defined by gauge condition  $G_1$ , one picks up  $d(A_1^{(1)}, A_2) + d(A_1^{(2)}, A_2)$  since  $A_2$  is the gauge-equivalent configuration with minimum distance both for  $A_1^{(1)}$  and  $A_1^{(2)}$ . When integrating over  $G_2$ , however, one only picks up  $d(A_1^{(1)}, A_2)$ , since  $A_1^{(1)}$  is the configuration with minimum distance to  $A_2$  while  $A_1^{(2)}$  is not.

### 1.5.3 The Distance between General Gauges

We have seen that the set of unique gauges,  $\mathcal{G}_U$ , can be promoted to a metric space. Since most popular gauges are plagued by Gribov copies (and conditions which provide only incomplete gauge-fixing inevitably introduce ambiguities), the more important question is whether the set of *all* valid gauges can be equipped with a metric.

Straightforward generalizations of (1.85) could be

$$d'(G_1, G_2) = \frac{1}{Z_{G_1}} \int_{G_1^A} \mathcal{D}_{G_1} A_1 e^{-S_{\text{YM}}[A_1]} \sum_{g_{12}} \|A_1 - g_{12} A_1\| \quad (1.93)$$

$$d''(G_1, G_2) = \frac{1}{Z_{G_1}} \int_{G_1^A} \mathcal{D}_{G_1} A_1 e^{-S_{\text{YM}}[A_1]} \min_{g_{12}} \|A_1 - g_{12} A_1\| \quad (1.94)$$

where we include summation/integration over respectively minimization with respect to all gauge transformation  $g_{12}$  which yield gauge-equivalent configurations  $A_2 \in G_2^A$ . Unfortunately these definitions are extremely problematic.

We noted that (1.85) is well-defined (employing the usual existence standards for path integrals in quantum field theory and excluding extremely pathological cases) since for each  $A_1 \in G_1^A$  there is precisely one  $g_{12} A_1 = A_2 \in G_2^A$  and accordingly the integrand is under control. In contrast to that, (1.93) may contain a divergent series or integral for certain  $A_1$  (if there are infinitely many gauge-equivalent configurations contained in  $G_2^A$ ). While (1.94) does not encounter this problem, it potentially violates symmetry. An example for this is given in figure 1.12.

So we will choose a different route which is based on partitioning general gauges into unique gauges. This leads to the introduction of a *distance measure* which has some, but not all properties of a metric. Note that on the set of subsets of a given metric space the Hausdorff distance

$$d_H(X, Y) = \max\left\{\sup_{x \in X} \inf_{y \in Y} d(x, y), \sup_{y \in Y} \inf_{x \in X} d(x, y)\right\} \quad (1.95)$$

induces a metric (see also figure 1.13.a).

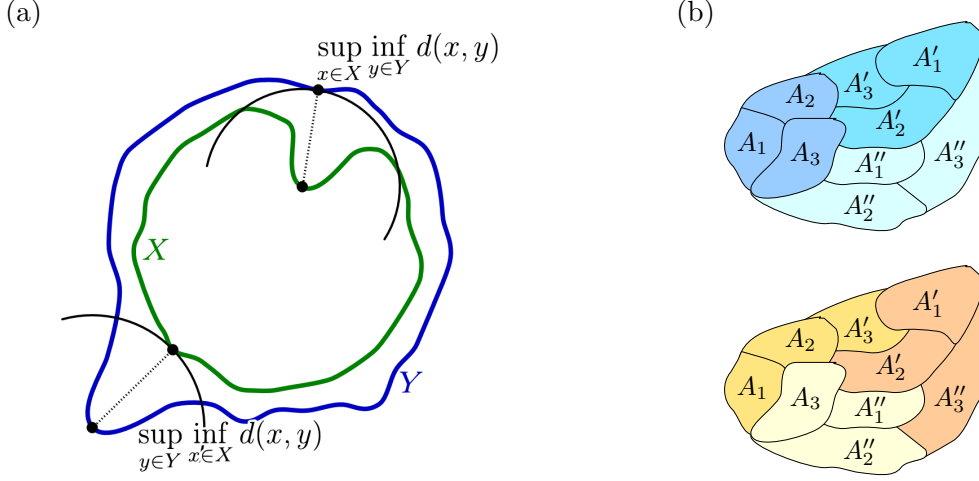


Figure 1.13: Moving on beyond metric spaces: (a) On the set of subsets of a given metric space, the Hausdorff distance (1.95) induces a metric (figure taken from [169]). (b) The partitioning of general gauges is not unique. This is illustrated for a theory with three orbits  $O_i$  which each contain three gauge-equivalent configurations  $A_i$ ,  $A'_i$  and  $A''_i$ ,  $i = 1, 2, 3$ . A possible partitioning is given by  $\{\{A_1, A_2, A_3\}, \{A'_1, A'_2, A'_3\}, \{A''_1, A''_2, A''_3\}\}$ , but in principle this is completely equivalent to  $\{\{A_1, A_2, A'_3\}, \{A'_1, A'_2, A''_3\}, \{A''_1, A''_2, A_3\}\}$ . In order to establish a distance measure one has to minimize (1.97) with respect to all possible ways to partition a composite gauge.

For the present case, however, matters are more delicate due to the fact that a general gauge is characterized not as a subset, but as an equivalence class of positive semidefinite functions on  $\mathcal{G}$  (with elements which are from now on always regarded as being properly normalized to unity). Thus we define:

A partitioning  $\mathcal{P}_G$  of a general gauge  $G$  into unique gauges is characterized by a family  $(G_t)_{t \in T}$  of unique gauges (with a suitable index set  $T$ ) and a corresponding family of coefficients  $(c_t)_{t \in T}$ ,  $c_t \geq 0$ , such that

$$G^{\mathcal{A}} = \bigcup_{t \in T} G_t^{\mathcal{A}} \quad \text{and} \quad \mathcal{D}_G A|_{\tilde{A}} = \sum_{t \in T} c_t \mathcal{D}_{G_t} A|_{\tilde{A}} \quad (1.96)$$

for all  $\tilde{A} \in G^{\mathcal{A}}$ . Partitionings which differ only by a constant factor in  $c_t$  may be identified (since constant factors are absorbed in the normalization of functional integrals); accordingly we impose the normalization condition  $\sum_{t \in T} c_t = 1$ .

The partitioning of general gauges into unique gauges is typically non-unique. Even in the most simple (finite or countable) situations there are many ways to partition a general gauge, as illustrated in figure 1.13.(b).

It is now straightforward to define the distance between partitionings  $\mathcal{P}_{G_1}$  and  $\mathcal{P}_{G_2}$ ,

$$d_P(\mathcal{P}_{G_1}, \mathcal{P}'_{G_2}) = \sum_{t \in T, t' \in T'} c_t c'_{t'} d(G_t, G_{t'}) \quad (1.97)$$

with  $d$  on the rhs denoting the distance (1.85) in  $\mathcal{G}_U$ . The distance between the general gauges  $G_1$  and  $G_2$  is defined as the minimum of all these distances w.r.t. all partitionings  $\mathcal{P}$  and  $\mathcal{P}'$ ,

$$d(G_1, G_2) = \min_{\mathcal{P}, \mathcal{P}'} d_P(G_1^{\mathcal{P}}, G_2^{\mathcal{P}'}). \quad (1.98)$$

This quantity is nonnegative and vanishes only for gauges which (up to a set of measure zero) coincide. It is symmetric as well; however it is not clear whether (and in view of the argument illustrated in figure 1.13.(b) actually unlikely that) the triangle inequality is fulfilled as well.

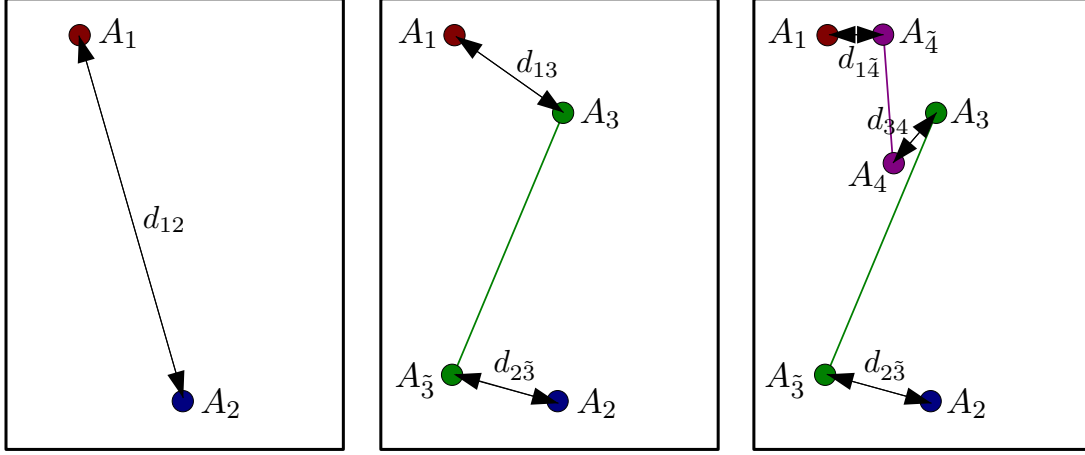


Figure 1.14: In a space with points identified, one can take shortcuts und thus violate the naive triangle inequality. With the identifications  $A_3 \simeq A_{\bar{3}}$  and  $A_4 \simeq A_{\bar{4}}$  on has  $d_{12} > d_{13} + d_{2\bar{3}} > d_{1\bar{4}} + d_{3\bar{4}} + d_{2\bar{3}}$ , i.e. the naive triangle inequality does not hold.

#### 1.5.4 Metric Considerations regarding Topologically Nontrivial Spaces

Als already discussed in subsection 1.2 it can become necessary to identify certain points in  $\mathcal{A}$ -space. Due to this modification, ist is not straightforward to connect embeddings of the FMR in  $\mathcal{A}$ -space with unique gauges. While a unique gauge can be obtained by removing a sufficient number of gauge copies, this process is quite arbitrary and particular features of the FMR are lost.

Therefore we will at least comment on (though not study in depth) the metric properties of a space which has been obtained by performing such identifications. Starting with a Banach space  $(\mathcal{A}, \|\cdot\|)$  we will study the space  $\mathcal{A}'$  which is obtained by identifying all gauge-equivalent configurations with the same norm. Such a space is well-suited to describe the FMR of a specific gauge, defined by globally minimizing that particular norm.<sup>32</sup>

It is obvious that the metric structure of  $\mathcal{A}$  can not be transferred to  $\mathcal{A}'$  in a straightforward way. Loosely speaking, with that huge amount of identified configurations, one could take shortcuts and thus violate the triangle inequality, as illustrated in figure 1.14.

Thus we refine the definition of distance in  $\mathcal{A}$  to one in  $\mathcal{A}'$  by setting

$$d'(A'_1, A'_2) := \min_{i_1, i_2, \dots}^{\text{id}} \left( \|A_1^{\text{id}} - A_2^{\text{id}}\|, \|A_1^{\text{id}} - A_{i_1}\| + \|A_{i_1}^{\text{id}} - A_2^{\text{id}}\|, \right. \\ \left. \|A_1^{\text{id}} - A_{i_1}\| + \|A_{i_1}^{\text{id}} - A_{i_2}\| + \|A_{i_2}^{\text{id}} - A_2^{\text{id}}\|, \dots \right), \quad (1.99)$$

where  $\|\cdot\|$  denotes the norm in  $\mathcal{A}$ . The minimum  $\min_{i_1, i_2, \dots}^{\text{id}}$  is taken w.r.t. all configurations with are identified in the process  $\mathcal{A} \rightarrow \mathcal{A}'$  and w.r.t *all* configuration  $A_{i_k} \in \mathcal{A}$ .

We now prove that (1.99) indeed defines a metric in  $\mathcal{A}'$ : It is non-negative, and it is zero if there exist identifications  $\text{id}_1, \text{id}_2$  with  $A_1^{\text{id}_1} = A_2^{\text{id}_2}$ , i.e. if  $A'_1 = A'_2$ . It is clearly symmetric, and the triangle inequality is fulfilled already by construction. The only challenge is to show if  $d'(A'_1, A'_2) = 0$  *only if*  $A'_1 = A'_2$ . For any given argument of the minimum appearing on the rhs of (1.99), this is clear, since

$$d_n := \|A_1^{\text{id}} - A_{i_1}\| + \|A_{i_1}^{\text{id}} - A_{i_2}\| + \dots + \|A_{i_n}^{\text{id}} - A_2\| \quad (1.100)$$

<sup>32</sup>Unfortunately,  $\mathcal{A}'$  as defined here is not sufficient to study the metric properties of the set of all (embeddings of) FMRs, since different gauges  $G$  and thus (the embedding of) their FMRs are in general defined via different norms  $\|\cdot\|_G$ . Nevertheless the following considerations may be helpful in order to perform the next step – to establish a distance measure between FMRs.

equals zero only if there exist identifications  $\text{id}_k$  such that

$$A_1^{\text{id}_0} = A_{i_1}, \quad A_{i_1}^{\text{id}_1} = A_{i_2}, \quad \dots, \quad A_{i_n}^{\text{id}_n} = A_2, \quad (1.101)$$

i.e. if there exists an identification  $\text{id}_f$  with  $A_1^{\text{id}_f} = A_2$  which implies  $A'_1 = A'_2$ .

The limit  $\lim_{n \rightarrow \infty} d_n$ , however, may be zero even if  $d_n \neq 0$  for all  $n \in \mathbb{N}$ . In this case also  $d'(A'_1, A'_2)$  could be zero even for  $A'_1 \neq A'_2$ . To exclude this possibility, we establish two inequalities:

- Since we have identified only points of  $\mathcal{A}$  with equal norm, the inequality

$$d'(A'_1, A'_2) \geq | \|A_1\| - \|A_2\| | \quad (1.102)$$

always holds. This is seen best, as illustrated in figure 1.15.(a), if configurations are grouped on hyperspheres with radius  $\|A\|$ . Due to identification, one can “jump” on each hypersphere. Between them, however, the shortest route can at best be in radial direction. Therefore inequality (1.102) cannot be circumvented.

- To derive the second inequality, we define the distance  $d$  of two gauge orbits  $O_1 \in \mathcal{O}$  and  $O_2 \in \mathcal{O}$  in  $\mathcal{A}$  as

$$d(O_1, O_2) := \min_{A_1 \in O_1, A_2 \in O_2} \|A_1 - A_2\|. \quad (1.103)$$

At first glance, one could guess that this does not define a metric, since it might seem possible, as depicted in figure 1.15.(b), to circumvent the triangle equation by a clever choice of orbits. This, however, is not true.

Gauge orbits are in some sense *parallel* (see for example [223]), with a common direction defined by the set of all local gauge transformations  $\mathbb{G}(x)$ . If we perform the same gauge transformation  $g$  on two configurations  $A_1 \in O_1$  and  $A_2 \in O_2$ , we obtain

$$\begin{aligned} d({}^g A_1, {}^g A_2) &= \|{}^g A_1 - {}^g A_2\| \\ &= \left\| U_g^\dagger A_1 U_g + U_g^\dagger \partial U_g - U_g^\dagger A_2 U_g - U_g^\dagger \partial U_g \right\| \\ &= \left\| U_g^\dagger A_1 U_g - U_g^\dagger A_2 U_g \right\| = \left\| U_g^\dagger (A_1 - A_2) U_g \right\| \\ &= \|A_1 - A_2\| = d(A_1, A_2). \end{aligned} \quad (1.104)$$

This implies that we can choose, for example,  $A_1 \in O_1$  freely and find  $A_2 \in O_2$  and  $A_3 \in O_3$  such that

$$d(A_1, A_2) = d(O_1, O_2) \quad \text{and} \quad d(A_2, A_3) = d(O_2, O_3). \quad (1.105)$$

In that case, as illustrated in figure 1.15.(b), all three points lie in a hyperplane defined by the base point  $A_1$  and the normal direction  $\mathbb{G}(x)$ . (If this wasn't the case, we could employ suitable local gauge transformations on  $A_2$  or  $A_3$  to further reduce the distances.)

Thus we also have  $d(A_1, A_3) = d(O_1, O_3)$ , and since the distance defined for the points  $A_i \in \mathcal{A}$ ,  $i = 1, 2, 3$  fulfills the triangle inequality, the same is true for (1.103) defined in  $O_i \in \mathcal{O}$ . Since the transition  $\mathcal{A} \rightarrow \mathcal{A}'$  only identifies certain configurations on the *same* orbit, we clearly have

$$d'(A'_1, A'_2) \geq d(O_1, O_2) \quad (1.106)$$

From both inequalities (1.102) and (1.106) it follows that  $d'(A'_1, A'_2) = 0$  only if  $\|A_1\| = \|A_2\|$  and  $O_1 = O_2$ , i.e. if  $A'_1 = A'_2$ .  $\square$



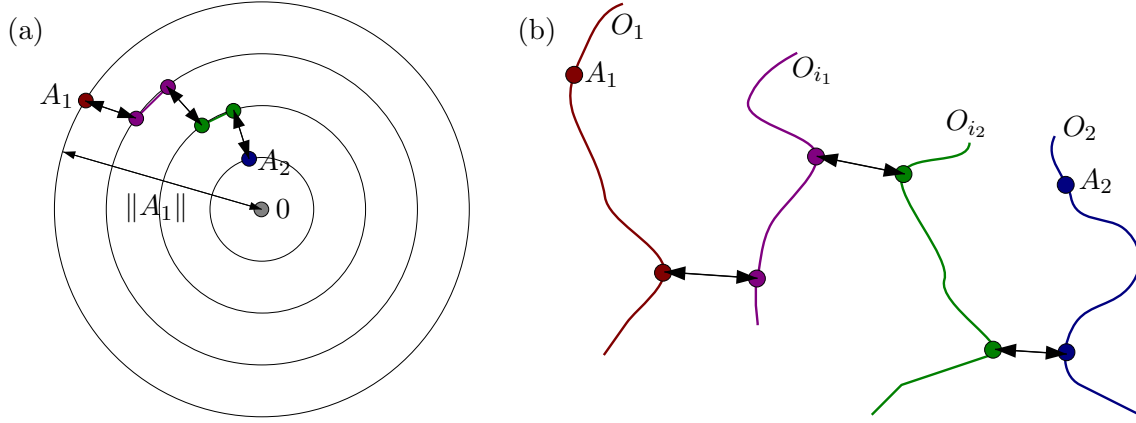


Figure 1.15: (a) Even with identifications, the distance between two points in  $A_1 \in \mathcal{A}$  and  $A_2 \in \mathcal{A}$  cannot become smaller than the radial distance  $||A_1|| - ||A_2||$ . (b) One could think that the triangle inequality for the distance between orbits, as defined in (1.103), does not hold, since one can take “shortcuts”, as depicted here. This is, however, not true, since gauge orbits are in some sense “parallel”, as expressed in (1.104). Therefore shortcuts between orbits as (wrongly) sketched in this figure are not possible.

### 1.5.5 Further Comments on the Distance between Gauges

Since the metric space of unique gauges is (to the knowledge of the present author) a new concept, one should add a few remarks regarding definition (1.85) and the reasons for introducing such a space at all.

First, why employ (1.85) and not, as it may seem more appropriate at first glance, a definition based on a minimum? This could be something like  $d(G_1, G_2) = \min_{A_1, A_2} ||A_1 - A_2||$ , where the minimum is taken with respect to all configurations  $A_1$  which belong to gauge  $G_1$  and all gauge-equivalent configurations  $A_2$  which belong to gauge  $G_2$ .

There are, however, several reasons why not to employ such a definition:

- Any quantity characterizing something important in a gauge theory should not be sensitive to changes on a set of zero measure, but this definition of a distance obviously is.
- A single configuration with large action (i.e. a small contribution to the partition function) could set the distance, which does not seem “natural”.
- Since all linear gauges contain the configuration  $A = 0$ , the distance between all linear gauges would be zero, thus they would have to be identified.

In addition (1.85) has a form which could be evaluated (with some modifications in the formulation) in lattice gauge theory via Monte-Carlo simulations.

But are there any purposes for which the concept of such a distance could turn out to be useful? Presumably it does not allow to calculate observables, so from a very strict point of view it is not even physics. On the other hand, gauge theories obviously have physical content. They are often approached via gauge-fixing, where the relation between different gauges is often not clear.

A distance measure could help to classify and organize gauges, i.e. create a “map” of gauges. Moreover, even if the value in physics is limited,  $\mathcal{G}_U$  and the distance between general gauges might still be interesting objects to be studied in mathematics.

### 1.5.6 $\mathbb{Z}_2$ Gauge-like Theory on One Plaquette

As a very simple example for our considerations we study a  $\mathbb{Z}_2$ -based gauge-like theory on one plaquette with four links  $U_i \in \{-1, +1\}$ ,  $i = 1, 2, 3, 4$ . The action is chosen as

$$S_{\mathbb{Z}_2}[\mathbf{U}] = -h U_1 U_2 U_3 U_4 \quad (1.107)$$

with a fixed constant  $h > 0$ . Since the only gauge-invariant quantity one can form is the product of the four link variables, one only has the “physically” distinct cases  $S = -h$  and  $S = +h$ . Thus any transformation which changes the sign of an even number of links leaves “physics” invariant and is accordingly just a gauge transformation.

Obviously there are only two gauge orbits which each contain eight configurations,

$$O^{(1)} = \{(1, 1, 1, 1), (1, 1, -1, -1), (1, -1, 1, -1), (-1, 1, 1, -1), \\ (1, -1, -1, 1), (-1, 1, -1, 1), (-1, -1, 1, 1), (-1, -1, -1, -1)\} \quad (1.108)$$

$$O^{(2)} = \{(-1, 1, 1, 1), (1, -1, 1, 1), (1, 1, -1, 1), (1, 1, 1, -1), \\ (1, -1, -1, -1), (-1, 1, -1, -1), (-1, -1, 1, -1), (-1, -1, -1, 1)\} \quad (1.109)$$

The whole configuration space is given as  $\mathcal{A} = O^{(1)} \cup O^{(2)}$ . Since (1.85) and all consequences are given in continuum language, we have to do some reformulations. Thus we define the metric in this (configuration) space as

$$d(\mathbf{U}^1, \mathbf{U}^2) = \frac{1}{2} \sum_{k=1}^4 |U_k^1 - U_k^2| \in \{0, 1, 2, 3, 4\}. \quad (1.110)$$

With this metric in the base space at hand we can begin to establish also a metric of unique gauges.

#### Unique Gauges

A properly normalized unique gauge has to contain precisely one configuration from each of the orbits, so there are  $8 \cdot 8 = 64$  unique gauges  $G_{i,j}$ , which contain the configuration  $U_i^{(1)} \in O^{(1)}$  and  $U_j^{(2)} \in O^{(2)}$ . The distance between such gauges is given by

$$d(G_{i,j}, G_{k,\ell}) = \frac{1}{Z} \left( d(U_i^{(1)}, U_k^{(1)}) e^h + d(U_j^{(2)}, U_\ell^{(2)}) e^{-h} \right) \quad (1.111)$$

$$\text{with } Z = e^{-S[O^{(1)}]} + e^{-S[O^{(2)}]} = e^h + e^{-h} = 2 \cosh h \quad (1.112)$$

For example, the distance between

$$G_{1,3} = \{(1, 1, 1, 1), (1, 1, -1, 1)\} \quad \text{and} \quad G_{2,7} = \{(1, 1, -1, -1), (-1, -1, 1, -1)\}$$

turns out to be

$$d(G_{1,3}, G_{2,8}) = \frac{1}{Z} \left( d((1, 1, 1, 1), (1, 1, -1, -1)) e^h + d((1, 1, -1, 1), (-1, -1, 1, -1)) e^{-h} \right) \\ = \frac{1}{2 \cosh h} \left( 2e^h + 4e^{-h} \right) = \frac{2e^h + 4e^{-h}}{e^h + e^{-h}} = \frac{2 + 4e^{-2h}}{1 + e^{-2h}}. \quad (1.113)$$

The maximum distance between two such gauges is

$$d_{\max} = \frac{1}{Z} \left( 4e^h + 4e^{-h} \right) = 4. \quad (1.114)$$

### General Gauges

General gauges can be characterized by 16-tuples

$$\boldsymbol{\omega} = (\omega_1^{(1)}, \omega_2^{(1)}, \dots, \omega_8^{(1)}; \omega_1^{(2)}, \dots, \omega_8^{(2)}) \in (\mathbb{R}_0^+)^{16} \quad (1.115)$$

where  $\omega_i^{(k)}$  denotes the weight that particular gauge attributes to the configuration  $U_i^{(k)}$ . A “vector”  $\boldsymbol{\omega}$  defines a simple measure on  $\mathcal{A}$ , but also on the subset

$$G^{\mathcal{A}} = \left\{ U_i^{(k)} \in \mathcal{A} : \omega_i^{(k)} \neq 0 \right\}. \quad (1.116)$$

Since gauges are actually *equivalence classes*, we can choose one representative by imposing a normalization condition. Since valid gauges have to attribute equal weight to both orbits, one immediately obtains a second condition as well,

$$\sum_{i=1}^8 \omega_i^{(1)} = \sum_{i=1}^8 \omega_i^{(2)} = 1. \quad (1.117)$$

Accordingly the range permitted for  $\boldsymbol{\omega}$  is not complete  $(\mathbb{R}_0^+)^{16}$ , but the cartesian product of two eight-dimensional unit simplices.

Two particular gauges could be defined by

$$\begin{aligned} G_1 \sim \boldsymbol{\omega}_1 &= \left( \frac{1}{2}, \frac{1}{2}, 0, \dots, 0; \frac{3}{4}, \frac{1}{4}, 0, \dots, 0 \right), \\ G_2 \sim \boldsymbol{\omega}_2 &= \left( \frac{3}{4}, \frac{1}{4}, 0, \dots, 0; \frac{1}{2}, \frac{1}{2}, 0, \dots, 0 \right). \end{aligned}$$

This gauges  $G_k$  can now be partitioned into unique gauges by giving coefficients  $c_{i,j}^k$  for the unique gauges  $G_{i,k}$ ,  $i = 1, \dots, 8$ ,  $j = 1, \dots, 8$ . Since we demand nonnegativity, only the four unique gauges  $G_{1,1}$ ,  $G_{1,2}$ ,  $G_{2,1}$  and  $G_{2,2}$  qualify as basis elements; accordingly we have  $c_{i,j}^k = 0$  for  $i \notin \{1, 2\}$  or  $j \notin \{1, 2\}$ .

Only  $G_{1,1}$  and  $G_{1,2}$  contain the configuration  $U_1^{(1)}$  which has weight  $\frac{1}{2}$  in  $G_1$ . Thus one has the condition  $c_{1,1}^1 + c_{1,2}^1 = \frac{1}{2}$ , and by analogous reasoning one can conclude that partitioning  $G_1$  and  $G_2$  corresponds to solving the linear systems

$$\begin{aligned} c_{1,1}^1 + c_{1,2}^1 &= \frac{1}{2} & c_{1,1}^2 + c_{1,2}^2 &= \frac{3}{4} \\ c_{2,1}^1 + c_{2,2}^1 &= \frac{1}{2} & c_{2,1}^2 + c_{2,2}^2 &= \frac{1}{4} \\ c_{1,1}^1 + c_{2,1}^1 &= \frac{3}{4} & c_{1,1}^2 + c_{2,1}^2 &= \frac{1}{2} \\ c_{1,2}^1 + c_{2,2}^1 &= \frac{1}{4} & c_{1,2}^2 + c_{2,2}^2 &= \frac{1}{2}. \end{aligned} \quad (1.118)$$

In general such systems will be underdetermined (at most 16 equations for up to 64 coefficients) and thus contain free parameters. In this easy setup, however, both systems have a unique solution,

$$c_{1,1}^1 = c_{2,1}^1 = \frac{3}{8}, \quad c_{1,2}^1 = c_{2,2}^1 = \frac{1}{8}, \quad c_{1,1}^2 = c_{1,2}^2 = \frac{3}{8}, \quad c_{2,1}^2 = c_{2,2}^2 = \frac{1}{8}. \quad (1.119)$$

One finds the following distances between the relevant unique gauges:

$d$	$G_{1,1}$	$G_{1,2}$	$G_{2,1}$	$G_{2,2}$
$G_{1,1}$	0	$\frac{e^{-h}}{\cosh h}$	$\frac{e^h}{\cosh h}$	2
$G_{1,2}$	$\frac{e^{-h}}{\cosh h}$	0	2	$\frac{e^h}{\cosh h}$
$G_{2,1}$	$\frac{e^h}{\cosh h}$	2	0	$\frac{e^{-h}}{\cosh h}$
$G_{2,2}$	2	$\frac{e^h}{\cosh h}$	$\frac{e^{-h}}{\cosh h}$	0

The distance between  $G_1$  and  $G_2$  is now easy to determine,

$$\begin{aligned} d(G_1, G_2) &= c_{1,1}^1 c_{1,1}^2 d(G_{1,1}, G_{1,1}) + c_{1,1}^1 c_{1,2}^2 d(G_{1,1}, G_{1,2}) + \dots + c_{2,2}^1 c_{2,2}^2 d(G_{2,2}, G_{2,2}) \\ &= \frac{9+3+3+1}{64} \frac{e^h}{\cosh h} + \frac{9+3+3+1}{64} \frac{e^{-h}}{\cosh h} + 2 \frac{9+3+3+1}{64} = \frac{1}{4} \frac{e^h + e^{-h}}{\cosh h} + \frac{1}{2} = 1. \end{aligned} \quad (1.120)$$

## Chapter 2

# The Dyson-Schwinger Approach

*A physicist working without a lattice is something like a trapeze artist working without a net. There is an ever present danger that a false move will lead to a fatal result.*

Lee Smolin, *Three Roads to Quantum Gravity*

*Ihr kennt's ma's glaub'n, die größte Hetz  
hålt ma in Wårheit ohne Netz!*

Rainhard Fendrich, *Zeitgeisterfahrer*

How could we solve a quantum field theory? One possible strategy is to look for a way to directly calculate all observables with arbitrary precision (or at least with controlled error). This is the path of lattice gauge theory, as briefly discussed in subsection 1.1.4, where expectation values  $\langle O \rangle$  are calculated by discretization of the functional integrals (1.29).

Other strategies, however, might employ some intermediate steps. One such possible step could be to determine the *Green functions* of the theory. Green functions describe the propagation and interaction of the fields present in a theory. If all the Green functions are known, the theory can also be regarded as being solved, since with this knowledge, all physical quantities can be calculated as well.

While the reader is expected to have some basic knowledge of Green functions, still some of the most essential basics are summarized in section 2.1. Different Green functions of the same theory are connected by certain equations of motion, the *Dyson-Schwinger equations*, which are discussed in section 2.2. Both sections follow closely the presentation given in [63] and partially [109], adapted to suit the aims of this thesis.

To give a concrete example, we derive in sec. 2.3 – in the context of finite-temperature Yang-Mills theory – the equation for a particular two-point function which we will again need in chapter 5.

The particularities of gauge theories manifest themselves as identities which have to be obeyed by Green functions. These are Ward, Ward-Takahashi and Slavnov-Taylor identities, which are briefly discussed in section 2.4.

One can use the Dyson-Schwinger equation to generate the perturbation series of a theory, one can solve them numerically, which typically requires truncations or approximations – a path followed in chapter 4 for the quark propagator equation. In the deep infrared, however, another approach is possible. In the absence of all other momentum scales (external parameters or dynamically generated masses) propagators can be expanded in asymptotic series.

Employing this expansion, the Dyson-Schwinger equations can be solved analytically for leading orders; from these solutions and consistency conditions, the leading infrared behaviour of propagators and also higher-order Green functions can be extracted – a method which is discussed in section 2.5.

## 2.1 The Green Function Formalism

### 2.1.1 Full Green Functions and the Generating Functional

Green functions ( $N$ -point functions) are defined as time-ordered expectation values of fields

$$G_{i_1 \dots i_N}(x_1, \dots, x_N) = \langle \mathcal{T} \phi_{i_1}(x_1) \dots \phi_{i_N}(x_N) \rangle. \quad (2.1)$$

In this section we employ the compact DeWitt notation: All particle properties (type, spin or polarization, charge, color, ...) except sometimes position/momentum are summarized by a single collective index  $i_k$ . Repeated indices are summed/integrated over; the functional integral over all fields  $\phi_1, \dots, \phi_N$  is often just written as  $\int \mathcal{D}\phi$ .

Graphically particles are represented by a solid line — with a collective index explicitly given when necessary.  $N$ -point functions are drawn as gray blobs with  $N$  legs, e.g.

$$\langle \mathcal{T} \phi_i(x_1) \phi_j(x_2) \phi_k(x_3) \rangle = \text{diagram of a gray blob with three legs labeled } i, j, k. \quad (2.2)$$

It is often convenient to introduce sources (or sinks)  $J$  in the generating functional<sup>1</sup>

$$Z = \langle 0|0 \rangle = \int \mathcal{D}\phi e^{iS[\Phi]} \rightarrow Z[J] = \langle 0|e^{i(\phi, J)}|0 \rangle = \int \mathcal{D}\phi e^{iS[\Phi] + i(\phi, J)} \quad (2.3)$$

with  $(\phi, J) = \phi_i J_i = \int d^d x \phi_i(x) J_i(x) = \int d^d x (\phi_1(x) J_1(x) + \dots + \phi_n(x) J_n(x))$ . In the vacuum all sources vanish, but one can set them to zero in the very last step of a calculation and make use of them in intermediate steps. Sources and sinks are drawn as crosses  $\times$ . Employing (2.3), the generating functional can be written as a (formal) power series in the sources,

$$\begin{aligned} Z[J] = & 1 + i \sum_i \int d^d x_1 G_i(x_1) J_i(x_1) - \frac{1}{2!} \sum_{ij} \int d^2 d(x_1, x_2) G_{ij}(x_1, x_2) J_i(x_1) J_j(x_2) \\ & - \frac{i}{3!} \sum_{ijk} \int d^3 d(x_1, x_2, x_3) G_{ijk}(x_1, x_2, x_3) J_i(x_1) J_j(x_2) J_k(x_3) + \dots \end{aligned}$$

$$\text{diagram of a gray blob} = 1 + i \sum_i \text{diagram of a gray blob with one leg } i \text{ and a cross} - \frac{1}{2!} \sum_{ij} \text{diagram of a gray blob with two legs } i, j \text{ and crosses} - \frac{i}{3!} \sum_{ijk} \text{diagram of a gray blob with three legs } i, j, k \text{ and crosses} + \dots \quad (2.4)$$

and indeed any particular Green function can be obtained by taking an appropriate derivative with respect to the sources and afterwards setting all sources to zero, e.g.

$$\left[ \frac{\delta^2 Z}{\delta(iJ_i) \delta(iJ_j)} \right]_{J=0} = \left[ \frac{\delta^2}{\delta(iJ_i) \delta(iJ_j)} \text{diagram of a gray blob} \right]_{J=0} = \text{diagram of a gray blob with two legs } i, j. \quad (2.5)$$

This is similar to the technique of generating functions, well-known from the theory of orthogonal polynomials and special functions (see for example chapter 34 of [18]). Thus the name *generating functional* for  $Z[J]$  is justified.

Typically one can give a perturbative expansion for Green functions. Note, however, that the full Green functions considered so far contain disconnected parts. These parts are mostly unwanted, because they describe independent processes which are better described separately and combined (if necessary) at the very end. This is achieved by introducing new types of Green functions.

$$\text{diagram of a gray blob with four legs } i, j, k, \ell = \dots + \text{diagram of a gray blob with two legs } i, j \text{ and a loop with legs } k, \ell + \dots$$

<sup>1</sup>Note that this prescription can be also be interpreted as a Fourier transform  $Z[J] = \int \frac{\mathcal{D}[\phi_1 \dots \phi_N]}{(2\pi)^{N/2}} \tilde{Z}[\phi] e^{i(\phi, J)}$ .

### 2.1.2 Connected Green Functions

Disconnected parts of the Green functions can be removed by transforming the generating functional  $Z[J]$  to another functional which we will denote by  $W[J]$ . Any full Green function can be decomposed in a connected piece (which we draw as a shaded blob) and a remainder. We do this explicitly for the 1-point function and obtain

$$i \text{---} \text{blob} = i \text{---} \text{shaded blob} \cdot \text{blob} \iff \frac{\delta Z[J]}{\delta(iJ_i)} = \frac{\delta W}{\delta(iJ_i)} Z[J] \quad (2.6)$$

Equation 2.6 is a functional differential equation which can be easily solved to yield  $Z[J] = e^{iW[J]}$  or  $W[J] = -i \ln Z[J]$ , respectively.

One can – for a given order – check explicitly that this is indeed a useful definition in order to remove all connected parts. For example, for the one to three-point functions one finds

$$\begin{aligned} \frac{\delta \ln Z}{\delta(iJ_i)} &= \frac{1}{Z} \frac{\delta Z}{\delta(iJ_i)} = \left\langle \frac{\delta Z}{\delta(iJ_i)} \right\rangle = G_i, \\ \frac{\delta^2 \ln Z}{\delta(iJ_i) \delta(iJ_j)} &= -\frac{1}{Z^2} \frac{\delta Z}{\delta(iJ_i)} \frac{\delta Z}{\delta(iJ_j)} + \frac{1}{Z} \frac{\delta^2 Z}{\delta(iJ_i) \delta(iJ_j)} = \left\langle \frac{\delta^2 Z}{\delta(iJ_i) \delta(iJ_j)} \right\rangle - \left\langle \frac{\delta Z}{\delta(iJ_i)} \right\rangle \left\langle \frac{\delta Z}{\delta(iJ_j)} \right\rangle = G_{ij} - G_i G_j, \\ \frac{\delta^3 \ln Z}{\delta(iJ_i) \delta(iJ_j) \delta(iJ_k)} &= \frac{2}{Z^3} \frac{\delta Z}{\delta(iJ_i)} \frac{\delta Z}{\delta(iJ_j)} \frac{\delta Z}{\delta(iJ_k)} - \frac{1}{Z^2} \frac{\delta^2 Z}{\delta(iJ_i) \delta(iJ_k)} \frac{\delta Z}{\delta(iJ_j)} - \frac{1}{Z^2} \frac{\delta Z}{\delta(iJ_i)} \frac{\delta^2 Z}{\delta(iJ_j) \delta(iJ_k)} \\ &\quad - \frac{1}{Z^2} \frac{\delta^2 Z}{\delta(iJ_i) \delta(iJ_j)} \frac{\delta Z}{\delta(iJ_k)} + \frac{1}{Z} \frac{\delta^3 Z}{\delta(iJ_i) \delta(iJ_j) \delta(iJ_k)} \\ &= G_{ijk} - (G_{ij} G_k - G_i G_j G_k) - (G_{ik} G_j - G_i G_j G_k) - (G_{jk} G_i - G_i G_j G_k) - G_i G_j G_k. \end{aligned}$$

Graphically, this means that all diagrams contained in such a Green function must be *connected*, thus the  $N$ -point functions

$$W_{i_1 i_2 \dots i_N} = G_{i_1 i_2 \dots i_N}^{(c)} = \frac{\delta^N W}{\delta(iJ_{i_1}) \delta(iJ_{i_2}) \dots \delta(iJ_{i_N})} \quad (2.7)$$

are called *connected Green functions*. 2-point connected Green functions  $G_{ij}^{(c)}$  are called *propagators* and typically denoted by  $D_{ij}$ . Propagators will play an essential role in our following considerations.

The same way  $Z$  is the generating functional for the full Green functions,  $W$  is the generating functional of the connected Green functions,

$$W[J] = \sum_{N=1}^{\infty} \frac{i^N}{N!} \sum_{i_1 \dots i_N} \int d^N x (x_1 \dots x_N) G_{i_1 \dots i_N}^{(c)}(x_1, \dots, x_N) J_{i_1}(x_1) \dots J_{i_N}(x_N)$$

$$\text{blob} = i \sum_i \text{shaded blob with } i \text{ line} - \frac{1}{2!} \sum_{ij} \text{shaded blob with } i, j \text{ lines} - \frac{i}{3!} \sum_{ijk} \text{shaded blob with } i, j, k \text{ lines} + \dots \quad (2.8)$$

To transform expressions formulated in terms of  $Z$  to the corresponding ones formulated in terms of  $W$ , one can use the identity

$$\frac{1}{Z[J]} \frac{\delta}{\delta(iJ_i)} (Z[J] f[J]) = \frac{1}{Z[J]} \left( \frac{\delta W}{\delta(iJ_i)} e^{W[J]} f[J] + Z[J] \frac{\delta f[J]}{\delta(iJ_i)} \right) = \frac{\delta W[J]}{\delta(iJ_i)} f[J] + \frac{\delta f[J]}{\delta(iJ_i)},$$

which holds for arbitrary functions  $f$  of the sources and can thus be written as an operator equation

$$\frac{1}{Z} \frac{\delta}{\delta(iJ_i)} Z = \frac{\delta W}{\delta(iJ_i)} + \frac{\delta}{\delta(iJ_i)}. \quad (2.9)$$

### 2.1.3 Proper (1PI) Green Functions

Connected Green functions are useful, but often it is desirable to go one step further and study only Green functions which are *one-particle irreducible* (1PI), also called *proper* Green functions. This property means that one cannot cut a diagram into two (or more) disconnected parts by cutting a single line.

The consequences of one-particle irreducibility are deeper than they may seem at first glance. In particular, such irreducibility implies that a 1PI function must not have external legs (since one could cut one of them and thus produce a disconnected piece). 1PI functions are “amputated”, i.e. connected to the outside world via vertices (which could even be drawn explicitly on the blobs).

The “leglessness” implies that one can “stick together” a connected and a 1PI function, but not two functions of the same type (or a full and a connected function).<sup>2</sup> It further implies that the generating functional  $\Gamma$  of the proper functions cannot depend on sources  $J$ . Instead it depends on fields, more precisely on classical fields, defined as

$$\phi_i^{(\text{cl})} = \langle \phi_i \rangle = \frac{\delta W[J]}{\delta (iJ_i)} = i \text{---} \text{blob} . \quad (2.10)$$

The term *classical* stems from the fact that (according to Ehrenfest’s theorem) the expectation values of the field operators  $\phi_i$  obey the classical equations of motion. While  $\phi_i^{(\text{cl})} \neq \phi_i$ , nevertheless the superscript  $(\text{cl})$  is typically dropped when there is no potential for confusion (and sometimes even when there is).

Picking out a leg in a connected diagram pulls out a 1PI piece which is connected to 0, 1, 2 or more one-particle reducible, but still connected pieces. In detail this means

$$\begin{aligned} \text{---} \text{blob} &= \text{---} \times + \text{---} \text{---} \text{blob} + \text{---} \text{---} \text{blob} \text{---} \text{blob} + \frac{1}{2} \text{---} \text{---} \text{blob} \begin{array}{c} \text{---} \text{blob} \\ \text{---} \text{blob} \end{array} + \dots \\ \phi_i^{(\text{cl})} &= \Delta_{ij} \left( iJ_j + i\Gamma_j + i\Sigma_{jk}\phi_k^{(\text{cl})} + \frac{i}{2}\Gamma_{jkl}\phi_k^{(\text{cl})}\phi_l^{(\text{cl})} + \dots \right), \end{aligned} \quad (2.11)$$

where we have denoted the proper 2-point function appearing here by  $\Sigma_{jk}$ . It is convenient to combine the “proper self-energy”  $\Sigma$  with the inverse bare propagator  $\Delta^{-1}$ . Multiplying (2.11) with  $(-i)\Delta^{-1}$  and slightly rearranging terms yields

$$0 = J_i + \Gamma_i + \underbrace{(\Sigma + i\Delta^{-1})_{ij}}_{=: \Gamma_{ij}} \phi_j^{(\text{cl})} + \frac{1}{2} \Gamma_{ijk} \phi_k^{(\text{cl})} \phi_j^{(\text{cl})} + \dots \quad (2.12)$$

Defining yet another generating functional  $\Gamma$ ,

$$\begin{aligned} \Gamma[\phi^{(\text{cl})}] &= \sum_{N=1}^{\infty} \frac{1}{N!} \sum_{i_1 \dots i_N} \int d^N(x_1 \dots x_N) \Gamma_{i_1 \dots i_N}(x_1, \dots, x_N) \phi_{i_1}^{(\text{cl})}(x_1) \dots \phi_{i_N}^{(\text{cl})}(x_N) \\ \text{---} \text{blob} &= \sum_i \text{---} \text{blob} \text{---} \text{blob}_i + \frac{1}{2!} \sum_{ij} \text{---} \text{blob} \text{---} \text{blob}_i \text{---} \text{blob}_j + \frac{1}{3!} \sum_{ijk} \text{---} \text{blob} \text{---} \text{blob}_i \text{---} \text{blob}_j \text{---} \text{blob}_k + \dots, \end{aligned} \quad (2.13)$$

<sup>2</sup>Of course one can always connect two 1PI functions by a bare propagator or attach a full or connected function to an appropriate bare vertex.



we can write (2.11) as

$$0 = J_i + \frac{\delta\Gamma[\phi]}{\delta\phi_i} = \frac{i}{\text{---}\times\text{---}} + \frac{i}{\text{---}\bigcirc\text{---}}. \quad (2.14)$$

Relations (2.10) and (2.14) can be summarized by a *Legendre transform* [110]

$$i\Gamma[\phi^{(\text{cl})}] = W[J] - i\phi_i^{(\text{cl})} J_i, \quad (2.15)$$

which again makes clear that classical fields are dual to the sources. Correspondingly, connected and 1PI functions are in many respects inverse to each other.<sup>3</sup> This can be made most explicit for two-point functions, where a functional derivative of (2.14) with respect to a source  $J_k$  gives (employing the functional version of the chain rule)

$$0 = \delta_{ki} + \frac{\delta}{\delta J_k} \frac{\delta\Gamma[\phi]}{\delta\phi_i} = \delta_{ki} + \frac{\delta\phi_j}{\delta J_k} \frac{\delta}{\delta\phi_j} \frac{\delta\Gamma[\phi]}{\delta\phi_i} \stackrel{(2.10)}{=} \delta_{ki} + i \frac{\delta^2 W}{\delta(iJ_k)\delta(iJ_j)} \frac{\delta^2 \Gamma}{\delta\phi_j \delta\phi_i}, \quad (2.16)$$

i.e.  $W_{kj}\Gamma_{ji} = i\delta_{ki}$  with (as usual) a summation/integration over the multi-index  $j$  implied. Separating again the inverse free propagator  $\Delta^{-1}$  from the self-energy part  $\Sigma$ , one can rewrite this relation as

$$\begin{aligned} \frac{\delta^2 W}{\delta(iJ_i)\delta(iJ_j)} &= \frac{i}{\text{---}\bigcirc\text{---}} \frac{j}{\text{---}} = \Delta_{ij} - i\Delta_{ik}\Sigma_{kl}\Delta_{lj} - \Delta_{ik}\Sigma_{kl}\Delta_{lm}\Sigma_{mn}\Delta_{nj} + i\dots \\ &= \frac{i}{\text{---}} \frac{j}{\text{---}} + \frac{i}{\text{---}\bigcirc\text{---}} \frac{j}{\text{---}} + \frac{i}{\text{---}\bigcirc\text{---}} \frac{j}{\text{---}\bigcirc\text{---}} + \dots \\ &= [\Delta \{1 - i\Sigma\Delta + (-i\Sigma\Delta)^2 + (-i\Sigma\Delta)^3 + \dots\}]_{ij} = \left[ \frac{\Delta}{1 + i\Sigma\Delta} \right]_{ij} = \left[ \frac{i}{i\Delta^{-1} - \Sigma} \right]_{ij}, \end{aligned} \quad (2.17)$$

which emphasizes the role of  $W_{ij} = \frac{\delta^2 W}{\delta(iJ_i)\delta(iJ_j)} = G_{ij}^{(c)} = D_{ij}$  as a dressed propagator and  $\Sigma_{ij} = \Gamma_{ij} - i(\Delta^{-1})_{ij}$  as corresponding self-energy. By introducing appropriate sources and a corresponding Legendre transform, the formalism of 1PI functions can be extended to 2PI and general  $n$ PI functions, see appendix A of [63].

### Derivatives of Propagators

In the derivation of Dyson-Schwinger equations (to be discussed in section 2.2) one repeatedly has to take derivatives of propagators with respect to classical fields. Making use of the fact that propagators are the inverse<sup>4</sup> of 1PI two-point functions, one obtains the important relation<sup>5</sup>

$$\begin{aligned} \frac{\delta}{\delta\phi_j} D_{ik} &= -D_{i\nu_1} \frac{\delta^3 \Gamma}{\delta\phi_{\nu_1} \delta\phi_j \delta\phi_{\nu_2}} D_{\nu_2 k}, \\ \frac{\delta}{\delta\phi_j} \frac{i}{\text{---}\bigcirc\text{---}} \frac{k}{\text{---}} &= - \frac{i}{\text{---}\bigcirc\text{---}} \nu_1 \frac{j}{\text{---}\bigcirc\text{---}} \nu_2 \frac{k}{\text{---}\bigcirc\text{---}}. \end{aligned} \quad (2.18)$$

<sup>3</sup>This is a consequence of the Legendre transform, which translates a function of physical dimension  $p^{-n}$  to a function of dimension  $p^n$ . Thus in contrast to a popular misconception, the proper functions are *not* a subset of the connected functions, but objects of a different type.

<sup>4</sup>Note that this is meant as *matrix inversion* of 1PI two-point functions. If two or more fields mix, one has to invert the matrix of propagators in order to obtain the 1PI functions and vice versa. This is already true at tree-level, where one has to perform a matrix inversion to obtain the propagators of mixing fields from the action

<sup>5</sup>This is the functional analogue to the matrix equation  $\frac{d}{d\lambda} M^{-1} = -M^{-1} \frac{dM}{d\lambda} M^{-1}$ , which can be proven by taking the derivative of the equation  $MM^{-1} = \mathbb{1}$ . For commuting objects  $f$  this relation reduces to the elementary formula  $(\frac{1}{f})' = -\frac{f'}{f^2}$ .

### Expressing Connected Functions in Terms of Proper Functions and Propagators

Typically, when studying a quantum field theory, one is only interested in propagators and 1PI functions. Full Green functions can be obtained as trivial products of connected functions, and connected functions can be expressed in terms of proper functions and propagators:

Taking successive derivatives of (2.16) with respect to sources  $J_{i_k}$  and making use of lower-order relations yields

$$\text{Diagram 1} = \text{Diagram 2}, \quad (2.19)$$

$$\text{Diagram 3} = \text{Diagram 4} + \text{Diagram 5} + \text{Diagram 6} + \text{Diagram 7} + \text{Diagram 8}, \quad (2.20)$$

and correspondingly for connected  $n$ -point functions of higher order.

#### 2.1.4 A Note on Fermionic Fields

In the formalism considered so far we have assumed that all fields  $\phi_i$  and  $\phi_j$  commute, i.e. are bosonic. Fermionic fields can be incorporated as well (in a straightforward way, except some worrying about signs going wrong). Having fermionic fields  $\bar{\psi}_i, \psi_i$  (which always come in pairs) means that one has to introduce anticommuting sources ( $\bar{\eta}_i \eta_i = -\eta_i \bar{\eta}_i$ ), and the generating functional is (employing Grassmann variables) extended to

$$Z[J, \bar{\eta}, \eta] = \int \mathcal{D}[\phi, \bar{\psi}, \psi] e^{iS[\phi, \bar{\psi}, \psi] + i(J, \phi) + i(\bar{\eta}, \psi) + i(\eta, \bar{\psi})}. \quad (2.21)$$

The diagrammatic notation is useful as well, one only has to care about the direction of fermion flow (typically indicated by arrows on propagators) and the order of legs, see chapter 4 of [63].

#### 2.1.5 The Role of the Vacuum

Green functions are defined as *vacuum* expectation values. When introducing sources, we leave the vacuum and thus instead of (2.1) we obtain modified expectation values

$$G_{\phi_1 \dots \phi_N}^{(J)}(x_1, \dots, x_N) = \langle \mathcal{T} \phi_1(x_1) \dots \phi_N(x_N) \rangle_J = \langle J | \mathcal{T} \phi_1(x_1) \dots \phi_N(x_N) | J \rangle. \quad (2.22)$$

We always have to distinguish the general theory (with nonvanishing sources, here denoted by a subscript  $J$  or a superscript  $(J)$ ) and the vacuum theory, where the symmetries of the vacuum are imposed on all Green functions. In the case of QCD, a quark-antighost two-point function can easily exist in the general theory (including sources),

$$G_{q\bar{c}}^{(J)}(x_1, x_2) = \text{Diagram 1} = \text{Diagram 2} + \text{Diagram 3} + \text{Diagram 4} + \dots, \quad (2.23)$$

while in the vacuum such a function is prohibited by various symmetries, i.e. conservation laws (charge conservation, baryon number conservation, ghost number conservation, to name just a few). One can deduce from another important vacuum symmetry, namely translation invariance, that Green functions (2.1) may only depend on relative, but not on absolute positions, e.g.

$$G_{ij}^{(J)}(x_1, x_2) \xrightarrow{J \rightarrow 0} G_{ij}(x_1 - x_2). \quad (2.24)$$

## 2.2 The Dyson-Schwinger Equations

*To define precisely the set of functions  $q(t)$  which contribute essentially in this limit is a nontrivial mathematical matter. [...] The careful reader is referred to the literature on this point. A physicist will, however, proceed without fear [...]*

C. Itzykson and J.-B. Zuber in [109], p.428

*Dyson-Schwinger equations* (DSEs), often also called *Schwinger-Dyson equations*, are fundamental equations of any given quantum field theory. Since they are the quantum analog to the Euler-Lagrange equations of classical systems, they are also often referred to as *equations of motion*. DSEs can be used to generate – in a weak-coupling expansion – all Feynman diagrams of perturbation theory. They are even more useful, however, to study *nonperturbative* phenomena of quantum field theory. This makes them natural candidates for studies of QCD in the strong-coupling regime.

Therefore, they complement lattice-based or exact renormalization group approaches to strong QCD and are an important method for obtaining analytic statements as well as numerical results. The latter ones usually heavily rely on truncations, approximations and clever ansätze.

Unfortunately, as far as we are aware, there exists no easily accessible pedagogic introduction to this subject. Standard textbooks on quantum field theory like [158] or [109] discuss DSEs only in a very condensed and abstract way (and several other textbooks don't discuss them at all). There are only a few texts that treat this topic in more detail, especially [63, 142, 167]. All of them have their virtues, but none of them seems to be completely appropriate as a first introduction to the subject. In addition, being out of print, they are difficult to access.

Topical reviews like [13], [123] or [80], which heavily rely on DSEs, focus for obvious reasons on recent results and not on the basics that are of course well-known to the authors. Accordingly, they tend to start on an already quite advanced level, assuming knowledge which can be hardly expected from a beginner in the field.

So the basics about DSEs are scattered among various sources, a situation that can easily discourage students from working with this powerful tool. It may even be a reason why DSEs at the present time receive less attention than they deserve in the community of field theorists and particle physicists (even though they began to gain increasing popularity during the last few years).

To fill this gap at least partially, we examine the principles behind DSEs quite in detail and from various points of view. We motivate them diagrammatically, before deriving them in a more formal, abstract way. This will be done first for a general quantum field theory. In the next section we will give a concrete example, employing the Lagrangian of high-temperature Yang-Mills theory as a starting point.

### 2.2.1 From the Action to Equations of Motion

Both classical and quantum theories are initially defined by giving an Lagrangian (or, equally good, a Hamiltonian, with a Legendre transformation mediating the transition from one formulation to the other<sup>6</sup>). In classical theories, one can derive from a Lagrange function  $L(q_i, \dot{q}_i)$  equations of motion by the variational principle. Demanding the stationarity condition  $\delta S = 0$  yields the differential equations

$$\frac{d}{dt} \frac{\partial L}{\partial \dot{q}_i} - \frac{\partial L}{\partial q_i} = 0. \quad (2.25)$$

---

<sup>6</sup>The Lagrangian formulation heavily dominates quantum field theory. This is mostly due to the fact that symmetries of the system are more transparent in the Lagrangian than in the Hamiltonian. Since quantum theory relies so heavily on symmetries, the choice of the Lagrangian is quite natural.

In classical field theories with a Lagrangian density  $\mathcal{L}(\phi_i, \partial_\mu \phi_i)$  which depends on fields  $\phi_i$  and their derivatives, one obtains

$$\partial_\mu \frac{\partial \mathcal{L}}{\partial (\partial_\mu \phi_i)} - \frac{\partial \mathcal{L}}{\partial \phi_i} = 0, \quad (2.26)$$

which are partial differential equations. The Maxwell equations of electromagnetism can be obtained by this formalism (by setting  $\mathcal{L} = \frac{1}{4} F_{\mu\nu} F^{\mu\nu}$  with the field strength tensor  $F_{\mu\nu} \sim \partial_\mu A_\nu - \partial_\nu A_\mu$ ) as well as the Einstein field equations of General Relativity, employing the Einstein-Hilbert Lagrangian  $\mathcal{L} = \sqrt{|\det g|} R(g)$ .

Also the equations of motion of relativistic quantum mechanics like the Klein-Gordon equation or the Dirac equation can be obtained from the variational principle; they are also partial differential equations, which describe the evolution of fields. It is well-known, however, that relativistic quantum mechanics has a limited range of validity (demonstrated clearly, for example, in Klein's paradox) and one has to move on to quantum field theory in order to access fundamental features of particle physics.

By allowing creation and annihilation of particles (i.e. field excitations), we lose the concept of a well-defined particle number. From Heisenberg's uncertainty principle, combined with mass-energy equivalence, even the vacuum, when observed closely enough, can contain a huge number of virtual particles. Thus we cannot expect to obtain just a closed system of differential equations which describe the motion of a given number of particles. So what is the best thing which we can hope to get?

As already discussed in section 2.1, propagation and interaction of quantum fields can be described in terms of *Green functions*, where full propagators are 2-point functions  $G_{(2)}$ , dressed vertices are best described as 3- or 4-point 1PI functions  $\Gamma_{(3)}$  or  $\Gamma_{(4)}$ , and the interaction of a larger number of fields is similarly described by higher 1PI  $n$ -point functions.

What comes closest to a trajectory or the time evolution of a single particle wave function is a propagator. So what we can hope to get is an equation for the propagator, which will probably be coupled to other objects of the theory, i.e. other Green functions. Let us try to imagine how this coupling could look like for the quark propagator of QCD.

We examine a quark of momentum  $p$  going from some state  $i$  to some state  $j$ . As already discussed, such condensed indices can contain in principle contain all of information; here it is sufficient to read them just as different states of the same particle.

The full propagator  $S(p)$  describes everything the quark could possibly "do" on its path from  $i$  to  $j$ , as long as no other external particles are involved in the process. In particular, this contains the possibility of the particle doing nothing special at all. So the full propagator will certainly contain the bare one, as depicted in figure 2.1.a.

In an interacting theory, that's of course not the whole story. The quark can interact with gluons, which is described on tree level with the bare quark-gluon vertex  $\gamma^\mu t^a$ . So if anything has to happen at all, the quark first has to emit a gluon (to which we ascribe the momentum  $k = p - q$ ). This is depicted in figure 2.1.b.

After that, the quark can again propagate in all possible ways (described again by the full quark propagator  $S(q)$ ), but also the gluon can propagate in all ways possible for a gluon,  $D_{\mu\nu}^{ab}(k)$ , which is illustrated in figure 2.1.c.

After these propagations, the gluon has eventually to be reabsorbed by the quark, which can happen in various different ways, described by the dressed quark-gluon vertex  $\Gamma^{\nu,b}(p, q, k)$ . This is illustrated in figure 2.1.d.

The quark can still propagate any way it likes,  $S(p)$ , until it finally arrives in state  $j$ , as depicted in figure 2.1.e. We note that the second interesting diagram on the right-hand side (the interesting one) necessarily contains a closed loop. As usual in quantum theory, we have to permit all possible intermediate states, i.e. integrate over all values for the momentum  $q$ .

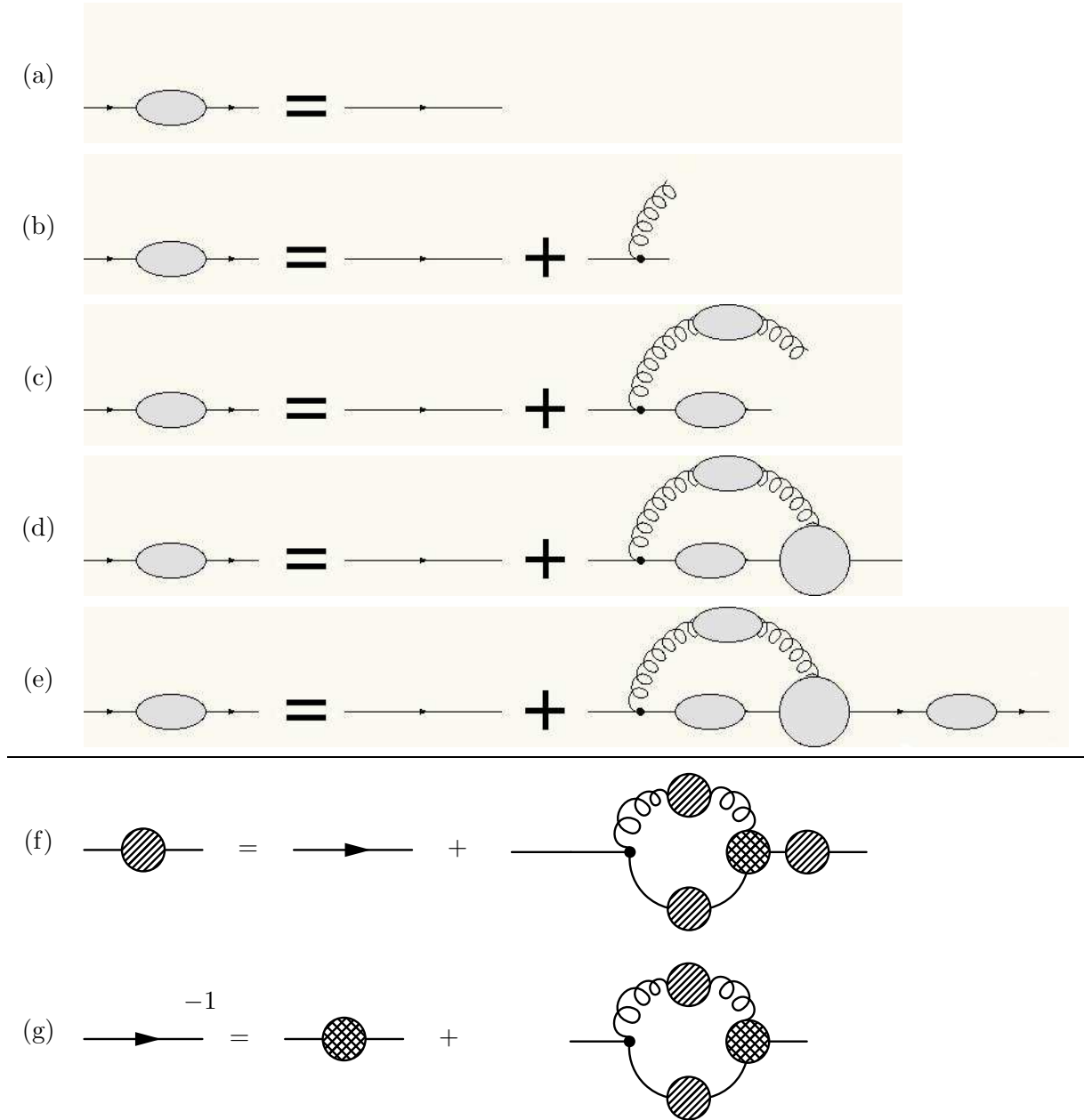


Figure 2.1: Heuristic derivation of the Dyson-Schwinger equation for the quark propagator, where during the first steps we denote Green functions of any type uniformly by gray blobs: A quark can either (a) propagate without interaction or (b) propagate freely and emit a gluon (c) propagate again, as does the gluon, (d) re-absorb the gluon in any way and (e) propagate to the final state.

So far this “derivation” does not care about the type of Green functions involved. The considerations of section 2.1 make clear that all the two-point functions are connected functions (i.e. propagators) while the dressed quark-gluon vertex has to be a 1PI function. Adopting the more concise notation of the previous section, the equation takes the form given in (f). Note that by using (2.19) this equation could be cast in a more compact, yet more opaque form which involves only connected Green functions.

Multiplying this equation from the left by the inverse free quark propagator and from the right with the quark 2-point 1PI function yields the form given in (g). A simple rearrangement of terms gives the quark gap equation in standard form displayed in figure 4.1.

Thus we would expect the resulting equation to take the form

$$S(p) = S_0(p) + S_0(p) \int d^4q \gamma^\mu t^a D_{\mu\nu}^{ab}(p-q) \Gamma^{\nu,b}(p, q, k) S(-q) S(p). \quad (2.27)$$

This equation, obtained by heuristic reasoning, is indeed correct (up to factors of  $i$ , since we did not care about the precise definition of the propagators), though not written in the most useful way. Still, we already see some of the most prominent features of such equations:

- Since the quantity we were initially looking for appears both outside and inside the integral, we encounter some sort of *integral equation*, and we can guess that the best procedure to solve it may be iteration (i.e. start with some guess for  $S$ , put it into the integral, get a new form of  $S$ , put it again into the integral. . .)
- The equation for the two-point function  $S$  contains the three-point function  $\Gamma^{\nu,b}$ . Analogously every  $n$ -point function couples to one or more  $m$ -point functions with  $m > n$ . Thus one cannot expect to obtain a closed system, but instead (countably) infinitely many equations (“an infinite tower of equations”).

Equation 2.27 or, equivalently, figure 2.1.f has not yet been cast in the most convenient form. For example while we cannot avoid having both  $S(p)$  and  $S(q)$  in the equation, we can still reduce the number of propagators present. This is achieved by multiplying (2.27) from the left with  $S_0^{-1}(p)$  and from the right with  $S^{-1}(p)$ . The equation now reads

$$S_0^{-1}(p) = S^{-1}(p) + \int d^4q \gamma^\mu t^a D_{\mu\nu}^{ab}(p-q) \Gamma^{\nu,b}(p, q, k) S(-q), \quad (2.28)$$

which is depicted in figure 2.1.g. Simple rearrangement of terms and multiplication with  $i$  yields (4.1) which is the basic equation in chapter 4.

### 2.2.2 The Formal Derivation of DSEs

The easiest way to (formally) derive the Dyson-Schwinger equations is by exploiting the fact that – given suitable boundary conditions – the integral of a derivative vanishes.<sup>7</sup>

$$\begin{aligned} 0 &= \int \mathcal{D}\phi \frac{\delta}{\delta\phi_k} e^{iS[\phi] + iJ_i\phi_i} = \int \mathcal{D}\phi \left( i \frac{\delta S}{\delta\phi_k} [\phi] + i J_k \right) e^{iS[\phi] + iJ_i\phi_i} \\ &= i \left( \frac{\delta S}{\delta\phi_k} \left[ \frac{\delta}{\delta(iJ)} \right] + J_k \right) \int \mathcal{D}\phi e^{iS[\phi] + iJ_i\phi_i} = i \left( \frac{\delta S}{\delta\phi_k} \left[ \frac{\delta}{\delta(iJ)} \right] + J_k \right) Z[J], \end{aligned} \quad (2.29)$$

so we have

$$\left( \frac{\delta S}{\delta\phi_k} \left[ \frac{\delta}{\delta(iJ)} \right] + J_k \right) Z[J] = 0 \quad (2.30)$$

The resulting equation can be rewritten with (2.9) as

$$\left( \frac{\delta S}{\delta\phi_k} \left[ \frac{\delta W}{\delta(iJ)} + \frac{\delta}{\delta(iJ)} \right] + J_k \right) = 0. \quad (2.31)$$

---

<sup>7</sup>This is not a trivial assumption. The integral is an integral over a *function space*, and it is not obvious how to define the boundary of such a space. It is even far less obvious that the contributions from the boundary of such an infinite-dimensional space indeed vanish unless the measure includes a factor which strongly suppresses large field configurations. A Gaussian measure  $\mathcal{D}\phi \exp(-\|\phi\|^2)$  can be expected to do the job, but at the same time includes an unwanted perturbative limitation in the derivation of equations which are expected to describe the full nonperturbative behaviour of the theory.

A more rigorous way to derive the DSEs is to use the invariance with respect to infinitesimal field translations, as demonstrated in [109, 167]. But even in this case the use of perturbative methods cannot yet be completely avoided at an intermediate stage. As stated in [13]: “In neither direction, from the combinatorics of interactions to the generating functional nor the other way round, from generating functionals to DSEs, can the derivation of both as yet be fully divorced from perturbation theory.”



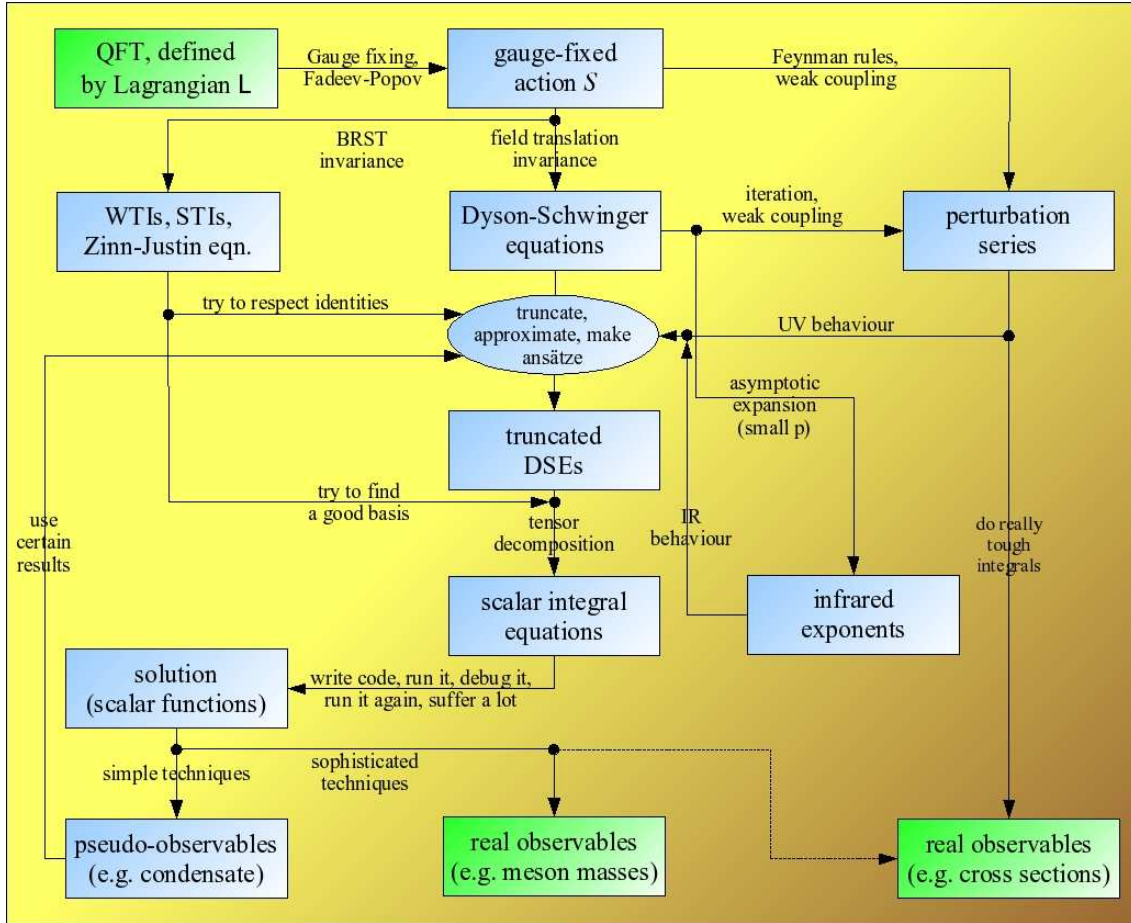


Figure 2.2: Sketch of the procedure necessary to extract physical quantities from Dyson-Schwinger equations

Using (2.14) to express  $J$  as  $-\frac{\delta\Gamma}{\delta\phi}$ , recognizing  $\frac{\delta W}{\delta(iJ)}$  as the classical field and employing the functional chain rule (see (2.16)) one obtains

$$\frac{\delta\Gamma[\phi]}{\delta\phi_k} = \frac{\delta S}{\delta\phi_k} \left[ \phi + i \frac{\delta^2 W}{\delta(iJ)\delta(iJ_j)} \frac{\delta}{\delta\phi_j} \right]. \quad (2.32)$$

The Euclidean version of these functional equations is given by (see for example [13]):

$$\left( -\frac{\delta S}{\delta\phi_k} \left[ \frac{\delta}{\delta J} \right] + J_k \right) Z[J] = 0, \quad (2.33)$$

$$-\frac{\delta S}{\delta\phi_k} \left[ \frac{\delta W}{\delta J} + \frac{\delta}{\delta J} \right] + J_k = 0, \quad (2.34)$$

$$\frac{\delta\Gamma[\phi]}{\delta\phi_k} - \frac{\delta S}{\delta\phi_k} \left[ \phi + \frac{\delta^2 W}{\delta J \delta J_j} \frac{\delta}{\delta\phi_j} \right] = 0. \quad (2.35)$$

Actual DSEs can now be obtained from these equations by acting with functional derivatives on them. The path required to extract physics from the Dyson-Schwinger equations is illustrated schematically in figure 2.2.

Version (2.32) respectively (2.35) of these equations will turn out to be the most useful one for our purposes – but all of them are presumably quite opaque for readers with little experience in field theory. Indeed, equations (2.30) to (2.35) have been described in [63] as “so elegant that one is probably at a loss as what to do with them” – thus we will proceed with a comprehensive example.



## 2.3 DSEs for Finite-Temperature Coulomb-Gauge YM Theory

In order to give a concrete example for procedure outlined in the last section, we explicitly show the derivation of a particular Dyson-Schwinger equation which we will employ (together with others) in section 5.3 to extract infrared critical exponents.

### 2.3.1 Action and Fields

Our starting point is the action (defined in  $s$  spatial dimensions)

$$\begin{aligned}
S = \int d^s z \Big[ & \frac{1}{2} \pi_k^{\text{tr},d}(z) \pi_k^{\text{tr},d}(z) + \frac{1}{2} (\partial_k \varphi^d(z)) (\partial_k \varphi^d(z)) + i (\partial_k \varphi^d(z)) (\partial_k A_0^d(z)) \\
& - i \tilde{g} f^{def} \pi_k^{\text{tr},d}(z) A_k^{\text{tr},e}(z) A_0^f(z) + i \tilde{g} f^{def} (\partial_k \varphi^d(z)) A_k^{\text{tr},e}(z) A_0^f(z) \\
& + (\partial_k \bar{c}^d(z)) (\partial_k c^d(z)) + \tilde{g} f^{def} (\partial_k \bar{c}^d(z)) A_k^{\text{tr},e}(z) c^f(z) \Big], \tag{2.36}
\end{aligned}$$

which contains the fields  $A_0$ ,  $\varphi$ ,  $A^{\text{tr}}$ ,  $\pi^{\text{tr}}$ ,  $c$  and  $\bar{c}$ . The superscript tr denotes transversality, i.e. the conditions  $k_i A_i^{\text{tr}} = 0$  and  $k_i \pi_i^{\text{tr}} = 0$  are imposed. In diagrams, these fields are depicted as

$$\begin{aligned}
A_0 &= \text{~~~~~} & A^{\text{tr}} &= \text{~~~~~} & c &= \cdots \blacktriangleright \cdots \\
\varphi &= \text{-----} & \pi^{\text{tr}} &= \text{~~~~~} & \bar{c} &= \cdots \blacktriangleleft \cdots
\end{aligned} \tag{2.37}$$

Space indices (lower latin indices) run from 1 to  $s$ , color indices (upper latin indices) from 1 to  $N_C^2 - 1$ . Here we state this action in ad-hoc fashion, but in chapter 5 it will turn out to be the action for Coulomb-gauge Yang-Mills theory in first-order formalism in the infinite-temperature limit, with  $\tilde{g} = g \sqrt{T}$  being the (dimensionful) effective coupling.

This action is interesting (and slightly tricky to handle) because some of the fields may mix. For example the propagator  $D_{\pi_i^{\text{tr}} A_j^{\text{tr}}}^{ab}$  does not vanish, so an  $A^{\text{tr}}$ -field can go into a  $\pi^{\text{tr}}$ -field. (This is already possible at tree-level). In the case of mixing fields, the relation between connected and 1PI Green functions is more complicated: The relation

$$\frac{\delta^2 W}{\delta J_i \delta J_j} = \left( \frac{\delta^2 \Gamma}{\delta \Phi_i \delta \Phi_j} \right)^{-1}$$

only holds as a *matrix equation*, thus with the abbreviations

$$D_{\Phi_i \Phi_j} := \frac{\delta^2 W}{\delta J_i \delta J_j} \quad \text{and} \quad \Gamma_{\Phi_1 \Phi_2} := \frac{\delta^2 \Gamma}{\delta \Phi_1 \delta \Phi_2} \tag{2.38}$$

one has

$$\begin{pmatrix} D_{A^{\text{tr}} A^{\text{tr}}} & D_{A^{\text{tr}} \pi^{\text{tr}}} \\ D_{A^{\text{tr}} \pi^{\text{tr}}} & D_{\pi^{\text{tr}} \pi^{\text{tr}}} \end{pmatrix} = \begin{pmatrix} \Gamma_{A^{\text{tr}} A^{\text{tr}}} & \Gamma_{A^{\text{tr}} \pi^{\text{tr}}} \\ \Gamma_{A^{\text{tr}} \pi^{\text{tr}}} & \Gamma_{\pi^{\text{tr}} \pi^{\text{tr}}} \end{pmatrix}^{-1} \tag{2.39}$$

$$\begin{pmatrix} D_{A_0 A_0} & D_{A_0 \varphi} \\ D_{\varphi A_0} & D_{\varphi \varphi} \end{pmatrix} = \begin{pmatrix} \Gamma_{A_0 A_0} & \Gamma_{A_0 \varphi} \\ \Gamma_{\varphi A_0} & \Gamma_{\varphi \varphi} \end{pmatrix}^{-1}, \tag{2.40}$$

e.g.

$$D_{A^{\text{tr}} \pi^{\text{tr}}} = \frac{\Gamma_{A^{\text{tr}} \pi^{\text{tr}}}}{\Gamma_{A^{\text{tr}} A^{\text{tr}}} \Gamma_{\pi^{\text{tr}} \pi^{\text{tr}}} - \Gamma_{A^{\text{tr}} \pi^{\text{tr}}}^2}, \quad D_{A_0 A_0} = \frac{\Gamma_{\varphi \varphi}}{\Gamma_{A_0 A_0} \Gamma_{\varphi \varphi} - \Gamma_{A_0 \varphi}^2}. \tag{2.41}$$

This has to be taken into account when determining propagators from the corresponding 1PI functions.

### 2.3.2 The Generating Equation

We now want to derive the Dyson-Schwinger equations for some of the two-point 1PI-functions. The basic equation for this is (2.32) [with a slightly different convention for factors of  $i$ ] which we now have a closer look at. On the right hand side we have the derivative of  $\Gamma$  with respect to a classical field, e.g.  $A_0$  – a quantity we know nothing about a priori. On the right hand side, however, there is an expression we can easily determine – the derivative of the action  $S$  with respect to a field, with some substitutions done in the argument. In our case we immediately find

$$\begin{aligned} \frac{\delta S}{\delta A_0^a(x)} &= \int d^s z \left[ i(\partial_k \varphi^d(z)) (\delta^{ad} \partial_k^{(z)} \delta(z-x)) - i\tilde{g} f^{def} \pi_k^{\text{tr},d}(z) A_k^{\text{tr},e}(z) \delta^{af} \delta(z-x) \right. \\ &\quad \left. + i\tilde{g} f^{def} (\partial_k^{(z)} \varphi^d(z)) A_k^{\text{tr},e}(z) \delta^{af} \delta(z-x) \right] \\ &= \int d^s z \delta(z-x) \left[ -i\partial_{(z)}^2 \varphi^a(z) - i\tilde{g} f^{dea} \pi_k^{\text{tr},d}(z) A_k^{\text{tr},e}(z) + i\tilde{g} f^{dea} (\partial_k^{(z)} \varphi^d(z)) A_k^{\text{tr},e}(z) \right] \\ &= -i\partial_{(x)}^2 \varphi^a(x) - i\tilde{g} f^{ade} \pi_k^{\text{tr},d}(x) A_k^{\text{tr},e}(x) + i\tilde{g} f^{ade} (\partial_k^{(x)} \varphi^d(x)) A_k^{\text{tr},e}(x), \end{aligned} \quad (2.42)$$

where we have used “partial integration” and cyclicity of the structure constants,  $f^{dea} = f^{ade}$ . In order to obtain an equation for  $\frac{\delta \Gamma}{\delta A_0}$  we substitute for all instances of the fields  $\Phi_k$  the corresponding classical fields  $\Phi_k^{\text{cl}}$  plus the derivative term  $\frac{\delta^2 W}{\delta J_k \delta J_j} \frac{\delta}{\delta \Phi_j}$  with the multi-index  $j$  summed/integrated over.<sup>8</sup> With the abbreviation

$$D_{\Phi_i \Phi_j}^{a \ b}(x, y) \quad \text{for} \quad \frac{\delta^2 W}{\delta J_i^a(x) \delta J_j^b(y)}$$

we find (dropping again the cumbersome superscript “cl”)

$$\begin{aligned} \frac{\delta \Gamma}{\delta A_0^a(x)} &= \frac{\delta S}{\delta A_0^a(x)} \left[ \Phi + \frac{\delta^2 W}{\delta J \delta J} \frac{\delta}{\delta \Phi_j} \right] = -i\partial_{(x)}^2 \varphi^a(x) - i\partial_{(x)}^2 \cancel{D_{\varphi \Phi_1}^{a \ s'}(x, x') \frac{\delta}{\delta \Phi_1^{a'}(x')}} \\ &\quad - i\tilde{g} f^{ade} \left( \pi_k^{\text{tr},d}(x) + D_{\pi_k^{\text{tr}} \Phi_1}^{d \ d'}(x, x') \frac{\delta}{\delta \Phi_1^{d'}(x')} \right) \left( A_k^{\text{tr},e}(x) + \cancel{D_{A_k^{\text{tr}} \Phi_2}^{a \ a'}(x, x'') \frac{\delta}{\delta \Phi_1^{a'}(x'')}} \right) \\ &\quad + i\tilde{g} f^{ade} \left( \partial_k^{(x)} \varphi^d(x) + \left[ \partial_k^{(x)} D_{\varphi \Phi_1}^{d \ d'}(x, x') \right] \frac{\delta}{\delta \Phi_1^{d'}(x')} \right) \left( A_k^{\text{tr},e}(x) + \cancel{D_{A_k^{\text{tr}} \Phi_2}^{a \ a'}(x, x'') \frac{\delta}{\delta \Phi_1^{a'}(x'')}} \right), \\ &= -i\partial_{(x)}^2 \varphi^a(x) - i\tilde{g} f^{ade} \pi_k^{\text{tr},d}(x) A_k^{\text{tr},e}(x) - i\tilde{g} f^{ade} D_{\pi_k \Phi_1}^{d \ d'}(x, x') \frac{\delta A_k^{\text{tr},e}(x)}{\delta \Phi_1^{d'}(x')} \\ &\quad + i\tilde{g} f^{ade} (\partial_k^{(x)} \varphi^d(x)) A_k^{\text{tr},e}(x) + i\tilde{g} f^{ade} \left[ \partial_k^{(x)} D_{\varphi \Phi_1}^{d \ d'}(x, x') \right] \frac{\delta A_k^{\text{tr},e}(x)}{\delta \Phi_1^{d'}(x')}, \end{aligned} \quad (2.43)$$

where we have dropped all terms where functional derivatives have nothing to act on. The remaining functional derivatives yield

$$\frac{\delta A_k^{\text{tr},e}(x)}{\delta \Phi_1^{d'}(x')} = \delta_{\Phi_1 A_k^{\text{tr}}} \delta^{d'e} \delta(x-x'), \quad (2.44)$$

i.e. they vanish unless the initially unspecified field  $\Phi_1$  is an  $A_{\text{tr}}$ -field with the correct properties. With this constraint we obtain

$$\begin{aligned} \frac{\delta \Gamma}{\delta A_0^a(x)} &= -i\partial_{(x)}^2 \varphi^a(x) - i\tilde{g} f^{ade} \pi_k^{\text{tr},d}(x) A_k^{\text{tr},e}(x) - i\tilde{g} f^{ade} D_{\pi_k^{\text{tr}} A_k^{\text{tr}}}^{d \ e}(x, x) \\ &\quad + i\tilde{g} f^{ade} (\partial_k^{(x)} \varphi^d(x)) A_k^{\text{tr},e}(x) + i\tilde{g} f^{ade} \left[ \partial_k^{(x)} D_{\varphi A_k^{\text{tr}}}^{d \ e}(x, x') \right]_{x'=x} \end{aligned} \quad (2.45)$$

<sup>8</sup>As we will see soon, the derivative generates the loop terms which incorporate the quantum nature of the theory. We have set  $\hbar = 1$ ; otherwise we would explicitly find a factor of  $\hbar$  in front of the derivative term, and for  $\hbar \rightarrow 0$  we would obtain the classical theory without any loops present.

as the generating equation for (certain) 1PI DSEs. Note that the propagators connect the point  $x$  with itself, so we have indeed obtained a closed loop. Displayed graphically (absorbing signs and prefactors into the graphs), this equation takes the form

In many cases such equations contain propagators which vanish in the vacuum, but as discussed in subsection 2.1.5, they make perfect sense in the presence of sources. In our case, the  $\pi^{\text{tr}}$  and the  $A^{\text{tr}}$  fields mix, but the dressed  $\varphi - A^{\text{tr}}$  propagator vanishes in the vacuum since transverse and scalar fields do not mix.

### 2.3.3 DSE for a Two-Point Function (in Position Space)

In order to obtain the DSE for a two-point 1PI function, we take a derivative of (2.45) with respect to another field, in our case either  $A_0$  or  $\varphi$ . (All other cases are trivial either due to the non-mixing of transverse and scalar fields or due to ghost number conservation).

For the derivative with respect to  $A_0$  we find (employing (2.18) in order to take derivatives of propagators with respect to fields)

$$\begin{aligned} \frac{\delta^2 \Gamma}{\delta A_0^a(x) \delta A_0^b(y)} &= i\tilde{g} f^{ade} \int dw D_{\pi_k^{\text{tr}} \Phi_1}^{d d'}(x, w_1) \frac{\delta^3 \Gamma}{\delta \Phi_1^{d'}(w_1) \delta A_0^b(y) \delta \Phi_2^{e'}(w_2)} D_{\Phi_2 A_k^{\text{tr}}}^{e' e}(w_2, x) \\ &\quad - i\tilde{g} f^{ade} \int dw \left[ \partial_k^{(x)} D_{\varphi \Phi_1}^{d d'}(x, w_1) \right] \frac{\delta^3 \Gamma}{\delta \Phi_1^{d'}(w_1) \delta A_0^b(y) \delta \Phi_2^{e'}(w_2)} D_{\Phi_2 A_k^{\text{tr}}}^{e' e}(w_2, x) \\ &\quad \text{with } \int dw = \int d^s w_1 \int d^s w_2, \end{aligned} \quad (2.46)$$

which, written diagrammatically, takes the form

$\Phi_1$  and  $\Phi_2$  run over all fields, so written in detail, (2.49) reads (recall that we still work in the presence of sources, so also propagators like  $D_{A_0 \bar{c}}$  make sense):

Putting this equation to the vacuum removes most of the mixed propagators. The equation obtained this way is exact, but contains lots of (completely unknown) three-point functions.

### 2.3.4 Truncated DSE (in position space)

In order to make the problem tractable, we will resort to a drastic approximation: We replace all three-point functions by the corresponding bare vertices,

$$\frac{\delta^3 \Gamma}{\delta \Phi_1 \delta \Phi_2 \delta \Phi_3} \rightarrow \frac{\delta^3 S}{\delta \Phi_1 \delta \Phi_2 \delta \Phi_3}, \quad (2.48)$$

and accordingly dismiss those three-point functions which have no tree-level counterpart. In our case the only relevant vertices are those with an  $A_0$  (amputated) leg, i.e. the  $\pi^{\text{tr}}\text{-}A^{\text{tr}}\text{-}A_0$  and the  $\varphi\text{-}A^{\text{tr}}\text{-}A_0$  vertex. Employing these vertices together with only those propagators which do not vanish in the vacuum due to symmetries<sup>9</sup> yields<sup>10</sup>

$$(2.49)$$

Written in more detail, taking a derivative of (2.42) with respect to  $A_i^{\text{tr},f}(u)$  yields

$$\begin{aligned} \frac{\delta^2 S}{\delta A_0^a(x) \delta A_i^{\text{tr},f}(u)} &= -i\tilde{g} f^{ade} \pi_k^{\text{tr},d}(x) \delta_{ik} \delta^{ef} \delta(x-u) + i\tilde{g} f^{ade} (\partial_k^{(x)} \varphi^d(x)) \delta_{ik} \delta^{ef} \delta(x-u) \\ &= -i\tilde{g} f^{adf} \pi_i^{\text{tr},d}(x) \delta(x-u) + i\tilde{g} f^{adf} (\partial_i^{(x)} \varphi^d(x)) \delta(x-u) \end{aligned} \quad (2.50)$$

and thus we obtain

$$\begin{aligned} \frac{\delta^3 S}{\delta A_0^a(x) \delta A_i^{\text{tr},f}(u) \delta \pi_j^{\text{tr},g}(v)} &= -i\tilde{g} f^{adf} \delta_{ij} \delta^{dg} \delta(x-v) \delta(x-u) \\ &= i\tilde{g} f^{afg} \delta_{ij} \delta(x-v) \delta(x-u) \end{aligned} \quad (2.51)$$

$$\begin{aligned} \frac{\delta^3 S}{\delta A_0^a(x) \delta A_i^{\text{tr},f}(u) \delta \varphi^g(v)} &= i\tilde{g} f^{adf} \delta_{ij} \delta^{dg} \delta(x-v) \delta(x-u) \\ &= -i\tilde{g} f^{afg} \left( \partial_i^{(x)} \delta(x-v) \right) \delta(x-u). \end{aligned} \quad (2.52)$$

The appropriately truncated version of (2.46) (corresponding to the diagrammatic expression stated in (2.49)) reads

$$\begin{aligned} \Gamma_{00}^{ab}(x, y) &\equiv \left. \frac{\delta^2 \Gamma}{\delta A_0^a(x) \delta A_0^b(y)} \right|_{J=0} \\ &= i\tilde{g} f^{ade} \int dw D_{\pi_k^{\text{tr}} \pi_i^{\text{tr}}}^{d, d'}(x, w_1) \frac{\delta^3 S}{\delta \pi_i^{\text{tr}, d'}(w_1) \delta A_0^b(y) \delta A_j^{\text{tr}, e'}(w_2)} D_{A_j^{\text{tr}} A_k^{\text{tr}}}^{e', e}(w_2, x) \\ &\quad + i\tilde{g} f^{ade} \int dw D_{\pi_k^{\text{tr}} A_i^{\text{tr}}}^{d, d'}(x, w_1) \frac{\delta^3 S}{\delta A_i^{\text{tr}, d'}(w_1) \delta A_0^b(y) \delta \pi_j^{\text{tr}, e'}(w_2)} D_{\pi_j^{\text{tr}} A_k^{\text{tr}}}^{e', e}(w_2, x) \\ &\quad - i\tilde{g} f^{ade} \int dw \left[ \partial_k^{(x)} D_{\varphi \varphi}^{d, d'}(x, w_1) \right] \frac{\delta^3 S}{\delta \varphi^{d'}(w_1) \delta A_0^b(y) \delta A_j^{\text{tr}, e'}(w_2)} D_{A_j^{\text{tr}} A_k^{\text{tr}}}^{e', e}(w_2, x). \end{aligned} \quad (2.53)$$

<sup>9</sup>Of course one could have the situation that a propagator still vanishes even if it is not forced to do so by a conservation law. In fact, in chapter 5 we will consistently set  $D_{A^{\text{tr}} \pi^{\text{tr}}} = 0$ .

<sup>10</sup>It is easy to check that no other combinations are possible. For example the  $\varphi$ -field could change into a  $A_0$ -field, but since we need an external  $A_0$  and since there is no vertex with two (amputated)  $A_0$  legs, such a diagram does not exist in our truncation.

By plugging (2.51) and (2.52) into this equation we obtain

$$\begin{aligned}
\Gamma_{00}^{ab}(x, y) &= i\tilde{g} f^{ade} \int dw D_{\pi_k^{\text{tr}} \pi_i^{\text{tr}}}^{d d'}(x, w_1) i\tilde{g} f^{be' d'} \delta_{ij} \delta(y - w_1) \delta(y - w_2) D_{A_j^{\text{tr}} A_k^{\text{tr}}}^{e' e}(w_2, x) \\
&\quad + i\tilde{g} f^{ade} \int dw D_{\pi_k^{\text{tr}} A_i^{\text{tr}}}^{d d'}(x, w_1) i\tilde{g} f^{bd' e'} \delta_{ij} \delta(y - w_1) \delta(y - w_2) D_{\pi_j^{\text{tr}} A_k^{\text{tr}}}^{e' e}(w_2, x) \\
&\quad - i\tilde{g} f^{ade} \int dw \left[ \partial_k^{(x)} D_{\varphi\varphi}^{d d'}(x, w_1) \right] (-i) \tilde{g} f^{be' d'} \left( \partial_i^{(y)} \delta(y - w_1) \right) \delta(y - w_2) D_{A_j^{\text{tr}} A_k^{\text{tr}}}^{e' e}(w_2, x) \\
&= \tilde{g}^2 f^{ade} f^{bd' e'} D_{\pi_k^{\text{tr}} \pi_i^{\text{tr}}}^{d d'}(x, y) D_{A_i^{\text{tr}} A_k^{\text{tr}}}^{e' e}(y, x) - \tilde{g}^2 f^{ade} f^{bd' e'} D_{\pi_k^{\text{tr}} A_i^{\text{tr}}}^{d d'}(x, y) D_{\pi_i^{\text{tr}} A_k^{\text{tr}}}^{e' e}(y, x) \\
&\quad + \tilde{g}^2 f^{ade} f^{bd' e'} \int d^s w_1 \left[ \partial_k^{(x)} D_{\varphi\varphi}^{d d'}(x, w_1) \right] \left( \partial_i^{(y)} \delta(y - w_1) \right) D_{A_i^{\text{tr}} A_k^{\text{tr}}}^{e' e}(y, x). \tag{2.54}
\end{aligned}$$

In order to exploit the remaining delta functional, we employ

$$\partial_i^{(y)} \delta(y - w_1) = -\partial_i^{(w_1)} \delta(y - w_1), \tag{2.55}$$

and with “partial integration” (which yields another minus sign) we find

$$\begin{aligned}
\Gamma_{00}^{ab}(x, y) &= \tilde{g}^2 f^{ade} f^{bd' e'} D_{\pi_k^{\text{tr}} \pi_i^{\text{tr}}}^{d d'}(x, y) D_{A_i^{\text{tr}} A_k^{\text{tr}}}^{e' e}(y, x) - \tilde{g}^2 f^{ade} f^{bd' e'} D_{\pi_k^{\text{tr}} A_i^{\text{tr}}}^{d d'}(x, y) D_{\pi_i^{\text{tr}} A_k^{\text{tr}}}^{e' e}(y, x) \\
&\quad + \tilde{g}^2 f^{ade} f^{bd' e'} \int d^s w_1 \left[ \partial_k^{(x)} \partial_i^{(w_1)} D_{\varphi\varphi}^{d d'}(x, w_1) \right] \delta(y - w_1) D_{A_i^{\text{tr}} A_k^{\text{tr}}}^{e' e}(y, x). \\
&= \tilde{g}^2 f^{ade} f^{bd' e'} D_{\pi_k^{\text{tr}} \pi_i^{\text{tr}}}^{d d'}(x, y) D_{A_i^{\text{tr}} A_k^{\text{tr}}}^{e' e}(y, x) - \tilde{g}^2 f^{ade} f^{bd' e'} D_{\pi_k^{\text{tr}} A_i^{\text{tr}}}^{d d'}(x, y) D_{\pi_i^{\text{tr}} A_k^{\text{tr}}}^{e' e}(y, x) \\
&\quad + \tilde{g}^2 f^{ade} f^{bd' e'} \left[ \partial_k^{(x)} \partial_i^{(y)} D_{\varphi\varphi}^{d d'}(x, y) \right] D_{A_i^{\text{tr}} A_k^{\text{tr}}}^{e' e}(y, x). \tag{2.56}
\end{aligned}$$

Due to translational invariance the propagators can only depend on the relative position  $x - y$ , not on  $x$  and  $y$  individually. They are diagonal in color space, so we can also factor out an appropriate color Kronecker delta,

$$\begin{aligned}
D_{A_i^{\text{tr}} A_k^{\text{tr}}}^{a b}(x, y) &= \delta^{ab} D_{A_i^{\text{tr}} A_k^{\text{tr}}}(x - y) & \Gamma_{00}^{ab}(x, y) &= \delta^{ab} \Gamma_{00}(x - y), \\
D_{\pi_i^{\text{tr}} \pi_k^{\text{tr}}}^{a b}(x, y) &= \delta^{ab} D_{\pi_i^{\text{tr}} \pi_k^{\text{tr}}}(x - y), & D_{\varphi\varphi}^{ab}(x, y) &= \delta^{ab} D_{\varphi\varphi}(x - y), \\
D_{\pi_i^{\text{tr}} A_k^{\text{tr}}}^{a b}(x, y) &= \delta^{ab} D_{\pi_i^{\text{tr}} A_k^{\text{tr}}}(x - y). \tag{2.57}
\end{aligned}$$

Thus the implied sum over  $d'$  and  $e'$  in (2.56) is trivial. The structure constants fulfill

$$f^{ade} f^{bde} = N_C \delta^{ab}, \tag{2.58}$$

so we can cancel the  $\delta^{ab}$  on both sides of the equation and end up with

$$\begin{aligned}
\Gamma_{00}(x - y) &= N_C \tilde{g}^2 D_{\pi_k^{\text{tr}} \pi_i^{\text{tr}}}(x - y) D_{A_i^{\text{tr}} A_k^{\text{tr}}}(y - x) \\
&\quad - N_C \tilde{g}^2 D_{\pi_k^{\text{tr}} A_i^{\text{tr}}}(x - y) D_{\pi_i^{\text{tr}} A_k^{\text{tr}}}(y - x) \\
&\quad + N_C \tilde{g}^2 \left[ \partial_k^{(x)} \partial_i^{(y)} D_{\varphi\varphi}(x - y) \right] D_{A_i^{\text{tr}} A_k^{\text{tr}}}(y - x). \tag{2.59}
\end{aligned}$$

which is precisely the algebraic transcription of (2.49).

This can be regarded as the final result – the truncated DSE for  $\Gamma_{00}$ . We note, however, that (2.49) is formulated in position space. It is typically more convenient to handle such equations in momentum space where also the known transversality properties can be incorporated with ease. Thus the next (and already final) step will be to transform (2.59) to momentum space.

### 2.3.5 Truncated DSE in momentum space

We rewrite (2.59) in terms of Fourier transforms,

$$\begin{aligned}
\int \frac{d^s k}{(2\pi)^s} e^{ik(x-y)} \Gamma_{00}(k) &= N_C \tilde{g}^2 \int \frac{d^s p}{(2\pi)^s} e^{ip(x-y)} D_{\pi_k^{\text{tr}} \pi_i^{\text{tr}}}(p) \int \frac{d^s q}{(2\pi)^s} e^{iq(y-x)} D_{A_i^{\text{tr}} A_k^{\text{tr}}}(q) \\
&\quad - N_C \tilde{g}^2 \int \frac{d^s p}{(2\pi)^s} e^{ip(x-y)} D_{\pi_k^{\text{tr}} A_i^{\text{tr}}}(p) \int \frac{d^s q}{(2\pi)^s} e^{iq(y-x)} D_{\pi_i^{\text{tr}} A_k^{\text{tr}}}(q) \\
&\quad + N_C \tilde{g}^2 \underbrace{\left[ \partial_k^{(x)} \partial_i^{(y)} \int \frac{d^s p}{(2\pi)^s} e^{ip(x-y)} D_{\varphi\varphi}(p) \right]}_{= - \int \frac{d^s p}{(2\pi)^s} e^{ip(x-y)} p_i p_k D_{\varphi\varphi}(p)} \int \frac{d^s q}{(2\pi)^s} e^{iq(y-x)} D_{A_i^{\text{tr}} A_k^{\text{tr}}}(q) \\
&= N_C \tilde{g}^2 \int \frac{d^s q}{(2\pi)^s} \int \frac{d^s p}{(2\pi)^s} e^{i(p-q)(x-y)} D_{\pi_k^{\text{tr}} \pi_i^{\text{tr}}}(p) D_{A_i^{\text{tr}} A_k^{\text{tr}}}(q) \\
&\quad - N_C \tilde{g}^2 \int \frac{d^s q}{(2\pi)^s} \int \frac{d^s p}{(2\pi)^s} e^{i(p-q)(x-y)} D_{\pi_k^{\text{tr}} A_i^{\text{tr}}}(p) D_{\pi_i^{\text{tr}} A_k^{\text{tr}}}(q) \\
&\quad + N_C \tilde{g}^2 \int \frac{d^s q}{(2\pi)^s} \int \frac{d^s p}{(2\pi)^s} e^{i(p-q)(x-y)} p_i p_k D_{\varphi\varphi}(p) D_{A_i^{\text{tr}} A_k^{\text{tr}}}(q) \quad (2.60)
\end{aligned}$$

and decide to substitute  $p \rightarrow k = p - q$ , which yields

$$\begin{aligned}
\int \frac{d^s k}{(2\pi)^s} e^{ik(x-y)} \Gamma_{00}(k) &= N_C \tilde{g}^2 \int \frac{d^s k}{(2\pi)^s} e^{ik(x-y)} \int \frac{d^s q}{(2\pi)^s} D_{\pi_k^{\text{tr}} \pi_i^{\text{tr}}}(k+q) D_{A_i^{\text{tr}} A_k^{\text{tr}}}(q) \quad (2.61) \\
&\quad - N_C \tilde{g}^2 \int \frac{d^s k}{(2\pi)^s} e^{ik(x-y)} \int \frac{d^s q}{(2\pi)^s} D_{\pi_k^{\text{tr}} A_i^{\text{tr}}}(k+q) D_{\pi_i^{\text{tr}} A_k^{\text{tr}}}(q) \\
&\quad + N_C \tilde{g}^2 \int \frac{d^s k}{(2\pi)^s} e^{ik(x-y)} \int \frac{d^s q}{(2\pi)^s} (q+k)_i (q+k)_k D_{\varphi\varphi}(k+q) D_{A_i^{\text{tr}} A_k^{\text{tr}}}(q).
\end{aligned}$$

Assuming the Fourier transform is well-defined<sup>11</sup>, we can just “leave out” the Fourier operator  $\int \frac{d^s k}{(2\pi)^s} e^{ik(x-y)}$  on both sides of the equation and read off the momentum space equation

$$\begin{aligned}
\Gamma_{00}(k) &= N_C \tilde{g}^2 \int \frac{d^s q}{(2\pi)^s} D_{\pi_k^{\text{tr}} \pi_i^{\text{tr}}}(k+q) D_{A_i^{\text{tr}} A_k^{\text{tr}}}(q) \\
&\quad - N_C \tilde{g}^2 \int \frac{d^s q}{(2\pi)^s} D_{\pi_k^{\text{tr}} A_i^{\text{tr}}}(k+q) D_{\pi_i^{\text{tr}} A_k^{\text{tr}}}(q) \\
&\quad + N_C \tilde{g}^2 \int \frac{d^s q}{(2\pi)^s} (q+k)_i (q+k)_k D_{\varphi\varphi}(k+q) D_{A_i^{\text{tr}} A_k^{\text{tr}}}(q). \quad (2.62)
\end{aligned}$$

In general we would now have to perform a tensor decomposition (see appendix B) of all objects involved in this equation in order to extract scalar equations. In the present case, however, we can exploit one additional fact – the transversality<sup>12</sup> of certain propagators,

$$\begin{aligned}
D_{A_i^{\text{tr}} A_k^{\text{tr}}}(q) &= \hat{P}_{ik}(q) D_{\mathbf{A}\mathbf{A}}(q), \\
D_{\pi_i^{\text{tr}} \pi_k^{\text{tr}}}(q) &= \hat{P}_{ik}(q) D_{\boldsymbol{\pi}\boldsymbol{\pi}}(q), \\
D_{A_i^{\text{tr}} \pi_k^{\text{tr}}}(q) &= \hat{P}_{ik}(q) D_{\mathbf{A}\boldsymbol{\pi}}(q) \\
\text{with } \hat{P}_{ik}(q) &= \delta_{ik} - \frac{q_i q_k}{q^2}. \quad (2.63)
\end{aligned}$$

<sup>11</sup>Otherwise the equality of integrals would allow no statement about the equality of integrands.

<sup>12</sup>See chapter 3 for a more detailed discussion of transversality in the Coulomb gauge.

The corresponding contractions and traces read

$$\begin{aligned}
\hat{P}_{ki}(q+k)\hat{P}_{ik}(q) &= \left( \delta_{ki} - \frac{(q+k)_i(q+k)_k}{(q+k)^2} \right) \left( \delta_{ki} - \frac{q_k q_i}{q^2} \right) \\
&= \delta_{kk} - \frac{q_i q_i}{q^2} - \frac{(q+k)_i(q+k)_i}{(q+k)^2} + \frac{q_i(q+k)_i q_k(q+k)_k}{q^2(q+k)^2} \\
&= s - 2 + \frac{(q^2 + q \cdot k)^2}{q^2(q+k)^2} = \frac{(s-2)q^2(q+k)^2 + (q^2 + q \cdot k)^2}{q^2(q+k)^2}
\end{aligned} \tag{2.64}$$

and (employing the projection property  $q_i \hat{P}_{ik}(q) = 0$  and  $\hat{P}_{ik}(q) q_k = 0$ )

$$\begin{aligned}
(q+k)_i \hat{P}_{ik}(q)(q+k)_k &= k_i \hat{P}_{ik}(q) k_k = k_i k_i - \frac{k_i q_i q_k k_k}{q^2} \\
&= k^2 - \frac{(k \cdot q)^2}{q^2} = \frac{k^2 q^2 - (k \cdot q)^2}{q^2}.
\end{aligned} \tag{2.65}$$

With these results, (2.62) takes the form

$$\begin{aligned}
\Gamma_{00}(k) &= N_C \tilde{g}^2 \int \frac{d^s q}{(2\pi)^s} \frac{(s-2)q^2(q+k)^2 + (q^2 + q \cdot k)^2}{q^2(q+k)^2} D_{\pi\pi}(k+q) D_{AA}(q) \\
&\quad - N_C \tilde{g}^2 \int \frac{d^s q}{(2\pi)^s} \frac{(s-2)q^2(q+k)^2 + (q^2 + q \cdot k)^2}{q^2(q+k)^2} D_{\pi A}(k+q) D_{\pi A}(q) \\
&\quad + N_C \tilde{g}^2 \int \frac{d^s q}{(2\pi)^s} \frac{k^2 q^2 - (k \cdot q)^2}{q^2} D_{AA}(q).
\end{aligned} \tag{2.66}$$

which is the final result. For the other propagators one finds similar equations, and the system of bare-vertex truncated propagator equations could be solved numerically (by iteration) for a fixed value of  $s$  by introducing spherical coordinates in the momentum integrals. In chapter 5 we will follow a different route and use the equations to extract infrared critical exponents.

The derivation of DSEs for other actions follows the same algorithmic procedure (but one might have to take into account additional combinatorial factors). The derivation becomes significantly lengthier for quartic interactions, since the canonical substitution required in (2.32) transforms

$$\begin{aligned}
\frac{\delta S}{\delta \phi_1} &= \cdots + \gamma_{1ijk} \phi_i \phi_j \phi_k \quad \text{into} \\
\frac{\delta \Gamma}{\delta \phi_1} &= \cdots + \gamma_{1ijk} \left( \phi_i + D_{i\nu} \frac{\delta}{\delta \phi_\nu} \right) \left( \phi_j + D_{j\mu} \frac{\delta}{\delta \phi_\mu} \right) \left( \phi_k + D_{k\lambda} \frac{\delta}{\delta \phi_\lambda} \right) \\
&= \cdots + \gamma_{1ijk} \left( \phi_i \phi_j \phi_k + \phi_i D_{jk} + D_{i\nu} \frac{\delta}{\delta \phi_\nu} (\phi_j \phi_k) + D_{i\nu} \frac{\delta}{\delta \phi_\nu} D_{jk} \right) \\
&= \cdots + \gamma_{1ijk} (\phi_i \phi_j \phi_k + \phi_i D_{jk} + \phi_j D_{ik} + \phi_k D_{ij} - D_{i\nu} D_{j\mu} \Gamma_{\mu\nu\lambda} D_{\lambda k}) \\
&= \cdots + \text{diagram 1} + \text{diagram 2} + \text{diagram 3} + \text{diagram 4} + \text{diagram 5},
\end{aligned} \tag{2.67}$$

which includes a two-loop term containing three propagators and one three-point 1PI function. Acting with a functional derivative on this term will generate four new terms (three with two three-point functions and one with one four-point function). By now a Mathematica package exists which automates the combinatorics involved in the derivation of DSEs [10].



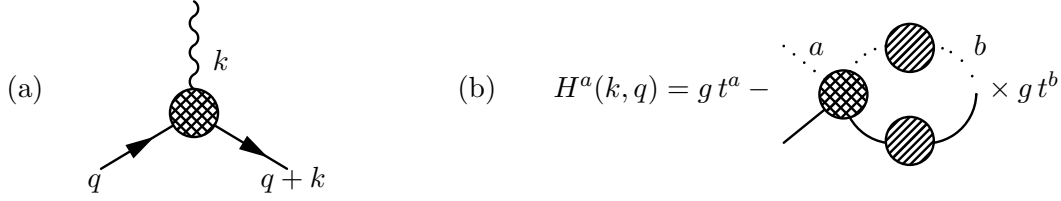


Figure 2.3: (a) momentum flow in the fermion-photon vertex, (b) definition of the amplitude  $H$  in (2.70)

## 2.4 Ward-Takahashi and Slavnov-Taylor Identities

In gauge theories, the initial gauge invariance yields identities also for the gauge-fixed theory. These identities are (partly depending on the context) known as Ward, Ward–Takahashi, Slavnov–Taylor or Zinn–Justin identities. These identities can be derived from the invariance of the measure, but the more elegant technique is to use the BRST transformation, discussed in sec. 1.2.2.

The Slavnov-Taylor identities are valid for renormalized quantities as well and thus they are an important tool in proving renormalizability.<sup>13</sup> They also imply that the different renormalization constants are not all independent.

### 2.4.1 Restrictions on Propagators and Vertices

The Ward-Takahashi or Slavnov-Taylor identities yield exact constraints on solution of QED, Yang-Mills theory or QCD, and the amount these identities are violated indicates to which amount gauge invariance itself is violated.

Green functions with (in case of 1PI functions amputated) gauge field legs are still restricted by identities which are a consequence of original gauge invariance. Since the vector bosons, being transverse, have only two physical degrees of freedom, one obtains restrictions for “sticking” external momenta in place of the gauge fields.

In the general linear covariant gauge, the most simple of these identities reads (see section 2.5 of [140])

$$q^\mu q^\nu D_{\mu\nu}^{ab}(q) = -i\xi \delta^{ab}. \quad (2.68)$$

It is more interesting to study the identities for vertices, in particular the fermion-photon respectively the quark-gluon vertex. For the fermion-photon vertex the relevant identity reads (with  $k$  denoting the photon momentum)

$$k_\mu \Gamma^\mu(k, q) = S^{-1}(k+q) - S^{-1}(q). \quad (2.69)$$

In the case of covariant Yang-Mills theory this is modified to

$$k_\mu \Gamma^{a,\mu}(k, q) (1 + b(k^2)) = H^a(k, q) S^{-1}(k+q) - S^{-1}(q) H^a(k, q), \quad (2.70)$$

where  $b$  denotes the ghost self-energy and  $H^a$  is an amplitude which contains the quark-ghost scattering kernel. Unfortunately (2.70) is complicated to handle (mostly because it contains the essentially unknown amplitude  $H$ ). Still the identity (2.69) is believed to hold approximately also in the non-Abelian context and it will be used in section 4.2 to motivate certain vertex ansätze.

<sup>13</sup>This is typically done inductively in the order of loop expansion, so strictly speaking it is proven to every order of perturbation theory, but not necessarily in the complete nonperturbative context.



## Chapter 3

# QCD in the Coulomb Gauge

As already stated in sections 1.2 and 1.4, the Coulomb gauge is defined by the gauge condition  $\nabla \cdot \mathbf{A} = 0$ , which reads in more detail

$$\partial_i^{(x)} A_i^a(x) t^a = 0. \quad (3.1)$$

In contrast to the covariant gauge-fixing condition  $\partial_\mu A^\mu = 0$ , there is no reference to the  $A_0^a$  components and one has no derivative with respect to  $x_0 = ct$ . This difference has a large impact on the properties of the theory.

Even among the “physical gauges”, the Coulomb gauge has a special status. On the one hand, there are several problems and difficulties, both technical and fundamental issues, which have to be discussed in this chapter. On the other hand it is commonly believed that the Coulomb gauge permits the most direct physical interpretation of results and mechanisms.

This is related to the fact that the gauge condition is more “physical” (three-dimensional transversality of the gauge fields) than other conditions, but presumably also to the related fact that time is not treated on equal footing with space coordinates. While the covariant framework certainly has considerable merits, the special role of time as compared to space is sometimes blurred.

In sec. 3.1 we start with some fundamental issues, including the tree level propagators and mixing of scalar fields, the infamous energy divergences of Coulomb gauge, the reformulation by introducing auxiliary fields (first-order formalism) and questions of renormalization.

In sec. 3.2 we discuss the remnant  $g(t)$  symmetry, which leads to some quite special and peculiar features of Coulomb gauge, including the physical state space.

Sec. 3.3 gives a synopsis of the Hamiltonian formulation of QCD, including the  $(1+1)$ -dimensional case for which analytic solutions are available.

In sec. 3.4 we summarize various results which come from perturbative, functional, variational and lattice calculations, including a brief discussion of infrared exponents.

In sec. 3.5 this chapter is concluded by a discussion of interpolating gauges, which were introduced as a tool to regularize and renormalize the Coulomb gauge. While they turned out to be at best partially fit for this task (due to problems in the limiting process), they are nevertheless an interesting topic for themselves.

### 3.1 Some Fundamental Issues

*Computations in the Coulomb gauge never seem particularly enjoyable or uplifting. Too many trivial things can and do go wrong, and the compilation of Feynman integrals seems to take forever.*

G. Leibbrandt and J. Williams in [130]

#### 3.1.1 Coulomb-Gauge Propagators

From the Coulomb-gauge partition function (1.36) one can (after integrating out the Nakanishi-Lautrup field  $b$  and performing some partial integration) directly read off the tree-level propagators by inspecting the quadratic part of the action:

$$\begin{aligned} D_{ij}^{(0)}(k) &= \frac{1}{k^2} \hat{P}_{ij}(k) & \text{with} & & \hat{P}_{ij}(k) &= \delta_{ij} - \frac{k_i k_j}{k^2} \\ D_{i0}^{(0)}(k) &= D_{0j}^{(0)}(k) = 0 & & & D_{00}^{(0)}(k) &= \frac{1}{k^2} \\ S_F^{(0)}(k) &= \frac{1}{\not{k} - m} & & & D_{c\bar{c}}^{(0)}(k) &= \frac{1}{k^2} \end{aligned} \quad (3.2)$$

Both the Faddeev-Popov-ghost propagator and the  $A_0$ - $A_0$  propagator  $D_{00}$  have the purely instantaneous  $\frac{1}{k^2}$  form. Thus the “unphysical” time-like gluons and the “even more unphysical” Faddeev-Popov ghost are (at tree-level) static, fixed on their timeslice.<sup>1</sup>

Loop corrections modify parts of this picture. While, due to ghost number conservation, the ghost propagator stays instantaneous at any order in perturbation theory,  $D_{00}$  can, due to intermediate loops, acquire a non-instantaneous part, as sketched in figure 3.1.

On the level of full propagators, however, due to remnant symmetry discussed in sec. 3.2.1 one expects the transverse gluons to become instantaneous themselves, which confines *all* color-charged fields to their respective timeslice. While this effect has not been explicitly studied for the gluonic sector, we will discuss this issue in chapter 4 when we study the quark propagator.

#### 3.1.2 Coulomb-Gauge Vertices

While both  $A_0$  and  $A_i$  couple to the quark the same way (since the quark does not directly feel the effect of gauge-fixing) other vertices are significantly modified – or at least one has to take greater care than in the covariant case which types of gluons can be coupled together:

The  $A_0$  does not directly couple to the FP-ghost. A three-gluon vertex can connect three transverse gluons, two transverse gluons and one Coulomb gluon  $A_0$ , one transverse gluon and two  $A_0$ , but not (due to antisymmetry requirements) three  $A_0$ . Analogously a four-gluon vertex can either connect four transverse gluons or two transverse and two Coulomb gluons; no other combination is permitted. A table of all tree-level propagators and vertices present in the Coulomb gauge is given in figure 3.2.

---

<sup>1</sup>Even without performing a single line of actual calculation, one can see how this comes about.  $A_0$  appears in the Yang-Mills action linearly or quadratically only in the term  $F_{0i}^2$ . The mixed propagators are removed since partial integration yields

$$(\partial_i A_0)(\partial_0 A_i) \rightarrow -A_0 \partial_i \partial_0 A_i = -A_0 \partial_0 \partial_i A_i,$$

which vanishes due to  $\partial_i A_i = 0$ . The term quadratic in  $A_0$ ,

$$(\partial_i A_0)(\partial_i A_0) \rightarrow -A_0 \partial_i \partial_i A_0$$

only contains spatial derivatives, and in contrast to Landau gauge this fact is not altered by the gauge-fixing term (which knows nothing about  $A_0$ ). Similarly the quadratic ghost part has the form  $\bar{c} \partial_i \partial_i c$ , thus the propagator extracted from this is instantaneous as well.

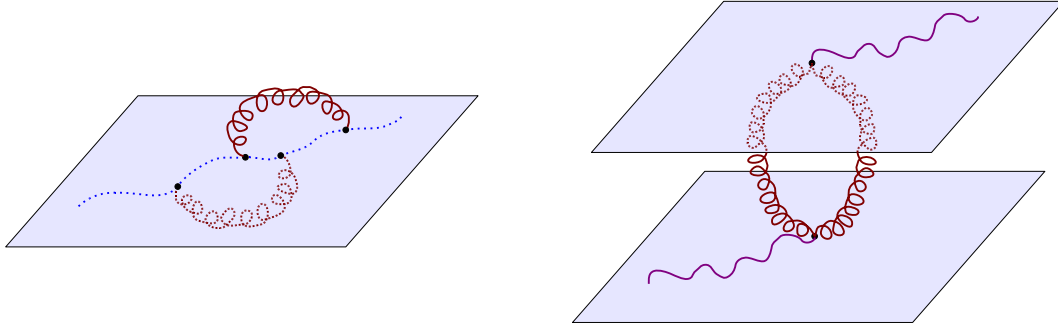


Figure 3.1: Ghosts in Coulomb gauge have a purely instantaneous tree-level propagator. Since ghost number is conserved, even with loop corrections included, the ghost (dotted line) is still confined to one time-slice. The Coulomb gluon  $A_0$  (wavy lines), however, is not restricted by such a conservation law. It can split into two transverse gluons (curly lines), which propagate in time, so  $D_{00}$  could, in principle, acquire a non-instantaneous piece.

### 3.1.3 Further Notes on Propagators and 1PI Functions

We now give a more rigorous treatment of the propagator extraction [233], which also illustrates the inversion properties of two-point connected and 1PI Green functions, discussed in sec. 2.1.3. We now restrict ourselves to the Yang-Mills part, since the quark sector is not directly altered by the procedure.

The Ward identity

$$\Gamma(A_i, A_0, b) = \tilde{\Gamma}(A_i, A_0) + \int d^4x \, i(\partial_i b) A_i, \quad (3.3)$$

completely fixes the dependence of  $\Gamma$  on  $b$ . From this, we find

$$\frac{\delta \Gamma}{\delta b} = -i \partial_i A_i \quad (3.4)$$

Now we separate  $A_i$  into its transverse and longitudinal parts,

$$A_i = A_i^{\text{tr}} + \partial_i s. \quad (3.5)$$

The transverse part does not mix with any of the scalars, so we only have to consider three scalar fields, namely  $A_0$ ,  $s$  and  $b$ . The dependence of  $\Gamma$  on  $b$  is given by

$$\Gamma(A_i^{\text{tr}}, A_0, s, b) = \tilde{\Gamma}(A_i^{\text{tr}}, A_0, s) + \int d^4x \, i(\partial_i b) (\partial_i s). \quad (3.6)$$

To find the propagators it is sufficient to consider the terms in  $\Gamma$  that are quadratic in the fields. For the three scalar fields  $A_0$ ,  $s$  and  $b$ , this is a  $[3 \times 3]$ -matrix. From the dependence of  $\Gamma$  on  $b$ , the elements of this matrix that involve  $b$  are given by

$$\Gamma_{sb} = \Gamma_{bs} = i \mathbf{k}^2, \quad \Gamma_{b0} = \Gamma_{0b} = \Gamma_{bb} = 0. \quad (3.7)$$

The matrix thus has the particular form

$$\Gamma^{(2)} = \begin{pmatrix} \Gamma_{00} & \Gamma_{0s} & 0 \\ \Gamma_{s0} & \Gamma_{ss} & i \mathbf{k}^2 \\ 0 & i \mathbf{k}^2 & 0 \end{pmatrix}. \quad (3.8)$$

$$\begin{aligned}
\left[ D_{A_0 A_0}^{(0)} \right]^{ab}(k) &= \text{wavy line} = \frac{\delta^{ab}}{\mathbf{k}^2} \\
\left[ D_{\mathbf{A}^T \mathbf{A}^T}^{(0)} \right]_{ij}^{ab}(k) &= \text{coiled line} = \frac{\delta^{ab}}{k^2} \hat{P}_{ij}(\mathbf{k}) \\
\left[ G^{(0)} \right]^{ab}(k) &= \text{dotted line with arrow} = \frac{\delta^{ab}}{\mathbf{k}^2} \\
\left[ S_F^{(0)} \right](k) &= \text{solid line with arrow} = \frac{1}{\not{k} - m} \\
\left[ \Gamma_{\bar{q} A_0 q}^{(0)} \right]^a &= \text{vertex with wavy line} = i g t^a \gamma_0 \\
\left[ \Gamma_{\bar{q} \mathbf{A}^T q}^{(0)} \right]_i^a &= \text{vertex with coiled line} = i g t^a \gamma_i \\
\left[ \Gamma_{\bar{c} \mathbf{A}^T c}^{(0)} \right]_i^{abc}(p) &= \text{vertex with coiled line and arrow} = g f^{abc} p_i \\
\left[ \Gamma_{\mathbf{A}^T \mathbf{A}^T \mathbf{A}^T}^{(0)} \right]_{ijk}^{abc}(p, q, r) &= \text{triple coiled line vertex} = g f^{abc} \begin{bmatrix} \delta_{ij}(r-p)_k \\ + \delta_{jk}(p-q)_i \\ + \delta_{ki}(q-r)_j \end{bmatrix} \\
\left[ \Gamma_{\mathbf{A}^T A_0 \mathbf{A}^T}^{(0)} \right]_{jk}^{abc}(p, q) &= \text{vertex with coiled and wavy lines} = g f^{abc} \delta_{jk} (p_0 - q_0) \\
\left[ \Gamma_{A_0 \mathbf{A}^T A_0}^{(0)} \right]_i^{abc}(p, q) &= \text{vertex with wavy and coiled lines} = g f^{abc} (p - q)_i \\
\left[ \Gamma_{\mathbf{A}^T \mathbf{A}^T \mathbf{A}^T \mathbf{A}^T}^{(0)} \right]_{ijkl}^{abcd} &= \text{quadruple coiled line vertex} = -i g^2 \begin{bmatrix} f^{abe} f^{cde} (\delta_{ik} \delta_{jl} - \delta_{il} \delta_{jk}) \\ + f^{ace} f^{bde} (\delta_{ij} \delta_{kl} - \delta_{il} \delta_{jk}) \\ + f^{ade} f^{bce} (\delta_{ij} \delta_{kl} - \delta_{ik} \delta_{jl}) \end{bmatrix} \\
\left[ \Gamma_{\mathbf{A}^T A_0 \mathbf{A}^T A_0}^{(0)} \right]_{jk}^{abcd} &= \text{vertex with wavy and coiled lines} = i g^2 [f^{abe} f^{cde} + f^{ace} f^{bde}] \delta_{jk}
\end{aligned}$$

Figure 3.2: All tree-level propagators and vertices relevant for Coulomb gauge QCD. (Note in particular that the ghost- $A_0$  and the triple- $A_0$  vertex are absent.)

with determinant  $\det \Gamma^{(2)} = \mathbf{k}^4 \Gamma_{00}$ . The propagators are obtained by inverting  $\Gamma^{(2)}$ , which yields

$$D \equiv W^{(2)} = \left( \Gamma^{(2)} \right)^{-1} = \begin{pmatrix} \frac{1}{\Gamma_{00}} & 0 & -\frac{\Gamma_{0s}}{i\mathbf{k}^2 \Gamma_{00}} \\ 0 & 0 & \frac{1}{i\mathbf{k}^2} \\ -\frac{\Gamma_{s0}}{i\mathbf{k}^2 \Gamma_{00}} & \frac{1}{i\mathbf{k}^2} & -\frac{\Gamma_{00}\Gamma_{ss} - \Gamma_{0s}\Gamma_{s0}}{i\mathbf{k}^4 \Gamma_{00}} \end{pmatrix} \quad (3.9)$$

Since  $D_{0s} = D_{s0} = 0$  there is no mixing between  $A_i$  and  $A_0$ . From  $D_{ss} = 0$  we see that the  $A_i$ - $A_i$ -propagator is indeed transverse. One also obtains

$$D_{00} = \frac{1}{\Gamma_{00}}. \quad (3.10)$$

In addition one has found the propagators involving the  $b$ -field. They are all non-zero, but they are usually not needed because  $b$  does not appear in any vertex.

### 3.1.4 Energy Divergences

A main feature of Coulomb gauge is that one has to deal with instantaneous propagators. At tree-level, the ghost and the Coulomb gluon have propagators of the form

$$D_{cc}^{(0)} = D_{00}^{(0)} = \frac{1}{\mathbf{k}^2}. \quad (3.11)$$

Also the full propagators of those fields contain an instantaneous part or are even fully instantaneous. Instantaneous propagators (which correspond to static potentials) give rise to severe problems. The first one is a conceptual one:

Instantaneous interactions threaten one of the cornerstones of quantum field theory – causality. As it will be discussed in sec. 3.2.4, instantaneous effects never show up in the physical sector – provided everything is handled correctly. As soon as truncations are employed, however, one cannot exclude the possibility of finding causality-violating effects also in observables.

A second problem is both conceptual and technical: In any loop we have to integrate over both 3-momentum and the momentum zero- (respectively four-)component. In Coulomb gauge one can construct loops which contain *only* instantaneous propagators. It is obvious that the integral

$$\int_{\mathbb{R}^3} d^3k \int_{-\infty}^{\infty} \frac{dk_4}{\mathbf{k}^2 (\mathbf{p} - \mathbf{k})^2} \quad (3.12)$$

diverges, since an  $k_4$ -independent expression is integrated over the infinite domain  $(-\infty, \infty)$ . But also integrals like

$$\int_{\mathbb{R}^3} d^3k \int_{-\infty}^{\infty} \frac{dk_4 k_4^2}{(\mathbf{k}^2 + k_4^2) (\mathbf{p} - \mathbf{k})^2}, \quad (3.13)$$

which stem from loops with just one instantaneous propagator are *energy-divergent*. These divergences cannot be handled by standard regularization/renormalization techniques (and indeed the renormalizability of the Coulomb gauge is a delicate issue, see sec. 3.1.6).

While energy divergences are obviously present in single diagrams, they are expected to cancel when diagrams are correctly combined. This is, however, hard to show explicitly even in perturbation theory. The energy divergences have been shown to cancel up to two loops [15], but a general proof is still missing. A more convenient way to handle this issue is the *first order formalism*, which is discussed in 3.1.5 and is more closely related to the Hamiltonian formalism (sec. 3.3).



### Split Dimensional Regularization

There is a proposal to regularize energy divergences by a procedure called *split dimensional regularization* (SDIM) [130], where *two* parameters  $\omega$  and  $\sigma$  are introduced,

$$\int d^3q dq_4 \quad \rightarrow \quad \int d^{2\omega}q d^{2\sigma}q_4. \quad (3.14)$$

The regularization parameters can in principle even be complex; the four-dimensional world is recovered in the limit  $\omega \rightarrow \frac{3}{2}$ ,  $\sigma \rightarrow \frac{1}{2}$ . The SDIM procedure has been employed also in the context of negative dimensional regularization (NDIM; see appendix C.1) [189], but it cannot be regarded as a generally accepted solution of the problem of energy divergences [207].

#### 3.1.5 The First-Order Formalism

It is often convenient to reformulate Coulomb gauge QCD by introducing an additional field, which plays roughly the role of a color-electric field. While this increases the number of fields, it simplifies the structure of vertices, and many features (like the cancellation of energy divergences on perturbative level) are easier to treat in this *first order formalism*.

Typically, quantum field theory is treated in the standard *second order* formalism. However, there is the – sometimes advantageous – possibility to switch to the phase-space or *first order* formalism. To do this, an auxiliary field  $\pi_i^a$  is introduced which plays a role related to the color-electric field. Employing the field-theoretical version of the identity

$$e^{+a^2} = \frac{1}{\sqrt{\pi}} \int_{-\infty}^{\infty} e^{-x^2+2ax} dx \quad (3.15)$$

(which can be shown easily by completing the square and performing Gaussian integration) one obtains the action

$$S = \int d^4x \left[ i\pi_i^a (\partial_0 A_i^a - D_i^{ab} A_0^b) + \frac{1}{2} (\pi_i^a \pi_i^a + B_i^a B_i^a) + (\partial_i \bar{c}^a) D_i^{ab} c^b + i(\partial_i b^a) A_i^a \right]. \quad (3.16)$$

In contrast to the initial action one has only first derivatives acting on the gauge fields, and the quartic  $A_0$ - $A_0$ - $A_i$ - $A_i$  vertex has been converted to a quadratic piece of the action. The price for this is the additional  $\pi$ -field, which one has also to integrate over in the path integral.

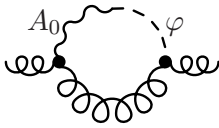
While the fields in first- and second-order formalism are related by simple identities, matters are more complicated for functional derivatives and sources. This unfortunately quite technical issue has been settled in [200] for general field theories with focus on Coulomb gauge QCD.

It is often convenient to separate the  $\pi$ -field into a transverse and a longitudinal part by setting

$$\pi_i^a = \pi_i^{\text{tr},a} + \partial_i \varphi^a. \quad (3.17)$$

The gluon and the  $\pi$ -fields mix both on tree-level and for full propagators. Since scalar and transverse parts do not mix, one has to consider only  $A^{\text{tr}}$ - $\pi^{\text{tr}}$  and  $A_0$ - $\varphi$  transitions. The  $A_0$ - $\varphi$  propagator has precisely the same form and appears at the same places as the  $\bar{c}$ - $c$  propagator.

Since  $A_0$ - $\varphi$  is bosonic while  $\bar{c}$ - $c$  is fermionic, the energy-divergent contributions are expected to cancel, which is easy to make explicit at one-loop order. When denoting the external momentum by  $p$ , the internal by  $k$  and the energy-convergent function from the transverse gluon propagator by  $F(p, k)$ , we find for a graph contributing to the gluon self-energy



$$\begin{aligned}
 & \sim \int d^4k F(p, k) \frac{k_0^2}{k_0^2 + \mathbf{k}^2} \left( \delta_{ij} - \frac{k_i k_j}{\mathbf{k}^2} \right) \\
 &= \int d^4k F(p, k) \frac{k_0^2 + \mathbf{k}^2 - \mathbf{k}^2}{k_0^2 + \mathbf{k}^2} \left( \delta_{ij} - \frac{k_i k_j}{\mathbf{k}^2} \right) \\
 &= \int d^4k F(p, k) \left[ \underbrace{\left( \delta_{ij} - \frac{k_i k_j}{\mathbf{k}^2} \right)}_{=: I_4} - \underbrace{\frac{\mathbf{k}^2}{k_0^2 + \mathbf{k}^2} \left( \delta_{ij} - \frac{k_i k_j}{\mathbf{k}^2} \right)}_{\text{energy-convergent}} \right]
 \end{aligned} \tag{3.18}$$

The integral containing  $I_{\text{gh}}$  is up to the sign what one obtains from the ghost contribution to the self-energy, while the part containing  $I_4$  is cancelled by the energy-divergent part of the diagram containing the four-gluon vertex.

### 3.1.6 Renormalization of the Coulomb Gauge

Renormalization in the Lagrangian formalism has been discussed in [153] (in a rather traditional approach which employs Zinn-Justin equations, an expansion of the effective action and recursive relations), but since no consistent regularization has been employed and the topic of energy divergences has been left untouched, the status of this piece of work is somehow unclear. In a follow-up article [154] some of the gaps have been filled, but still the question of renormalizability cannot be regarded as settled [233].

In order to prove the renormalizability of the Coulomb gauge, interpolating gauges have been used [31], but as discussed in section 3.5 the status of the limiting process remains unclear. A problem with the interpolating gauges is that the ghost- $A_0$  vertex is proportional to the regularization parameter  $\eta$ . This leads to some of the difficulties discussed in section 3.5.

For many purposes (including the possible proof of renormalizability) it would be beneficial to have a “minimal” regularization procedure which only modifies the propagators, leaving all the vertices untouched. Such a regulator has been proposed in [32], it takes the form

$$\mathcal{L}_{\text{reg}} = \mathcal{L}_{\text{Coul}} + \eta \left( i \dot{\varphi} \dot{A}_0 + \dot{\bar{c}} \dot{c} \right) \tag{3.19}$$

Obviously, on tree-level only the gluon and the ghost propagator are affected by this prescription. In contrast to interpolating gauges, however, for  $\eta \neq 0$  the Lagrangian (3.19) does not describe a gauge-fixed Yang-Mills theory. In particular BRST invariance is broken.

Consequently, the most difficult part in using (3.19) is to show that BRST invariance is regained in the limit  $\eta \rightarrow 0$ , and this is still work in progress [233].

Nevertheless there are certain results about behaviour of Coulomb gauge under renormalization group flow (implicitly assuming that the theory is indeed renormalizable). In particular it is known that  $g^2 D_{00}$  is a renormalization group invariant [226], which singles out the Coulomb-gluon propagator as a particularly interesting object (which is one of the foundations of the analysis done in chapter 4). The feature of renormalization group invariance is not shared by the ghost propagator,  $g^2 \langle c \bar{c} \rangle$  is no renormalization group invariant.

## 3.2 Why Coulomb Gauge is Special

*Yet, despite its headstart in an Abelian context, application of the Coulomb gauge to non-Abelian models remains as puzzling and problematic today as ever.*

George Leibbrandt in [129]

### 3.2.1 The Remnant Symmetry

Gauge condition (3.1) is obviously left invariant by time dependent gauge transformation  $g(t)$ . Since this symmetry is a “leftover” of the original full gauge symmetry, the term *remnant symmetry* has been coined. It is intimately connected to the property of a “physical” state space, as discussed in section 3.2.2.

Presence of this symmetry implies that – even without the Gribov problem – one physical state does not correspond to just one, but to infinitely many configurations which are related by particular time-dependent gauge transformations. Gauge-fixing is incomplete with a one-parameter family of transformations left open. In the introduction to [31] the number of such parameters has been called “degree of arbitrariness” and denoted by  $\sigma$ . The Coulomb gauge has  $\sigma = 1$ , while the Weyl gauge (left invariant by all gauge transformations  $g(\mathbf{x})$ ) has  $\sigma = 3$ .

A consequence of this “arbitrariness” is that one has to be careful when speaking about “the” Coulomb gauge, since one can fix the remnant symmetry and about a gauge which still respects the Coulomb gauge condition (3.1) but does presumably not have all the properties discussed in this chapter. To have a more accurate terminology at hand we will distinguish the *physical Coulomb gauge* where  $g(t)$  remains unfixed from *Coulomb-like gauges* where  $g(t)$  is either explicitly removed (by demanding additional conditions) or spontaneously broken (by the calculational process employed).

The remnant symmetry is responsible for many of the outstanding features of the Coulomb gauge, in particular the property of being “physical”. It is tied closely to the fact that correlators of colored fields vanish identically for unequal times.

At tree-level, the ghost and part the Coulomb gluon propagator are static, containing a delta functional in time direction,  $\delta(t)$ . A remainder of the Coulomb gluon, the transverse gluon and the quark propagator, however, are not instantaneous at tree-level.

### Consequences in Perturbation Theory

Perturbation theory breaks the remnant symmetry, since tree-level transverse gluon and quark propagator contain instances of the momentum zero-component. This can be interpreted in (at least) three ways:

- The remnant symmetry could be removed (spontaneously broken) by some mechanism which leaves its traces already in perturbation theory. A “self-completion” of the Coulomb gauge (i.e. automatic removal of the remnant symmetry) has been advocated in [208]; the arguments will be discussed in subsection 3.2.5.
- It cannot be excluded that the Coulomb gauge constitutes no valid gauge at all. In particular the proof of renormalizability of this gauge is still missing.

- Typically, if an approximation method violates an important symmetry of a theory, this should raise serious doubt about the approximation method, not the theory. The fact that perturbation theory and Coulomb gauge QCD are in some sense incompatible is not completely surprising. If we mean by confinement that colored objects have no physical existence of their own, this principle is already to a large extent built into the construction of non-Abelian gauge theories, since in a gauge average, color non-singlets vanish. For unequal times, Coulomb gauge inherits the property that all correlators between color non-singlets are gauge-averaged away as well.

### Consequences on the Lattice

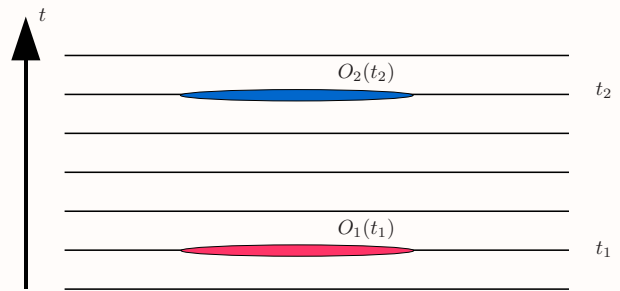
On the lattice the Coulomb gauge is fixed on each timeslice. The remnant symmetry appears as the freedom to impose further conditions on the time-like links. For example one could choose all these links  $U_4$  such that the average distance to the unit element  $\mathbb{1}_{\text{SU}(3)}$  is minimal. This has been done for example in [60], but presumably corresponds (in the language of subsection 3.2.1) to the reduction of the physical Coulomb gauge to a Coulomb-like gauge.

Even when the remnant symmetry is not explicitly fixed, it is still somehow problematic to choose from each sampled orbit only one configuration to represent the Coulomb gauge. Since the path integral representation contains an integration over infinitely many configurations, linked by time-dependent gauge transformations, also the Monte Carlo average should include a statistically significant number of configurations from each orbit. The proposal for a new type of interpolating gauge, made in subsection 3.5.6 is based on this condition.

### 3.2.2 The Physical State Space

In Coulomb gauge, gauge-fixing is done on each time-slice separately. Typically it is argued that this leads to a “physical”, i.e. positive definite state space with only gauge-invariant objects propagating in time – while Lorenz invariance is not manifest, unitarity is.

This property is understood best on the lattice in a setup as illustrated on the right. On intermediate timeslices, the correlator  $\langle O_1(t_1)O_2(t_2) \rangle$  involves only the action itself, which is initially gauge-invariant. Since gauge-fixing has been done separately on each timeslice, it can also be undone on all intermediate slices without affecting the typically gauge-dependent operators  $O_1$  and  $O_2$ , defined at  $t = t_1$  and  $t = t_2$ .



In the unfixed theory, only physical, i.e. gauge-invariant states propagate, while all gauge-dependent quantities are washed out by averaging over all possible gauges. So while  $O_1$  and  $O_2$  may be extremely “obscure”, in particular involving strongly gauge-dependent effects, only the physically relevant part will propagate and thus enter the correlator.

As a consequence, in completely unregularized Coulomb gauge one expects the unequal-time correlators of all color-charged fields and composite operators (gluons, quarks, diquarks, ...) to vanish; they do not propagate in the strict sense.

### 3.2.3 The Color-Coulomb Potential

The full  $A_0$ - $A_0$  propagator consists of an instantaneous and a non-instantaneous “polarization” piece,

$$-g^2 D_{00}(\mathbf{x}, t_x, \mathbf{y}, t_y) = V_C(\mathbf{x} - \mathbf{y}) \delta(t_x - t_y) + P_{\text{non-inst}}(\mathbf{x} - \mathbf{y}, t_x - t_y). \quad (3.20)$$

Little is known about the non-instantaneous piece; it may even vanish in full theory due to the arguments given in sec. 3.2.2. For the instantaneous piece (which is expected to be dominant even if the non-instantaneous part does not vanish) some results are available.

$V_C$  can be expressed in terms of the Laplacian and the inverse Faddeev-Popov operator,

$$V_C(\mathbf{x} - \mathbf{y}) = \int_{\mathbb{R}^3} d^3z \langle 0 | \mathcal{M}_{xz}^{-1}[A] (\nabla^2 \mathcal{M}^{-1}[A])_{z,y} | 0 \rangle. \quad (3.21)$$

Inserting a complete set of states (with  $|0\rangle$  denoting the vacuum) we obtain

$$V_C(\mathbf{x} - \mathbf{y}) = \int_{\mathbb{R}^3} d^3z \langle 0 | \mathcal{M}_{xz}^{-1}[A] (\nabla^2 \mathcal{M}^{-1}[A])_{z,y} | 0 \rangle \quad (3.22)$$

$$\begin{aligned} &= \int_{\mathbb{R}^3} d^3z \langle 0 | \mathcal{M}_{xz}^{-1} | 0 \rangle \nabla_z^2 \langle 0 | \mathcal{M}_{zy}^{-1} | 0 \rangle \quad (\text{disconnected}) \\ &+ \underbrace{\sum_{n=1}^{\infty} \int_{\mathbb{R}^3} d^3z \langle 0 | \mathcal{M}_{xz}^{-1} | n \rangle \nabla_z^2 \langle n | \mathcal{M}_{zy}^{-1} | 0 \rangle}_{\text{should fall off exponentially due to mass gap}}. \quad (\text{connected}) \end{aligned} \quad (3.23)$$

The connected part contains intermediate massive states (since Yang-Mills theory has a mass gap) and thus falls off exponentially. Thus for large distances we have a contribution only from the disconnected part, which can be expressed in terms of the ghost propagator  $G = \langle 0 | \mathcal{M}^{-1} | 0 \rangle$ ,

$$(\text{disconn.}) = \int_{\mathbb{R}^3} d^3z G(\mathbf{x} - \mathbf{z}) \nabla_z^2 G(\mathbf{z} - \mathbf{y}) \xrightarrow{\text{FT}} G^2(\mathbf{k}^2) \mathbf{k}^2. \quad (3.24)$$

We now write the ghost propagator in the form

$$G(\mathbf{k}^2) = \frac{d(\mathbf{k}^2)}{\mathbf{k}^2} \quad (3.25)$$

and thus can express the color-Coulomb potential in the form

$$V_{\text{coul}}(\mathbf{k}^2) = G^2(\mathbf{k}^2) \mathbf{k}^2 = \frac{d^2(\mathbf{k}^2)}{\mathbf{k}^2} \rightarrow \alpha(\mathbf{k}^2) \frac{d^2(\mathbf{k}^2)}{\mathbf{k}^2} \quad (3.26)$$

with a form factor  $\alpha$  which is expected to approach one for  $\mathbf{k}^2 \rightarrow 0$ .

Employing variational methods it has been shown [228] that the color-Coulomb potential  $V_C$  lies (asymptotically for large distances) above the Wilson potential (*Zwanziger inequality*). Thus, if the (physical) Wilson potential is confining,  $V_C$  is confining as well – *no confinement without Coulomb confinement*.

Since the Wilson potential is presumably linearly rising (as also indicated by numerous lattice studies) and a more than linearly rising potential would pose severe problems, it is reasonable to expect

$$V_C(\mathbf{k}^2) \sim \frac{\sigma_C}{(\mathbf{k}^2)^2} \quad (3.27)$$

with a constant  $\sigma_C$  (the Coulomb string tension) for small  $\mathbf{k}^2$ . The determination of  $\sigma_C$  on the lattice is reviewed in sec. 3.4.1, a possible form of  $V_C$  for large  $\mathbf{k}^2$  is discussed in sec. 4.1.2.

The Zwanziger inequality is particularly intriguing since  $V_C$  is just a piece of a two-point function while the Wilson potential is defined via a path-ordered exponential,  $e^{\mathcal{P} \int A_\mu dx^\mu}$ , and thus contains contributions from  $n$ -point functions of arbitrarily large  $n$ .

### 3.2.4 Causality in the Coulomb gauge

Instantaneous propagators, as found for  $D_{00}^{(0)}(k)$  as well as for (at least for the dominant piece of)  $D_{00}(k)$  correspond to a static potential. While static potentials are a perfectly valid concept in the framework of nonrelativistic (quantum) mechanics, in the strict sense they do not make sense in relativistic (quantum) field theory, since any instantaneous interaction violates the concepts relativity is built on.

So at first glance the instantaneous propagators of Coulomb gauge seem to be an embarrassment. Here we have to keep in mind that in the gauge-dependent sector of the theory almost anything (including the sudden appearance of scalar fermions) can happen. So only physical effects have to obey causality, not necessarily gauge-dependent quantities.

This means however that all acausal effects in Coulomb gauge have to cancel in a way to guarantee causality for observables. This can be seen from various points of view [233]:

- If one is doing ordinary perturbation theory then one can use BRST invariance in the interpolating gauge (see section 3.5). Leaving aside the question of a discontinuity at the Coulomb gauge (which would only affect zero-momentum quantities) then one passes from the Coulomb gauge to the (Lorentz-invariant) Landau gauge by varying a gauge parameter. The gauge parameter appears in the BRST-exact part of the action, and one can easily show that the expectation value of a (BRST-invariant) observable is independent of the gauge parameter.
- In the operator formalism one can show that the Dirac-Schwinger consistency condition (see for example ref [41]) is satisfied by the Coulomb-gauge Hamiltonian. [As a historical note: Schwinger originally constructed the Coulomb-gauge Hamiltonian by requiring that this consistency condition be satisfied.]
- If Gribov copies are handled correctly, the result will be consistent with Lorentz invariance. In the operator formalism that means that the wave functional must satisfy the boundary condition that results from identifying gauge-equivalent points on the boundary of the Gribov region. This is supposed to be achieved at the non-perturbative level by imposing the horizon condition [221, 222], see also section 5.2.

### 3.2.5 Further Notes on the Remnant Symmetry

Repeatedly the status of the remnant symmetry is under discussion. In [208] it has been argued that in the functional approach, the Coulomb-gauge is self-completing in the sense that the system itself chooses a way how to remove the symmetry under time-dependent gauge transformations  $g(t)$ . In this section we want to point out some possible problems in the derivation given there.

As it will be discussed in sec. 3.5, one can deduce the condition

$$\int_{\mathbb{R}^3} d^3x \partial_0 A_0 = 0 \quad \Longleftrightarrow \quad I := \int_{\mathbb{R}^3} d^3x A_0 = C \quad (3.28)$$

with some constant  $C$  for the Coulomb endpoint of certain interpolating gauges. In [208], time reversal has been invoked to argue that  $C = 0$ . Time reversal allows immediate statements about the propagator  $\langle A_0 A_0 \rangle$  (which has to be an even function of the zero-component of momentum), but it seems questionable to deduce further information about  $A_0$  from it. Thus, instead of simply setting  $C = 0$ , it would seem necessary to integrate  $C$  over all permitted values to obtain a valid representation of the path integral [233].

Assuming this problem could be circumvented, we soon run into the next difficulty. The conclusion in [208] relies on the assumption that imposing a condition on a system that already fulfills that condition should not have any effect – so if the Coulomb gauge already fulfills some time-dependent gauge condition  $G[A] = 0$ , imposing this condition once more shouldn't change anything.

While such reasoning is certainly true in ordinary geometry and algebra, one has to be cautious when translating it to functional analysis. The reason for this is that imposing the same condition twice involves the square of a  $\delta$ -distribution – an *a priori* undefined (and in general undefinable) object.

Let us go through the usual procedure to see at which point problems may arise when imposing two gauge conditions on a system. We find for a functional integral restricted by the condition  $G_1[A] = 0$  the expression

$$\begin{aligned} \int \mathcal{D}A e^{iS[A]} &= \int \mathcal{D}U \int \mathcal{D}A e^{iS[A]} \delta(G[U A]) \det \frac{\delta G_1[U A]}{\delta U} \\ &= \int \mathcal{D}U \int \mathcal{D}[U A] e^{iS[U A]} \delta(G_1[U A]) \det \frac{\delta G_1[U A]}{\delta U} \end{aligned}$$

For a linear gauge condition,  $\det \frac{\delta G_1[U A]}{\delta U}$  is independent of  $U$ , but (in the non-Abelian theory) it still depends on  $A$ , so let us set

$$J_{G_1}[U A] := \det \frac{\delta G_1[U A]}{\delta U}.$$

The measure  $\mathcal{D}A$  and the action  $S$  are both invariant under gauge transformation, so we obtain

$$\int \mathcal{D}A e^{iS[A]} = \int \mathcal{D}U \cdot \int \mathcal{D}^U A e^{iS[U A]} \delta(G_1[U A]) J_{G_1}[U A].$$

Now we can rename  $^U A \rightarrow A$  everywhere and obtain

$$\int \mathcal{D}A e^{iS[A]} = \int \mathcal{D}U \cdot \int \mathcal{D}A e^{iS[A]} \delta(G_1[A]) J_G[A].$$

where  $\int \mathcal{D}U$  can be absorbed in an overall normalization factor. Now let us impose the condition  $G_2[A] = 0$ ,

$$\int \mathcal{D}A e^{iS[A]} = \int \mathcal{D}U \cdot \int \mathcal{D}V \int \mathcal{D}A e^{iS[A]} \delta(G_1[A]) \delta(G_2[V A]) J_{G_2}[A] \det \frac{\delta G[V A]}{\delta V}.$$

As before, the determinant does not depend on  $V$ , the integral measure and the action are both invariant under gauge transformations, so we have

$$\int \mathcal{D}A e^{iS[A]} = \int \mathcal{D}U \cdot \int \mathcal{D}V \int \mathcal{D}^V A e^{iS[V A]} \delta(G_1[A]) \delta(G_2[V A]) J_{G_1}[A] J_{G_2}[V A]. \quad (3.29)$$

Now, however, we run into problems. In general we cannot factor out the  $V$ -integral, since we have no way to rewrite  $\delta(G_1[A])$  and  $J_{G_1}[A]$  in terms of  $^V A$ . This would be only possible if  $G_1$  and  $G_2$  were completely independent gauge conditions (as for example a purely spatial and a purely temporal one). Without the ability to separate the  $V$ -integration from the rest of the integral, we lose the ability of rewriting (3.29) in terms of local fields.

We could argue (rather handwavingly) that for  $G_1 = G_2$ , in (3.29) indeed  $A$  can be replaced by  $^V A$ , since the two conditions are equivalent everywhere. When doing this, we may again rename  $^V A \rightarrow A$  and factor out  $\int \mathcal{D}V$ . After performing this (highly questionable) operation, we end up with

$$\int \mathcal{D}A e^{iS[A]} = \int \mathcal{D}U \int \mathcal{D}V \cdot \int \mathcal{D}A e^{iS[A]} \delta^2(G_1[A]) J_{G_1}^2[A],$$



an object that contains the square of a delta functional<sup>2</sup> and the squared Jacobian, which, as we will explain, may be problematic as well:

The regions where the Jacobian diverges are believed to dominate the behaviour of such functional integrals (the Gribov-Zwanziger confinement scenario of sec. 1.3.2). This may be regarded similar to the case of an integrable singularity that dominates the value of an integral.

It is well known already from standard calculus that a product of two integrable singular functions is not necessarily integrable anymore. For example, while for  $f(x) = 1/\sqrt{x}$

$$\int_0^1 f(x) dx = \int_0^1 \frac{dx}{\sqrt{x}} = \frac{1}{1 - \frac{1}{2}} = 2$$

exists, the integral

$$\int_0^1 f^2(x) dx = \int_0^1 \frac{dx}{x} = -\lim_{a \rightarrow 0} \ln a$$

clearly diverges.

So while one Jacobian may provide the key to understanding confinement, two of them are likely to invalidate the functional approach altogether. One can of course hope that the ill-defined square of delta and the probably ill-defined square of Jacobians cancel precisely in the way necessary to obtain a sensible result – but it seems unjustified to draw any conclusions from such a hope.

While expression (3.29) is probably well-defined for compatible gauge conditions  $G_1$  and  $G_2$ , it seems impossible to rewrite it in terms of local fields. This should not come as a big surprise. While, for example, the condition  $\partial_i A_i = 0$  can be handled in a local way, the completely equivalent condition  $(\partial_i A_i)^2 = 0$  cannot be directly implemented with standard methods.

Assuming that all problems pointed out so far could be circumvented, the final conclusion still exhibits a logical loophole. To shortly summarize the argument, it goes along the lines of

1. One cannot impose two time-dependent gauge conditions on the Coulomb gauge. (This would clearly mean overfixing the gauge.)
2. A certain choice of time-dependent gauge fixing (which seems most obvious to us) cannot be imposed. We just checked.
3. Therefore, the system must already fulfill another (probably highly nontrivial) gauge condition, which it has chosen itself.
4. Thus the remnant symmetry has been removed, the Coulomb gauge has completed itself.

The problem with this reasoning is that it implicitly assumes that some sort of time-dependent gauge-fixing condition has to be chosen in any case. It seems likely, however, that one simply cannot impose an additional constraint on the physical Coulomb gauge without losing its most important properties and ending up just with a non-unitary Coulomb-like gauge. Due to these arguments, the claimed “self-completion” of the Coulomb gauge seems highly questionable.

---

<sup>2</sup>When continuing with the usual Faddeev-Popov procedure, the problem of squared deltas seems less severe, since delta distributions are effectively replaced by Gaussians, which can be multiplied with ease. For the Coulomb gauge, however, one has to take the width  $\xi$  of the Gaussian to zero, so the original problem is recovered.

### 3.3 Hamiltonian Formulation of Coulomb Gauge QCD

*Coulomb gauge Yang-Mills theory (and by extension quantum chromodynamics) is a fascinating, yet frustrating endeavor.*

P. Watson & H. Reinhardt in [211]

#### 3.3.1 Gauß' Law

The Non-Abelian version of Gauß' law,

$$\nabla \cdot \mathbf{E}^a = \rho_{\text{quark}}^a - g f^{abc} A_k^b E_k^c, \quad (3.30)$$

has to be fulfilled. In Coulomb gauge, Gauß' law can be obtained directly by integrating out the  $A_0$  field, while in other gauges it only enters the game when finally projecting to the physical subspace.

As explained for example in [9], the quark color charge  $\rho_{\text{quark}}^a$  which is in the fundamental representation cannot be neutralized by gluons which have charge in the adjoint representation. Thus color-electric field lines either have to connect two quarks or extend to infinity.<sup>3</sup>

In the canonical approach, described for example in [162], the gauge fields  $A_\mu^a$  are considered as (cartesian) coordinates with conjugate moment defined as

$$\Pi_\mu^a(x) := \frac{\delta S}{\delta(\partial_0 A_\mu^a(x))} = \begin{cases} E_i^a(x) & \text{for } \mu = i \in \{1, 2, 3\} \\ 0 & \text{for } \mu = 0. \end{cases} \quad (3.31)$$

In order to avoid problems with the result  $\Pi_i^a(x) \equiv 0$ , the Weyl gauge condition  $A_0^a(x) \equiv 0$  is imposed. Doing so, one obtains the Hamiltonian

$$H = \frac{1}{2} \int d^3x (\mathbf{\Pi}^2(x) + \mathbf{B}^2(x)), \quad (3.32)$$

where the chromomagnetic field is defined as  $B_i^a = \varepsilon_{ijk} F_{jk}^a(x)$ . Canonical quantization is performed by imposing canonically the equal-time commutation relation

$$[A_i^a(\mathbf{x}), \Pi_j^b(\mathbf{y})] = \delta_{ij} \delta^{ab} \delta^3(\mathbf{x} - \mathbf{y}), \quad (3.33)$$

which promotes the classical canonical momentum to an operator,

$$\Pi_i^a(x) \rightarrow \hat{\Pi}_i^a(x) = \frac{1}{i} \frac{\delta}{\delta A_i^a(x)}. \quad (3.34)$$

It is Gauß' law,

$$\left( \delta^{ab} \partial_i + g f^{acb} A_i^c \right) \Pi_i(x) \varphi(x) = -g \rho_q(x) \psi(x), \quad (3.35)$$

which is responsible for the separation of gauge-invariant (physical) and gauge-dependent degrees of freedom. Consequently it has to be imposed on the wave functional in order to obtain the physical state space.

Gauß' law is identically fulfilled in Coulomb gauge, therefore it is typically more convenient to fix the gauge to Coulomb gauge than to work with a constraint on the wave functional.

---

<sup>3</sup>In principle there is a third possibility. As discussed in [161] in the context of classical electrodynamics, one can place curves of infinite length in a finite domain (for example by wrapping up a curve on a torus in an irrational manner), and such half-infinite or infinite curves would in principle be suitable as electric respectively magnetic field lines which neither end on charges resp. close nor extend to infinity. This can be translated to color-electric and color-magnetic field lines as well. It is very unlikely however that such – extremely unstable – configurations have any physical relevance.

### 3.3.2 The Operator Ordering Problem

The Weyl gauge Yang-Mills Hamiltonian given in (1.13) in some sense corresponds to the use of cartesian coordinates in  $A$ -space and thus has the most simple form. Switching to another gauge corresponds to a change to curvilinear coordinates, and as usual, operators take a different (and usually more complicated) form in such coordinates.

As derived in [51] one finds for the Yang-Mills Hamiltonian in a linear gauge the expression

$$H = \frac{1}{2} \int d^3r \{ [E_i^a(\mathbf{r})]^2 + [B_i^a(\mathbf{r})]^2 \}_W + \mathcal{V}_1 + \mathcal{V}_2, \quad (3.36)$$

$$\mathcal{V}_1 = \frac{1}{8} g^2 \int d^3r \langle \mathbf{r}, a' | (\mathcal{F}_k D_k)^{-1} \mathcal{F}_j | \mathbf{r}, a \rangle \langle \mathbf{r}, b | (\mathcal{F}_{k'} D_{k'})^{-1} \mathcal{F}_j t^a t^{a'} | \mathbf{r}, b \rangle \quad (3.37)$$

$$\mathcal{V}_2 = \frac{1}{8} g^2 \int d^3r \int d^3r' \langle \mathbf{r}', a' | [\delta_{ii'} - D_{i'}(\mathcal{F}_k D_k)^{-1} \mathcal{F}_i] | \mathbf{r}, b \rangle \times \langle \mathbf{r}, a | [\delta_{ii'} - D_i(\mathcal{F}_{k'} D_{k'})^{-1} \mathcal{F}_{i'}] | \mathbf{r}', b' \rangle \langle \mathbf{r}, b | t^a (\mathcal{F}_{\bar{k}} D_{\bar{k}})^{-1} \mathcal{F}_j \mathcal{F}_j^\dagger (D_{\bar{k}'}^\dagger \mathcal{F}_{\bar{k}'}^\dagger)^{-1} t^{a'} | \mathbf{r}', b' \rangle \quad (3.38)$$

where  $W$  denotes Weyl ordering<sup>4</sup> and the quantities  $\mathcal{F}_j$  are defined via the gauge condition  $F[A_i] = 0$  by

$$F^a[A_i, \mathbf{r}] = \int d^3r' \langle \mathbf{r}, a | \mathcal{F}_j | \mathbf{r}', b \rangle A_j^b(\mathbf{r}', t). \quad (3.39)$$

The two nonlocal terms, conventionally denoted by  $\mathcal{V}_1$  and  $\mathcal{V}_2$  are related to ambiguities certain in energy-divergent two-loop diagrams in the functional approach.

This result is rederived in [165] within the path integral formalism and supplemented by an additional term which shows up in the presence of fermions. See also [225] for a pedagogical derivation of the continuum and the lattice Coulomb gauge Hamiltonian.

### 3.3.3 Connection between Hamiltonian and Functional Formalism

The main advantage of the Hamiltonian formalism is that it allows (due to employing a positive definite space of states) the use of the variational principle. As in ordinary quantum mechanics one can choose an ansatz for the wave functional and minimize the expectation value of the Hamiltonian, see e.g. [162].

A disadvantage of this method is that it is hard to find a connection to the usual functional formalism, as can be seen from the following argument<sup>5</sup>:

In the Hamiltonian approach one chooses an initial time-slice  $t = t_i$  and imposes the Weyl gauge condition  $A_0 = 0$ . The remaining gauge freedom is employed in order to choose  $\mathbf{A}$  transverse. Employing transverse gluons as degrees of freedom, unitary time evolution is used to reach all other time-slices. While the Coulomb gauge condition  $\nabla_i A_i = 0$  is fulfilled for all times, the Weyl gauge condition cannot be simultaneously fulfilled.

Accordingly one finds in general  $A_0 \neq 0$  for  $t \neq t_i$ . Still, as it is obvious by the choice  $A_0 = 0$  at  $t = t_i$ , the correlator  $\langle A_0(\mathbf{x}, t) A_0(\mathbf{x}', t') \rangle$ , which vanishes for  $t = t' = t_i$  has not the same meaning as in the functional approach, where  $D_{00}$  does not vanish, but instead diverges for small momenta at *each* timeslice.

While one can hope that transverse gluons behave in a similar way in the Hamiltonian and the path-integral approach, there is no rigorous argument for that (in particular since also transverse gluons are just would-be physical particles).

<sup>4</sup>Weyl-ordering means the symmetric ordering of equal-time operators, i.e.  $[\hat{x}\Phi(\hat{x}, \hat{p})]_W = \frac{1}{2}\{\hat{x}, \Phi(\hat{x}, \hat{p})\}_W$  and  $[\hat{p}\Phi(\hat{x}, \hat{p})]_W = \frac{1}{2}\{\hat{p}, \Phi(\hat{x}, \hat{p})\}_W$ , in particular  $[\hat{x}\hat{p}]_W = [\hat{p}\hat{x}]_W = \frac{1}{2}(\hat{x}\hat{p} + \hat{p}\hat{x})$ . See [69] for a one-page tutorial.

<sup>5</sup>While the first-order formalism is in some aspects closer in spirit to the Hamiltonian approach, there is still no immediate correspondence known between the quantities in those two (in principle equivalent) ways to write down the theory.

### 3.3.4 (1 + 1)-dimensional Coulomb Gauge

QCD in two dimensions [191], called the *'t Hooft model* can be solved exactly, it has been discussed further in [43, 76, 28] and various other publications. While such a model has little to do with the real (3 + 1)-dimensional world, it can still be an interesting playground to test various techniques or see how certain mechanisms may work in principle.

Even though it is possible to solve  $\text{QCD}_{1+1}$  analytically, these calculations are not necessarily possible in an arbitrary gauge, and indeed already in the Landau gauge no way of solving the theory is known so far. Typically,  $\text{QCD}_{1+1}$  is considered in the axial gauge, but a solution can be obtained in the Coulomb gauge as well.

The Coulomb gauge condition reads

$$\frac{\partial A_1}{\partial x_1} = 0, \quad (3.40)$$

which implies that  $A_1$  is constant on each timeslice and that the Faddeev-Popov operator takes the form

$$M^{ab} = -\frac{\partial}{\partial x_1} \left( \delta^{ab} \frac{\partial}{\partial x_1} + g f^{acb} A_1^c \right), \quad (3.41)$$

which is now just an ordinary differential operator. When restricting the system to the interval  $-\frac{L}{2} \leq x_1 \leq \frac{L}{2}$ , one can give an expansion of the wave functional in Fourier modes,

$$\psi(x_1) = \sum_n \psi_n e^{ik_n x_1} \quad \text{with } k_n = \frac{2\pi n}{L}. \quad (3.42)$$

The propagators of  $A_0$  and the Faddeev-Popov ghost are given by

$$\langle A_0(x_1) A_0(y_1) \rangle = \left\langle \frac{1}{-D_1^2} \right\rangle \quad (3.43)$$

$$\langle c(x_1) \bar{c}(y_1) \rangle = \left\langle \frac{1}{-\partial_1 D_1} \right\rangle \quad (3.44)$$

where we have  $D_1[A] = \partial_1 + gA_1 \times$  and the average is with respect to  $A_1$ . Since  $A_1$  is independent of  $x_1$ , one can diagonalize these operators by Fourier transform, so

$$\begin{aligned} D_{A_0 A_0}(k_1) &= \left\langle \frac{1}{(k_1 + igA_1 \times)^2} \right\rangle \\ D_{\text{gh}}(k_1) &= \left\langle \frac{1}{k_1(k_1 + igA_1 \times)} \right\rangle \end{aligned} \quad (3.45)$$

We now integrate  $A_1$  over the Gribov region, which is the region where the eigenvalues of the Faddeev-Popov operator  $k_1(k_1 + igA_1 \times)$  are non-negative. For this purpose, we quantize (as above) in a periodic box of length  $L$ , so  $k_1 = 2\pi n/L$ , where  $n$  is an integer. We first consider the gauge group to be  $\text{SU}(2)$ . One easily finds that the eigenvalues of  $igA_1 \times$  are given by 0 and  $\pm|gA_1|$ . The case  $k_1 = 0$  is trivial.

The Gribov horizon is determined by the first non-trivial zero eigenvalue. This occurs for  $n = \pm 1$ , at  $|gA| = 2\pi/L$ . Thus  $A_1$  is integrated over the sphere  $|A_1| \leq 2\pi/gL$ . We now take the infinite-volume limit  $L \rightarrow \infty$ , while keeping a typical momentum  $k_1$  finite. In this case we have  $A_1 \rightarrow 0$ , and the  $A_0$  and ghost propagators approach their free values,  $D_{A_0 A_0}(k_1) = D_{\text{gh}}(k_1) = 1/k_1^2$ . This result does not change for  $\text{SU}(N)$  with  $N > 2$ . The restriction to the Gribov region (which in this case coincides with the Fundamental Modular Region) was essential in deriving this result.

For an up-to-date review on (1 + 1)-dimensional Yang-Mills theory in the Hamiltonian approach and implications for Dyson-Schwinger equations see [164].

### 3.4 Selected Results on the Coulomb Gauge

We now briefly summarize several results on Coulomb gauge QCD which are typically closely connected to the investigations performed in this thesis. The methods used to obtain them range from perturbative over functional to lattice approaches.

#### 3.4.1 On the Lattice: Propagators and the Coulomb String Tension

While gauge-fixing on the lattice is a cumbersome procedure [87, 134], it is nevertheless performed by several groups and yields valuable insights (and sometimes important numerical parameters) also for functional approaches.

In the brief review [54], lattice simulations in Coulomb gauge are divided into those from the *classical area*, which examine propagators and the color-Coulomb potential, and the *modern area*, where mainly the eigenvalue spectrum of the Faddeev-Popov operator is investigated. While both issues are relevant for questions of confinement, the “classical” results are more intimately linked to the questions discussed in this thesis.

Several lattice studies show a blowup of ghost and  $A_0$ - $A_0$  propagator, while the transverse gluon propagator is suppressed [59, 58, 61, 127] in accordance with the Coulomb gauge version of the Gribov-Zwanziger scenario. Gauge-fixed lattice studies allow also the determination of the Coulomb string tension  $\sigma_C$  [171, 150, 145, 146, 202, 203]. Zwanziger’s inequality (see sec. 3.2.3) implies  $\sigma_C \leq \sigma_W$ , and indeed most studies find

$$\sigma_C \approx (2 \div 3)\sigma_W. \quad (3.46)$$

Thus typical values are  $\sigma_C \approx 0.5 \text{ MeV}^2$ . In the high-temperature (“deconfined”) phase, one finds magnetic scaling (see the expositions given in chapter 5 and section VI.C to VI.E of [145])

$$\sqrt{\sigma_C} \sim g^2(T) T. \quad (3.47)$$

Coulomb-gauge lattice studies also reveal the close connection between a finite string tension and the presence of center vortices [92, 93].

#### 3.4.2 The Transverse Gluon Energy and Gribov’s Formula

The dispersion relation of transverse gluons is significantly modified as compared to the one of transverse photons. While for large momenta one finds  $E(\mathbf{k}) \approx |\mathbf{k}|$ , the infrared region is strikingly different.

While a photon of low momentum has also low energy, a low-momentum gluon is expected to have a large energy which diverges towards infinity for  $\mathbf{k}^2 \rightarrow 0$  (i.e. for increasingly large distance). A simple formula which describes this behaviour has been proposed by Gribov [95],

$$E(\mathbf{k}) = \sqrt{\mathbf{k}^2 + \frac{m^4}{\mathbf{k}^2}}. \quad (3.48)$$

It contains a mass parameter  $m$  (conventionally called the Gribov mass) which is dynamically generated (similar to  $\Lambda_{\text{QCD}}$ ) from the initially scale-free theory. The energy has a minimum at  $|\mathbf{k}| = m$ ; and for smaller momenta it increases again; at some point one has  $\frac{\partial E}{\partial k} > c = 1$ , which makes obvious that (3.48) does not describe a *physical* particle.

The fits of numerical results, either from the lattice [60] or from the Hamiltonian approach [79, 163] to (3.48) or similar forms like

$$E(\mathbf{k}) = |\mathbf{k}| + \frac{\Lambda^2}{|\mathbf{k}|} \quad (3.49)$$

works reasonably well, so (3.48) or (3.49) can be used as a starting point for further calculations. While (3.48) has been *postulated* in [95], its form can be derived from the Gribov-Zwanziger Lagrangian (1.64), see also sec. 5.2.

### 3.4.3 Perturbative Expansion and Dyson-Schwinger Equations

While there have been perturbative calculations in Coulomb gauge by Leibbrandt, Zwanziger, Andrasi, Doust, Taylor and others, the situation has remained – mostly due to the problems outlined in sections 3.1 and 3.2 – somehow unsatisfactory for many years.

The problem has been taken up by Watson and Reinhardt, who have in a couple of articles [210, 208, 209, 211, 160, 212] done a systematic investigation of one-loop perturbative two-point functions and their Dyson-Schwinger equations. The tools employed encompass Schwinger parameterization, differential equations for certain integrals and integration by parts.

### 3.4.4 Infrared Exponents in the Coulomb Gauge

Infrared exponents have been briefly discussed for covariant gauges in section 2.5, and in the context of covariant gauges, they turn out to be a powerful tool for the analysis of propagators and vertex functions. It won't come as a surprise that, as so many tools developed for the covariant formalism, the study of these exponents can be transferred to the non-covariant setup, but becomes significantly more cumbersome and allows less general statements.

The origin of these problems is, once again, that even in the conformal region and even in the case of the simplest nontrivial objects of the theory there are at least two scales present, namely (given some Euclidean momentum  $p$ )  $p^2$  and  $p_4^2$ . This is true for the pure Coulomb gauge and (though presumably in a less severe way) in the (Weyl-)Landau-Coulomb interpolating gauge.

While some ideas to define a general asymptotic expansion in several variables are outlined in appendix C.3, they are not yet directly applicable to the current situation. Actually the most straightforward approach is to neglect in the system of Dyson-Schwinger equations all diagrams which have no instantaneous piece. This has been done in [12], where it has turned out that, truncated such severely, the first-order system is incompatible with the expected  $1/k^4$ -behaviour of  $D_{00}(k)$ . Also inclusion of straightforward vertex dressing (not taking into account more complicated tensor structures) did not provide a remedy.

Coulomb-gauge infrared exponents are easier to handle at finite temperature: In this setup the zeroth momentum components  $p_0$  are replaced by the Matsubara frequencies  $n 2\pi T$  (see section 5.1). In the high-temperature limit the 0<sup>th</sup> Matsubara frequency is expected to dominate; thus one can factor out the scale  $g^2 T$  from all equations and work with only one scale  $p^2$ . This path is followed in section 5.3.

### 3.4.5 The Gluon Chain Model

The existence of a linearly rising color-Coulomb potential answers certain questions concerning confinement, but as well gives rise to other puzzles:

- If, as the lattice data indicates,  $\sigma_C$  is indeed significantly larger than  $\sigma_W$ , there has to be a mechanism which reduces the Coulomb string tension to the physical one.
- The color-Coulomb potential is radially symmetric; thus it does not describe the formation of a string between two distant color charges. Somehow the Coulomb gluons have to be collimated to such a string.

A possible explanation for both these effects is provided by the *gluon chain model* [91, 90] in which two fundamental color charges are connected by a chain of constituent gluons which interact via the color-Coulomb potential, but partially screen it at the same time. This model potentially explains both the formation of a string and the reduction of the Coulomb string tension to the Wilson value.



### 3.5 Interpolating Gauges and their Limits

As discussed in [31], a whole class of *interpolating gauges* is given by the condition<sup>6</sup>

$$\eta \partial_0 A_0 - \partial_i A_i = 0, \quad \eta \in [0, 1]. \quad (3.50)$$

These gauges are essentially Landau-like (in particular perturbatively unique, i.e. unique up to Gribov copies) for  $\eta > 0$ , but already non-covariant for  $\eta < 1$ . The most striking difference is that they have two different ghost-gluon vertices which allow the definition of two running couplings [84].

#### 3.5.1 Tree-Level Propagators

Employing the Fadeev-Popov method for the gauge condition (3.50) the gauge-fixing and ghost part of the Lagrangian take the form

$$\mathcal{L}_{\text{gf,gh}} = \frac{1}{2\xi} (\partial' \cdot A)^2 + \partial' \bar{c} \cdot D[A]c$$

with  $\partial' = (\eta \partial_0, \nabla)$ . Including this in the Lagrangian, the gluon and ghost propagator for Landau-Coulomb interpolating gauge can be easily read off (note that in [31] a different metric has been chosen which alters some of the expressions),

$$D_{ij}^{(0)}(k) = -i \left\{ \frac{1}{k^2} \left( \delta_{ij} - \frac{k_i k_j}{\mathbf{k}^2} \right) - \frac{k_i k_j}{\mathbf{k}^2} \frac{\eta^2 k_0^2}{(\eta k_0^2 - \mathbf{k}^2)^2} \right\},$$

$$D_{0i}^{(0)}(k) = i \frac{\eta k_0 k_i}{(\eta k_0^2 - \mathbf{k}^2)^2}, \quad D_{00}^{(0)}(k) = i \frac{\mathbf{k}^2}{(\eta k_0^2 - \mathbf{k}^2)^2}, \quad D_{\text{gh}}^{(0)}(k) = -i \frac{1}{\eta k_0^2 - \mathbf{k}^2}.$$

The fermion propagator is unaffected by the choice of gauge fixing. One notes that  $D_{0i}^{(0)}$  vanishes for  $\eta \rightarrow 0$  while  $D_{00}^{(0)}(k)$  and  $D_{\text{gh}}^{(0)}(k)$  become instantaneous. For  $\eta > 0$  one has to include the mixed propagator, but there are no problems with energy divergences.

The only tree-level vertex directly affected by the interpolation procedure is the ghost- $A_0$  vertex which is proportional to  $\eta$  and thus formally vanishes in the Coulomb limit  $\eta \rightarrow 0$ . However, as we will see in sec. 3.5.3, certain diagrams which contain such a vertex survive in the Coulomb limit.

#### 3.5.2 Access to the Physical Coulomb Gauge?

Even though one is left only with the Coulomb gauge condition in the limit  $\eta \rightarrow 0$  (and no other explicit condition is present), the nature of the limit is far from being obvious. Essentially there are three main possibilities:

1. The endpoint is the physical Coulomb gauge. This implies that the limit  $\eta \rightarrow 0$  of the interpolating gauge is extremely singular since the dimensionality of the gauge condition changes discontinuously.
2. The endpoint is only one Coulomb-like gauge, where  $\nabla \cdot \mathbf{A} = 0$  holds, but the  $g(t)$ -symmetry has been removed.
3. The endpoint defines no valid gauge at all.

---

<sup>6</sup>An extension of this interpolation process which includes also the Maximal Abelian Gauge as a particular limit has been established in [44] and discussed further in [45].



### An Additional Constraint

While none of these possibilities can be rigorously excluded, there seems to be some evidence for the second scenario. Integration of (3.50) over space yields (with periodic boundary conditions or for fields vanishing sufficiently rapidly at infinity)

$$\int d^3x (\eta \partial_0 A_0 + \partial_i A_i) = \eta \int d^3x \partial_0 A_0 + \underbrace{\int d^3x \partial_i A_i}_{=0 \text{ due to Gau\ss' theorem}} = \eta \partial_0 \int d^3x A_0 = 0. \quad (3.51)$$

For  $\eta \neq 0$  one can divide this condition by  $\eta$  and obtains the constraint

$$\partial_0 \int d^3x A_0 = 0 \quad (3.52)$$

which holds for all  $\eta > 0$  and thus also in the limit  $\eta \rightarrow 0$ . This implies that the value of the integral over  $A_0$  is constant over all time-slices, in contrast to the physical Coulomb gauge, where the  $g(t)$ -symmetry allows to choose  $\int d^3x A_0$  independently on each time-slice.

### Existence of Stronger Constraints?

One can ask whether not only (3.52) but also the significantly stronger condition

$$\partial_0^{(x)} A_0(x) = 0 \quad (3.53)$$

holds for the Coulomb endpoint of the interpolating gauge. This, however, is quite unlikely, since for  $\eta \ll 1$ , large fluctuations of  $\partial_0 A_0$  can be compensated by small fluctuations of  $\partial_i A_i$ .

Consider two independent linear gauge conditions<sup>7</sup>  $F[A] = 0$  and  $G[A] = 0$ , where

$$F[A] + G[A] = 0 \quad \text{provides perturbatively complete gauge-fixing.} \quad (3.54)$$

In this case (since only rescaling is involved [31, 84]) an interpolation prescription

$$\eta F[A] + G[A] = 0, \quad \eta \in [0, 1] \quad (3.55)$$

provides complete gauge fixing as well for  $\eta > 0$ . We now assume that the limit  $\eta \rightarrow 0^+$  can enforce  $F[A] = 0$  and  $G[A] = 0$  individually. Certainly

$$G_0 := \{A \mid F[A] = G[A] = 0\} \subset \{A \mid F[A] + G[A] = 0\} =: G_1 \quad (3.56)$$

holds, and this inclusion is proper, since in general there exist configurations  $A$  which fulfill

$$F[A(x)] = -G[A(x)] = f(x) \neq 0. \quad (3.57)$$

These configurations do not only exist, but they are expected to constitute a “large” part of  $G_2$ , since among those configurations with  $F[A(x)] = f(x)$ , configurations with  $F[A(x)] \equiv 0$  are a subset of measure zero. Thus  $G_0$  is only a “small” subset of  $G_1$ , and if (3.54) holds, than a significant number of gauge orbits has been completely removed from the path integral.

Thus, if (3.53) indeed held for the Coulomb endpoint of the interpolating gauge, this would imply that either Landau gauge is already perturbative incomplete (for which there is no evidence) or that the gauge-fixing for  $\eta \rightarrow 0$  is overcomplete and the endpoint does not describe a valid gauge any more. It is also impossible to impose the lattice versions of  $\nabla \cdot \mathbf{A} = 0$  and (3.53) at the same time [134].

---

<sup>7</sup>The argument indeed only holds for independent gauge conditions, not for choices like  $F[A] = G[A] = \frac{1}{2} \partial_\mu A^\mu$ .

$$\sim \frac{1}{(\eta^{1/2})^2} \eta^2 \frac{1}{(\eta^{1/2})^2} = 1$$

Figure 3.3: For this graph, where all internal propagators are of the form  $\frac{1}{p^2 + \eta p_0^2}$ , we find  $(\eta^{-1/2})^2$  from rescaling,  $(\eta^{-1/2})^2$  from two powers of  $p_0$  and  $\eta^2$  from the vertices. Thus this diagram is proportional to  $\eta^0 = 1$  and does not vanish for  $\eta \rightarrow 0$  even though it has no corresponding counterpart in the physical Coulomb gauge.

### 3.5.3 Rescaling of Momenta and Further Hints at Discontinuities

Regularizing diagrams which contain  $A_0$ - or ghost propagators (which are instantaneous in the Coulomb gauge) with (3.50) gives rise to integrals of the form (in the Euclidean setup)

$$I := \int \frac{dp_4}{(p^2 + \eta p_4^2) ((p + k)^2 + \eta(p_4 + k_4)^2)}. \quad (3.58)$$

They are energy-divergent in the formal Coulomb limit  $\eta \rightarrow 0$ . As long as we have  $\eta > 0$ , however, we can rescale such an integral by  $p_4 \rightarrow \frac{p_4}{\sqrt{\eta}}$ , which yields

$$I = \frac{1}{\sqrt{\eta}} \int \frac{dp_4}{(p^2 + p_4^2) ((p + k)^2 + (p_4 + \sqrt{\eta} k_4)^2)}. \quad (3.59)$$

Even in the limit  $\eta \rightarrow 0$ , the rescaled  $p_4$ -integral itself poses no problem – the divergence has been shifted to the divergent prefactor  $\frac{1}{\sqrt{\eta}}$ . Thus this procedure offers an alternative way to regularize energy divergences.

The rescaling of momenta with  $\frac{1}{\sqrt{\eta}}$  is a general procedure, thus one can directly read off the power of  $\eta$  for a given diagram. (Each loop contributes  $\eta^{-1/2}$ , each power of  $p_4$  as well, and there might be explicit powers of  $\eta$  from mixed gluon propagators or ghost- $A_0$  vertices.)

In order to access to the physical Coulomb gauge with the limit  $\eta \rightarrow 0$ , one would expect certain diagrams to vanish during the limiting process – those diagrams which are absent in the physical Coulomb gauge (like those containing a mixed propagator  $D_{0i}$  or a ghost- $A_0$  vertex). As already noted in [31] this is not the case:

The diagram depicted in 3.3 (a contribution to the self-energy of the transverse gluon) does not vanish in the Coulomb limit  $\eta \rightarrow 0$  though it contains ghost- $A_0$  vertices and is thus absent in the physical Coulomb gauge.

Of course one cannot exclude the possibility of intricate cancellations between several diagrams which are absent for  $\eta = 0$ , but there is no strong argument in favor of this possibility. It is more likely to interpret this as a further hint that the Coulomb limit of the interpolating gauge is not the physical Coulomb gauge. This can presumably be characterized by breaking of the  $g(t)$  symmetry by the limiting process<sup>8</sup> and thus one finds only one particular Coulomb-like gauge.

<sup>8</sup>This might be similar to what is known from spin models. The  $\uparrow$ - $\downarrow$  symmetry of the Ising model is broken by application of an external magnetic field  $h$ , and in the thermodynamic limit (i.e. for an infinitely large system) this breaking survives the limiting process  $h \rightarrow 0$ .

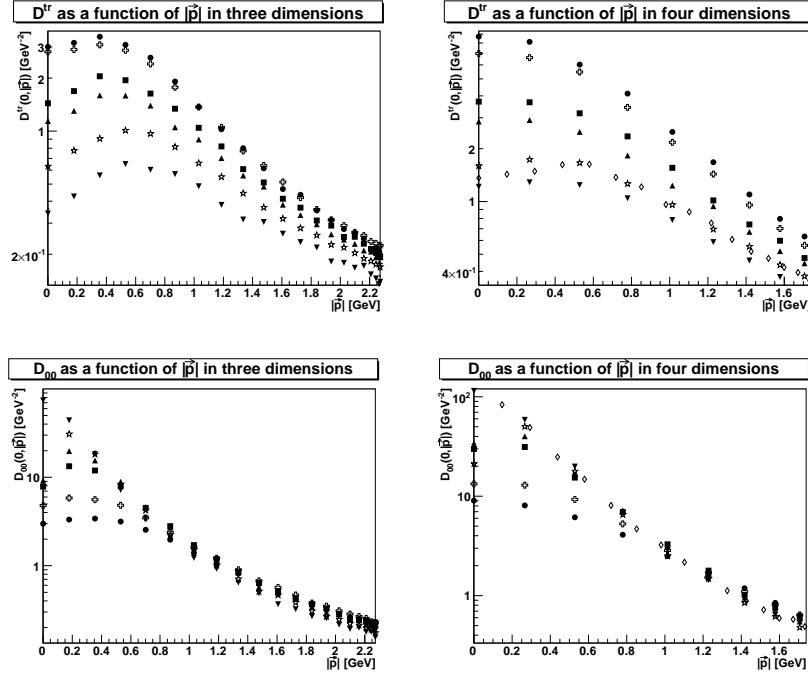


Figure 3.4: Results from [55]: The gluonic correlators  $D^{\text{tr}}(0, |\mathbf{p}|)$  and  $D_{00}(0, |\mathbf{p}|)$  in three (left) and four (right) dimensions. Circles indicate data for  $\eta = 1$  (Landau gauge), crosses are used for  $\eta = \frac{1}{2}$ , squares for  $\eta = \frac{1}{10}$ , triangles for  $\eta = \frac{1}{20}$ , stars for  $\eta = \frac{1}{100}$  and upside-down triangles represent results at  $\eta = 0$  (Coulomb gauge).

### 3.5.4 Interpolating Gauges on the Lattice

Interpolating gauges as defined by (3.50) have also been studied on the lattice [135, 55]. The results for three and four dimensions, as illustrated in figure 3.4, confirm the picture proposed in [84], where for  $\lambda > 0$  the interpolating gauge is in some sense a deformed Landau gauge.

There is evidence for a limiting momentum scale  $\mathbf{k}_{\text{lim}}^2$  (depending on the interpolation parameter  $\eta$ ) below which the gauge is essentially Landau-like, while for  $\mathbf{k}^2 > \mathbf{k}_{\text{lim}}^2$  one finds Coulomb-like behaviour. This is particularly intriguing for  $D_{00}$ , a quantity which looks radically different in Landau respectively Coulomb gauge<sup>9</sup>:

- In Landau gauge,  $D_{00}(k)$  is contained in the full gluon propagator  $D_{\mu\nu}(k)$ , consequently (see sec. 1.3) it is supposed to *vanish* for  $k^2 \rightarrow 0$ .
- In Coulomb gauge, on the other hand,  $D_{00}(k)$  does *not* describe the propagation of would-be physical gluons, but instead gives a confining, essentially static potential which is supposed to *diverge* for  $\mathbf{k}^2 \rightarrow 0$ .

In the interpolating gauge,  $D_{00}$  is starting to blow up for  $\mathbf{k}^2$  becoming smaller until  $\mathbf{k}_{\text{lim}}^2$  is reached. For  $\mathbf{k}^2$  decreasing further,  $D_{00}(k)$  starts to approach zero (as the Landau-like behaviour dictates – but see also [56]).

The apparent existence of an  $\eta$ -dependent threshold momentum, below which the behaviour of the interpolating gauge is essentially Landau-like, vaporizes all attempts to perform an infrared analysis (along the lines of sec. 2.5) of this interpolating gauge. In the deep infrared one will find Landau-like behaviour for all  $\eta > 0$ ; it remains unclear to what extent the Coulomb endpoint of this gauge coincides with the physical Coulomb gauge.

<sup>9</sup>Note that at some instances one has statements about the dependence on  $\mathbf{k}^2$ , at other instances about the dependence on  $k^2 = -(k_4^2 + \mathbf{k}^2)$ . For  $k_4 = 0$  these scales agree (up to the minus sign which can easily be absorbed). Actually it might be reasonable to check the dependence on the “interpolating” momentum scales  $k'^2 = -(\eta^2 k_4^2 + \mathbf{k}^2)$  and  $k' \cdot k = -(\eta k_4^2 + \mathbf{k}^2)$  as well.

### 3.5.5 A Picture of the Interpolation Process

The interpolation prescription (3.50) can be extended to include also the Weyl gauge,

$$\frac{1-\lambda}{2} \partial_0 A_0 - \frac{1+\lambda}{2} \partial_i A_i = 0, \quad \lambda \in [-1, 1], \quad (3.60)$$

and doing so is actually helpful for the following discussions. For  $\lambda = -1$  one has the Weyl gauge condition, for  $\lambda = 0$  the covariant and for  $\lambda = 1$  the Coulomb gauge condition. Quantum fluctuations can be handled by introducing [in terms of (1.32)] a continuous function  $\xi(\lambda)$  with  $\xi(-1) = \xi(1) = 0$  and  $\xi(0) = \xi_0$ , where  $\xi_0$  is chosen according to the type of covariant gauge one wants to access (like  $\xi_0 = 0$  for Landau and  $\xi_0 = 1$  for Feynman gauge).

For  $\lambda = 1$  a one-parameter family of gauge transformations  $g(t)$  is left open, for  $\lambda = -1$  it is a three-parameter family  $g(\mathbf{x})$  while for  $\lambda \in (-1, 1)$  the gauge fixing is unique (up to Gribov copies). With the words of [31], the “degree of arbitrariness”  $\sigma$  varies according to

$$\sigma(\lambda) = \begin{cases} 3 & \text{for } \lambda = -1 \\ 0 & \text{for } -1 < \lambda < 1 \\ 1 & \text{for } \lambda = +1 \end{cases} \quad (3.61)$$

As already discussed in some length, it is highly questionable whether the limits  $\lambda \rightarrow -1^+$  and  $\lambda \rightarrow 1^-$  indeed yield the corresponding gauge, i.e. if the limits are continuous.

We now try to find an illustrative picture of the interpolation process and give certain conjectures about the endpoints of these interpolation: To do this, we work in the metric space of *gauges*  $\mathcal{G}$  (which is not the space  $\mathcal{A}$  of configurations!) as introduced in sec. 1.5. Each point in this space represents a perturbatively unique gauge ( $\sigma = 0$ ), while hypersurfaces are incomplete gauges with  $\sigma > 0$ .

On the hypersurface  $C$  of all formal Coulomb gauges (i.e. all valid gauges which fulfill (3.1), but with  $g(t)$ -invariance removed one way or the other), the condition

$$\left\langle \int d^4x (\nabla \cdot \mathbf{A})^2 \right\rangle = 0 \quad (3.62)$$

is precisely met.<sup>10</sup> The physical Coulomb gauge  $G_C^{(\text{phys})}$  encompasses *all* of these gauges in the sense that any given Coulomb-like gauge  $G_C^*$  can be partitioned in a way such that all unique gauges contained in  $\mathcal{P}_{G_C^*}$  are also contained in an appropriate partitioning of  $G_C^{(\text{phys})}$ .

Assuming reasonable continuity properties (some of which can be derived from the considerations in 1.5 and the fact that a distance functional  $d$  is continuous) the hypersurface  $C$  is surrounded by a continuum of other hypersurfaces which contain gauges that are “almost” Coulomb-like. This means they fulfill

$$\left\langle \int d^4x (\nabla \cdot \mathbf{A})^2 \right\rangle = c_C \quad (3.63)$$

with  $c_C$  being small (but strictly positive) close to  $C$ . The further we move away from  $C$ , the larger values for  $c_C$  we will find. Loosely speaking, these are hypersurfaces of constant, but decreasing “Coulombness”. The same way we have a hypersurface  $W$  with  $\left\langle \int d^4x (\partial_0 A_0)^2 \right\rangle = 0$  and hypersurfaces of decreasing “Weylness” with

$$\left\langle \int d^4x (\partial_0 A_0)^2 \right\rangle = c_W \quad (3.64)$$

and  $c_W \in \mathbb{R}^+$ .

---

<sup>10</sup>With  $\langle \dots \rangle$  we denote the correctly normalized expectation value with respect to all configurations which belong to the relevant gauge.

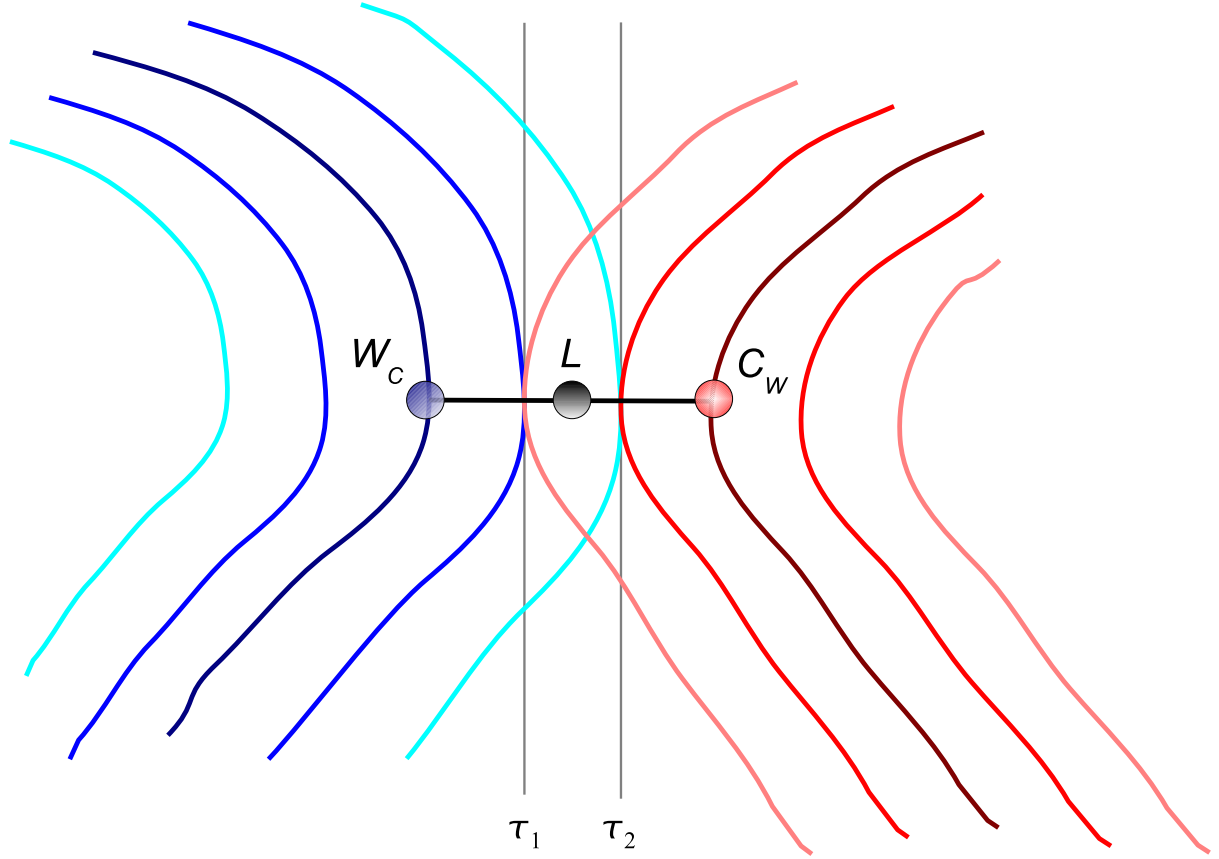


Figure 3.5: The curve  $\gamma_\lambda$  of Weyl-Landau-Coulomb interpolating gauge connects the Weyl gauge  $W_C$  which is most Coulomb-like and the Coulomb gauge  $C_W$  which is most Weyl-like. The Landau gauge  $L$  lies between these two gauges. For any point on the interpolation line, the tangent hyperplanes  $\tau_i$  of the hypersurfaces  $\langle \int d^4x (\nabla \cdot \mathbf{A})^2 \rangle = \text{const}$  and  $\langle \int d^4x (\partial_0 A_0)^2 \rangle = \text{const}$  coincide, and the tangent to  $\gamma_\lambda$  is a normal vector.

While the numbers  $c_C$  from (3.63) and  $c_W$  from (3.64) do not define a metric in the strict sense, they still serve as a “distance measure” which allows to classify “how far a certain gauge is away” from Coulomb respectively Weyl gauge.

The Landau gauge strictly fulfills

$$\partial_\mu A^\mu \equiv \partial_0 A_0 - \partial_i A_i = 0 \quad \Longleftrightarrow \quad \partial_0 A_0 = \partial_i A_i. \quad (3.65)$$

Thus we find

$$c_W^{(\text{Landau})} = \left\langle \int d^4x (\partial_0 A_0)^2 \right\rangle = \left\langle \int d^4x (\partial_i A_i)^2 \right\rangle = c_C^{(\text{Landau})}, \quad (3.66)$$

i.e. the Landau gauge is located “right in the middle” between the two gauge hypersurfaces  $C$  and  $W$ .

The interpolation process (3.60) with  $\lambda \in (-1, 1)$  defines a curve  $\gamma_\lambda$  in  $\mathcal{G}$  which starts for  $\lambda = -1^+$  infinitesimally close to  $W$  and comes for  $\lambda = +1^-$  infinitesimally close to  $C$ . This is sketched graphically in figure 3.5.

While the interpolation process inevitably leaves  $C$  (unless  $\partial_0 A_0 = \nabla \cdot \mathbf{A} = 0$  defined a valid gauge, a possibility which has been discarded in sec. 3.5.2), condition (3.60) still constrains  $(\partial_0 A_0)^2$ . Thus an infinitesimal interpolation step  $\lambda \rightarrow \lambda + \varepsilon$  reduces  $c_C$  while it increases  $c_W$  – but in a controlled, possibly even minimal way:

**Conjecture 3.5.1:** An infinitesimal interpolation step  $\lambda \rightarrow \lambda + \varepsilon$  in (3.60) selects among all paths which reduce  $c_C^{(0)}$  to  $c_C^{(\varepsilon)} < c_C^{(0)}$  the one which minimizes the increase of  $c_W$ .

According to this conjecture,  $\gamma_\lambda$  intersects both the hypersurfaces of constant “Weylness” and those of constant “Coulombness” orthogonally. Thus  $\gamma_\lambda$  can be regarded as a geodesic in  $\mathcal{G}$ , which connects the hypersurfaces  $W$  and  $C$  in the shortest possible way. The gauges obtained for  $\lambda \rightarrow -1^+$  and  $\lambda \rightarrow 1^-$  are thus expected to lie on  $W$  respectively on  $C$ , but as close to each other as possible.<sup>11</sup>

**Conjecture 3.5.2:** The endpoint  $\lambda \rightarrow +1^-$  of the Weyl-Landau-Coulomb interpolating gauge, denoted by  $C_W$ , is the one gauge which, among all gauges fulfilling the Coulomb gauge condition  $\nabla \cdot \mathbf{A} = 0$ , minimizes the functional  $\langle \int d^4x (\partial_0 A_0)^2 \rangle$ .

Analogously we conjecture that for  $\lambda \rightarrow -1^+$ , the endpoint  $W_C$  of the Landau-Weyl interpolating gauge is the gauge that, while strictly fulfilling the Weyl gauge condition  $\partial_0 A_0 = 0$ , minimizes the functional  $\langle \int d^4x (\nabla \cdot \mathbf{A})^2 \rangle$  as compared to all other types of Weyl gauge.<sup>12</sup>

Loosely speaking: According to this conjecture, the Coulomb endpoint of the interpolating gauge (3.60) is the one formal Coulomb gauge which is most “Weyl-like” – and vice versa.

If these considerations turn out to be correct, the Landau gauge, obtained for  $\lambda = 0$ , is located not only half way between  $C$  and  $W$ , but also on  $\gamma_\lambda$  half way between  $C_W$  and  $W_C$ .

The considerations so far are based on the distance measures (3.63) and (3.64). All results should also translate to the original distance defined in sec. 1.5, therefore we propose that also the following statement holds:

**Conjecture 3.5.3:** The endpoints  $\lambda \rightarrow \pm 1^\mp$  of the Weyl-Landau-Coulomb interpolating gauge are those gauges  $G_C \in C$  and  $G_W \in W$  which minimize  $d(G_C, G_W)$ , when employing the distance  $d$  from (1.98),

$$d(C_W, W_C) \leq d(G_C, G_W) \quad \text{for all } G_C \in C \text{ and } G_W \in W. \quad (3.67)$$

---

<sup>11</sup>Note that we still have to *assume* that the gauges  $\lambda \rightarrow \pm 1^\mp$  exist. If  $\mathcal{G}$  was a complete metric space (which remains to be proven) the existence of the endpoint gauges could be established the following way:

1. Define a sequence of gauges by the choice  $\lambda = -1 + \frac{1}{n}$  respectively  $\lambda = 1 - \frac{1}{n}$ ,  $n \in \mathbb{N}$ .
2. Show that this is a Cauchy sequence.
3. Since in a complete space each Cauchy sequence converges, also the limit element belongs to  $\mathcal{G}$  and thus is a valid gauge.

While the steps 1 and 3 are straightforward, we expect enormous difficulties to be associated with step 2, the proof of the Cauchy property.

<sup>12</sup>We note that  $\gamma_\lambda$  can be built up from infinitesimal parameter shifts and the increase of (3.64) is supposedly minimal for each such shift. Thus *locally* conjecture 3.5.2 is an immediate corollary of conjecture 3.5.1. *Globally*, however, one cannot a priori exclude the possibility that such a steepest descent-like procedure does not yield an optimal result.

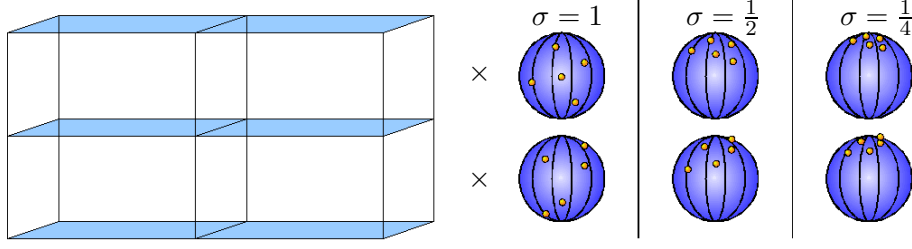


Figure 3.6: An illustration of the “retraction” process of random time-dependent gauge transformations to the north pole (= the position of the identity) for  $\sigma \rightarrow 0$

### 3.5.6 Proposal of a New Type of Interpolating Gauge

As discussed in some length, the interpolation prescription (3.50) is expected to remove the remnant symmetry in the Coulomb limit (by implicitly imposing an additional constraint); therefore it is probably at best discontinuously connected to the physical Coulomb gauge.

Taking into account the importance of the remnant symmetry it would be desirable to have a procedure at hand which *gradually* removes the remnant symmetry in an essentially continuous way. Here we sketch a possible path how such a procedure could be implemented on the lattice:

1. Generate (typically via importance-sampling Monte-Carlo simulations) an ensemble of independent gauge configurations; gauge-fix each one to the configuration which satisfies (the lattice version of)  $\nabla \cdot \mathbf{A} = 0$  and fulfills a further condition which removes remnant symmetry (e.g. minimizes the lattice version of  $\int d^4x (\partial_0 A_0(x))^2$ ). In the following we denote these configurations by  $\{U_{i,\min}^C\}_{i=1,\dots,N_{\text{conf}}}$ .
2. Generate a set of random time-dependent gauge transformations

$$\left\{g(t)_i^j\right\} = \left\{e^{i\theta_i^{a,j}(t)\frac{\lambda^a}{2}}\right\}_{i=1,\dots,N_{\text{conf}}}^{j=1,\dots,N_{\text{rem}}}, \quad (3.68)$$

characterized by time dependent parameters  $\theta_i^{a,j}(t)$ ,  $a = 1, \dots, N_C^2 - 1$ . These configuration should be “small”, i.e. continuously connected to unity (in contrast to “large” gauge transformations which play an important role in the discussion of instantons).

3. Choose a gauge-variant quantity  $X[U]$  (e.g. a particular Green function). Introduce a parameter  $\sigma$ , set  $\sigma = 1$  and choose a fixed  $q \in (0, 1)$ . Repeat the following process  $N_{\text{interp}}$  times:
  - Produce configurations  $U_{i,\sigma}^{j,C} = e^{i\sigma\theta_i^{a,j}(t)\frac{\lambda^a}{2}} U_{i,\min}^C$  ( $i = 1, \dots, N_{\text{conf}}$ ;  $j = 1, \dots, N_{\text{rem}}$ ).
  - Evaluate  $\langle X[U] \rangle_\sigma$  with the ensemble of all these  $N_{\text{conf}} \cdot N_{\text{rem}}$  configurations.
  - Scale down  $\sigma$  by  $\sigma \rightarrow q\sigma$ .
4. Check whether  $\langle X[U] \rangle_\sigma$  depends on  $\sigma$  and whether the extrapolation  $\sigma \rightarrow 0$  coincides with the results for  $\langle X[U] \rangle$  when taking the expectation value w.r.t.  $\{U_{i,\min}^C\}_{i=1,\dots,N_{\text{conf}}}$ .

In case of  $\mathbb{G} = \text{SU}(2)$  a geometric interpretation of this procedure is relatively straightforward. Geometrically  $\text{SU}(2)$  is equivalent to a three-sphere. Without loss of generality we can place the identity element  $\mathbb{1}$  at the north pole and  $(-\mathbb{1})$  at the south pole. Starting from a minimal configuration  $U_{i_0,\min}^C$  all links between two distinct time-slices are multiplied by the same random group elements. For  $\sigma = 1$  these elements are randomly distributed over the whole sphere, while for  $\sigma \rightarrow 0$  they are contracted towards the north pole. The process is illustrated in figure 3.6.



## Chapter 4

# The Coulomb-Gauge Gap Equation

We now turn to our main source of information about the quark sector of Coulomb gauge QCD, the Dyson-Schwinger equation for the (inverse) quark propagator. Since this equation determines the dynamically generated mass (i.e. the mass gap between physical objects and the vacuum), it is often called a *gap equation*.

### 4.1 Gap Equation and Propagators

The (unrenormalized) quark gap equation reads

$$iS^{-1}(p) = \gamma^\mu p_\mu - m + ig^2 C_F \int_{\mathbb{R}^4} \frac{d^4 q}{(2\pi)^4} \gamma^\nu S(q) \Gamma^\mu(q, p) D_{\mu\nu}(k) \quad (4.1)$$

where we have set  $k = p - q$ . It is schematically illustrated in figure 4.1 and involves the fully dressed quark propagator (appearing on the right-hand side of the equation as well)  $S$ , the fully dressed gluon propagator  $D_{\mu\nu}$ , a bare quark gluon vertex  $\gamma^\nu$  and a dressed vertex  $\Gamma^\mu$ .

#### 4.1.1 Structure of the Quark Propagator

In covariant gauges, the quark propagator has two independent Dirac tensor structures. As well known, the inverse bare propagator is given by

$$iS_0^{-1}(p) = \not{p} - m + i\varepsilon. \quad (4.2)$$

The full (dressed) propagator can be described in similar way, if one introduces two scalar functions  $A(p^2)$  and  $B(p^2)$ , which describe the “vector” and the “scalar” part of the propagator.

$$iS^{-1}(p) = \not{p} A(p^2) - B(p^2) + i\varepsilon. \quad (4.3)$$

In the non-covariant case, unfortunately, the description gets more involved. As discussed in appendix B, in Coulomb gauge (and other situations which explicitly separate time from space) the number of independent scalar structures increases to four.

In our case, we set

$$iS^{-1} = \gamma^0 p_0 A - B - \gamma^i p_i C + \gamma^0 p_0 \gamma^i p_i D + i\varepsilon \quad (4.4)$$

where  $A = A(\mathbf{p}^2, p_0^2)$  and analogously for the scalar functions  $B$ ,  $C$  and  $D$ .<sup>1</sup> The contraction of  $\gamma^0$  with  $p_0$  and the fact that the scalar coefficients may depend only on the square of  $p_0$  ensures

---

<sup>1</sup>The component  $D$  does not appear in a straightforward decomposition of the covariant expression. It vanishes at tree level and thus does not introduce perturbative divergences (see for example discussion in [168], p.42f). For these reasons it is often neglected

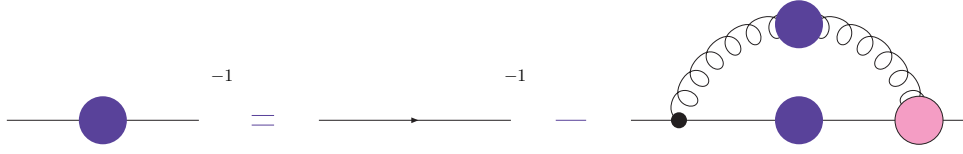


Figure 4.1: Diagrammatic representation of the quark gap equation

that time reversal invariance is respected. From (4.4) we obtain<sup>2</sup>

$$S(p) = i \frac{\gamma^0 p_0 A + B - \gamma^i p_i C + \gamma^0 p_0 \gamma^i p_i D}{p_0^2 A^2 - B^2 - \mathbf{p}^2 C^2 + \mathbf{p}^2 p_0^2 D^2}. \quad (4.5)$$

A Wick rotation  $p_0 \rightarrow -ip_4$  gives  $p_0^2 \rightarrow -p_4^2$  and thus

$$S_E(p) = i \frac{\gamma^4 p_4 A + B - \gamma^i p_i C - \gamma^4 p_4 \gamma^i p_i D}{p_4^2 A^2 + B^2 + \mathbf{p}^2 C^2 + \mathbf{p}^2 p_4^2 D^2}. \quad (4.6)$$

For convenience we introduce the abbreviation

$$d_{\text{quad,E}} := p_4^2 A^2 + B^2 + \mathbf{p}^2 C^2 + \mathbf{p}^2 p_4^2 D^2 \quad (4.7)$$

for the quadratic form that appears as denominator in Euclidean formulation.

#### 4.1.2 Parameterization of the Gluon Propagator

Due to non-covariance, in the expression  $\gamma^\mu D_{\mu\nu} \Gamma^\nu$  the spatial and the temporal components have to be disentangled. This implies that the gluon propagator components  $D_{00}$  and  $D_{ij}$  can (and, as already discussed in chapter 3 do) have a different form.

##### The Mixed Gluon Propagator – $D_{i0}$ and $D_{0j}$

Formally such a decomposition also includes the mixed propagator  $D_{i0}$  (and  $D_{0j}$ , which because of gluon exchange symmetry has to have the same structure). Due to rotational and time reversal invariance  $D_{i0}(k)$  has to be proportional<sup>3</sup> to both to  $k_0$  and  $k_i$ .

$$D_{i0}(k) = D_{0i}(k) = V_M(\mathbf{k}^2, k_0^2) k_0 k_i. \quad (4.8)$$

Since the transversality condition  $k_i A_i = 0$  is imposed in Coulomb gauge<sup>4</sup> one also has for the propagator

$$k_i D_{i0}(k) = k_i \langle A_i A_0 \rangle = \langle k_i A_i A_0 \rangle = \langle 0 \rangle = 0. \quad (4.9)$$

Combining this with (4.8), one obtains

$$\mathbf{k}^2 k_0 V_M(\mathbf{k}^2, k_0^2) = 0, \quad (4.10)$$

which immediately shows that  $V_M(\mathbf{k}^2, k_0^2) \equiv 0$  for  $\mathbf{k} \neq \mathbf{0}$  and  $k_0 \neq 0$ . While, as discussed in appendix A.4, this equation has a nontrivial distributional solution, the physical relevance of this formally possible solution is highly questionable and thus we set  $D_{i0} = D_{0j} = 0$  in the following. Accordingly, the relevant parts of the gluon propagator are  $D_{00}(k)$  and  $D_{ij}(k)$ .

<sup>2</sup>The causal prescription  $+\mathrm{i}\varepsilon$  is from now on implicitly understood. Also note that from  $\not{p} \not{p} = p^2$  it follows in Minkowski space that  $\not{p} \not{p} \equiv \gamma^i \gamma^j p_i p_j = -\mathbf{p}^2$ .

<sup>3</sup>Note that  $k$  is the only vector available for construction of all terms, and both indices of  $D_{i0}$  have to be taken by objects with the correct transformation properties, so the proportionality to  $k_i k_0$  immediately follows.

<sup>4</sup>This is true also in the more formal treatment (briefly mentioned in subsection 1.2.1) which makes use of the Nakanishi-Lautrup field  $b$ . Since  $b$  has no “real” dynamics (there is no kinetic term and no propagator) it can be integrated out for any correlator not explicitly containing it. This imposes the transversality condition on spatial gluons  $A_i$

### The Coulomb Gluons – $D_{00}$

As discussed already in chapter 3,  $D_{00}$  contains an instantaneous part which is believed to be dominant in the infrared as well as a possible non-instantaneous part. Since (to the knowledge of the present author) no information on the non-instantaneous part is available and since it is believed to be subdominant anyhow, we choose to neglect it in the following.

For the instantaneous part, we eliminate the renormalization-flow invariant coupling  $g$  in favor of the running coupling  $\alpha$ ,

$$D_{00}(\mathbf{k}^2, k_0^2) = \frac{i}{g^2} 4\pi V_C(\mathbf{k}^2) \quad \text{with} \quad V_C(\mathbf{k}^2) = \frac{\alpha(\mathbf{k}^2)}{\mathbf{k}^2} \quad (4.11)$$

The form of  $\alpha$  is known in two limits:

- Far in the ultraviolet,  $\mathbf{k}^2 \gg \Lambda_{\text{QCD}}^2$ , one has to find

$$\alpha(\mathbf{k}^2) \simeq \frac{12\pi}{(11N_c - 2N_f) \ln \frac{\mathbf{k}^2}{\Lambda_{\text{QCD}}^2}} \quad \text{i.e.} \quad \lim_{\mathbf{k}^2 \rightarrow \infty} \ln \left( \frac{\mathbf{k}^2}{\Lambda_{\text{QCD}}^2} \right) \alpha(\mathbf{k}^2) = \frac{12\pi}{11N_c - 2N_f} \quad (4.12)$$

in order to recover the results of perturbation theory.

- In the deep infrared,  $\mathbf{k}^2 \ll \Lambda_{\text{QCD}}^2$ , one has

$$\alpha(\mathbf{k}^2) \simeq \frac{2\sigma_C}{\mathbf{k}^2} \quad \text{i.e.} \quad \lim_{\mathbf{k}^2 \rightarrow 0} \mathbf{k}^2 \alpha(\mathbf{k}^2) = 2\sigma_C \quad (4.13)$$

with the Coulomb string tension  $\sigma_C$ , which can be obtained from lattice calculations.

A potential which interpolates between these asymptotic forms has been given by Richardson [166],

$$\alpha(\mathbf{k}^2) = \frac{12\pi}{(11N_c - 2N_f) \ln \left( 1 + \frac{\mathbf{k}^2}{\Lambda^2} \right)}. \quad (4.14)$$

For  $\mathbf{k}^2 \gg \Lambda$  one can neglect the term 1 within the logarithm and recover (4.12) with  $\Lambda = \Lambda_{\text{QCD}}$ , while for  $\mathbf{k}^2 \ll \Lambda_{\text{QCD}}^2$  one can expand the logarithm, which gives

$$\alpha(\mathbf{k}^2) \simeq \frac{12\pi \Lambda^2}{(11N_c - 2N_f) \mathbf{k}^2}. \quad (4.15)$$

In order to recover (4.13), one has to choose

$$\Lambda^2 = \frac{11N_c - 2N_f}{6\pi} \sigma_C \quad \begin{matrix} N_c = 3 \\ N_f = 3 \\ \downarrow \\ = \end{matrix} \quad \frac{9}{2\pi} \sigma_C. \quad (4.16)$$

The advantage of this approach is that since only one physical scale enters the calculation, the influence of this scales is easy to check. The disadvantage of this approach is that only one physical scale enters the calculation, and that for current lattice values of the string tension [145, 203],

$$\sigma_c = 0.300 \div 0.550 \text{ GeV}^2 \quad (4.17)$$

one finds  $\Lambda_{\text{QCD}} = 0.650 \div 0.890 \text{ GeV}$ , which is an extremely large value compared to what is typically given in the literature,  $\Lambda_{\text{QCD}} = 0.150 \div 0.300 \text{ GeV}$ , [40, 72]. It is unclear whether gauge and renormalization ambiguities can make up for that difference.

### The Transverse Gluons – $D_{ij}$

The transverse gluon propagator  $D_{ij}$  has to contain a transverse projector, so the most general parameterization has the form

$$D_{ij} = \frac{i}{g^2} V_T(\mathbf{k}^2, k_0^2) \left( \delta_{ij} - \frac{k_i k_j}{\mathbf{k}^2} \right) \quad (4.18)$$

with a function  $V_T$ . Along the lines of [121, 124] we choose

$$V_T(\mathbf{k}^2, k_0^2) = \frac{Z(\mathbf{k}^2, k_0^2)}{k_0^2 - \omega_g^2(\mathbf{k}^2)} \quad (4.19)$$

$$\omega_g^2(\mathbf{k}^2) = \left( |\mathbf{k}| + \frac{\Lambda^2}{|\mathbf{k}|} \right)^2 = \mathbf{k}^2 + 2\Lambda^2 + \frac{\Lambda^4}{\mathbf{k}^2} \quad (4.20)$$

with a scale  $\Lambda$  which is chosen equal to  $\Lambda_{\text{QCD}}$  and a dressing function  $Z$ . Since in the gap equation the dressing of  $D_{ij}$  cannot be disentangled from the dressing of the vertex  $\Gamma^j$  we set  $Z(\mathbf{k}^2, k_0^2) \equiv 1$  for now; other choices are discussed in sec. 4.3.3. For  $Z = 1$  the ansatz (4.20) has the following features

1. For  $\mathbf{k}^2 \gg \Lambda^2$  one can neglect  $\frac{\Lambda^2}{|\mathbf{k}|}$  compared to  $|\mathbf{k}|$ . Thus one recovers  $\omega_g \sim |\mathbf{k}|$  as by perturbation theory in the regime of small coupling, i.e. large momenta.
2. For  $\mathbf{k}^2 \ll \Lambda^2$  the  $\frac{\Lambda^2}{|\mathbf{k}|}$  term is dominant and for  $\mathbf{k} \rightarrow 0$  the gluon energy (which is up to a constant factor equal to  $\frac{1}{\omega_g}$ ) diverges. As discussed in subsection 1.3 this can be interpreted as a manifestation of gluon confinement.
3. Also in the intermediate momentum regime, this ansatz is in good agreement both with lattice results [60] and with results from Hamiltonian calculations [78, 79].

#### 4.1.3 The Resulting Gap Equation

With the harsh truncation  $\Gamma^\mu(q, p) \rightarrow \gamma^\mu$  and by plugging the parameterizations (4.4), (4.11) and (4.18) into (4.1) one can obtain a set of scalar equations by projecting on single propagator tensor components. After working out everything in Minkowski space, one can hope to safely Wick-rotate all integrals to Euclidean space.

For realistic choices of (4.11) and (4.18) the integrals appearing in the gap equation are UV-divergent and thus have to be renormalized. One finds (see [124] and also appendix A.3) the renormalized gap equation

$$iS^{-1}(p) = Z_{(\mu)} \gamma^\mu p_\mu - Z_m m + ig^2 C_F \int_{\mathbb{R}^4} \frac{d^4 q}{(2\pi)^4} \gamma^\nu S(q) \Gamma^\mu(q, p) D_{\mu\nu}(k). \quad (4.21)$$

In Coulomb gauge the renormalization constant  $Z_0$  can be different from  $Z_i$  (which is equal for  $i = 1, 2, 3$ ). In practical calculations, renormalization is performed by momentum subtraction: One considers the subtracted quantities  $A(\mathbf{p}^2, p_4^2) - A(\boldsymbol{\mu}^2, \mu_4^2)$  for a renormalization point  $(\boldsymbol{\mu}, \mu_4)$  far in the ultraviolet. This subtraction reduces the renormalization constants to their tree-level expressions,

$$Z_{(0)} = 1, \quad Z_{(i)} = 1, \quad mZ_m = m_0. \quad (4.22)$$

#### 4.1.4 Applications of the Quark Propagator: the Mass Function

Any solution for the functions  $A$ ,  $B$ ,  $C$ ,  $D$  can be employed (together with an appropriate ansatz for the quark-quark scattering kernel) in a Bethe-Salpeter equation (relativistic two-particle bound-state equation, see sec. 4.4) in order to obtain information about mesons. A more ambitious (and significantly more difficult) way to use the propagator is within a Faddeev equation (the corresponding three-body equation) to study baryons.

However, one often wants to make quick statements about (pseudo)physical numbers without invoking a bound-state equation. Therefore, one usually introduces a *mass function*  $M(\mathbf{p}^2, p_0^2)$ , which can be interpreted as the momentum-dependent mass of a “constituent quark”.

The idea behind the definition of this function is that (4.3) can be rewritten as

$$iS^{-1}(p) = A(p^2) \left( \not{p} - \frac{B(p^2)}{A(p^2)} \right) + i\varepsilon. \quad (4.23)$$

This reveals that for the dressed propagator the quantity  $\frac{B}{A}$  plays a role similar to the mass  $m$  in the bare propagator (4.2) and thus one can set  $M(p^2) := \frac{B(p^2)}{A(p^2)}$  and hope that this quantity describes bare plus dynamically generated mass.

In the non-covariant formalism such considerations are less straightforward, one has to examine the poles of the  $p_0$ -integrated propagator  $S$ . The position of the poles can be set in correspondence with a constituent quark mass. From (4.5) we obtain<sup>5</sup>

$$\begin{aligned} S(\mathbf{p}) &= -i \int_{-\infty}^{\infty} \frac{\gamma^0 p_0 A + B - \gamma^i p_i C + \gamma^0 p_0 \gamma^i p_i D}{(A^2 + \mathbf{p}^2 D^2) p_0^2 - B^2 - \mathbf{p}^2 C^2} dp_0 \\ &\stackrel{\text{sym}}{=} -i \int_{-\infty}^{\infty} \frac{B - \gamma^i p_i C}{A^2 + \mathbf{p}^2 D^2} \cdot \frac{dp_0}{p_0^2 - \frac{B^2 + \mathbf{p}^2 C^2}{A^2 + \mathbf{p}^2 D^2}}. \end{aligned} \quad (4.24)$$

To proceed further with this expression we have to make some assumptions about the  $p_0^2$ -dependence of the coefficient functions  $A$ ,  $B$ ,  $C$  and  $D$ . According to the argument given in section 3.2 one expects such functions to be  $p_0$ -independent in the strict Coulomb gauge – an expectation largely confirmed by the numerical results presented in section 4.3.

Assuming such  $p_0$ -independence, the integral can be done analytically,

$$\begin{aligned} S(\mathbf{p}) &= -i \frac{B - \gamma^i p_i C}{A^2 + \mathbf{p}^2 D^2} \int_{-\infty}^{\infty} \frac{dp_0}{\left(p_0 - \sqrt{\frac{B^2 + \mathbf{p}^2 C^2}{A^2 + \mathbf{p}^2 D^2}}\right) \left(p_0 + \sqrt{\frac{B^2 + \mathbf{p}^2 C^2}{A^2 + \mathbf{p}^2 D^2}}\right)} \\ &\stackrel{\text{causal prescr.}}{=} -i \frac{B - \gamma^i p_i C}{A^2 + \mathbf{p}^2 D^2} \lim_{\varepsilon \rightarrow 0} \int_{-\infty}^{\infty} \frac{dp_0}{\left(p_0 - \sqrt{\frac{B^2 + \mathbf{p}^2 C^2}{A^2 + \mathbf{p}^2 D^2}} + i\varepsilon\right) \left(p_0 + \sqrt{\frac{B^2 + \mathbf{p}^2 C^2}{A^2 + \mathbf{p}^2 D^2}} - i\varepsilon\right)} \end{aligned} \quad (4.25)$$

We now set  $\kappa := \sqrt{\frac{B^2 + \mathbf{p}^2 C^2}{A^2 + \mathbf{p}^2 D^2}}$  and  $f(p_0) := \frac{1}{(p_0 - \kappa + i\varepsilon)(p_0 + \kappa - i\varepsilon)}$ . Residue calculus yields

$$\begin{aligned} I_\varepsilon &:= \int_{-\infty}^{\infty} \frac{dp_0}{(p_0 - (\kappa - i\varepsilon))(p_0 - (-\kappa + i\varepsilon))} = 2\pi i \{ \text{Res}(f, -\kappa + i\varepsilon) - \text{Res}(f, \kappa - i\varepsilon) \} \\ &= 2\pi i \left\{ \frac{1}{p_0 - \kappa + i\varepsilon} \Big|_{p_0 \rightarrow -\kappa + i\varepsilon} - \frac{1}{p_0 + \kappa - i\varepsilon} \Big|_{p_0 \rightarrow \kappa - i\varepsilon} \right\} = \pi i \left\{ \frac{1}{-\kappa + i\varepsilon} - \frac{1}{\kappa - i\varepsilon} \right\} \\ &= -\frac{\pi i}{2(\kappa - i\varepsilon)} \xrightarrow{\varepsilon \rightarrow 0} -\frac{\pi i}{2} \frac{1}{\kappa} = -\frac{\pi i}{2} \sqrt{\frac{A^2 + \mathbf{p}^2 D^2}{B^2 + \mathbf{p}^2 C^2}} \end{aligned} \quad (4.26)$$

<sup>5</sup>Note that the coefficients depend on  $p_0^2$ , i.e. only on even combinations of  $p_0$ . Thus one can immediately apply some symmetry arguments to get rid of antisymmetric parts of such an expression.

This yields

$$S(\mathbf{p}) = -\frac{\pi}{2} \frac{B - \gamma^i p_i C}{\sqrt{A^2 + \mathbf{p}^2 D^2} \sqrt{B^2 + \mathbf{p}^2 C^2}}, \quad (4.27)$$

which suggests that either  $\frac{B}{C}$  or  $\frac{A}{D}$  might be regarded as the mass of such a constituent quark. Since  $\frac{A}{D}$  is not defined at tree-level and  $D$  might even vanish identically we define the mass function (for the Wick-rotated system) as

$$M(\mathbf{p}^2, p_4^2) := \frac{B(\mathbf{p}^2, p_4^2)}{C(\mathbf{p}^2, p_4^2)}. \quad (4.28)$$

It turns out that with the form (4.11) for  $D_{00}$  both  $B$  and  $C$  are divergent quantities which have to be regularized in order to obtain sensible results. Such a regularization can be achieved for example by the substitution

$$\mathbf{k}^2 \rightarrow \mathbf{k}^2 + \mu_{\text{IR}}^2 \quad (4.29)$$

with  $\mu_{\text{IR}}^2 > 0$ . While both  $B$  and  $C$  diverge for  $\mu_{\text{IR}} \rightarrow 0$ , the ratio  $M = B/C$  remains well-defined. We now attempt to separate  $B$  and  $C$  into a divergent (for  $\mu_{\text{IR}} \rightarrow 0$ ) and a regular part [5],

$$B = B_{\text{div}} + B_{\text{reg}}, \quad C = C_{\text{div}} + C_{\text{reg}}. \quad (4.30)$$

Obviously this is ambiguous in general, since any  $\mu_{\text{IR}}$ -finite quantity can be freely shifted between the divergent and the regular part. Such a separation is only possible with additional assumptions about analyticity properties. We now assume that  $B$ ,  $C$  and the mass  $M$  can be expanded in the form

$$B = \frac{B^{(-1)}}{\mu_{\text{IR}}} + B^{(0)} + B^{(1)} \mu_{\text{IR}} + \mathcal{O}(\mu_{\text{IR}}^2) \quad (4.31)$$

$$C = \frac{C^{(-1)}}{\mu_{\text{IR}}} + C^{(0)} + C^{(1)} \mu_{\text{IR}} + \mathcal{O}(\mu_{\text{IR}}^2) \quad (4.32)$$

$$M = M^{(0)} + M^{(1)} \mu_{\text{IR}} + \mathcal{O}(\mu_{\text{IR}}^2). \quad (4.33)$$

Then we have

$$M^{(0)} = \lim_{\mu_{\text{IR}} \rightarrow 0} \frac{B}{C} = \frac{B^{(-1)}}{C^{(-1)}}, \quad \text{i.e.} \quad B^{(-1)} = M^{(0)} C^{(-1)}. \quad (4.34)$$

So on the one hand, the ratio of the divergent parts determines the mass and the regular parts seem to drop out completely. On the other hand, using this result, we find

$$M^{(0)} + M^{(1)} \mu_{\text{IR}} + \mathcal{O}(\mu_{\text{IR}}^2) = \frac{\frac{M^{(0)} C^{(-1)}}{\mu_{\text{IR}}} + B^{(0)} + B^{(1)} \mu_{\text{IR}} + \mathcal{O}(\mu_{\text{IR}}^2)}{\frac{C^{(-1)}}{\mu_{\text{IR}}} + C^{(0)} + C^{(1)} \mu_{\text{IR}} + \mathcal{O}(\mu_{\text{IR}}^2)}. \quad (4.35)$$

Rearrangement yields (note that from multiplication with  $\mu_{\text{IR}}^{-1}$  we lose one order of  $\mu_{\text{IR}}$  which we can keep track of)

$$\cancel{\frac{M^{(0)} C^{(-1)}}{\mu_{\text{IR}}}} + M^{(0)} C^{(0)} + M^{(1)} C^{(-1)} + \mathcal{O}(\mu_{\text{IR}}) = \cancel{\frac{M^{(0)} C^{(-1)}}{\mu_{\text{IR}}}} + B^{(0)} + \mathcal{O}(\mu_{\text{IR}}), \quad (4.36)$$

i.e. for  $\mu_{\text{IR}} \rightarrow 0$  we find

$$M^{(0)} = \frac{B^{(0)}}{C^{(0)}} - \frac{M^{(1)} C^{(-1)}}{C^{(0)}}. \quad (4.37)$$

So the regular parts are closely related to the mass as well, and if  $M^{(1)}$  was to vanish, the mass could be expressed solely in terms of the regular parts.

## 4.2 The Quark-Gluon Vertex

### 4.2.1 Naive Decomposition

The considerations in appendix B show that the quark-gluon vertex in Coulomb gauge formally has 32 components. One expects the Slavnov-Taylor identities to fix the longitudinal components, so making use these identities will reduce the number of independent components.

Unfortunately already for covariant gauges the Slavnov-Taylor identities are too complicated to be directly incorporated and the issue further complicated in the non-covariant formalism. Therefore, at this point, we only employ the most naive basis (which is most transparent, but not well-suited for exploiting Ward-like identities). In this basis the full tensor structure of the quark-gluon vertex is given by

$$\begin{aligned} \Gamma_0^a(p, q) = t^a & \left( \Gamma_{0a}^A \mathbb{1} + \Gamma_{0b}^S \gamma^0 + \Gamma_{0c}^A (\not{p} - \not{q}) + \Gamma_{0d}^A (\not{p} + \not{q}) + \Gamma_{0e}^S (\not{p} - \not{q}) \gamma^0 \right. \\ & \left. + \Gamma_{0f}^S (\not{p} + \not{q}) \gamma^0 + \Gamma_{0g}^A [\not{p}, \not{q}] + \Gamma_{0h}^S [\not{p}, \not{q}] \gamma^0 \right) \end{aligned} \quad (4.38)$$

for the 0-component of the vertex and

$$\begin{aligned} \Gamma_i^a(p, q) = t^a & \left\{ \left( \Gamma_{1a}^S \mathbb{1} + \Gamma_{1b}^A \gamma^0 + \Gamma_{1c}^S (\not{p} - \not{q}) + \Gamma_{1d}^S (\not{p} + \not{q}) + \Gamma_{1e}^A (\not{p} - \not{q}) \gamma^0 \right. \right. \\ & \left. \left. + \Gamma_{1f}^A (\not{p} + \not{q}) \gamma^0 + \Gamma_{1g}^S [\not{p}, \not{q}] + \Gamma_{1h}^A [\not{p}, \not{q}] \gamma^0 \right) \gamma_i \right. \\ & + \left( \Gamma_{2a}^S \mathbb{1} + \Gamma_{2b}^A \gamma^0 + \Gamma_{2c}^S (\not{p} - \not{q}) + \Gamma_{2d}^S (\not{p} + \not{q}) + \Gamma_{2e}^A (\not{p} - \not{q}) \gamma^0 \right. \\ & \left. + \Gamma_{2f}^A (\not{p} + \not{q}) \gamma^0 + \Gamma_{2g}^S [\not{p}, \not{q}] + \Gamma_{2h}^A [\not{p}, \not{q}] \gamma^0 \right) p_i \\ & + \left( \Gamma_{3a}^S \mathbb{1} + \Gamma_{3b}^A \gamma^0 + \Gamma_{3c}^S (\not{p} - \not{q}) + \Gamma_{3d}^S (\not{p} + \not{q}) + \Gamma_{3e}^A (\not{p} - \not{q}) \gamma^0 \right. \\ & \left. + \Gamma_{3f}^A (\not{p} + \not{q}) \gamma^0 + \Gamma_{3g}^S [\not{p}, \not{q}] + \Gamma_{3h}^A [\not{p}, \not{q}] \gamma^0 \right) q_i \end{aligned} \quad (4.39)$$

for the spatial part.

As discussed in section B.3, time reversal invariance gives an additional constraint concerning symmetry properties of the coefficient functions. More precisely, all functions with superscript  $S$  must be symmetric in the combined time components of momenta  $p$  and  $q$ , those with superscript  $A$  antisymmetric. A decomposition of the gap equation, employing the naive decomposition of the vertex and heavily using the computer algebra system FORM [199], is given in section A.5.

### 4.2.2 The Ball-Chiu and the Curtis-Pennington Vertex

For QED in the linear covariant gauge, Ball and Chiu [25, 26] have given a basis for the tensor decomposition of the fermion-photon vertex. In principle one has to deal with twelve spinor components, but four of them (the so-called “longitudinal part”) are determined by the corresponding Ward-Takashi identity. Using this basis (which is particularly well-suited for one-loop perturbative calculations) Curtis and Pennington [62] have constructed a vertex which respects multiplicative renormalizability and which is widely used in the covariant case.

In spite of some effort invested there, the translation to the non-covariant case, in particular the Coulomb gauge (where renormalizability is an unsettled issue), did not yield satisfying results. Apart from various conceptual problems, the resulting expressions turned out to be too involved to be useful for the numerical calculations performed in sec. 4.3.



### 4.2.3 Restrictions from Ward Identities

The quark-gluon vertex is restricted by its Slavnov-Taylor identity which contains the quark-ghost scattering kernel [140] and is considered as too complicated to be put to practical use.

So we modestly try to obtain some information from the Abelian Ward-Takahashi identity

$$(p_\mu - q_\mu)\Gamma^\mu = S^{-1}(p) - S^{-1}(q), \quad (4.40)$$

which is assumed to hold approximately also in the non-Abelian case. Employing the parameterization (4.4) for the quark propagator  $S$  and denoting the gluon momentum by  $k = p - q$ , we obtain

$$\begin{aligned} k_\mu \Gamma^\mu &\equiv k_0 \Gamma^0 + k_i \Gamma^i = -i \left\{ \gamma^0 (p_0 A(p) - q_0 A(q)) - (B(p) - B(q)) \right. \\ &\quad \left. - \gamma^j (p_j C(p) - q_j C(q)) + \gamma^0 \gamma^j (p_0 p_j D(p) - q_0 q_j D(q)) \right\} \end{aligned} \quad (4.41)$$

We are in particular interested in the case when  $p \approx q$  i.e. when the gluon momentum is small compared to all other scales. In this case we can set  $q = p - k$  and neglect in the following all terms of second or higher order in  $k$ . Moreover we can expect that for small  $k_0$  and  $k_i$  we can (assuming sufficient regularity properties) reliably use the linear approximation

$$\begin{aligned} A(q_0^2, \mathbf{q}^2) &\approx A(p_0^2, \mathbf{p}^2) + A_{p_0^2} ((p_0 - k_0)^2 - p_0^2) + A_{\mathbf{p}^2} ((\mathbf{p} - \mathbf{k})^2 - \mathbf{p}^2) \\ &= A(p_0^2, \mathbf{p}^2) + A_{p_0^2} (p_0^2 - 2p_0 k_0 + k_0^2 - p_0^2) + A_{\mathbf{p}^2} (\mathbf{p}^2 - 2\mathbf{p} \cdot \mathbf{k} + \mathbf{k}^2 - \mathbf{p}^2) \\ &= A(p_0^2, \mathbf{p}^2) - 2 \left( A_{p_0^2} p_0 k_0 + A_{\mathbf{p}^2} (\mathbf{p} \cdot \mathbf{k}) \right) =: A(p_0^2, \mathbf{p}^2) - 2 dA \end{aligned} \quad (4.42)$$

where we have used the abbreviations

$$A_{p_0^2} := \left. \frac{\partial A(x_1, x_2)}{\partial x_1} \right|_{(x_1, x_2) = (p_0^2, \mathbf{p}^2)} \quad (4.43)$$

$$A_{\mathbf{p}^2} := \left. \frac{\partial A(x_1, x_2)}{\partial x_2} \right|_{(x_1, x_2) = (p_0^2, \mathbf{p}^2)}. \quad (4.44)$$

The same is done for the functions  $B$ ,  $C$  and  $D$  and we obtain

$$\begin{aligned} k_\mu \Gamma^\mu &\approx -i \left\{ \gamma^0 (2p_0 dA + k_0 A(p) - \cancel{2k_0 dA}) - 2dB - \gamma^j (2p_j dC + k_j C(p) - \cancel{2k_j dC}) \right. \\ &\quad \left. + \gamma^0 \gamma^j (2p_0 p_j dD + p_0 k_j D(p) - \cancel{2p_0 k_j dD}) + p_i k_0 D(p) - \cancel{2p_i k_0 dD} \right\} \\ &= -i \left\{ k_0 \left[ 2\gamma^0 p_0^2 A_{p_0^2} + \gamma_0 A(p) - 2p_0 B_{p_0^2} - 2 \cancel{p_0 p_0} C_{p_0^2} + 2\gamma^0 p_0^2 \cancel{p_0} D_{p_0^2} \right] \right. \\ &\quad \left. + k_i \left[ 2\gamma^0 p_0^2 A_{\mathbf{p}^2} - 2p^i B_{\mathbf{p}^2} - 2 \cancel{p^i p^i} C_{\mathbf{p}^2} - \gamma^i C(p) + 2\gamma^0 p_0 \cancel{p^i} D_{\mathbf{p}^2} + \gamma^0 p_0 \gamma^i D(p) \right] \right\} \\ &\stackrel{(\text{also})}{=} -i (k_0 i\Gamma^0 + k_i i\Gamma^i), \end{aligned} \quad (4.45)$$

where we have neglected all terms of  $\mathcal{O}(k^2)$ . (Note that  $dA(p)$  defined in (4.42) is  $\mathcal{O}(k)$  and the same is of course true for  $dB(p)$ ,  $dC(p)$  and  $dD(p)$ .) So we find for small  $k$

$$i\Gamma^0 \approx \gamma_0 A(p) + 2\gamma^0 p_0^2 A_{p_0^2} - 2p_0 B_{p_0^2} - 2 \cancel{p_0 p_0} C_{p_0^2} + 2\gamma^0 p_0^2 \cancel{p_0} D_{p_0^2}, \quad (4.46)$$

$$i\Gamma^i \approx -\gamma^i C(p) + \gamma^0 p_0 \gamma^i D(p) + 2\gamma^0 p_0^2 A_{\mathbf{p}^2} - 2p^i B_{\mathbf{p}^2} - 2 \cancel{p^i p^i} C_{\mathbf{p}^2} + 2\gamma^0 p_0 \cancel{p^i} D_{\mathbf{p}^2}. \quad (4.47)$$

In the crudest approximation we can neglect all the derivatives  $A_{p_0^2}$ ,  $A_{\mathbf{p}^2}$ ,  $B_{p_0^2}$ ,  $\dots$ . Doing so, we find

$$\Gamma^0 \sim \gamma_0 A(p), \quad \Gamma^i \sim \gamma^i (C(p) - \gamma^0 p_0 D(p)). \quad (4.48)$$

As described in sec. 4.3, for a bare-vertex truncation we find an infrared-finite function  $A$ , which is close to one. While the calculations including  $D$  are not stable, there are indications that this component is small or vanishes altogether, while the coefficient  $C$  diverges  $\sim \frac{1}{\mu_{\text{IR}}}$ . From this simple analysis we could conclude that  $\Gamma^0$  may stay almost bare in a more advanced vertex ansatz, while the spatial part  $\Gamma^i$  has to be endowed with an infrared-divergent part.

While inclusion of the derivatives does not seriously affect the result for  $\Gamma^i$ , matters are more subtle for  $\Gamma^0$ , where one encounters the derivatives of the infrared divergent functions  $B$  and  $C$ . The vertex thus can only stay finite if

$$B_{p_0^2} + \not{p} C_{p_0^2} \leq \mathcal{O}(\mu_{\text{IR}}^0) = \mathcal{O}(1), \quad (4.49)$$

One possibility for this is that  $B_{p_0^2}$  and  $C_{p_0^2}$  both vanish. If they don't, one can neglect terms  $\mathcal{O}(1)$  as compared to the infrared-divergent functions and obtains

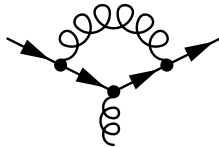
$$B_{p_0^2} \approx -\not{p} C_{p_0^2} \quad \xrightarrow{\text{(square)}} \quad B_{p_0^2} \approx \not{p}^2 C_{p_0^2}. \quad (4.50)$$

This relation can be checked for numerical solutions of the system, and a violation for  $p \approx q$  would indicate inconsistencies with a IR-finite vertex  $\Gamma^0$ .

#### 4.2.4 Perturbative Investigation of the Vertex


At one-loop order, there are contributions to the vertex from the diagrams

“Abelian” =



and

“Non-Abelian” =



(4.51)

The first of these diagrams is present also in the Abelian context, while the other one is genuinely non-Abelian. Most perturbative investigations focus on the Abelian diagram, but the non-Abelian one is enhanced by a factor of  $N_C^2$  [141].

As outlined in sec. C.1.2, all integrals that appear in these two diagrams can be derived from two “master integrals”, which, in principle, could be evaluated with the means of NDIM. The practical calculation, however, is extremely involved and has not been accomplished so far.

#### 4.2.5 Other Forms for the Quark-Gluon Vertex

The Slavnov-Taylor identity for the quark-gluon vertex in Landau gauge is given by [140]

$$G^{-1}(k^2) i k_\mu \Gamma_\mu(q, k) = S^{-1}(p) H(q, p) - \overline{H}(q, p) S^{-1}(q), \quad (4.52)$$

with  $G(k^2)$  denoting the ghost dressing function and  $H(q, p)$  denoting the ghost-quark scattering kernel. In [81], an approximate solution has been given in the form

$$\Gamma_\nu(q, k) = V_\nu^{\text{abel}}(p, q, k) W^{\text{-abel}}(p^2, q^2, k^2) \quad (4.53)$$

where  $V_\nu^{\text{abel}}$  carries the tensor structure and is chosen as a Ball-Chiu or Curtis-Pennington vertex. The function  $W^{\text{-abel}}$  is introduced in order to ensure that (i) the quark mass function ( $p^2$ ) is independent of the renormalization point and (ii) the anomalous dimension of the mass function known from perturbation theory is recovered in the UV-limit.

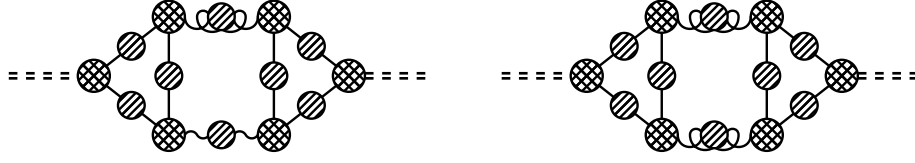


Figure 4.2: Two diagrams contributing to the mass of the  $\eta'$  meson.

#### 4.2.6 Considerations on an Infrared-divergent Vertex $\Gamma_i$

As it has been shown in [7], in Landau gauge the quark-gluon vertex has infrared-divergent components. This is not surprising, since the Landau-gauge gluon propagator is infrared vanishing and the ghosts – responsible for confinement in the Yang-Mills sector – do not directly interact with quarks. Thus another element has to carry the necessary infrared divergence which should lead to the expected vanishing of the quark propagator in the infrared.

Due to the similarities of 3-dimensional Landau and 4-dimensional Coulomb gauge, it does not seem unreasonable to expect also the spatial part of the Coulomb-gauge vertex,  $\Gamma_i$ , to be infrared divergent. On the other hand, since the Coulomb gluons already provide (over)confinement, such a divergence is not necessary to explain quark confinement. One-gluon exchange is sufficient for that.

In the following we summarize and discuss several arguments in regarding possible infrared divergent structures contained in the quark-gluon vertex.

- **The Hamiltonian Formalism:** In the Hamiltonian formalism, discussed in sec. 3.3, the quark-gluon vertex enters at certain off-diagonal elements of the Hamiltonian<sup>6</sup>,

	$ q\rangle$	$ qA\rangle$	$ q\bar{q}\rangle$	$ q\bar{q}A\rangle$	$\dots$
$\langle q $	$H_q$	*			$\dots$
$\langle qA $	*	$H_{qA}$			$\dots$
$\langle q\bar{q} $			$H_{qq}$	*	$\dots$
$\langle q\bar{q}A $			*	$H_{qqA}$	$\dots$
$\vdots$	$\vdots$	$\vdots$	$\vdots$	$\vdots$	$\ddots$

(4.54)

here marked with an asterik \*. A uniformly infrared-divergent vertex would break diagonal dominance of the operator which would be rather unexpected.

- **Meson Equations:** In the quark gap equation (4.1) one encounters a combination of a bare spatial quark-gluon vertex, a (presumably  $\sim \mathbf{k}^2$  infrared-suppressed) transverse gluon propagator and a dressed spatial quark-gluon vertex. To trigger chiral symmetry breaking and yield an effect comparable to that of the Coulomb gluons,  $\Gamma_i$  would have to carry a divergence of order  $\mathbf{k}^{-6}$ .

On the other hand, in meson diagrams as depicted in figure 4.2.6, one finds a combination of one transverse gluon propagator and *two* dressed quark-gluon vertices. Here a vertex  $\Gamma_i \sim \mathbf{k}^{-6}\gamma_i$  would yield an interaction diverging like  $\mathbf{k}^{-10}$ , which is hard to accomodify with the framework of relativistic quantum field theory.

<sup>6</sup>The author is grateful to Felipe Llanes-Estrada for bringing that fact to his attention.

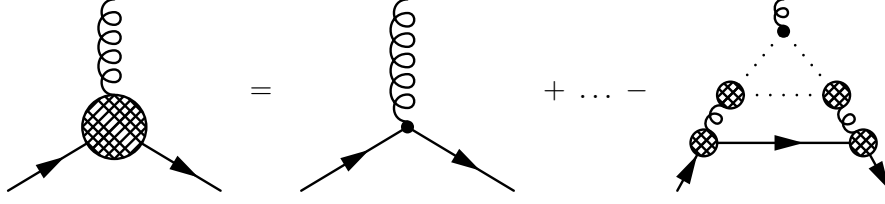


Figure 4.3: Part of the skeleton expansion of the vertex DSE in Landau gauge (all internal propagators are dressed)

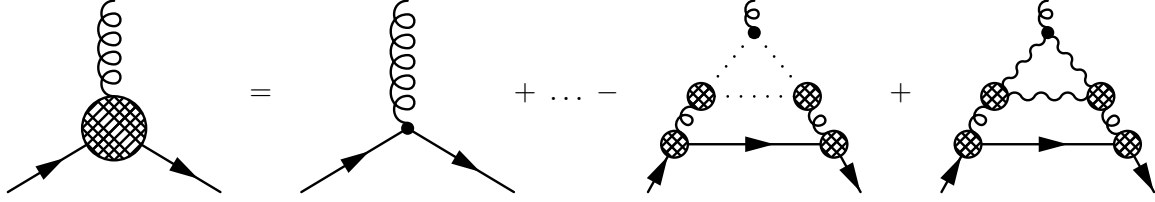


Figure 4.4: Part of the skeleton expansion of the vertex DSE in Coulomb gauge (all internal propagators are dressed)

- **Origin of the Divergence:** The infrared divergence of the Landau-gauge quark-gluon vertex is closely connected to the diagram depicted in figure 4.2.6, which is obtained in a skeleton expansion of the vertex Dyson-Schwinger equation.

In Coulomb gauge, a corresponding skeleton expansion contains additional terms, in particular those explicitly displayed in figure 4.2.6. The two diagrams are expected to (at least to some extent) cancel each other, thus (at least partially) removing the source of infrared divergence present in Landau gauge.

Consequently, while there might be infrared divergences in the Coulomb gauge quark-gluon vertex, one should not expect that they are of the same type as those found in Landau gauge.

- **Consistency of the Skeleton Expansion:** In Coulomb gauge the vertex DSE contains a  $q\bar{q}A_0A_0$  four point function. A skeleton expansion of this function is given by

(all internal propagators being dressed). In order for the skeleton expansion to make sense, the second term should not be more infrared singular than the first one.

Thus the combined effect of

- introduction of one additional  $D_{00}$ -propagator,
- replacement of a  $\Gamma_0$  vertex by the combination  $\Gamma_i D_{ij} \Gamma_{j00}^{(3g)}$ , performed twice
- and one additional momentum integration

should not be an increase the power of infrared divergence. This is hard to accomplish with a strongly infrared divergent  $\Gamma_i$ -vertex.

### 4.3 Truncation Schemes and Numerical Results

Having obtained the general form of the quark gap equation in extended rainbow truncation, we now turn to a discussion of the numerical solution of this equation.

#### 4.3.1 The Instantaneous Approximation

The Coulomb gap equation with an infrared-divergent kernel has first been studied numerically in the pioneering work of [1] and [6]. At that time the only way to have a chance of solve this equation was to employ severe truncations. So not the standard rainbow truncation ( $\Gamma_i \rightarrow \gamma_i$ ,  $\Gamma_0 \rightarrow \gamma_0$ ) was employed, but more drastically, the influence of the transverse gluon propagator has been neglected completely by setting  $\gamma_i \rightarrow 0$ .

In this case  $D$  drops out and one obtains  $A(\mathbf{p}^2, p_0^2) \equiv 1$ . When employing a purely instantaneous ansatz for  $D_{00}$  one can show that  $B$  and  $C$  do not depend on  $p_0$ . Thus the  $p_0$  integration in the integral equations can be done analytically and one is left with two coupled integral equations for two functions of only one variable  $\mathbf{p}^2$ .

Later the solution of the instantaneous approximation has also been used as an input in the Bethe-Salpeter equation (see sec. 4.4) for studies of meson properties [11]. While being quantitatively far off, this approach nevertheless yields a couple of interesting results: The Gell-Mann–Oakes–Renner relation  $M_\pi \propto m_{\text{quark}}^2$  is nicely fulfilled, the mass of the unphysical diquarks diverges if the infrared cutoff is removed, while meson masses, but also diquark radii remain finite. The latter result can be invoked as a justification for quark-diquark ansätze to describe baryons [75].

#### 4.3.2 Inclusion of Transverse Gluons and Retardation

**Previous Work** The treatment of the Coulomb gauge gap equation has been extended to include transverse gluons and possible retardation effects [121] (neglecting the component  $D$  of the quark propagator).

The numerical procedure has been significantly improved in [124]: The integral equations were solved by iteration, employing the  $\varepsilon$ -algorithm to accelerate convergence; the momentum integrals were performed by iterated adaptive Gauß-Kronrod integration,

The initial hope of the project was to obtain quantitatively reasonable results, in particular a “constituent quark mass”<sup>7</sup>  $m_{\text{CQ}} \approx 350 \text{ MeV}$  as opposed to  $m_{\text{CQ}} \approx 100 \text{ MeV}$  obtained in the instantaneous approximation with a bare-vertex truncation.

This has not been achieved: The inclusion of transverse gluons, employing a bare vertex  $\gamma_i t^a$  as an approximation to  $\Gamma_i^a$ , and the explicit treatment of possible retardation effects ( $A(\mathbf{p}^2) \rightarrow A(\mathbf{p}^2, p_0^2)$  etc.) did not significantly change the picture. In particular the value of the mass function stayed almost the same; the  $p_0^2$ -dependency was small (for  $A$ ) or essentially absent (for  $B$  and  $C$ ).

**New Results** On second thought, the results found in [121, 124] are not particular surprising. In the deep infrared the transverse gluons vanish  $\sim \mu_{\text{IR}}^2$ , while the Coulomb gluons diverge  $\sim \mu_{\text{IR}}^{-4}$ .

So in the (numerically performed) limit  $\mu_{\text{IR}} \rightarrow 0$  the effect of the transverse gluons is expected to vanish, while the instantaneous part of  $D_{00}$  (which is of course  $p_0^2$ -independent) completely dominates the system. Depending on the point of view, the  $p_0^2$ -independence of the propagator components can either be regarded as very deep (a direct manifestation of the remnant symmetry, as discussed in sec. 3.2.1) or as rather trivial (a simple consequence of comparing powers of  $\mu_{\text{IR}}$ ).<sup>8</sup>

<sup>7</sup>The constituent quark mass is usually defined as  $m_{\text{CQ}} := M(\mathbf{0}^2)$  or as  $m_{\text{CQ}} := M(\mathbf{p}_*^2)$  where  $M(\mathbf{p}_*^2) = \mathbf{p}_*^2$ .

<sup>8</sup>It has been explicitly checked that also for strongly  $p_0^2$ -dependent initial guesses the same  $p_0^2$ -independent solutions arise. Thus a propagator  $\sim \delta(t)$  is not only permitted by the system. but actually enforced.

$$\begin{aligned}
A(\mathbf{p}^2, p_4^2) &= 1 - \frac{4\pi}{p_4} \int_0^\infty dq q^2 \int_{\mathbb{R}} dq_4 \frac{q_4 A(\mathbf{q}^2, q_4^2)}{d_{\text{quad},E}} \int_{-1}^1 d(\cos \vartheta) V_C(\mathbf{k}^2) \\
&\quad + \frac{2}{p_4} \int_0^\infty dq q^2 \int_{\mathbb{R}} dq_4 \frac{q_4 A(\mathbf{q}^2, q_4^2)}{d_{\text{quad},E}} \int_{-1}^1 d(\cos \vartheta) V_T(\mathbf{k}^2, k_4^2) \\
B(\mathbf{p}^2, p_4^2) &= m_0 + 4\pi \int_0^\infty dq q^2 \int_{\mathbb{R}} dq_4 \frac{B(\mathbf{q}^2, q_4^2)}{d_{\text{quad},E}} \int_{-1}^1 d(\cos \vartheta) V_C(\mathbf{k}^2) \\
&\quad + 2 \int_0^\infty dq q^2 \int_{\mathbb{R}} dq_4 \frac{B(\mathbf{q}^2, q_4^2)}{d_{\text{quad},E}} \int_{-1}^1 d(\cos \vartheta) V_T(\mathbf{k}^2, k_4^2) \\
C(\mathbf{p}^2, p_4^2) &= 1 + \frac{4\pi}{p} \int_0^\infty dq q^3 \int_{\mathbb{R}} dq_4 \frac{C(\mathbf{q}^2, q_4^2)}{d_{\text{quad},E}} \int_{-1}^1 d(\cos \vartheta) V_C(\mathbf{k}^2) \cos \vartheta \\
&\quad - 2 \int_0^\infty dq q^4 \int_{\mathbb{R}} dq_4 \frac{C(\mathbf{q}^2, q_4^2)}{d_{\text{quad},E}} \int_{-1}^1 d(\cos \vartheta) \frac{V_T(\mathbf{k}^2, k_4^2) (1 + \cos^2 \vartheta)}{\mathbf{k}^2} \\
&\quad + \frac{2}{p} \int_0^\infty dq q^3 \int_{\mathbb{R}} dq_4 \frac{(p^2 + q^2) C(\mathbf{q}^2, q_4^2)}{d_{\text{quad},E}} \int_{-1}^1 d(\cos \vartheta) \frac{V_T(\mathbf{k}^2, k_4^2) \cos \vartheta}{\mathbf{k}^2} \\
D(\mathbf{p}^2, p_4^2) &= 0 + \frac{4\pi}{p p_4} \int_0^\infty dq q^3 \int_{\mathbb{R}} dq_4 \frac{q_4 D(\mathbf{q}^2, q_4^2)}{d_{\text{quad},E}} \int_{-1}^1 d(\cos \vartheta) V_C(\mathbf{k}^2) \cos \vartheta \\
&\quad + \frac{2}{p_4} \int_0^\infty dq q^4 \int_{\mathbb{R}} dq_4 \frac{q_4 D(\mathbf{q}^2, q_4^2)}{d_{\text{quad},E}} \int_{-1}^1 d(\cos \vartheta) \frac{V_T(\mathbf{k}^2, k_4^2) (1 + \cos^2 \vartheta)}{\mathbf{k}^2} \\
&\quad - \frac{2}{p p_4} \int_0^\infty dq q^3 \int_{\mathbb{R}} dq_4 \frac{(p^2 + q^2) q_4 D(\mathbf{q}^2, q_4^2)}{d_{\text{quad},E}} \int_{-1}^1 d(\cos \vartheta) \frac{V_T(\mathbf{k}^2, k_4^2) \cos \vartheta}{\mathbf{k}^2}
\end{aligned}$$

Exteq 1: Coulomb gauge gap equation in rainbow truncation. Contributions displayed in gray drop out for symmetry reasons when the non-instantaneous part of  $D_{00}$  is neglected, provided the functions  $A$  and  $D$  are even in  $p_0$ . The quantity  $d_{\text{quad},E}$  is defined in (4.7).

Building on the code developed in [124] the system of equations given in exteq. 1 has been analyzed in greater detail.<sup>9</sup> The standard setup uses  $m_0 = 0.0037 \text{ MeV}$ ,  $N_C = N_f = 3$  and  $\sigma_C = \sigma_C^{(\text{std})} := 0.4107 \text{ GeV}^2$ , which yields  $\Lambda_{\text{QCD}}^2 = 0.588284 \text{ GeV}^2$ . The calculations have been performed on a  $N_{p\text{-points}} \times N_{p_4\text{-points}}$  point grid with points  $(|\mathbf{p}|_k, p_{4,j})$  set according to the rule

$$\begin{aligned}
|\mathbf{p}|_k &= p_{\min} \left( \frac{p_{\max}}{p_{\min}} \right)^{k/(N_{p\text{-points}}-1)} & k &= 0, \dots, N_{p\text{-points}} - 1 \\
p_{4,j} &= p_{4,\min} \left( \frac{p_{4,\max}}{p_{4,\min}} \right)^{j/(N_{p_4\text{-points}}-1)} & j &= 0, \dots, N_{p_4\text{-points}} - 1
\end{aligned} \tag{4.56}$$

with  $N_{p_4\text{-points}} = N_{p\text{-points}} = 48$  and

$$p_{\min} = p_{4,\min} = 0.0015 \text{ GeV}, \quad p_{\max} = p_{4,\max} = 60000 \text{ GeV}. \tag{4.57}$$

The renormalization point has been chosen as  $\mu \equiv |\boldsymbol{\mu}| = \mu_4 = 45000 \text{ GeV}$ , the infrared regulator has typically been set to  $\mu_{\text{IR}}^2 = 10^{-4} \text{ GeV}^2$ . In order to accelerate the iteration process, often the value of  $\mu_{\text{IR}}^2$  has been scaled down during the calculation, starting from  $\mu_{\text{IR}}^2 = 0.1 \text{ GeV}^2$  until the desired value has been reached.

<sup>9</sup>The straightforward bare vertex truncation employed in the following corresponds to the substitution  $\Gamma_{0b}^S \rightarrow 1$ ,  $\Gamma_{1a}^S \rightarrow 1$  while all other components of (4.38) and (4.39) are set to zero. This truncation reduces the full gap equation (given in extended equations 3 to 6 on pages 157ff) to extended equation 1.



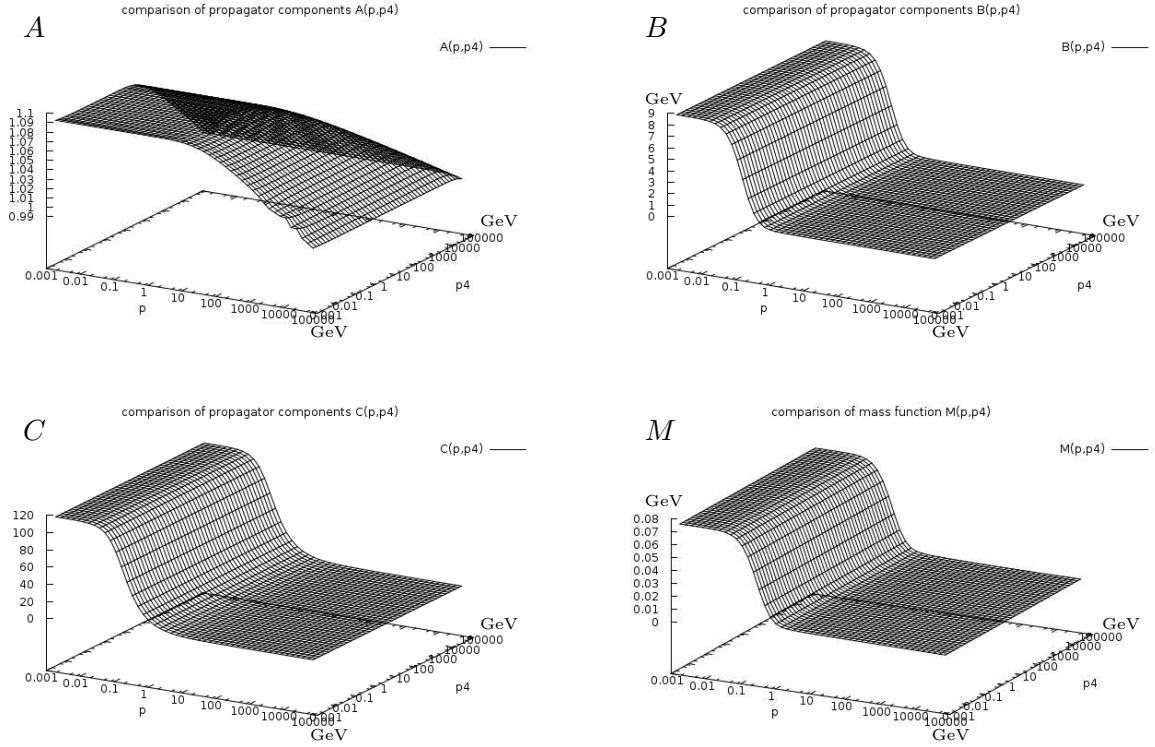


Figure 4.5: Propagator components  $A$ ,  $B$ ,  $C$  and the mass function  $M = \frac{B}{C}$  for the standard setup (employing  $D \equiv 0$ ,  $m_0 = 3.7$  MeV,  $\sigma_C = \sigma_C^{(\text{std})}$ ,  $\mu_{\text{IR}}^2 = 10^{-4}$ )

The standard setup produces the results illustrated in figure 4.5. The dependence on  $\mu_{\text{IR}}$  is illustrated in figure 4.6. One easily notices the divergent behaviour  $B \sim \frac{1}{\mu_{\text{IR}}}$  and  $C \sim \frac{1}{\mu_{\text{IR}}}$ , while the ration  $M := \frac{B}{C}$  seems to converge nicely.

The results for some other values of the Coulomb string tension  $\sigma_C$  and the current quark mass  $m_0$  are given in figures 4.7 and 4.8. While these results qualitatively show the expected behaviour ( $M \sim \sqrt{\sigma_C}$ ,  $M = m_0 + (\text{dynamically generated mass})$ ), the agreement is not particularly good, which may hint at possible numerical problems (see also the discussion in sec 4.3.4).

### 4.3.3 Explorative Study of an Infrared Divergent Vertex $\Gamma_i$

As mentioned in the previous section, the mere inclusion of transverse gluons and retardation effects does not produce quantitatively sensible results. So the truncation scheme employed so far seems to be too harsh. While it cannot be excluded that the Coulomb-gluon diagram has to be significantly modified (by employing additional tensor structures of  $\Gamma_0$  or taking into account the possible non-instantaneous parts of  $D_{00}$ ) the fact that  $g^2 D_{00}$  is already a renormalization group invariant makes it seem more likely that the transverse gluon diagram has to be changed.

Since there is quite some information available on  $D_{ij}$  (see sec. 4.1.2) it is most likely that  $\Gamma_i$  has to be enhanced. As discussed in sec. 4.2.6, there is some evidence for (as well as against) an infrared-divergent spatial vertex  $\Gamma_i$

The Ward-Takahashi identity discussed in sec. 4.2.3 suggests  $\Gamma_i \sim \gamma_i C$ , so the vertex would diverge  $\sim \frac{1}{\mu_{\text{IR}}}$ . The results for the modification  $\Gamma_i \sim \gamma_i C(q^2)$  are given in figure 4.9. While this modification definitely affects the propagator, it does not happen the way initially hoped for. Instead of enhancing the constituent quark mass, this change further suppresses  $m_{\text{CQ}}$  by roughly a factor of 2.5. This might or might not change when employing the full Slavnov-Taylor identity.



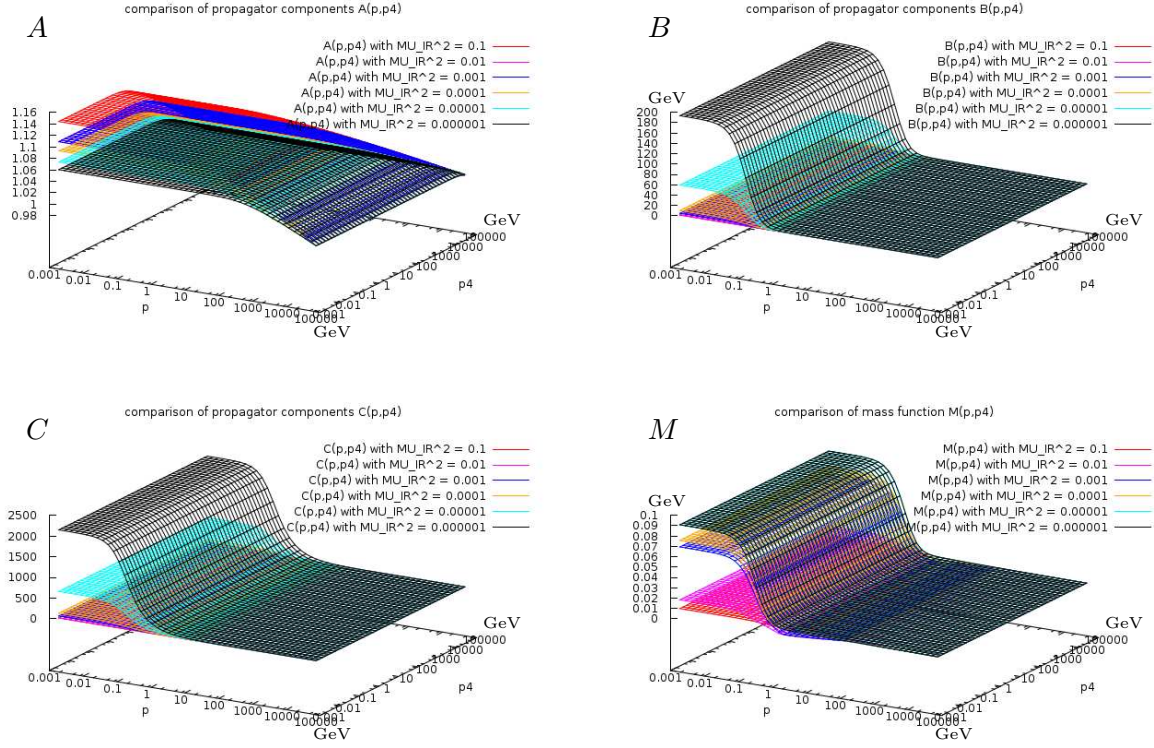


Figure 4.6: Propagator components  $A$ ,  $B$ ,  $C$  and the mass function  $M = \frac{B}{C}$  for  $\mu_{\text{IR}}^2 = 10^{-k} \text{ GeV}^2$ ,  $k = 1, 2, 3, 4, 5, 6$ ; otherwise as in fig. 4.5.

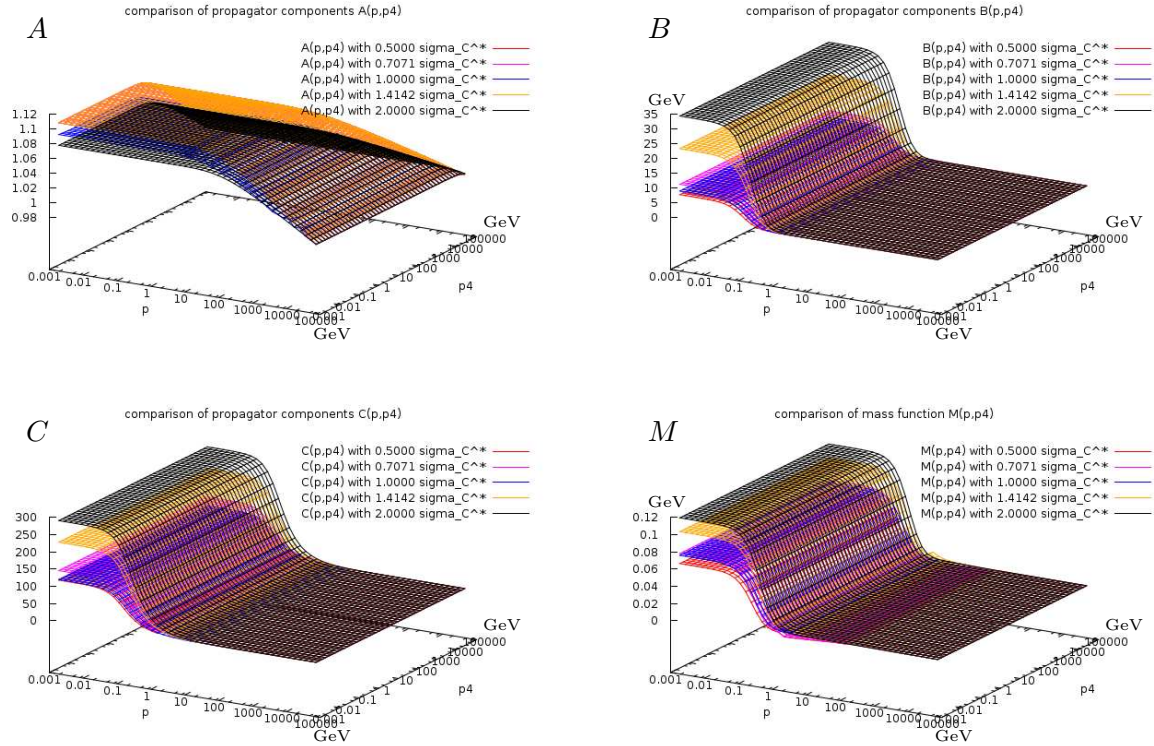


Figure 4.7: Propagator components  $A$ ,  $B$ ,  $C$  and the mass function  $M = \frac{B}{C}$  for different values of the Coulomb string tension  $\sigma_C = (\sqrt{2})^n \sigma_C^{(\text{std})}$ ,  $n = -2, -1, 0, 1, 2$ ; otherwise as in fig. 4.5

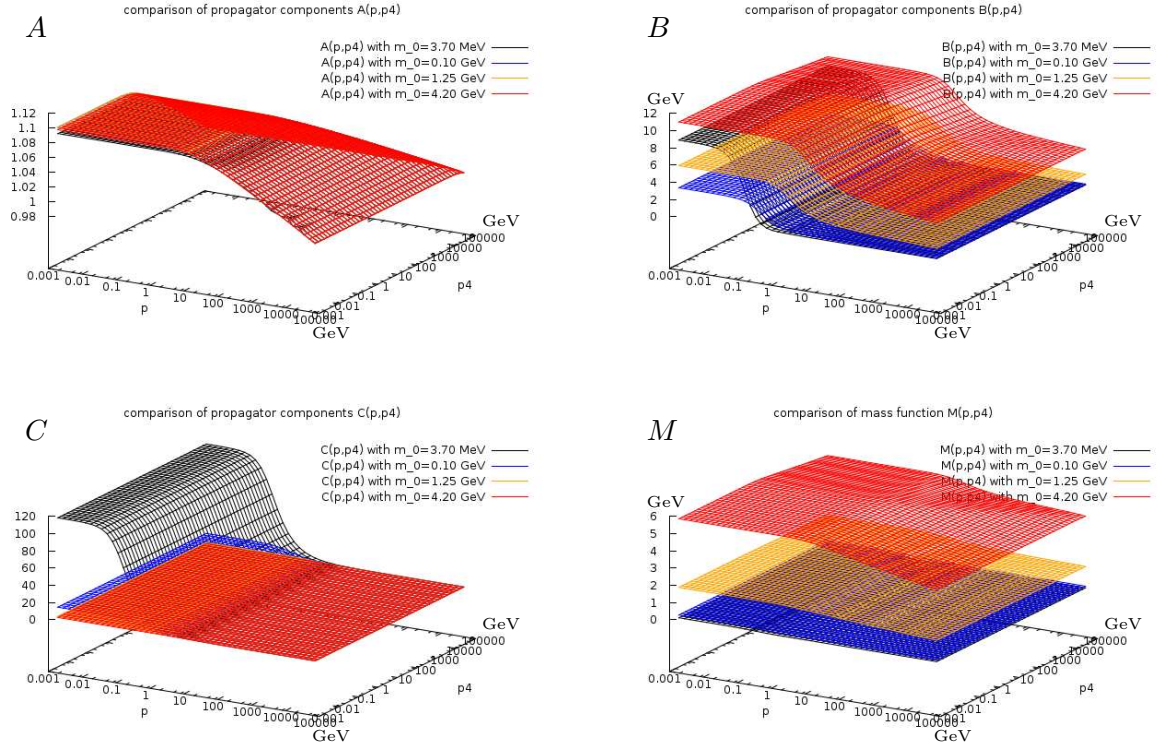


Figure 4.8: Propagator components  $A$ ,  $B$ ,  $C$  and the mass function  $M = \frac{B}{C}$  for different values of the bare quark mass, otherwise as in fig. 4.5

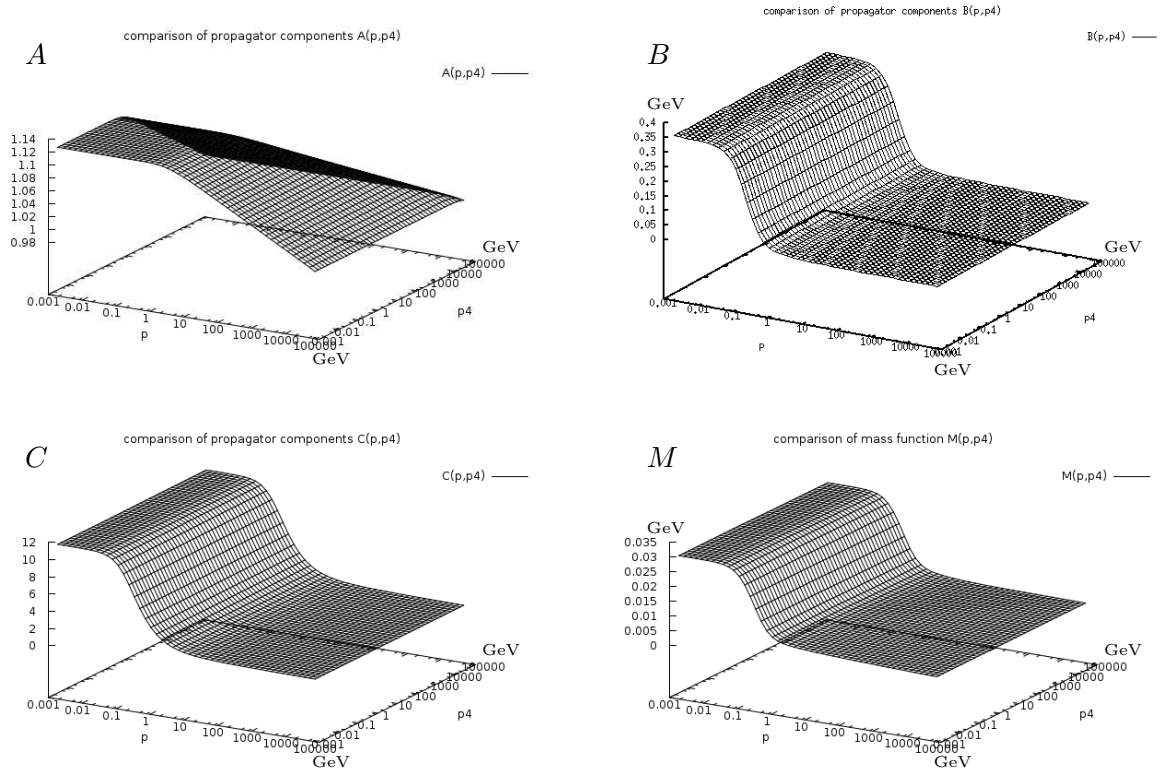


Figure 4.9: Propagator components  $A$ ,  $B$ ,  $C$  and the mass function  $M = \frac{B}{C}$  for an IR-divergent spatial vertex  $\Gamma_i \sim C \gamma_i$ , otherwise as in fig. 4.5



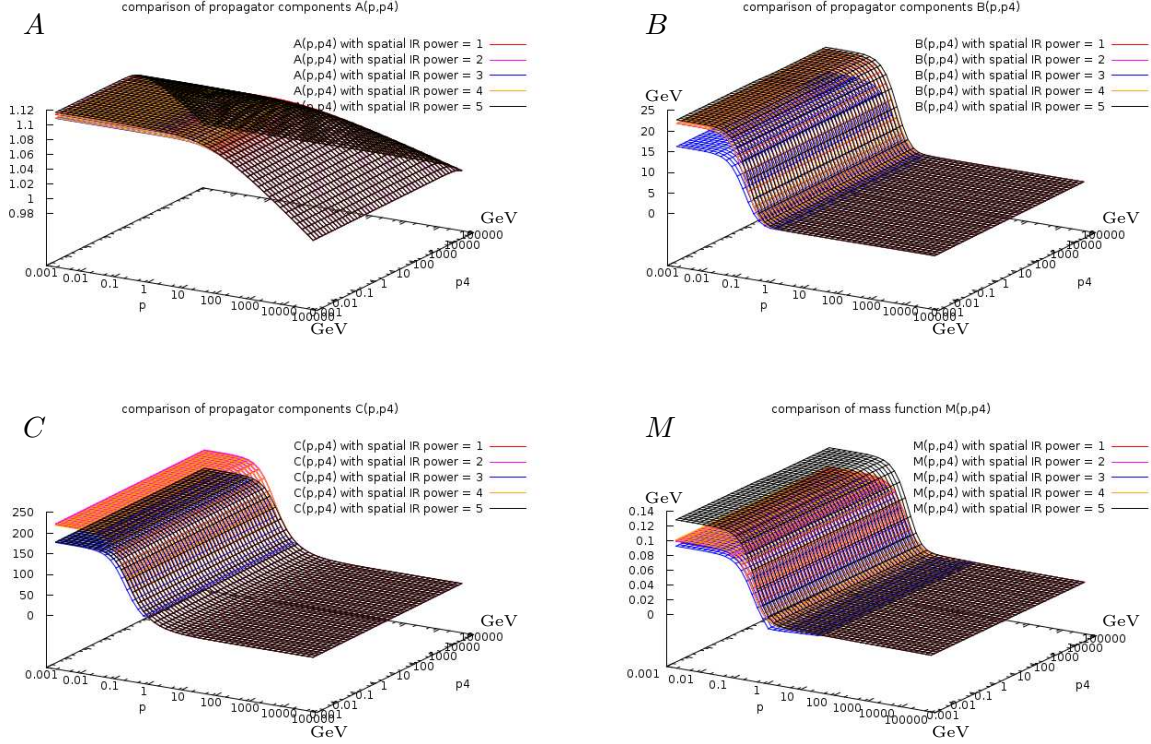


Figure 4.10: Propagator components  $A$ ,  $B$ ,  $C$  and the mass function  $M = \frac{B}{C}$  for an IR-divergent vertex  $\Gamma_i - \gamma_i \sim \frac{1}{|\mathbf{k}|^\alpha} \gamma_i$ ,  $\alpha = 1, 2, 3, 4, 5$ , otherwise as in fig. 4.5

In order to investigate other forms of infrared-divergent spatial vertices, we have chosen a dressing

$$\Gamma_i = \left( 1 + 2\pi \left( \frac{\Lambda_{\text{QCD}}}{|\mathbf{k}|} \right)^\alpha \right) \gamma_i \quad (4.58)$$

with  $\alpha \in \{1, 2, 3, 4, 5, 6\}$ . Since the transverse gluons are suppressed  $\sim \mu_{\text{IR}}^2$  in the infrared and since a divergence  $\sim \mu_{\text{IR}}^{-4}$  is present from the Coulomb gluons, one would expect such a dressing to have little effect for  $\alpha \leq 5$ . Indeed, the results given in figure 4.10 show some enhancement of the mass function, but the results are still numerically far off from what to expect for a reasonable constituent quark mass.

For  $\alpha = 6$ , the iteration did not converge. The final form of the propagator functions when terminating the calculation after several weeks is illustrated in figure 4.11. There are some indications of numerical instabilities (fluctuations in  $A$ , a “buckling-up” of  $C$ ) and a mysterious  $p_4^2$ -dependence of  $B$ ,  $C$  and  $M$ . The constituent quark mass did steadily rise during the iteration process; at the termination time it had reached  $m_{\text{CQ}} \approx 2.5 \text{ GeV}$ .

This can be interpreted as sign (in addition to the arguments given in sec. 4.2.6) that a uniformly strongly infrared divergent vertex introduces severe problems and presumably has to be dismissed. It might be possible to reduce  $\alpha$  slightly below  $\alpha = 6$  or tinker with the prefactors in order to obtain a finite result of the correct magnitude, but this would require extreme fine-tuning with correspondingly little or no significance.

When changing (4.58) to

$$\Gamma_i = \left( 1 + 2\pi \left( \frac{\Lambda_{\text{QCD}}}{\sqrt{\mathbf{k}^2 + k_4^2}} \right)^\alpha \right) \gamma_i, \quad (4.59)$$

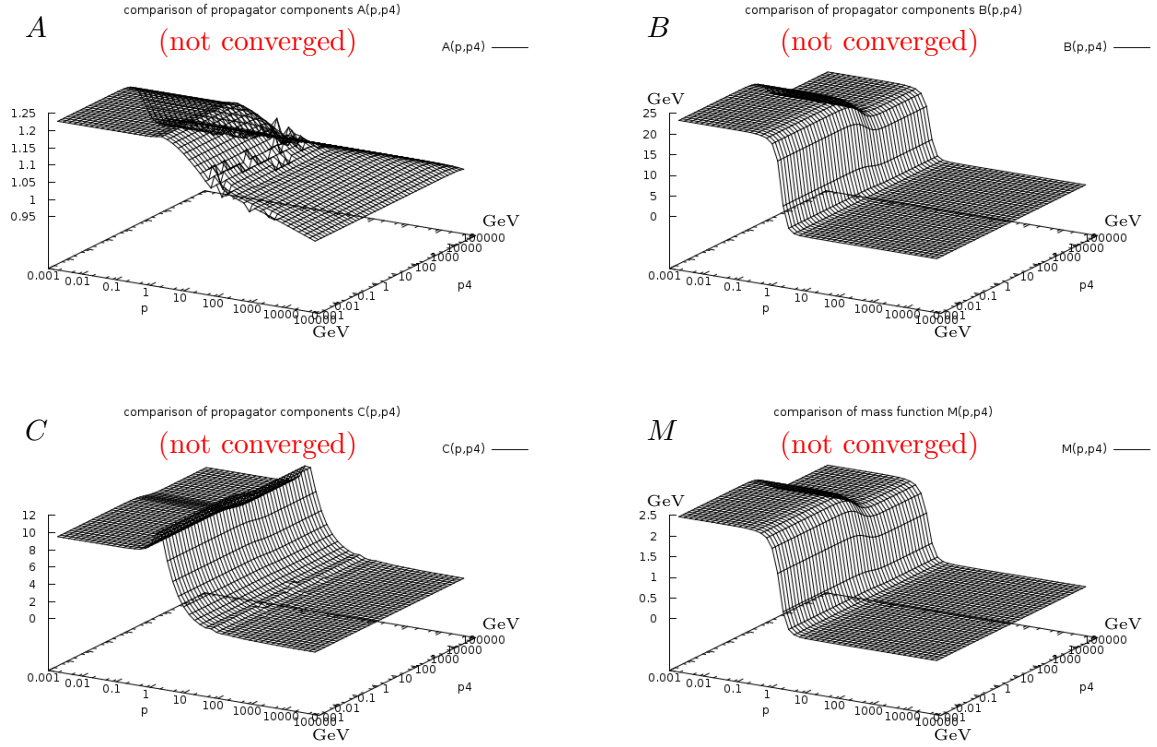


Figure 4.11: Propagator components  $A$ ,  $B$ ,  $C$  and the mass function  $M = \frac{B}{C}$  (not converged and unlikely to converge) for an IR-divergent vertex  $\Gamma_i - \gamma_i \sim \frac{1}{|k|^6} \gamma_i$ , otherwise as in fig. 4.5.

one obtains the results given in figure 4.12. In this case, the constituent quark mass is even *reduced* as compared to the calculations performed with a bare vertex.

One should note that the value of such ad-hoc ansätze is usually extremely limited: Even if such an ansatz yields reasonable values for certain observables, this does by no means imply that the form of the vertex is indeed correct. Basically such calculations may give some hints at how to possibly restrict a vertex, but without further theoretical foundations they have little explanatory power.

#### 4.3.4 Some Notes on the Numerical Challenges

The solution of the gap equation by iteration and numerical integration turned out to be extremely involved:

- Even the extremely elaborate algorithm developed in [124] repeatedly ran into problems or instabilities when the system of equations was somehow altered to test a different ansatz for one of the components. In particular the appropriate choice of relative and absolute error thresholds turned out to be highly nontrivial. In part this is a consequence of certain components diverging  $\sim \frac{1}{\mu_{\text{IR}}}$ . An error threshold which works fine for some value of  $\mu_{\text{IR}}^2$  might be inappropriate when  $\mu_{\text{IR}}^2$  is scaled further down. Since the calculations are extremely involved, so is the evaluation of different threshold strategies, and accordingly an satisfying strategy has not yet been found.
- In [124] a procedure called “freezing” has been proposed in order to accelerate convergence of the iteration: When using the “freezing” technique, those grid points for which the change due to iteration is below a given threshold are “frozen”, i.e. not changed any further.

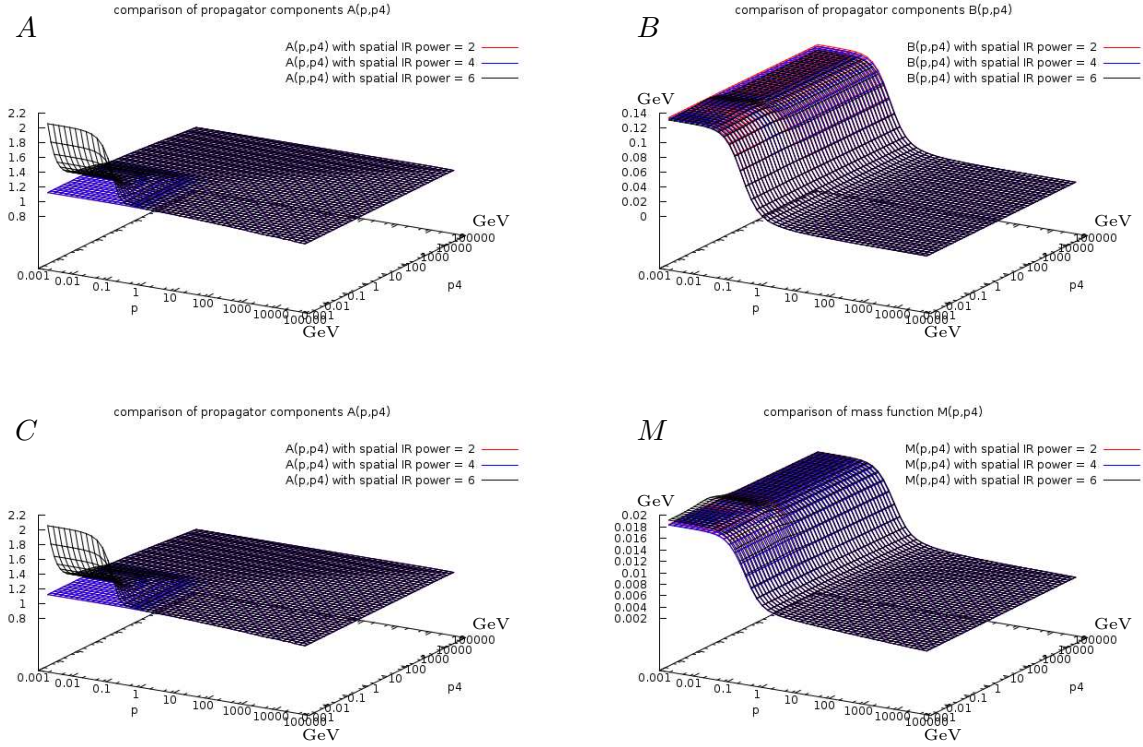


Figure 4.12: Propagator components  $A$ ,  $B$ ,  $C$  and the mass function  $M = \frac{B}{C}$  for an IR-divergent vertex  $\Gamma_i - \gamma_i \sim \frac{1}{|k|^\alpha} \gamma_i$ ,  $\alpha = 2, 4, 6$ , otherwise as in fig. 4.5

While this procedure produces a considerable speedup, it destroys the self-consistency of the system and can produce unwanted results. In particular it can lead to a “buckling-up” of the mass function. This effect became more severe for smaller values of  $\mu_{\text{IR}}$ ; for most calculations presented in the following, the freezing technique has not been used.

- The calculation turned out to be not stable when the  $D$ -component of the propagator was included. This is presumably a purely numerical effect, and there is some numerical evidence that  $D$  is negligible or vanishes completely. Also conceptually,  $D$  is intimately related to the mixed gluon propagators  $D_{i0}$  and  $D_{0j}$  which vanish in the Coulomb gauge. Still this topic should be subject to further investigations.
- Presumably the numerical treatment of a two-dimensional integral by iterated one-dimensional integrations is not optimal. An investigation of alternative techniques is currently performed [128].

#### 4.3.5 Conclusions

Apart from numerical challenges, the picture obtained for the Coulomb gauge gap equation remains shadowy. On the one hand side, a serious modification of the bare-vertex truncated version employed in [121, 124] seems to be necessary, on the other hand simple ansätze as employed in sec. 4.3.3 do not improve the situation.

The numerical results as well as some of the general considerations given in sec. 4.2.6 indicate that the spatial vertex is not globally divergent. Still it is likely that some components of  $\Gamma_i$  diverge for  $|k|^2 \rightarrow 0$  – though it’s not obvious from general considerations that this divergence will be strong enough to overcompensate the infrared suppression of the transverse gluons and produce an interaction of order  $\frac{1}{k^4}$ .

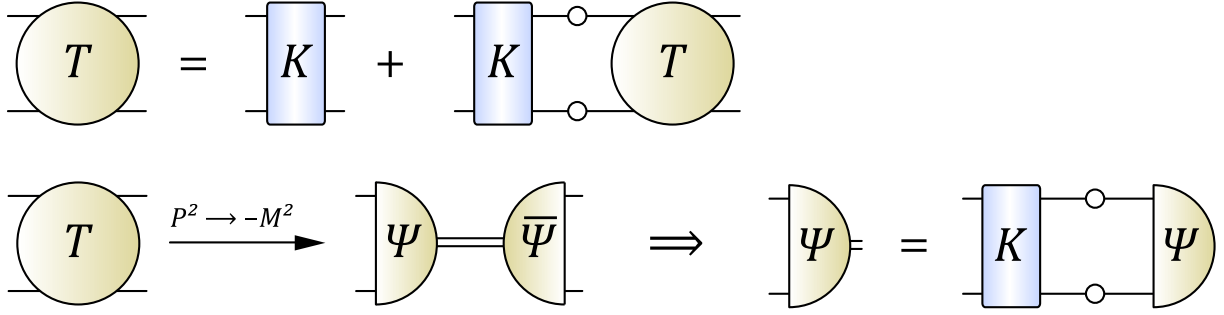


Figure 4.13: A graphical illustration of the relativistic two-body bound state equation (homogeneous Bethe-Salpeter equation), from [74].

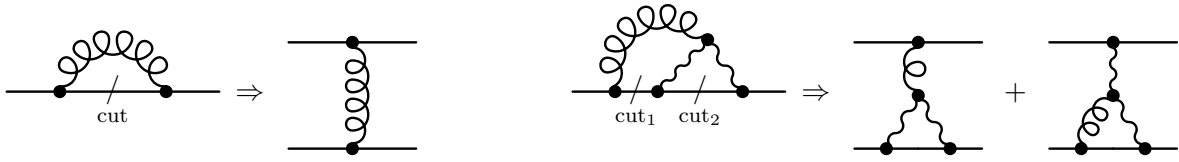


Figure 4.14: Prescription how to construct a scattering diagram from a self-energy diagram such that chiral symmetry is respected in a combined DSE/BSE approach, illustrated for rainbow-ladder and a more elaborate vertex ansatz.

#### 4.4 A Note on Mesons

When the quark propagator is known it can be used to obtain meson properties with the help of the Bethe-Salpeter equation (BSE; the relativistic generalization of the Schrödinger equation for two-body bound states [172]).

The general structure of the BSE for a quark-antiquark state is displayed in figure 4.13. It is obtained by projecting on a pole (corresponding to a bound state) of a quark-antiquark four-point function.

The equation contains (apart from the Bethe-Salpeter amplitude  $\Psi$  which roughly corresponds to the wave function in nonrelativistic quantum mechanics and which one typically wants to determine) two dressed quark propagators and the quark-antiquark scattering kernel.

This kernel is an unknown four-point function, for which of course an ansatz has to be made. This ansatz and the ansatz employed in the gap equation for the quark-gluon vertex have to be consistent in a quite particular way to ensure that chiral symmetry is respected [144]:

In order to obtain the form of the scattering kernel one has to add up the diagrams obtained by all possible ways to cut a single internal quark propagator line. This is illustrated in figure 4.14 for the rainbow truncation (which yields the so-called ladder truncation for the scattering kernel, thus “rainbow-ladder”) and a more elaborate vertex ansatz which includes a three-gluon vertex.

In principle the quark propagator obtained in sec. 4.3 could be used in the Bethe-Salpeter equation to compute meson properties. Due to the severe problems still present at the stage of the gap equation and due to lack of knowledge how to choose a reliable ansatz for the quark-gluon vertex (and thus also for the  $q\bar{q}q\bar{q}$  scattering kernel), however, this would appear to be a quite premature step.

## Chapter 5

# Finite Temperature Theory

The Coulomb gauge is well-suited for the studies at finite (i.e. non-zero) temperature. The reason is simple: In order to treat a system at temperature  $T$  one has to introduce a heat bath which defines a preferred rest frame, thus covariance is broken.<sup>1</sup> The loss of (manifest) covariance is the price one pays anyway when working in the Coulomb gauge, so finite- $T$  introduces no additional drawback.

Thus we use to opportunity to translate some ideas and methods to finite temperature. In section 5.1 we summarize some basic challenges of finite- $T$  QCD, we also review several methods to approach them, including consecutive effective field theories, as proposed in [39]. and methods to treat them.

In sec. 5.2 we use the local action proposed in [231] in order to obtained nonperturbative contributions to several thermodynamic observables, including free energy, anomaly and bulk viscosity. The physics behind this method is that the functional cut-off at the Gribov horizon suppresses the infrared components of the gluon field [95], so that the infrared divergences of finite-temperature field theory found by Linde [133] do not arise [218].

In sec. 5.3 we examine a different topic, employing the standard first-order pure gauge action. For the Dyson-Schwinger equations obtained in a bare-vertex truncation we look for infrared asymptotic power-law solutions and interestingly obtain a slightly overconfining color-Coulomb potential in  $s = 3$  spatial dimensions. Some mathematical aspects of such overconfining solutions are discussed in appendix C.2.

We close the chapter with a brief outlook on the inclusion of quarks, presented in sec. 5.4.

---

<sup>1</sup>One definitely loses *manifest* covariance. One could argue that when performing a boost, one would have to boost the heat bath as well in order to keep covariance – but we regard this as a rather unphysical setup. For example the microwave background defines (in good approximation) a heat bath with  $T \approx 2.7$  K and thus a rest frame. Any boost with respect to this rest frame will introduce a Doppler shift and thus anisotropies – which renders the definition of temperature questionable. In order to compensate this effect one would have to boost the whole known universe...



## 5.1 General Remarks on Finite Temperature QCD

### 5.1.1 Rise and Fall of the Quark-Gluon Plasma

As already mentioned in sec. 1.1, one of the most striking properties of QCD is *asymptotic freedom*. For large momentum  $p$ , the coupling  $g(p)$  is small, so quarks and gluons can be treated as if they were almost free particles — in particular, they can be treated with the sophisticated methods of perturbation theory.

While the situation is obviously different in the regime of low energies (which is most relevant for nuclear physics), it was natural to expect that a perturbative description could be applied to QCD at sufficiently high temperatures. After all, high temperature  $T$  implies high average particle momentum and thus a small coupling, i.e. almost free particles.

For this scenario, the term “quark-gluon plasma” was coined [177], and one could expect a phase transition where, on a certain curve in the  $\mu$ - $T$ -space (where  $\mu$  denotes the chemical potential), hadrons melt into such a plasma.

This phase transition offered a natural solution to a problem posed by Hagedorn, [100], who found that due to an exponential increase of the number of accessible states, the temperature of a hadron could not exceed a certain limit  $T_H \approx 160\text{MeV}$ .

The picture of hadrons melting into a plasma of (almost) free quarks and gluons, however, turned out to be too naive. In principle, this should have been clear at least since 1980, when it was shown [133, 98] that at order  $g^6$  a natural barrier arises for any perturbative description. Even earlier than that, the simple fact that the infinite-temperature limit of four-dimensional Yang-Mills theory is a three-dimensional *confining* Yang-Mills theory could and should have been regarded as a sign that any straightforward perturbative approach to high-temperature QCD was necessarily doomed.

It took however more than 20 years until it (slowly) began to be accepted that the high-temperature phase of QCD has little to do with a conventional plasma. The results of the RHIC experiments, [179], showed clearly that also above the phase transition, bound state phenomena cannot be neglected, and the description as a perfect fluid is much more accurate than the one as a weakly interacting plasma.

While the term “quark-gluon plasma” is still widely used, one begins to speak (more accurately, though somehow using an oxymoron) of a “strongly coupled quark gluon plasma” [27, 180], or even a “quark-gluon soup”.

With the experimental results which are — for certain observables — an order of magnitude away from the predictions for a weakly coupled plasma (see for example data on the elliptic flow in [143]) an accurate description of the high-temperature phase remains a challenge for theoretical physics. One conclusion, however, seems to be clear: In the high- $T$  regime, perturbation theory has to be replaced or at least supplemented by nonperturbative methods.

### 5.1.2 How to Study High Temperatures

It is useful to rescale thermodynamic quantities with appropriate powers of the temperature. In particular, the free energy per unit volume,<sup>2</sup> the pressure, and the energy per unit volume

$$w = \frac{\ln Z}{V}, \quad p = \frac{w}{\beta}, \quad e = -\frac{\partial w}{\partial \beta} \quad (5.1)$$

are rescaled to

$$w_r = \frac{w}{T^3}, \quad p_r = \frac{p}{T^4}, \quad e_r = \frac{e}{T^4}. \quad (5.2)$$

The *anomaly*  $A = e - 3p$  is rescaled to

$$A_r = \frac{A}{T^4} = \frac{e - 3p}{T^4}. \quad (5.3)$$

---

<sup>2</sup>In statistical mechanical usage the “free energy” is given by  $F = -wVT$ .

According to [120], up to a perturbative contribution, the *bulk viscosity*  $\zeta$  for hot gauge theories is given by the logarithmic derivative of the anomaly,

$$\zeta = \frac{1}{9\omega_0} \left\{ T^5 \frac{\partial}{\partial T} \left( \frac{e - 3p}{T^4} \right) + 16 |\varepsilon_V| \right\}, \quad (5.4)$$

where  $\omega_0$  denotes a perturbative scale and  $\varepsilon_V$  is a perturbative contribution. This formula can be derived from the Kubo formula of linear response theory. That the viscosity is linear in the trace of the energy-momentum tensor  $\Theta_{\mu\nu}$  (instead of quadratic) is not surprising in view of the Schwinger-Dirac relations, as discussed for example in [41].

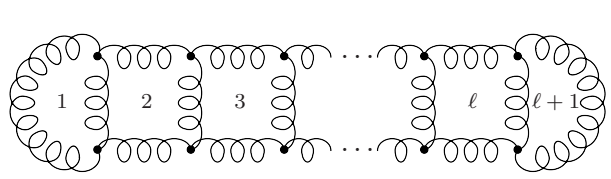
### 5.1.3 The Perturbative Problem in the Infrared

Perturbative calculations at finite temperature are dramatically different from those at  $T = 0$ . One of the most striking differences is that one cannot determine the order of a graph by simply counting the number of vertices. Actually a vacuum or propagator graph may be nonanalytic in  $g^2$ .

While ultraviolet divergences are regulated exactly the same way as in the zero-temperature theory, with no additional effort necessary, for  $T > 0$  additional *infrared* divergences appear. They come from Matsubara frequency  $n = 0$ , which has the infrared divergences of 3-dimensional Euclidean gauge theory that are even more severe than in 4 dimensions. For this reason the Gribov horizon, which affects primarily infrared components of the gauge field, is more important at finite and high  $T$  than at  $T = 0$ .

Here, however, another subtlety of thermal field theory comes to rescue: Thermal fluctuations give rise to self-energy, which, in the static limit  $\mathbf{p} \rightarrow \mathbf{0}$  corresponds to a mass  $m$ . At first glance, there are two natural candidates for the scale of such a mass, the electric screening mass  $m_{\text{el}} \sim gT$  and the magnetic screening mass  $m_{\text{mag}} \sim g^2 T$ .

The mass which is dynamically generated appears in the value for ladder diagrams (see sec. 8.7 of [118]). For this type of diagram we obtain (ignoring the complicated tensorial structure)



$$\sim \begin{cases} g^{2\ell} T^4 & \text{for } \ell = 1, 2 \\ g^6 T^4 \ln \frac{T}{m} & \text{for } \ell = 3 \\ g^6 T^4 \left( \frac{g^2 T}{m} \right)^{\ell-3} & \text{for } \ell > 3. \end{cases} \quad (5.5)$$

If  $m$  were independent of  $g$  or, like  $m_{\text{el}}$ , of order  $gT$ , we could proceed with perturbation theory without serious problems, since an increasing number of loops would always correspond to an increasing power of the coupling  $g$ . It turns out, however, that  $m$  is (in the best case) of the order of the *magnetic* screening mass,  $m_{\text{mag}} \sim g^2 T$ .

Thus for any value  $\ell \geq 3$  one has contributions of order  $g^6$ , the perturbative procedure becomes impracticable unless a suitable resummation technique is available — and such a technique has not been found up to now.

### 5.1.4 Direct Perturbative Approach

We have seen that the perturbative treatment of the QCD free energy runs into fundamental problems at order  $g^6$ . Still, one can expect that for sufficiently small values of  $g$  (i.e. for sufficiently high temperatures) the possible perturbative description (to order  $g^5$ ) still provides a good description.

This is indeed the case (although, as we will see in section 5.1.9, only at ridiculously high temperatures). Unfortunately, even these calculations turn out to be highly involved. We summarize here known results, which are also collected in [118], but specialize them to the case of pure gauge theory.

Zeroth order just gives the Stefan-Boltzmann law for SU(N) gauge theory,

$$\frac{p^{(0)}}{T^4} = -(N^2 - 1) \frac{\pi^2}{45}. \quad (5.6)$$

For the second-order contribution, one obtains, [178, 50],

$$\frac{p^{(2)}}{T^4} = -(N^2 - 1) \frac{\pi^2}{9} C_A \left( \frac{g}{4\pi} \right)^2 \quad (5.7)$$

with  $C_A$  denoting the Casimir of the adjoint representation, and  $C_A = N$  for SU(N). Due to non-analyticity, one has a contribution of  $\mathcal{O}(g^3)$ , calculated in [117],

$$\frac{p^{(3)}}{T^4} = (N^2 - 1) \frac{\pi^2}{9} C_A^{3/2} \frac{16}{\sqrt{3}} \left( \frac{g}{4\pi} \right)^3. \quad (5.8)$$

The  $g^4 \ln g$  contribution has been calculated in [195], the full  $g^4$  term has been obtained in [19, 20]

$$\begin{aligned} \frac{p^{(4)}}{T^4} = (N^2 - 1) \frac{\pi^2}{9} C_A^2 \left( \frac{g}{4\pi} \right)^4 & \left\{ 24 \ln \left( \frac{C_A}{3} \frac{g}{2\pi} \right) \right. \\ & \left. - \left[ \frac{22}{3} \ln \frac{\mu(T)}{2\pi T} + \frac{38}{3} \frac{\zeta'(-3)}{\zeta(-3)} - \frac{148}{3} \frac{\zeta'(-1)}{\zeta(-1)} - 4\gamma_E + \frac{64}{5} \right] \right\} \end{aligned} \quad (5.9)$$

where  $\gamma_E$  denotes the Euler-Mascheroni constant and  $\zeta$  the Riemann zeta function.

At order  $g^5$ , one obtains, [219]

$$\begin{aligned} \frac{p^{(5)}}{T^4} = (N^2 - 1) \frac{\pi^2}{9} \left( \frac{g}{4\pi} \right)^5 & \sqrt{\frac{C_A}{3}} C_A^2 \\ & \cdot \left[ 176 \ln \frac{\mu(T)}{2\pi T} + 176 \gamma_E - 24 \pi^2 + 494 + 264 \ln 2 \right]. \end{aligned} \quad (5.10)$$

### 5.1.5 Effective Field Theory

The result of order  $g^5$  is the last one obtained in strict perturbation theory. It has been rederived by Braaten and Nieto [39], using an effective field theory method that is built on the idea of dimensional reduction [17, 38].

The problem of infrared divergences is addressed by two effective theories that are constructed “below” perturbative QCD. We know that there are three important scales present, namely

$$\begin{array}{lll} 2\pi T & \dots & \text{scale of “hard modes”} \\ g T & \dots & \text{chromoelectric scale} \\ g^2 T & \dots & \text{chromomagnetic scale.} \end{array}$$

Thus it makes sense to describe each scale in a somewhat different way. To do this, two cutoff scales  $\Lambda_E$  and  $\Lambda_M$  are introduced, that have to satisfy

$$2\pi T \gg \Lambda_E \geq g T \gg \Lambda_M \geq g^2 T. \quad (5.11)$$

The region with  $p > \Lambda_E$  can be reliably described by perturbative QCD, and for this contribution to the free energy, called  $f_E$ , one obtains a power series in  $g^2$  with coefficients that can depend on  $\ln \frac{T}{\Lambda_E}$ . For  $\Lambda_E > p > \Lambda_M$ , with the hard modes integrated out, an effective three-dimensional theory, called *electrostatic QCD* (EQCD) is introduced,

$$\mathcal{L}_{\text{EQCD}} = \frac{1}{4} F_{ij}^a F_{ij}^a + \frac{1}{2} (D_i A_0)^a (D_i A_0)^a + \frac{1}{2} m_E^2 A_0^a A_0^a + \frac{1}{8} \lambda_E (A_0^a A_0^a)^2 + \delta \mathcal{L}_{\text{EQCD}}, \quad (5.12)$$

$$\Lambda_E \frac{2\pi T \quad \text{pQCD} \quad f_E = T^3 \sum_{k=0}^{\infty} a_k (g^2)^k}{gT \quad \text{EQCD} \quad f_M = (gT)^3 \sum_{k=0}^{\infty} b_k g^k}$$

$$\Lambda_M \frac{g^2 T \quad \text{MQCD} \quad f_G = (g^2 T)^3 \sum_{k=0}^{\infty} c_k g^k}{g^2 T \quad \text{MQCD} \quad f_G = (g^2 T)^3 \sum_{k=0}^{\infty} c_k g^k}$$

Figure 5.1: The scales of perturbative QCD (pQCD), electrostatic QCD (EQCD), magnetostatic QCD (MQCD) and the different contributions  $f_E$ ,  $f_M$  and  $f_G$  to the free energy. The coefficients  $a_k$  and  $b_k$  are polynomials in logarithms of ratios of scales,  $a_k = P_k(\ln \frac{T}{\Lambda_E})$ ,  $b_k = Q_k(\ln \frac{\Lambda_E}{gT}, \ln \frac{gT}{\Lambda_M})$ . While the coefficients  $a_k$  and  $b_k$  can be determined, at least in principle, in perturbation theory, this is not possible for  $c_k$ .

where  $F_{ij}^a = \partial_i A_j^a - \partial_j A_i^a + g_E f^{abc} A_i^b A_j^c$  denotes the magnetostatic field strength tensor and  $\delta\mathcal{L}_{\text{EQCD}}$  contains all other local (3-dimensional) gauge-invariant operators of dimension three or higher that can be constructed from  $A_i$  and  $A_0$ . The parameters  $g_E$ ,  $m_E$ ,  $\lambda_E$  are determined by matching to perturbative QCD, in particular one has  $m_E \sim m_{\text{el}} \sim gT$ .

This theory still allows perturbative treatment, making use of an expansion in the dimensionless quantities  $\frac{g_E^2}{m_E} \sim g$ ,  $\frac{\lambda_E}{m_E}$  etc. This gives for the contribution  $f_M$  to the free energy a power series in  $g$ , with coefficients that depend on  $\ln \frac{\Lambda_E}{gT}$  and  $\ln \frac{gT}{\Lambda_M}$ . The whole series is multiplied by the common factor  $(gT)^3 T$ . The infrared cutoff  $\Lambda_M$  of EQCD is the UV cutoff of another theory, *magnetostatic QCD* (MQCD),

$$\mathcal{L}_{\text{MQCD}} = \frac{1}{4} F_{ij}^a F_{ij}^a + \delta\mathcal{L}_{\text{MQCD}}, \quad (5.13)$$

with  $\delta\mathcal{L}_{\text{MQCD}}$  denoting all gauge-invariant operators of dimension 5 or higher. This theory is confining and thus truly nonperturbative, but according to [39], this contribution to the free energy, called  $f_G$ , can still be expanded in a power series in  $g$ , which is multiplied by a general factor  $(g^2 T)^3$ . However the value of the coefficient cannot be determined perturbatively. Since the (well-established) nomenclature may seem slightly misleading at first glance, we have tried to give a graphical representation in fig. 5.1.

MQCD is genuinely nonperturbative, its degrees of freedom are  $(2+1)$ -dimensional glueballs. In [38] it was suggested to calculate the contributions from this scale directly by lattice methods.

With the effective field theory, it is possible to compute the  $g^6 \ln g$  contribution [112]. The contribution obtained this way has to be regarded as partly conjectural, since it relies on assumptions about the cancellation patterns. In addition the argument inside the logarithm is not clearly defined until the full  $g^6$  contribution is known.

The result thus relies on a supposed structure of cancellation patterns. In addition, it is believed to be reliable only for sufficiently high temperatures (which could, however, mean down to  $T \approx 2T_C$ ), since description by a three-dimensional theory is valid only for such temperatures. With these caveats in mind, one obtains for pure  $SU(3)$  gauge theory

$$\frac{p^{(6)}}{T^4} = \frac{8\pi^2}{45} \left( \frac{g^2}{4\pi^2} \right)^3 \left\{ \left[ -659.2 + 742.5 \ln \frac{\mu(T)}{2\pi T} \right] \ln \frac{g^2}{4\pi^2} \right. \\ \left. - 475.6 \ln \frac{g^2}{4\pi^2} - \frac{1815}{16} \ln^2 \frac{\mu(T)}{2\pi T} + 2932.9 \ln \frac{\mu(T)}{2\pi T} + q_c^{(0)} \right\} \quad (5.14)$$

with a yet undetermined coefficient  $q_c^{(0)}$  for the pure  $g^6$  contribution. (See also [173, 175].)

This coefficient consists of both perturbative contributions (from pQCD and EQCD) and nonperturbative contributions (from MQCD). It was estimated in [112] by a fit to four-dimensional lattice data for the pressure.<sup>3</sup>

Some of the perturbative contributions of order  $g^6$  are known by now [126, 174], but others remain unknown. The nonperturbative coefficient has been determined by three-dimensional lattice calculations and matching to perturbative four-loop calculations in [104] (see also [105] for some cases with  $N \neq 3$ ) and [68]. One obtains

$$w_{\text{np}}^{(6)} = g_3^6 \frac{(N^2 - 1) N^2}{(4\pi)^4} B_G \quad (5.15)$$

with  $g_3^2 = g^2 T(1 + \mathcal{O}(g^2))$  and the constant

$$B_G = -0.2 \pm 0.4^{\text{MC}} \pm 0.4^{\text{SQ}}, \quad (5.16)$$

where the first error stems from the Monte Carlo simulation, the second one from the Stochastic Quantization procedure employed to obtain the final result. Note that  $B_G = 0$  is compatible with this result.

### 5.1.6 Functional Approaches

Due to the limitations of perturbation theory, nonperturbative methods definitely deserve a closer look — moreover the effective field theory approach also relies on the ability to calculate certain quantities nonperturbatively. As in the zero-temperature case, also for finite temperature, fundamental aspects of Yang-Mills theory and QCD are accessible to functional methods based on Dyson-Schwinger equations (DSEs), [137, 136].

For certain asymptotic situations (deep ultraviolet, deep infrared, infinite temperature limit) several analytic results can be obtained; but in general numerical studies of truncated DSE systems are necessary.

In addition to the standard truncations, finite temperature calculations require also some treatment of the Matsubara series. Usually it is replaced by a finite sum, even though this means that the limit of four-dimensional zero-temperature theory is now technically hard to access.

At the present level, these restrictions make it difficult to obtain precise quantitative results. Nevertheless there is reasonable confidence about the qualitative picture that arises from these studies. Both from infrared exponents and from numerical results one sees that the soft modes are not significantly affected by the presence of hard modes, thus the confining property of the theory cannot be expected to be lost in the high-temperature phase.

Consequently, while the over-screening (which would attribute an infinite amount of energy to free color charges) of chromoelectric gluons is reduced to screening (as it is the case for electric charges in a conventional plasma), chromomagnetic gluons remain over-screened and thus confined, which renders any description of such gluons as almost free (quasi-)particles meaningless.

While the functional method yields considerable insight into propagators and related quantities, unfortunately the pressure (and quantities derived from it) are, up to now, difficult to access in this approach. Nevertheless the results obtained so far by functional methods provide additional evidence for the picture of bound states playing an important role even at very high temperature and part of the gluon spectrum (the chromomagnetic sector) being confined at any temperature.

---

<sup>3</sup>The problem with such a procedure is that in the regime where lattice data is available, the contributions of higher order may also be large.

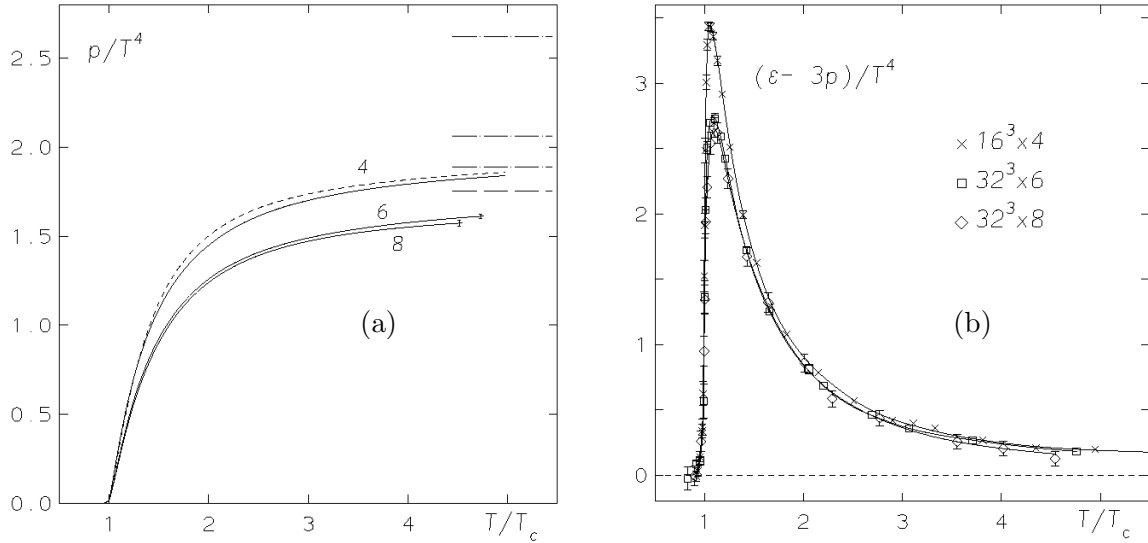


Figure 5.2: (a) Rescaled pressure of SU(3) lattice gauge theory where  $T_c$  is the transition temperature, and  $N_\tau = 4, 6, 8$ , (b) rescaled anomaly of SU(3) lattice gauge theory; both from [37]

### 5.1.7 Lattice Gauge Theory

Lattice Gauge Theory is generally considered the most rigorous approach to nonperturbative QCD, and so it is natural to also study thermodynamics on the lattice.

The drawbacks of the method, however, are known as well: To reliably approach the thermodynamic and the continuum limits, extrapolations which require calculations with various different lattice sizes are necessary. The inclusion of fermions is expensive, especially if good chiral properties are required.

Despite these drawbacks, lattice data is (apart from possible experiments) the thing one usually compares any other calculation to. For pure SU(3) gauge theory, the problem of determining the equation of state is regarded as solved since the publication of [37], where results are further confirmed in [155]. (Note, however, that there remain certain doubts about the accuracy of the infinite-volume limit, see [88].) The results for the pressure and the anomaly are displayed in figure 5.2.

### 5.1.8 Other Approaches

It has been observed [159] from lattice data [37] that  $(e - 3p)/T^4 \times T^2$  is approximately constant in a broad range above  $T_c$ . From this and physical reasoning the formula

$$p_{\text{pure glue}}(T) \approx f_{\text{pert}}(T^4 - T_c^2 T^2) \quad (5.17)$$

has been obtained. It is notable that no  $T^3$  correction is apparent.

An active area of research is the AdS/CFT duality [139] and AdS/QCD duality [2]. The duality at finite temperatures can be studied by putting a black hole into the AdS space (for a pedagogical introduction to these concepts see [157]).

In this connection it is interesting to note that a formula similar to Pisarski's has recently been obtained from this duality and the (truncated) entropy density of the horizon of a deformed Euclidean AdS<sub>5</sub> black hole [16].

The role of different channels in the deconfinement transition, particularly coexistence of hadron clusters with the quark-gluon plasma has been elucidated in [217].

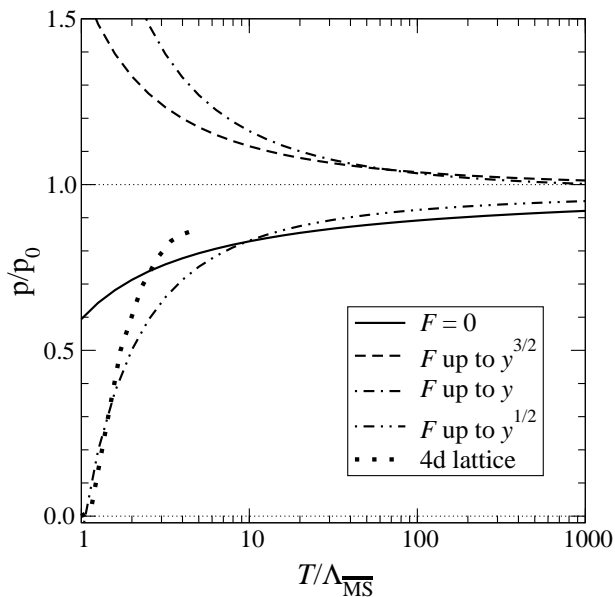


Figure 5.3: The convergence of an (optimized) perturbation series for “long-distance contribution” to the pressure, from [111]. The order of the expansion is characterized by the dimensionless parameter  $y \sim \frac{g^2 T^2}{g_3^4}$ , where  $g_3^2$  denotes the gauge coupling in the effective three-dimensional theory. The perturbative contribution  $F$  to the free energy contains a factor  $\left(\frac{g_3^2}{T}\right)^3$ , inclusion of lower powers of  $y$  corresponds to higher orders in perturbation theory.

### 5.1.9 Comparison of Results

Knowing that perturbation theory is limited to some fixed order in  $g$ , we can still estimate how good the possible perturbative description actually is. Ways to judge this are to check whether contributions from higher orders are small compared to those from lower orders or to compare perturbative expressions to results of lattice calculations.

Unfortunately, both methods suggest that the convergence is extremely poor for temperatures of the order of several  $T_c$ , where  $T_c$  is the transition temperature, and to obtain good convergence one has to look at least at the electroweak scale, [219, 112]. A plot of the results of optimized perturbation theory is given in fig. 5.3.

It has been conjectured, [125], that the results of order  $g^6$  are not significantly changed by higher orders (since one can hope to have obtained at order  $g^6$  the main contribution from each scale; perhaps also due to the fact that originally large terms of higher orders cancel against each other). To the knowledge of the author, however, there is no strong evidence to support this conjecture.

From the existing data one cannot even exclude the unsettling possibility that for “physical” temperatures the perturbation series already begins to diverge at some order  $n \leq 6$ . This would mean that contributions from higher orders are of comparable magnitude to those of low order and no systematic cancellations occur. If this were indeed the case, we could not expect to have any reliable perturbative description for temperatures which are accessible in current experiments.

One should mention that there is an additional ambiguity in the perturbative results. All terms beyond the Stefan-Boltzmann contribution contain some power of the running coupling  $g$ . Thus, for all practical calculations there is some dependence on the scale  $\mu$ , at which  $g(\mu)$  is evaluated. Traditionally, one chooses  $\mu(T) = 2\pi T$  in the high-temperature regime, but there are alternative approaches, for example application of the *principle of minimal sensitivity*, [182, 35, 108]. We will discuss this question in more detail in section 5.2.3.



## 5.2 Pure Gauge Theory with an Extended Action

### 5.2.1 Equation of State from a Local Action

An alternative approach that combines nonperturbative elements with perturbative expansions has been developed in [231, 230, 232], which we now briefly describe.

The basic physical idea is that the infrared divergences of finite-temperature perturbation theory do not arise when the domain of functional integration is cut-off at the Gribov horizon. The cut-off will be done in Coulomb gauge which is well adapted to finite-temperature calculations. Indeed both the gauge condition,  $\partial_i A_i(\mathbf{x}, t) = 0$ , and the cut-off at the Gribov horizon are applied to 3-dimensional configurations on each time slice  $t$ , and are entirely independent of the temporal extent of the lattice  $0 \leq t \leq \beta$ , where  $\beta = 1/kT$ .

The functional cut-off at the Gribov horizon is effected at first by adding a non-local term  $S_{NL}(A)$  to the action [221, 224]. The non-local term then gets replaced by a local, renormalizable term  $S_L$  in the action by means of an integration over a multiplet of auxiliary Fermi and Bose ghost pairs,

$$\exp[-S_{NL}(A)] = \int \mathcal{D}\varphi \mathcal{D}\bar{\varphi} \mathcal{D}\omega \mathcal{D}\bar{\omega} \exp[-S_L(\varphi, \bar{\varphi}, \omega, \bar{\omega})]. \quad (5.18)$$

The BRST symmetry is explicitly broken by this term, an effect which, alternatively, may be interpreted as spontaneous BRST breaking [138]. Although the breaking of BRST invariance precludes the definition of observables as elements of the cohomology of the BRST-operator, the equivalence to the canonical formulation has been established [231], thereby ensuring the physical foundation of the approach, including unitarity. Here the physicality of the Coulomb gauge plays an essential role. The new term in the action depends on a mass parameter  $m$  which appears in the Lagrangian density

$$\mathcal{L}_m = -\frac{m^4}{2Ng^2}(D-1)(N^2-1) + \frac{m^2}{(2N)^{1/2}g} [D_i(\varphi - \bar{\varphi})_i + g(D_i c \times \bar{\omega}_i)]^{aa}. \quad (5.19)$$

The adjoint part of the Bose ghost  $(\varphi - \bar{\varphi})_i$  mixes with the gauge field  $A_i$  through the term  $D_i(\varphi - \bar{\varphi})_i = (\partial_i + gA_i \times)(\varphi - \bar{\varphi})_i$ . At tree level one obtains a gluon propagator,

$$D = \frac{1}{k_0^2 + E^2(\mathbf{k})}, \quad (5.20)$$

that satisfies the Gribov dispersion relation

$$E(\mathbf{k}) = \sqrt{\mathbf{k}^2 + \frac{m^4}{\mathbf{k}^2}}. \quad (5.21)$$

The functional cut-off at the Gribov horizon imposes the condition that the free energy  $W$  or quantum effective action  $\Gamma$  be stationary with respect to  $m$ ,

$$\frac{\partial W}{\partial m} = -\frac{\partial \Gamma}{\partial m} = 0. \quad (5.22)$$

This ‘‘horizon condition’’ has the form of a non-perturbative gap equation that determines the Gribov mass  $m = m(T, \Lambda_{QCD})$ , and thereby provides a new vacuum, around which a perturbative expansion is again possible.

In a semi-perturbative approach [231] one calculates all quantities perturbatively in  $g$ , including  $\Gamma$ , taking  $m$  to be a quantity of order  $g^0$ , and then one substitutes for  $m$  the non-perturbative solution to the gap equation (5.22). We shall find that this method can be a good approximation only at extremely high energies. Nevertheless as a matter of principle, it is a significant success that for thermodynamic observables this procedure gives finite results precisely at the order,  $g^6$  at which ordinary perturbation theory diverges.

### 5.2.2 The Gap Equation

In lowest non-trivial order in the semi-perturbative method [231], the gap equation (5.22) reads after separation into an  $m^*$ -dependent and a  $T$ -dependent part

$$\frac{1}{2} \ln \frac{1}{m^*} + \int_0^\infty \frac{dx}{u(x)} \frac{1}{e^{m^* u(x)} - 1} = \frac{3\pi^2}{N g^2(\mu)} - \frac{1}{4} \ln \frac{e\mu^2(T)}{2T^2} \quad (5.23)$$

where  $m^* \equiv m_r = m/T$  is the rescaled Gribov mass and

$$u(x) \equiv \sqrt{x^2 + \frac{1}{x^2}} \quad (5.24)$$

is the reduced dispersion relation. An important source of ambiguity, shared with other (semi)-perturbative approaches, is the choice of the temperature-dependent scale  $\mu(T)$  at which the coupling  $g$  is evaluated.

### 5.2.3 Choice of the Renormalization Scale

We consider the coupling  $g^2(\mu)$  at some renormalization scale  $\mu(T)$ . For a certain temperature  $T$ , the optimal renormalization scale should be chosen equal to the scale that governs the behaviour of the system. For field theory at high temperatures, this scale is expected to be equal to the lowest Matsubara frequency, i.e.  $2\pi T$ ; for small  $T$  it should be constant.

Since we are considering a confining theory with a mass gap, for low temperatures the optimal renormalization scale is not expected to go to zero. For a system at very low (even zero) temperature, the most characteristic scale is not the very small average kinetic energy, but instead the mass of the lightest physical object, which is some bound state (a hadron in full QCD, a glueball in pure gauge theory). Actually, as long as we are in the confining region (i.e. below  $T = T_c$ ), the mass of bound states will always be “more important” than the thermal energy. These restrictions, together with some conditions of “naturalness”, can be summarized by demanding that the renormalization scale  $\mu(T)$  should fulfill:

- (I)  $\mu(T) \approx \mu_0 = \text{const}$  for  $T \ll T_c$ ,
- (II)  $\mu(T) \approx 2\pi T$  for  $T \gg T_c$ ,
- (III) continuous,
- (IV) monotonically rising for all  $T$ ,
- (V) convex for all  $T$

Conditions (I) and (II) might be replaced or supplemented by the asymptotic conditions

$$\begin{aligned} \text{(I')} \quad & \lim_{T \rightarrow 0} (\mu(T) - \mu_0) = 0, \quad \lim_{T \rightarrow 0} \frac{\mu(T) - \mu_0}{T} = 0, \\ \text{(II')} \quad & \lim_{T \rightarrow \infty} T^n (\mu(T) - 2\pi T) = 0 \quad \text{for all } n \in \mathbb{N}_0 \end{aligned} \quad (5.25)$$

Due to the phase transition at  $T = T_c \approx \Lambda_{\text{QCD}}$ , a simple choice is

$$\mu(T) = \begin{cases} \mu_{0,l}(T) := 2\pi \Lambda_{\overline{MS}} & \text{for } T < \Lambda_{\overline{MS}} \\ \mu_{0,h}(T) := 2\pi T & \text{for } T \geq \Lambda_{\overline{MS}}. \end{cases} \quad (5.26)$$

This choice is supported by the fact that  $2\pi \Lambda_{\overline{MS}}$  is in the order of magnitude of glueball masses. Another reasonable choice is

$$\mu(T) = 2\pi T + 2\pi \Lambda_{\overline{MS}} e^{-T/\Lambda_{\overline{MS}}}. \quad (5.27)$$

This form, however, is less favorable for numerical reasons, thus we have exclusively used (5.26) in the numerical studies performed in section 5.2.4. Both forms are plotted in fig. 5.4.

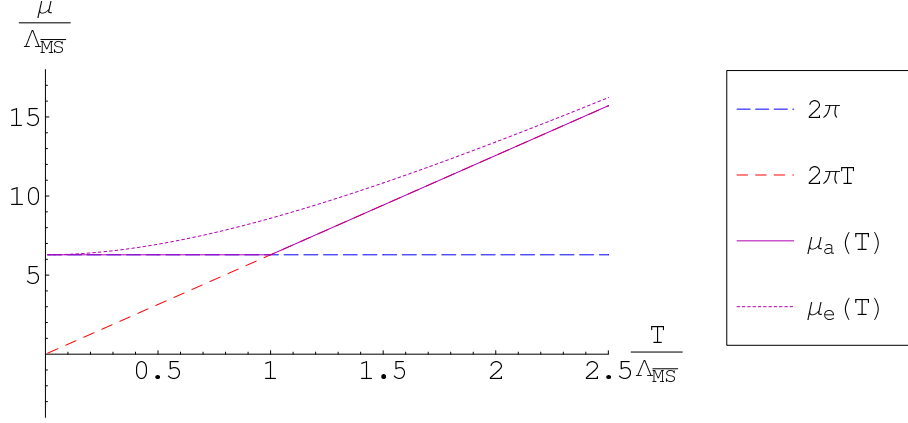


Figure 5.4: Graph of the renormalization scale  $\mu(T)$ : We show the piecewise linear form  $\mu_a(T)$  from (5.26) and the exponential form  $\mu_e(T)$  from (5.27) together with the asymptotics  $\mu_{0,1}(T) = 2\pi\Lambda_{\text{QCD}}$  and  $\mu_{0,h}(T) = 2\pi T$ .

### 5.2.4 Computational Methods

The gap equation (5.23) is an implicit equation for  $m^*(T)$ , which, in contrast to “genuine” integral equations, can be solved independently for each temperature  $T$ . Our results have been obtained in Mathematica<sup>4</sup> by combining a numerical equation solver with adaptive Gauß-Legendre integration.

The derivatives necessary to obtain anomaly and bulk viscosity (see equations (5.42) and (5.47)) can be done either numerically or analytically. The second way unfortunately involves additional integrals, which can again only be evaluated numerically. (See appendix C.4.1 for details.)

While both methods are potentially susceptible to numerical problems, they are of very different nature. Actually, the results of both methods agree remarkably well, inspiring confidence in the stability of the result.

All calculations directly involving  $T$  have been performed on logarithmic temperature scale. This allows direct implementation of logarithmic derivatives, reduces numerical errors as compared to calculations on a linear scale and enables one to reach significantly higher temperatures.

For all quantities under consideration, we could obtain asymptotic expressions by expansion in the coupling  $g^2$ . In general, we use, [126],

$$\frac{1}{g^2(\mu)} \stackrel{2\text{-loop}}{=} 2b_0 \ln \frac{\mu}{\Lambda_{\overline{\text{MS}}}} + \frac{b_0}{b_1} \ln \left( 2 \ln \frac{\mu}{\Lambda_{\overline{\text{MS}}}} \right), \quad (5.28)$$

$$\mu \frac{dg^2}{d\mu} = \beta(g^2) \stackrel{2\text{-loop}}{=} \frac{\beta_0}{(4\pi)^2} g^4(\mu) + \frac{\beta_1}{(4\pi)^4} g^6(\mu) \quad (5.29)$$

with the coefficients

$$\beta_0 \equiv -2(4\pi)^2 b_0 = \frac{-22C_A + 8T_f}{N} \stackrel{\text{pure SU}(3)}{=} -22, \quad (5.30)$$

$$\beta_1 \equiv -2(4\pi)^4 b_1 = \frac{-68C_A^2 + 40C_A T_f + 24C_F T_f}{N} \stackrel{\text{pure SU}(3)}{=} -204 \quad (5.31)$$

and the group-theoretical factors  $C_A = N$  and  $C_F = N^2 - 1$ .  $T_f$  is equal to half the number of quark flavors and thus vanishes in pure gauge. While the results in subsection 5.2.5 are given for the one-loop form (easily obtained by setting  $\beta_1 = b_1 = 0$  in (5.28) and (5.29)), there are only minor changes when switching to the two-loop form.

<sup>4</sup>The author is grateful to Roman Scoccimarro for providing the first version of the program.

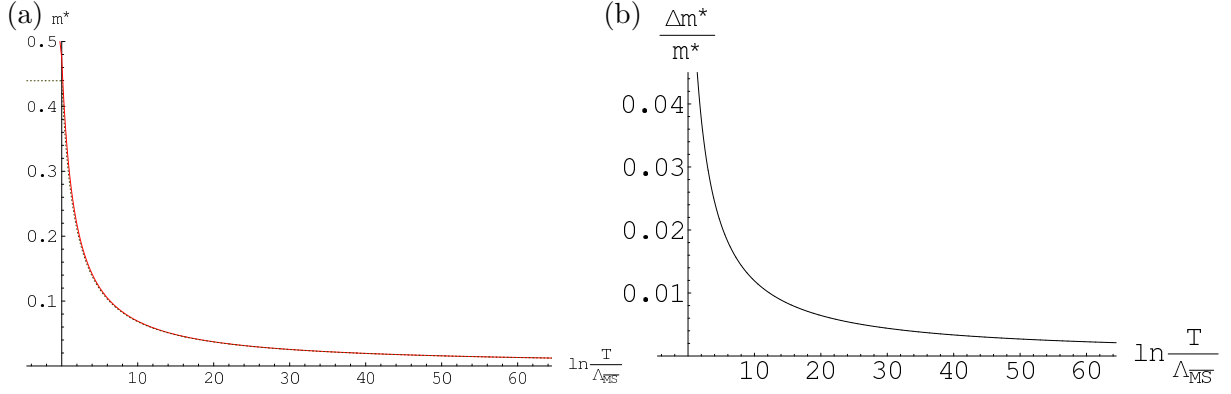


Figure 5.5: The rescaled Gribov mass  $m^* = \frac{m}{T}$ : (a) **solid** – numerical solution, dotted – asymptotic expression from (5.32); (b) relative deviation  $\Delta m_{\text{rel}}^* = (m_{\text{num}}^* - m_{\text{asy}}^*)/m_{\text{asy}}^*$

### 5.2.5 Results

We now summarize the results obtained by numerically solving the gap equation and the corresponding asymptotic expressions.

#### Gribov Mass

Solving the gap equation yields  $m(T)$ . An expansion gives to leading order in  $g^2$

$$m^*(T) \sim \frac{N}{2^{3/2} 3 \pi} g^2(\mu). \quad (5.32)$$

The numerical result and this asymptotic form are displayed in fig. 5.5. The agreement is excellent down to the phase transition (below which the formalism is probably not applicable anyhow), thus higher-order corrections to the Gribov mass are small.

#### Free Energy and Pressure

For the pressure  $p$  and the free energy  $w$  we obtain

$$\frac{p}{T^4} \equiv \frac{w}{T^3} = (N^2 - 1) \left[ \frac{3}{2N} \frac{m^{*4}}{g^2(\mu)} + \frac{1}{3\pi^2 T^4} K(m) \right], \quad (5.33)$$

$$K(m) := \int_0^\infty \frac{dk}{E(k)} \frac{k^4 - m^4}{e^{\beta E(k)} - 1}, \quad (5.34)$$

with  $k = |\mathbf{k}|$ . An expansion for  $K(m)$  is not completely straightforward due to a nonanalyticity in  $m^4$ , but, as shown in [231], it can be performed and yields the asymptotic expression

$$w \sim (N^2 - 1) \frac{\pi^2}{45} \left( 1 - \frac{5}{18} \left( \frac{N g^2}{4\pi^2} \right)^3 \right) T^3. \quad (5.35)$$

The full solution and the asymptotic form are given in fig. 5.6, where we have subtracted the Stefan-Boltzmann part, denoted by  $w_{\text{SB}}$ . In contrast to the case of  $m$ , higher-order corrections are obviously not small for  $w$  since agreement between the full (numerical) and the asymptotic result is not good below  $T \approx 10^6 \Lambda_{\text{MS}}$ .

It is instructive to see that  $K(m)$  can also be evaluated by using an intermediate cutoff. While more cumbersome, this method allows us to identify contributions from different scales and thus gives some idea how to relate this result to the one obtained by effective theory approaches (see section 5.1.5).

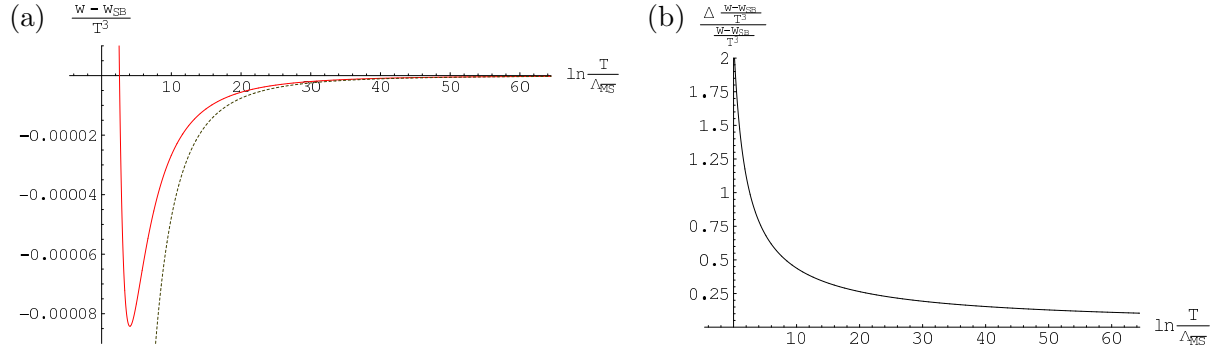


Figure 5.6: The rescaled reduced free energy  $w_r - w_{r,SB}$ : (a) **solid** – numerical solution, dotted – asymptotic expression from (5.35); (b) relative deviation  $\Delta w_{r,rel} = (w_{r,num} - w_{r,asy})/(w_{r,asy} - w_{r,SB}) = (w_{num} - w_{asy})/(w_{asy} - w_{SB})$

To do this, we introduce a cutoff  $\Lambda$  with  $m \ll \Lambda \ll T$ , which separates contributions from the scale  $m \sim g^2 T$  and from the scale  $2\pi T$ . Doing so, we obtain

$$K(m) = \underbrace{\int_0^\Lambda \frac{dk}{E(k)} \frac{k^4 - m^4}{e^{\beta E(k)} - 1}}_{K_1} + \underbrace{\int_\Lambda^\infty \frac{dk}{E(k)} \frac{k^4 - m^4}{e^{\beta E(k)} - 1}}_{K_2}, \quad (5.36)$$

where

$$\begin{aligned} K_1 &= m^4 \int_0^{\Lambda/m} dx \frac{x^4 - 1}{u(x) (e^{\beta m u(x)} - 1)} \\ &\approx m^3 T \int_0^{\Lambda/m} dx \frac{x^4 - 1}{u^2(x)} = m^3 T \int_0^{\Lambda/m} dx x^2 \frac{x^4 - 1}{x^4 + 1} \\ &= m^3 T \left\{ \int_0^{\Lambda/m} dx x^2 - 2 \int_0^{\Lambda/m} \frac{x^2}{x^4 + 1} dx \right\}. \end{aligned} \quad (5.37)$$

The first integral is trivial; for the second we can replace the upper limit  $\Lambda/m$  by  $\infty$  and apply residue calculus to obtain

$$K_1 = \frac{T}{3} \Lambda^3 - \frac{\pi}{\sqrt{2}} m^3 T. \quad (5.38)$$

For  $K_2$  we obtain

$$K_2 \approx \int_\Lambda^\infty \frac{dk}{k} \frac{k^4}{e^{\beta k} - 1} = T^4 \int_{\Lambda/T}^\infty dy \frac{y^3}{e^y - 1} = T^4 \left\{ \int_0^\infty dy \frac{y^3}{e^y - 1} - \int_0^{\Lambda/T} dy \frac{y^3}{e^y - 1} \right\}. \quad (5.39)$$

The first integral is the well-known Planck integral. In the second one we can again expand the exponential, since  $y \leq \frac{\Lambda}{T} \ll 1$ , and obtain

$$K_2 \approx T^4 \left\{ \frac{\pi^4}{15} - \int_0^{\Lambda/T} dy y^2 \right\} = T^4 \frac{\pi^4}{15} - \frac{T}{3} \Lambda^3. \quad (5.40)$$

This gives

$$K = K_1 + K_2 = T^4 \frac{\pi^4}{15} - \frac{\pi}{\sqrt{2}} m^3 T. \quad (5.41)$$

The cutoff-dependent parts in  $K_1$  and  $K_2$  precisely cancel, leaving a clear separation of the Stefan-Boltzmann contribution from  $k \sim T$  and the contribution from the scale  $k \sim m \sim g^2 T$ .

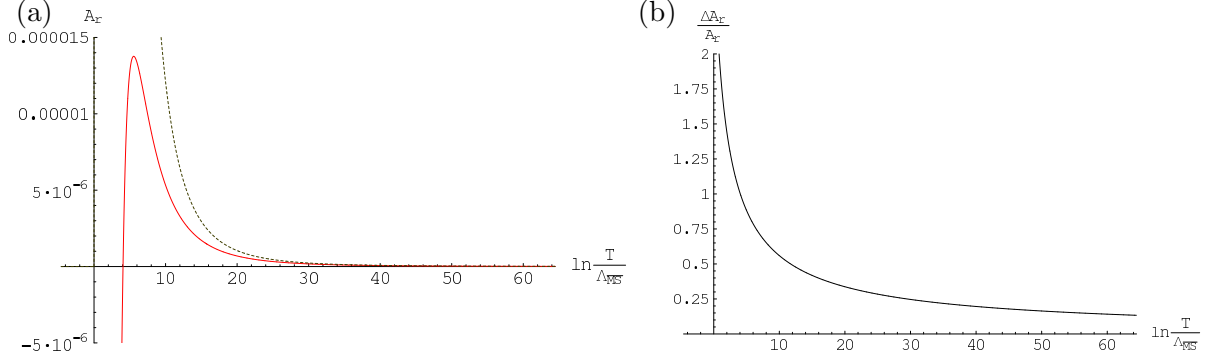


Figure 5.7: The rescaled anomaly  $A_r$ : (a) **solid** – numerical solution, dotted – asymptotic expression from (5.45); (b) relative deviation  $\Delta A_{r,\text{rel}} = (A_{r,\text{num}} - A_{r,\text{asy}})/A_{r,\text{asy}}$

### Energy and Anomaly

From the free energy or the pressure, we can calculate the rescaled anomaly via

$$A_r = \frac{e - 3p}{T^4} = T \frac{d}{dT} \frac{p}{T^4} = \frac{d}{d(\ln \frac{T}{\Lambda})} \frac{p}{T^4}, \quad (5.42)$$

(with some arbitrary scale  $\Lambda$ ) since from (5.1), we have

$$\begin{aligned} T \frac{d}{dT} \frac{p}{T^4} &\equiv T \frac{d}{dT} \frac{w}{T^3} = \frac{\partial w}{\partial T} - 3 \frac{w}{T^3} \\ &= \frac{T^2 \frac{\partial w}{\partial T} - 3wT}{T^4} = \frac{e - 3p}{T^4}. \end{aligned} \quad (5.43)$$

It is also obvious that the energy can be directly obtained from the anomaly by using the relation  $e = 3p + A$ . Thus we do not show separate graphs for  $e$ . From (5.42) it is also clear that *all* deviations from the Stefan-Boltzmann pressure  $p_{r,\text{SB}} = \frac{\pi^4}{15}$  are encoded in the anomaly, since integration gives

$$p_r(T) = p_{r,\text{SB}} - \int_T^\infty \frac{A_r(T')}{T'} dT'. \quad (5.44)$$

From (5.35), (5.42), and (5.29) we obtain

$$A_r \sim -(N^2 - 1) \frac{N^3}{3456 \pi^4} g^4(\mu) \beta(g^2) \frac{T}{\mu} \frac{d\mu}{dT} \quad (5.45)$$

for the asymptotic expansion. The numerical result and the asymptotic form are shown in fig. 5.7. Again higher-order corrections are large except for extremely high temperatures.

### Bulk Viscosity

In formula (5.4) there is one ambiguity, the choice of the scale  $\omega_0$ . According to [119] a reasonable range of values is  $\omega_0 = (0.5 \div 1.5)$  GeV. Neglecting the perturbative contribution from  $\varepsilon_V$ , we obtain

$$\zeta = \frac{1}{9\omega_0} T^5 \frac{d}{dT} \frac{e - 3p}{T^4}. \quad (5.46)$$

The rescaled bulk viscosity is given by

$$\zeta_r = \frac{1}{9\omega_0} T \frac{d}{dT} A_r. \quad (5.47)$$

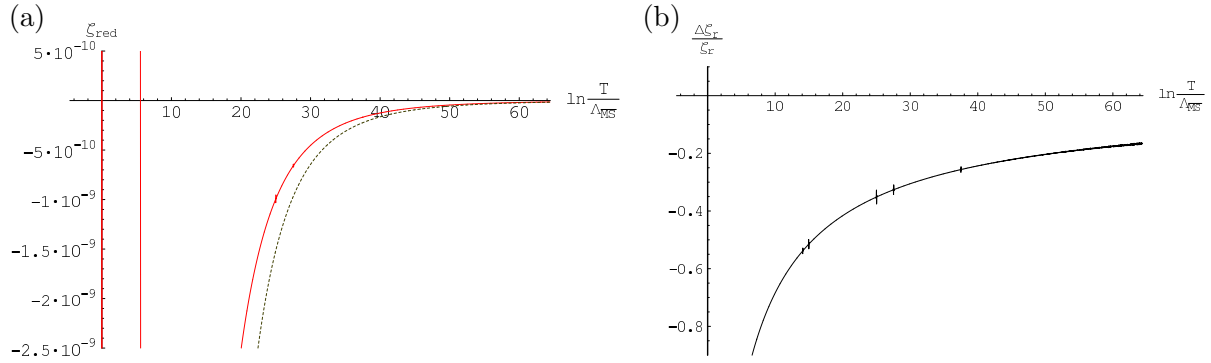


Figure 5.8: The rescaled bulk viscosity: (a) **solid** – numerical solution  $\zeta_{r,\text{num}}$ , dotted – asymptotic expression  $\zeta_{r,\text{asy}}$  from (5.45); (b) relative deviation  $\Delta\zeta_{r,\text{rel}} = (\zeta_{r,\text{num}} - \zeta_{r,\text{asy}})/\zeta_{r,\text{asy}}$

In the asymptotic expression, correction terms originating from  $\frac{T}{\mu} \frac{d\mu}{dT}$  become quite complicated. Since they are relatively unimportant for reasonable choice of  $\mu(T)$  (and even vanish identically for the simple form (5.26)) we only give the simplified expression, where we have set  $\frac{T}{\mu} \frac{d\mu}{dT} = 1$ ,

$$\zeta_r \sim -\frac{1}{9\omega_0} \frac{N^3(N^2-1)}{3456\pi^4} \left\{ 2g^2(\mu) \beta(g^2) + g^4(\mu) \frac{d\beta(g^2)}{dg^2} \right\} \beta(g^2). \quad (5.48)$$

Graphs for the numerical solution and the asymptotic expression are shown in fig. 5.8 for the choice  $\omega_0 = 5\Lambda_{\overline{\text{MS}}}$ .

The behaviour close to  $T = \Lambda_{\overline{\text{MS}}}$  is strongly influenced by the choice of  $\mu(T)$ . Apart from that however the viscosity  $\zeta_r$  rises significantly when the temperature approaches the critical temperature from above, in agreement with [119].

### 5.2.6 Discussion and Outlook

#### Access to the nonperturbative sector

Various results make clear that finite-temperature QCD contains in principle a perturbatively accessible sector, which, starting at order  $(g^2T)^3$ , interacts with a genuine nonperturbative sector. At least formally an expansion in powers of the coupling  $g$  is possible also for non-perturbative contributions.

According to the Gribov-Zwanziger scenario (see sec. 1.3.2) the vicinity of the Gribov horizon dominates the nonperturbative aspects of the theory. So correctly taking into account this region should give access to the nonperturbative sector of the theory at high temperatures as well. Indeed, the cutoff at the Gribov horizon employed in this article gives a finite nonperturbative contribution to the free energy at order  $g^6$ , where the nonperturbative sector of the theory begins to spoil direct perturbative approaches.

The nonperturbative sector (described by MQCD in the picture of section 5.1.5) is also accessible to lattice calculations. Comparison of our analytic result (5.35) with the lattice expressions (5.15) and (5.16) gives

$$w_{\text{np, analyt}}^{(6)} = -\frac{(N^2-1)N^3}{10368\pi^4} g^6 T^3, \quad (5.49)$$

$$w_{\text{np, lattice}}^{(6)} = -\frac{(N^2-1)N^3}{1280\pi^4} (1 \pm 4) g^6 T^3. \quad (5.50)$$

These results are compatible, though the errors of the lattice calculations are too large at the moment to allow a definite statement about the quality of agreement.



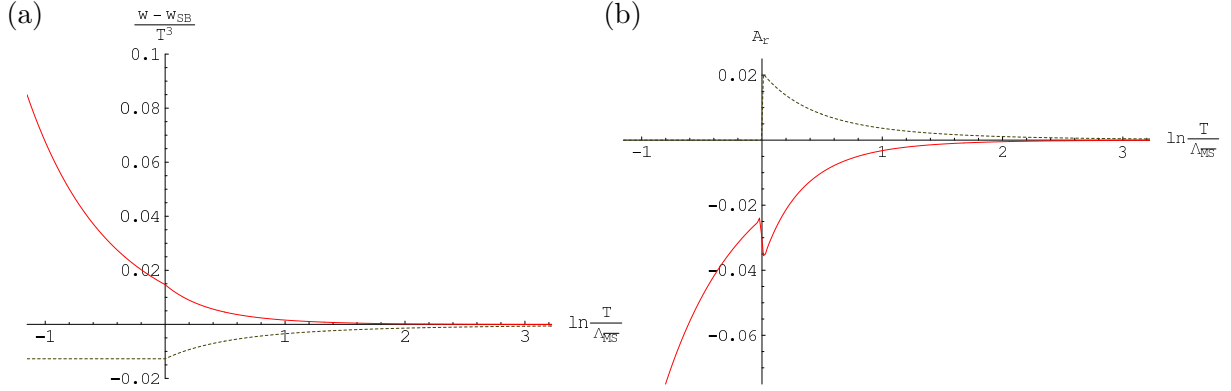


Figure 5.9: (a) The rescaled free energy and (b) the rescaled anomaly  $\frac{e-3p}{T^4}$  in the low-temperature region (solid – numerical solution, dotted – asymptotic expression from (5.45))

### Convergence of the series?

As already mentioned in section 5.1.9, the convergence of perturbation series is extremely poor for temperatures  $\mathcal{O}(\text{GeV})$  or below. As discussed in [35], this can be traced back to the poor convergence of contributions from the EQCD sector, which begin to contribute at order  $g^3$ .

A similar behaviour seems to be true for the contribution from MQCD. While a formal expansion in  $g$  is possible (and for very high temperatures  $T \geq 10^{10}\text{GeV}$  the agreement is reasonably good), the expansion has little to do with the full result for low temperatures. From the low-temperature graphs displayed in fig. 5.9 it is likely that higher-order corrections cannot be small compared to the leading term.

This suggests that either the convergence is extremely poor or that there is even no convergence at all (which would not be surprising, since asymptotic series are in general not convergent). If the expansion in  $g$  of the QCD free energy yields a divergent asymptotic series, one would have the following scenario: For each temperature  $T$  there is an “optimal order”  $n$  beyond which the series leaves the “path of apparent convergence”. For low temperatures and thus large couplings this order may be so small that no partial sum of the perturbation series can serve as a satisfactory approximation.

### Further Steps

The studies performed so far leave open several questions that are worth further investigation: Higher-order calculations in the semi-perturbative formalism could help to further clarify the connection of our approach to the sequence of theories discussed in subsection 5.1.5. They could also help to reveal if (5.49) is indeed the full contribution to order  $g^6$  from the magnetostatic sector or if there are additional contributions from (formally) higher orders as well, which are not present in the lowest-order approximation to the gap equation (5.23).

Such calculations could also shed some more light on the question of (apparent) convergence, as just discussed in subsection 5.2.6. Of course also determination of the full  $g^6$  contribution to the free energy (conceptually possible in the framework of effective theories) would be very helpful for further statements about convergence issues.

Our results indicate that the semi-perturbative method of calculation is reliable only at extremely high  $T$ . A more advanced approach to the nonperturbative sector could involve solving the Dyson-Schwinger equation for the system with local action and auxiliary Fermi and Bose ghost pairs [231] or, alternatively, studying bound-state equations for glueballs in MQCD. Those objects, which determine higher-order contributions from this sector are closely related (though not strictly identical) to chromomagnetic glueballs in the four-dimensional theory.

### 5.3 Coulomb-Gauge Infrared Exponents at Finite Temperature

As briefly mentioned in sec. 3.4.4 and discussed in detail in [12], infrared exponents are tricky to handle in the Coulomb gauge due to the presence of several independent scales. In principle different infrared limits have to be distinguished: Even if one has  $p^2 \rightarrow 0$  and  $p_0^2 \rightarrow 0$ , one could have completely different behaviour depending on the ratio  $\frac{p_0^2}{p^2}$ .<sup>5</sup>

Thus in this section (and accordingly in [132]) we perform a rather drastic step. Since, as outlined in sec. 5.1, also the “deconfined” phase seems to retain many features of (chromomagnetic) confinement, we examine infrared exponents for very large temperatures, where the scale  $p_0^2$  is replaced by Matsubara frequencies  $n 2\pi T$ ,  $n \in \mathbb{N}_0$ , which decouple from the deep infrared for  $n \geq 1$ .

#### 5.3.1 Local action

Our starting point is the Yang-Mills action in  $d = s + 1$  dimensions, gauge-fixed to the Coulomb gauge,

$$S_{\text{YM,Coul}} = \int d^{s+1}x \left( \frac{1}{4} F_{\mu\nu}^2 - i(\partial_i b) A_i + (\partial_i \bar{c}) D_i c \right) \quad (5.51)$$

where  $F_{\mu\nu} = \partial_\mu A_\nu - \partial_\nu A_\mu + g A_\mu \times A_\nu$ , and  $(A_\mu \times A_\nu)^a \equiv f^{abc} A_\mu^b A_\nu^c$ ; the gauge-covariant derivative is given by  $D_i c = D_i[A]c \equiv \partial_i c + g A_i \times c$ . We will now modify the action (5.51) in four ways:

- We apply the on-shell formalism, so the Nakanishi-Lautrup field  $b$  is integrated out in order to directly impose the transversality condition

$$\partial_i A_i = 0. \quad (5.52)$$

- We turn to finite temperature, so the temporal integral has the limits  $\int_0^\beta dx_0$ , where  $\beta = \frac{1}{T}$  and  $T$  is the temperature. Integrals over  $k_0$  will be replaced by a sum over Matsubara frequencies,  $\int dk_0 \rightarrow T \sum_n$ .
- We neglect all but the 0<sup>th</sup> Matsubara frequency,<sup>6</sup> which is the same as dropping all time derivatives,  $\partial_0 \rightarrow 0$ , in the action, and replacing  $\int_0^\beta dx_0 \rightarrow \frac{1}{T}$ , so the action simplifies to

$$S_1 = \frac{1}{T} \int d^s x \left( \frac{1}{2} (D_i A_0)^2 + \frac{1}{4} F_{ij}^2 + \partial_i \bar{c} D_i c \right). \quad (5.53)$$

- We rewrite the theory in the *first-order formalism* (see sec. 3.1.5), by introducing a new field  $\pi_i^a$  by a Gaussian identity, so the action reads

$$S_2 = \frac{1}{T} \int d^s x \left[ i\pi_i (-D_i A_0) + \frac{1}{2} \pi_i^2 + \frac{1}{4} F_{ij}^2 + \partial_i \bar{c} D_i c \right]. \quad (5.54)$$

The new field (which can be interpreted as the momentum conjugate to  $A_i^a$  and thus plays the role of a color-electric field) is decomposed into transverse and longitudinal parts,  $\pi_i = \pi'_i - \partial_i \varphi$ , where  $\pi'_i$  is transverse,  $\partial_i \pi'_i = 0$ , which gives the action that will be used to derive the DSEs,

$$S = \frac{1}{T} \int d^s x \left[ i(\pi'_i - \partial_i \varphi)(-D_i A_0) + \frac{1}{2} (\pi'_i)^2 + \frac{1}{2} (\partial_i \varphi)^2 + \frac{1}{4} F_{ij}^2 + \partial_i \bar{c} D_i c \right]. \quad (5.55)$$

<sup>5</sup>In general one encounters all problems present for functions of two real variables, where not only in general  $\lim_{x \rightarrow 0} \lim_{y \rightarrow 0} f(x, y) \neq \lim_{y \rightarrow 0} \lim_{x \rightarrow 0} f(x, y)$ , but the limit  $\lim_{(x_n, y_n) \rightarrow (0,0)} f(x_n, y_n)$  may even depend on the precise path on which the origin is approached.

<sup>6</sup>Note that the Linde problem [133] has its origin in the zeroth Matsubara frequency as well.

### 5.3.2 Definition of propagators and proper 2-point functions

If we confine ourselves to the zero Matsubara frequency, propagators only depend on the spatial momentum. The propagators of the transverse fields are defined as

$$\begin{aligned}\langle A_i^a(x) A_j^b(y) \rangle &= \int \frac{d^s k}{(2\pi)^s} e^{ik \cdot (x-y)} \delta^{ab} P_{ij}^T(k) D_{AA}(k), \\ \langle \pi_i'^a(x) \pi_j^b(y) \rangle &= \int \frac{d^s k}{(2\pi)^s} e^{ik \cdot (x-y)} \delta^{ab} P_{ij}^T(k) D_{\pi\pi}(k),\end{aligned}\quad (5.56)$$

where  $P_{ij}^T(k)$  is the transverse projector,

$$P_{ij}^T(k) = \delta_{ij} - \frac{k_i k_j}{k^2}. \quad (5.57)$$

The propagator  $\langle \pi_i'(x) A_j(y) \rangle$  is proportional to  $k_0$  both at tree-level and for the power-law ansätze employed in sec. 5.3.4. Thus it has vanishing zero-Matsubara component in this context, and will be neglected in the asymptotic infrared limit,

$$\langle \pi_i'(x) A_j(y) \rangle = 0. \quad (5.58)$$

This removes the mixing of the transverse fields, so the proper functions are given as the one-dimensional inverse of the propagators,

$$\Gamma_{\mathbf{AA}}(k) = \frac{D_{\pi'\pi'}}{D_{\mathbf{AA}} D_{\pi'\pi'} - D_{\mathbf{A}\pi'}^2} \rightarrow \frac{1}{D_{\mathbf{AA}}(k)}, \quad (5.59)$$

$$\Gamma_{\pi'\pi'}(k) = \frac{D_{\mathbf{AA}}}{D_{\mathbf{AA}} D_{\pi'\pi'} - D_{\mathbf{A}\pi'}^2} \rightarrow \frac{1}{D_{\pi'\pi'}(k)}. \quad (5.60)$$

On the other hand, the scalar Bose fields do mix. Their propagators are defined by

$$\begin{aligned}\langle A_0^a(x) A_0^b(y) \rangle &= \int \frac{d^s k}{(2\pi)^s} e^{ik \cdot (x-y)} \delta^{ab} D_{A_0 A_0}(k), \\ \langle A_0^a(x) \varphi^b(y) \rangle &= \int \frac{d^s k}{(2\pi)^s} e^{ik \cdot (x-y)} \delta^{ab} D_{A_0 \varphi}(k), \\ \langle \varphi^a(x) \varphi^b(y) \rangle &= \int \frac{d^s k}{(2\pi)^s} e^{ik \cdot (x-y)} \delta^{ab} D_{\varphi \varphi}(k),\end{aligned}\quad (5.61)$$

the Faddeev-Popov ghost propagator is defined by

$$\langle c^a(x) \bar{c}^b(y) \rangle = \int \frac{d^s k}{(2\pi)^s} e^{ik \cdot (x-y)} \delta^{ab} D_{c\bar{c}}(k). \quad (5.62)$$

While the inversion of the ghost propagator (in order to obtain the proper 2-point function) is simple,

$$\Gamma_{\bar{c}c}(k) = \frac{1}{D_{c\bar{c}}(k)}, \quad (5.63)$$

for the other scalar fields the proper 2-point functions are two-dimensional matrix inverses of the propagators,

$$\Gamma_{A_0 A_0}(k) = \frac{D_{\varphi \varphi}(k)}{\Delta(k)}, \quad \Gamma_{\varphi \varphi}(k) = \frac{D_{A_0 A_0}(k)}{\Delta(k)}, \quad \Gamma_{A_0 \varphi}(k) = -\frac{D_{\varphi A_0}(k)}{\Delta(k)}, \quad (5.64)$$

where

$$\Delta \equiv D_{\varphi \varphi} D_{A_0 A_0} - D_{A_0 \varphi}^2. \quad (5.65)$$

### 5.3.3 Truncated Dyson-Schwinger equations

The derivation of the Dyson-Schwinger equations for the theory described by (5.55) is straightforward, yet tedious; see the exemplary derivation given in sec. 2.3.

To simplify this endeavour we neglect the cubic and quartic pieces of  $F_{ij}$  in (5.55), since the scalar fields  $A_0$ ,  $\varphi$ ,  $c$  and  $\bar{c}$  are expected to be dominant in the infrared; loops containing a three- or four-gluon vertex (and the corresponding amount of transverse propagators) are supposed to be subdominant..

To further simplify the equations (and since little is known about the dressed vertices of this theory anyway), we employ a truncation in which dressed vertices are replaced by bare ones. (Note that in [12] a more general ansatz for the vertices did not change the general picture.) A graphical representation of the resulting DSEs is given in Figure 5.10.

With these truncations, the equation for  $\Gamma_{\mathbf{AA}}$  reads

$$P_{ij}^T(k)\Gamma_{\mathbf{AA}}(k) = P_{ij}^T(k) k^2 + g^2 T N P_{im}^T(k) I_{mn} P_{nj}^T(k), \quad (5.66)$$

where the temperature  $T$  stems from the Matsubara sum (of which we keep only the zeroth term). The loop integral  $I_{mn}(k)$  is sandwiched between transverse projectors  $P^T(k)$ , and is given by

$$I_{mn}(k) \equiv \int \frac{d^s p}{(2\pi)^s} \left[ D_{\pi_m \pi_n}(p) D_{A_0 A_0}(p+k) + p_m p_n \left( D_{\varphi A_0}(p) D_{A_0 \varphi}(p+k) + D_{c\bar{c}}(p) D_{c\bar{c}}(p+k) \right) \right],$$

where the propagator of the color-electric field has the decomposition

$$D_{\pi_m \pi_n}(p) = P_{mn}^T(p) D_{\pi' \pi'}(p) + p_m p_n D_{\varphi \varphi}(p). \quad (5.67)$$

The DS equation for  $\Gamma_{\pi' \pi'}$  reads

$$P_{ij}^T(k)\Gamma_{\pi' \pi'}(k) = P_{ij}^T(k) + g^2 T N P_{im}^T(k) J_{mn} P_{nj}^T(k) \quad (5.68)$$

where the loop integral is given by

$$J_{mn}(k) \equiv \int \frac{d^s p}{(2\pi)^s} P_{mn}^T(p) D_{\mathbf{AA}}(p) D_{A_0 A_0}(p+k). \quad (5.69)$$

We further obtain the equation for  $\Gamma_{A_0 A_0}$ ,

$$\Gamma_{A_0 A_0}(k) = g^2 T N \int \frac{d^s p}{(2\pi)^s} P_{ij}^T(p) D_{\mathbf{AA}}(p) D_{\pi_j \pi_i}(p+k), \quad (5.70)$$

where  $D_{\pi_j \pi_i}$  is given in (5.67). The DS equation for  $\Gamma_{\varphi \varphi}$  reads

$$\Gamma_{\varphi \varphi}(k) = k^2 + g^2 T N \int \frac{d^s p}{(2\pi)^s} k_i k_j P_{ij}^T(p) D_{\mathbf{AA}}(p) D_{A_0 A_0}(p+k), \quad (5.71)$$

the DS equation for  $\Gamma_{\varphi A_0}$  is given by

$$\Gamma_{\varphi A_0}(k) = i k^2 + g^2 T N \int \frac{d^s p}{(2\pi)^s} P_{ij}^T(p) D_{\mathbf{AA}}(p) k_i k_j D_{A_0 \varphi}(p+k). \quad (5.72)$$

Finally the equation for  $\Gamma_{\bar{c}c}$  reads

$$\Gamma_{\bar{c}c}(k) = k^2 - g^2 T N \int \frac{d^s p}{(2\pi)^s} P_{ij}^T(p) D_{\mathbf{AA}}(p) k_i k_j D_{c\bar{c}}(p+k). \quad (5.73)$$

The tree-level terms in equations (5.66) to (5.73) do not directly affect the infrared asymptotic behaviour for essentially two reasons:

- The scalar fields are expected to be infrared-enhanced. Accordingly we impose the horizon condition [221, 224] on the Faddeev-Popov ghosts and (since we expect at least qualitatively analogous behaviour) also on the bosonic fields. As a consequence, the tree-level part in (5.70) to (5.73) is cancelled by quantum fluctuations.
- The DS equations for the transverse fields contain at least one (uncancelled) loop with at least one scalar propagator, which will – due to infrared enhancement – dominate the tree-level part.

### 5.3.4 Definition of infrared critical exponents

The only dimensionful parameter in the DSEs is  $g^2T$ , which in spatial dimension  $s$  provides a mass scale  $m$  defined by

$$m^{4-s} = g^2T. \quad (5.74)$$

As an ansatz we look for a solution to the DSE for the one-Matsubara frequency propagator that is a simple power law in the spatial momentum,

$$\begin{aligned} D_{\mathbf{A}\mathbf{A}}(k) &\sim \frac{b_{\mathbf{A}}m^{2\alpha_{\mathbf{A}}}}{(k^2)^{1+\alpha_{\mathbf{A}}}}; & D_{\pi'\pi'}(k) &\sim \frac{b_{\pi'}m^{2\alpha_{\pi'}}}{(k^2)^{\alpha_{\pi'}}}; \\ D_{c\bar{c}}(k) &\sim \frac{b_{\text{gh}}m^{2\alpha_{\text{gh}}}}{(k^2)^{1+\alpha_{\text{gh}}}}; & D_{A_0A_0}(k) &\sim \frac{b_0m^{2\alpha_0}}{(k^2)^{1+\alpha_0}}; \\ D_{\varphi A_0}(k) &\sim \frac{-ib_m m^{2\alpha_m}}{(k^2)^{1+\alpha_m}}; & D_{\varphi\varphi}(k) &\sim \frac{b_{\varphi}m^{2\alpha_{\varphi}}}{(k^2)^{1+\alpha_{\varphi}}}. \end{aligned} \quad (5.75)$$

In the following it will be sometimes convenient to write  $\alpha_{\pi'} = 1 + \hat{\alpha}_{\pi'}$ . The mass  $m$  cancels out of all equations because of engineering dimensions.

### 5.3.5 Infrared asymptotic DS equations

In the DS equations, we take the external momentum  $k$  and the loop momentum  $p$  to be small compared to the other scales in the theory, and we take the infrared asymptotic form of the propagators. This will yield a finite system of equations which will provide a self-consistent infrared limit of the propagators.

The infrared asymptotic equations read<sup>7</sup> (with loop integrals  $I_{S(V,S)}$ ,  $I_{S(V,V)}$  etc. to be defined in sec. 5.3.5) for  $\Gamma_{A_0A_0}$

$$\frac{b_{\varphi}}{b_0b_{\varphi} + b_m^2} = b_{\mathbf{A}}b_{\varphi}I_{S(V,S)}(\alpha_{\mathbf{A}}, \alpha_{\varphi}) + b_{\mathbf{A}}b_{\pi'}I_{S(V,V)}(\alpha_{\mathbf{A}}, \hat{\alpha}_{\pi'}); \quad (5.76)$$

for  $\Gamma_{\varphi A_0}$ ,

$$\frac{b_m}{b_0b_{\varphi} + b_m^2} = -b_{\mathbf{A}}b_mI_{S(V,S)}(\alpha_{\mathbf{A}}, \alpha_m); \quad (5.77)$$

for  $\Gamma_{\varphi\varphi}$ ,

$$\frac{b_0}{b_0b_{\varphi} + b_m^2} = b_{\mathbf{A}}b_0I_{S(V,S)}(\alpha_{\mathbf{A}}, \alpha_0); \quad (5.78)$$

---

<sup>7</sup>We have checked explicitly that in the infrared, given the DS equations of Figure 5.10, both the assumption  $D_{\varphi\varphi}D_{A_0A_0} \ll D_{A_0\varphi}^2$  and  $D_{\varphi\varphi}D_{A_0A_0} \gg D_{A_0\varphi}^2$  lead to a contradiction for this system of equations. Thus  $D_{\varphi\varphi}D_{A_0A_0}$  and  $D_{A_0\varphi}^2$  have the same infrared behavior. A possibility we have not further explored in this article is a cancellation  $b_0b_{\varphi} + b_m^2 = 0$ .

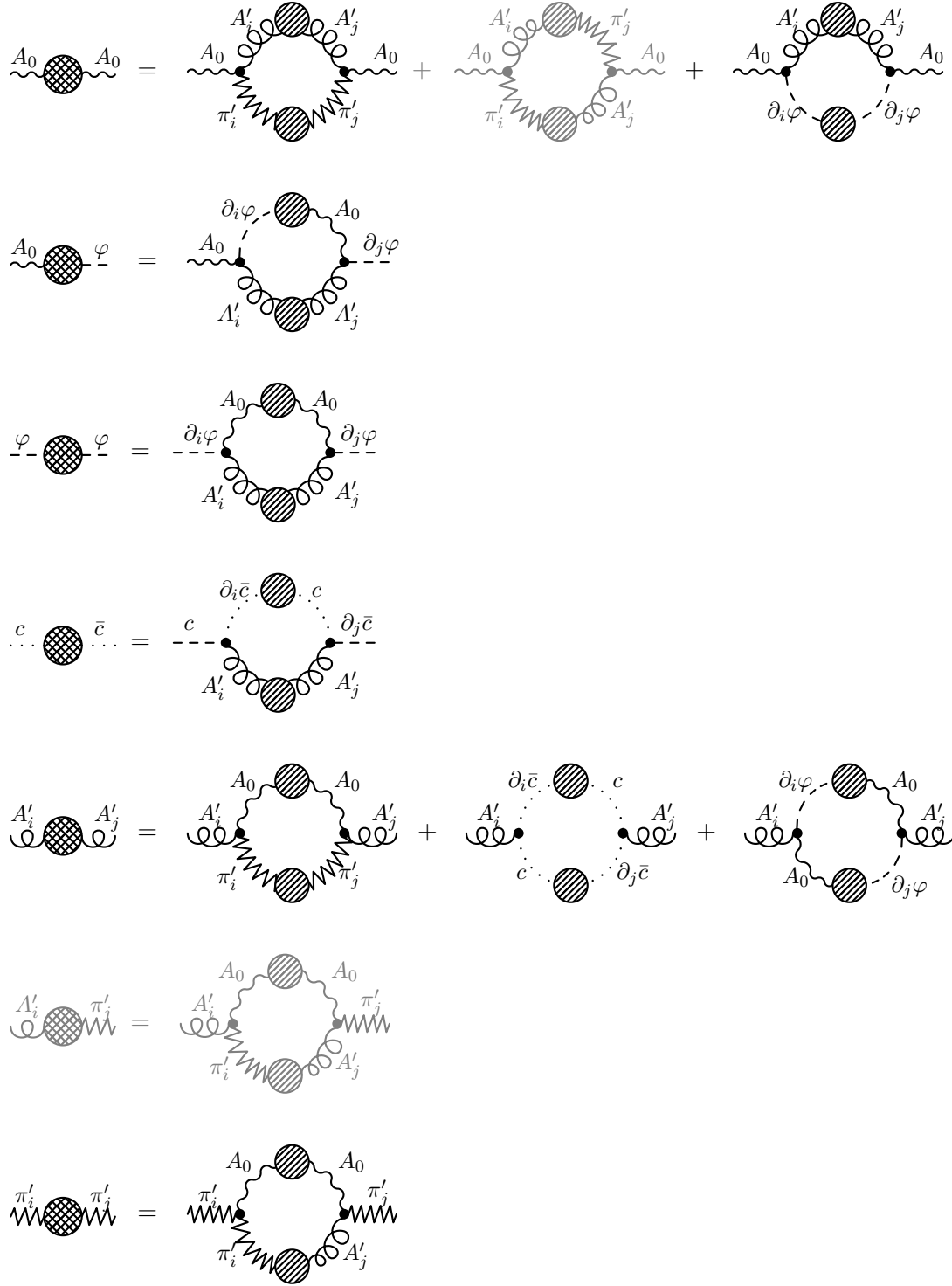


Figure 5.10: The system of bare vertex truncated Dyson-Schwinger equations in the first-order formalism, where the tree-level terms have (for the transverse fields) been neglected or (for the scalar fields) removed by imposing the horizon condition. Prefactors and signs have been absorbed in the graphs. Diagrams and equations drawn in gray drop out in the approximation (5.58).

for  $\Gamma_{\mathbf{A}\mathbf{A}}$ ,

$$\begin{aligned} 1 = & b_{\mathbf{A}} b_0 b_{\pi'} I_{V(V,S)}(\hat{\alpha}_{\pi'}, \alpha_0) + b_{\mathbf{A}} b_0 b_{\varphi} I_{V(S,S)}(\alpha_0, \alpha_{\varphi}) \\ & - b_{\mathbf{A}} b_m^2 I_{V(S,S)}(\alpha_m, \alpha_m) + b_{\mathbf{A}} b_{\text{gh}}^2 I_{V(S,S)}(\alpha_{\text{gh}}, \alpha_{\text{gh}}). \end{aligned} \quad (5.79)$$

for  $\Gamma_{\pi'\pi'}$ ,

$$1 = b_{\mathbf{A}} b_0 b_{\pi'} I_{V(V,S)}(\alpha_{\mathbf{A}}, \alpha_0); \quad (5.80)$$

for  $\Gamma_{\bar{c}c}$ ,

$$1 = -b_{\mathbf{A}} b_{\text{gh}}^2 I_{S(V,S)}(\alpha_{\mathbf{A}}, \alpha_{\text{gh}}). \quad (5.81)$$

**Symmetry of the infrared asymptotic equations** There is a two-parameter continuous symmetry transformation that these equations inherit from the cubic interaction terms  $\pi_i g A_i \times A_0$  and  $\partial_i \bar{c} g A_i \times c$ , namely

$$\begin{aligned} A_i & \rightarrow \exp(i\beta) A_i; & A_0 & \rightarrow \exp(i\gamma) A_0; & c & \rightarrow \exp(i\gamma) c \\ \pi_i & \rightarrow \exp[-i(\beta + \gamma)] \pi_i; & \bar{c} & \rightarrow \exp[-i(\beta + \gamma)] \bar{c}. \end{aligned} \quad (5.82)$$

As a consequence of this symmetry, the infrared asymptotic DS equations are invariant under the transformations of the asymptotic propagators

$$\begin{aligned} b_{\mathbf{A}} & \rightarrow \exp(2i\beta) b_{\mathbf{A}}; & b_{\pi'} & \rightarrow \exp[-2i(\beta + \gamma)] b_{\pi'} \\ b_{\text{gh}} & \rightarrow \exp(-i\beta) b_{\text{gh}}; & b_0 & \rightarrow \exp(2i\gamma) b_0; \\ b_m & \rightarrow \exp(-i\beta) b_m; & b_{\varphi} & \rightarrow \exp[-2i(\beta + \gamma)] b_{\varphi}. \end{aligned} \quad (5.83)$$

Because of this 2-parameter symmetry the DS equations provide only 4 relations among the 6  $b$ -coefficients.

**Definition of loop integrals** We now define the symbols that represent the loop integrals,

$$I_{S(V,S)}(\alpha_{\mathbf{A}}, \alpha_{\varphi}) \equiv N k^{-s+2\alpha_{\mathbf{A}}+2\alpha_{\varphi}+2} \int \frac{d^s p}{(2\pi)^s} \frac{k^2 p^2 - (p \cdot k)^2}{(p^2)^{2+\alpha_{\mathbf{A}}} [(k-p)^2]^{1+\alpha_{\varphi}}}, \quad (5.84)$$

$$I_{V(V,S)}(\alpha_{\mathbf{A}}, \alpha_0) \equiv \frac{N k^{-s+2\alpha_{\mathbf{A}}+2\alpha_0+2}}{s-1} \int \frac{d^s p}{(2\pi)^s} \frac{(s-2)k^2 p^2 + (p \cdot k)^2}{(p^2)^{2+\alpha_{\mathbf{A}}} [(k-p)^2]^{1+\alpha_0}}, \quad (5.85)$$

$$I_{S(V,V)}(\alpha_{\mathbf{A}}, \hat{\alpha}_{\pi'}) \equiv N k^{-s+2\alpha_{\mathbf{A}}+2\hat{\alpha}_{\pi'}+4} \int \frac{d^s p}{(2\pi)^s} \frac{(s-2)(k-p)^2 p^2 + [(k-p) \cdot p]^2}{(p^2)^{2+\alpha_{\mathbf{A}}} [(k-p)^2]^{2+\hat{\alpha}_{\pi'}}}, \quad (5.86)$$

$$I_{V(S,S)}(\alpha_0, \alpha_{\varphi}) \equiv \frac{N k^{-s+2\alpha_0+2\alpha_{\varphi}}}{s-1} \int \frac{d^s p}{(2\pi)^s} \frac{k^2 p^2 - (p \cdot k)^2}{(p^2)^{1+\alpha_0} [(k-p)^2]^{1+\alpha_{\varphi}}}. \quad (5.87)$$

One sees by inspection that two of the symbols are related by

$$I_{V(S,S)}(\alpha_0, \alpha_{\varphi}) = (s-1)^{-1} I_{S(V,S)}(\alpha_0 - 1, \alpha_{\varphi}). \quad (5.88)$$

The symbols have the value (see also appendix C.4.2)

$$I_{S(V,S)}(\alpha_{\mathbf{A}}, \alpha_{\text{gh}}) = \frac{N(s-1)}{2(4\pi)^{s/2}} \frac{\Gamma(2 + \alpha_{\mathbf{A}} + \alpha_{\text{gh}} - s/2)}{\Gamma(2 + \alpha_{\mathbf{A}})} \frac{\Gamma(s/2 - \alpha_{\text{gh}}) \Gamma(s/2 - \alpha_{\mathbf{A}} - 1)}{\Gamma(1 + \alpha_{\text{gh}}) \Gamma(s - \alpha_{\text{gh}} - \alpha_{\mathbf{A}} - 1)}, \quad (5.89)$$

$$I_{V(V,S)}(\alpha_{\mathbf{A}}, \alpha_0) = \frac{N c_1}{4(4\pi)^{s/2}} \frac{\Gamma(2 + \alpha_{\mathbf{A}} + \alpha_0 - s/2)}{\Gamma(2 + \alpha_{\mathbf{A}})} \frac{\Gamma(s/2 - \alpha_0 - 1) \Gamma(s/2 - \alpha_{\mathbf{A}} - 1)}{\Gamma(1 + \alpha_0) \Gamma(s - \alpha_0 - \alpha_{\mathbf{A}} - 1)}, \quad (5.90)$$

where

$$c_1 \equiv (s-1)(4\alpha_{\mathbf{A}} + 3) - (2\alpha_{\mathbf{A}} + 2\alpha_0 + 3)(2\alpha_{\mathbf{A}} + 1), \quad (5.91)$$



$$I_{S(V,V)}(\alpha_{\mathbf{A}}, \hat{\alpha}_{\pi'}) = \frac{N c_2}{4(4\pi)^{s/2}} \frac{\Gamma(2 + \alpha_{\mathbf{A}} + \hat{\alpha}_{\pi'} - s/2)}{\Gamma(2 + \alpha_{\mathbf{A}})} \frac{\Gamma(s/2 - \hat{\alpha}_{\pi'} - 1) \Gamma(s/2 - \alpha_{\mathbf{A}} - 1)}{\Gamma(2 + \hat{\alpha}_{\pi'}) \Gamma(s - \alpha_{\mathbf{A}} - \hat{\alpha}_{\pi'} - 2)} \quad (5.92)$$

where

$$c_2 \equiv (s - 1) [s - 1 + (1 + 2\alpha_{\mathbf{A}})(1 + 2\hat{\alpha}_{\pi'})], \quad (5.93)$$

and

$$I_{V(S,S)}(\alpha_0, \alpha_{\varphi}) = \frac{N}{2(4\pi)^{s/2}} \frac{\Gamma(1 + \alpha_0 + \alpha_{\varphi} - s/2)}{\Gamma(1 + \alpha_0)} \frac{\Gamma(s/2 - \alpha_{\varphi}) \Gamma(s/2 - \alpha_0)}{\Gamma(1 + \alpha_{\varphi}) \Gamma(s - \alpha_{\varphi} - \alpha_0)}. \quad (5.94)$$

**Check of loop integrals** We obtain a useful check on the evaluation of the loop integrals by rewriting<sup>8</sup> the numerator of the integrand of  $I_{S(V,V)}$ ,

$$\mathcal{N} \equiv \text{Tr}[(q^2 - qq)(p^2 - pp)], \quad (5.95)$$

where  $q = k - p$ . We have

$$\begin{aligned} T &= q^2(s-1)p^2 - q \cdot (p^2 - pp) \cdot q \\ &= \frac{q^2}{k^2} k^2(s-1)p^2 - k \cdot (p^2 - pp) \cdot k \\ &= \frac{q^2}{k^2} \text{Tr}[(k^2 - kk)(p^2 - pp)] + \left(\frac{q^2}{k^2} - 1\right) k \cdot (p^2 - pp) \cdot k, \end{aligned} \quad (5.96)$$

which, by comparison with (5.84) through (5.87), leads to the identity

$$\begin{aligned} I_{S(V,V)}(\alpha_{\mathbf{A}}, \hat{\alpha}_{\pi'}) &= (s-1)I_{V(V,S)}(\alpha_{\mathbf{A}}, \hat{\alpha}_{\pi'}) + I_{S(V,S)}(\alpha_{\mathbf{A}}, \hat{\alpha}_{\pi'}) \\ &\quad - (s-1)I_{V(S,S)}(1 + \alpha_{\mathbf{A}}, 1 + \hat{\alpha}_{\pi'}). \end{aligned} \quad (5.97)$$

As a precise check, it has been verified that this relation between the 4 integrals is satisfied by the 4 values just given.

### 5.3.6 Determination of infrared critical exponents

**4 power-relations among infrared critical exponents** There are 6 infrared critical exponents and 6 DS equations. By equating powers of momentum on both sides of the DS equations, one obtains relations between the infrared critical exponents. From the equation for  $\Gamma_{\bar{c}c}$ , one obtains

$$2\alpha_{\text{gh}} + \alpha_{\mathbf{A}} = (s-4)/2; \quad (5.98)$$

from the equation for  $\Gamma_{\varphi\varphi}$ ,

$$\alpha_0 + \alpha_{\varphi} + \alpha_{\mathbf{A}} = (s-4)/2; \quad (5.99)$$

from the equation for  $\Gamma_{\varphi A_0}$ ,

$$2\alpha_m + \alpha_{\mathbf{A}} = (s-4)/2; \quad (5.100)$$

from the equation for  $\Gamma_{\pi'\pi'}$ ,

$$\alpha_0 + \alpha_{\pi'} + \alpha_{\mathbf{A}} = (s-4)/2. \quad (5.101)$$

---

<sup>8</sup>In the following the expression  $p_1 p_2$  denotes the dyadic product of the  $s$ -vectors  $p_1$  and  $p_2$ . In a less compact way, one would write (5.95) as

$$\mathcal{N} \equiv \text{Tr}_s \left[ \left( |q|^2 \mathbb{1}_s - \mathbf{q} \mathbf{q}^\top \right) \left( |p|^2 \mathbb{1}_s - \mathbf{p} \mathbf{p}^\top \right) \right],$$

where  $\mathbf{p}$  and  $\mathbf{q}$  are column vectors and  $\top$  denotes transposition.

These 4 power relations come from the 4 DS equations that have only one term on the right-hand side. They leave undetermined two infrared critical exponents which we may choose to be  $\alpha_{\text{gh}}$  and  $\alpha_0$ . The remaining infrared critical exponents may be expressed in terms of these by

$$\begin{aligned}\alpha_{\mathbf{A}} &= (s-4)/2 - 2\alpha_{\text{gh}}, \\ \alpha_m &= \alpha_{\text{gh}}, \\ \alpha_{\pi'} &= \alpha_\varphi = 2\alpha_{\text{gh}} - \alpha_0.\end{aligned}\tag{5.102}$$

The equation

$$\alpha_0 + \alpha_\varphi = 2\alpha_m,\tag{5.103}$$

which follows from the above, relates the critical exponents of  $D_{A_0 A_0} \sim 1/k^{2+2\alpha_0}$ ,  $D_{\varphi\varphi} \sim 1/k^{2+2\alpha_\varphi}$  and  $D_{\varphi\alpha_0} \sim 1/k^{2+\alpha_\varphi+\alpha_0}$ . Thus the infrared critical exponents  $\alpha_0$  and  $\alpha_\varphi$  characterize the elementary fields  $A_0$  and  $\varphi$ .

**Equations for  $\alpha_0$  and  $\alpha_{\text{gh}}$**  When the above 4 power relations on the 6 critical exponents (the 6  $\alpha$ 's) are satisfied, the power relations among the remaining 2 DS equations are satisfied identically. The 6 DS equations also provide 6 relations among the 6  $b$ -coefficients. However, because of the 2-parameter symmetry invariance (5.83), of these 6 equations, only 4 are independent conditions on the  $b$ -coefficients. The remaining two equations provide consistency conditions that determine the two missing relations among the infrared critical exponents, as we now show. Thus all 6 infrared critical exponents are determined.

From (5.77) and (5.78) we obtain an equation relating critical exponents,

$$I_{S(V,S)}(\alpha_{\mathbf{A}}, \alpha_{\text{gh}}) = -I_{S(V,S)}(\alpha_{\mathbf{A}}, \alpha_0),\tag{5.104}$$

where we have used  $\alpha_{\text{gh}} = \alpha_m$ .

The remaining relation between critical exponents is obtained as follows. From (5.77) and (5.81) and power relation  $\alpha_{\text{gh}} = \alpha_m$  we obtain

$$b_{\text{gh}}^2 = b_0 b_\varphi + b_m^2.\tag{5.105}$$

This equation allows us to write (5.76) as

$$b_\varphi = b_{\mathbf{A}} b_\varphi b_{\text{gh}}^2 I_{S(V,S)}(\alpha_{\mathbf{A}}, \alpha_\varphi) + b_{\mathbf{A}} b_{\pi'} b_{\text{gh}}^2 I_{S(V,V)}(\alpha_{\mathbf{A}}, \hat{\alpha}_{\pi'})\tag{5.106}$$

or, by (5.81),

$$\frac{b_{\pi'}}{b_\varphi} = \frac{-I_{S(V,S)}(\alpha_{\mathbf{A}}, \alpha_{\text{gh}}) - I_{S(V,S)}(\alpha_{\mathbf{A}}, \alpha_\varphi)}{I_{S(V,V)}(\alpha_{\mathbf{A}}, \hat{\alpha}_{\pi'})} \equiv F_1.\tag{5.107}$$

Likewise (5.105) allows us to write (5.79) as

$$\begin{aligned}1 &= b_{\mathbf{A}} b_0 b_{\pi'} I_{V(V,S)}(\hat{\alpha}_{\pi'}, \alpha_0) + b_{\mathbf{A}} b_0 b_\varphi I_{V(S,S)}(\alpha_0, \alpha_\varphi) \\ &\quad + b_{\mathbf{A}} (b_0 b_\varphi - b_{\text{gh}}^2) I_{V(S,S)}(\alpha_m, \alpha_m) + b_{\mathbf{A}} b_{\text{gh}}^2 I_{V(S,S)}(\alpha_{\text{gh}}, \alpha_{\text{gh}}).\end{aligned}\tag{5.108}$$

With  $\alpha_m = \alpha_{\text{gh}}$ , there is a partial cancellation between the last two terms which are the contribution from bose and fermi ghost loops respectively, and we obtain

$$\begin{aligned}1 &= b_{\mathbf{A}} b_0 b_{\pi'} I_{V(V,S)}(\hat{\alpha}_{\pi'}, \alpha_0) \\ &\quad + b_{\mathbf{A}} b_0 b_\varphi [I_{V(S,S)}(\alpha_0, \alpha_\varphi) + I_{V(S,S)}(\alpha_{\text{gh}}, \alpha_{\text{gh}})].\end{aligned}\tag{5.109}$$

This gives, by (5.80)

$$\frac{b_{\pi'}}{b_\varphi} = \frac{I_{V(S,S)}(\alpha_0, \alpha_\varphi) + I_{V(S,S)}(\alpha_{\text{gh}}, \alpha_{\text{gh}})}{I_{V(V,S)}(\alpha_{\mathbf{A}}, \alpha_0) - I_{V(V,S)}(\hat{\alpha}_{\pi'}, \alpha_0)} \equiv F_2.\tag{5.110}$$

From equations (5.107) and (5.110) we obtain the final equation that determines the infrared critical exponents.

$$F_1 - F_2 = 0. \quad (5.111)$$

Equations (5.104) and (5.111) together with the above power relations given previously determine the remaining two infrared critical exponents,  $\alpha_0$  and  $\alpha_{\text{gh}}$ .

**General Remarks on the Equations** The driving force of the system seems to be equation (5.104). Upon canceling common factors, this equation reads, from (5.89),

$$\frac{-\Gamma(2 + \alpha_{\mathbf{A}} + \alpha_{\text{gh}} - s/2) \Gamma(s/2 - \alpha_{\text{gh}})}{\Gamma(1 + \alpha_{\text{gh}}) \Gamma(s - \alpha_{\text{gh}} - \alpha_{\mathbf{A}} - 1)} = \frac{\Gamma(2 + \alpha_{\mathbf{A}} + \alpha_0 - s/2) \Gamma(s/2 - \alpha_0)}{\Gamma(1 + \alpha_0) \Gamma(s - \alpha_0 - \alpha_{\mathbf{A}} - 1)}. \quad (5.112)$$

We eliminate  $\alpha_{\mathbf{A}}$  using  $\alpha_{\mathbf{A}} = -2\alpha_{\text{gh}} + (s - 4)/2$  and obtain

$$\frac{-\Gamma(-\alpha_{\text{gh}}) \Gamma(s/2 - \alpha_{\text{gh}})}{\Gamma(1 + \alpha_{\text{gh}}) \Gamma((s + 2)/2 + \alpha_{\text{gh}})} = \frac{\Gamma(\alpha_0 - 2\alpha_{\text{gh}}) \Gamma(s/2 - \alpha_0)}{\Gamma(1 + \alpha_0) \Gamma((s + 2)/2 + 2\alpha_{\text{gh}} - \alpha_0)}. \quad (5.113)$$

Note that

$$-\Gamma(-\alpha_{\text{gh}}) = \frac{\Gamma(1 - \alpha_{\text{gh}})}{\alpha_{\text{gh}}}, \quad (5.114)$$

so this factor is positive for  $0 < \alpha_{\text{gh}} < 1$ . Now let  $s$  be fixed in the interval

$$1 < s \leq 3 \quad (5.115)$$

and let  $\alpha_0$  be fixed in the interval

$$0 < \alpha_0 < s/2 \leq 3/2. \quad (5.116)$$

Then for  $\alpha_{\text{gh}}$  in the interval

$$0 < \alpha_{\text{gh}} < \alpha_0/2 \leq 3/4 \quad (5.117)$$

both sides of (5.113) are positive and finite. Moreover, by (5.114), when  $\alpha_{\text{gh}}$  approaches its lower limit, namely 0, the LHS of (5.113) approaches  $+\infty$  while the RHS is finite, and when  $\alpha_{\text{gh}}$  approaches its upper limit, namely  $\alpha_0/2$ , the RHS approaches  $+\infty$  while the LHS remains finite. Since there are no further poles or other discontinuities present in the stated interval, for every  $\alpha_0 \in (0, s/2)$  there exists (at least) one solution  $\alpha_{\text{gh}}$ .

This tells us that to solve (5.113) numerically we should take  $\alpha_0$  as the independent variable and we are assured that there exists a solution for

$$\alpha_{\text{gh}} = \alpha_{\text{gh}}(\alpha_0), \quad (5.118)$$

both variables being in the stated intervals.

**Analytic Statements** We may in fact solve (5.113) analytically for  $\alpha_0$  close to its end-points,  $\alpha_0 = \epsilon$  and  $\alpha_0 = s/2 - \epsilon$ , where  $\epsilon$  is small. Suppose first that  $\alpha_0 = \epsilon$ . Then the inequality  $0 < \alpha_{\text{gh}} < \epsilon/2$  implies that  $\alpha_{\text{gh}}$  is also small. In this limit (5.113) approaches

$$\frac{-\Gamma(-\alpha_{\text{gh}}) \Gamma(s/2)}{\Gamma(1) \Gamma((s + 2)/2)} = \frac{\Gamma(\epsilon - 2\alpha_{\text{gh}}) \Gamma(s/2)}{\Gamma(1) \Gamma((s + 2)/2)}. \quad (5.119)$$

With  $-\Gamma(-\alpha_{\text{gh}}) \approx 1/\alpha_{\text{gh}}$ , and  $\Gamma(\epsilon - 2\alpha_{\text{gh}}) \approx 1/(\epsilon - 2\alpha_{\text{gh}})$ , we may equate the singular pole terms

$$\frac{1}{\alpha_{\text{gh}}} = \frac{1}{\epsilon - 2\alpha_{\text{gh}}}, \quad (5.120)$$

and with  $\epsilon = \alpha_0$ , this has the solution

$$\alpha_{\text{gh}}(\alpha_0) = \alpha_0/3 \quad \alpha_0 \approx 0. \quad (5.121)$$

Now suppose that  $\alpha_0 = s/2 - \epsilon$ . Then since the RHS of (5.113) blows up like  $1/\epsilon$ ,  $\alpha_{\text{gh}}$  must be small, so (5.113) approaches

$$\frac{-\Gamma(-\alpha_{\text{gh}}) \Gamma(s/2)}{\Gamma(1) \Gamma((s+2)/2)} = \frac{\Gamma(s/2) \Gamma(\epsilon)}{\Gamma(1+s/2) \Gamma(1)}. \quad (5.122)$$

We again equate singular pole terms

$$\frac{1}{\alpha_{\text{gh}}} = \frac{1}{\epsilon} \quad (5.123)$$

which, with  $\epsilon = s/2 - \alpha_0$ , gives

$$\alpha_{\text{gh}}(\alpha_0) = s/2 - \alpha_0 \quad \alpha_0 \approx s/2 - \epsilon. \quad (5.124)$$

We have now determined that  $\alpha_{\text{gh}}(\alpha_0)$  vanishes at  $\alpha_0 = 0, s/2$ , and we have determined its slope at these two points. We approximate  $\alpha_{\text{gh}}(\alpha_0)$  in its interval by an interpolation. We write

$$\alpha_{\text{gh}} = \alpha_0(s/2 - \alpha_0)f(\alpha_0), \quad (5.125)$$

where  $f(\alpha_0)$  is a positive function whose values at  $\alpha_0 = 0$  and  $\alpha_0 = s/2$  are determined by the slope of  $\alpha_{\text{gh}}(\alpha_0)$  at these two points which are given respectively by  $1/3$  and  $-1$ .

A linear interpolation for  $f(\alpha_0)$  yields an approximate solution to (5.113),

$$\alpha_{\text{gh}}(\alpha_0) \approx \alpha_0 \left( \frac{s}{2} - \alpha_0 \right) \frac{2}{3s} \left( 1 + \frac{4\alpha_0}{s} \right), \quad (5.126)$$

and comparison with the numerical results in subsection 5.3.6 shows that this is a reasonable approximation (with less than 10% deviation) even for intermediate values of  $\alpha_0$ .

**Numerical Results** A full analytic solution of (5.104) and (5.111) has not been obtained so far. To find a solution at least numerically, one can follow one of two strategies:

- One equation (preferably (5.104)) can be solved for one variable (yielding  $\alpha_{\text{gh}}^{(1)}(\alpha_0)$ ) and this function can be substituted into both  $F_1$  from (5.107) and  $F_2$  from (5.110), yielding two functions of one variable  $F_i(\alpha_0, \alpha_{\text{gh}}(\alpha_0))$ ,  $i = 1, 2$ . Intersection points of these functions are solutions of the system of equations.
- Equations (5.104) and (5.111) each implicitly define a (possibly multi-valued) function  $\alpha_{\text{gh}}^{(i)}(\alpha_0)$ ,  $i = 1, 2$ . One can obtain each of these functions separately and find the solutions of the system as intersection points in a two-dimensional plot.

The second strategy is more cumbersome, yet it gives a better understanding of the conditioning of the system and the relationship between solutions for various values of  $s$ . While a solution for (5.104) is easy to find, solving (5.111) requires more effort, since it defines a multivalued function with several potentially relevant branches.

We have employed the `findroot` routine of *Mathematica* 5.2 and 7.0.0 with a wide variety of initial guesses in order to find all branches. (In the color version different starting points can be recognized for having different shades of blue and green.) The corresponding plots are given in Figures 5.11 to 5.13. For comparison also the  $F_1$  vs.  $F_2$  plot for these three cases is given in Figure 5.14.

The two-dimensional plot is particularly interesting in the case  $s = 2$  (Figure 5.12), since it shows that the system of equations is relatively ill-conditioned and the intersection point (i.e.

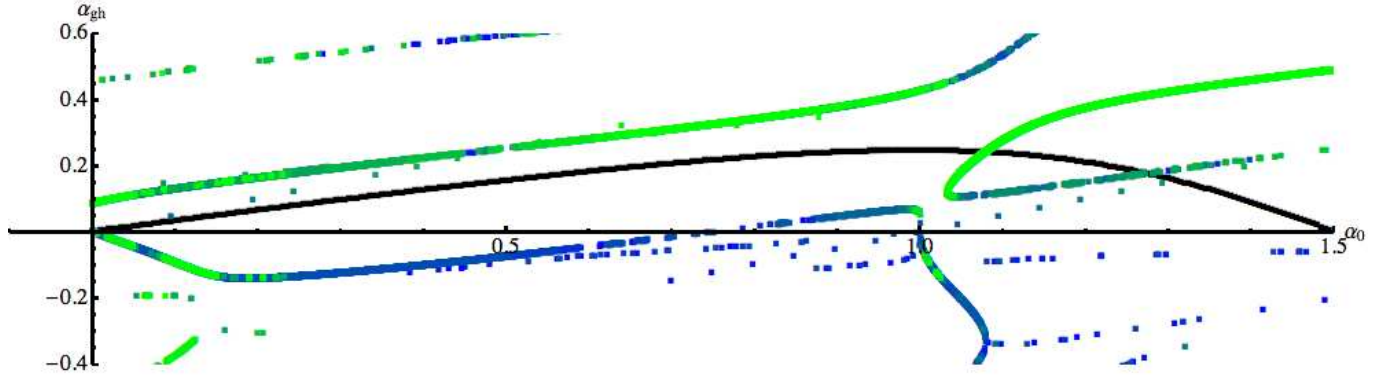


Figure 5.11: Solution of equations (5.104) and (5.111) for  $s = 3$ : We plot  $\alpha_{\text{gh}}(\alpha_0)$  from (5.104) and from (5.111). The relevant solution of the first first equation is represented by a solid black line. The second equation gives rise to a multivalued function: The graphs are composed of single dots; different shades of blue and green (in the color version) indicate different initial guesses. Note that single points which do not belong to any branch of the function typically correspond to values in which the `findroot` routine got stuck.

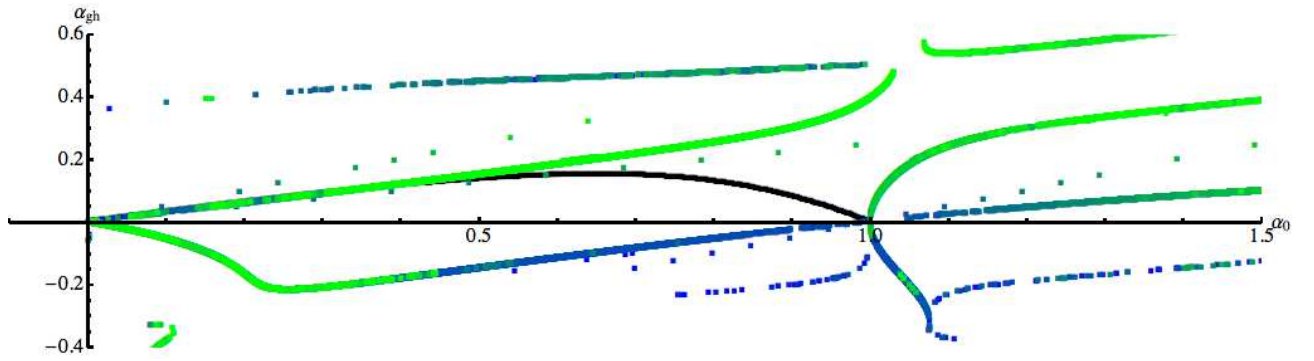


Figure 5.12: Solution of equations (5.104) and (5.111) for  $s = 2$ , otherwise as in Figure 5.11.

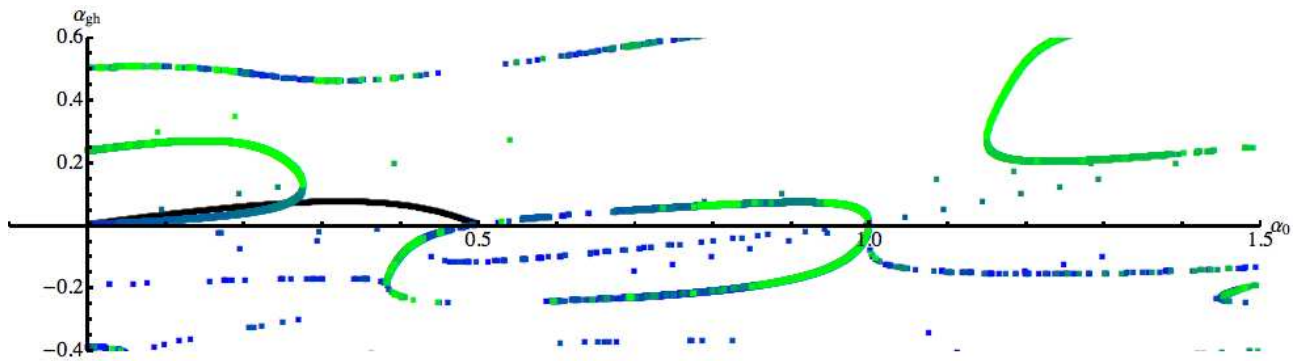


Figure 5.13: Solution of equations (5.104) and (5.111) for  $s = 1$ , otherwise as in Figure 5.11.

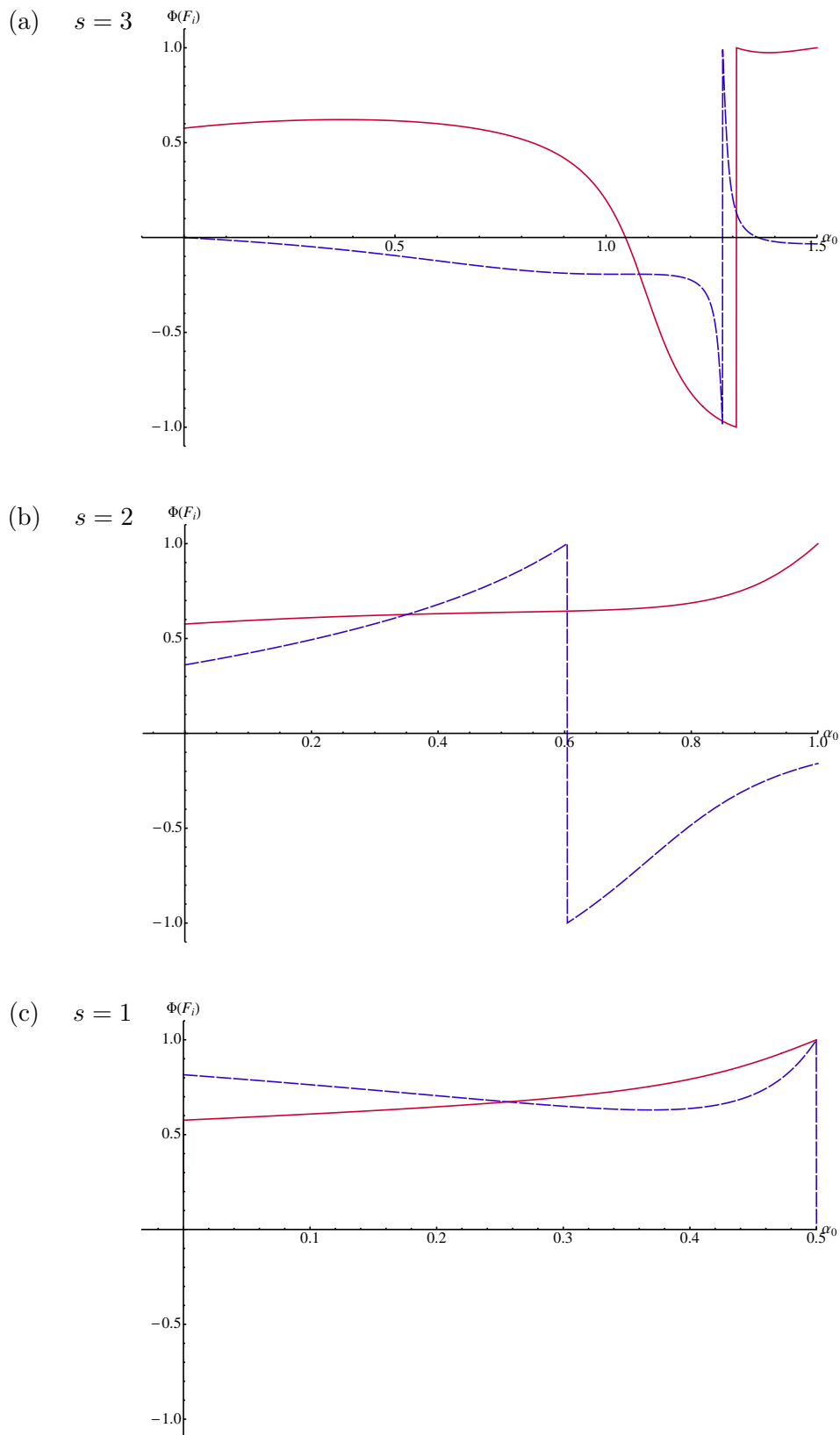


Figure 5.14: Solution of equations (5.104) and (5.111) for (a)  $s = 3$ , (b)  $s = 2$  and (c)  $s = 1$ : We display  $F_1$  (solid) and  $F_2$  (dashed) for as functions of  $\alpha_0$  with  $\alpha_{\text{gh}}(\alpha_0)$  from (5.104). We have employed the mapping  $\Phi(x) = \frac{2}{\pi} \arctan \frac{x}{\pi}$  to compactify the range  $(-\infty, \infty)$  to  $(-1, 1)$ . Solutions are determined by intersection points. Note that horizontal lines correspond to odd-order poles, so there is no solution for  $s = 3$  at  $\alpha_0 \approx 1.31$  and no solution for  $s = 2$  at  $\alpha_0 \approx 0.605$ .

	$\alpha_0$	$\alpha_{\text{gh}}$	$\alpha_{\mathbf{A}}$	$\alpha_{\pi'}$
$s = 3$	1.07945	0.240044	-0.980087	-0.599366
$s = 2$	0.351045	0.105460	-1.21092	-0.140125
$s = 1$	0.256229	0.068302	-1.63660	-0.119625

Table 5.1: Infrared exponents, obtained from the smallest solution of equations (5.104) and (5.111) for different values of  $s$ . Note that from (5.102) we have  $\alpha_m = \alpha_{\text{gh}}$  and  $\alpha_\varphi = \alpha_{\pi'}$ .

	$\alpha_0^{(1)}$	$\alpha_0^{(2)}$	$\alpha_0^{(3)}$	$\alpha_{\text{gh}}^{(1)}$
$s = 1.06$	—	—	0.512478	—
$s = 1.05$	0.131834	0.202188	0.510570	0.0408666
$s = 1.04$	0.093892	0.224380	0.508586	0.0298297
$s = 1.03$	0.065958	0.236660	0.506537	0.0212898
$s = 1.02$	0.041940	0.245122	0.504421	0.0137068
$s = 1.01$	0.020197	0.251402	0.502242	0.0066706

Table 5.2: Infrared exponents, obtained from the smallest of equations (5.104) and (5.111) for different values of  $s$  close to  $s = 1$ . The exponent  $\alpha_{\text{gh}}$  is only given for the solution close to  $\alpha_0 = 0$ . (Note that relation (5.121) is fulfilled quite well for this solution.)

the solution) would be sensitive even to small perturbations. (Such perturbations are of course absent in the present truncation, but could be introduced, for example, by vertex dressing.)

For  $s = 3$  and  $s = 2$ , the physical values are expected to be given by the smallest solution for  $\alpha_0$ , as summarized in Table 5.1.

For  $s = 1$  the situation is somehow different since strictly speaking our equations are not well-defined (because the transverse projectors vanish for  $s = 1$ ). So instead of plainly taking the value obtained for  $s = 1$  we instead study the solutions for  $s = 1 + \varepsilon$  with some small, but positive number  $\varepsilon$ . For  $s = 1.06$  there is only one solution at  $\alpha_0 = 0.512478$ .

When we lower  $s$  to  $s \approx 1.0541071910$ , in addition to the previous solution (which has now moved to  $\alpha_0 \approx 0.51136$ ) another solution arises at  $\alpha_0 \approx 0.17026$ . This solution splits into two independent solutions for smaller values of  $s$ ; the smaller solution approaches zero for  $s \rightarrow 1^+$ , as indicated by the values given in Table 5.2.

This is also illustrated in Figure 5.15 which, together with Figure 5.14.(c) gives a good impression of what is going on: For  $s < 1.0541071910$  there is a region around  $\alpha_0 \approx 0.17026$  where  $F_2 > F_1$ . For  $s = 1 + \varepsilon$  with  $0 < \varepsilon < 0.0541071910$  we have  $F_2(0) = 0$  and  $F_1(0) > 0$ , so there has to be an intersection point. For  $s = 1$ , however, we find  $F_2(0) > F_1(0)$ . The family of functions  $\{F_2\}_{s=1+\varepsilon, \varepsilon>0}$  seems to converge pointwise, but not uniformly towards  $F_2|_{s=1}$  when  $\varepsilon$  approaches zero from above.

### 5.3.7 Relations among the $b$ -coefficients

Having determined the 6 infrared critical exponents, the  $\alpha$ 's, we turn to the  $b$ -coefficients. There are 6 DS equations and 6 coefficients  $b_{\mathbf{A}}, b_{\pi'}, b_{\text{gh}}, b_0, b_m, b_\varphi$ . However, as we have seen, only 4 of the equations for the  $b$ 's are independent, so there are 4 relations satisfied by the  $b$ 's. These are, from (5.81),

$$b_{\mathbf{A}} b_{\text{gh}}^2 = \frac{-1}{I_{S(V,S)}(\alpha_{\mathbf{A}}, \alpha_{\text{gh}})}; \quad (5.127)$$

from (5.80)

$$b_{\mathbf{A}} b_0 b_{\pi'} = \frac{1}{I_{V(V,S)}(\alpha_{\mathbf{A}}, \alpha_0)}; \quad (5.128)$$



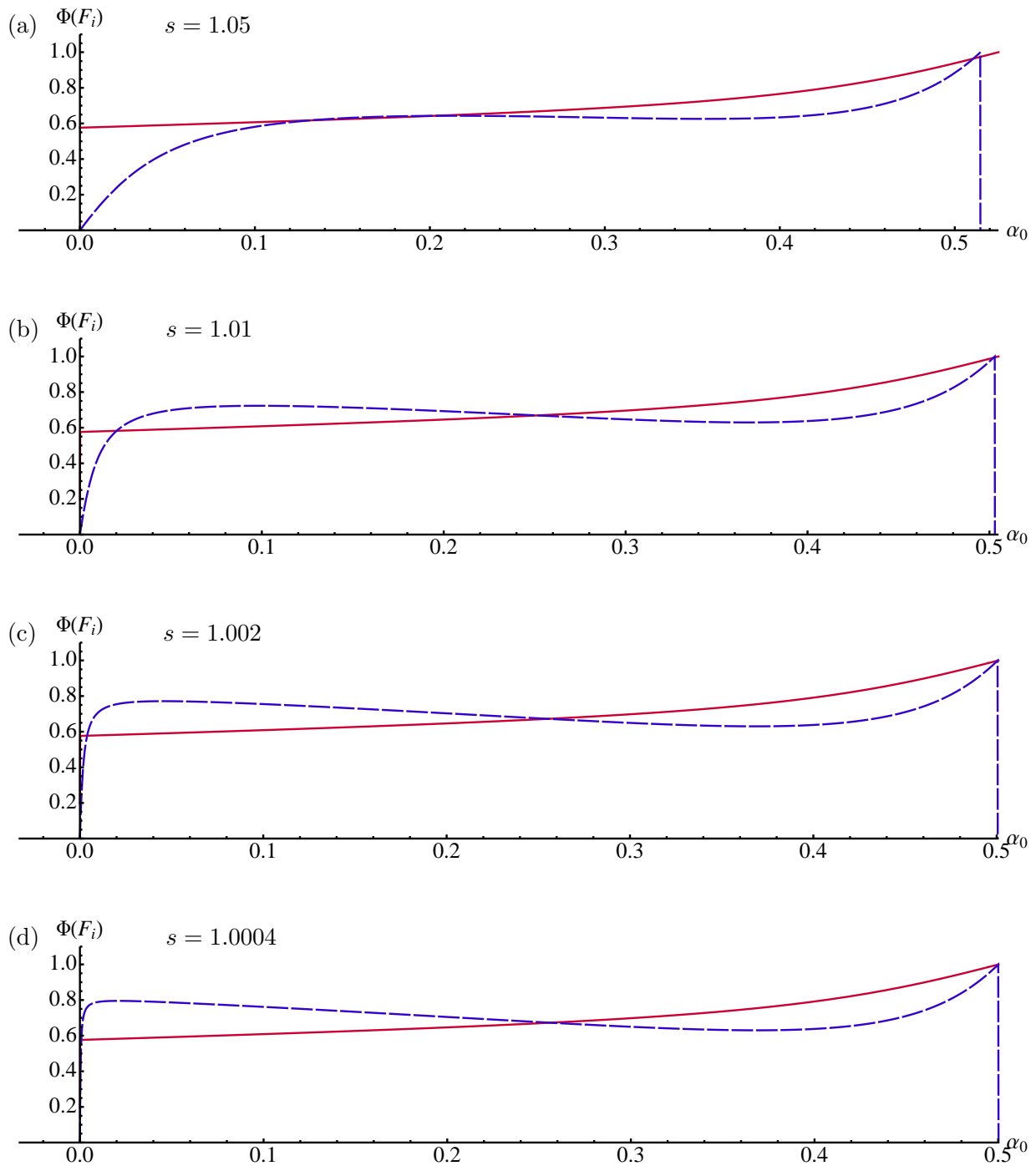


Figure 5.15: Solution of equations (5.104) and (5.111) for (a)  $s = 1.05$ , (b)  $s = 1.01$ , (c)  $s = 1.002$  and (d)  $s = 1.0004$ , otherwise as in Figure 5.14. One clearly notes that (as also suggested by Table 5.2) there is a solution which approaches  $\alpha_0 = \alpha_{\text{gh}} = 0$  for  $s \rightarrow 1^+$  but vanishes for  $s = 1$ .

eq. (5.107)

$$\frac{b_{\pi'}}{b_{\varphi}} = F_2(\alpha_0); \quad (5.129)$$

and eq. (5.105),

$$b_{\text{gh}}^2 = b_0 b_{\varphi} + b_m^2. \quad (5.130)$$

The last two equations determine the triple products

$$b_{\mathbf{A}} b_0 b_{\varphi} = \frac{1}{F_2(\alpha) I_{V(V,S)}(\alpha_{\mathbf{A}}, \alpha_0)} \quad (5.131)$$

$$b_{\mathbf{A}} b_m^2 = \frac{-1}{F_2(\alpha) I_{V(V,S)}(\alpha_{\mathbf{A}}, \alpha_0)} + \frac{-1}{I_{S(V,S)}(\alpha_{\mathbf{A}}, \alpha_{\text{gh}})}. \quad (5.132)$$

### 5.3.8 Range of Validity

So far we have only taken into account the zeroth Matsubara frequency, thus working effectively in the infinite-temperature limit. However, since infrared properties of the theory are governed by the zero frequency contribution also at finite temperatures (for all  $T \neq 0$ , even those in the confined phase) the results obtained so far may be more general than initially stated.

All Matsubara frequencies  $\omega_n$  with  $n \geq 1$  effectively introduce mass terms in the non-instantaneous propagators, so all such contributions decouple from the deep infrared where critical exponents are valid. Also in loop terms massive contributions show up only pairwise, so taking into account only the 0<sup>th</sup> Matsubara frequency yields a closed system.

The only instance where zero and nonzero Matsubara frequencies could directly be intertwined is imposing the horizon condition – an issue which should be the subject of closer investigation.

### 5.3.9 Discussion of the Infrared Exponents

We now turn to the discussion of the results given in table 5.1. The horizon condition tells us that the ghost propagator  $D_{\text{gh}} \sim \frac{b_{\text{gh}}}{(k^2)^{1+\alpha_{\text{gh}}}}$  is enhanced in the infrared, so we are interested in solutions which fulfill

$$\alpha_{\text{gh}} > 0.$$

As one sees from the black curves in Figs. 2, 3 and 4, this is true for our solution in the whole interval  $0 < \alpha_0 < \frac{s}{2}$  which is the interval of physical interest.

The most interesting quantity in Coulomb gauge Yang-Mills theory is presumably the color-Coulomb potential, given in momentum space by

$$D_{A_0 A_0}(k) \sim \frac{b_0 m^{2\alpha_0}}{(k^2)^{1+\alpha_0}}. \quad (5.133)$$

It is linearly rising in position space for  $\alpha_0|_s = (s-1)/2$ .

For  $s = 3$ , this gives  $\alpha_0|_3 = 1$ , and the result we obtain lies slightly above this value, at  $\alpha_0 = 1.07945$ . This corresponds to a slightly more than linearly rising potential<sup>9</sup>. The transverse gluon propagator  $D_{\mathbf{A}\mathbf{A}}(k)$  vanishes at  $k = 0$  if  $\alpha_{\mathbf{A}} < -1$ . From Table 5.1 we have  $\alpha_{\mathbf{A}}|_{s=3} = -0.980087$ , which corresponds to  $D_{\mathbf{A}\mathbf{A}}(k)$  that is weakly divergent at  $k = 0$ . This value is close to  $\alpha_{\mathbf{A}} = -1$ , which corresponds to a finite value for  $D_{\mathbf{A}\mathbf{A}}(k = 0)$ , and a small

---

<sup>9</sup>Note that the color-Coulomb potential is not a gauge-invariant quantity, so the arguments which forbid more-than linearly rising potentials in relativistic field theory do not directly apply; also the asymptotic inequality between Wilson and color-Coulomb potential in [228] would be satisfied. As discussed in section C.2.1, the mathematical aspects of such potentials are under control. Still it would be very surprising if in reality  $D_{A_0 A_0}$  were more than linearly rising.

change caused by an improved truncation could also change this to  $\alpha_{\mathbf{A}} < -1$ , corresponding to a gluon propagator  $D_{\mathbf{A}\mathbf{A}}(k)$  that vanishes at  $k = 0$ .

For  $s = 2$ , the value from Table 5.1,  $\alpha_0 = 0.351045$ , lies below the linearly rising case,  $\alpha_0 = (s - 1)/2 = 0.5$ . However as can be seen from Figure 5.12, the system is badly conditioned so that, if properly dressed vertices or terms neglected in our truncation even slightly modify the system of equations, then any value  $\alpha_0 \in (0, 0.55)$  [which determines a value of  $\alpha_{\text{gh}} \in (0, 0.146)$ ] could qualify as a possible solution. This includes the linearly rising case. From Table 5.1 we find  $\alpha_{\mathbf{A}} = -1.21092 < -1$ , which implies that  $D_{\mathbf{A}\mathbf{A}}(k)$  vanishes at  $k = 0$ , but the uncertainty of  $\alpha_0$ , due to ill-conditioning, extends to all critical exponents, including  $\alpha_{\mathbf{A}}$ .

For  $s = 1$ , the system is exactly solvable analytically. Since our equations do not strictly apply at  $s = 1$  (see discussion in Sec. 5.3.6) we have examined numerically the limit  $s \rightarrow 1^+$  (see Table 5.2 and Figure 5.15). The results obtained this way are consistent with eq. (5.121) which is valid for small  $\alpha_0$ . For  $s \rightarrow 1^+$  this solution converges towards

$$\alpha_0 = \alpha_{\text{gh}} = 0. \quad (5.134)$$

These values agree with the analytic solution presented in Appendix B. By (5.102) this would correspond to  $\alpha_{\mathbf{A}} = -\frac{3}{2}$ , but transverse propagators are not well-defined for  $s = 1$ , so this infrared critical exponent is undefined for the theory at  $s = 1$ .

Because of the symmetry (5.83) the coefficient  $b_0$  is undetermined in the infrared asymptotic limit and must be fixed by subdominant terms that we have neglected. This is unfortunate because according to (5.74) and (5.75), for  $\alpha_0 = 1$ , the quantity  $b_0(g^2T)^{2\alpha_0}$  represents the color-Coulomb string tension and one would have liked to make a comparison with lattice determinations of this quantity [93, 145, 148, 147, 203].

**Conclusion** An ideal theory of confinement would explain in simple terms why there is a linearly rising Wilson potential and, in the Coulomb-gauge scenario, why there is a linearly rising color-Coulomb potential, with a Coulomb string tension  $\sigma_{\text{coul}}(T)$  that increases with  $T$  even in the deconfined phase [93] – a goal not achieved here. (The solutions are obtained from complicated equations involving  $\Gamma$ -functions which have to be solved numerically).

Nevertheless it remains true that the numerical value obtained for  $s = 3$  space dimensions is numerically close to a linearly rising potential, with  $V(r) \sim r^{2+2\alpha_0-s} = r^{1.15890}$ . In  $s = 2$  spatial dimensions the agreement is not as good but this may be due to the ill-conditioning of the equations. Finally, as  $s$  approaches 1 spatial dimension, the smallest solution approaches the exact analytic result.

The interpretation of the overconfining solutions for  $s = 3$ , however, is not clear. As discussed in appendix C.2, such solutions are mathematically well-defined, but their physical meaning is obscure. In the field line-picture, a  $\frac{1}{r}$ -potential (in  $s = 3$  spatial dimensions) corresponds to the field lines equally distributed among all angular regions, while the linearly rising potential corresponds to all field lines collimated in a string. A more-than-linearly rising potential would accordingly imply an enhancement of the field lines.

For a physical potential such a behaviour can be excluded on very general grounds. For a gauge-variant quantity (as the color-Coulomb potential), there are no arguments which are so strict. Still a more-than-linearly rising behavior would be extremely surprising, so it is more likely that this is an artifact of our truncation.

## 5.4 Quarks at Finite Temperature – a Brief Remark

The formalism used in chapter 4 can also be transferred to finite temperature. As in the pure gauge case, the frequency integrals are replaced by Matsubara sums (which look slightly different for fermions [118]). Working in the instantaneous approximation, one finds

$$L := T \sum_{q_0} \frac{i q_0 \gamma_0 + C(\mathbf{q}^2) q_i \gamma_i - B(\mathbf{q}^2)}{q_0^2 + C^2(\mathbf{q}^2) \mathbf{q}^2 + B^2(\mathbf{q}^2)} \stackrel{\text{symm.}}{=} T \underbrace{(C(\mathbf{q}^2) q_i \gamma_i - B(\mathbf{q}^2))}_{=: N(\mathbf{q}^2)} \sum_{q_0} \frac{1}{q_0^2 + \Delta^2(\mathbf{q}^2)}. \quad (5.135)$$

with  $\Delta^2(\mathbf{q}^2) := C^2(\mathbf{q}^2) \mathbf{q}^2 + B^2(\mathbf{q}^2)$ . Summation of this series can be done analytically, by using the product representation of the hyperbolic sine (cf. [231]),

$$\sinh y = \frac{y}{\pi} \prod_{n=1}^{\infty} \left( 1 + \frac{y^2}{n^2 \pi^2} \right). \quad (5.136)$$

From this, we obtain for  $y > 0$

$$\frac{\partial}{\partial y} \ln \sinh y = \frac{\partial}{\partial y} \left\{ \ln \frac{y}{\pi} + \sum_{n=1}^{\infty} \ln \left[ 1 + \frac{y^2}{(n\pi)^2} \right] \right\} = \frac{1}{y} + \sum_{n=1}^{\infty} \frac{2y}{(n\pi)^2 + y^2}, \quad (5.137)$$

on the other hand, we have

$$\frac{\partial}{\partial y} \ln \sinh y = \frac{\cosh y}{\sinh y} = \frac{e^y + e^{-y}}{e^y - e^{-y}} = 1 + \frac{2e^{-y}}{e^y - e^{-y}} = 1 + \frac{2}{e^{2y} - 1}. \quad (5.138)$$

Comparison yields

$$\sum_{n=1}^{\infty} \frac{2y}{(n\pi)^2 + y^2} = \frac{2}{e^{2y} - 1} + 1 - \frac{1}{y} \quad (5.139)$$

With this, we find

$$\begin{aligned} L &= T \sum_{q_0} \frac{N(\mathbf{q}^2)}{q_0^2 + \Delta^2(\mathbf{q}^2)} = T \sum_{n \in \mathbb{Z}} \frac{N(\mathbf{q}^2)}{\left(\frac{2\pi}{\beta}\right)^2 \left(\frac{2n+1}{2}\right)^2 + \Delta^2(\mathbf{q}^2)} \\ &= 2N(\mathbf{q}^2) T \sum_{n=0}^{\infty} \frac{1}{\frac{\pi^2}{\beta^2} (2n+1)^2 + \Delta^2(\mathbf{q}^2)} = 2N(\mathbf{q}^2) \beta \sum_{n=0}^{\infty} \frac{1}{\pi^2 (2n+1)^2 + \Delta^2(\mathbf{q}^2) \beta^2} \\ &\stackrel{2\mathbb{N}_0+1 \equiv \mathbb{N}-2\mathbb{N}}{=} 2N(\mathbf{q}^2) \beta \left\{ \sum_{n=1}^{\infty} \frac{1}{\pi^2 n^2 + \Delta^2(\mathbf{q}^2) \beta^2} - \sum_{n=1}^{\infty} \frac{1}{\pi^2 (2n)^2 + \Delta^2(\mathbf{q}^2) \beta^2} \right\} \\ &= \frac{N(\mathbf{q}^2)}{\Delta(\mathbf{q}^2)} \left\{ \sum_{n=1}^{\infty} \frac{2\Delta(\mathbf{q}^2)\beta}{(n\pi)^2 + \Delta^2(\mathbf{q}^2)\beta^2} - \frac{1}{2} \sum_{n=1}^{\infty} \frac{2\left(\frac{\Delta(\mathbf{q}^2)\beta}{2}\right)}{(n\pi)^2 + \left(\frac{\Delta(\mathbf{q}^2)\beta}{2}\right)^2} \right\} \\ &\stackrel{(5.139)}{=} \frac{N(\mathbf{q}^2)}{\Delta(\mathbf{q}^2)} \left\{ \frac{2}{e^{2\Delta(\mathbf{q}^2)\beta} - 1} + 1 - \frac{1}{\Delta(\mathbf{q}^2)\beta} - \frac{1}{2} \left( \frac{2}{e^{\Delta(\mathbf{q}^2)\beta} - 1} + 1 - \frac{2}{\Delta(\mathbf{q}^2)\beta} \right) \right\} \\ &= \frac{N(\mathbf{q}^2)}{\Delta(\mathbf{q}^2)} \left\{ \frac{2}{e^{2\Delta(\mathbf{q}^2)\beta} - 1} + 1 - \cancel{\frac{1}{\Delta(\mathbf{q}^2)\beta}} - \frac{1}{e^{\Delta(\mathbf{q}^2)\beta} - 1} - \frac{1}{2} + \cancel{\frac{1}{\Delta(\mathbf{q}^2)\beta}} \right\} \\ &= \frac{N(\mathbf{q}^2)}{\Delta(\mathbf{q}^2)} \left\{ \frac{1}{2} + \frac{1}{e^{\Delta(\mathbf{q}^2)\beta} - 1} \left[ \frac{2}{e^{\Delta(\mathbf{q}^2)\beta} + 1} - 1 \right] \right\} = \frac{N(\mathbf{q}^2)}{\Delta(\mathbf{q}^2)} \left\{ \frac{1}{2} - \frac{1}{e^{\Delta(\mathbf{q}^2)\beta} + 1} \right\} \\ &= \frac{C(\mathbf{q}^2) q_i \gamma_i - B(\mathbf{q}^2)}{\sqrt{C^2(\mathbf{q}^2) \mathbf{q}^2 + B^2(\mathbf{q}^2)}} \left\{ \frac{1}{2} - \frac{1}{e^{\beta \sqrt{C^2(\mathbf{q}^2) \mathbf{q}^2 + B^2(\mathbf{q}^2)}} + 1} \right\} \quad (5.140) \end{aligned}$$

In order to treat the full problem, including transverse gluons and “retardation” effects (i.e. a possible dependency of the propagators on the Matsubara index  $n$ ) one would have to truncate the series and presumably have to use numerical methods as employed for example in [137, 136].



# Epilogue

The picture of confinement in Coulomb gauge QCD in the functional approach remains incomplete and inconclusive. While there is considerable potential for a physical understanding of confinement, severe problems remain unsolved. They include fundamental issues (like the still missing proof of renormalizability), conceptional challenges (like the question how to reasonably truncate the quark-gluon vertex) and technical problems which mostly stem from the non-covariant formulation of the gauge-fixed theory.

This is particularly true in the quark sector: Truncation strategies and numerical treatment of the Coulomb gauge gap equation remain highly unsatisfactory. In spite of considerable effort already invested in the improvement of the numerical procedure [121, 124, 128], the computational costs of such calculations are still unreasonably large. Even worse, it is not at all clear whether the numerical problems associated with this equation (even in the relatively simple bare-vertex form) are really under control.

The quantitative results are unsettling; and while there are reasons to believe that corrections in the spatial quark-gluon vertex might be a remedy, information about the form of such corrections is hard to obtain. The trial-and-error model-building approach which is sometimes employed in analogous covariant problems has to be dismissed in this case both due to the increased complexity of the problem and due to the large computational cost associated with each calculation.

In addition, even if phenomenologically successful forms of the vertex could be found that way, one could draw only very limited conclusions from such calculations without further theoretical justification. If, however, sound results on the structure of the Coulomb gauge quark-gluon vertex were available, the gap equation would be a good opportunity to test them. Unfortunately, even in this case, as soon as additional tensor structures are included, the computational effort to solve the equation increases considerably, maybe beyond the point of any reasonable cost-benefit ratio.

All in all, while the calculations performed in the instantaneous approximation [1, 6, 11] yield considerable qualitative insight in the structure of the equation, studies of the full system, including transverse gluons and retardation effects, offer little additional understanding for an unreasonably high price.

The situation is different in the pure gauge sector, here investigated in the framework of finite temperature. The extension of techniques and ideas initially developed in a confining setup to the “deconfined” phase is promising, even if also there some issues (as the overconfining solutions obtained in sec. 5.3) will have to be settled in order to obtain reliable statements.

A question that still remains largely unanswered is how to relate the properties of different gauges and how to connect scenarios (in particular those for confinement) which exist in these gauges. Some connections have been mentioned in sec. 1.3.3, but certainly a more general scheme would be desirable. Interpolating gauges, as discussed for a particular case in sec. 3.5 may have their merits, but their range of applicability is more limited than it had been initially hoped for. A distance-based classification scheme as sketched in sec. 1.5 offers a completely different point of view – but only further investigation can show if this topic has the potential to be more than just a mostly mathematical plaything.





# Appendix A

## The Quark Gap Equation: Remarks and Details

In this appendix we summarize our conventions and present the detailed decomposition of the quark gap equation in bare vertex truncation. In addition, we include a complete decomposition of the gap equation with the full quark-gluon vertex (in the naive basis given by (4.38) and (4.39)), some details on the renormalization procedure and a discussion of the mixed gluon propagator.

### A.1 Conventions

#### A.1.1 Natural Units

Usually we will employ natural units,

$$\hbar = c = k_B = 1, \quad (\text{A.1})$$

unless explicitly noted otherwise. Units will typically be expressed in terms of energy,

$$[\text{energy}] = [\text{momentum}] = [\text{mass}] = [\text{temperature}] = \text{MeV}, \quad [\text{length}] = [\text{time}] = \frac{1}{\text{MeV}}. \quad (\text{A.2})$$

#### A.1.2 Indices

Greek indices  $\mu, \nu, \dots$  (which may appear as *covariant* or *contravariant*) take values 0, 1, 2, 3, while latin indices take the values 1, 2, 3. An index which appears in the same term both as covariant and contravariant is summed over, using the Minkowski metric tensor

$$g_{\mu\nu} = g^{\mu\nu} = \text{diag}(1, -1, -1, -1). \quad (\text{A.3})$$

A latin index which appears twice as a *subscript* is summed over employing the Euclidean metric  $\delta_{ij}$ .<sup>1</sup> The contraction of two three-vectors is often written in index-free notation as  $a^\mu b_\mu = \mathbf{a} \cdot \mathbf{b}$  and  $a_i b_i = \mathbf{a} \cdot \mathbf{b}$ . So one has, for example,

$$\mathbf{a} \cdot \mathbf{b} = a^\mu b_\mu = a^0 b_0 + a^i b_i = a_0 b_0 - a_i b_i = a_0 a_0 - \mathbf{a} \cdot \mathbf{b}. \quad (\text{A.4})$$

A scalar product of the type  $\mathbf{a} \cdot \mathbf{a}$  is often abbreviated as  $\mathbf{a}^2$ , and we write  $a = |\mathbf{a}| = \sqrt{\mathbf{a}^2}$ . We accept the ambiguity that  $a$  may either denote a four-vector  $a = (a_0, \mathbf{a})$  or the modulus of a three-vector,  $a = |\mathbf{a}|$  since the potential for confusion is small.

---

<sup>1</sup>Note that this is a slight abuse of notation, since position vectors, augmented by a 0<sup>th</sup> component, naturally fit into the four-dimensional as *contravariant* vectors. However, the use of superscripts is cumbersome, and typically there is no potential for confusion or sign errors if one consequently sticks to subscripts for 3D indices.

## A.2 The Quark Gap Equation with a Bare Vertex

We now proceed with the gap equation in bare vertex truncation.

### A.2.1 Inversion of the Quark Propagator

First we show that the inverse of (4.4) is indeed given by (4.5). For convenience we define<sup>2</sup>

$$d_{q,M}(p) := p_0^2 A_p^2 - B_p^2 - \mathbf{p}^2 C_p^2 + p_0^2 \mathbf{p}^2 D_p^2 \quad (\text{A.5})$$

$$\hat{S}(p) := -i d_{q,M}(p) S(p) = \gamma_0 p_0 A_p + B_p - \gamma_i p_i C_p + \gamma_0 p_0 \gamma_i p_i D_p \quad (\text{A.6})$$

$$\widehat{S^{-1}}(p) := i S^{-1}(p) = \gamma_0 p_0 A_p - B_p - \gamma_j p_j C_p + \gamma_0 p_0 \gamma_j p_j D_p \quad (\text{A.7})$$

and obtain for the product of  $\hat{S}$  and  $\widehat{S^{-1}}$

$$\begin{aligned} \hat{S}(p) \widehat{S^{-1}}(p) &= (\gamma_0 p_0 A + B - \gamma_i p_i C + \gamma_0 p_0 \gamma_i p_i D) (\gamma_0 p_0 A - B - \gamma_j p_j C + \gamma_0 p_0 \gamma_j p_j D) \\ &= \cancel{\gamma_0^2 p_0^2 A^2} - \cancel{\gamma_0 p_0 A B} - \gamma_0 \gamma_j p_0 p_j A C + \cancel{\gamma_0^2 \gamma^j p_0^2 p_j A D} \\ &\quad + \cancel{\gamma_0 p_0 A B} - B^2 - \gamma_j p_j B C + \cancel{\gamma_0 p_0 \gamma_j p_j B D} \\ &\quad - \gamma_i \gamma_0 p_0 p_i A C + \cancel{\gamma_i p_i B C} + \gamma_i \gamma_j p_i p_j C^2 - \gamma_i \gamma_0 \gamma_j p_0 p_i p_j C D \\ &\quad + \gamma_0 \gamma_i \gamma_0 p_0^2 p_i A D - \cancel{\gamma_0 p_0 \gamma_i p_i B D} - \gamma_0 \gamma_i \gamma_j p_0 p_i p_j C D + \gamma_0 \gamma_i \gamma_0 \gamma_j p_0^2 p_i p_j D^2 \\ &= p_0^2 A^2 - B^2 + \gamma_i \gamma_j p_i p_j C^2 - \gamma_0^2 \gamma_i \gamma_j p_0^2 p_i p_j D^2 \\ &\quad - \{\gamma_0, \gamma_i\} p_0 p_i A C + \gamma_0 \{\gamma_0, \gamma_i\} p_0^2 p_i A D - \{\gamma_0, \gamma_i\} \gamma_j p_0 p_i p_j C D \end{aligned} \quad (\text{A.8})$$

From the defining properties of the  $\gamma$  matrices one can conclude that

$$\{\gamma_0, \gamma_i\} = 2g_{0i} = 0, \quad (\text{A.9})$$

$$\begin{aligned} \not{p} \not{p} &= \gamma_i \gamma_j p_i p_j = \frac{1}{2} (\gamma_i \gamma_j p_i p_j + \gamma_j \gamma_i p_j p_i) = \frac{1}{2} \{\gamma_i, \gamma_j\} p_i p_j \\ &= \frac{1}{2} 2g_{ij} p_i p_j = (-\delta_{ij}) p_i p_j = -p_i p_i = -\mathbf{p}^2 \end{aligned} \quad (\text{A.10})$$

and thus one finds  $\hat{S}(p) \widehat{S^{-1}}(p) = p_0^2 A_p^2 - B_p^2 - \mathbf{p}^2 C_p^2 + p_0^2 \mathbf{p}^2 D_p^2 = d_{q,M}(p)$  and we obtain

$$S(p) S^{-1}(p) = \frac{i}{d_{q,M}(p)} \hat{S}(p) \left( -i \widehat{S^{-1}}(p) \right) = \frac{\hat{S} \widehat{S^{-1}}}{d_{q,M}(p)} = 1 \quad (\text{A.11})$$

which justifies (4.5).

### A.2.2 Expansion of the Gap Equation

We now proceed with the reduction of (4.1) to scalar equations in the bare-vertex truncation  $\Gamma^\mu(q, p) \rightarrow \gamma^\mu$ . Employing (4.11) and (4.18), the gap equation takes the form

$$\begin{aligned} iS^{-1}(p) &\equiv \gamma_0 p_0 A_p - B_p - \gamma_i p_i C_p + \gamma_0 \gamma_i p_0 p_i D_p \quad (\text{A.12}) \\ &= \gamma^\mu p_\mu - m - \frac{C_F}{(2\pi)^4} \int d^4 q \gamma_0 S(q) \gamma_0 \frac{4\pi \alpha(\mathbf{k}^2)}{\mathbf{k}^2} - \frac{C_F}{(2\pi)^4} \int d^4 q \gamma_i S(q) \gamma_j \hat{P}_{ij}(k) V_T(k) \\ &\equiv \gamma_0 p_0 - \gamma_i p_i - m - \frac{i C_F}{(2\pi)^4} \int \frac{d^4 q}{d_{q,M}(q)} \left\{ \gamma_0^2 \gamma_0 q_0 A_q + \gamma_0^2 B_q \right. \\ &\quad \left. - \gamma_0 \gamma_k \gamma_0 q_k C_q + \gamma_0^2 \gamma_k \gamma_0 q_0 q_k D_q \right\} \frac{4\pi \alpha(\mathbf{k}^2)}{\mathbf{k}^2} \\ &\quad - \frac{i C_F}{(2\pi)^4} \int \frac{d^4 q}{d_{q,M}(q)} \left\{ \gamma_i \gamma_0 \gamma_j q_0 A_q + \gamma_i \gamma_j B_q \right. \\ &\quad \left. - \gamma_i \gamma_k \gamma_j q_k C_q + \gamma_i \gamma_0 \gamma_k \gamma_j q_0 q_k D_q \right\} \hat{P}_{ij}(k) V_T(k) \end{aligned}$$

---

<sup>2</sup>To have a more compact notation, we employ the abbreviation  $A_p \equiv A(p) \equiv A_M(\mathbf{p}^2, p_0^2)$ . Most times the M for Minkowskian is dropped; we may also drop the argument altogether if it is clear from the context.

Employing (in the first term containing  $C_q$ ) the relation  $\gamma_0 \gamma_k \gamma_0 = -\gamma_0^2 \gamma_k = -\gamma_k$  we obtain

$$\begin{aligned} \gamma_0 p_0 A_p - B_p - \gamma_i p_i C_p + \gamma_0 \gamma_i p_0 p_i D_p &= \gamma_0 p_0 - \gamma_i p_i - m \\ &- \frac{i C_F}{(2\pi)^4} \int \frac{d^4 q}{d_{q,M}(q)} \{ \gamma_0 q_0 A_q + B_q + \gamma_k q_k C_q + \gamma_k \gamma_0 q_0 q_k D_q \} \frac{4\pi \alpha(\mathbf{k}^2)}{\mathbf{k}^2} \\ &- \frac{i C_F}{(2\pi)^4} \int \frac{d^4 q}{d_{q,M}(q)} \{ \gamma_i \gamma_0 \gamma_j q_0 A_q + \gamma_i \gamma_j B_q - \gamma_i \gamma_k \gamma_j q_k C_q + \gamma_i \gamma_0 \gamma_k \gamma_j q_0 q_k D_q \} \hat{P}_{ij}(k) V_T(k), \end{aligned} \quad (\text{A.13})$$

which is the basic equation for the following steps.

### A.2.3 Projection onto Basis Elements

In order to obtain scalar equations we multiply (A.13) with the tensor basis elements of  $iS^{-1}(p)$ , namely  $\gamma_0 p_0$ ,  $\mathbb{I}$ ,  $\gamma_i p_i$  and  $\gamma_0 \gamma_i p_0 p_i$ , and take Dirac traces of the resulting equations. The necessary traces have been summarized in subsection A.2.6.

#### Equation for $A$ :

$\gamma_0 p_0 \times$  (A.13) reads

$$\begin{aligned} p_0^2 A_p - \gamma_0 p_0 B_p - \gamma_0 \gamma_i p_0 p_i C_p + \gamma_i p_0^2 p_i D_p &= p_0^2 - \gamma_0 \gamma_i p_0 p_i - \gamma_0 p_0 m \\ &- \frac{i C_F}{(2\pi)^4} \int \frac{d^4 q}{d_{q,M}(q)} \{ p_0 q_0 A_q - \gamma_0 p_0 B_q + \gamma_0 \gamma_k p_0 q_0 q_k C_q + \gamma_0 \gamma_k \gamma_0 p_0 q_0 q_k D_q \} \frac{4\pi \alpha(\mathbf{k}^2)}{\mathbf{k}^2} \\ &- \frac{i C_F}{(2\pi)^4} \int \frac{d^4 q}{d_{q,M}(q)} \{ \gamma_0 \gamma_i \gamma_0 \gamma_j p_0 q_0 A_q + \gamma_0 \gamma_i \gamma_j p_0 B_q - \gamma_0 \gamma_i \gamma_k \gamma_j p_0 q_k C_q \\ &\quad + \gamma_0 \gamma_i \gamma_0 \gamma_k \gamma_j p_0 q_0 q_k D_q \} \hat{P}_{ij}(k) V_T(k). \end{aligned} \quad (\text{A.14})$$

Taking  $\frac{1}{4} \text{tr}$  of this expression yields (employing (A.62))

$$p_0^2 A_p = p_0^2 - \frac{i C_F}{(2\pi)^4} \int \frac{d^4 q}{d_{q,M}(q)} p_0 q_0 A_q \frac{4\pi \alpha(\mathbf{k}^2)}{\mathbf{k}^2} - \frac{i C_F}{(2\pi)^4} \int \frac{d^4 q}{d_{q,M}(q)} \delta_{ij} p_0 q_0 A_q \hat{P}_{ij}(k) V_T(k) \quad (\text{A.15})$$

and with

$$\delta_{ij} \hat{P}_{ij}(k) = \delta_{ij} \left( \delta_{ij} - \frac{k_i k_j}{\mathbf{k}^2} \right) = \delta_{ii} - \frac{\mathbf{k}^2}{\mathbf{k}^2} = 3 - 1 = 2 \quad (\text{A.16})$$

we obtain

$$A_p = 1 - \frac{1}{p_0} \frac{i C_F}{(2\pi)^4} \int \frac{d^4 q}{d_{q,M}(q)} q_0 A_q \frac{4\pi \alpha(\mathbf{k}^2)}{\mathbf{k}^2} - \frac{2}{p_0} \frac{i C_F}{(2\pi)^4} \int \frac{d^4 q}{d_{q,M}(q)} q_0 A_q V_T(k). \quad (\text{A.17})$$

#### Equation for $B$ :

Taking  $\frac{1}{4} \text{tr}$  of (A.13) yields

$$\begin{aligned} -B_p &= -m - \frac{i C_F}{(2\pi)^4} \int \frac{d^4 q}{d_{q,M}(q)} B_q \frac{4\pi \alpha(\mathbf{k}^2)}{\mathbf{k}^2} - \frac{i C_F}{(2\pi)^4} \int \frac{d^4 q}{d_{q,M}(q)} \frac{1}{4} \text{tr}(\gamma_i \gamma_j) B_q \hat{P}_{ij}(k) V_T(k) \\ &\stackrel{(\text{A.61})}{=} -m - \frac{i C_F}{(2\pi)^4} \int \frac{d^4 q}{d_{q,M}(q)} B_q \frac{4\pi \alpha(\mathbf{k}^2)}{\mathbf{k}^2} + \frac{i C_F}{(2\pi)^4} \int \frac{d^4 q}{d_{q,M}(q)} B_q \delta_{ij} \hat{P}_{ij}(k) V_T(k), \end{aligned} \quad (\text{A.18})$$

i.e. (employing (A.16))

$$B_p = m + \frac{i C_F}{(2\pi)^4} \int \frac{d^4 q}{d_{q,M}(q)} B_q \frac{4\pi \alpha(\mathbf{k}^2)}{\mathbf{k}^2} - \frac{2i C_F}{(2\pi)^4} \int \frac{d^4 q}{d_{q,M}(q)} B_q V_T(k). \quad (\text{A.19})$$

**Equation for  $C$ :**

$\gamma_\ell p_\ell \times (\text{A.13})$  reads

$$\begin{aligned} & \gamma_\ell \gamma_0 p_0 p_\ell A_p - \gamma_\ell p_\ell B_p - \gamma_\ell \gamma_i p_i p_\ell C_p + \gamma_\ell \gamma_0 \gamma_i p_0 p_\ell p_i D_p = \gamma_\ell \gamma_0 p_0 p_\ell - \gamma_\ell \gamma_i p_i p_\ell - \gamma_\ell p_\ell m \\ & - \frac{i C_F}{(2\pi)^4} \int \frac{d^4 q}{d_{q,M}(q)} \{ \gamma_\ell \gamma_0 p_\ell q_0 A_q + \gamma_\ell p_\ell B_q + \gamma_\ell \gamma_k p_\ell q_k C_q + \gamma_\ell \gamma_k \gamma_0 p_\ell q_0 q_k D_q \} \frac{4\pi \alpha(\mathbf{k}^2)}{\mathbf{k}^2} \\ & - \frac{i C_F}{(2\pi)^4} \int \frac{d^4 q}{d_{q,M}(q)} \left\{ \gamma_\ell \gamma_i \gamma_0 \gamma_j p_\ell q_0 A_q + \gamma_\ell \gamma_i \gamma_j p_\ell B_q - \gamma_\ell \gamma_i \gamma_k \gamma_j p_\ell q_k C_q \right. \\ & \quad \left. + \gamma_\ell \gamma_i \gamma_0 \gamma_k \gamma_j p_\ell q_0 q_k D_q \right\} \hat{P}_{ij}(k) V_T(k). \end{aligned} \quad (\text{A.20})$$

Taking  $\frac{1}{4} \text{tr}(\text{A.20})$  yields with the general results of subsection A.2.6, and in particular (A.64)

$$\begin{aligned} -\frac{1}{4} \text{tr}(\gamma_\ell \gamma_i) p_\ell p_i C_p &= -\frac{1}{4} \text{tr}(\gamma_\ell \gamma_i) p_i p_\ell - \frac{i C_F}{(2\pi)^4} \int \frac{d^4 q}{d_{q,M}(q)} \frac{1}{4} \text{tr}(\gamma_\ell \gamma_k) p_\ell q_k C_q \frac{4\pi \alpha(\mathbf{k}^2)}{\mathbf{k}^2} \\ & \quad + \frac{i C_F}{(2\pi)^4} \int \frac{d^4 q}{d_{q,M}(q)} \frac{1}{4} \text{tr}(\gamma_\ell \gamma_i \gamma_k \gamma_j) p_\ell q_k C_q \hat{P}_{ij}(k) V_T(k); \\ \delta_{\ell i} p_\ell p_i C_p &= \frac{1}{4} \delta_{\ell i} p_i p_\ell + \frac{i C_F}{(2\pi)^4} \int \frac{d^4 q}{d_{q,M}(q)} \delta_{\ell k} p_\ell q_k C_q \frac{4\pi \alpha(\mathbf{k}^2)}{\mathbf{k}^2} \\ & \quad + \frac{i C_F}{(2\pi)^4} \int \frac{d^4 q}{d_{q,M}(q)} (\delta_{\ell i} \delta_{kj} - \delta_{\ell k} \delta_{ij} + \delta_{\ell j} \delta_{ik}) p_\ell q_k C_q \hat{P}_{ij}(k) V_T(k). \end{aligned} \quad (\text{A.21})$$

The contractions in the last term read

$$\begin{aligned} & (\delta_{\ell i} \delta_{kj} - \delta_{\ell k} \delta_{ij} + \delta_{\ell j} \delta_{ik}) p_\ell q_k \hat{P}_{ij}(k) \\ &= p_\ell \delta_{\ell i} \hat{P}_{ij}(k) \delta_{kj} q_k - p_\ell \delta_{\ell k} q_k \delta_{ij} \hat{P}_{ij}(k) + p_\ell \delta_{\ell j} \hat{P}_{ij}(k) \delta_{ik} q_k \\ &= 2 p_i \hat{P}_{ij}(k) q_j - p_\ell \delta_{\ell k} q_k \underbrace{\delta_{ij} \hat{P}_{ii}(k)}_{\substack{=2 \\ (\text{A.16})}} = 2 \underbrace{p_i \delta_{ij} q_j}_{=\mathbf{p} \cdot \mathbf{q}} - 2 \frac{p_i k_i k_j q_j}{\mathbf{k}^2} - 2 \underbrace{p_\ell \delta_{\ell k} q_k}_{=\mathbf{p} \cdot \mathbf{q}} = -2 \frac{(\mathbf{p} \cdot \mathbf{k})(\mathbf{q} \cdot \mathbf{k})}{\mathbf{k}^2} \end{aligned} \quad (\text{A.22})$$

Thus we find

$$\mathbf{p}^2 C_p = \mathbf{p}^2 + \frac{i C_F}{(2\pi)^4} \int \frac{d^4 q}{d_{q,M}(q)} (\mathbf{p} \cdot \mathbf{q}) C_q \frac{4\pi \alpha(\mathbf{k}^2)}{\mathbf{k}^2} - \frac{2i C_F}{(2\pi)^4} \int \frac{d^4 q}{d_{q,M}(q)} \frac{(\mathbf{p} \cdot \mathbf{k})(\mathbf{q} \cdot \mathbf{k})}{\mathbf{k}^2} C_q V_T(k), \quad (\text{A.23})$$

which after division by  $p^2 = \mathbf{p}^2$  reads

$$C_p = 1 + \frac{i C_F}{(2\pi)^4} \frac{1}{p^2} \int \frac{d^4 q}{d_{q,M}(q)} (\mathbf{p} \cdot \mathbf{q}) C_q \frac{4\pi \alpha(\mathbf{k}^2)}{\mathbf{k}^2} - \frac{2i C_F}{(2\pi)^4} \frac{1}{p^2} \int \frac{d^4 q}{d_{q,M}(q)} \frac{(\mathbf{p} \cdot \mathbf{k})(\mathbf{q} \cdot \mathbf{k})}{\mathbf{k}^2} C_q V_T(k). \quad (\text{A.24})$$

**Equation for  $D$ :**

$\gamma_0 \gamma_\ell p_0 p_\ell \times (\text{A.13})$  reads after straightforward simplifications

$$\begin{aligned} & -\gamma_\ell p_0^2 p_\ell A_p - \gamma_0 \gamma_\ell p_0 p_\ell B_p - \gamma_0 \gamma_\ell \gamma_i p_0 p_\ell p_i C_p - \gamma_\ell \gamma_i p_0^2 p_\ell p_i D_p \\ &= -\gamma_\ell p_0^2 p_\ell - \gamma_0 \gamma_\ell \gamma_i p_i p_\ell - \gamma_0 \gamma_\ell p_0 p_\ell m \\ & \quad - \frac{i C_F}{(2\pi)^4} \int \frac{d^4 q}{d_{q,M}(q)} \left\{ -\gamma_\ell p_0 p_\ell q_0 A_q + \gamma_0 \gamma_\ell p_0 p_\ell B_q \right. \\ & \quad \left. + \gamma_0 \gamma_\ell \gamma_k p_0 p_\ell q_k C_q + \gamma_\ell \gamma_k p_0 p_\ell q_0 q_k D_q \right\} \frac{4\pi \alpha(\mathbf{k}^2)}{\mathbf{k}^2} \\ & \quad - \frac{i C_F}{(2\pi)^4} \int \frac{d^4 q}{d_{q,M}(q)} \left\{ \gamma_\ell \gamma_i \gamma_j p_0 p_\ell q_0 A_q + \gamma_0 \gamma_\ell \gamma_i \gamma_j p_0 p_\ell B_q \right. \\ & \quad \left. - \gamma_0 \gamma_\ell \gamma_i \gamma_k \gamma_j p_0 p_\ell q_k C_q + \gamma_\ell \gamma_i \gamma_k \gamma_j p_0 p_\ell q_0 q_k D_q \right\} \hat{P}_{ij}(k) V_T(k). \end{aligned} \quad (\text{A.25})$$

Taking  $\frac{1}{4}\text{tr}(\text{A.25})$  yields

$$\begin{aligned}
-\frac{1}{4}\text{tr}(\gamma_\ell \gamma_i) p_0^2 p_\ell p_i D_p &= -\frac{i C_F}{(2\pi)^4} \int \frac{d^4 q}{d_{q,M}(q)} \frac{1}{4} \text{tr}(\gamma_\ell \gamma_k) p_0 p_\ell q_0 q_k D_q \frac{4\pi \alpha(\mathbf{k}^2)}{\mathbf{k}^2} \\
&\quad - \frac{i C_F}{(2\pi)^4} \int \frac{d^4 q}{d_{q,M}(q)} \text{tr}(\gamma_\ell \gamma_i \gamma_k \gamma_j) p_0 p_\ell q_0 q_k D_q \hat{P}_{ij}(k) V_T(k), \\
p_0^2 \delta_{\ell i} p_\ell p_i D_p &= \frac{i C_F}{(2\pi)^4} \int \frac{d^4 q}{d_{q,M}(q)} \delta_{\ell k} p_0 p_\ell q_0 q_k D_q \frac{4\pi \alpha(\mathbf{k}^2)}{\mathbf{k}^2} \\
&\quad - \frac{i C_F}{(2\pi)^4} \int \frac{d^4 q}{d_{q,M}(q)} p_0 q_0 (\delta_{\ell i} \delta_{kj} - \delta_{\ell k} \delta_{ij} + \delta_{\ell j} \delta_{ik}) p_\ell q_k \hat{P}_{ij}(k) D_q V_T(k),
\end{aligned} \tag{A.26}$$

and by (A.22) we have

$$p_0^2 \mathbf{p}^2 D_p = \frac{i C_F}{(2\pi)^4} \int \frac{d^4 q}{d_{q,M}(q)} p_0 q_0 (\mathbf{p} \cdot \mathbf{q}) D_q \frac{4\pi \alpha(\mathbf{k}^2)}{\mathbf{k}^2} + \frac{2i C_F}{(2\pi)^4} \int \frac{d^4 q}{d_{q,M}(q)} p_0 q_0 \frac{(\mathbf{p} \cdot \mathbf{k})(\mathbf{q} \cdot \mathbf{k})}{\mathbf{k}^2} D_q V_T(k), \tag{A.27}$$

respectively

$$D_p = \frac{i C_F}{(2\pi)^4} \frac{1}{p_0 p^2} \int \frac{d^4 q}{d_{q,M}(q)} q_0 (\mathbf{p} \cdot \mathbf{q}) D_q \frac{4\pi \alpha(\mathbf{k}^2)}{\mathbf{k}^2} + \frac{2i C_F}{(2\pi)^4} \frac{1}{p_0 p^2} \int \frac{d^4 q}{d_{q,M}(q)} q_0 \frac{(\mathbf{p} \cdot \mathbf{k})(\mathbf{q} \cdot \mathbf{k})}{\mathbf{k}^2} D_q V_T(k). \tag{A.28}$$

#### A.2.4 Symmetry and Wick-Rotation

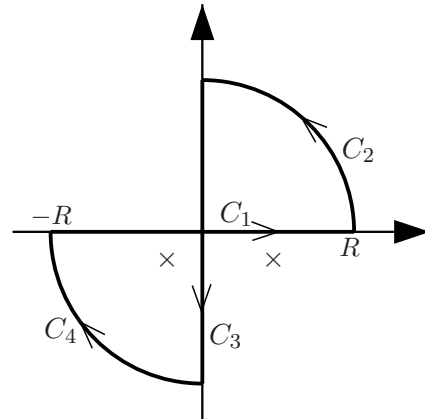
Due to rotational and time reversal symmetry the propagator functions  $A_q$  etc. are expected to depend only on  $\mathbf{q}^2$  and  $q_0$ . Thus, due to total antisymmetry in  $q_0$  the first integral on the right-hand side of (A.17) and (A.28) vanishes and we end up with the final Minkowski equations

$$\begin{aligned}
A_p &= 1 - \frac{2}{p_0} \frac{i C_F}{(2\pi)^4} \int \frac{d^4 q}{d_{q,M}(q)} q_0 A_q V_T(k), \\
B_p &= m + \frac{i C_F}{(2\pi)^4} \int \frac{d^4 q}{d_{q,M}(q)} B_q \frac{4\pi \alpha(\mathbf{k}^2)}{\mathbf{k}^2} - \frac{2i C_F}{(2\pi)^4} \int \frac{d^4 q}{d_{q,M}(q)} B_q V_T(k), \\
C_p &= 1 + \frac{i C_F}{(2\pi)^4} \frac{1}{p^2} \int \frac{d^4 q}{d_{q,M}(q)} (\mathbf{p} \cdot \mathbf{q}) C_q \frac{4\pi \alpha(\mathbf{k}^2)}{\mathbf{k}^2} - \frac{2i C_F}{(2\pi)^4} \frac{1}{p^2} \int \frac{d^4 q}{d_{q,M}(q)} \frac{(\mathbf{p} \cdot \mathbf{k})(\mathbf{q} \cdot \mathbf{k})}{\mathbf{k}^2} C_q V_T(k), \\
D_p &= \frac{2i C_F}{(2\pi)^4} \frac{1}{p_0 p^2} \int \frac{d^4 q}{d_{q,M}(q)} q_0 \frac{(\mathbf{p} \cdot \mathbf{k})(\mathbf{q} \cdot \mathbf{k})}{\mathbf{k}^2} D_q V_T(k).
\end{aligned} \tag{A.29}$$

To proceed further, we Wick-rotate these equations to Euclidean space. From Cauchy's theorem we have for any function  $f$  with poles (indicated by  $\times$ ) only in the sectors  $-\frac{\pi}{2} < \arg z < 0$  and  $\frac{\pi}{2} < \arg z < \pi$

$$0 = \int_{C_1} f(z) dz + \int_{C_2} f(z) dz + \int_{C_3} f(z) dz + \int_{C_4} f(z) dz.$$

The paths  $C_1$  and  $C_3$  can be parameterized by  $z_1(t) = t$ ,  $t \in (-R, R)$ ,  $dz = dt$  and  $z_3(t) = -it$ ,  $t \in (-R, R)$ ,  $dz = -i dt$ . If  $f$  vanishes sufficiently rapidly at infinity, the contributions from  $C_2$  and  $C_4$  drop out for  $R \rightarrow \infty$ .



Thus we have

$$\int_{-\infty}^{\infty} f(t) dt = - \int_{-\infty}^{\infty} f(-it) (-i dt) \Big|_{\substack{u = -t \quad \infty \rightarrow -\infty \\ du = -dt \quad -\infty \rightarrow \infty}} = \int_{-\infty}^{\infty} f(iu) i d(iu) \quad (\text{A.30})$$

and under the aforementioned conditions the substitution  $q_4 = i q_0$ ,  $q_0 = -i q_4$ ,  $i dq_0 = d(iq_4) = dq_4$  is valid. The Wick-rotated version of (A.29) is

$$A_E(\mathbf{p}^2, p_4^2) = 1 - \frac{2C_F}{(2\pi)^4} \frac{1}{p_4} \int_{-\infty}^{\infty} dq_4 \int_{\mathbb{R}^3} d^3 q \frac{q_4 A_E(\mathbf{q}^2, q_4^2) V_T(\mathbf{k}^2, k_4^2)}{d_{q,E}(\mathbf{q}^2, q_4^2)}, \quad (\text{A.31})$$

$$B_E(\mathbf{p}^2, p_4^2) = m + \frac{4\pi C_F}{(2\pi)^4} \int_{-\infty}^{\infty} dq_4 \int_{\mathbb{R}^3} d^3 q \frac{B_E(\mathbf{q}^2, q_4^2) \alpha(\mathbf{k}^2)}{\mathbf{k}^2 d_{q,E}(\mathbf{q}^2, q_4^2)} - \frac{2C_F}{(2\pi)^4} \int_{-\infty}^{\infty} dq_4 \int_{\mathbb{R}^3} d^3 q \frac{B_E(\mathbf{q}^2, q_4^2) V_T(\mathbf{k}^2, k_4^2)}{d_{q,E}(\mathbf{q}^2, q_4^2)}, \quad (\text{A.32})$$

$$C_E(\mathbf{p}^2, p_4^2) = 1 + \frac{4\pi C_F}{(2\pi)^4} \frac{1}{p^2} \int_{-\infty}^{\infty} dq_4 \int_{\mathbb{R}^3} d^3 q \frac{(\mathbf{p} \cdot \mathbf{q}) C_E(\mathbf{q}^2, q_4^2) \alpha(\mathbf{k}^2)}{\mathbf{k}^2 d_{q,E}(\mathbf{q}^2, q_4^2)} - \frac{2C_F}{(2\pi)^4} \frac{1}{p^2} \int_{-\infty}^{\infty} dq_4 \int_{\mathbb{R}^3} d^3 q \frac{(\mathbf{p} \cdot \mathbf{k})(\mathbf{q} \cdot \mathbf{k}) C_E(\mathbf{q}^2, q_4^2) V_T(\mathbf{k}^2, k_4^2)}{\mathbf{k}^2 d_{q,E}(\mathbf{q}^2, q_4^2)}, \quad (\text{A.33})$$

$$D_E(\mathbf{p}^2, p_4^2) = \frac{2C_F}{(2\pi)^4} \frac{1}{p_4 p^2} \int_{-\infty}^{\infty} dq_4 \int_{\mathbb{R}^3} d^3 q \frac{q_4 (\mathbf{p} \cdot \mathbf{k})(\mathbf{q} \cdot \mathbf{k}) D_E(\mathbf{q}^2, q_4^2) V_T(\mathbf{k}^2, k_4^2)}{\mathbf{k}^2 d_{q,E}(\mathbf{q}^2, q_4^2)} \quad (\text{A.34})$$

with the Euclidean propagator functions, obtained from their Minkowski counterparts as

$$\{A, B, C, D\}_E(\mathbf{p}^2, p_4^2) = \{A, B, C, D\}_M(\mathbf{p}^2, -p_4^2), \quad (\text{A.35})$$

and the quadratic form

$$d_{q,E}(\mathbf{q}^2, q_4^2) = d_{q,M}(\mathbf{q}^2, -q_4^2) \quad (\text{A.36})$$

### A.2.5 Introduction of Spherical Coordinates

In order to deal with the spatial triple integrals in (A.31) to (A.34) we introduce three-dimensional spherical coordinates  $(q, \vartheta, \varphi)$ ,  $d^3 q = q^2 dq d(\cos \vartheta) d\varphi$ . We choose  $\mathbf{p}$  to be aligned along the preferred axis, i.e.  $\mathbf{p} \cdot \mathbf{q} = pq \cos \vartheta$ . The  $\varphi$ -integration is straightforward and yields a factor of  $2\pi$ . So we find

$$A_E(\mathbf{p}^2, p_4^2) = 1 - \frac{2C_F}{(2\pi)^3} \frac{1}{p_4} \int_{-\infty}^{\infty} dq_4 q_4 \int_0^{\infty} dq \frac{q^2 A_E(q^2, q_4^2)}{d_{q,E}(q^2, q_4^2)} \int_{-1}^1 d(\cos \vartheta) V_T(\mathbf{k}^2, k_4^2), \quad (\text{A.37})$$

$$B_E(\mathbf{p}^2, p_4^2) = m + \frac{4\pi C_F}{(2\pi)^3} \int_{-\infty}^{\infty} dq_4 \int_0^{\infty} dq \frac{q^2 B_E(q^2, q_4^2)}{d_{q,E}(q^2, q_4^2)} \int_{-1}^1 d(\cos \vartheta) \frac{\alpha(\mathbf{k}^2)}{\mathbf{k}^2} - \frac{2C_F}{(2\pi)^3} \int_{-\infty}^{\infty} dq_4 \int_0^{\infty} dq \frac{q^2 B_E(q^2, q_4^2)}{d_{q,E}(q^2, q_4^2)} \int_{-1}^1 d(\cos \vartheta) V_T(\mathbf{k}^2, k_4^2). \quad (\text{A.38})$$

where  $\mathbf{k}^2 = (\mathbf{p} - \mathbf{q})^2 = \mathbf{p}^2 + \mathbf{q}^2 - 2\mathbf{p} \cdot \mathbf{q} = p^2 + q^2 - 2pq \cos \vartheta$ .

The equations for  $C$  and  $D$  contain the particular combination  $\frac{(\mathbf{p} \cdot \mathbf{k})(\mathbf{q} \cdot \mathbf{k})}{\mathbf{k}^2}$  for which we obtain

$$\begin{aligned} (\mathbf{p} \cdot \mathbf{k})(\mathbf{q} \cdot \mathbf{k}) &= [\mathbf{p} \cdot (\mathbf{p} - \mathbf{q})] [\mathbf{q} \cdot (\mathbf{p} - \mathbf{q})] = [\mathbf{p}^2 - \mathbf{p} \cdot \mathbf{q}] [\mathbf{p} \cdot \mathbf{q} - \mathbf{q}^2] \\ &= (\mathbf{p}^2 + \mathbf{q}^2) (\mathbf{p} \cdot \mathbf{q}) - \mathbf{p}^2 \mathbf{q}^2 - (\mathbf{p} \cdot \mathbf{q})^2 \\ &= (p^2 + q^2) pq \cos \vartheta - p^2 q^2 - p^2 q^2 \cos^2 \vartheta \\ &= pq \{ (p^2 + q^2) \cos \vartheta - pq - pq \cos^2 \vartheta \} \\ &= pq \{ (p^2 + q^2 - 2pq \cos \vartheta) \cos \vartheta - pq + pq \cos^2 \vartheta \} \\ &= pq \{ \mathbf{k}^2 \cos \vartheta - pq + pq \cos^2 \vartheta \}. \end{aligned} \quad (\text{A.39})$$

Thus we find

$$\frac{(\mathbf{p} \cdot \mathbf{k})(\mathbf{q} \cdot \mathbf{k})}{\mathbf{k}^2} = pq \left\{ \cos \vartheta + \frac{pq}{\mathbf{k}^2} (\cos^2 \vartheta - 1) \right\} \quad (\text{A.40})$$

and therefore we have

$$\begin{aligned} C_E(\mathbf{p}^2, p_4^2) = & 1 + \frac{4\pi C_F}{(2\pi)^3} \frac{1}{p} \int_{-\infty}^{\infty} dq_4 \int_0^{\infty} dq \frac{q^3 C_E(q^2, q_4^2)}{d_{q,E}(q^2, q_4^2)} \int_{-1}^1 d(\cos \vartheta) \frac{\cos \vartheta \alpha(\mathbf{k}^2)}{\mathbf{k}^2} \\ & - \frac{2 C_F}{(2\pi)^3} \frac{1}{p} \int_{-\infty}^{\infty} dq_4 \int_0^{\infty} dq \frac{q^3 C_E(\mathbf{q}^2, q_4^2)}{d_{q,E}(\mathbf{q}^2, q_4^2)} \int_{-1}^1 d(\cos \vartheta) \cos \vartheta V_T(\mathbf{k}^2, k_4^2) \\ & - \frac{2 C_F}{(2\pi)^4} \int_{-\infty}^{\infty} dq_4 \int_0^{\infty} dq \frac{q^4 C_E(q^2, q_4^2)}{d_{q,E}(q^2, q_4^2)} \int_{-1}^1 d(\cos \vartheta) \frac{(\cos^2 \vartheta - 1) V_T(\mathbf{k}^2, k_4^2)}{\mathbf{k}^2}, \end{aligned} \quad (\text{A.41})$$

$$\begin{aligned} D_E(\mathbf{p}^2, p_4^2) = & \frac{2 C_F}{(2\pi)^3} \frac{1}{p_4 p} \int_{-\infty}^{\infty} dq_4 q_4 \int_0^{\infty} dq \frac{q^3 D_E(q^2, q_4^2)}{d_{q,E}(q^2, q_4^2)} \int_{-1}^1 d(\cos \vartheta) \cos \vartheta V_T(\mathbf{k}^2, k_4^2) \\ & + \frac{2 C_F}{(2\pi)^3} \frac{1}{p_4} \int_{-\infty}^{\infty} dq_4 q_4 \int_0^{\infty} dq \frac{q^4 D_E(q^2, q_4^2)}{d_{q,E}(q^2, q_4^2)} \int_{-1}^1 d(\cos \vartheta) \frac{(\cos^2 \vartheta - 1) V_T(\mathbf{k}^2, k_4^2)}{\mathbf{k}^2} \end{aligned} \quad (\text{A.42})$$

It is possible to rewrite the integral over  $p_4$  by changing the domain of integration,

$$\begin{aligned} \int_{-\infty}^{\infty} f(q_4) dq_4 &= \int_{-\infty}^0 f(q_4) dq_4 + \int_0^{\infty} f(q_4) dq_4 = \int_0^{\infty} f(-q_4) dq_4 + \int_0^{\infty} f(q_4) dq_4 \\ &= \int_0^{\infty} \{f(q_4) + f(-q_4)\} dq_4. \end{aligned} \quad (\text{A.43})$$

This yields

$$\begin{aligned} A_E(\mathbf{p}^2, p_4^2) = & 1 - \frac{2 C_F}{(2\pi)^3} \frac{1}{p_4} \int_0^{\infty} dq_4 q_4 \int_0^{\infty} dq \frac{q^2 A_E(q^2, q_4^2)}{d_{q,E}(q^2, q_4^2)} \\ & \cdot \int_{-1}^1 d(\cos \vartheta) \{V_T(\mathbf{k}^2, (p_4 - q_4)^2) - V_T(\mathbf{k}^2, (p_4 + q_4)^2)\}, \end{aligned} \quad (\text{A.44})$$

$$\begin{aligned} B_E(\mathbf{p}^2, p_4^2) = & m + \frac{8\pi C_F}{(2\pi)^3} \int_0^{\infty} dq_4 \int_0^{\infty} dq \frac{q^2 B_E(q^2, q_4^2)}{d_{q,E}(q^2, q_4^2)} \int_{-1}^1 d(\cos \vartheta) \frac{\alpha(\mathbf{k}^2)}{\mathbf{k}^2} \\ & - \frac{2 C_F}{(2\pi)^3} \int_0^{\infty} dq_4 \int_0^{\infty} dq \frac{q^2 B_E(q^2, q_4^2)}{d_{q,E}(q^2, q_4^2)} \\ & \cdot \int_{-1}^1 d(\cos \vartheta) \{V_T(\mathbf{k}^2, (p_4 - q_4)^2) + V_T(\mathbf{k}^2, (p_4 + q_4)^2)\}, \end{aligned} \quad (\text{A.45})$$

$$\begin{aligned} C_E(\mathbf{p}^2, p_4^2) = & 1 + \frac{8\pi C_F}{(2\pi)^3} \frac{1}{p} \int_0^{\infty} dq_4 \int_0^{\infty} dq \frac{q^3 C_E(q^2, q_4^2)}{d_{q,E}(q^2, q_4^2)} \int_{-1}^1 d(\cos \vartheta) \frac{\cos \vartheta \alpha(\mathbf{k}^2)}{\mathbf{k}^2} \\ & - \frac{2 C_F}{(2\pi)^3} \frac{1}{p} \int_0^{\infty} dq_4 \int_0^{\infty} dq \frac{q^3 C_E(\mathbf{q}^2, q_4^2)}{d_{q,E}(\mathbf{q}^2, q_4^2)} \\ & \cdot \int_{-1}^1 d(\cos \vartheta) \cos \vartheta \{V_T(\mathbf{k}^2, (p_4 - q_4)^2) + V_T(\mathbf{k}^2, (p_4 + q_4)^2)\} \\ & - \frac{2 C_F}{(2\pi)^3} \int_0^{\infty} dq_4 \int_0^{\infty} dq \frac{q^4 C_E(q^2, q_4^2)}{d_{q,E}(q^2, q_4^2)} \\ & \cdot \int_{-1}^1 d(\cos \vartheta) \frac{(\cos^2 \vartheta - 1) \{V_T(\mathbf{k}^2, (p_4 - q_4)^2) + V_T(\mathbf{k}^2, (p_4 + q_4)^2)\}}{\mathbf{k}^2} \end{aligned} \quad (\text{A.46})$$



and

$$\begin{aligned}
D_E(\mathbf{p}^2, p_4^2) = & \frac{2C_F}{(2\pi)^3} \frac{1}{p_4 p} \int_0^\infty dq_4 q_4 \int_0^\infty dq \frac{q^3 C_E(q^2, q_4^2)}{d_{q,E}(q^2, q_4^2)} \\
& \cdot \int_{-1}^1 d(\cos \vartheta) \cos \vartheta \{V_T(\mathbf{k}^2, (p_4 - q_4)^2) - V_T(\mathbf{k}^2, (p_4 + q_4)^2)\} \\
& + \frac{2C_F}{(2\pi)^3} \frac{1}{p_4} \int_{-\infty}^\infty dq_4 q_4 \int_0^\infty dq \frac{q^4 C_E(q^2, q_4^2)}{d_{q,E}(q^2, q_4^2)} \\
& \cdot \int_{-1}^1 d(\cos \vartheta) \frac{(\cos^2 \vartheta - 1) \{V_T(\mathbf{k}^2, (p_4 - q_4)^2) - V_T(\mathbf{k}^2, (p_4 + q_4)^2)\}}{\mathbf{k}^2}.
\end{aligned} \tag{A.47}$$

Employing the abbreviations

$$I_{\text{ang}}^{\text{C0}} := \int_{-1}^1 d(\cos \vartheta) \frac{\alpha(\mathbf{k}^2)}{\mathbf{k}^2}, \tag{A.48}$$

$$I_{\text{ang}}^{\text{C1}} := \int_{-1}^1 d(\cos \vartheta) \frac{\cos \vartheta \alpha(\mathbf{k}^2)}{\mathbf{k}^2}, \tag{A.49}$$

$$I_{\text{ang}}^{T0-} := \int_{-1}^1 d(\cos \vartheta) V_T(\mathbf{k}^2, (p_4 - q_4)^2), \tag{A.50}$$

$$I_{\text{ang}}^{T0+} := \int_{-1}^1 d(\cos \vartheta) V_T(\mathbf{k}^2, (p_4 + q_4)^2), \tag{A.51}$$

$$I_{\text{ang}}^{T1-} := \int_{-1}^1 d(\cos \vartheta) \cos \vartheta V_T(\mathbf{k}^2, (p_4 - q_4)^2), \tag{A.52}$$

$$I_{\text{ang}}^{T1+} := \int_{-1}^1 d(\cos \vartheta) \cos \vartheta V_T(\mathbf{k}^2, (p_4 + q_4)^2), \tag{A.53}$$

$$I_{\text{ang}}^{T\mathbf{k}-} := \int_{-1}^1 d(\cos \vartheta) \frac{(\cos^2 \vartheta - 1) V_T(\mathbf{k}^2, (p_4 - q_4)^2)}{\mathbf{k}^2}, \tag{A.54}$$

$$I_{\text{ang}}^{T\mathbf{k}+} := \int_{-1}^1 d(\cos \vartheta) \frac{(\cos^2 \vartheta - 1) V_T(\mathbf{k}^2, (p_4 + q_4)^2)}{\mathbf{k}^2} \tag{A.55}$$

we can rewrite (A.37) to (A.47) as

$$A_E(\mathbf{p}^2, p_4^2) = 1 - \frac{2C_F}{(2\pi)^3} \frac{1}{p_4} \int_0^\infty dq_4 q_4 \int_0^\infty dq \frac{q^2 A_E(q^2, q_4^2)}{d_{q,E}(q^2, q_4^2)} (I_{\text{ang}}^{T0-} - I_{\text{ang}}^{T0+}), \tag{A.56}$$

$$\begin{aligned}
B_E(\mathbf{p}^2, p_4^2) = & m + \frac{8\pi C_F}{(2\pi)^3} \int_0^\infty dq_4 \int_0^\infty dq \frac{q^2 B_E(q^2, q_4^2)}{d_{q,E}(q^2, q_4^2)} I_{\text{ang}}^{\text{C0}} \\
& - \frac{2C_F}{(2\pi)^3} \int_0^\infty dq_4 \int_0^\infty dq \frac{q^2 B_E(q^2, q_4^2)}{d_{q,E}(q^2, q_4^2)} (I_{\text{ang}}^{T0-} + I_{\text{ang}}^{T0+}),
\end{aligned} \tag{A.57}$$

$$\begin{aligned}
C_E(\mathbf{p}^2, p_4^2) = & 1 + \frac{8\pi C_F}{(2\pi)^3} \frac{1}{p} \int_0^\infty dq_4 \int_0^\infty dq \frac{q^3 C_E(q^2, q_4^2)}{d_{q,E}(q^2, q_4^2)} I_{\text{ang}}^{\text{C1}} \\
& - \frac{2C_F}{(2\pi)^3} \frac{1}{p} \int_0^\infty dq_4 \int_0^\infty dq \frac{q^3 C_E(q^2, q_4^2)}{d_{q,E}(q^2, q_4^2)} (I_{\text{ang}}^{T1-} + I_{\text{ang}}^{T1+}) \\
& - \frac{2C_F}{(2\pi)^3} \int_0^\infty dq_4 \int_0^\infty dq \frac{q^4 C_E(q^2, q_4^2)}{d_{q,E}(q^2, q_4^2)} (I_{\text{ang}}^{T\mathbf{k}-} + I_{\text{ang}}^{T\mathbf{k}+}),
\end{aligned} \tag{A.58}$$

$$\begin{aligned}
D_E(\mathbf{p}^2, p_4^2) = & \frac{2C_F}{(2\pi)^3} \frac{1}{p_4 p} \int_0^\infty dq_4 q_4 \int_0^\infty dq \frac{q^3 D_E(q^2, q_4^2)}{d_{q,E}(q^2, q_4^2)} (I_{\text{ang}}^{T1-} - I_{\text{ang}}^{T1+}) \\
& + \frac{2C_F}{(2\pi)^3} \frac{1}{p_4} \int_{-\infty}^\infty dq_4 q_4 \int_0^\infty dq \frac{q^4 D_E(q^2, q_4^2)}{d_{q,E}(q^2, q_4^2)} (I_{\text{ang}}^{T\mathbf{k}-} - I_{\text{ang}}^{T\mathbf{k}+}).
\end{aligned} \tag{A.59}$$

### A.2.6 Some Important Dirac Traces

In the analysis of the gap equation one encounters traces of up to six gamma matrices. As well-known (and easy to show with the help of  $\gamma_5 = i\gamma_0\gamma_1\gamma_2\gamma_3$ ), Dirac traces of an odd number of gamma matrices always vanish in  $D = 4$ ,

$$\text{tr}(\gamma_0) = \text{tr}(\gamma_i) = \text{tr}(\gamma_0\gamma_i\gamma_j) = \text{tr}(\gamma_i\gamma_j\gamma_k) = \dots = 0. \quad (\text{A.60})$$

For the trace of two gamma matrices one finds

$$\begin{aligned} \gamma_i\gamma_j + \gamma_j\gamma_i &= 2g_{ij}\mathbb{1}_D = -2\delta_{ij}\mathbb{1}_D & \Big| \frac{1}{4}\text{tr} \\ \frac{1}{4}\text{tr}(\gamma_i\gamma_j) + \frac{1}{4}\text{tr}(\gamma_j\gamma_i) &= -\frac{1}{2}\delta_{ij}\text{tr}(\mathbb{1}_D) & \Big| \text{tr}(\gamma_j\gamma_i) \stackrel{\text{cycl.}}{=} \text{tr}(\gamma_i\gamma_j) \\ \frac{1}{2}\text{tr}(\gamma_i\gamma_j) &= -2\delta_{ij} \end{aligned}$$

and

$$\begin{aligned} \gamma_0\gamma_i + \gamma_i\gamma_0 &= 2g_{0i}\mathbb{1}_D = 0 & \Big| \frac{1}{4}\text{tr} \\ \frac{1}{4}\text{tr}(\gamma_0\gamma_i) + \frac{1}{4}\text{tr}(\gamma_i\gamma_0) &= 0 & \Big| \text{tr}(\gamma_i\gamma_0) \stackrel{\text{cycl.}}{=} \text{tr}(\gamma_0\gamma_i) \\ \frac{1}{2}\text{tr}(\gamma_0\gamma_i) &= 0, \end{aligned}$$

i.e.

$$\frac{1}{4}\text{tr}(\gamma_i\gamma_j) = -\delta_{ij} \quad \text{and} \quad \frac{1}{4}\text{tr}(\gamma_0\gamma_i) = 0. \quad (\text{A.61})$$

Expressions which contain at least two instances of  $\gamma_0$  can be simplified by repeated use of the anticommutation relation  $\gamma_0\gamma_i = -\gamma_i\gamma_0$  until one obtains an expression with  $\gamma_0^2$  which is equal to  $\mathbb{1}_D$ . Thus we find

$$\frac{1}{4}\text{tr}(\gamma_0\gamma_i\gamma_0\gamma_j) = -\frac{1}{4}\text{tr}(\gamma_i\gamma_0\gamma_0\gamma_j) = -\frac{1}{4}\text{tr}(\gamma_i\gamma_j) \stackrel{(\text{A.61})}{=} \delta_{ij}. \quad (\text{A.62})$$

For three spatial gamma matrices and one instance of  $\gamma^0$  we have

$$\text{tr}(\gamma_0\gamma_i\gamma_j\gamma_k) \stackrel{\text{cycl.}}{=} \text{tr}(\gamma_i\gamma_j\gamma_k\gamma_0) = -\text{tr}(\gamma_i\gamma_j\gamma_0\gamma_k) = \text{tr}(\gamma_i\gamma_0\gamma_j\gamma_k) = -\text{tr}(\gamma_0\gamma_i\gamma_j\gamma_k), \quad (\text{A.63})$$

so  $\text{tr}(\gamma_0\gamma_i\gamma_j\gamma_k)$  has to vanish. This is, by basically the same argument, true for the trace of any expression which contains precisely one instance of  $\gamma_0$  and an odd number of spatial gamma matrices. One  $\gamma_0$  and an even number of spatial gamma matrices constitute in total an odd number of matrices, thus the trace vanishes as well. Thus we can conclude: *The trace of any product which contains an odd number of  $\gamma_0$  vanishes.*

The most involved trace which we actually have to evaluate (i.e. which cannot be further simplified by the arguments given above) contains four spatial gamma matrices,

$$\begin{aligned} T &:= \text{tr}(\gamma_i\gamma_j\gamma_k\gamma_\ell) = \text{tr}(\gamma_i\gamma_j(2g_{k\ell} - \gamma_\ell\gamma_k)) \\ &= 2g_{k\ell}\text{tr}(\gamma_i\gamma_j) - \text{tr}(\gamma_i\gamma_j\gamma_\ell\gamma_k) \\ &= -2\delta_{k\ell}\text{tr}(\gamma_i\gamma_j) - \text{tr}(\gamma^i(2g_{j\ell} - \gamma_\ell\gamma_j)\gamma_k) \\ &= 8\delta_{k\ell}\delta_{ij} - 2g_{j\ell}\text{tr}(\gamma_i\gamma_k) + \text{tr}(\gamma_i\gamma_\ell\gamma_j\gamma_k) \\ &= 8\delta^{k\ell}\delta^{ij} + 2\delta_{j\ell}\text{tr}(\gamma_i\gamma_k) + \text{tr}((2g_{i\ell} - \gamma_\ell\gamma_i)\gamma_j\gamma_k) \\ &= 8\delta_{k\ell}\delta_{ij} - 8\delta_{j\ell}\delta_{ik} + 2g_{i\ell}\text{tr}(\gamma_j\gamma_k) - \text{tr}(\gamma_\ell\gamma_i\gamma_j\gamma_k) \\ &= 8\delta_{k\ell}\delta_{ij} - 8\delta_{j\ell}\delta_{ik} - 2\delta_{i\ell}\text{tr}(\gamma_j\gamma_k) - \text{tr}(\gamma_i\gamma_j\gamma_k\gamma_\ell) \\ &= 8\delta_{k\ell}\delta_{ij} - 8\delta_{j\ell}\delta_{ik} + 8\delta_{i\ell}\delta_{jk} - T \end{aligned}$$

One has obtained an algebraic equation for  $T$  from which one can read off

$$\frac{1}{4}\text{tr}(\gamma_i\gamma_j\gamma_k\gamma_\ell) = \delta_{k\ell}\delta_{ij} - \delta_{j\ell}\delta_{ik} + \delta_{i\ell}\delta_{jk}. \quad (\text{A.64})$$

### A.3 Renormalization of the Quark Gap Equation

The renormalization of the gap equation (4.1) is discussed in detail in subsection 2.4.4 of [124]. Since in that thesis the discussion is given in German and in order to have a self-contained presentation, we repeat here the arguments which lead to (4.21), effectively just giving a translation, slightly reformulated and extended by some additional comments:

In order to find the correct renormalization, we examine the renormalized integral equations for vector, axial vector and pseudoscalar quark-meson vertex functions [5]

$$\Gamma_\mu(p, p') = Z_{(\mu)}\gamma_\mu + \int \frac{d^4q}{(2\pi)^4} S(p' + q)\Gamma_\mu(p' + q, p + q)S(p + q)K(p + q, p' + q, q), \quad (\text{A.65})$$

$$\Gamma_{\mu 5}(p, p') = Z_{(\mu)5}\gamma_\mu\gamma_5 + \int \frac{d^4q}{(2\pi)^4} S(p' + q)\Gamma_{\mu 5}(p' + q, p + q)S(p + q)K(p + q, p' + q, q), \quad (\text{A.66})$$

$$\Gamma_5(p, p') = Z_5\gamma_5 + \int \frac{d^4q}{(2\pi)^4} S(p' + q)\Gamma_5(p' + q, p + q)S(p + q)K(p + q, p' + q, q) \quad (\text{A.67})$$

with  $K$  denoting the quark-antiquark scattering kernel which plays a key role in the Bethe-Salpeter equation (the relativistic bound state equation for two particles, see also sec. 4.4). In full untruncated QCD the eight renormalization constants  $Z_{(\mu)}$  and  $Z_{(\mu)5}$  are equal. This equality does not hold in the instantanous approximation (but it is expected to be restored when transverse gluons are taken into account). Therefore the model can be regarded as non-covariant approximation to a covariantly renormalized one-gluon exchange model. Since quark loops are neglected, all contributions to the axial U(1) anomaly vanish. Therefore the vertex functions are connected via the non-anomalous Ward identities

$$(p' - p)^\mu \Gamma_\mu(p', p) = iS^{-1}(p') - iS^{-1}(p), \quad (\text{A.68})$$

$$(p' - p)^\mu \Gamma_{\mu 5}(p', p) = iS^{-1}(p')\gamma_5 + \gamma_5 iS^{-1}(p) + 2m_0\Gamma_5(p', p). \quad (\text{A.69})$$

with  $m_0$  denoting the bare quark mass. In ladder approximation the scattering kernel is approximated by (cf. sec. 4.1.2)

$$\begin{aligned} K(p + q, p' + q, q) &\approx k(q) = iC_F g^2 \gamma_\mu \otimes \gamma_\nu D_{\mu\nu} \\ &= -i4\pi C_F \gamma_0 \otimes \gamma_0 V_C(\mathbf{q}^2) + i4\pi C_F \gamma_i \otimes \gamma_j \left( \delta^{ij} - \frac{q_i q_j}{\mathbf{q}^2} \right) V_T(q) \end{aligned} \quad (\text{A.70})$$

This yields for the axial vector function

$$\begin{aligned} (p' - p)^\mu \Gamma_{\mu 5}(p', p) &= iS^{-1}(p')\gamma_5 + \gamma_5 iS^{-1}(p) + 2m_0\Gamma_5(p', p) \\ &= Z_{(\mu)5}\gamma_\mu\gamma_5(p - p')^\mu + \int \frac{d^4q}{(2\pi)^4} S(p' + q)[iS^{-1}(p' + q)\gamma_5 \\ &\quad + \gamma_5 iS^{-1}(p + q) + 2m_0\Gamma_5(p' + q, p + q)]S(p + q)k(q) \end{aligned} \quad (\text{A.71})$$

The properties of the gamma matrices are used to obtain

$$\begin{aligned} &iS^{-1}(p')\gamma_5 + \gamma_5 iS^{-1}(p) + 2m_0\Gamma_5(p', p) \\ &= \gamma_5 \left( Z_{(\mu)5}\gamma_\mu p'^\mu - Z_5 m_0 + \int \frac{d^4q}{(2\pi)^4} S(p + q)k(q) \right) \\ &\quad + \left( Z_{(\mu)5}\gamma_\mu p'^\mu - Z_5 m_0 + \int \frac{d^4q}{(2\pi)^4} S(p' + q)k(q) \right) \gamma_5 + 2m_0\Gamma_5(p', p). \end{aligned} \quad (\text{A.72})$$

Now one can cancel the term  $2m_0\Gamma_5(p', p)$  on both sides of this equation, the dependency on the momenta  $p$  and  $p'$  is completely separated in this form. Thus one can directly read off

$$iS^{-1}(p) = Z_{(\mu)5}\gamma_\mu p'^\mu - Z_5 m_0 + \int \frac{d^4q}{(2\pi)^4} S(p' + q)k(q). \quad (\text{A.73})$$

Since in the present approximation the properties of the vertex functions do not change under parity transformations, one has

$$Z_{(\mu)5} = Z_{(\mu)} = \begin{cases} Z_0 & \text{for } \mu = 0 \\ Z_{(i)} & \text{for } \mu = i \in \{1, 2, 3\} \end{cases} \quad (\text{A.74})$$

The  $D$  component of the propagator has not been considered in [124], but since this component of the propagator does not acquire an ultraviolet divergent piece, no renormalization of this function is necessary. Therefore the discussion of renormalization remains unchanged.

## A.4 The Mixed Gluon Propagator in Coulomb Gauge

We have omitted the mixed gluon propagator from our discussion in chapter 4, since (4.10) suggests that it vanishes identically. However, strictly speaking this equation has a nontrivial distribution-valued solution, namely

$$V_M(\mathbf{k}^2, k_0^2) = f(k_0^2) \delta(\mathbf{k}^2) \quad (\text{A.75})$$

with an arbitrary generalized function  $f$ . To show that this is indeed a solution, we multiply (4.10) with a generic test function  $\varphi \in C_0^\infty(\mathbb{R}_0^+ \times \mathbb{R})$  and integrate it over  $\mathbb{R}_0^+ \times \mathbb{R}$ .

$$\iint_{\mathbb{R}_0^+ \times \mathbb{R}} \mathbf{k}^2 k_0 V_M(\mathbf{k}^2, k_0^2) \varphi(\mathbf{k}^2, k_0) d(\mathbf{k}^2, k_0) = 0. \quad (\text{A.76})$$

The validity of this equation for arbitrary test functions  $\varphi$  is equivalent to the validity of (4.10). If we choose  $V_M$  according to (A.75), this yields<sup>3</sup>

$$\begin{aligned} T_1 &:= \iint_{\mathbb{R}_0^+ \times \mathbb{R}} \mathbf{k}^2 k_0 \delta(\mathbf{k}^2) f(k_0^2) \varphi(\mathbf{k}^2, k_0) d(\mathbf{k}^2, k_0) \\ &= \frac{1}{2} \int_{-\infty}^{\infty} [\mathbf{k}^2 k_0 f(k_0^2) \varphi(\mathbf{k}^2, k_0)]_{\mathbf{k}^2=0} dk_0 = 0 \end{aligned} \quad (\text{A.77})$$

for arbitrary  $\varphi$ . We also note that a similar term  $V_M(\mathbf{k}^2, k_0^2) = g(\mathbf{k}^2) \delta(k_0^2)$  with a *regular* function  $g$  does not provide a solution, since for this we find

$$\begin{aligned} T_2 &:= \iint_{\mathbb{R}_0^+ \times \mathbb{R}} \mathbf{k}^2 k_0 \delta(k_0^2) g(\mathbf{k}^2) \varphi(\mathbf{k}^2, k_0) d(\mathbf{k}^2, k_0) \\ &= \frac{1}{2} \iint_{\mathbb{R}_0^+ \times \mathbb{R}_0^+} \mathbf{k}^2 \delta(k_0^2) g(\mathbf{k}^2) \left[ \varphi\left(\mathbf{k}^2, \sqrt{k_0^2}\right) + \varphi\left(\mathbf{k}^2, -\sqrt{k_0^2}\right) \right] d(\mathbf{k}^2, k_0^2) \\ &= \frac{1}{4} \int_0^\infty \mathbf{k}^2 g(\mathbf{k}^2) [\varphi(\mathbf{k}^2, 0) + \varphi(\mathbf{k}^2, 0)] d(\mathbf{k}^2) = \frac{1}{2} \int_0^\infty \mathbf{k}^2 g(\mathbf{k}^2) \varphi(\mathbf{k}^2, 0) d(\mathbf{k}^2), \end{aligned} \quad (\text{A.78})$$

which, in general, is different from zero. Also terms involving delta derivatives  $\delta^{(n)}(\mathbf{k}^2)$  with  $n \geq 1$  do not lead to the vanishing of (A.76) for arbitrary test function  $\varphi$ .

While such zero-mode contributions are possible from a mathematical point of view, their physical relevance is highly questionable. The matrix of 1PI-functions  $\Gamma^{(2)}$ , given in (3.8) does not have an inverse for  $\mathbf{k}^2 = 0$ . The matrix itself stays well-defined, but its rank drops to two. Taking into account that the 1PI functions are regarded as “more fundamental” than propagators, this is no real problem, but it precludes the clean treatment of propagators at  $\mathbf{k}^2 = 0$ .

---

<sup>3</sup>We remind our readers of the convention  $\int_0^b \varphi(x) \delta(x) dx = \frac{1}{2} \varphi(0)$  for  $b > 0$ . This choice is suggested by the properties of symmetric delta families (“Delta-Scharen”), where one obtains  $\lim_{\varepsilon \rightarrow 0} \int_0^b \varphi(x) \delta_\varepsilon^{(k)}(x) dx = \frac{1}{2} \varphi(0)$  for arbitrary test functions  $\varphi$  and  $k = 1, 2$ .

$$\begin{aligned}
I_{C0} &:= \frac{4\pi}{d_{\text{quad,E}}} \int_{-1}^1 d(\cos \vartheta) V_C(\mathbf{k}^2, k_4^2) & I_{T0} &:= \frac{1}{d_{\text{quad,E}}} \int_{-1}^1 d(\cos \vartheta) V_T(\mathbf{k}^2, k_4^2) \\
I_{C1} &:= \frac{4\pi}{d_{\text{quad,E}}} \int_{-1}^1 d(\cos \vartheta) V_C(\mathbf{k}^2, k_4^2) \cos \vartheta & I_{T1} &:= \frac{1}{d_{\text{quad,E}}} \int_{-1}^1 d(\cos \vartheta) V_T(\mathbf{k}^2, k_4^2) \cos \vartheta \\
I_{C2} &:= \frac{4\pi}{d_{\text{quad,E}}} \int_{-1}^1 d(\cos \vartheta) V_C(\mathbf{k}^2, k_4^2) \cos^2 \vartheta & I_{T2} &:= \frac{1}{d_{\text{quad,E}}} \int_{-1}^1 d(\cos \vartheta) V_T(\mathbf{k}^2, k_4^2) \cos^2 \vartheta \\
I_{M0} &:= \frac{1}{d_{\text{quad,E}}} \int_{-1}^1 d(\cos \vartheta) V_M(\mathbf{k}^2, k_4^2) & I_{T0k} &:= \frac{1}{d_{\text{quad,E}}} \int_{-1}^1 d(\cos \vartheta) \frac{V_T(\mathbf{k}^2, k_4^2)}{\mathbf{k}^2} \\
I_{M1} &:= \frac{1}{d_{\text{quad,E}}} \int_{-1}^1 d(\cos \vartheta) V_M(\mathbf{k}^2, k_4^2) \cos \vartheta & I_{T1k} &:= \frac{1}{d_{\text{quad,E}}} \int_{-1}^1 d(\cos \vartheta) \frac{V_T(\mathbf{k}^2, k_4^2) \cos \vartheta}{\mathbf{k}^2} \\
I_{M2} &:= \frac{1}{d_{\text{quad,E}}} \int_{-1}^1 d(\cos \vartheta) V_M(\mathbf{k}^2, k_4^2) \cos^2 \vartheta & I_{T2k} &:= \frac{1}{d_{\text{quad,E}}} \int_{-1}^1 d(\cos \vartheta) \frac{V_T(\mathbf{k}^2, k_4^2) \cos^2 \vartheta}{\mathbf{k}^2} \\
& & I_{T3k} &:= \frac{1}{d_{\text{quad,E}}} \int_{-1}^1 d(\cos \vartheta) \frac{V_T(\mathbf{k}^2, k_4^2) \cos^3 \vartheta}{\mathbf{k}^2}
\end{aligned}$$

Exteq 2: Integrals (respectively integral operators) which appear in the decomposition of the (Weyl-Landau-)Coulomb gauge gap equation, summarized in extended equations 3 to 10.

## A.5 Complete Decomposition of the Quark Gap Equation

Here we give the full decomposition of the quark gap equation, obtained by plugging the parameterizations (4.4), (4.11), (4.18), (4.38) and (4.39) into (4.1) and projecting on single propagator tensor components by taking appropriate Dirac traces and Wick-rotating all integrals to Euclidean space.

We explicitly keep the (formally present) mixed propagator, which is presumably irrelevant in the Coulomb gauge, but becomes important for example in the Landau-Coulomb interpolating gauge.

As in sec. A.2.5, in the four-dimensional integral  $\int_{\mathbb{R}^4} d^4q$ , the component  $p_4$  is naturally treated individually, but for the remaining three-dimensional integral is rewritten in spherical coordinates  $(q, \vartheta, \varphi)$  with  $\mathbf{p}$ -direction as preferred axis are introduced. In these coordinates, the  $\varphi$ -integration is trivial, so there remain the integrations over  $q = |\mathbf{q}|$  and the  $\vartheta$  which satisfies  $\mathbf{p} \cdot \mathbf{q} = pq \cos \vartheta$ .

To have a compact notation for  $\vartheta$ -integrals (angular integrals) at hand, we define several expressions which – depending on the ansätze for the vertex functions – can be read either as Lebesgue integrals or as integral operators. If the vertex dressing functions  $\Gamma_{ix}^X$ ,  $i \in \{0, 1, 2, 3\}$ ,  $x \in \{a, \dots, h\}$ ,  $X \in \{S, A\}$  are independent of the angle  $\theta$ , these expressions can be evaluated as simple definite integrals (which typically require regularization). If the vertex dressing functions depend on  $\theta$  (i.e. on the scalar product  $\mathbf{p} \cdot \mathbf{q}$ ), they have to be interpreted as *integral operators* which act to the right.

Putting everything together and setting  $V_M(\mathbf{k}^2, k_0^2) = 0$  (Coulomb gauge case) yields the scalar integral equations given in exteq 3-6. Inclusion of the mixed propagator (relevant for example for the Landau-Coulomb interpolating gauge) gives exteq 7-10. Both the intimidating length of these equations and the fact that the knowledge about the vertex functions  $\Gamma_{ix}^X$  is extremely limited indicate that a solution can only be obtained for dramatic simplifications.

$$\begin{aligned}
A(p) = & 1 + \frac{C_F}{(2\pi)^3} \frac{1}{p_4} \int_0^\infty dq q^2 \int_{\mathbb{R}} dq_4 \left\{ I_{C0} \left( -B_{(q)} \Gamma_{0a}^A - C_{(q)} \Gamma_{0c}^A q^2 + C_{(q)} \Gamma_{0d}^A q^2 \right. \right. \\
& - A_{(q)} \Gamma_{0b}^S q_4 + D_{(q)} \Gamma_{0e}^S q^2 q_4 - D_{(q)} \Gamma_{0f}^S q^2 q_4) \\
& + I_{C1} (C_{(q)} \Gamma_{0c}^A p q + C_{(q)} \Gamma_{0d}^A p q - D_{(q)} \Gamma_{0e}^S p q q_4 - D_{(q)} \Gamma_{0f}^S p q q_4) \\
& + I_{T0} (2B_{(q)} \Gamma_{1b}^A + B_{(q)} \Gamma_{2e}^A p^2 + B_{(q)} \Gamma_{2f}^A p^2 + B_{(q)} \Gamma_{3e}^A p^2 + B_{(q)} \Gamma_{3f}^A p^2 + 2C_{(q)} \Gamma_{1e}^A q^2 \\
& - 2C_{(q)} \Gamma_{1f}^A q^2 - C_{(q)} \Gamma_{2b}^A q^2 + B_{(q)} \Gamma_{2e}^A q^2 - B_{(q)} \Gamma_{2f}^A q^2 + C_{(q)} \Gamma_{3b}^A q^2 - B_{(q)} \Gamma_{3e}^A q^2 \\
& + B_{(q)} \Gamma_{3f}^A q^2 + 2C_{(q)} \Gamma_{2h}^A p^2 q^2 + 2C_{(q)} \Gamma_{3h}^A p^2 q^2 + 2A_{(q)} \Gamma_{1a}^S q_4 - A_{(q)} \Gamma_{2c}^S p^2 q_4 \\
& - A_{(q)} \Gamma_{2d}^S p^2 q_4 - A_{(q)} \Gamma_{3c}^S p^2 q_4 - A_{(q)} \Gamma_{3d}^S p^2 q_4 - 2D_{(q)} \Gamma_{1c}^S q^2 q_4 + 2D_{(q)} \Gamma_{1d}^S q^2 q_4 \\
& - D_{(q)} \Gamma_{2a}^S q^2 q_4 - A_{(q)} \Gamma_{2c}^S q^2 q_4 + A_{(q)} \Gamma_{2d}^S q^2 q_4 + D_{(q)} \Gamma_{3a}^S q^2 q_4 + A_{(q)} \Gamma_{3c}^S q^2 q_4 \\
& - A_{(q)} \Gamma_{3d}^S q^2 q_4 + 2D_{(q)} \Gamma_{2g}^S p^2 q^2 q_4 + 2D_{(q)} \Gamma_{3g}^S p^2 q^2 q_4) \\
& + I_{T1} (-2C_{(q)} \Gamma_{1e}^A p q - 2C_{(q)} \Gamma_{1f}^A p q + C_{(q)} \Gamma_{2b}^A p q - 2B_{(q)} \Gamma_{2e}^A p q + C_{(q)} \Gamma_{3b}^A p q \\
& + 2B_{(q)} \Gamma_{3f}^A p q + 2D_{(q)} \Gamma_{1c}^S p q q_4 + 2D_{(q)} \Gamma_{1d}^S p q q_4 + D_{(q)} \Gamma_{2a}^S p q q_4 + 2A_{(q)} \Gamma_{2c}^S p q q_4 \\
& + D_{(q)} \Gamma_{3a}^S p q q_4 - 2A_{(q)} \Gamma_{3d}^S p q q_4) \\
& + I_{T2} (-2C_{(q)} \Gamma_{2h}^A p^2 q^2 - 2C_{(q)} \Gamma_{3h}^A p^2 q^2 - 2D_{(q)} \Gamma_{2g}^S p^2 q^2 q_4 - 2D_{(q)} \Gamma_{3g}^S p^2 q^2 q_4) \\
& + I_{T0k} (-B_{(q)} \Gamma_{2e}^A p^4 - B_{(q)} \Gamma_{2f}^A p^4 - B_{(q)} \Gamma_{3e}^A p^4 - B_{(q)} \Gamma_{3f}^A p^4 + C_{(q)} \Gamma_{2b}^A p^2 q^2 - 2B_{(q)} \Gamma_{2e}^A p^2 q^2 \\
& + C_{(q)} \Gamma_{3b}^A p^2 q^2 + 2B_{(q)} \Gamma_{3f}^A p^2 q^2 - 2C_{(q)} \Gamma_{2h}^A p^4 q^2 - 2C_{(q)} \Gamma_{3h}^A p^4 q^2 + C_{(q)} \Gamma_{2b}^A q^4 - B_{(q)} \Gamma_{2e}^A q^4 \\
& + B_{(q)} \Gamma_{2f}^A q^4 - C_{(q)} \Gamma_{3b}^A q^4 + B_{(q)} \Gamma_{3e}^A q^4 - B_{(q)} \Gamma_{3f}^A q^4 - 2C_{(q)} \Gamma_{2h}^A p^2 q^4 + 2C_{(q)} \Gamma_{3h}^A p^2 q^4 \\
& + A_{(q)} \Gamma_{2c}^S p^4 q_4 + A_{(q)} \Gamma_{2d}^S p^4 q_4 + A_{(q)} \Gamma_{3c}^S p^4 q_4 + A_{(q)} \Gamma_{3d}^S p^4 q_4 + D_{(q)} \Gamma_{2a}^S p^2 q^2 q_4 \\
& + 2A_{(q)} \Gamma_{2c}^S p^2 q^2 q_4 + D_{(q)} \Gamma_{3a}^S p^2 q^2 q_4 - 2A_{(q)} \Gamma_{3d}^S p^2 q^2 q_4 - 2D_{(q)} \Gamma_{2g}^S p^4 q^2 q_4 \\
& - 2D_{(q)} \Gamma_{3g}^S p^4 q^2 q_4 + D_{(q)} \Gamma_{2a}^S q^4 q_4 + A_{(q)} \Gamma_{2c}^S q^4 q_4 - A_{(q)} \Gamma_{2d}^S q^4 q_4 - D_{(q)} \Gamma_{3a}^S q^4 q_4 \\
& - A_{(q)} \Gamma_{3c}^S q^4 q_4 + A_{(q)} \Gamma_{3d}^S q^4 q_4 - 2D_{(q)} \Gamma_{2g}^S p^2 q^4 q_4 + 2D_{(q)} \Gamma_{3g}^S p^2 q^4 q_4) \\
& + I_{T1k} (-C_{(q)} \Gamma_{2b}^A p^3 q + 4B_{(q)} \Gamma_{2e}^A p^3 q + 2B_{(q)} \Gamma_{2f}^A p^3 q - C_{(q)} \Gamma_{3b}^A p^3 q + 2B_{(q)} \Gamma_{3e}^A p^3 q \\
& - 3C_{(q)} \Gamma_{2b}^A p q^3 + 4B_{(q)} \Gamma_{2e}^A p q^3 - 2B_{(q)} \Gamma_{2f}^A p q^3 + C_{(q)} \Gamma_{3b}^A p q^3 - 2B_{(q)} \Gamma_{3e}^A p q^3 \\
& + 4C_{(q)} \Gamma_{2h}^A p^3 q^3 - D_{(q)} \Gamma_{2a}^S p^3 q q_4 - 4A_{(q)} \Gamma_{2c}^S p^3 q q_4 - 2A_{(q)} \Gamma_{2d}^S p^3 q q_4 - D_{(q)} \Gamma_{3a}^S p^3 q q_4 \\
& - 2A_{(q)} \Gamma_{3c}^S p^3 q q_4 - 3D_{(q)} \Gamma_{2a}^S p q^3 q_4 - 4A_{(q)} \Gamma_{2c}^S p q^3 q_4 + 2A_{(q)} \Gamma_{2d}^S p q^3 q_4 + D_{(q)} \Gamma_{3a}^S p q^3 q_4 \\
& + 2A_{(q)} \Gamma_{3c}^S p q^3 q_4 + 4D_{(q)} \Gamma_{2g}^S p^3 q^3 q_4) \\
& + I_{T2k} (2C_{(q)} \Gamma_{2b}^A p^2 q^2 - 4B_{(q)} \Gamma_{2e}^A p^2 q^2 + 2C_{(q)} \Gamma_{2h}^A p^4 q^2 + 2C_{(q)} \Gamma_{3h}^A p^4 q^2 + 2C_{(q)} \Gamma_{2h}^A p^2 q^4 \\
& - 2C_{(q)} \Gamma_{3h}^A p^2 q^4 + 2D_{(q)} \Gamma_{2a}^S p^2 q^2 q_4 + 4A_{(q)} \Gamma_{2c}^S p^2 q^2 q_4 + 2D_{(q)} \Gamma_{2g}^S p^4 q^2 q_4 \\
& + 2D_{(q)} \Gamma_{3g}^S p^4 q^2 q_4 + 2D_{(q)} \Gamma_{2g}^S p^2 q^4 q_4 - 2D_{(q)} \Gamma_{3g}^S p^2 q^4 q_4) \\
& \left. + I_{T3k} (-4C_{(q)} \Gamma_{2h}^A p^3 q^3 - 4D_{(q)} \Gamma_{2g}^S p^3 q^3 q_4) \right\}
\end{aligned}$$

Exteq 3: Gap equation for the propagator component  $A(p) \equiv A(\mathbf{p}^2, p_0^2)$ . The parametrization of the propagator is given in (4.4), the vertex coefficient functions  $\Gamma_{0a}^A, \dots$  are defined in (4.38) and (4.39); the integral operators  $I_{C0}, \dots$  are introduced in extended equation 2.

$$\begin{aligned}
B_{(p)} = & m + C_1 \int_0^\infty dq q^2 \int_{\mathbb{R}} dq_4 \left\{ I_{C0} (B_{(q)} \Gamma_{0b}^S + C_{(q)} \Gamma_{0e}^S q^2 - C_{(q)} \Gamma_{0f}^S q^2 \right. \\
& - A_{(q)} \Gamma_{0a}^A q_4 + D_{(q)} \Gamma_{0c}^A q^2 q_4 - D_{(q)} \Gamma_{0d}^A q^2 q_4) \\
& + I_{C1} (-C_{(q)} \Gamma_{0e}^S p q - C_{(q)} \Gamma_{0f}^S p q - D_{(q)} \Gamma_{0c}^A p q q_4 - D_{(q)} \Gamma_{0d}^A p q q_4) \\
& + I_{T1} (-2C_{(q)} \Gamma_{1c}^S p q - 2C_{(q)} \Gamma_{1d}^S p q - C_{(q)} \Gamma_{2a}^S p q + 2B_{(q)} \Gamma_{2c}^S p q - C_{(q)} \Gamma_{3a}^S p q \\
& - 2B_{(q)} \Gamma_{3d}^S p q - 2D_{(q)} \Gamma_{1e}^A p q q_4 - 2D_{(q)} \Gamma_{1f}^A p q q_4 + D_{(q)} \Gamma_{2b}^A p q q_4 + 2A_{(q)} \Gamma_{2e}^A p q q_4 \\
& + D_{(q)} \Gamma_{3b}^A p q q_4 - 2A_{(q)} \Gamma_{3f}^A p q q_4) \\
& + I_{T2} (2C_{(q)} \Gamma_{2g}^S p^2 q^2 + 2C_{(q)} \Gamma_{3g}^S p^2 q^2 - 2D_{(q)} \Gamma_{2h}^A p^2 q^2 q_4 - 2D_{(q)} \Gamma_{3h}^A p^2 q^2 q_4) \\
& + I_{T0} (2B_{(q)} \Gamma_{1a}^S - B_{(q)} \Gamma_{2c}^S p^2 - B_{(q)} \Gamma_{2d}^S p^2 - B_{(q)} \Gamma_{3c}^S p^2 - B_{(q)} \Gamma_{3d}^S p^2 + 2C_{(q)} \Gamma_{1c}^S q^2 \\
& - 2C_{(q)} \Gamma_{1d}^S q^2 + C_{(q)} \Gamma_{2a}^S q^2 - B_{(q)} \Gamma_{2c}^S q^2 + B_{(q)} \Gamma_{2d}^S q^2 - C_{(q)} \Gamma_{3a}^S q^2 + B_{(q)} \Gamma_{3c}^S q^2 \\
& - B_{(q)} \Gamma_{3d}^S q^2 - 2C_{(q)} \Gamma_{2g}^S p^2 q^2 - 2C_{(q)} \Gamma_{3g}^S p^2 q^2 - 2A_{(q)} \Gamma_{1b}^A q_4 - A_{(q)} \Gamma_{2e}^A p^2 q_4 \\
& - A_{(q)} \Gamma_{2f}^A p^2 q_4 - A_{(q)} \Gamma_{3e}^A p^2 q_4 - A_{(q)} \Gamma_{3f}^A p^2 q_4 + 2D_{(q)} \Gamma_{1e}^A q^2 q_4 - 2D_{(q)} \Gamma_{1f}^A q^2 q_4 \\
& - D_{(q)} \Gamma_{2b}^A q^2 q_4 - A_{(q)} \Gamma_{2e}^A q^2 q_4 + A_{(q)} \Gamma_{2f}^A q^2 q_4 + D_{(q)} \Gamma_{3b}^A q^2 q_4 + A_{(q)} \Gamma_{3e}^A q^2 q_4 \\
& - A_{(q)} \Gamma_{3f}^A q^2 q_4 + 2D_{(q)} \Gamma_{2h}^A p^2 q^2 q_4 + 2D_{(q)} \Gamma_{3h}^A p^2 q^2 q_4) \\
& + I_{T0k} (B_{(q)} \Gamma_{2c}^S p^4 + B_{(q)} \Gamma_{2d}^S p^4 + B_{(q)} \Gamma_{3c}^S p^4 + B_{(q)} \Gamma_{3d}^S p^4 - C_{(q)} \Gamma_{2a}^S p^2 q^2 + 2B_{(q)} \Gamma_{2c}^S p^2 q^2 \\
& - C_{(q)} \Gamma_{3a}^S p^2 q^2 - 2B_{(q)} \Gamma_{3d}^S p^2 q^2 + 2C_{(q)} \Gamma_{2g}^S p^4 q^2 + 2C_{(q)} \Gamma_{3g}^S p^4 q^2 - C_{(q)} \Gamma_{2a}^S q^4 \\
& + B_{(q)} \Gamma_{2c}^S q^4 - B_{(q)} \Gamma_{2d}^S q^4 + C_{(q)} \Gamma_{3a}^S q^4 - B_{(q)} \Gamma_{3c}^S q^4 + B_{(q)} \Gamma_{3d}^S q^4 + 2C_{(q)} \Gamma_{2g}^S p^2 q^4 \\
& - 2C_{(q)} \Gamma_{3g}^S p^2 q^4 + A_{(q)} \Gamma_{2e}^A p^4 q_4 + A_{(q)} \Gamma_{2f}^A p^4 q_4 + A_{(q)} \Gamma_{3e}^A p^4 q_4 + A_{(q)} \Gamma_{3f}^A p^4 q_4 \\
& + D_{(q)} \Gamma_{2b}^A p^2 q^2 q_4 + 2A_{(q)} \Gamma_{2e}^A p^2 q^2 q_4 + D_{(q)} \Gamma_{3b}^A p^2 q^2 q_4 - 2A_{(q)} \Gamma_{3f}^A p^2 q^2 q_4 \\
& - 2D_{(q)} \Gamma_{2h}^A p^4 q^2 q_4 - 2D_{(q)} \Gamma_{3h}^A p^4 q^2 q_4 + D_{(q)} \Gamma_{2b}^A q^4 q_4 + A_{(q)} \Gamma_{2e}^A q^4 q_4 - A_{(q)} \Gamma_{2f}^A q^4 q_4 \\
& - D_{(q)} \Gamma_{3b}^A q^4 q_4 - A_{(q)} \Gamma_{3e}^A q^4 q_4 + A_{(q)} \Gamma_{3f}^A q^4 q_4 - 2D_{(q)} \Gamma_{2h}^A p^2 q^4 q_4 + 2D_{(q)} \Gamma_{3h}^A p^2 q^4 q_4) \\
& + I_{T1k} (C_{(q)} \Gamma_{2a}^S p^3 q - 4B_{(q)} \Gamma_{2c}^S p^3 q - 2B_{(q)} \Gamma_{2d}^S p^3 q + C_{(q)} \Gamma_{3a}^S p^3 q - 2B_{(q)} \Gamma_{3c}^S p^3 q \\
& + 3C_{(q)} \Gamma_{2a}^S p q^3 - 4B_{(q)} \Gamma_{2c}^S p q^3 + 2B_{(q)} \Gamma_{2d}^S p q^3 - C_{(q)} \Gamma_{3a}^S p q^3 + 2B_{(q)} \Gamma_{3c}^S p q^3 \\
& - 4C_{(q)} \Gamma_{2g}^S p^3 q^3 - D_{(q)} \Gamma_{2b}^A p^3 q q_4 - 4A_{(q)} \Gamma_{2e}^A p^3 q q_4 - 2A_{(q)} \Gamma_{2f}^A p^3 q q_4 - D_{(q)} \Gamma_{3b}^A p^3 q q_4 \\
& - 2A_{(q)} \Gamma_{3e}^A p^3 q q_4 - 3D_{(q)} \Gamma_{2b}^A p q^3 q_4 - 4A_{(q)} \Gamma_{2e}^A p q^3 q_4 + 2A_{(q)} \Gamma_{2f}^A p q^3 q_4 \\
& + D_{(q)} \Gamma_{3b}^A p q^3 q_4 + 2A_{(q)} \Gamma_{3e}^A p q^3 q_4 + 4D_{(q)} \Gamma_{2h}^A p^3 q^3 q_4) \\
& + I_{T2k} (-2C_{(q)} \Gamma_{2a}^S p^2 q^2 + 4B_{(q)} \Gamma_{2c}^S p^2 q^2 - 2C_{(q)} \Gamma_{2g}^S p^4 q^2 - 2C_{(q)} \Gamma_{3g}^S p^4 q^2 \\
& - 2C_{(q)} \Gamma_{2g}^S p^2 q^4 + 2C_{(q)} \Gamma_{3g}^S p^2 q^4 + 2D_{(q)} \Gamma_{2b}^A p^2 q^2 q_4 + 4A_{(q)} \Gamma_{2e}^A p^2 q^2 q_4 \\
& + 2D_{(q)} \Gamma_{2h}^A p^4 q^2 q_4 + 2D_{(q)} \Gamma_{3h}^A p^4 q^2 q_4 + 2D_{(q)} \Gamma_{2h}^A p^2 q^4 q_4 - 2D_{(q)} \Gamma_{3h}^A p^2 q^4 q_4) \\
& \left. + I_{T3k} (4C_{(q)} \Gamma_{2g}^S p^3 q^3 - 4D_{(q)} \Gamma_{2h}^A p^3 q^3 q_4) \right\}
\end{aligned}$$

Exteq 4: Gap equation for the propagator component  $B_{(p)} \equiv B(\mathbf{p}^2, p_0^2)$  in Coulomb gauge. The notation is explained in extended equation 3.



$$\begin{aligned}
C_{(p)} = 1 &+ \frac{C_1}{p} \int_0^\infty dq q^2 \int_{\mathbb{R}} dq_4 \left\{ I_{C0} (B_{(q)} \Gamma_{0e}^S p + B_{(q)} \Gamma_{0f}^S p + 2C_{(q)} \Gamma_{0h}^S p q^2 \right. \\
&+ A_{(q)} \Gamma_{0c}^A p q_4 + A_{(q)} \Gamma_{0d}^A p q_4 - 2D_{(q)} \Gamma_{0g}^A p q^2 q_4) \\
&+ I_{C1} (C_{(q)} \Gamma_{0b}^S q - B_{(q)} \Gamma_{0e}^S q + B_{(q)} \Gamma_{0f}^S q - D_{(q)} \Gamma_{0a}^A q q_4 - A_{(q)} \Gamma_{0c}^A q q_4 + A_{(q)} \Gamma_{0d}^A q q_4) \\
&+ I_{C2} (-2C_{(q)} \Gamma_{0h}^S p q^2 + 2D_{(q)} \Gamma_{0g}^A p q^2 q_4) \\
&+ I_{T0} (-B_{(q)} \Gamma_{2a}^S p - B_{(q)} \Gamma_{3a}^S p - 2C_{(q)} \Gamma_{2c}^S p q^2 + 2B_{(q)} \Gamma_{2g}^S p q^2 + 2C_{(q)} \Gamma_{3d}^S p q^2 \\
&- 2B_{(q)} \Gamma_{3g}^S p q^2 + A_{(q)} \Gamma_{2b}^A p q_4 + A_{(q)} \Gamma_{3b}^A p q_4 - 2D_{(q)} \Gamma_{2e}^A p q^2 q_4 - 2A_{(q)} \Gamma_{2h}^A p q^2 q_4 \\
&+ 2D_{(q)} \Gamma_{3f}^A p q^2 q_4 + 2A_{(q)} \Gamma_{3h}^A p q^2 q_4) \\
&+ I_{T1} (B_{(q)} \Gamma_{2a}^S q - B_{(q)} \Gamma_{3a}^S q + C_{(q)} \Gamma_{2c}^S p^2 q + C_{(q)} \Gamma_{2d}^S p^2 q + C_{(q)} \Gamma_{3c}^S p^2 q + C_{(q)} \Gamma_{3d}^S p^2 q \\
&+ C_{(q)} \Gamma_{2c}^S q^3 - C_{(q)} \Gamma_{2d}^S q^3 - C_{(q)} \Gamma_{3c}^S q^3 + C_{(q)} \Gamma_{3d}^S q^3 - A_{(q)} \Gamma_{2b}^A q q_4 + A_{(q)} \Gamma_{3b}^A q q_4 \\
&+ D_{(q)} \Gamma_{2e}^A p^2 q q_4 + D_{(q)} \Gamma_{2f}^A p^2 q q_4 + D_{(q)} \Gamma_{3e}^A p^2 q q_4 + D_{(q)} \Gamma_{3f}^A p^2 q q_4 + D_{(q)} \Gamma_{2e}^A q^3 q_4 \\
&- D_{(q)} \Gamma_{2f}^A q^3 q_4 - D_{(q)} \Gamma_{3e}^A q^3 q_4 + D_{(q)} \Gamma_{3f}^A q^3 q_4) \\
&+ I_{T2} (-2B_{(q)} \Gamma_{2g}^S p q^2 + 2B_{(q)} \Gamma_{3g}^S p q^2 + 2A_{(q)} \Gamma_{2h}^A p q^2 q_4 - 2A_{(q)} \Gamma_{3h}^A p q^2 q_4) \\
&+ I_{T0k} (2B_{(q)} \Gamma_{1c}^S p^3 + 2B_{(q)} \Gamma_{1d}^S p^3 + B_{(q)} \Gamma_{2a}^S p^3 + B_{(q)} \Gamma_{3a}^S p^3 - 2C_{(q)} \Gamma_{1a}^S p q^2 + 2B_{(q)} \Gamma_{1c}^S p q^2 \\
&- 2B_{(q)} \Gamma_{1d}^S p q^2 + B_{(q)} \Gamma_{2a}^S p q^2 - B_{(q)} \Gamma_{3a}^S p q^2 + 4C_{(q)} \Gamma_{1g}^S p^3 q^2 + 2C_{(q)} \Gamma_{2c}^S p^3 q^2 - 2B_{(q)} \Gamma_{2g}^S p^3 q^2 \\
&+ 2C_{(q)} \Gamma_{3c}^S p^3 q^2 - 2B_{(q)} \Gamma_{3g}^S p^3 q^2 + 2C_{(q)} \Gamma_{2c}^S p q^4 - 2B_{(q)} \Gamma_{2g}^S p q^4 - 2C_{(q)} \Gamma_{3c}^S p q^4 + 2B_{(q)} \Gamma_{3g}^S p q^4 \\
&+ 2A_{(q)} \Gamma_{1e}^A p^3 q_4 + 2A_{(q)} \Gamma_{1f}^A p^3 q_4 - A_{(q)} \Gamma_{2b}^A p^3 q_4 - A_{(q)} \Gamma_{3b}^A p^3 q_4 + 2D_{(q)} \Gamma_{1b}^A p q^2 q_4 \\
&+ 2A_{(q)} \Gamma_{1e}^A p q^2 q_4 - 2A_{(q)} \Gamma_{1f}^A p q^2 q_4 - A_{(q)} \Gamma_{2b}^A p q^2 q_4 + A_{(q)} \Gamma_{3b}^A p q^2 q_4 - 4D_{(q)} \Gamma_{1h}^A p^3 q^2 q_4 \\
&+ 2D_{(q)} \Gamma_{2e}^A p^3 q^2 q_4 + 2A_{(q)} \Gamma_{2h}^A p^3 q^2 q_4 + 2D_{(q)} \Gamma_{3e}^A p^3 q^2 q_4 + 2A_{(q)} \Gamma_{3h}^A p^3 q^2 q_4 + 2D_{(q)} \Gamma_{2e}^A p q^4 q_4 \\
&+ 2A_{(q)} \Gamma_{2h}^A p q^4 q_4 - 2D_{(q)} \Gamma_{3e}^A p q^4 q_4 - 2A_{(q)} \Gamma_{3h}^A p q^4 q_4) \\
&+ I_{T1k} (2C_{(q)} \Gamma_{1a}^S p^2 q - 6B_{(q)} \Gamma_{1c}^S p^2 q - 2B_{(q)} \Gamma_{1d}^S p^2 q - 3B_{(q)} \Gamma_{2a}^S p^2 q - B_{(q)} \Gamma_{3a}^S p^2 q + 2C_{(q)} \Gamma_{1a}^S q^3 \\
&- 2B_{(q)} \Gamma_{1c}^S q^3 + 2B_{(q)} \Gamma_{1d}^S q^3 - B_{(q)} \Gamma_{2a}^S q^3 + B_{(q)} \Gamma_{3a}^S q^3 - 4C_{(q)} \Gamma_{1g}^S p^2 q^3 - 6C_{(q)} \Gamma_{2c}^S p^2 q^3 \\
&+ 4B_{(q)} \Gamma_{2g}^S p^2 q^3 + 2C_{(q)} \Gamma_{3d}^S p^2 q^3 - C_{(q)} \Gamma_{2c}^S q^5 + C_{(q)} \Gamma_{2d}^S q^5 + C_{(q)} \Gamma_{3c}^S q^5 - C_{(q)} \Gamma_{3d}^S q^5 \\
&- 2D_{(q)} \Gamma_{1b}^A p^2 q q_4 - 6A_{(q)} \Gamma_{1e}^A p^2 q q_4 - 2A_{(q)} \Gamma_{1f}^A p^2 q q_4 + 3A_{(q)} \Gamma_{2b}^A p^2 q q_4 + A_{(q)} \Gamma_{3b}^A p^2 q q_4 \\
&- 2D_{(q)} \Gamma_{1b}^A q^3 q_4 - 2A_{(q)} \Gamma_{1e}^A q^3 q_4 + 2A_{(q)} \Gamma_{1f}^A q^3 q_4 + A_{(q)} \Gamma_{2b}^A q^3 q_4 - A_{(q)} \Gamma_{3b}^A q^3 q_4 \\
&+ 4D_{(q)} \Gamma_{1h}^A p^2 q^3 q_4 - 6D_{(q)} \Gamma_{2e}^A p^2 q^3 q_4 - 4A_{(q)} \Gamma_{2h}^A p^2 q^3 q_4 + 2D_{(q)} \Gamma_{3f}^A p^2 q^3 q_4 - D_{(q)} \Gamma_{2e}^A q^5 q_4 \\
&+ D_{(q)} \Gamma_{2f}^A q^5 q_4 + D_{(q)} \Gamma_{3e}^A q^5 q_4 - D_{(q)} \Gamma_{3f}^A q^5 q_4 - p^4 q (C_{(q)} (\Gamma_{2c}^S + \Gamma_{2d}^S + \Gamma_{3c}^S + \Gamma_{3d}^S) \\
&+ D_{(q)} (\Gamma_{2e}^A + \Gamma_{2f}^A + \Gamma_{3e}^A + \Gamma_{3f}^A) q_4)) \\
&+ I_{T2k} (-2C_{(q)} \Gamma_{1a}^S p q^2 + 4B_{(q)} \Gamma_{1c}^S p q^2 + 2B_{(q)} \Gamma_{2a}^S p q^2 - 4C_{(q)} \Gamma_{1g}^S p^3 q^2 + 2C_{(q)} \Gamma_{2c}^S p^3 q^2 \\
&+ 2C_{(q)} \Gamma_{2d}^S p^3 q^2 + 2B_{(q)} \Gamma_{2g}^S p^3 q^2 + 2B_{(q)} \Gamma_{3g}^S p^3 q^2 + 2C_{(q)} \Gamma_{2c}^S p q^4 - 2C_{(q)} \Gamma_{2d}^S p q^4 + 2B_{(q)} \Gamma_{2g}^S p q^4 \\
&- 2B_{(q)} \Gamma_{3g}^S p q^4 + 2D_{(q)} \Gamma_{1b}^A p q^2 q_4 + 4A_{(q)} \Gamma_{1e}^A p q^2 q_4 - 2A_{(q)} \Gamma_{2b}^A p q^2 q_4 + 4D_{(q)} \Gamma_{1h}^A p^3 q^2 q_4 \\
&+ 2D_{(q)} \Gamma_{2e}^A p^3 q^2 q_4 + 2D_{(q)} \Gamma_{2f}^A p^3 q^2 q_4 - 2A_{(q)} \Gamma_{2h}^A p^3 q^2 q_4 - 2A_{(q)} \Gamma_{3h}^A p^3 q^2 q_4 + 2D_{(q)} \Gamma_{2e}^A p q^4 q_4 \\
&- 2D_{(q)} \Gamma_{2f}^A p q^4 q_4 - 2A_{(q)} \Gamma_{2h}^A p q^4 q_4 + 2A_{(q)} \Gamma_{3h}^A p q^4 q_4) \\
&+ I_{T3k} (4C_{(q)} \Gamma_{1g}^S p^2 q^3 - 4B_{(q)} \Gamma_{2g}^S p^2 q^3 - 4D_{(q)} \Gamma_{1h}^A p^2 q^3 q_4 + 4A_{(q)} \Gamma_{2h}^A p^2 q^3 q_4) \Big\}
\end{aligned}$$

Exteq 5: Gap equation for the propagator component  $C_{(p)} \equiv C(\mathbf{p}^2, p_0^2)$  in Coulomb gauge. The notation is explained in extended equation 3.

$$\begin{aligned}
D_{(p)} = & \frac{C_1}{p p_4} \int_0^\infty dq q^2 \int_{\mathbb{R}} dq_4 \left\{ I_{C0} (B_{(q)} \Gamma_{0c}^A p + B_{(q)} \Gamma_{0d}^A p + 2C_{(q)} \Gamma_{0g}^A p q^2 \right. \\
& - A_{(q)} \Gamma_{0e}^S p q_4 - A_{(q)} \Gamma_{0f}^S p q_4 + 2D_{(q)} \Gamma_{0h}^S p q^2 q_4) \\
& + I_{C1} (C_{(q)} \Gamma_{0a}^A q - B_{(q)} \Gamma_{0c}^A q + B_{(q)} \Gamma_{0d}^A q + D_{(q)} \Gamma_{0b}^S q q_4 + A_{(q)} \Gamma_{0e}^S q q_4 - A_{(q)} \Gamma_{0f}^S q q_4) \\
& + I_{C2} (-2C_{(q)} \Gamma_{0g}^A p q^2 - 2D_{(q)} \Gamma_{0h}^S p q^2 q_4) \\
& + I_{T0} (-B_{(q)} \Gamma_{2b}^A p - B_{(q)} \Gamma_{3b}^A p - 2C_{(q)} \Gamma_{2e}^A p q^2 + 2B_{(q)} \Gamma_{2h}^A p q^2 + 2C_{(q)} \Gamma_{3f}^A p q^2 \\
& - 2B_{(q)} \Gamma_{3h}^A p q^2 - A_{(q)} \Gamma_{2a}^S p q_4 - A_{(q)} \Gamma_{3a}^S p q_4 + 2D_{(q)} \Gamma_{2c}^S p q^2 q_4 + 2A_{(q)} \Gamma_{2g}^S p q^2 q_4 \\
& - 2D_{(q)} \Gamma_{3d}^S p q^2 q_4 - 2A_{(q)} \Gamma_{3g}^S p q^2 q_4) \\
& + I_{T1} (B_{(q)} \Gamma_{2b}^A q - B_{(q)} \Gamma_{3b}^A q + C_{(q)} \Gamma_{2f}^A p^2 q + C_{(q)} \Gamma_{3e}^A p^2 q + C_{(q)} \Gamma_{3f}^A p^2 q - C_{(q)} \Gamma_{2f}^A q^3 \\
& - C_{(q)} \Gamma_{3e}^A q^3 + C_{(q)} \Gamma_{3f}^A q^3 + C_{(q)} \Gamma_{2e}^A q (p^2 + q^2) + A_{(q)} \Gamma_{2a}^S q q_4 - A_{(q)} \Gamma_{3a}^S q q_4 \\
& - D_{(q)} \Gamma_{2d}^S p^2 q q_4 - D_{(q)} \Gamma_{3c}^S p^2 q q_4 - D_{(q)} \Gamma_{3d}^S p^2 q q_4 + D_{(q)} \Gamma_{2d}^S q^3 q_4 + D_{(q)} \Gamma_{3c}^S q^3 q_4 \\
& - D_{(q)} \Gamma_{3d}^S q^3 q_4 - D_{(q)} \Gamma_{2c}^S q (p^2 + q^2) q_4) \\
& + I_{T2} (-2B_{(q)} \Gamma_{2h}^A p q^2 + 2B_{(q)} \Gamma_{3h}^A p q^2 - 2A_{(q)} \Gamma_{2g}^S p q^2 q_4 + 2A_{(q)} \Gamma_{3g}^S p q^2 q_4) \\
& + I_{T0k} (-2B_{(q)} \Gamma_{1e}^A p^3 - 2B_{(q)} \Gamma_{1f}^A p^3 + B_{(q)} \Gamma_{2b}^A p^3 + B_{(q)} \Gamma_{3b}^A p^3 + 2C_{(q)} \Gamma_{1b}^A p q^2 - 2B_{(q)} \Gamma_{1e}^A p q^2 \\
& + 2B_{(q)} \Gamma_{1f}^A p q^2 + B_{(q)} \Gamma_{2b}^A p q^2 - B_{(q)} \Gamma_{3b}^A p q^2 - 4C_{(q)} \Gamma_{1h}^A p^3 q^2 - 2B_{(q)} \Gamma_{2h}^A p^3 q^2 \\
& + 2C_{(q)} \Gamma_{3e}^A p^3 q^2 - 2B_{(q)} \Gamma_{3h}^A p^3 q^2 - 2B_{(q)} \Gamma_{2h}^A p q^4 - 2C_{(q)} \Gamma_{3e}^A p q^4 + 2B_{(q)} \Gamma_{3h}^A p q^4 \\
& + 2C_{(q)} \Gamma_{2e}^A p q^2 (p^2 + q^2) + 2A_{(q)} \Gamma_{1c}^S p^3 q_4 + 2A_{(q)} \Gamma_{1d}^S p^3 q_4 + A_{(q)} \Gamma_{2a}^S p^3 q_4 + A_{(q)} \Gamma_{3a}^S p^3 q_4 \\
& + 2D_{(q)} \Gamma_{1a}^S p q^2 q_4 + 2A_{(q)} \Gamma_{1c}^S p q^2 q_4 - 2A_{(q)} \Gamma_{1d}^S p q^2 q_4 + A_{(q)} \Gamma_{2a}^S p q^2 q_4 - A_{(q)} \Gamma_{3a}^S p q^2 q_4 \\
& - 4D_{(q)} \Gamma_{1g}^S p^3 q^2 q_4 - 2A_{(q)} \Gamma_{2g}^S p^3 q^2 q_4 - 2D_{(q)} \Gamma_{3c}^S p^3 q^2 q_4 - 2A_{(q)} \Gamma_{3g}^S p^3 q^2 q_4 - 2A_{(q)} \Gamma_{2g}^S p q^4 q_4 \\
& + 2D_{(q)} \Gamma_{3c}^S p q^4 q_4 + 2A_{(q)} \Gamma_{3g}^S p q^4 q_4 - 2D_{(q)} \Gamma_{2c}^S p q^2 (p^2 + q^2) q_4) \\
& + I_{T1k} (-2C_{(q)} \Gamma_{1b}^A p^2 q + 6B_{(q)} \Gamma_{1e}^A p^2 q + 2B_{(q)} \Gamma_{1f}^A p^2 q - 3B_{(q)} \Gamma_{2b}^A p^2 q - B_{(q)} \Gamma_{3b}^A p^2 q - C_{(q)} \Gamma_{2f}^A p^4 q \\
& - C_{(q)} \Gamma_{3e}^A p^4 q - C_{(q)} \Gamma_{3f}^A p^4 q - 2C_{(q)} \Gamma_{1b}^A q^3 + 2B_{(q)} \Gamma_{1e}^A q^3 - 2B_{(q)} \Gamma_{1f}^A q^3 - B_{(q)} \Gamma_{2b}^A q^3 + B_{(q)} \Gamma_{3b}^A q^3 \\
& + 4C_{(q)} \Gamma_{1h}^A p^2 q^3 + 4B_{(q)} \Gamma_{2h}^A p^2 q^3 + 2C_{(q)} \Gamma_{3f}^A p^2 q^3 + C_{(q)} \Gamma_{2f}^A q^5 + C_{(q)} \Gamma_{3e}^A q^5 - C_{(q)} \Gamma_{3f}^A q^5 \\
& - C_{(q)} \Gamma_{2e}^A q (p^4 + 6p^2 q^2 + q^4) - 2D_{(q)} \Gamma_{1a}^S p^2 q q_4 - 6A_{(q)} \Gamma_{1c}^S p^2 q q_4 - 2A_{(q)} \Gamma_{1d}^S p^2 q q_4 \\
& - 3A_{(q)} \Gamma_{2a}^S p^2 q q_4 - A_{(q)} \Gamma_{3a}^S p^2 q q_4 + D_{(q)} \Gamma_{2d}^S p^4 q q_4 + D_{(q)} \Gamma_{3c}^S p^4 q q_4 + D_{(q)} \Gamma_{3d}^S p^4 q q_4 \\
& - 2D_{(q)} \Gamma_{1a}^S q^3 q_4 - 2A_{(q)} \Gamma_{1c}^S q^3 q_4 + 2A_{(q)} \Gamma_{1d}^S q^3 q_4 - A_{(q)} \Gamma_{2a}^S q^3 q_4 + A_{(q)} \Gamma_{3a}^S q^3 q_4 \\
& + 4D_{(q)} \Gamma_{1g}^S p^2 q^3 q_4 + 4A_{(q)} \Gamma_{2g}^S p^2 q^3 q_4 - 2D_{(q)} \Gamma_{3c}^S p^2 q^3 q_4 - D_{(q)} \Gamma_{2d}^S q^5 q_4 - D_{(q)} \Gamma_{3c}^S q^5 q_4 \\
& + D_{(q)} \Gamma_{3d}^S q^5 q_4 + D_{(q)} \Gamma_{2c}^S q (p^4 + 6p^2 q^2 + q^4) q_4) \\
& + I_{T2k} (2C_{(q)} \Gamma_{1b}^A p q^2 - 4B_{(q)} \Gamma_{1e}^A p q^2 + 2B_{(q)} \Gamma_{2b}^A p q^2 + 4C_{(q)} \Gamma_{1h}^A p^3 q^2 + 2C_{(q)} \Gamma_{2f}^A p^3 q^2 \\
& + 2B_{(q)} \Gamma_{2h}^A p^3 q^2 + 2B_{(q)} \Gamma_{3h}^A p^3 q^2 - 2C_{(q)} \Gamma_{2f}^A p q^4 + 2B_{(q)} \Gamma_{2h}^A p q^4 - 2B_{(q)} \Gamma_{3h}^A p q^4 \\
& + 2C_{(q)} \Gamma_{2e}^A p q^2 (p^2 + q^2) + 2D_{(q)} \Gamma_{1a}^S p q^2 q_4 + 4A_{(q)} \Gamma_{1c}^S p q^2 q_4 + 2A_{(q)} \Gamma_{2a}^S p q^2 q_4 \\
& + 4D_{(q)} \Gamma_{1g}^S p^3 q^2 q_4 - 2D_{(q)} \Gamma_{2d}^S p^3 q^2 q_4 + 2A_{(q)} \Gamma_{2g}^S p^3 q^2 q_4 + 2A_{(q)} \Gamma_{3g}^S p^3 q^2 q_4 + 2D_{(q)} \Gamma_{2d}^S p q^4 q_4 \\
& + 2A_{(q)} \Gamma_{2g}^S p q^4 q_4 - 2A_{(q)} \Gamma_{3g}^S p q^4 q_4 - 2D_{(q)} \Gamma_{2c}^S p q^2 (p^2 + q^2) q_4) \\
& + I_{T3k} (-4C_{(q)} \Gamma_{1h}^A p^2 q^3 - 4B_{(q)} \Gamma_{2h}^A p^2 q^3 - 4D_{(q)} \Gamma_{1g}^S p^2 q^3 q_4 - 4A_{(q)} \Gamma_{2g}^S p^2 q^3 q_4) \Big\}
\end{aligned}$$

Exteq 6: Gap equation for the propagator component  $D_{(p)} \equiv D(\mathbf{p}^2, p_0^2)$  in Coulomb gauge. The notation is explained in extended equation 3.

$$\begin{aligned}
A_{(p)} = & [\text{rhs of exteq 3}] + \frac{C_F}{(2\pi)^3} \frac{1}{p_4} \int_0^\infty dq q^2 \int_{\mathbb{R}} dq_4 \left\{ I_{M0} (B_{(q)} \Gamma_{0e}^S p^2 p_4 + B_{(q)} \Gamma_{0f}^S p^2 p_4 + B_{(q)} \Gamma_{1c}^S p^2 p_4 \right. \\
& + B_{(q)} \Gamma_{1d}^S p^2 p_4 + B_{(q)} \Gamma_{2a}^S p^2 p_4 + B_{(q)} \Gamma_{3a}^S p^2 p_4 - C_{(q)} \Gamma_{0b}^S p_4 q^2 + B_{(q)} \Gamma_{0e}^S p_4 q^2 - B_{(q)} \Gamma_{0f}^S p_4 q^2 \\
& - C_{(q)} \Gamma_{1a}^S p_4 q^2 + B_{(q)} \Gamma_{1c}^S p_4 q^2 - B_{(q)} \Gamma_{1d}^S p_4 q^2 + B_{(q)} \Gamma_{2a}^S p_4 q^2 - B_{(q)} \Gamma_{3a}^S p_4 q^2 + 2C_{(q)} \Gamma_{0h}^S p^2 p_4 q^2 \\
& + 2C_{(q)} \Gamma_{1g}^S p^2 p_4 q^2 + C_{(q)} \Gamma_{2c}^S p^2 p_4 q^2 - C_{(q)} \Gamma_{2d}^S p^2 p_4 q^2 + C_{(q)} \Gamma_{3c}^S p^2 p_4 q^2 - C_{(q)} \Gamma_{3d}^S p^2 p_4 q^2 \\
& + C_{(q)} \Gamma_{2c}^S p_4 q^4 - C_{(q)} \Gamma_{2d}^S p_4 q^4 - C_{(q)} \Gamma_{3c}^S p_4 q^4 + C_{(q)} \Gamma_{3d}^S p_4 q^4 - B_{(q)} \Gamma_{0e}^S p^2 q_4 - B_{(q)} \Gamma_{0f}^S p^2 q_4 \\
& - B_{(q)} \Gamma_{1c}^S p^2 q_4 - B_{(q)} \Gamma_{1d}^S p^2 q_4 - B_{(q)} \Gamma_{2a}^S p^2 q_4 - B_{(q)} \Gamma_{3a}^S p^2 q_4 + A_{(q)} \Gamma_{1e}^A p^2 p_4 q_4 \\
& + A_{(q)} \Gamma_{1f}^A p^2 p_4 q_4 - A_{(q)} \Gamma_{2b}^A p^2 p_4 q_4 - A_{(q)} \Gamma_{3b}^A p^2 p_4 q_4 + C_{(q)} \Gamma_{0b}^S q^2 q_4 - B_{(q)} \Gamma_{0e}^S q^2 q_4 \\
& + B_{(q)} \Gamma_{0f}^S q^2 q_4 + C_{(q)} \Gamma_{1a}^S q^2 q_4 - B_{(q)} \Gamma_{1c}^S q^2 q_4 + B_{(q)} \Gamma_{1d}^S q^2 q_4 - B_{(q)} \Gamma_{2a}^S q^2 q_4 + B_{(q)} \Gamma_{3a}^S q^2 q_4 \\
& - 2C_{(q)} \Gamma_{0h}^S p^2 q^2 q_4 - 2C_{(q)} \Gamma_{1g}^S p^2 q^2 q_4 - C_{(q)} \Gamma_{2c}^S p^2 q^2 q_4 + C_{(q)} \Gamma_{2d}^S p^2 q^2 q_4 - C_{(q)} \Gamma_{3c}^S p^2 q^2 q_4 \\
& + C_{(q)} \Gamma_{3d}^S p^2 q^2 q_4 + D_{(q)} \Gamma_{0a}^A p_4 q^2 q_4 + D_{(q)} \Gamma_{1b}^A p_4 q^2 q_4 + A_{(q)} \Gamma_{1e}^A p_4 q^2 q_4 - A_{(q)} \Gamma_{1f}^A p_4 q^2 q_4 \\
& - A_{(q)} \Gamma_{2b}^A p_4 q^2 q_4 + A_{(q)} \Gamma_{3b}^A p_4 q^2 q_4 - 2D_{(q)} \Gamma_{0g}^A p^2 p_4 q^2 q_4 - 2D_{(q)} \Gamma_{1h}^A p^2 p_4 q^2 q_4 \\
& + D_{(q)} \Gamma_{2e}^A p^2 p_4 q^2 q_4 - D_{(q)} \Gamma_{2f}^A p^2 p_4 q^2 q_4 + D_{(q)} \Gamma_{3e}^A p^2 p_4 q^2 q_4 - D_{(q)} \Gamma_{3f}^A p^2 p_4 q^2 q_4 \\
& - C_{(q)} \Gamma_{2c}^S q^4 q_4 + C_{(q)} \Gamma_{2d}^S q^4 q_4 + C_{(q)} \Gamma_{3c}^S q^4 q_4 - C_{(q)} \Gamma_{3d}^S q^4 q_4 + D_{(q)} \Gamma_{2e}^A p_4 q^4 q_4 - D_{(q)} \Gamma_{2f}^A p_4 q^4 q_4 \\
& - D_{(q)} \Gamma_{3e}^A p_4 q^4 q_4 + D_{(q)} \Gamma_{3f}^A p_4 q^4 q_4 + A_{(q)} \Gamma_{0d}^A p_4 (p^2 - q^2) q_4 + A_{(q)} \Gamma_{0c}^A p_4 (p^2 + q^2) q_4 \\
& - A_{(q)} \Gamma_{0c}^A p^2 q_4^2 - A_{(q)} \Gamma_{0d}^A p^2 q_4^2 - A_{(q)} \Gamma_{1e}^A p^2 q_4^2 - A_{(q)} \Gamma_{1f}^A p^2 q_4^2 + A_{(q)} \Gamma_{2b}^A p^2 q_4^2 + A_{(q)} \Gamma_{3b}^A p^2 q_4^2 \\
& - D_{(q)} \Gamma_{0a}^A q^2 q_4^2 - A_{(q)} \Gamma_{0c}^A q^2 q_4^2 + A_{(q)} \Gamma_{0d}^A q^2 q_4^2 - D_{(q)} \Gamma_{1b}^A q^2 q_4^2 - A_{(q)} \Gamma_{1e}^A q^2 q_4^2 + A_{(q)} \Gamma_{1f}^A q^2 q_4^2 \\
& + A_{(q)} \Gamma_{2b}^A q^2 q_4^2 - A_{(q)} \Gamma_{3b}^A q^2 q_4^2 + 2D_{(q)} \Gamma_{0g}^A p^2 q^2 q_4^2 + 2D_{(q)} \Gamma_{1h}^A p^2 q^2 q_4^2 - D_{(q)} \Gamma_{2e}^A p^2 q^2 q_4^2 \\
& + D_{(q)} \Gamma_{2f}^A p^2 q^2 q_4^2 - D_{(q)} \Gamma_{3e}^A p^2 q^2 q_4^2 + D_{(q)} \Gamma_{3f}^A p^2 q^2 q_4^2 - D_{(q)} \Gamma_{2e}^A q^4 q_4^2 + D_{(q)} \Gamma_{2f}^A q^4 q_4^2 \\
& + D_{(q)} \Gamma_{3e}^A q^4 q_4^2 - D_{(q)} \Gamma_{3f}^A q^4 q_4^2) \\
& + I_{M1} (C_{(q)} \Gamma_{0b}^S p p_4 q - 2B_{(q)} \Gamma_{0e}^S p p_4 q + C_{(q)} \Gamma_{1a}^S p p_4 q - 2B_{(q)} \Gamma_{1c}^S p p_4 q - 2B_{(q)} \Gamma_{2a}^S p p_4 q \\
& - C_{(q)} \Gamma_{2c}^S p^3 p_4 q - C_{(q)} \Gamma_{2d}^S p^3 p_4 q - C_{(q)} \Gamma_{3c}^S p^3 p_4 q - C_{(q)} \Gamma_{3d}^S p^3 p_4 q - 3C_{(q)} \Gamma_{2c}^S p p_4 q^3 \\
& + C_{(q)} \Gamma_{2d}^S p p_4 q^3 + C_{(q)} \Gamma_{3c}^S p p_4 q^3 + C_{(q)} \Gamma_{3d}^S p p_4 q^3 - C_{(q)} \Gamma_{0b}^S p q q_4 + 2B_{(q)} \Gamma_{0e}^S p q q_4 \\
& - C_{(q)} \Gamma_{1a}^S p q q_4 + 2B_{(q)} \Gamma_{1c}^S p q q_4 + 2B_{(q)} \Gamma_{2a}^S p q q_4 + C_{(q)} \Gamma_{2c}^S p^3 q q_4 + C_{(q)} \Gamma_{2d}^S p^3 q q_4 \\
& + C_{(q)} \Gamma_{3c}^S p^3 q q_4 + C_{(q)} \Gamma_{3d}^S p^3 q q_4 - D_{(q)} \Gamma_{0a}^A p p_4 q q_4 - 2A_{(q)} \Gamma_{0c}^A p p_4 q q_4 - D_{(q)} \Gamma_{1b}^A p p_4 q q_4 \\
& - 2A_{(q)} \Gamma_{1e}^A p p_4 q q_4 + 2A_{(q)} \Gamma_{2b}^A p p_4 q q_4 - D_{(q)} \Gamma_{2e}^A p^3 p_4 q q_4 - D_{(q)} \Gamma_{2f}^A p^3 p_4 q q_4 - D_{(q)} \Gamma_{3e}^A p^3 p_4 q q_4 \\
& - D_{(q)} \Gamma_{3f}^A p^3 p_4 q q_4 + 3C_{(q)} \Gamma_{2c}^S p q^3 q_4 - C_{(q)} \Gamma_{2d}^S p q^3 q_4 - C_{(q)} \Gamma_{3c}^S p q^3 q_4 - C_{(q)} \Gamma_{3d}^S p q^3 q_4 \\
& - 3D_{(q)} \Gamma_{2e}^A p p_4 q^3 q_4 + D_{(q)} \Gamma_{2f}^A p p_4 q^3 q_4 + D_{(q)} \Gamma_{3e}^A p p_4 q^3 q_4 + D_{(q)} \Gamma_{3f}^A p p_4 q^3 q_4 + D_{(q)} \Gamma_{0a}^A p q q_4^2 \\
& + 2A_{(q)} \Gamma_{0c}^A p q q_4^2 + D_{(q)} \Gamma_{1b}^A p q q_4^2 + 2A_{(q)} \Gamma_{1e}^A p q q_4^2 - 2A_{(q)} \Gamma_{2b}^A p q q_4^2 + D_{(q)} \Gamma_{2e}^A p^3 q q_4^2 \\
& + D_{(q)} \Gamma_{2f}^A p^3 q q_4^2 + D_{(q)} \Gamma_{3e}^A p^3 q q_4^2 + D_{(q)} \Gamma_{3f}^A p^3 q q_4^2 + 3D_{(q)} \Gamma_{2e}^A p q^3 q_4^2 - D_{(q)} \Gamma_{2f}^A p q^3 q_4^2 \\
& - D_{(q)} \Gamma_{3e}^A p q^3 q_4^2 - D_{(q)} \Gamma_{3f}^A p q^3 q_4^2) \\
& + I_{M2} (-2C_{(q)} \Gamma_{0h}^S p^2 p_4 q^2 - 2C_{(q)} \Gamma_{1g}^S p^2 p_4 q^2 + 2C_{(q)} \Gamma_{2c}^S p^2 p_4 q^2 + 2C_{(q)} \Gamma_{2d}^S p^2 p_4 q^2 \\
& + 2C_{(q)} \Gamma_{0h}^S p^2 q^2 q_4 + 2C_{(q)} \Gamma_{1g}^S p^2 q^2 q_4 - 2C_{(q)} \Gamma_{2c}^S p^2 q^2 q_4 - 2C_{(q)} \Gamma_{2d}^S p^2 q^2 q_4 + 2D_{(q)} \Gamma_{0g}^A p^2 p_4 q^2 q_4 \\
& + 2D_{(q)} \Gamma_{1h}^A p^2 p_4 q^2 q_4 + 2D_{(q)} \Gamma_{2e}^A p^2 p_4 q^2 q_4 + 2D_{(q)} \Gamma_{2f}^A p^2 p_4 q^2 q_4 - 2D_{(q)} \Gamma_{0g}^A p^2 q^2 q_4^2 \\
& - 2D_{(q)} \Gamma_{1h}^A p^2 q^2 q_4^2 - 2D_{(q)} \Gamma_{2e}^A p^2 q^2 q_4^2 - 2D_{(q)} \Gamma_{2f}^A p^2 q^2 q_4^2) \}
\end{aligned}$$

Exteq 7: Gap equation for the propagator component  $A_{(p)} \equiv A(\mathbf{p}^2, p_0^2)$  in Weyl-Landau-Coulomb interpolating gauge. The notation is explained in extended equation 3.

$$\begin{aligned}
B_{(p)} = & [\text{rhs of exteq 4}] + \frac{C_F}{(2\pi)^3} \frac{1}{p_4} \int_0^\infty dq q^2 \int_{\mathbb{R}} dq_4 \left\{ I_{M0} (B_{(q)} \Gamma_{0c}^A p^2 p_4 + B_{(q)} \Gamma_{0d}^A p^2 p_4 - B_{(q)} \Gamma_{1e}^A p^2 p_4 \right. \\
& - B_{(q)} \Gamma_{1f}^A p^2 p_4 + B_{(q)} \Gamma_{2b}^A p^2 p_4 + B_{(q)} \Gamma_{3b}^A p^2 p_4 - C_{(q)} \Gamma_{0a}^A p_4 q^2 + B_{(q)} \Gamma_{0c}^A p_4 q^2 - B_{(q)} \Gamma_{0d}^A p_4 q^2 \\
& + C_{(q)} \Gamma_{1b}^A p_4 q^2 - B_{(q)} \Gamma_{1e}^A p_4 q^2 + B_{(q)} \Gamma_{1f}^A p_4 q^2 + B_{(q)} \Gamma_{2b}^A p_4 q^2 - B_{(q)} \Gamma_{3b}^A p_4 q^2 + 2C_{(q)} \Gamma_{0g}^A p^2 p_4 q^2 \\
& - 2C_{(q)} \Gamma_{1h}^A p^2 p_4 q^2 + C_{(q)} \Gamma_{2e}^A p^2 p_4 q^2 - C_{(q)} \Gamma_{2f}^A p^2 p_4 q^2 + C_{(q)} \Gamma_{3e}^A p^2 p_4 q^2 - C_{(q)} \Gamma_{3f}^A p^2 p_4 q^2 \\
& + C_{(q)} \Gamma_{2e}^A p_4 q^4 - C_{(q)} \Gamma_{2f}^A p_4 q^4 - C_{(q)} \Gamma_{3e}^A p_4 q^4 + C_{(q)} \Gamma_{3f}^A p_4 q^4 - B_{(q)} \Gamma_{0c}^S p^2 p_4 q_4 - B_{(q)} \Gamma_{0d}^S p^2 p_4 q_4 \\
& + B_{(q)} \Gamma_{1e}^S p^2 p_4 q_4 + B_{(q)} \Gamma_{1f}^S p^2 p_4 q_4 - B_{(q)} \Gamma_{2b}^S p^2 p_4 q_4 - B_{(q)} \Gamma_{3b}^S p^2 p_4 q_4 - A_{(q)} \Gamma_{0e}^S p^2 p_4 q_4 - A_{(q)} \Gamma_{0f}^S p^2 p_4 q_4 \\
& + A_{(q)} \Gamma_{1c}^S p^2 p_4 q_4 + A_{(q)} \Gamma_{1d}^S p^2 p_4 q_4 + A_{(q)} \Gamma_{2a}^S p^2 p_4 q_4 + A_{(q)} \Gamma_{3a}^S p^2 p_4 q_4 + C_{(q)} \Gamma_{0a}^A q^2 q_4 \\
& - B_{(q)} \Gamma_{0c}^A q^2 q_4 + B_{(q)} \Gamma_{0d}^A q^2 q_4 - C_{(q)} \Gamma_{1b}^A q^2 q_4 + B_{(q)} \Gamma_{1e}^A q^2 q_4 - B_{(q)} \Gamma_{1f}^A q^2 q_4 - B_{(q)} \Gamma_{2b}^A q^2 q_4 \\
& + B_{(q)} \Gamma_{3b}^A q^2 q_4 - 2C_{(q)} \Gamma_{0g}^A p^2 q^2 q_4 + 2C_{(q)} \Gamma_{1h}^A p^2 q^2 q_4 - C_{(q)} \Gamma_{2e}^A p^2 q^2 q_4 + C_{(q)} \Gamma_{2f}^A p^2 q^2 q_4 \\
& - C_{(q)} \Gamma_{3e}^A p^2 q^2 q_4 + C_{(q)} \Gamma_{3f}^A p^2 q^2 q_4 - D_{(q)} \Gamma_{0b}^S p_4 q^2 q_4 - A_{(q)} \Gamma_{0e}^S p_4 q^2 q_4 + A_{(q)} \Gamma_{0f}^S p_4 q^2 q_4 \\
& + D_{(q)} \Gamma_{1a}^S p_4 q^2 q_4 + A_{(q)} \Gamma_{1c}^S p_4 q^2 q_4 - A_{(q)} \Gamma_{1d}^S p_4 q^2 q_4 + A_{(q)} \Gamma_{2a}^S p_4 q^2 q_4 - A_{(q)} \Gamma_{3a}^S p_4 q^2 q_4 \\
& + 2D_{(q)} \Gamma_{0h}^S p^2 p_4 q^2 q_4 - 2D_{(q)} \Gamma_{1g}^S p^2 p_4 q^2 q_4 - D_{(q)} \Gamma_{2c}^S p^2 p_4 q^2 q_4 + D_{(q)} \Gamma_{2d}^S p^2 p_4 q^2 q_4 \\
& - D_{(q)} \Gamma_{3c}^S p^2 p_4 q^2 q_4 + D_{(q)} \Gamma_{3d}^S p^2 p_4 q^2 q_4 - C_{(q)} \Gamma_{2e}^A q^4 q_4 + C_{(q)} \Gamma_{2f}^A q^4 q_4 + C_{(q)} \Gamma_{3e}^A q^4 q_4 \\
& - C_{(q)} \Gamma_{3f}^A q^4 q_4 - D_{(q)} \Gamma_{2c}^S p_4 q^4 q_4 + D_{(q)} \Gamma_{2d}^S p_4 q^4 q_4 + D_{(q)} \Gamma_{3c}^S p_4 q^4 q_4 - D_{(q)} \Gamma_{3d}^S p_4 q^4 q_4 \\
& + A_{(q)} \Gamma_{0e}^S p^2 q_4^2 + A_{(q)} \Gamma_{0f}^S p^2 q_4^2 - A_{(q)} \Gamma_{1c}^S p^2 q_4^2 - A_{(q)} \Gamma_{1d}^S p^2 q_4^2 - A_{(q)} \Gamma_{2a}^S p^2 q_4^2 - A_{(q)} \Gamma_{3a}^S p^2 q_4^2 \\
& + D_{(q)} \Gamma_{0b}^S q^2 q_4^2 + A_{(q)} \Gamma_{0e}^S q^2 q_4^2 - A_{(q)} \Gamma_{0f}^S q^2 q_4^2 - D_{(q)} \Gamma_{1a}^S q^2 q_4^2 - A_{(q)} \Gamma_{1c}^S q^2 q_4^2 + A_{(q)} \Gamma_{1d}^S q^2 q_4^2 \\
& - A_{(q)} \Gamma_{2a}^S q^2 q_4^2 + A_{(q)} \Gamma_{3a}^S q^2 q_4^2 - 2D_{(q)} \Gamma_{0h}^S p^2 q^2 q_4^2 + 2D_{(q)} \Gamma_{1g}^S p^2 q^2 q_4^2 + D_{(q)} \Gamma_{2c}^S p^2 q^2 q_4^2 \\
& - D_{(q)} \Gamma_{2d}^S p^2 q^2 q_4^2 + D_{(q)} \Gamma_{3c}^S p^2 q^2 q_4^2 - D_{(q)} \Gamma_{3d}^S p^2 q^2 q_4^2 + D_{(q)} \Gamma_{2c}^S q^4 q_4^2 - D_{(q)} \Gamma_{2d}^S q^4 q_4^2 \\
& - D_{(q)} \Gamma_{3c}^S q^4 q_4^2 + D_{(q)} \Gamma_{3d}^S q^4 q_4^2) \\
& + I_{M1} (C_{(q)} \Gamma_{0a}^A p p_4 q - 2B_{(q)} \Gamma_{0c}^A p p_4 q - C_{(q)} \Gamma_{1b}^A p p_4 q + 2B_{(q)} \Gamma_{1e}^A p p_4 q - 2B_{(q)} \Gamma_{2b}^A p p_4 q \\
& - C_{(q)} \Gamma_{2e}^A p^3 p_4 q - C_{(q)} \Gamma_{2f}^A p^3 p_4 q - C_{(q)} \Gamma_{3e}^A p^3 p_4 q - C_{(q)} \Gamma_{3f}^A p^3 p_4 q - 3C_{(q)} \Gamma_{2e}^A p p_4 q^3 \\
& + C_{(q)} \Gamma_{2f}^A p p_4 q^3 + C_{(q)} \Gamma_{3e}^A p p_4 q^3 + C_{(q)} \Gamma_{3f}^A p p_4 q^3 - C_{(q)} \Gamma_{0a}^A p q q_4 + 2B_{(q)} \Gamma_{0c}^A p q q_4 \\
& + C_{(q)} \Gamma_{1b}^A p q q_4 - 2B_{(q)} \Gamma_{1e}^A p q q_4 + 2B_{(q)} \Gamma_{2b}^A p q q_4 + C_{(q)} \Gamma_{2e}^A p^3 q q_4 + C_{(q)} \Gamma_{2f}^A p^3 q q_4 \\
& + C_{(q)} \Gamma_{3e}^A p^3 q q_4 + C_{(q)} \Gamma_{3f}^A p^3 q q_4 + D_{(q)} \Gamma_{0b}^S p p_4 q q_4 + 2A_{(q)} \Gamma_{0e}^S p p_4 q q_4 - D_{(q)} \Gamma_{1a}^S p p_4 q q_4 \\
& - 2A_{(q)} \Gamma_{1c}^S p p_4 q q_4 - 2A_{(q)} \Gamma_{2a}^S p p_4 q q_4 + D_{(q)} \Gamma_{2c}^S p^3 p_4 q q_4 + D_{(q)} \Gamma_{2d}^S p^3 p_4 q q_4 + D_{(q)} \Gamma_{3c}^S p^3 p_4 q q_4 \\
& + D_{(q)} \Gamma_{3d}^S p^3 p_4 q q_4 + 3C_{(q)} \Gamma_{2e}^A p q^3 q_4 - C_{(q)} \Gamma_{2f}^A p q^3 q_4 - C_{(q)} \Gamma_{3e}^A p q^3 q_4 - C_{(q)} \Gamma_{3f}^A p q^3 q_4 \\
& + 3D_{(q)} \Gamma_{2c}^S p p_4 q^3 q_4 - D_{(q)} \Gamma_{2d}^S p p_4 q^3 q_4 - D_{(q)} \Gamma_{3c}^S p p_4 q^3 q_4 - D_{(q)} \Gamma_{3d}^S p p_4 q^3 q_4 - D_{(q)} \Gamma_{0b}^S p q q_4^2 \\
& - 2A_{(q)} \Gamma_{0e}^S p q q_4^2 + D_{(q)} \Gamma_{1a}^S p q q_4^2 + 2A_{(q)} \Gamma_{1c}^S p q q_4^2 + 2A_{(q)} \Gamma_{2a}^S p q q_4^2 - D_{(q)} \Gamma_{2c}^S p^3 q q_4^2 \\
& - D_{(q)} \Gamma_{2d}^S p^3 q q_4^2 - D_{(q)} \Gamma_{3c}^S p^3 q q_4^2 - D_{(q)} \Gamma_{3d}^S p^3 q q_4^2 - 3D_{(q)} \Gamma_{2c}^S p q^3 q_4^2 + D_{(q)} \Gamma_{2d}^S p q^3 q_4^2 \\
& + D_{(q)} \Gamma_{3c}^S p q^3 q_4^2 + D_{(q)} \Gamma_{3d}^S p q^3 q_4^2) \\
& + I_{M2} (-2C_{(q)} \Gamma_{0g}^A p^2 p_4 q^2 + 2C_{(q)} \Gamma_{1h}^A p^2 p_4 q^2 + 2C_{(q)} \Gamma_{2e}^A p^2 p_4 q^2 + 2C_{(q)} \Gamma_{2f}^A p^2 p_4 q^2 \\
& + 2C_{(q)} \Gamma_{0g}^A p^2 q^2 q_4 - 2C_{(q)} \Gamma_{1h}^A p^2 q^2 q_4 - 2C_{(q)} \Gamma_{2e}^A p^2 q^2 q_4 - 2C_{(q)} \Gamma_{2f}^A p^2 q^2 q_4 - 2D_{(q)} \Gamma_{0h}^S p^2 p_4 q^2 q_4 \\
& + 2D_{(q)} \Gamma_{1g}^S p^2 p_4 q^2 q_4 - 2D_{(q)} \Gamma_{2c}^S p^2 p_4 q^2 q_4 - 2D_{(q)} \Gamma_{2d}^S p^2 p_4 q^2 q_4 + 2D_{(q)} \Gamma_{0h}^S p^2 q^2 q_4^2 \\
& - 2D_{(q)} \Gamma_{1g}^S p^2 q^2 q_4^2 + 2D_{(q)} \Gamma_{2c}^S p^2 q^2 q_4^2 + 2D_{(q)} \Gamma_{2d}^S p^2 q^2 q_4^2) \}
\end{aligned}$$

Exteq 8: Gap equation for the propagator component  $B_{(p)} \equiv B(\mathbf{p}^2, p_0^2)$  in Weyl-Landau-Coulomb interpolating gauge. The notation is explained in extended equation 3.

$$\begin{aligned}
C_{(p)} = & [\text{rhs of exteq 5}] + \frac{C_F}{(2\pi)^3} \frac{1}{p_4} \int_0^\infty dq q^2 \int_{\mathbb{R}} dq_4 \left\{ I_{M0} (B_{(q)} \Gamma_{0a}^A p p_4 + B_{(q)} \Gamma_{1b}^A p p_4 + B_{(q)} \Gamma_{2e}^A p^3 p_4 \right. \\
& + B_{(q)} \Gamma_{2f}^A p^3 p_4 + B_{(q)} \Gamma_{3e}^A p^3 p_4 + B_{(q)} \Gamma_{3f}^A p^3 p_4 + 2C_{(q)} \Gamma_{0c}^A p p_4 q^2 - 2B_{(q)} \Gamma_{0g}^A p p_4 q^2 \\
& - 2C_{(q)} \Gamma_{1f}^A p p_4 q^2 + 2B_{(q)} \Gamma_{1h}^A p p_4 q^2 + B_{(q)} \Gamma_{2e}^A p p_4 q^2 + B_{(q)} \Gamma_{2f}^A p p_4 q^2 - B_{(q)} \Gamma_{3e}^A p p_4 q^2 \\
& - B_{(q)} \Gamma_{3f}^A p p_4 q^2 + 2C_{(q)} \Gamma_{2h}^A p^3 p_4 q^2 + 2C_{(q)} \Gamma_{3h}^A p^3 p_4 q^2 + 2C_{(q)} \Gamma_{2h}^A p p_4 q^4 - 2C_{(q)} \Gamma_{3h}^A p p_4 q^4 \\
& - B_{(q)} \Gamma_{0a}^A p q_4 - B_{(q)} \Gamma_{1b}^A p q_4 - B_{(q)} \Gamma_{2e}^A p^3 q_4 - B_{(q)} \Gamma_{2f}^A p^3 q_4 - B_{(q)} \Gamma_{3e}^A p^3 q_4 - B_{(q)} \Gamma_{3f}^A p^3 q_4 \\
& + A_{(q)} \Gamma_{0b}^S p p_4 q_4 + A_{(q)} \Gamma_{1a}^S p p_4 q_4 - A_{(q)} \Gamma_{2c}^S p^3 p_4 q_4 - A_{(q)} \Gamma_{2d}^S p^3 p_4 q_4 - A_{(q)} \Gamma_{3c}^S p^3 p_4 q_4 \\
& - A_{(q)} \Gamma_{3d}^S p^3 p_4 q_4 - 2C_{(q)} \Gamma_{0c}^A p q^2 q_4 + 2B_{(q)} \Gamma_{0g}^A p q^2 q_4 + 2C_{(q)} \Gamma_{1f}^A p q^2 q_4 - 2B_{(q)} \Gamma_{1h}^A p q^2 q_4 \\
& - B_{(q)} \Gamma_{2e}^A p q^2 q_4 - B_{(q)} \Gamma_{2f}^A p q^2 q_4 + B_{(q)} \Gamma_{3e}^A p q^2 q_4 + B_{(q)} \Gamma_{3f}^A p q^2 q_4 - 2C_{(q)} \Gamma_{2h}^A p^3 q^2 q_4 \\
& - 2C_{(q)} \Gamma_{3h}^A p^3 q^2 q_4 - 2D_{(q)} \Gamma_{0e}^S p p_4 q^2 q_4 - 2A_{(q)} \Gamma_{0h}^S p p_4 q^2 q_4 + 2D_{(q)} \Gamma_{1d}^S p p_4 q^2 q_4 \\
& + 2A_{(q)} \Gamma_{1g}^S p p_4 q^2 q_4 - A_{(q)} \Gamma_{2c}^S p p_4 q^2 q_4 - A_{(q)} \Gamma_{2d}^S p p_4 q^2 q_4 + A_{(q)} \Gamma_{3c}^S p p_4 q^2 q_4 + A_{(q)} \Gamma_{3d}^S p p_4 q^2 q_4 \\
& + 2D_{(q)} \Gamma_{2g}^S p^3 p_4 q^2 q_4 + 2D_{(q)} \Gamma_{3g}^S p^3 p_4 q^2 q_4 - 2C_{(q)} \Gamma_{2h}^A p q^4 q_4 + 2C_{(q)} \Gamma_{3h}^A p q^4 q_4 \\
& + 2D_{(q)} \Gamma_{2g}^S p p_4 q^4 q_4 - 2D_{(q)} \Gamma_{3g}^S p p_4 q^4 q_4 - A_{(q)} \Gamma_{0b}^S p q_4^2 - A_{(q)} \Gamma_{1a}^S p q_4^2 + A_{(q)} \Gamma_{2c}^S p^3 q_4^2 \\
& + A_{(q)} \Gamma_{2d}^S p^3 q_4^2 + A_{(q)} \Gamma_{3c}^S p^3 q_4^2 + A_{(q)} \Gamma_{3d}^S p^3 q_4^2 + 2D_{(q)} \Gamma_{0e}^S p q^2 q_4^2 + 2A_{(q)} \Gamma_{0h}^S p q^2 q_4^2 \\
& - 2D_{(q)} \Gamma_{1d}^S p q^2 q_4^2 - 2A_{(q)} \Gamma_{1g}^S p q^2 q_4^2 + A_{(q)} \Gamma_{2c}^S p q^2 q_4^2 + A_{(q)} \Gamma_{2d}^S p q^2 q_4^2 - A_{(q)} \Gamma_{3c}^S p q^2 q_4^2 \\
& - A_{(q)} \Gamma_{3d}^S p q^2 q_4^2 - 2D_{(q)} \Gamma_{2g}^S p^3 q^2 q_4^2 - 2D_{(q)} \Gamma_{3g}^S p^3 q^2 q_4^2 - 2D_{(q)} \Gamma_{2g}^S p q^4 q_4^2 + 2D_{(q)} \Gamma_{3g}^S p q^4 q_4^2) \\
& + I_{M1} (-B_{(q)} \Gamma_{0a}^A p_4 q - B_{(q)} \Gamma_{1b}^A p_4 q - C_{(q)} \Gamma_{0c}^A p^2 p_4 q - C_{(q)} \Gamma_{0d}^A p^2 p_4 q - C_{(q)} \Gamma_{1e}^A p^2 p_4 q - C_{(q)} \Gamma_{1f}^A p^2 p_4 q \\
& + C_{(q)} \Gamma_{2b}^A p^2 p_4 q - 3B_{(q)} \Gamma_{2e}^A p^2 p_4 q - B_{(q)} \Gamma_{2f}^A p^2 p_4 q + C_{(q)} \Gamma_{3b}^A p^2 p_4 q - B_{(q)} \Gamma_{3e}^A p^2 p_4 q \\
& + B_{(q)} \Gamma_{3f}^A p^2 p_4 q - C_{(q)} \Gamma_{0c}^A p_4 q^3 + C_{(q)} \Gamma_{0d}^A p_4 q^3 - C_{(q)} \Gamma_{1e}^A p_4 q^3 + C_{(q)} \Gamma_{1f}^A p_4 q^3 + C_{(q)} \Gamma_{2b}^A p_4 q^3 \\
& - B_{(q)} \Gamma_{2e}^A p_4 q^3 + B_{(q)} \Gamma_{2f}^A p_4 q^3 - C_{(q)} \Gamma_{3b}^A p_4 q^3 + B_{(q)} \Gamma_{3e}^A p_4 q^3 - B_{(q)} \Gamma_{3f}^A p_4 q^3 - 4C_{(q)} \Gamma_{2h}^A p^2 p_4 q^3 \\
& + B_{(q)} \Gamma_{0a}^A q p_4 + B_{(q)} \Gamma_{1b}^A q p_4 + C_{(q)} \Gamma_{0c}^A p^2 q p_4 + C_{(q)} \Gamma_{0d}^A p^2 q p_4 + C_{(q)} \Gamma_{1e}^A p^2 q p_4 + C_{(q)} \Gamma_{1f}^A p^2 q p_4 \\
& - C_{(q)} \Gamma_{2b}^A p^2 q p_4 + 3B_{(q)} \Gamma_{2e}^A p^2 q p_4 + B_{(q)} \Gamma_{2f}^A p^2 q p_4 - C_{(q)} \Gamma_{3b}^A p^2 q p_4 + B_{(q)} \Gamma_{3e}^A p^2 q p_4 - B_{(q)} \Gamma_{3f}^A p^2 q p_4 \\
& - A_{(q)} \Gamma_{0b}^S p_4 q p_4 - A_{(q)} \Gamma_{1a}^S p_4 q p_4 + D_{(q)} \Gamma_{0e}^S p^2 p_4 q p_4 + D_{(q)} \Gamma_{0f}^S p^2 p_4 q p_4 + D_{(q)} \Gamma_{1c}^S p^2 p_4 q p_4 \\
& + D_{(q)} \Gamma_{1d}^S p^2 p_4 q p_4 + D_{(q)} \Gamma_{2a}^S p^2 p_4 q p_4 + 3A_{(q)} \Gamma_{2c}^S p^2 p_4 q p_4 + A_{(q)} \Gamma_{2d}^S p^2 p_4 q p_4 + D_{(q)} \Gamma_{3a}^S p^2 p_4 q p_4 \\
& + A_{(q)} \Gamma_{3c}^S p^2 p_4 q p_4 - A_{(q)} \Gamma_{3d}^S p^2 p_4 q p_4 + C_{(q)} \Gamma_{0c}^A q^3 p_4 - C_{(q)} \Gamma_{0d}^A q^3 p_4 + C_{(q)} \Gamma_{1e}^A q^3 p_4 - C_{(q)} \Gamma_{1f}^A q^3 p_4 \\
& - C_{(q)} \Gamma_{2b}^A q^3 p_4 + B_{(q)} \Gamma_{2e}^A q^3 p_4 - B_{(q)} \Gamma_{2f}^A q^3 p_4 + C_{(q)} \Gamma_{3b}^A q^3 p_4 - B_{(q)} \Gamma_{3e}^A q^3 p_4 + B_{(q)} \Gamma_{3f}^A q^3 p_4 \\
& + 4C_{(q)} \Gamma_{2h}^A p^2 q^3 p_4 + D_{(q)} \Gamma_{0e}^S p_4 q^3 p_4 - D_{(q)} \Gamma_{0f}^S p_4 q^3 p_4 + D_{(q)} \Gamma_{1c}^S p_4 q^3 p_4 - D_{(q)} \Gamma_{1d}^S p_4 q^3 p_4 \\
& + D_{(q)} \Gamma_{2a}^S p_4 q^3 p_4 + A_{(q)} \Gamma_{2c}^S p_4 q^3 p_4 - A_{(q)} \Gamma_{2d}^S p_4 q^3 p_4 - D_{(q)} \Gamma_{3a}^S p_4 q^3 p_4 - A_{(q)} \Gamma_{3c}^S p_4 q^3 p_4 + A_{(q)} \Gamma_{3d}^S p_4 q^3 p_4 \\
& - 4D_{(q)} \Gamma_{2g}^S p^2 p_4 q^3 p_4 + A_{(q)} \Gamma_{0b}^S p q_4^2 + A_{(q)} \Gamma_{1a}^S p q_4^2 - D_{(q)} \Gamma_{0e}^S p^2 q q_4^2 - D_{(q)} \Gamma_{0f}^S p^2 q q_4^2 - D_{(q)} \Gamma_{1c}^S p^2 q q_4^2 \\
& - D_{(q)} \Gamma_{1d}^S p^2 q q_4^2 - D_{(q)} \Gamma_{2a}^S p^2 q q_4^2 - 3A_{(q)} \Gamma_{2c}^S p^2 q q_4^2 - A_{(q)} \Gamma_{2d}^S p^2 q q_4^2 - D_{(q)} \Gamma_{3a}^S p^2 q q_4^2 - A_{(q)} \Gamma_{3c}^S p^2 q q_4^2 \\
& + A_{(q)} \Gamma_{3d}^S p^2 q q_4^2 - D_{(q)} \Gamma_{0e}^S q^3 q_4^2 + D_{(q)} \Gamma_{0f}^S q^3 q_4^2 - D_{(q)} \Gamma_{1c}^S q^3 q_4^2 + D_{(q)} \Gamma_{1d}^S q^3 q_4^2 - D_{(q)} \Gamma_{2a}^S q^3 q_4^2 \\
& - A_{(q)} \Gamma_{2c}^S q^3 q_4^2 + A_{(q)} \Gamma_{2d}^S q^3 q_4^2 + D_{(q)} \Gamma_{3a}^S q^3 q_4^2 + A_{(q)} \Gamma_{3c}^S q^3 q_4^2 - A_{(q)} \Gamma_{3d}^S q^3 q_4^2 + 4D_{(q)} \Gamma_{2g}^S p^2 q^3 q_4^2) \\
& + I_{M2} (2B_{(q)} \Gamma_{0g}^A p p_4 q^2 + 2C_{(q)} \Gamma_{1e}^A p p_4 q^2 + 2C_{(q)} \Gamma_{1f}^A p p_4 q^2 - 2B_{(q)} \Gamma_{1h}^A p p_4 q^2 - 2C_{(q)} \Gamma_{2b}^A p p_4 q^2 \\
& + 2B_{(q)} \Gamma_{2e}^A p p_4 q^2 - 2B_{(q)} \Gamma_{2f}^A p p_4 q^2 - 2C_{(q)} \Gamma_{2h}^A p^3 p_4 q^2 - 2C_{(q)} \Gamma_{3h}^A p^3 p_4 q^2 + 4C_{(q)} \Gamma_{2h}^A p^2 p_4 q^3 \\
& - 2C_{(q)} \Gamma_{2h}^A p p_4 q^4 + 2C_{(q)} \Gamma_{3h}^A p p_4 q^4 - 2B_{(q)} \Gamma_{0g}^A p q^2 q_4 - 2C_{(q)} \Gamma_{1e}^A p q^2 q_4 - 2C_{(q)} \Gamma_{1f}^A p q^2 q_4 \\
& + 2B_{(q)} \Gamma_{1h}^A p q^2 q_4 + 2C_{(q)} \Gamma_{2b}^A p q^2 q_4 - 2B_{(q)} \Gamma_{2e}^A p q^2 q_4 + 2B_{(q)} \Gamma_{2f}^A p q^2 q_4 + 2C_{(q)} \Gamma_{2h}^A p^3 q^2 q_4 \\
& + 2C_{(q)} \Gamma_{3h}^A p^3 q^2 q_4 + 2A_{(q)} \Gamma_{0h}^S p p_4 q^2 q_4 - 2D_{(q)} \Gamma_{1c}^S p p_4 q^2 q_4 - 2D_{(q)} \Gamma_{1d}^S p p_4 q^2 q_4 - 2A_{(q)} \Gamma_{1g}^S p p_4 q^2 q_4 \\
& - 2D_{(q)} \Gamma_{2a}^S p p_4 q^2 q_4 - 2A_{(q)} \Gamma_{2c}^S p p_4 q^2 q_4 + 2A_{(q)} \Gamma_{2d}^S p p_4 q^2 q_4 - 2D_{(q)} \Gamma_{2g}^S p^3 p_4 q^2 q_4 \\
& - 2D_{(q)} \Gamma_{3g}^S p^3 p_4 q^2 q_4 - 4C_{(q)} \Gamma_{2h}^A p^2 q^3 p_4 + 4D_{(q)} \Gamma_{2g}^S p^2 p_4 q^3 p_4 + 2C_{(q)} \Gamma_{2h}^A p q^4 p_4 - 2C_{(q)} \Gamma_{3h}^A p q^4 p_4 \\
& - 2D_{(q)} \Gamma_{2g}^S p p_4 q^4 p_4 + 2D_{(q)} \Gamma_{3g}^S p p_4 q^4 p_4 - 2A_{(q)} \Gamma_{0h}^S p q^2 q_4^2 + 2D_{(q)} \Gamma_{1c}^S p q^2 q_4^2 + 2D_{(q)} \Gamma_{1d}^S p q^2 q_4^2 \\
& + 2A_{(q)} \Gamma_{1g}^S p q^2 q_4^2 + 2D_{(q)} \Gamma_{2a}^S p q^2 q_4^2 + 2A_{(q)} \Gamma_{2c}^S p q^2 q_4^2 - 2A_{(q)} \Gamma_{2d}^S p q^2 q_4^2 + 2D_{(q)} \Gamma_{2g}^S p^3 q^2 q_4^2 \\
& + 2D_{(q)} \Gamma_{3g}^S p^3 q^2 q_4^2 - 4D_{(q)} \Gamma_{2g}^S p^2 q^3 q_4^2 + 2D_{(q)} \Gamma_{2g}^S p q^4 q_4^2 - 2D_{(q)} \Gamma_{3g}^S p q^4 q_4^2) \}
\end{aligned}$$

Exteq 9: Gap equation for the propagator component  $C_{(p)} \equiv C(\mathbf{p}^2, p_0^2)$  in Weyl-Landau-Coulomb interpolating gauge. The notation is explained in extended equation 3.

$$\begin{aligned}
D_{(p)} = & [\text{rhs of exteq 6}] + \frac{C_F}{(2\pi)^3} \frac{1}{p^4} \int_0^\infty dq q^2 \int_{\mathbb{R}} dq_4 \left\{ I_{M0} \left( -B_{(q)} \Gamma_{0b}^S p p_4 + B_{(q)} \Gamma_{1a}^S p p_4 - B_{(q)} \Gamma_{2c}^S p^3 p_4 \right. \right. \\
& - B_{(q)} \Gamma_{2d}^S p^3 p_4 - B_{(q)} \Gamma_{3c}^S p^3 p_4 - B_{(q)} \Gamma_{3d}^S p^3 p_4 - 2C_{(q)} \Gamma_{0e}^S p p_4 q^2 + 2B_{(q)} \Gamma_{0h}^S p p_4 q^2 - 2C_{(q)} \Gamma_{1d}^S p p_4 q^2 \\
& + 2B_{(q)} \Gamma_{1g}^S p p_4 q^2 - B_{(q)} \Gamma_{2c}^S p p_4 q^2 - B_{(q)} \Gamma_{2d}^S p p_4 q^2 + B_{(q)} \Gamma_{3c}^S p p_4 q^2 + B_{(q)} \Gamma_{3d}^S p p_4 q^2 \\
& - 2C_{(q)} \Gamma_{2g}^S p^3 p_4 q^2 - 2C_{(q)} \Gamma_{3g}^S p^3 p_4 q^2 - 2C_{(q)} \Gamma_{2g}^S p p_4 q^4 + 2C_{(q)} \Gamma_{3g}^S p p_4 q^4 + B_{(q)} \Gamma_{0b}^S p q_4 \\
& - B_{(q)} \Gamma_{1a}^S p q_4 + B_{(q)} \Gamma_{2c}^S p^3 q_4 + B_{(q)} \Gamma_{2d}^S p^3 q_4 + B_{(q)} \Gamma_{3c}^S p^3 q_4 + B_{(q)} \Gamma_{3d}^S p^3 q_4 + A_{(q)} \Gamma_{0a}^A p p_4 q_4 \\
& - A_{(q)} \Gamma_{1b}^A p p_4 q_4 - A_{(q)} \Gamma_{2e}^A p^3 p_4 q_4 - A_{(q)} \Gamma_{2f}^A p^3 p_4 q_4 - A_{(q)} \Gamma_{3e}^A p^3 p_4 q_4 - A_{(q)} \Gamma_{3f}^A p^3 p_4 q_4 \\
& + 2C_{(q)} \Gamma_{0e}^S p q^2 q_4 - 2B_{(q)} \Gamma_{0h}^S p q^2 q_4 + 2C_{(q)} \Gamma_{1d}^S p q^2 q_4 - 2B_{(q)} \Gamma_{1g}^S p q^2 q_4 + B_{(q)} \Gamma_{2c}^S p q^2 q_4 \\
& + B_{(q)} \Gamma_{2d}^S p q^2 q_4 - B_{(q)} \Gamma_{3c}^S p q^2 q_4 - B_{(q)} \Gamma_{3d}^S p q^2 q_4 + 2C_{(q)} \Gamma_{2g}^S p^3 q^2 q_4 + 2C_{(q)} \Gamma_{3g}^S p^3 q^2 q_4 \\
& - 2D_{(q)} \Gamma_{0c}^A p p_4 q^2 q_4 - 2A_{(q)} \Gamma_{0g}^A p p_4 q^2 q_4 - 2D_{(q)} \Gamma_{1f}^A p p_4 q^2 q_4 - 2A_{(q)} \Gamma_{1h}^A p p_4 q^2 q_4 - A_{(q)} \Gamma_{2e}^A p p_4 q^2 q_4 \\
& - A_{(q)} \Gamma_{2f}^A p p_4 q^2 q_4 + A_{(q)} \Gamma_{3e}^A p p_4 q^2 q_4 + A_{(q)} \Gamma_{3f}^A p p_4 q^2 q_4 + 2D_{(q)} \Gamma_{2h}^A p^3 p_4 q^2 q_4 + 2D_{(q)} \Gamma_{3h}^A p^3 p_4 q^2 q_4 \\
& + 2C_{(q)} \Gamma_{2g}^S p q^4 q_4 - 2C_{(q)} \Gamma_{3g}^S p q^4 q_4 + 2D_{(q)} \Gamma_{2h}^A p p_4 q^4 q_4 - 2D_{(q)} \Gamma_{3h}^A p p_4 q^4 q_4 - A_{(q)} \Gamma_{0a}^A p q_4^2 \\
& + A_{(q)} \Gamma_{1b}^A p q_4^2 + A_{(q)} \Gamma_{2e}^A p^3 q_4^2 + A_{(q)} \Gamma_{2f}^A p^3 q_4^2 + A_{(q)} \Gamma_{3e}^A p^3 q_4^2 + A_{(q)} \Gamma_{3f}^A p^3 q_4^2 + 2D_{(q)} \Gamma_{0c}^A p q^2 q_4^2 \\
& + 2A_{(q)} \Gamma_{0g}^A p q^2 q_4^2 + 2D_{(q)} \Gamma_{1f}^A p q^2 q_4^2 + 2A_{(q)} \Gamma_{1h}^A p q^2 q_4^2 + A_{(q)} \Gamma_{2e}^A p q^2 q_4^2 + A_{(q)} \Gamma_{2f}^A p q^2 q_4^2 \\
& - A_{(q)} \Gamma_{3e}^A p q^2 q_4^2 - A_{(q)} \Gamma_{3f}^A p q^2 q_4^2 - 2D_{(q)} \Gamma_{2h}^A p^3 q^2 q_4^2 - 2D_{(q)} \Gamma_{3h}^A p^3 q^2 q_4^2 - 2D_{(q)} \Gamma_{2h}^A p q^4 q_4^2 \\
& + 2D_{(q)} \Gamma_{3h}^A p q^4 q_4^2) \\
& + I_{M1} (B_{(q)} \Gamma_{0b}^S p_4 q - B_{(q)} \Gamma_{1a}^S p_4 q + C_{(q)} \Gamma_{0e}^S p^2 p_4 q + C_{(q)} \Gamma_{0f}^S p^2 p_4 q - C_{(q)} \Gamma_{1c}^S p^2 p_4 q - C_{(q)} \Gamma_{1d}^S p^2 p_4 q \\
& - C_{(q)} \Gamma_{2a}^S p^2 p_4 q + 3B_{(q)} \Gamma_{2c}^S p^2 p_4 q + B_{(q)} \Gamma_{2d}^S p^2 p_4 q - C_{(q)} \Gamma_{3a}^S p^2 p_4 q + B_{(q)} \Gamma_{3c}^S p^2 p_4 q \\
& - B_{(q)} \Gamma_{3d}^S p^2 p_4 q + C_{(q)} \Gamma_{0e}^S p_4 q^3 - C_{(q)} \Gamma_{0f}^S p_4 q^3 - C_{(q)} \Gamma_{1c}^S p_4 q^3 + C_{(q)} \Gamma_{1d}^S p_4 q^3 - C_{(q)} \Gamma_{2a}^S p_4 q^3 \\
& + B_{(q)} \Gamma_{2c}^S p_4 q^3 - B_{(q)} \Gamma_{2d}^S p_4 q^3 + C_{(q)} \Gamma_{3a}^S p_4 q^3 - B_{(q)} \Gamma_{3c}^S p_4 q^3 + B_{(q)} \Gamma_{3d}^S p_4 q^3 + 4C_{(q)} \Gamma_{2g}^S p^2 p_4 q^3 \\
& - B_{(q)} \Gamma_{0b}^S q q_4 + B_{(q)} \Gamma_{1a}^S q q_4 - C_{(q)} \Gamma_{0e}^S p^2 q q_4 - C_{(q)} \Gamma_{0f}^S p^2 q q_4 + C_{(q)} \Gamma_{1c}^S p^2 q q_4 + C_{(q)} \Gamma_{1d}^S p^2 q q_4 \\
& + C_{(q)} \Gamma_{2a}^S p^2 q q_4 - 3B_{(q)} \Gamma_{2c}^S p^2 q q_4 - B_{(q)} \Gamma_{2d}^S p^2 q q_4 + C_{(q)} \Gamma_{3a}^S p^2 q q_4 - B_{(q)} \Gamma_{3c}^S p^2 q q_4 \\
& + B_{(q)} \Gamma_{3d}^S p^2 q q_4 - A_{(q)} \Gamma_{0a}^A p_4 q q_4 + A_{(q)} \Gamma_{1b}^A p_4 q q_4 + D_{(q)} \Gamma_{0c}^A p^2 p_4 q q_4 + D_{(q)} \Gamma_{0d}^A p^2 p_4 q q_4 \\
& - D_{(q)} \Gamma_{1e}^A p^2 p_4 q q_4 - D_{(q)} \Gamma_{1f}^A p^2 p_4 q q_4 + D_{(q)} \Gamma_{2b}^A p^2 p_4 q q_4 + 3A_{(q)} \Gamma_{2e}^A p^2 p_4 q q_4 + A_{(q)} \Gamma_{2f}^A p^2 p_4 q q_4 \\
& + D_{(q)} \Gamma_{3b}^A p^2 p_4 q q_4 + A_{(q)} \Gamma_{3e}^A p^2 p_4 q q_4 - A_{(q)} \Gamma_{3f}^A p^2 p_4 q q_4 - C_{(q)} \Gamma_{0e}^S q^3 q_4 + C_{(q)} \Gamma_{0f}^S q^3 q_4 \\
& + C_{(q)} \Gamma_{1c}^S q^3 q_4 - C_{(q)} \Gamma_{1d}^S q^3 q_4 + C_{(q)} \Gamma_{2a}^S q^3 q_4 - B_{(q)} \Gamma_{2c}^S q^3 q_4 + B_{(q)} \Gamma_{2d}^S q^3 q_4 - C_{(q)} \Gamma_{3a}^S q^3 q_4 \\
& + B_{(q)} \Gamma_{3c}^S q^3 q_4 - B_{(q)} \Gamma_{3d}^S q^3 q_4 - 4C_{(q)} \Gamma_{2g}^S p^2 q^3 q_4 + D_{(q)} \Gamma_{0c}^A p_4 q^3 q_4 - D_{(q)} \Gamma_{0d}^A p_4 q^3 q_4 \\
& - D_{(q)} \Gamma_{1e}^A p_4 q^3 q_4 + D_{(q)} \Gamma_{1f}^A p_4 q^3 q_4 + D_{(q)} \Gamma_{2b}^A p_4 q^3 q_4 + A_{(q)} \Gamma_{2e}^A p_4 q^3 q_4 - A_{(q)} \Gamma_{2f}^A p_4 q^3 q_4 \\
& - D_{(q)} \Gamma_{3b}^A p_4 q^3 q_4 - A_{(q)} \Gamma_{3e}^A p_4 q^3 q_4 + A_{(q)} \Gamma_{3f}^A p_4 q^3 q_4 - 4D_{(q)} \Gamma_{2h}^A p^2 p_4 q^3 q_4 + A_{(q)} \Gamma_{0a}^A q q_4^2 - A_{(q)} \Gamma_{1b}^A q q_4^2 \\
& - D_{(q)} \Gamma_{0c}^A p^2 q q_4^2 - D_{(q)} \Gamma_{0d}^A p^2 q q_4^2 + D_{(q)} \Gamma_{1e}^A p^2 q q_4^2 + D_{(q)} \Gamma_{1f}^A p^2 q q_4^2 - D_{(q)} \Gamma_{2b}^A p^2 q q_4^2 - 3A_{(q)} \Gamma_{2e}^A p^2 q q_4^2 \\
& - A_{(q)} \Gamma_{2f}^A p^2 q q_4^2 - D_{(q)} \Gamma_{3b}^A p^2 q q_4^2 - A_{(q)} \Gamma_{3e}^A p^2 q q_4^2 + A_{(q)} \Gamma_{3f}^A p^2 q q_4^2 - D_{(q)} \Gamma_{0c}^A q^3 q_4^2 + D_{(q)} \Gamma_{0d}^A q^3 q_4^2 \\
& + D_{(q)} \Gamma_{1e}^A q^3 q_4^2 - D_{(q)} \Gamma_{1f}^A q^3 q_4^2 - D_{(q)} \Gamma_{2b}^A q^3 q_4^2 - A_{(q)} \Gamma_{2e}^A q^3 q_4^2 + A_{(q)} \Gamma_{2f}^A q^3 q_4^2 + D_{(q)} \Gamma_{3b}^A q^3 q_4^2 \\
& + A_{(q)} \Gamma_{3e}^A q^3 q_4^2 - A_{(q)} \Gamma_{3f}^A q^3 q_4^2 + 4D_{(q)} \Gamma_{2h}^A p^2 q^3 q_4^2) \\
& + I_{M2} (-2B_{(q)} \Gamma_{0h}^S p p_4 q^2 + 2C_{(q)} \Gamma_{1c}^S p p_4 q^2 + 2C_{(q)} \Gamma_{1d}^S p p_4 q^2 - 2B_{(q)} \Gamma_{1g}^S p p_4 q^2 + 2C_{(q)} \Gamma_{2a}^S p p_4 q^2 \\
& - 2B_{(q)} \Gamma_{2c}^S p p_4 q^2 + 2B_{(q)} \Gamma_{2d}^S p p_4 q^2 + 2C_{(q)} \Gamma_{2g}^S p^3 p_4 q^2 + 2C_{(q)} \Gamma_{3g}^S p^3 p_4 q^2 - 4C_{(q)} \Gamma_{2g}^S p^2 p_4 q^3 \\
& + 2C_{(q)} \Gamma_{2g}^S p p_4 q^4 - 2C_{(q)} \Gamma_{3g}^S p p_4 q^4 + 2B_{(q)} \Gamma_{0h}^S p q^2 q_4 - 2C_{(q)} \Gamma_{1c}^S p q^2 q_4 - 2C_{(q)} \Gamma_{1d}^S p q^2 q_4 \\
& + 2B_{(q)} \Gamma_{1g}^S p q^2 q_4 - 2C_{(q)} \Gamma_{2a}^S p q^2 q_4 + 2B_{(q)} \Gamma_{2c}^S p q^2 q_4 - 2B_{(q)} \Gamma_{2d}^S p q^2 q_4 - 2C_{(q)} \Gamma_{2g}^S p^3 q^2 q_4 \\
& - 2C_{(q)} \Gamma_{3g}^S p^3 q^2 q_4 + 2A_{(q)} \Gamma_{0g}^A p p_4 q^2 q_4 + 2D_{(q)} \Gamma_{1e}^A p p_4 q^2 q_4 + 2D_{(q)} \Gamma_{1f}^A p p_4 q^2 q_4 + 2A_{(q)} \Gamma_{1h}^A p p_4 q^2 q_4 \\
& - 2D_{(q)} \Gamma_{2b}^A p p_4 q^2 q_4 - 2A_{(q)} \Gamma_{2e}^A p p_4 q^2 q_4 + 2A_{(q)} \Gamma_{2f}^A p p_4 q^2 q_4 - 2D_{(q)} \Gamma_{2h}^A p^3 p_4 q^2 q_4 - 2D_{(q)} \Gamma_{3h}^A p^3 p_4 q^2 q_4 \\
& + 4C_{(q)} \Gamma_{2g}^S p^2 q^3 q_4 + 4D_{(q)} \Gamma_{2h}^A p^2 p_4 q^3 q_4 - 2C_{(q)} \Gamma_{2g}^S p q^4 q_4 + 2C_{(q)} \Gamma_{3g}^S p q^4 q_4 - 2D_{(q)} \Gamma_{2h}^A p p_4 q^4 q_4 \\
& + 2D_{(q)} \Gamma_{3h}^A p p_4 q^4 q_4 - 2A_{(q)} \Gamma_{0g}^A p q^2 q_4^2 - 2D_{(q)} \Gamma_{1e}^A p q^2 q_4^2 - 2D_{(q)} \Gamma_{1f}^A p q^2 q_4^2 - 2A_{(q)} \Gamma_{1h}^A p q^2 q_4^2 \\
& + 2D_{(q)} \Gamma_{2b}^A p q^2 q_4^2 + 2A_{(q)} \Gamma_{2e}^A p q^2 q_4^2 - 2A_{(q)} \Gamma_{2f}^A p q^2 q_4^2 + 2D_{(q)} \Gamma_{2h}^A p^3 q^2 q_4^2 + 2D_{(q)} \Gamma_{3h}^A p^3 q^2 q_4^2 \\
& - 4D_{(q)} \Gamma_{2h}^A p^2 q^3 q_4^2 + 2D_{(q)} \Gamma_{2h}^A p q^4 q_4^2 - 2D_{(q)} \Gamma_{3h}^A p q^4 q_4^2) \}
\end{aligned}$$

Exteq 10: Gap equation for the propagator component  $D_{(p)} \equiv D(p^2, p_0^2)$  in Weyl-Landau-Coulomb interpolating gauge. The notation is explained in extended equation 3.

## Appendix B

# Elements of Tensor Decomposition

*We know that under the image revealed there is another which is truer to reality and under this image still another and yet again still another under this last one, right down to the true image of that reality, absolute, mysterious, which no one will ever see or perhaps right down to the decomposition of any image, of any reality.*

Michelangelo Antonioni

In the previous chapters, we have already encountered complicated objects like the quark-gluon vertex,



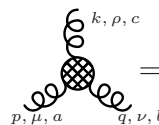
$$= \Gamma_{\alpha\beta}^{\mu,a}(p, q, k), \quad (\text{B.1})$$

which “lives” in a product space of Lorentz spacetime (index  $\mu$ ), color space (index  $a$ ) and Dirac space (spinor indices  $\alpha$  and  $\beta$ ). It is not always easy to handle such an object – especially if one has to rely on computers, which are notoriously bad in dealing with abstract spaces, but usually require all problems to be formulated either in matrix language or in terms of real scalar equations.

The problems we are dealing with tend to be strongly nonlinear, so matrices are usually not an option. Thus we now discuss, how (B.1) and others of its kind can be characterized by scalar functions. This also sets the stage for the reduction of the Dyson-Schwinger equations to a set of scalar equations. The solution of these equations for some special cases, employing tough numerics, will be discussed in chapter 4.

Here we confine ourselves to the discussion of how to disentangle the tensor components of such objects. In the present context, “tensor decomposition” actually refers to the task of organizing the Lorentz and Dirac structure of objects in a convenient way. While this may look slightly complicated for general objects, one should not forget that such “structural” problems are still easy as compared to the “dynamical” ones to be treated later.

In the following we will assume trivial color structure. This is strictly true for example the quark-gluon vertex, since the only admitted object with one color index is the set of generators  $t^a$ . For other objects the color structure could be more complicated than the one at tree-level. For example the three-gluon vertex could contain a color-antisymmetric and a color-symmetric part,



$$= \Gamma_{\mu\nu\rho}^{abc}(p, q, k) = f^{abc}\Gamma_{\mu\nu\rho}^{(A)}(p, q, k) + d^{abc}\Gamma_{\mu\nu\rho}^{(S)}(p, q, k), \quad (\text{B.2})$$

where  $\Gamma^{(A)}$  and  $\Gamma^{(S)}$  denote functions completely antisymmetric respectively symmetric in the momenta  $p$ ,  $q$  and  $k$ . However, even in this case, the color structure can be easily separated



from the rest. In addition there is good evidence that at least in this example the contribution from the color-symmetric part is negligible (and may even completely vanish).

For each Green function, momentum conservation holds, thus the number of momentum argument is reduced by one and we can use a factorization like

$$\Gamma_{\alpha\beta}^{\mu,a}(p, q, k) = t^a \delta(k + p - q) \Gamma_{\alpha\beta}^{\mu}(p, q). \quad (\text{B.3})$$

In the following, we will only discuss the decomposition of objects like  $\Gamma_{\alpha\beta}^{\mu}(p, q)$ , with results which can be applied to Abelian and non-Abelian gauge theories the same way. Thus we will often refer to the gauge bosons just as “photons”, even though at the end we will be most interested in them being gluons.

## B.1 Covariant Tensor Decomposition

To simplify matters we will discuss the question how to handle the tensor structure of general objects (usually Green functions) first in the covariant formalism. The result obtained here will also be useful in section B.3, where we extend our considerations to the case when the  $SO(3, 1)$  symmetry of spacetime is broken down to some lower symmetry group.

### B.1.1 General Considerations

In the following, we will primarily employ the fermion-photon vertex to illustrate ideas and techniques. On the one hand, we can directly transfer the results to the quark-gluon vertex (by attaching a  $t^a$  factor), on the other hand this is one of the most simple objects for which the tensor decomposition is not straightforward any more.

As it is probably well known to the reader, the bare fermion-photon vertex is given by  $\gamma^{\mu}$ . It is the task of the gamma matrices to connect the spinor structure of the attached fermions to the Lorentz vector structure of the photon. The object  $\gamma^{\mu}$  has one free Lorentz and two free Dirac indices, so the contraction with two spinors,  $\bar{\psi}\gamma^{\mu}\psi$ , transforms as a Lorentz vector.

However, the structure of the full vertex is strikingly more complicated than being just a bare  $\gamma_{\mu}$ . In general, it will depend on the particle momenta in a nontrivial way and involve more sophisticated combinations of gamma matrices.

For the fermion-photon vertex, there are two spin- $\frac{1}{2}$ -fermions involved, so in principle any element of the general Dirac matrix  $\Gamma$  (that is finally contracted with spinors to  $\bar{\psi}\Gamma\psi$ ) can appear in such an expression. Grouping these matrix elements according to their transformation properties and expressing them in terms of gamma matrices, we have

$$\begin{array}{lll} T_1 & = \mathbb{1} & T_6 & = \gamma_0\gamma_1 & T_{12} & = \gamma_1\gamma_2\gamma_3 \\ & & T_7 & = \gamma_0\gamma_2 & T_{13} & = \gamma_0\gamma_2\gamma_3 \\ T_2 & = \gamma_0 & T_8 & = \gamma_0\gamma_3 & T_{14} & = \gamma_0\gamma_1\gamma_3 \\ T_3 & = \gamma_1 & T_9 & = \gamma_1\gamma_2 & T_{15} & = \gamma_0\gamma_1\gamma_2 \\ T_4 & = \gamma_2 & T_{10} & = \gamma_1\gamma_3 & & \\ T_5 & = \gamma_3 & T_{11} & = \gamma_2\gamma_3 & T_{16} & = \gamma_0\gamma_1\gamma_2\gamma_3, \end{array}$$

We note that many of these expressions could be written in a more elegant way by employing  $\gamma_5 = \gamma_0\gamma_1\gamma_2\gamma_3$ , see for example section 3.4 in [158]. Rewriting it in this way also clearly reveals the separation into a scalar, a vector, a tensor, an axial vector and a pseudoscalar part.) So we obtain the structure

$$\Gamma^{\mu} = \sum_{k=1}^{16} A_k^{(\mu)}(p_1^0, p_1^1, p_1^2, p_1^3, p_2^0, p_2^1, p_2^2, p_2^3) T_k, \quad \mu = 0, 1, 2, 3. \quad (\text{B.4})$$

In total we need 64 functions  $A_k^{(\mu)}, \mathbb{R}^8 \rightarrow \mathbb{R}$ , to describe the structure of this vertex. These coefficient functions can be regarded as some sort of form factors, as they describe the intrinsic structure of the object under consideration.

The reader might have the impression that 64 is a quite large number for such a task, and he or she is absolutely right in this. The above reasoning, while indeed correct, does not take into account *covariance*. While the intimidating number of 64 coefficients is necessary in a theory where each dimension of space and time can be distinguished from all others (for example by the choice of gauge fixing or anisotropic background fields), in a covariant theory we can do much better than that.

As long as the system under consideration is Lorentz invariant, the objects  $\gamma$ ,  $p_1$  and  $p_2$  transform as Lorentz vectors, and due to this transformation properties, many of the functions  $A_k^{(\mu)}$  either vanish or appear only in certain combinations. More precisely, the transformation properties dictate that there is only one free Lorentz index left uncontracted. The only applicable objects with such an index are  $\gamma^\mu$ ,  $p_1^\mu$  and  $p_2^\mu$ . The scalar coefficient functions may – again due to covariance – only depend on the scalar products  $p_1 \cdot p_1$ ,  $p_2 \cdot p_2$  and  $p_1 \cdot p_2$ .

So all we have to do is to implement the rest of the Dirac structure. Any expression contained in an appropriate factor has to be a Lorentz scalar. Therefore we have to check which expressions with trivial Lorentz, but nontrivial Dirac structure we can form with the objects  $\gamma^\mu$ ,  $p_1^\mu$  and  $p_2^\mu$  at hand. These are  $\not{p}_1$ ,  $\not{p}_2$  and the product  $\not{p}_1 \not{p}_2$ .

There is also the possibility that the whole Dirac structure is carried by the Lorentz vector (i.e. it is either trivial or only  $\gamma^\mu$ ), so we also admit  $\mathbb{1}$  as a dummy in this part of the vertex structure. Combining these, we obtain the following twelve elements

$$\Gamma_i^\mu = f_i(p_1 \cdot p_1, p_2 \cdot p_2, p_1 \cdot p_2) \cdot \left\{ \begin{array}{c} \mathbb{1} \\ \not{p}_1 \\ \not{p}_2 \\ \not{p}_1 \not{p}_2 \end{array} \right\} \otimes \left\{ \begin{array}{c} \gamma^\mu \\ p_1^\mu \\ p_2^\mu \end{array} \right\}, \quad (\text{B.5})$$

and indeed, in the covariant case, the fermion-photon vertex is described by twelve components, i.e. twelve scalar functions. For example one specific term (in straightforward numbering the 10<sup>th</sup>) in this decomposition has the form

$$\begin{aligned} \Gamma_{10}^\mu &= f_{10}(p_1 \cdot p_1, p_2 \cdot p_2, p_1 \cdot p_2) && \text{Lorentz and Dirac scalar} \\ &\cdot \not{p}_1 \not{p}_2 && \text{Lorentz scalar with Dirac structure} \\ &\cdot \gamma^\mu && \text{Lorentz vector (can carry} \\ &&& \text{additional Dirac structure).} \end{aligned}$$

So instead of 64 functions  $\mathbb{R}^6 \rightarrow \mathbb{R}$ , we have merely 12 functions  $\mathbb{R}^3 \rightarrow \mathbb{R}$ , which fully describe the vertex. It should be noted that for performing actual calculations, it is usually convenient to group the elements of this naive basis in a more sophisticated way. For example, one can change from  $p_1^\mu$  and  $p_2^\mu$  to the symmetric and antisymmetric combination

$$(p_1 + p_2)^\mu \quad \text{and} \quad (p_1 - p_2)^\mu \quad (\text{B.6})$$

or use the straightforward identity

$$\gamma^\mu \gamma^\nu = \frac{1}{2} \{ \gamma^\mu, \gamma^\nu \} + \frac{1}{2} [ \gamma^\mu, \gamma^\nu ] = g^{\mu\nu} - i\sigma^{\mu\nu} \quad (\text{B.7})$$

to rewrite  $\not{p}_1 \not{p}_2$  as  $(p_1 \cdot p_2) \mathbb{1} - i\sigma^{\mu\nu} p_{1,\mu} p_{2,\nu}$ . For the fermion-photon vertex, in [25], Ball and Chiu have constructed a basis which is extremely well-suited for perturbative calculations. In many following publications, their or some slightly modified basis has been used.

### B.1.2 Extended Lorentz Structure

We know already that we can build our covariant tensors from the elements  $p_i^\mu$  and  $\gamma^\mu$ . If there are two or more free Lorentz indices, however, we also have to consider the metric tensor  $g^{\mu\nu}$ . For example, the tensor basis of the three-gluon vertex  $\Gamma^{\mu\nu\rho}$  consists (after stripping off color factors) of the following 14 elements:

$$\begin{aligned} p_1^\mu p_1^\nu p_1^\rho, & \quad p_1^\mu p_1^\nu p_2^\rho, \quad p_1^\mu p_2^\nu p_1^\rho, \quad p_1^\mu p_2^\nu p_2^\rho, \quad p_1^\mu g^{\nu\rho}, \quad p_1^\nu g^{\mu\rho}, \quad p_1^\rho g^{\mu\nu}, \\ p_2^\mu p_1^\nu p_1^\rho, & \quad p_2^\mu p_1^\nu p_2^\rho, \quad p_2^\mu p_2^\nu p_1^\rho, \quad p_2^\mu p_2^\nu p_2^\rho, \quad p_2^\mu g^{\nu\rho}, \quad p_2^\nu g^{\mu\rho}, \quad p_2^\rho g^{\mu\nu}, \end{aligned}$$

in contrast to  $4^3 = 64$  elements in four dimensions in straightforward decomposition. In  $D$  or more dimensions, also the Levi-Civita-tensor  $\varepsilon^{\mu_1 \dots \mu_D}$  may come into play (depending on whether there are any constraints on parity).

These additional tensors have to be taken into account when constructing a basis. For an object with trivial Dirac structure and  $m$  Lorentz indices we can construct  $N_p^m$  tensors out of  $N_p$  vectors without using the metric or Levi-Civita tensor. In general, if there are  $\nu_1$  indices left to be taken by momenta, there are  $N_p^{\nu_1}$  possibilities for that.

When we employ one metric tensor, we use up two indices, which can be selected in  $\binom{m}{2}$  ways. The remaining indices have to be taken by momenta, which is possible in  $N_p^{m-2}$  ways. For two metric tensors, we have  $\binom{m}{4}$  combinations of indices, which can be distributed in 3 distinguishable ways

$$g^{\mu\nu} g^{\rho\sigma}, \quad g^{\mu\rho} g^{\nu\sigma}, \quad g^{\mu\sigma} g^{\nu\rho},$$

and  $N_p^{m-4}$  momenta combinations. In general,  $\nu_2$  metric tensors take  $2\nu_2$  indices, which can be chosen in  $\binom{m}{2\nu_2}$  combinations. These indices can now be distributed in

$$(2\nu_2 - 1)!! = (2\nu_2 - 1)(2\nu_2 - 3) \dots 3 \cdot 1 \quad (\text{B.8})$$

distinguishable ways<sup>1</sup>, where we define as usual  $(-1)!! = 1$ . The remaining momenta can appear in  $N_p^{m-2k}$  combinations, and we end up with

$$\sum_{\nu_2=0}^{\lfloor \frac{m}{2} \rfloor} (2\nu_2 - 1)!! \binom{m}{2\nu_2} N_p^{m-2\nu_2} \quad (\text{B.9})$$

tensors in total, where  $\lfloor \dots \rfloor$  denotes the Gauß brackets, i.e. rounding down toward minus infinity.

There remains the possibility that there are  $\nu_3$  Levi-Civita-Tensors present, which take  $\nu_3 D$  indices in total. They can be chosen in  $\binom{m}{\nu_3 D}$  ways, and they have to be distributed in  $\nu_3$  groups of  $D$  members each, so there are

$$\binom{\nu_3 D}{\{D, \dots, D\}} = \frac{(\nu_3 D)!}{(D!)^{\nu_3}} \quad (\text{B.10})$$

possibilities to do so. Since the Levi-Civita tensors are undistinguishable, one has to divide by the number of possible arrangements, which happens to be  $\nu_3!$ . Thus we end up with

$$\binom{m}{\nu_3 D} \frac{(\nu_3 D)!}{(D!)^{\nu_3}} \frac{1}{\nu_3!} = \frac{m!}{\nu_3! (D!)^{\nu_3} (m - \nu_3 D)!} \quad (\text{B.11})$$

---

<sup>1</sup>The easiest way to see this is to choose one index, say  $\mu_1$  and attach it to the first metric tensor,  $g^{\mu_1 \nu_1}$ . The second position can now be taken by any of the remaining  $(2\nu_2 - 1)$  indices. After this has been done, there are  $\nu_2 - 2$  indices remaining, which we have to distribute among the remaining  $\nu_2 - 1$  metric tensors. Induction now yields that there are  $(2\nu_2 - 1)!!$  combinations in total. Even though the initial choice of  $\mu_1$  was arbitrary, this way of distributing indices still covers all possibilities, since  $\mu_1$  has to be attached to one metric tensor somewhere and the tensors are symmetric and identical.

combinations in total. For the general case (still with trivial Dirac structure) we have to combine the results we have found so far. If the  $m$  indices are distributed among  $\nu_1$  momenta,  $\nu_2$  metric tensors and  $\nu_3$  Levi-Civita tensors, one finds

$$N_p^{\nu_1} (2\nu_2 - 1)!! \binom{m}{2\nu_2} \frac{m!}{\nu_3! (D!)^{\nu_3} (m - \nu_3 D)!} \quad (\text{B.12})$$

components. To get the total number, one has to sum over all combinations of  $\nu_i \in \mathbb{N}_0$ , which satisfy the constraint  $\nu_1 + 2\nu_2 + D\nu_3 = m$ .

### B.1.3 Inclusion of Fermions

In subsection B.1.2 we have assumed trivial Dirac structure. The presence of spinors means considerable complication, in particular if there is more than one spinor pair present. We will denote the number of spinor pairs by  $n$ . Writing Dirac indices explicitly  $(\alpha_i, \beta_j)$ , contraction of an object  $\Gamma$  with spinors gives

$$\bar{\psi}_{\alpha_1}^{(1)} \dots \bar{\psi}_{\alpha_n}^{(n)} \Gamma_{\alpha_1 \dots \alpha_n \beta_1 \dots \beta_n} \psi_{\beta_1}^{(1)} \dots \psi_{\beta_n}^{(n)}. \quad (\text{B.13})$$

The Dirac structure of such an object is – in principle – encoded in a rank- $2n$  tensor that has  $D_\gamma^{2n}$  entries, where the gamma matrices are of dimension  $D_\gamma \times D_\gamma$ .

This is already the best we can do in the straightforward approach – if the spinor pairs all belong to different spin lines, i.e. if there are no identical particles involved. For undistinguishable particles, however, we know that exchange just gives an additional sign.

To simplify matters we examine only “half” of the tensor, for definiteness only the indices  $\alpha_1$  to  $\alpha_n$ . A rank- $n$  tensor in  $D_\gamma$  dimensions which is antisymmetric under exchange of  $m_1$  indices only has

$$\frac{D_\gamma^{n-m_1}}{m_1!} \prod_{r=0}^{m_1-1} (D_\gamma - r)$$

independent components<sup>2</sup>. In the general case, we collect the indices in sets of  $m_J$ ,  $J = 1, \dots, n_{\text{sp}}$  with

$$m_1 + m_2 + \dots + m_{n_{\text{sp}}} = n, \quad (\text{B.14})$$

where the tensor is antisymmetric with respect to exchange of indices which belong to the same set. Such a tensor has

$$\prod_{J=1}^{n_{\text{sp}}} \frac{1}{m_J!} \prod_{r=0}^{m_J-1} (D_\gamma - r) \quad (\text{B.15})$$

independent components. For any object that can be sensibly defined in a vacuum theory (e.g. Green functions, which are *vacuum* expectation values), the structure of incoming and outgoing fermions (or incoming fermions and antifermions) has to be the same. So the inclusion of the remaining “half” of the tensors, i.e. the indices  $\beta_1$  to  $\beta_n$  just gives us a square on our previous result. The whole structure found so far appears for each of the  $D^m$  components of the Lorentz tensor, so with  $n_{\text{sp}}$  different spinor particles, we end up with

$$N_{\text{tens}} = \left( \prod_{J=1}^{n_{\text{sp}}} \frac{1}{m_J!} \prod_{r=0}^{m_J-1} (D_\gamma - r) \right)^2 D^m \quad (\text{B.16})$$

<sup>2</sup>For an indexed object  $T_{\alpha_1 \dots \alpha_{m_1} \alpha_{m_1+1} \dots \alpha_n}$  in  $D_\gamma$  dimensions which is antisymmetric under exchange of the indices  $\alpha_1$  to  $\alpha_{m_1}$ , one can choose  $\alpha_1$  freely among the numbers 1 to  $D_\gamma$ . For  $\alpha_2$  the number chosen for  $\alpha_1$  is not available any more, so there are only  $(D_\gamma - 1)$  possibilities left, for  $\alpha_3$  there are only  $(D_\gamma - 2)$  and so on.

To find the number of independent components, we only count the combinations that are in canonical order  $\alpha_1 < \alpha_2 < \dots < \alpha_{m_1}$ . For each such combination, there exist  $(m_1! - 1)$  others which contain the same indices, but are not canonically ordered. Thus we have to divide  $D_\gamma(D_\gamma - 1) \dots (D_\gamma - m_1 + 1)$  by  $m_1!$ . The remaining indices  $\alpha_{m_1+1}$  to  $\alpha_n$  are not constrained by symmetry and thus give  $D_\gamma^{n-m_1}$  combinations, which have to be multiplied by the result obtained before.

elements in the direct decomposition. (The case of all spinors being different is still covered by the choice  $m_1 = m_2 = \dots = m_n = 1$ .)

Let us now see how much better covariant tensor decomposition can do. Again we separate the full object into a scalar coefficient function, a Lorentz scalar with Dirac structure and a Lorentz tensor with possible additional Dirac structure.

For the Lorentz tensor, we can use all momenta, but in addition there are also  $n_{\text{sp}}$  gamma vectors  $\gamma_i^\mu$ ,  $i = 1, \dots, n_{\text{sp}}$ , which connect to different Dirac spaces. Thus we have to substitute  $N_p \rightarrow N_p + n_{\text{sp}}$  in (B.12). These Lorentz tensors have to be multiplied by all possible Lorentz scalars that we can form – and here things start to become slightly involved.

For each of the spin lines, we can form all combinations  $\mathbb{1}, \not{p}_1, \dots$  which we already know from our example, the fermion-photon vertex. This gives  $(2^{N_p})^{n_{\text{sp}}}$  possibilities in total. However, there are other possibilities to form Lorentz scalars as well. For example  $\gamma_1 \cdot \gamma_2$  is perfectly valid and independent of everything we have found so far, since those objects on different spin lines and thus do not know of each other's Dirac structure. In general, we can couple each spin line to each other, but each combination can appear at most one time, since otherwise one could use the relation  $\not{p} \not{p} = p^2$  as well in this case, reducing the product  $(\gamma_1 \cdot \gamma_2)(\gamma_1 \cdot \gamma_2)$  to a multiple of unity in both Dirac spaces.

So we can select any number of elements from the set

$$\{\gamma_1 \cdot \gamma_2, \gamma_1 \cdot \gamma_3, \dots, \gamma_{n-1} \cdot \gamma_n\} \quad (\text{B.17})$$

which contains  $\frac{n_{\text{sp}}(n_{\text{sp}}-1)}{2}$  elements, thus in total we have  $2^{n_{\text{sp}}(n_{\text{sp}}-1)/2}$  possibilities of coupling spin lines. So we end up with

$$N_{\text{L-scal}} = 2^{n_{\text{sp}} N_p} 2^{n_{\text{sp}}(n_{\text{sp}}-1)/2} \quad (\text{B.18})$$

Lorentz scalars that may carry relevant Dirac structure.

#### B.1.4 The Number of Covariant Tensors

Now all that is left is to put everything together – and, in addition allow an arbitrary number of (pseudo)scalar legs being attached to the Green function. Scalar or pseudoscalar particles (ghosts, pions in an effective theory, ...) do not give rise to additional Lorentz or Dirac structure, but of course they may increase the total number of independent momenta, a number which we will denote by  $N_p$ .

Usually we will have  $N_p \geq m + 2n - 1$ , but sometimes one is also interested in collinear setups. In these cases, typically many elements of the initial tensor basis collapse into one single element of a significantly smaller basis. Combining the results of the previous subsections, we obtain:

The general covariant tensor decomposition of an object with  $N_p$  independent momenta,  $m$  external gauge bosons and  $n$  external spinor pairs (with  $n_{\text{sp}}$  spin lines), consists of

$$N_{\text{basis}} = 2^{n_{\text{sp}} \left( N_p + \frac{n_{\text{sp}}-1}{2} \right)} \sum_{\nu_1 + 2\nu_2 + D\nu_3 = m} (N_p + n_{\text{sp}})^{\nu_1} \cdot (2\nu_2 - 1)!! \binom{m}{2\nu_2} \frac{m!}{\nu_3! (D!)^{\nu_3} (m - \nu_3 D)!}$$

basis elements.

This is to be seen in contrast to

$$N_{\text{basis}} = \left( \prod_{J=1}^{n_{\text{sp}}} \frac{1}{m_J!} \prod_{r=0}^{m_J-1} (D_\gamma - r) \right)^2 D^m$$

elements for direct decomposition. Note in particular that for  $\nu_i = 0$  the corresponding factor

$$N_p^{\nu_1}, \quad (2\nu_2 - 1)!! \binom{m}{2\nu_2} \quad \text{or} \quad \frac{m!}{\nu_3! (D!)^{\nu_3} (m - \nu_3 D)!}$$

is equal to one, so for  $m = 0$  the whole sum (which represents the combinations due to Lorentz structure) is equal to one.

So let us apply this result to a few practically relevant cases:

- For the four-gluon vertex ( $N_p = 3$ ,  $m = 4$ ,  $n = n_{\text{sp}} = 0$ ) in  $D = 4$  dimensions we have the possibilities

$$\begin{aligned} &\{\nu_1 = 4, \nu_2 = \nu_3 = 0\}, \quad \{\nu_1 = 2, \nu_2 = 1, \nu_3 = 0\}, \\ &\{\nu_1 = 0, \nu_2 = 2, \nu_3 = 0\}, \quad \{\nu_1 = \nu_2 = 0, \nu_3 = 1\}. \end{aligned}$$

and thus find

$$\begin{aligned} N_{4g} = 2^0 &\left\{ 3^4 (-1)!! \binom{4}{0} \frac{4!}{0! (4!)^0 4!} + 3^2 1!! \binom{4}{2} \frac{4!}{0! (4!)^0 4!} + 3^0 3!! \binom{4}{4} \frac{4!}{0! (4!)^0 4!} \right. \\ &\left. + 3^0 (-1)!! \binom{4}{0} \frac{4!}{1! (4!)^1 (4-4)!} \right\} = 3^4 + 3^2 \binom{4}{2} + 3 + \frac{4!}{4!} = 139 \end{aligned}$$

tensor components.

- For the four-quark-scattering kernel ( $N_p = 3$ ,  $m = 0$ ,  $n = 2$ ) we find for identical quarks ( $n_{\text{sp}} = 1$ ,  $m_1 = 2$ )

$$N_{4q}^{(\text{id})} = 2^3 \cdot 1 = 8,$$

components, for distinguishable quarks ( $n_{\text{sp}} = 2$ ,  $m_1 = m_2 = 1$ )

$$N_{4q}^{(-\text{id})} = 2^{2(3+\frac{1}{2})} \cdot 1 = 128,$$

components.

- A Greens function with two quark and three gluon legs appears for example in the Dyson-Schwinger equation for the quark-gluon vertex. For such an object ( $N_p = 4$ ,  $m = 3$ ,  $n = n_{\text{sp}} = m_1 = 1$ ) we have to consider the combinations

$$\{\nu_1 = 3, \nu_2 = \nu_3 = 0\}, \quad \{\nu_1 = 1, \nu_2 = 1, \nu_3 = 0\},$$

which leads to

$$N_{2q3g} = 2^4 \left\{ (4+1)^3 + (4+1) \cdot 1!! \cdot \binom{3}{2} \right\} = 2240$$

covariant tensor structures.

We should note here this formula often overestimate the number of tensors actually needed. This is due to the fact that – depending on remnants of gauge symmetry – there may be further restrictions that reduce the number of independent tensors. The fermion-photon vertex, as our main example, consists of 12 tensors, but when using clever linear combinations, four of them are in fact completely fixed by the Ward-Takahashi identity (which is a remnant of gauge symmetry). Only eight independent tensors remain, thus eight scalar functions are sufficient to describe the vertex. The basis of Ball and Chiu [25] already takes into account this fact.

In addition we have assumed that all vector particles are gauge bosons of the same type. One could generalize the result to the case of different vector particles (in order to describe combined QCD-QED vertex functions, to include vector mesons in an effective theory, ...), but of course the resulting formula would look more cumbersome than the result given here.

## B.2 Limits of Tensor Decomposition

Tensor decomposition can reduce both the number of scalar coefficients and the number of variables they depend on (i.e. the dimension of their domain of definition). In general we are willing to accept even a higher number of functions if, for exchange, they depend on a lower number of variables – and we do so for good reasons.

When performing numerical computations, coefficient functions are usually represented on a grid.<sup>3</sup> The number of grid points depends exponentially on the dimension of the region that is sampled here. Usually operations (like iteration steps when solving integral equations) have to be performed for every grid point separately, and they often involve integration over the whole grid as well. So each additional dimension means a tremendous complication of the whole problem.

Additional tensor components, on the other hand, give – depending on the type of calculation – additional terms to evaluate or additional equations to solve. In this case, the rise of effort is only polynomial, in many cases it may even be (approximately) linear. So with  $N_T$  scalar functions  $\mathbb{R}^{N_D} \rightarrow \mathbb{R}$ , the computational cost is roughly proportional to  $N_T C^{N_D}$  with  $C$  being almost a constant. (For large values of  $N_D$ , the use of Monte-Carlo integration may slightly improve the situation.) With this estimate at hand, we can now examine in which cases the use of covariant tensor decomposition is advantageous and in which cases it is inferior to the direct approach.

We consider again with the fermion-photon vertex, but with some (pseudo-)scalar legs attached to it. In the straightforward approach, in  $D$ -dimensional spacetime, the scalar coefficient functions have  $D N_p$  arguments. In the covariant form, we have to use the scalar products of all momenta, which are

$$1 + 2 + \dots + N_p = \frac{N_p(N_p + 1)}{2} \quad (\text{B.19})$$

in total. Regarding the number of arguments as the characteristic measure for the usability of a certain method, the covariant formalism loses when  $\frac{1}{2} N_p(N_p + 1) > D N_p$ , i.e. when

$$N_p > 2D - 1. \quad (\text{B.20})$$

In four dimensions, this means that for more than seven independent momenta, the straightforward approach defeats the apparently more sophisticated covariant one. It is clear that covariant tensor decomposition gets better, the higher the dimensionality of the system is.

When we examine the number of scalar coefficient functions, the situation is even worse for the tensor decomposition. For  $n = n_{\text{sp}} = 1$  and  $m = 1$  we obtain

$$2^{N_p} (N_p + 1)$$

tensors, while for the direct decomposition, we have  $D^3$  coefficient functions. For  $D = 4$ , the inequality

$$2^{N_p} (N_p + 1) > D^3$$

is already fulfilled for  $N_p = 4$ , which gives  $80 > 64$  tensors. As we have previously discussed, the number of tensors is usually only secondary for questions of usability and performance. In the case  $D = 4$ ,  $N_p = 7$ , where straightforward and covariant method are tied with respect to the complexity of the scalar functions, we have 1024 covariant tensors versus 64 basis elements.

So the straightforward method can be expected to be roughly a factor 16 faster. The covariant method, however, may still give expressions that are more easily evaluated for example in perturbative calculations.

---

<sup>3</sup>Even if the representation is done in other ways, for example via expansion in a set of basis functions, still the dimensional arguments presented in this section apply.



## B.3 Non-Covariant Tensor Decomposition

Can we translate the tensor decomposition procedure also to the case where Lorentz symmetry is broken down to some lower symmetry? This is indeed possible, but of course the method is less efficient than in the covariant case.

### B.3.1 The Fermion-Photon Vertex with Broken Lorentz Invariance

As an illustrative example, we again study the fermion-photon vertex in four dimensions and examine cases, where some, but not all of the Lorentz symmetry is lost. (When all symmetry is gone, we are back at the case of straightforward decomposition.) In general we can note that we have to find all possible Dirac structures that are compatible with what is left of spacetime symmetry.

#### The Case $3 + 1$

As a first (and in our case most important) example, we study the situation when one direction is distinguished from all the others, a case denoted in the following by  $3 + 1$ . In gauge theories, this happens for example in the Coulomb gauge  $\nabla \cdot \mathbf{A} = 0$  or the Weyl gauge  $A_0 = 0$ .

For definiteness (and since we are particularly interested in the Coulomb gauge) we separate the 0-component from the rest. While

$$\gamma = \begin{pmatrix} \gamma^1 \\ \gamma^2 \\ \gamma^3 \end{pmatrix}, \quad \mathbf{p}_1 = \begin{pmatrix} p_1^1 \\ p_1^2 \\ p_1^3 \end{pmatrix} \quad \text{and} \quad \mathbf{p}_2 = \begin{pmatrix} p_2^1 \\ p_2^2 \\ p_2^3 \end{pmatrix}$$

still transform as 3-vectors (assuming here and in the following that all gamma matrices are properly contracted with spinors), i.e. under the three-dimensional rotation group  $SO(3)$ , the objects  $\gamma^0$ ,  $p_1^0$  and  $p_2^0$  feel no restriction of this type. (See later for a discussion of time reversal.) Also  $\Gamma^i$  with  $i \in \{1, 2, 3\}$  still has to transform as a Lorentz vector (assuming contraction with spinors), so we know the form

$$\Gamma^i = \sum_{\nu} f_{\nu}(\mathbf{p}_1^2, \mathbf{p}_2^2, \mathbf{p}_1 \cdot \mathbf{p}_2, p_1^0, p_2^0) \cdot \left( \begin{array}{l} \text{Lorentz scalar that} \\ \text{can carry some of} \\ \text{the Dirac structure} \end{array} \right) \otimes \left\{ \begin{array}{c} \gamma^i \\ p_1^i \\ p_2^i \end{array} \right\},$$

with  $\mathbf{p}_1^2$  used as a shorthand notation for  $\mathbf{p}_1 \cdot \mathbf{p}_1$ . On the other hand,  $\Gamma^0$  is a Lorentz scalar, so it has the simpler structure

$$\Gamma^0 = \sum_{\nu} g_{\nu}(\mathbf{p}_1^2, \mathbf{p}_2^2, \mathbf{p}_1 \cdot \mathbf{p}_2, p_1^0, p_2^0) \cdot \left( \begin{array}{l} \text{Lorentz scalar that carries} \\ \text{the whole Dirac structure} \end{array} \right).$$

Lorentz scalars that we can use for the “Dirac structure part” are  $\gamma_0$ ,  $\not{\mathbf{p}}_1 := p_1^i \gamma_i$  and  $\not{\mathbf{p}}_2 := p_2^i \gamma_i$  as well as any of their (in Dirac sense) nontrivial products and of course the trivial structure  $\mathbb{1}$ . We do not have to consider  $p_1^0$  and  $p_2^0$ , since they can always be absorbed in the scalar coefficient functions  $g_{\nu}$  (again, as we will discuss soon, under a caveat regarding time reversal symmetry).

Thus the “spatial part” of the vertex has 24 components,

$$\Gamma^i = \sum_{\nu} f_{\nu}(\mathbf{p}_1^2, \mathbf{p}_2^2, \mathbf{p}_1 \cdot \mathbf{p}_2, p_1^0, p_2^0) \cdot \left\{ \begin{array}{c} \mathbb{1} \\ \not{\mathbf{p}}_1 \\ \not{\mathbf{p}}_2 \\ \not{\mathbf{p}}_1 \not{\mathbf{p}}_2 \end{array} \right\} \otimes \left\{ \begin{array}{c} \mathbb{1} \\ \gamma^0 \end{array} \right\} \otimes \left\{ \begin{array}{c} \gamma^i \\ p_1^i \\ p_2^i \end{array} \right\}, \quad (\text{B.21})$$

while the “temporal” has 8,

$$\Gamma^0 = \sum_{\nu} g_{\nu}(\mathbf{p}_1^2, \mathbf{p}_2^2, \mathbf{p}_1 \cdot \mathbf{p}_2, p_1^0, p_2^0) \cdot \left\{ \begin{array}{c} \mathbb{1} \\ \mathbf{p}_1 \\ \mathbf{p}_2 \\ \mathbf{p}_1 \mathbf{p}_2 \end{array} \right\} \otimes \left\{ \begin{array}{c} \mathbb{1} \\ \gamma^0 \end{array} \right\}, \quad (\text{B.22})$$

which sum up to 32 components. This seems to be fine, since we had expected significantly more than 12 and significantly less than 64 tensor components.

There are two remarks which should be made at this point:

- The objects  $\gamma^0$  and  $p_i^0$  are not as independent as one may expect at first glance. Since most objects we study should respect time reversal invariance, each  $\gamma^0$  has to be accompanied by one  $p_i^0$ . More general, in each product the number of quantities that carry a 0-index has to be even. So for each scalar coefficient function we know whether it has to be symmetric or antisymmetric in the combination of all  $p_i^0$ .

These symmetry properties cannot be directly implemented in the definition of the vertex functions, since there is no general way to determine, for example, whether  $p_1^0$  or  $p_2^0$  carries the relevant symmetry properties.  $(p_1^0)^2$  is as symmetric with respect to time reversal as  $(p_1^0)^2$  or  $p_1^0 p_2^0$ . An antisymmetric vertex function of two momenta  $p_1$  and  $p_2$  could, for example, have the form

$$\begin{aligned} \Gamma^A(p_1, p_2) &= p_1^0 \Theta((p_1^0)^2 - (p_2^0)^2) f((p_1^0)^2, (p_2^0)^2) \\ &\quad + p_2^0 \Theta((p_2^0)^2 - (p_1^0)^2) g(p_1^0 p_2^0) \end{aligned} \quad (\text{B.23})$$

with arbitrary functions  $f, \mathbb{R}_{\geq 0}^2 \rightarrow \mathbb{R}$  and  $g, \mathbb{R} \rightarrow \mathbb{R}$ . For such an antisymmetric case, one could directly separate terms proportional to  $p_1^0$  and terms proportional to  $p_2^0$ , but this would increase the number of tensor components, and one would still have to keep in mind the symmetry of the coefficient functions.

For symmetric functions one could eliminate the symmetry constraint by admitting all products  $p_i^0 p_j^0$  as arguments of the coefficient functions. Unfortunately, this both significantly increases the number of arguments and introduces an unwanted degree of arbitrariness in the functional representation. When introducing the notation  $x = (p_1^0)^2$ ,  $y = (p_2^0)^2$  and  $z = p_1^0 p_2^0$ , one finds for example  $x^2 y^2 = x y z^2 = z^4$ .

- We note that there is another way, which, at first glance, could be expected to yield a basis for the tensor decomposition, namely the simple splitting of the full covariant expression. In the (3+1)-case, for example, one might expect that splitting expression (B.5) in temporal and spatial part should yield a basis for the non-covariant case 3 + 1 as well.

Doing this explicitly, we obtain (using a metric with  $g_{00} = g^{00} = 1$ ) the result given in table B.1. There we have

$$3 \cdot 2 + 6 \cdot 4 + 3 \cdot 8 = 54 \text{ expressions,}$$

but we see that not all of them are independent. Some terms even appear twice; they can be dismissed without second thoughts. Since we can (with the caveats regarding symmetry mentioned above) absorb any power of  $p_1^0$  and  $p_2^0$  in the scalar coefficient function, the new basis element  $\mathbb{1}$  can account for  $p_1^0, p_2^0, (p_1^0)^2 p_2^0$  and  $p_1^0 (p_2^0)^2$ . The same way we can absorb for example  $\mathbf{p}_1 \gamma^0 p_1^0 p_2^0$  and  $\mathbf{p}_1 \gamma^0 (p_2^0)^2$  into  $\mathbf{p}_1 \gamma^0$ .

$$\begin{aligned}
\gamma^\mu &\rightarrow \gamma^0, \gamma^i \\
p_1^\mu &\rightarrow p_1^0, p_1^i \\
p_2^\mu &\rightarrow p_2^0, p_2^i \\
\not{p}_1 \gamma^\mu &\rightarrow \not{p}_1 \gamma^0, p_1^0, \not{p}_1 \gamma^i, p_1^0 \gamma^0 \gamma^i \\
\not{p}_1 p_1^\mu &\rightarrow \not{p}_1 p_1^0, (p_1^0)^2 \gamma^0, \not{p}_1 p_1^i, p_1^0 \gamma^0 p_1^i \\
\not{p}_1 p_2^\mu &\rightarrow \not{p}_1 p_2^0, p_1^0 p_2^0 \gamma^0, \not{p}_1 p_2^i, p_1^0 \gamma^0 p_2^i \\
\not{p}_2 \gamma^\mu &\rightarrow \not{p}_2 \gamma^0, p_2^0, \not{p}_2 \gamma^i, p_2^0 \gamma^0 \gamma^i \\
\not{p}_2 p_1^\mu &\rightarrow \not{p}_2 p_1^0, p_1^0 p_2^0 \gamma^0, \not{p}_2 p_1^i, p_2^0 \gamma^0 p_1^i \\
\not{p}_2 p_2^\mu &\rightarrow \not{p}_2 p_2^0, (p_2^0)^2 \gamma^0, \not{p}_2 p_2^i, p_2^0 \gamma^0 p_2^i \\
\not{p}_1 \not{p}_2 \gamma^\mu &\rightarrow \not{p}_1 \not{p}_2 \gamma^0, \not{p}_1 p_2^0, \not{p}_2 p_1^0, p_1^0 p_2^0 \gamma^0, \\
&\quad \not{p}_1 \not{p}_2 \gamma^i, \not{p}_1 p_2^0 \gamma^0 \gamma^i, \not{p}_2 p_1^0 \gamma^0 \gamma^i, p_1^0 p_2^0 \gamma^i \\
\not{p}_1 \not{p}_2 p_1^\mu &\rightarrow \not{p}_1 \not{p}_2 p_1^0, \not{p}_1 \gamma^0 p_1^0 p_2^0, \not{p}_2 \gamma^0 (p_1^0)^2, (p_1^0)^2 p_2^0, \\
&\quad \not{p}_1 \not{p}_2 p_1^i, \not{p}_1 p_2^0 \gamma^0 p_1^i, \not{p}_2 p_1^0 \gamma^0 p_1^i, p_1^0 p_2^0 p_1^i \\
\not{p}_2 \not{p}_2 p_2^\mu &\rightarrow \not{p}_1 \not{p}_2 p_2^0, \not{p}_1 \gamma^0 (p_2^0)^2, \not{p}_2 \gamma^0 p_1^0 p_2^0, p_1^0 (p_2^0)^2, \\
&\quad \not{p}_1 \not{p}_2 p_2^i, \not{p}_1 p_2^0 \gamma^0 p_2^i, \not{p}_2 p_1^0 \gamma^0 p_2^i, p_1^0 p_2^0 p_2^i
\end{aligned}$$

Table B.1: Splitting the initial covariant tensor decomposition according to the  $SO(3)$  symmetry left in the  $3 + 1$  case.

Exploiting these reductions, we end up with the following basis elements:

$$\begin{aligned}
\Gamma^0 : & \quad \mathbb{1}, \gamma^0, \not{p}_1, \not{p}_2, \not{p}_1 \gamma^0, \not{p}_2 \gamma^0, \not{p}_1 \not{p}_2, \not{p}_1 \not{p}_2 \gamma^0 \\
\Gamma^i : & \quad \gamma^i, \gamma^0 \gamma^i, p_1^i, p_2^i, \gamma^0 p_1^i, \gamma^0 p_2^i, \not{p}_1 \gamma^i, \not{p}_2 \gamma^i, \\
& \quad \not{p}_1 p_1^i, \not{p}_1 p_2^i, \not{p}_2 p_1^i, \not{p}_2 p_2^i, \not{p}_1 \gamma^0 \gamma^i, \not{p}_2 \gamma^0 \gamma^i, \\
& \quad \not{p}_1 \gamma^0 p_1^i, \not{p}_1 \gamma^0 p_2^i, \not{p}_2 \gamma^0 p_1^i, \not{p}_2 \gamma^0 p_2^i, \not{p}_1 \not{p}_2 \gamma^i, \\
& \quad \not{p}_1 \not{p}_2 p_1^i, \not{p}_1 \not{p}_2 p_2^i
\end{aligned}$$

These are in total, however, only 29, not 32 elements. The components  $\not{p}_1 \not{p}_2 \gamma^0 \gamma^i$ ,  $\not{p}_1 \not{p}_2 \gamma^0 p_1^i$  and  $\not{p}_1 \not{p}_2 \gamma^0 p_2^i$  have not been created in the splitting procedure.

So just splitting the covariant expression does not give all Dirac structures that are compatible with the reduced symmetry of the non-covariant system, und thus this method is not valid for the generation of the non-covariant tensor decomposition.

### The Case $2 + 2$

What happens when we change the symmetry by effectively breaking each four-vector  $p = (p^0, p^1, p^2, p^3)^\top$  in two independent two-vectors? We set  $\bar{p} = (p^0, p^3)^\top$  and  $\underline{p} = (p^1, p^2)^\top$ ; in addition we stipulate that overlined indices ( $\bar{i}, \bar{j}, \dots$ ) can only take the values 0 and 3, while underlined indices ( $\underline{i}, \underline{j}, \dots$ ) can only take the values 1 and 2.

In this situation, which we will denote by  $2 + 2$ , Lorentz scalars relevant for Dirac structure are now given by  $\bar{p}_1, \bar{p}_2, \underline{p}_1, \underline{p}_2$ , their products and again the trivial structure  $\mathbb{1}$ . So we have

$$\begin{aligned}
\Gamma^{\bar{i}} &= \sum_\nu f_\nu \left( \begin{matrix} \bar{p}_1^2, \bar{p}_2^2, \bar{p}_1 \cdot \bar{p}_2 \\ \underline{p}_1^2, \underline{p}_2^2, \underline{p}_1 \cdot \underline{p}_2 \end{matrix} \right) \cdot \left\{ \begin{matrix} \mathbb{1} \\ \bar{p}_1 \\ \bar{p}_2 \\ \bar{p}_1 \bar{p}_2 \end{matrix} \right\} \otimes \left\{ \begin{matrix} \mathbb{1} \\ \underline{p}_1 \\ \underline{p}_2 \\ \underline{p}_1 \underline{p}_2 \end{matrix} \right\} \otimes \left\{ \begin{matrix} \gamma^{\bar{i}} \\ p_1^{\bar{i}} \\ p_2^{\bar{i}} \end{matrix} \right\} \\
\Gamma^{\underline{i}} &= \sum_\nu f_\nu \left( \begin{matrix} \bar{p}_1^2, \bar{p}_2^2, \bar{p}_1 \cdot \bar{p}_2 \\ \underline{p}_1^2, \underline{p}_2^2, \underline{p}_1 \cdot \underline{p}_2 \end{matrix} \right) \cdot \left\{ \begin{matrix} \mathbb{1} \\ \bar{p}_1 \\ \bar{p}_2 \\ \bar{p}_1 \bar{p}_2 \end{matrix} \right\} \otimes \left\{ \begin{matrix} \mathbb{1} \\ \underline{p}_1 \\ \underline{p}_2 \\ \underline{p}_1 \underline{p}_2 \end{matrix} \right\} \otimes \left\{ \begin{matrix} \gamma^{\underline{i}} \\ p_1^{\underline{i}} \\ p_2^{\underline{i}} \end{matrix} \right\}
\end{aligned}$$

Counting all these possibilities, we end up with  $2 \cdot 4 \cdot 4 \cdot 3 = 96$  tensor structures. This is significantly more than in the straightforward approach with no symmetry considered at all. So surely, we must have acted stupid somewhere on our way!

Well, perhaps not that stupid after all. Our scalar coefficient functions depend on six variables rather than on eight as in the general case. As already discussed, for this advantage, we can easily afford to pay the price of some additional tensor components.

Nevertheless, one can rightfully ask the question, where these many components actually come from, especially why there are *more* than in the case without symmetry.

There are two reasons for this.

- First, we note that an expression like  $\vec{p}_1 \vec{p}_2 \gamma^\tau$  contains a product of three gamma matrices, which can be chosen only from the set  $\{\gamma^0, \gamma^3\}$ . Therefore, using the Dirac algebra, it could be reduced to terms that only contain one gamma matrix,

$$\begin{aligned} \vec{p}_1 \vec{p}_2 \gamma^\tau &= (p_{1,0}\gamma^0 + p_{1,3}\gamma^3) (p_{2,0}\gamma^0 + p_{2,3}\gamma^3) \begin{pmatrix} \gamma^0 \\ \gamma^3 \end{pmatrix} \\ &= \begin{pmatrix} (p_{1,0}p_{2,0} - p_{1,3}p_{2,3})\gamma^0 + (p_{1,3}p_{2,0} - p_{1,0}p_{2,3})\gamma^3 \\ (p_{1,3}p_{2,0} - p_{1,0}p_{2,3})\gamma^0 + (p_{1,0}p_{2,0} - p_{1,3}p_{2,3})\gamma^3 \end{pmatrix} \end{aligned}$$

Including such the element  $\vec{p}_1 \vec{p}_2 \gamma^\tau$  is, however, still necessary in our approach, since the cross products  $(p_{1,0}p_{2,0} - p_{1,3}p_{2,3})$  and  $(p_{1,3}p_{2,0} - p_{1,0}p_{2,3})$  can't be built from the scalars  $\vec{p}_1 \cdot \vec{p}_1$ ,  $\vec{p}_1 \cdot \vec{p}_2$  and so forth. So while producing redundancy in Dirac space, such elements allow to reduce the number of arguments of the scalar coefficients.

- The basis is overcomplete not only in Dirac, but also in Lorentz space. The alert reader might have noted that we have used for example  $\bar{\psi}\gamma^\tau\psi$ ,  $p_1^\tau$  and  $p_2^\tau$  as basis of  $\mathbb{R}^2$  (later adding Dirac structure as good as we could).

In a two-dimensional vector space, however, there can be not more than two linearly independent vectors. So the basis  $((\bar{\psi}\gamma^\tau\psi, p_1^\tau, p_2^\tau))$  is *overcomplete*, producing several terms that – in Lorentz space – could be expressed by linear combinations of other basis elements.

We can justify this fact the same way we have already done for Dirac space. The redundancy in Lorentz space is again necessary to accomodate scalar functions with less than eight arguments.

### The Case $2 + 1 + 1$

For a systematic study of broken Lorentz invariance in four dimensions, there is one case left to check:  $2 + 1 + 1$  with one set of two-vectors  $\vec{p} = (p_1, p_2)^\top$ , and two independent sets of scalars. Here we use the symbols  $\iota, j$  for two-vector indices. Lorentz scalars with Dirac structure are given by  $\vec{p}_1, \vec{p}_2, \gamma_0, \gamma_3$ , their nontrivial products and the Dirac unit  $\mathbb{1}$ .

$$\begin{aligned} \Gamma^\iota &= \sum_\nu f_\nu \left( \begin{matrix} \vec{p}_1^\iota, \vec{p}_2^\iota, \vec{p}_1 \cdot \vec{p}_2, \\ p_1^0, p_1^3, p_2^0, p_2^3 \end{matrix} \right) \cdot \left\{ \begin{matrix} \mathbb{1} \\ \vec{p}_1 \\ \vec{p}_2 \\ \vec{p}_1 \vec{p}_2 \end{matrix} \right\} \otimes \left\{ \begin{matrix} \mathbb{1} \\ \gamma_0 \end{matrix} \right\} \otimes \left\{ \begin{matrix} \mathbb{1} \\ \gamma_3 \end{matrix} \right\} \otimes \left\{ \begin{matrix} \gamma^\iota \\ p_1^\iota \\ p_2^\iota \end{matrix} \right\}, \\ \left\{ \begin{matrix} \Gamma^0 \\ \Gamma^3 \end{matrix} \right\} &= \sum_\nu g_\nu \left( \begin{matrix} \vec{p}_1^\iota, \vec{p}_2^\iota, \vec{p}_1 \cdot \vec{p}_2, \\ p_1^0, p_1^3, p_2^0, p_2^3 \end{matrix} \right) \cdot \left\{ \begin{matrix} \mathbb{1} \\ \vec{p}_1 \\ \vec{p}_2 \\ \vec{p}_1 \vec{p}_2 \end{matrix} \right\} \otimes \left\{ \begin{matrix} \mathbb{1} \\ \gamma_0 \end{matrix} \right\} \otimes \left\{ \begin{matrix} \mathbb{1} \\ \gamma_3 \end{matrix} \right\}. \end{aligned}$$

There are  $16 \cdot 3 + 2 \cdot 16 = 80$  tensors, again significantly more than in the straightforward approach. The scalar coefficients, however, depend on seven rather than eight variables, so, as discussed in section B.2, in most cases it will still be advantageous to exploit the symmetry and work in this basis.

### B.3.2 The Number of Non-Covariant Tensors

After we have examined in detail a specific example, we face a more general question: How can we translate the result of subsection B.1.4 to the non-covariant case, where the initial Lorentz symmetry is broken down to a product of special orthogonal groups  $SO(N)$  respectively  $SO(N-1, 1)$ ? To be definite, we stipulate that the symmetry of  $\mathbb{R}^D$  is broken down to independent symmetries acting in  $n_V$  subspaces of dimension  $D_i \geq 2$ ,  $i = 1, \dots, n_V$ , while  $n_S$  one-dimensional subspaces are left behind.

In this setup we obtain

$$N_{\text{L-scal}, V} = \left[ 2^{n_{\text{sp}}} \left( N_p + \frac{n_{\text{sp}}-1}{2} \right) \right]^{n_V} \quad (\text{B.24})$$

Lorentz scalars from the “vector subspaces”. From the “scalar subspaces” we have  $n_S n_{\text{sp}}$  gamma matrices

$$\gamma_k^{ij}, \quad j = 1, \dots, n_S, \quad k = 1, \dots, n_{\text{sp}},$$

and each of them can either be employed or not, which gives  $2^{n_S n_{\text{sp}}}$  combinations in total.

This result for the Lorentz scalars has to be combined with the In addition, we have to count the possible Lorentz index distributions. There are  $m$  Lorentz indices, each of which can be chosen from  $n_V + n_S$  possibilities. In total, there are  $m^{n_V + n_S}$  combinations, which are distributed according to the multinomial coefficients

$$\binom{m}{\{k_1, \dots, k_{n_V}, \ell_1, \dots, \ell_{n_S}\}} = \frac{m!}{k_1! \dots k_{n_V}! \ell_1! \dots \ell_{n_S}!}.$$

Here  $k_i \in \mathbb{N}_0$  denotes the number of indices distributed to the  $i^{\text{th}}$  ( $2+$ )-dimensional subspace, while  $\ell_j \in \mathbb{N}_0$  is the similar number for the  $j^{\text{th}}$  one-dimensional subspace.

While those indices attributed to “scalar” values create no additional structure (except possible symmetry constraints on the coefficient functions), a “vector” value which is taken by  $k_i$  indices creates (according to our result for the covariant case)

$$\sum_{\nu_1 + 2\nu_2 + D\nu_3 = k_i} (N_p + n_{\text{sp}})^{\nu_1} (2\nu_2 - 1)!! \binom{k_i}{2\nu_2} \frac{m!}{\nu_3! (D_i!)^{\nu_3} (m - \nu_3 D_i)!} \quad (\text{B.25})$$

terms. In total we obtain:

The general decomposition of an object with  $N_p$  independent momenta,  $m$  free Lorentz indices and  $n$  spinor pairs (with  $n_{\text{sp}}$  different spin lines), when the symmetry of  $\mathbb{R}^D$  is broken down to those acting in  $n_S$  subspaces of dimension one and  $n_V$  of dimension  $D_i \geq 2$ , is given by

$$N_{\text{nc}} = 2^{n_{\text{sp}}} \left\{ n_V \left( N_p + \frac{n_{\text{sp}}-1}{2} \right) + n_S \right\} \cdot \sum'_{k_i, \ell_j} \binom{m}{\{k_1, \dots, k_{n_V}, \ell_1, \dots, \ell_{n_S}\}}$$

$$\prod_{i=1}^{n_V} \sum_{\nu_1 + 2\nu_2 + D\nu_3 = k_i} (N_p + n_{\text{sp}})^{\nu_1} (2\nu_2 - 1)!! \binom{k_i}{2\nu_2} \frac{m!}{\nu_3! (D_i!)^{\nu_3} (m - \nu_3 D_i)!}.$$

basis elements, where the prime indicates the condition  $k_1 + \dots + k_{n_V} + \ell_1 + \dots + \ell_{n_S} = m$  with  $k_i \in \mathbb{N}_0$  and  $\ell_j \in \mathbb{N}_0$ .

The scalar coefficient functions depend in this case on

$$n_S N_p + n_V \frac{N_p (N_p + 1)}{2}$$

arguments, again to be compared to  $DN_p$  in the case of straightforward decomposition. For  $n_S \neq 0$  typically there are symmetry constraints on the coefficient functions.

Again, we apply this formula to some practically relevant examples; where we focus on the case  $n_V = n_S = 1$ , relevant for the Coulomb gauge.

- For the quark propagator  $N_p = n = n_{\text{sp}} = 1$ ,  $m = 0$  we find

$$N_{\text{prop}} = 2^{1\{1(1+0)+1\}} = 4$$

components.

- For the quark-gluon vertex ( $N_p = 2$ ,  $n = n_{\text{sp}} = 1$ ,  $m = 1$ ) we have only to consider  $\nu_1 = 1$  (in the case  $k_1 = 1$ ,  $\ell_1 = 0$ ) and recover

$$N_{\text{qglvert}} = 2^{1\{1 \cdot (2+0)+1\}} \cdot \left\{ \binom{1}{\{1, 0\}} (2+1) + \binom{1}{\{0, 1\}} \cdot 1 \right\} = 32. \quad (\text{B.26})$$

- The quark-ghost scattering kernel appears in the Slavnov-Taylor identity for the quark-gluon vertex. This object has two quark and two ghost legs, with  $N_p = 3$ ,  $n = n_{\text{sp}} = 1$ ,  $m = 0$  we obtain

$$N_{\text{qc}} = 2^{1\{1 \cdot (3+0)+1\}} = 16$$

components.

- For the gluon propagator we have  $N_p = 1$ ,  $n = n_{\text{sp}} = 0$ ,  $m = 2$  and thus we have to consider the combinations  $\{k_1 = 0, \ell_1 = 2\}$ ,  $\{k_1 = \ell_1 = 1\}$  (which gives  $\{\nu_1 = 1, \nu_2 = \nu_3 = 0\}$ ) and  $\{k_2 = 2, \ell_1 = 0\}$  (which contains  $\{\nu_1 = 2, \nu_2 = \nu_3 = 0\}$  and  $\{\nu_1 = 0, \nu_2 = 1, \nu_3 = 0\}$ ). Combining these, we obtain

$$N_{\text{gg}} = 2^0 \cdot \left\{ \binom{2}{\{0, 2\}} + \binom{2}{\{1, 1\}} (1+0)^1 + \binom{2}{\{2, 0\}} [(1+0)^2 + (1+0)^0 1!!] \right\} = 5$$

For Coulomb gauge, this number is too large, since due to the transversality condition the five basis elements  $k_0 k_0$ ,  $k_i k_0$ ,  $k_0 k_j$ ,  $k_i k_j$  and  $\delta_{ij}$  are not independent. The coefficients of the mixed elements  $k_i k_0$  and  $k_0 k_j$  vanish, while the purely spatial parts are combined to the transverse projector

$$\hat{P}_{ij} = \delta_{ij} - \frac{k_i k_j}{\mathbf{k}^2}.$$

For a detailed discussion of this propagator, see chapters 3 and 4.

So while the final formula may look cumbersome, it is still useful to get a general overview over the maximum number of tensor components. The combinatorics involved are pretty straightforward and could be implemented with ease in a small program.

The numbers yielded by the formula are in general only upper bounds since further symmetries and identities will typically further restrict the number of (independent) components. In practice however for higher Green functions those identities are so difficult to implement, so that one will often have to use all components to describe an object.

# Appendix C

## Bits and Pieces

In this appendix we collect several notes and results. This includes a very short guide to the NDIM method in sec. C.1, a discussion of the Fourier transform of rising potentials in sec. C.2, some thoughts on asymptotic expansions in several variables in sec. C.3 and in sec. C.4 a more detailed exposition of calculations done in chapter 5.

### C.1 The Negative Dimensional Integration Method

Dimensional regularization [193, 36] which is by now treated in most textbooks on quantum field theory is an important tool to regularize quantum field theories. When one is working in  $D + \varepsilon$  or  $D - \varepsilon$  instead of  $D \in \mathbb{N}$  dimensions, certain integrals become convergent, and the renormalization process can be controlled by the limit  $\varepsilon \rightarrow 0$ .

This procedure has been extended to *negative dimensions* in order to obtain a *computational tool* in 1987 [101, 73], a technique picked up and further extended by Suzuki, Schmidt [183, 185, 184, 190, 186, 188, 187] and others [14]. It has been used in the context of asymptotic power-law integrals for example in [106] and subsequent pieces of work.

Basically one employs a Feynman-Schwinger-like parameterization of the propagators (see also section 2 of [33]),

$$\frac{1}{p^2 + i\varepsilon} = \int_0^\infty d\alpha e^{-\alpha(p^2 + i\varepsilon)}, \quad (\text{C.1})$$

and can, when continuing to negative dimensions, combine Gaussian integration, and the expansion of the remaining exponential with the multinomial expansion

$$(\alpha_1 + \alpha_2 + \dots + \alpha_N)^\nu = \sum_{n_1 + \dots + n_N = \nu} \frac{\Gamma(1 + \nu)}{n_1! n_2! \dots n_N!} \alpha_1^{n_1} \alpha_2^{n_2} \dots \alpha_N^{n_N}. \quad (\text{C.2})$$

Since in this procedure one typically finds  $\nu = -k - \frac{D}{2}$  with  $k \in \mathbb{N}_0$  and  $D$  as the number of dimensions, this expansion is only well-defined for appropriate values  $D \in -2\mathbb{N}_0 = \{0, -2, -4, -6, \dots\}$ .

The expression obtained this way can be compared with a direct expansion of the initial exponential. This yields a typically underdetermined system of linear equations. Depending on which indices are chosen as independent variables and which one as those to be solved for, one obtains different series, which are representations of hypergeometric functions, to be discussed in sec. C.1.1.

Those functions can be analytically continued back to positive values for the dimension  $D$ . Depending on how many propagators enter the game, there can be a vast number of hypergeometric series which might or might not be degenerate. All different series have to be taken into account in order to obtain the full solution of the original problem. The procedure is depicted graphically in figure C.1.



### C.1.1 Hypergeometric Functions

Hypergeometric functions which naturally arise in NDIM as well as other methods to evaluate loop integrals are a very general class of functions which contain also many elementary functions as special cases. To have a compact notation at hand, we first define the *Pochhammer symbols*

$$(a|n) \equiv (a)_n := \frac{\Gamma(a+n)}{\Gamma(a)}. \quad (\text{C.3})$$

They are well-defined for  $a \notin \mathbb{Z}_0^-$ , but even for  $a \in \mathbb{Z}_0^-$  and  $a+n \in \mathbb{Z}_0^-$  (i.e. for  $n$  being an sufficiently small integer) the poles “cancel”, i.e. one can consistently extend the definition of the symbol to include these cases. The identity

$$\frac{1}{(1-a|k)} = (-1)^k (a|-k) \quad (\text{C.4})$$

is particularly useful in order to perform analytic continuation of functions that include Pochhammer symbols, in particular hypergeometric functions.

The general hypergeometric function of one variable are defined as

$${}_mF_n \left( \begin{matrix} a_1, \dots, a_m \\ b_1, \dots, b_n \end{matrix} \middle| z \right) \equiv {}_mF_n(a_1, \dots, a_m; b_1, \dots, b_n; z) = \sum_{k=0}^{\infty} \frac{(a_1|k) \dots (a_m|k)}{k! (b_1|k) \dots (b_n|k)} z^k. \quad (\text{C.5})$$

Since the Pochhammer symbols behave asymptotically similar to factorials, each Pochhammer symbol in the numerator renders the series “less convergent”, each symbol in the denominator “more convergent”. Taking into account the factorial in the denominator one easily finds that such a series converges for all  $z \in \mathbb{C}$  if  $m \leq n$  and diverges for all  $z \neq 0$  if  $m > n+1$ . The most interesting case is thus  $m = n+1$  where one typically has a limited region of convergence (depending also on the parameters) and thus sometimes applications require to perform analytic continuation.

A particular well-known example is *Gauß’ hypergeometric series*

$${}_2F_1 \left( \begin{matrix} a, b \\ c \end{matrix} \middle| z \right) = \sum_{k=0}^{\infty} \frac{(a|k) (b|k)}{k! (c|k)} z^k. \quad (\text{C.6})$$

This series has radius of convergence  $R = 1$ , for  $|z| < 1$  it is absolutely convergent. On the circle  $|z| = 1$  the convergence depends on the coefficients  $a$ ,  $b$  and  $c$ . For  $z = 1$  it converges if  $\Re(c-a-b) > 0$  and one obtains

$${}_2F_1 \left( \begin{matrix} a, b \\ c \end{matrix} \middle| 1 \right) = \frac{\Gamma(c) \Gamma(c-a-b)}{\Gamma(c-a) \Gamma(c-b)}. \quad (\text{C.7})$$

Many elementary functions can be interpreted as special hypergeometric functions, e.g.

$$(1+z)^n = {}_2F_1 \left( \begin{matrix} -n, 1 \\ 1 \end{matrix} \middle| -z \right), \quad (\text{C.8})$$

$$\sqrt{1-z^2} = {}_2F_1 \left( \begin{matrix} \frac{1}{2}, -\frac{1}{2} \\ \frac{3}{2} \end{matrix} \middle| z^2 \right), \quad (\text{C.9})$$

$$\log(1+z) = z \cdot {}_2F_1 \left( \begin{matrix} 1, 1 \\ 2 \end{matrix} \middle| -z \right). \quad (\text{C.10})$$

The expansion of hypergeometric functions around integer and half-integer parameters is derived and discussed in [114, 116, 115, 107]. For the relationship between Feynman diagrams and hypergeometric functions see [113].

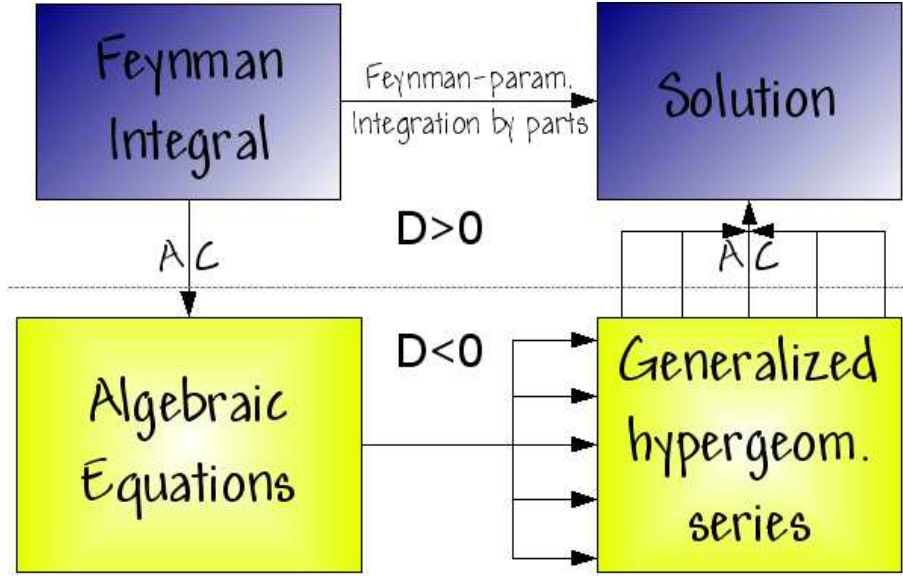


Figure C.1: Graphical illustration of the NDIM procedure, where AC denotes analytic continuation. The dotted line separates the region of  $D > 0$  (upper half) from  $D < 0$  (lower half).

### C.1.2 Application to Coulomb Gauge Problems

NDIM is a method which might be suitable to obtain approximations for Coulomb gauge vertex functions, at least in the context of split dimensional regularization as outlined in [189]. At one-loop level, all integrals that appear in the quark-gluon vertex can be derived from two “master integrals”

$$I_{\text{abelian}} = \int \frac{d^3q \, dq_0 \, (\mathbf{p} \cdot \mathbf{q})^{i_1} (\mathbf{p}' \cdot \mathbf{q})^{i_2} q_0^{i_3}}{(q^2)^{k_1} (q^2)^{k_2} ((q-p)^2 + m^2)^{k_3} ((q-p')^2 + m^2)^{k_4}} \quad (\text{C.11})$$

$$I_{\text{nonab.}} = \int \frac{d^3q \, dq_0 \, (\mathbf{p} \cdot \mathbf{q})^{i_1} (\mathbf{p}' \cdot \mathbf{q})^{i_2} (q^2)^{i_3} q_0^{i_4}}{(q^2 + m^2)^{k_1} ((\mathbf{q} - \mathbf{p})^2)^{k_2} ((\mathbf{q} - \mathbf{p}')^2)^{k_3} ((q-p)^2)^{k_4} ((q-p')^2)^{k_5}} \quad (\text{C.12})$$

In principle these integrals are accessible with NDIM, in practice severe problems arise. The first intimidating aspect is the sheer number of index combinations that have to be checked in order to obtain the full solution of the problem. For  $I_{\text{abelian}}$

$$\binom{25}{16} = 2042975$$

solutions have to be checked, and the number is even larger for  $I_{\text{nonab.}}$ . The vast majority does not contribute, remaining solutions tend to be highly degenerate, but still the calculations constitute a major effort.

Apparently the only feasible way to perform this task is to be to develop a specialized *expert system* which can automatically perform all steps which have to be repeated for each potential solution. This in turn requires to have high-performance *symbolic computation* power at hand.

Standard Computer algebra systems like Mathematica or Maple are presumably too slow for such tasks. Form [199] is very efficient, but lacks some capabilities which are required to build an expert system as sketched above. The most promising approach seems to be the use of a symbolic library like Ginac, <http://www.ginac.de/> (which has been developed as a library for C++ and is available via an interface also in Python) and to combine the full power of a general programming language with fast symbolic computation.

## C.2 Fourier Transform of Rising Potentials

As already mentioned in section 1.3.1 the Fourier transform of the linearly rising potential is plagued with conceptual and technical difficulties since neither the linearly rising function nor the  $\frac{1}{k^4}$ -potential belong to  $\mathcal{L}^1$ , the space of Lebesgue-integrable functions.

Thus an appropriate regularization procedure is necessary to define the Fourier-transform of such a linearly rising potential. In order to have a more general result at hand, we study the potential  $V(\mathbf{x}) = |\mathbf{x}|^{1+\alpha}$ , though most times we are only interested in the case  $\alpha = 0$ . For the Fourier transform we obtain (using  $r = |\mathbf{x}|$  and  $k = |\mathbf{k}|$  to simplify the notation)

$$\begin{aligned}
 V(\mathbf{k}^2, k_0) &= \int_{\mathbb{R}^4} d^4x e^{-i(k_0 x_0 - \mathbf{k} \cdot \mathbf{x})} \underbrace{\delta(x_0) \sigma |\mathbf{x}|^{1+\alpha}}_{=V(\mathbf{x}, x_0)} = \sigma \underbrace{\int_{-\infty}^{\infty} e^{-ik_0 x_0} \delta(x_0) dx_0}_{=1} \int_{\mathbb{R}^3} d^3x e^{i\mathbf{k} \cdot \mathbf{x}} |\mathbf{x}|^{1+\alpha} \\
 &= \left| \begin{array}{l} \text{introduction of spherical coordinates} \\ \text{with the } \mathbf{k}\text{-direction as preferred axis} \end{array} \right| = \sigma \int_{\mathbb{R}^3} e^{i\mathbf{k} \cdot \mathbf{x}} r^{1+\alpha} r^2 dr d(\cos \vartheta) d\varphi \\
 &= 2\pi\sigma \int_0^\infty dr \int_{-1}^1 d(\cos \vartheta) e^{ikr \cos \vartheta} r^{3+\alpha} = 2\pi\sigma \int_0^\infty dr r^{3+\alpha} \left. \frac{e^{ikr \cos \vartheta}}{ikr} \right|_{-1}^1 \\
 &= \frac{4\pi\sigma}{k} \int_0^\infty dr r^{2+\alpha} \frac{e^{ikr} - e^{-ikr}}{2i} = \frac{4\pi\sigma}{k} \int_0^\infty dr r^{2+\alpha} \sin(kr) \\
 &= \frac{4\pi\sigma}{k^{4+\alpha}} \int_0^\infty d(kr) (kr)^{2+\alpha} \sin(kr) = \frac{4\pi\sigma}{k^{4+\alpha}} \underbrace{\int_0^\infty t^{2+\alpha} \sin t dt}_{=: I_{\alpha,0}}. \tag{C.13}
 \end{aligned}$$

Reduction of the integral to a dimensionless quantity has revealed a momentum space potential  $\sim \frac{1}{k^{4+\alpha}}$ , but the expression contains (as it could be expected from the form of the problem) an ill-defined integral, which we call  $I_{\alpha,0}$ . Some regularization procedure is required to assign a value to this integral. Here we employ the popular  $e^{-\varepsilon t^2}$  prescription ( $\varepsilon > 0$ ,  $\varepsilon \rightarrow 0$ ) and define

$$I_{\alpha,\varepsilon} := \int_0^\infty e^{-\varepsilon t^2} t^{2+\alpha} \sin t dt. \tag{C.14}$$

For  $\alpha = 0$  (the linearly rising potential) we find

$$I_{0,\varepsilon} = \frac{1}{4\varepsilon^2} \left( 1 - \frac{\sqrt{\pi} e^{-1/(4\varepsilon)} (1 - 2\varepsilon) \operatorname{erf}\left(\frac{i}{2\sqrt{\varepsilon}}\right)}{2i\sqrt{\varepsilon}} \right) \xrightarrow{\varepsilon \rightarrow 0} -2. \tag{C.15}$$

The limit of this expression is obtained both analytically (with help of Mathematica) and numerically, as illustrated in figure C.2, and we end up with the confinement potential

$$V(\mathbf{k}^2, k_0) = -\frac{8\pi\sigma}{k^4}. \tag{C.16}$$

The general case can be evaluated as well provided  $\alpha$  is sufficiently large so that no non-integrable singularity evolves at  $t = 0$  (which would happen for  $\alpha \leq -4$ , a case so far from a linearly rising potential that we are not interested in it). In this case one has the limit

$$I_{\alpha,\varepsilon} = \frac{\varepsilon^{-2-\alpha/2}}{2} \Gamma\left(2 + \frac{\alpha}{2}\right) {}_1F_1\left(\begin{array}{c} 2 + \frac{\alpha}{2} \\ 3/2 \end{array} \middle| -\frac{1}{4\varepsilon}\right) \tag{C.17}$$

with the hypergeometric function  ${}_1F_1$ , discussed in appendix C.1.1. One finds

$$\lim_{\varepsilon \rightarrow 0^+} I_{\alpha,\varepsilon} = \frac{2^{2+\alpha} \sqrt{\pi} \Gamma\left(2 + \frac{\alpha}{2}\right)}{\Gamma\left(-\frac{1}{2} - \frac{\alpha}{2}\right)} =: C_{\text{FT}}(\alpha), \tag{C.18}$$

an expression which is plotted for  $-4 < \alpha < 4$  in figure C.3.

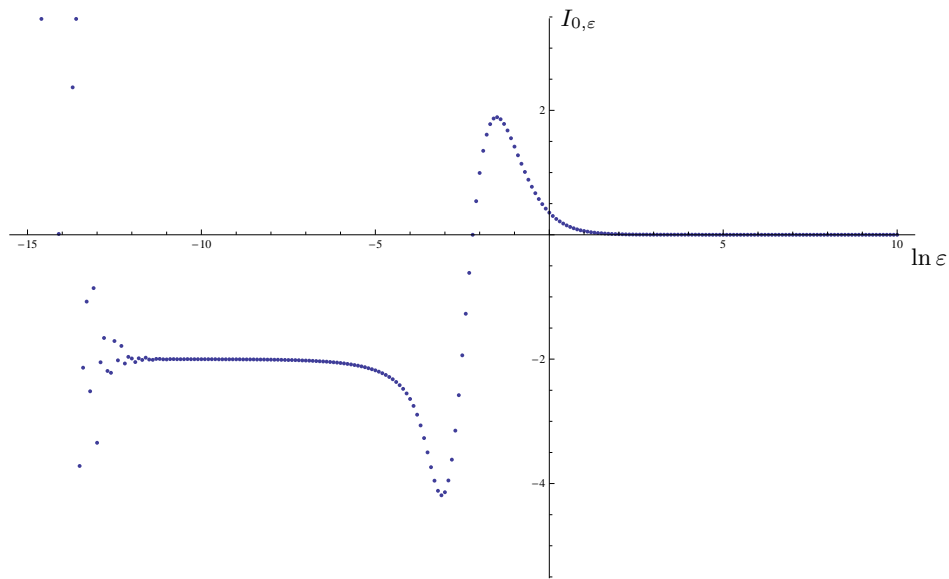


Figure C.2: Numerical check of  $I_{0,\varepsilon}$ , as defined in (C.15) for  $\alpha = 0$ , for  $\varepsilon \rightarrow 0$ . Note that for very small values of  $\varepsilon$ , the evaluation becomes unstable due to numerical cancellations.

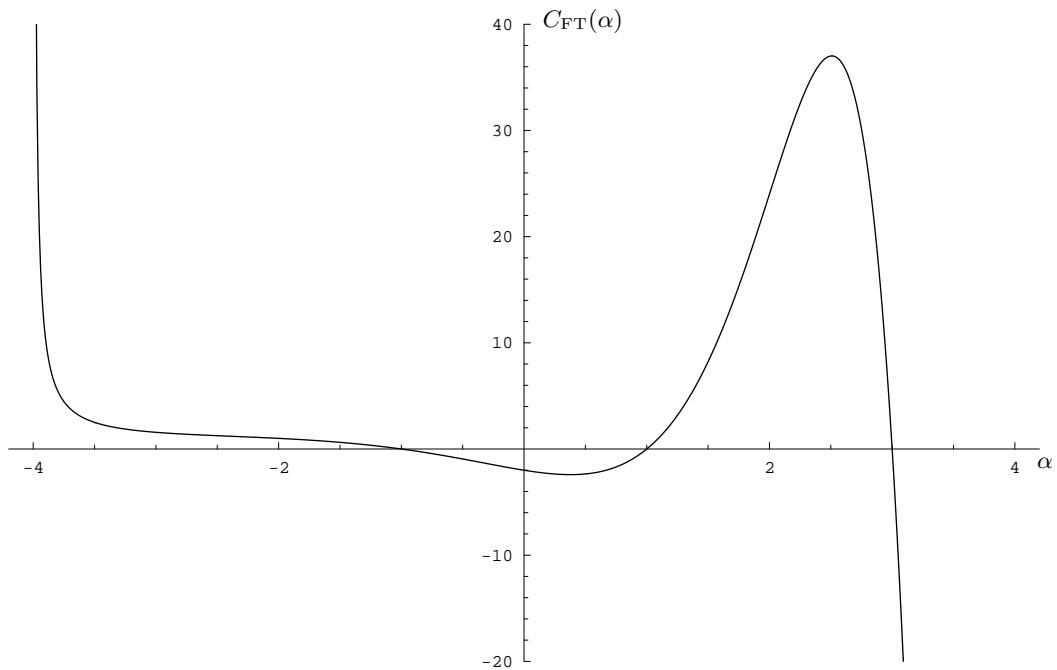


Figure C.3: Plot of  $C_{\text{FT}}(\alpha) = \lim_{\varepsilon \rightarrow 0^+} I_{\alpha,\varepsilon}$ , as defined in (C.15) and evaluated in (C.18). Note that  $\alpha = 0$ , where we find the value  $-2$ , corresponds to the linearly rising potential.

One finds that the regularization procedure yields a vanishing coefficient for  $\alpha = -1$  (the constant case),  $\alpha = 1$  (the harmonic oscillator potential) and  $\alpha = 3$ . Such a vanishing coefficient makes sense for  $V(\mathbf{x}) = \text{const}^1$  and the change of sign at  $\alpha = -1$  can be interpreted as transition between attractive and repulsive behaviour.

For  $V(\mathbf{x}) = |\mathbf{x}|^2$ , however, this regularization procedure fails since there is no reason for a vanishing coefficient and a sign change. So one should not trust the results obtained by this regularization for  $\alpha \geq 1$ . In the vicinity of the linearly rising potential ( $|\alpha| < 1$ ), the results can be considered as reasonable, and so the Fourier transform is (relatively) well-defined.

When we proceed to the inverse Fourier transform, matters are even more delicate, since we find

$$\begin{aligned}
V(x) &= \frac{1}{(2\pi)^4} \int_{\mathbb{R}^4} d^4k \, e^{i(k_0 x_0 - \mathbf{k} \cdot \mathbf{x})} \frac{4\pi\sigma C_{\text{FT}}(\alpha)}{k^{4+\alpha}} \\
&= \underbrace{\frac{1}{2\pi} \int_{-\infty}^{\infty} e^{ik_0 x_0} dk_0}_{=\delta(x_0)} \cdot \underbrace{\frac{1}{2\pi} \int_0^{2\pi} d\varphi}_{=1} \cdot \frac{1}{(2\pi)^2} \int_0^{\infty} dk \, k^2 \int_{-1}^1 d\cos(\vartheta) e^{-ikr \cos \vartheta} \frac{4\pi\sigma C_{\text{FT}}(\alpha)}{k^{4+\alpha}} \\
&= \delta(x_0) \frac{4\pi\sigma C_{\text{FT}}(\alpha)}{4\pi^2} \int_0^{\infty} \frac{dk}{k^{2+\alpha}} \left. \frac{e^{-ikr \cos \vartheta}}{-ikx} \right|_{-1}^1 = \delta(x_0) \frac{2\sigma C_{\text{FT}}(\alpha)}{\pi r} \int_0^{\infty} \frac{dk}{k^{3+\alpha}} \frac{e^{-ikr} - e^{ikr}}{-2i} \\
&= \delta(x_0) \frac{2\sigma C_{\text{FT}}(\alpha)}{\pi r} \int_0^{\infty} \frac{\sin(kr)}{k^{3+\alpha}} dk = \delta(x_0) \frac{2\sigma C_{\text{FT}}(\alpha)}{\pi r} \int_0^{\infty} r^{2+\alpha} \frac{\sin(kr)}{(kr)^{3+\alpha}} d(kr) \\
&= \delta(x_0) r^{1+\alpha} \frac{2\sigma C_{\text{FT}}(\alpha)}{\pi} \underbrace{\int_0^{\infty} \frac{\sin t}{t^{3+\alpha}} dt}_{=: J_{\alpha,0}} \tag{C.19}
\end{aligned}$$

Instead of a non-integrable singularity at infinity (which is alleviated by the oscillatory sine function introduced by the Fourier transform) the dimensionless integral  $J_{\alpha,0}$  contains (for  $\alpha \geq -1$ ) a non-integrable singularity at the origin which is not affected by the oscillations of the sine. In this case even a sophisticated regularization procedure can not be expected to yield a finite result for this integral.

The  $e^{-\varepsilon t^2}$  regularization is not suited here since it is designed to regulate singularities at infinity, so we choose as regularized integral<sup>2</sup>

$$J_{\alpha,\varepsilon} := \int_0^{\infty} e^{-\varepsilon^2/t^2} \frac{\sin t}{t^{3+\alpha}} dt \tag{C.20}$$

Evaluation of this integral yields for  $\varepsilon > 0$  and  $\alpha > -3$

$$J_{\alpha,\varepsilon} = \frac{1}{\varepsilon^{1+\alpha}} \frac{1}{2} \Gamma\left(\frac{1+\alpha}{2}\right) \underbrace{{}_0F_2\left(\frac{3}{2}, \frac{1-\alpha}{2} \middle| \frac{\varepsilon}{4}\right)}_{\xrightarrow{\varepsilon \rightarrow 0} 1} + \Gamma(-2-\alpha) \sin\left(\frac{\pi\alpha}{2}\right) \underbrace{{}_0F_2\left(\frac{3+\alpha}{2}, \frac{4+\alpha}{2} \middle| \frac{\varepsilon}{4}\right)}_{\xrightarrow{\varepsilon \rightarrow 0} 1} \tag{C.21}$$

The finite part has a removable singularity at  $\alpha = 0$ , and we find

$$\begin{aligned}
C_{\text{FT}^{-1},\text{fin}}(0) &:= \lim_{\alpha \rightarrow 0} \Gamma(-2-\alpha) \sin\left(\frac{\pi\alpha}{2}\right) = \lim_{\alpha \rightarrow 0} \frac{\Gamma(-\alpha)}{(-2-\alpha)(-1-\alpha)} \sin\left(\frac{\pi\alpha}{2}\right) \\
&= \lim_{\alpha \rightarrow 0} \frac{-\frac{1}{\alpha} + \mathcal{O}(1)}{(-2-\alpha)(-1-\alpha)} \left(\frac{\pi\alpha}{2} + \mathcal{O}(\alpha^3)\right) = \lim_{\alpha \rightarrow 0} \frac{-\frac{\pi}{2} + \mathcal{O}(\alpha)}{2 + \mathcal{O}(\alpha)} = -\frac{\pi}{4}, \tag{C.22}
\end{aligned}$$

<sup>1</sup>For a constant potential (i.e. vanishing force) the choice of the constant is arbitrary. Thus it can be set to zero without affecting physics (except possibly gravitational effects which are completely neglected here).

<sup>2</sup>We have checked explicitly that oscillatory regulators like  $\rho_\varepsilon(t) = \cos\left(\frac{\varepsilon^2}{t^2}\right)$  or  $\rho_\varepsilon(t) = \frac{t^2}{\varepsilon^2} \sin\left(\frac{\varepsilon^2}{t^2}\right)$  yield the same finite part as obtained by the following procedure (though they give a different coefficient for the divergent part).

which is precisely the constant required for consistency of the inverse Fourier transform. Therefore it is common practice to discard the divergent  $\frac{1}{\varepsilon}$  part and proceed only with the finite part. We now generalize this procedure to arbitrary  $\alpha \in (-1, 1)$ , dismissing the divergent  $\frac{1}{\varepsilon^{1+\alpha}}$  part. This yields

$$C_{\text{FT}^{-1}, \text{fin}}(\alpha) := \Gamma(-2 - \alpha) \sin\left(\frac{\pi\alpha}{2}\right), \quad (\text{C.23})$$

which has apart from the removable singularity at  $\alpha = 0$  no further peculiarities in the region  $|\alpha| < 1$ . Employing this (of course ad-hoc) procedure, we obtain

$$\begin{aligned} V(x) &= \delta(x_0) r^{1+\alpha} \frac{2\sigma}{\pi} C_{\text{FT}}(\alpha) C_{\text{FT}^{-1}, \text{fin}}(\alpha) \\ &= \delta(x_0) r^{1+\alpha} \sigma \frac{2^{3+\alpha} \sqrt{\pi} \Gamma(2 + \frac{\alpha}{2})}{\Gamma(-\frac{1}{2} - \frac{\alpha}{2})} \Gamma(-2 - \alpha) \frac{\sin(\frac{\alpha\pi}{2})}{\pi} \\ &= \delta(x_0) r^{1+\alpha} \sigma \frac{2^{3+\alpha} \sqrt{\pi} \Gamma(2 + \frac{\alpha}{2})}{\Gamma(-\frac{1}{2} - \frac{\alpha}{2})} \Gamma(-2 - \alpha) \frac{1}{\Gamma(\frac{\alpha}{2}) \Gamma(1 - \frac{\alpha}{2})} \\ &= \delta(x_0) r^{1+\alpha} \sigma \frac{2^{3+\alpha} \sqrt{\pi} (1 + \frac{\alpha}{2}) \frac{\alpha}{2} \Gamma(\frac{\alpha}{2}) (-\frac{1}{2} - \frac{\alpha}{2})}{\Gamma(-\frac{\alpha}{2} + \frac{1}{2})} \Gamma(-2 - \alpha) \frac{1}{\Gamma(\frac{\alpha}{2}) (-\frac{\alpha}{2}) \Gamma(-\frac{\alpha}{2})} \\ &= \delta(x_0) r^{1+\alpha} \sigma \frac{2^{1+\alpha} \sqrt{\pi} (2 + \alpha) (1 + \alpha)}{\Gamma(-\frac{\alpha}{2} + \frac{1}{2})} \Gamma(-2 - \alpha) \frac{1}{\Gamma(-\frac{\alpha}{2})} \\ &= \delta(x_0) r^{1+\alpha} \sigma \frac{\sqrt{\pi}}{2^{2(-\frac{\alpha}{2})-1} \Gamma(-\frac{\alpha}{2}) \Gamma(-\frac{\alpha}{2} + \frac{1}{2})} (2 + \alpha) (1 + \alpha) \Gamma(-2 - \alpha) \\ &= \delta(x_0) r^{1+\alpha} \sigma \frac{(-2 - \alpha) (-1 - \alpha) \Gamma(-2 - \alpha)}{\Gamma(-\alpha)} \\ &= \delta(x_0) r^{1+\alpha} \sigma. \end{aligned} \quad (\text{C.24})$$

Thus discarding the divergent part gives the correct transformation back to position space also for general  $\alpha \in (-1, 1)$ . We note that the coefficient  $C_{\text{FT}^{-1}, \text{fin}}(\alpha)$  has first-order poles at  $\alpha = \pm 1$  which compensate the vanishing coefficients  $C_{\text{FT}}$  in these cases.

Simply discarding the  $\frac{1}{\varepsilon^{1+\alpha}}$  term in the inverse Fourier transform is an extremely untidy procedure. It can be made at least somehow more rigorous by analytic continuation. We note that for  $0 < z < 2$  we find<sup>3</sup>

$$\int_0^\infty \frac{\sin t}{t^z} dt = \underbrace{\cos\left(\frac{\pi z}{2}\right) \Gamma(1 - z)}_{:= f_{\sin}(z)}. \quad (\text{C.25})$$

The meromorphic function  $f_{\sin}$  on the right-hand side is the analytic continuation of the integral from the interval  $(0, 2)$  to  $\mathbb{C} \setminus 2\mathbb{N}$ . While for  $z = 1, 3, 5, \dots$  the zeros of the cosine cancel the poles of the gamma function,  $f_{\sin}$  has first-order poles for  $z = 2, 4, 6, \dots$ .

For the most interesting case  $2 < z < 4$  the function  $f$  is clearly regular. One indeed obtains  $\lim_{z \rightarrow 3} f_{\sin}(z) = -\frac{\pi}{4}$ , and in general one has

$$f_{\sin}(3 + \alpha) = \underbrace{\cos\left(\frac{3\pi}{2} + \frac{\alpha\pi}{2}\right)}_{= \sin(\frac{\alpha\pi}{2})} \Gamma(-2 - \alpha) = C_{\text{FT}^{-1}, \text{fin}}(\alpha). \quad (\text{C.26})$$

The finite part, obtained by discarding the divergent  $\frac{1}{\varepsilon^{1+\alpha}}$  piece of the integral, is precisely identical to the expression obtained by analytic continuation.

---

<sup>3</sup>For  $z = 0$  we encounter the undefined integral  $\int_0^\infty \sin(t) dt$ , while for  $z \rightarrow 2^-$  the singularity at  $t = 0$  becomes non-integrable, since  $\frac{\sin(t)}{t^2} \sim \frac{1}{t}$  for small  $t$  and we have  $\int_\varepsilon^1 \frac{dt}{t} = -\ln \varepsilon \xrightarrow{\varepsilon \rightarrow 0} \infty$ .

### C.2.1 A Further Comment on Infrared Divergences in DSEs

Another aspect of the mathematical treatment of overconfining potentials has been given in [132]: We recall (see sec. 3.2.3) that in Coulomb gauge, the time-time component of the gluon propagator has an instantaneous part,

$$-g^2 D_{A_0 A_0}(x, t) = V_C(r) \delta(t) + V_{\text{non-inst.}}(x, t), \quad (\text{C.27})$$

known as the color-Coulomb potential  $V_C(r)$ , where  $r = |x|$ . When the gauge-invariant potential introduced by Wilson is confining,  $\lim_{r \rightarrow \infty} V_W(r) = \infty$ , it provides a lower bound on the color-Coulomb potential asymptotically at large  $r$ ,  $V_C(r) \geq V_W(r)$ , summarized by “no confinement without Coulomb confinement” [228].

In the confining phase we expect the Wilson potential to rise linearly,  $V_W(r) \sim \sigma r$ , where  $\sigma$  is the physical string tension, and in this case the color-Coulomb potential rises (at least) linearly,  $V_C(r) \sim \sigma_C r$ , where  $\sigma_C$  is the Coulomb string tension and  $\sigma_C \geq \sigma$ . Moreover in Coulomb gauge  $gA_0$  is a renormalization-group invariant [228], which implies that  $V_C(r)$  is also a renormalization-group invariant. Thus, as long as  $\sigma_{\text{coul}}$  is finite, it has a well-defined physical value in MeV which has been calculated in lattice gauge theory [93, 145, 148, 147, 203].

The linearly rising potential  $r$  corresponds in momentum space to  $1/k^4$ , so one encounters infrared divergences of the type  $\int d^3 k/k^4$  in the DS equations. To address this problem, we observe that the DS equations are originally derived in position space [from the functional identity for  $\delta\Gamma/\delta A(x)$ ], and moreover these equations remain free of infrared divergences when written in position space, even in the presence of long-range potentials. Indeed a loop integral such as

$$L(p) = \int \frac{d^s k}{(2\pi)^s} D_1(p-k) D_2(k), \quad (\text{C.28})$$

which is a convolution in momentum space, corresponds in position space to the ordinary product

$$L(r) = D_1(r) D_2(r). \quad (\text{C.29})$$

This product is well-defined for long-range potentials such as  $D_1(r) \sim r$ . This is the basic observation which gives a well-defined meaning to the DS equations for long-range forces.

One has the option of working entirely in position space. However, as a matter of convenience, we may also work in momentum space, as usual, once we provide a well-defined two-way translation between position and momentum space.

The Fourier transform of a long-range correlator such as  $D_1(r) = \sigma_C r$  is well-defined by providing a convergence factor, for example  $\exp(-\epsilon r^2)$ . Indeed the integral

$$D(k) = \int d^3 x \sigma_C r \exp(-ik \cdot x) \exp(-\epsilon r^2), \quad (\text{C.30})$$

has a finite limit for  $\epsilon \rightarrow 0$ ,

$$D(k) = -8\pi\sigma_C/k^4. \quad (\text{C.31})$$

The minus sign here is as it should be because  $\sigma_C r$  is an attractive potential. [The minus sign in (C.27) was in fact introduced to make  $V_C(r)$  a positive quantity.] We conclude that there is no difficulty in taking the Fourier transform of long-range potentials.

However the inverse Fourier transform poses an apparent difficulty because it has an infrared divergence of the form  $\int d^3 k/k^4$ . Moreover the DS equations which contain a loop integral (C.28) have infrared divergences of this type.

To address these problems, consider the inverse Fourier transform in  $s$  spatial dimensions

$$\int \frac{d^s k}{(2\pi)^s} \frac{\exp(ik \cdot x)}{(k^2)^\alpha} = \frac{\Gamma(s/2 - \alpha)}{2^{2\alpha} \pi^{s/2} \Gamma(\alpha)} r^{2\alpha-s}. \quad (\text{C.32})$$



It is free of infrared divergence provided that the parameter  $\alpha$  satisfies the bound  $\alpha < s/2$ . The integral has been evaluated by Gaussian integration after insertion of the identity,

$$\frac{1}{(k^2)^\alpha} = \frac{1}{\Gamma(\alpha)} \int_0^\infty d\beta \beta^{\alpha-1} \exp(-\beta k^2). \quad (\text{C.33})$$

[By this method of integration the convergence factor  $\exp(-\epsilon k^2)$  is not needed explicitly.] The last integral is convergent only for  $\alpha > 0$ . However the left hand side of (C.32) is well defined for all real  $\alpha$  satisfying the bound  $\alpha < s/2$  so, by analytic continuation, eq. (C.32) holds for all  $\alpha$  that satisfies this bound. Because  $1/r^{s-2\alpha}$  appears on the right hand side of (C.32), the restriction  $\alpha < s/2$  corresponds to a negative power of  $r$ .

To extend the inverse Fourier transform to longer range potentials such as  $r$  itself, which corresponds to a more infrared-singular power of  $k$ , we observe that such a more infrared-singular power may be written as a derivative,

$$\frac{1}{(k^2)^{1+\alpha}} = \frac{-1}{4\alpha(s/2 - \alpha - 1)} \frac{\partial^2}{\partial k_i^2} \frac{1}{(k^2)^\alpha}, \quad (\text{C.34})$$

and we take the inverse Fourier transform of the right hand side in the distribution sense. This gives

$$\begin{aligned} \int \frac{d^s k}{(2\pi)^s} \exp(ik \cdot x) \frac{1}{(k^2)^{1+\alpha}} &= \frac{-1}{4\alpha(s/2 - \alpha - 1)} \int \frac{d^s k}{(2\pi)^s} \exp(ik \cdot x) \frac{\partial^2}{\partial k_i^2} \frac{1}{(k^2)^\alpha} \\ &= \frac{x^2}{4\alpha(s/2 - \alpha - 1)} \int \frac{d^s k}{(2\pi)^s} \exp(ik \cdot x) \frac{1}{(k^2)^\alpha} \\ &= \frac{\Gamma(s/2 - \alpha - 1)}{2^{2(\alpha+1)} \pi^{s/2} \Gamma(\alpha + 1)} r^{2(\alpha+1)-s}, \end{aligned} \quad (\text{C.35})$$

where we have used (C.32) for  $\alpha < s/2$ , and  $r \equiv (x^2)^{1/2}$ . We now observe that (C.35) has the same form as (C.32), with the substitution  $\alpha \rightarrow \alpha + 1$ . Thus the result of giving  $1/(k^2)^{\alpha+1}$  a meaning as a distribution is quite simple: formula (C.32) is continued analytically from  $\alpha$  to  $\alpha + 1$ , so it is valid under the weaker restriction  $\alpha < s/2 + 1$ . By induction, formula (C.32) may be continued to  $\alpha < s/2 + n$ , where  $n$  is any integer.

Finally we note that the loop integral (C.28) that appears in the DS equation becomes well-defined by the same method. Indeed, suppose that  $D_1(k) = 1/(k^2)^{\alpha+1}$  is written as the derivative

$$D_1(k) = \frac{\partial^2}{\partial k_i^2} E_1(k) \quad (\text{C.36})$$

where  $E_1(k)$  is written above and is less singular than  $D_1(k)$ . Then the ill-defined loop integral (C.28) may be replaced by the well-defined expression

$$L(p) = \frac{\partial^2}{\partial p_i^2} \int \frac{d^s k}{(2\pi)^s} E_1(p-k) D_2(k). \quad (\text{C.37})$$

However there is no need to do this explicitly because the result of this substitution may be obtained, as before, by analytic continuation in  $\alpha$  of the original loop integral

$$L_{\text{original}} = \int \frac{d^s k}{(2\pi)^s} D_1(p-k) D_2(k). \quad (\text{C.38})$$

We conclude that instead of working in position space, where there are no infrared divergences, we may, as a matter of convenience, work directly in momentum space according to the following prescription: The standard loop integral (C.28) is performed for values of the critical exponents  $\alpha$  for which it is well defined. The result is then analytically continued in  $\alpha$  to the values of interest.

### C.3 Notes on a General Asymptotic Expansion

Finding a reliable asymptotic expression which takes both scales into account at the same time is a highly nontrivial task.<sup>4</sup> Even for  $p^2 = \mathbf{p}^2 + p_4^2$  being small, the ratio between  $\mathbf{p}^2$  and  $p_4^2$  can be of any order of magnitude. An asymptotic infrared expansion (that consequently makes use of power laws) is only reasonable for the smallest momentum scale present in the system.

Usually, in Coulomb gauge we are particularly interested in the case where  $\mathbf{p}^2$  is small. If at the same time  $p_4^2$  is large, we can simply give an asymptotic expansion in  $\mathbf{p}^2$  without having to care about  $p_4^2$  more than about any intrinsic scale present in the system. In this thesis, we will exclusively employ this type of infrared analysis.

We have to keep in mind, however, that an analysis performed that way has only limited range of applicability, since no statements can be made about the cases  $\mathbf{p}^2 \approx p_4^2$  and  $p_4^2 \ll \mathbf{p}^2$ . In interpolating gauges, it may be reasonable to employ the combination

$$p_\alpha^2 = \mathbf{p}^2 + \alpha p_4^2 \quad (\text{C.39})$$

as expansion parameter, again provided that this scale is much smaller than all other scales present in the system.

A more general approach to Coulomb gauge could involve an expansion in the quantity

$$p_{<}^2 := \frac{\mathbf{p}^2 p_4^2}{\mathbf{p}^2 + p_4^2} \dots \begin{cases} \approx \mathbf{p}^2 & \text{for } \mathbf{p}^2 \ll p_4^2 \\ \approx p_4^2 & \text{for } p_4^2 \ll \mathbf{p}^2 \\ = \frac{p^2}{2} & \text{for } \mathbf{p}^2 = p_4^2 = \frac{p^2}{2}, \end{cases} \quad (\text{C.40})$$

which picks out the smaller of the two momentum scales. This scale is complemented by

$$p_{>}^2 := \frac{\mathbf{p}^4 + p_4^4}{\mathbf{p}^2 + p_4^2} \dots \begin{cases} \approx \mathbf{p}^2 & \text{for } \mathbf{p}^2 \gg p_4^2 \\ \approx p_4^2 & \text{for } p_4^2 \gg \mathbf{p}^2 \\ = \frac{p^2}{2} & \text{for } \mathbf{p}^2 = p_4^2 = \frac{p^2}{2}. \end{cases} \quad (\text{C.41})$$

One always finds  $p_{<}^2 < p_{>}^2$  and for  $\frac{p^2}{p_4^2} \neq \mathcal{O}(1)$  one indeed has  $p_{<}^2 \ll p_{>}^2$ . Thus one could reasonably expect an expansion of the form

$$G(p) \sim \sum_{k=1}^{\infty} c_k (p_{<})^{\delta_k} \quad (\text{C.42})$$

with  $\delta_1 < \delta_2 < \dots$  to hold at least in most kinematic regions. Note also that

$$2p_{<}^2 + p_{>}^2 = \frac{\mathbf{p}^4 + 2\mathbf{p}^2 p_4^2 + p_4^4}{\mathbf{p}^2 + p_4^2} = \frac{(\mathbf{p}^2 + p_4^2)^2}{\mathbf{p}^2 + p_4^2} = \mathbf{p}^2 + p_4^2 = p^2 \quad (\text{C.43})$$

---

<sup>4</sup>The most straightforward generalization of the one-dimensional case would constitute of an expansion

$$F(\varepsilon, \delta) \sim \sum_{k=0}^{\infty} c_k \varphi_k(\varepsilon, \delta) = c_0 \varphi_0(\varepsilon, \delta) + c_1 \varphi_1(\varepsilon, \delta) + \dots$$

with

$$\lim_{\varepsilon, \delta} \frac{F(\varepsilon, \delta) - \sum_{k=0}^n c_k \varphi_k(\varepsilon, \delta)}{\varphi_n(\varepsilon, \delta)} = 0, \quad \lim_{\varepsilon, \delta} \frac{\varphi_{n+1}(\varepsilon, \delta)}{\varphi_n(\varepsilon, \delta)} = 0.$$

where  $\lim_{\varepsilon, \delta}$  denotes any of the limits  $(\varepsilon, \delta) \rightarrow (0, 0)$ ,  $\varepsilon \rightarrow 0$  while  $\delta \neq 0$  and  $\delta \rightarrow 0$  while  $\varepsilon \neq 0$ . A more modest approach could constitute of an expansion

$$F(\varepsilon, \delta) \sim \sum_{i,j} c_{ij} \varphi_i(\varepsilon) \psi_j(\delta)$$

with basis functions fulfilling  $\lim_{\varepsilon \rightarrow 0} \frac{\varphi_{n+1}(\varepsilon)}{\varphi_n(\varepsilon)} = 0$  and  $\lim_{\delta \rightarrow 0} \frac{\psi_{n+1}(\delta)}{\psi_n(\delta)} = 0$ . In general, such an expansion will only be able to grasp certain aspects of  $F$  in the asymptotic region  $\varepsilon \approx \delta \approx 0$ , the same way directional limits usually grasp only certain aspects of functions  $\mathbb{R}^2 \rightarrow \mathbb{R}$ .

Making use of this fact, a suitable expansion parameter for interpolating gauges may be

$$p_\alpha^2 = p_{<}^2 + \alpha(p_{<}^2 + p_{>}^2) = \frac{\alpha \mathbf{p}^2 + (1 + \alpha) \mathbf{p}^2 p_4^2 + \alpha p_4^2}{\mathbf{p}^2 + p_4^2} \rightarrow \begin{cases} p_{<}^2 & \text{for } \alpha \rightarrow 0 \\ p^2 & \text{for } \alpha \rightarrow 1. \end{cases} \quad (\text{C.44})$$

The main obstacle in establishing a procedure for infrared power counting in Coulomb gauge is that it is not always clear how to count the integration over the zero-component of momentum. To see this effect, we compare two integrals (with the external momentum  $p = (p_0, \mathbf{p})$  flowing through the corresponding diagrams). In the first one we consider a  $k_0$ -dependent propagator similar to the infrared-dominant part of the dressed transverse gluon,

$$\begin{aligned} I_1 &= \int d^3k dk_0 |\mathbf{p} - \mathbf{k}|^\alpha \frac{1}{\frac{\Lambda^4}{k^2} + k_0^2} = \int d^3k dk_0 |\mathbf{p} - \mathbf{k}|^\alpha \frac{k^2}{\Lambda^4} \frac{1}{1 + \frac{k^2 k_0^2}{\Lambda^4}} \\ &= \int d^3k |\mathbf{p} - \mathbf{k}|^\alpha \frac{k}{\Lambda^2} \int_{-\infty}^{\infty} d\left(\frac{k_0 k}{\Lambda^2}\right) \frac{1}{1 + \frac{k^2 k_0^2}{\Lambda^4}} = \frac{\pi}{\Lambda^2} \int d^3k k |\mathbf{p} - \mathbf{k}|^\alpha \sim \mathcal{O}(p^{4+\alpha}). \end{aligned} \quad (\text{C.45})$$

In the second integral we employ a  $k_0$ -dependent function similar to the tree-level transverse gluon propagator,

$$\begin{aligned} I_2 &= \int d^3k dk_0 |\mathbf{p} - \mathbf{k}|^\alpha \frac{1}{k^2 + k_0^2} = \int d^3k dk_0 |\mathbf{p} - \mathbf{k}|^\alpha \frac{1}{k^2} \frac{1}{1 + \frac{k_0^2}{k^2}} \\ &= \int d^3k |\mathbf{p} - \mathbf{k}|^\alpha \frac{1}{k} \int_{-\infty}^{\infty} d\left(\frac{k_0}{k}\right) \frac{1}{1 + \left(\frac{k_0}{k}\right)^2} = \pi \int d^3k \frac{|\mathbf{p} - \mathbf{k}|^\alpha}{k} \sim \mathcal{O}(p^{2+\alpha}). \end{aligned} \quad (\text{C.46})$$

In the first case we find

$$\int d^3k dk_0 \mathcal{O}(p^\alpha) \mathcal{O}(k^2) \sim \mathcal{O}(p^{4+\alpha}).$$

In the second case we find for  $k_0 \gg k$

$$\int d^3k dk_0 \mathcal{O}(p^\alpha) \mathcal{O}(k^0) \sim \mathcal{O}(p^{2+\alpha}),$$

which seems to suggest

$$\int d^3k dk_0 \sim \mathcal{O}(p^2).$$

For  $k_0 \ll k$  however we have

$$\int d^3k dk_0 \mathcal{O}(p^\alpha) \mathcal{O}(k^2) \sim \mathcal{O}(p^{2+\alpha}).$$

$$\int_{-\infty}^{\infty} \frac{dq_0}{(\Lambda^2 + q_0^2)^\alpha} = \frac{\sqrt{\pi} \Lambda^{1-2\alpha} \Gamma(\alpha - \frac{1}{2})}{\Gamma(\alpha)} \sim \Lambda^{1-2\alpha} \quad (\text{C.47})$$

$$\begin{aligned} \int_{-\infty}^{\infty} \frac{dq_0}{(\Lambda_1^2 + q_0^2)(\Lambda_2^2 + (p_0 - q_0)^2)} &= \frac{\pi(\Lambda_1 + \Lambda_2)}{\Lambda_1 \Lambda_2 (p_0^2 + (\Lambda_1 + \Lambda_2)^2)} \\ &\sim \frac{1}{\min(\Lambda_1, \Lambda_2) \max^2(p_0, \Lambda_1, \Lambda_2)} \end{aligned} \quad (\text{C.48})$$

with scales  $\Lambda_i$  related to  $|\mathbf{q}|$ ,  $|\mathbf{p}|$  or some external scale like  $\Lambda_{\text{QCD}}$ . Typically in a diagram containing a transverse gluon and a quark, one will have  $\Lambda_1 \sim |\mathbf{q}|$  and  $\Lambda_2 \sim \frac{\Lambda_{\text{QCD}}^2}{|\mathbf{p} - \mathbf{q}|}$ . Focussing on the extreme infrared (both for the loop momentum  $q$  and the external momentum  $p$ ) one has

$|\mathbf{q}| \ll p_0 \ll \frac{\Lambda_{\text{QCD}}^2}{|\mathbf{p}-\mathbf{q}|}$ , which allows to evaluate the asymptotics of (C.48). For the self-energy term in figure 4.1 one has to analyze the properties of integrals like

$$\int_0^{\Lambda_c} dq q \int_{-1}^1 d(\cos \vartheta) \frac{p^2 - 2pq \cos \vartheta + q^2}{\Lambda_{\text{QCD}}^2} \quad (\text{C.49})$$

with some cutoff  $\Lambda_c$ , introduced to separate the infrared region from other momentum scales. In addition to this analysis one has to determine consistency conditions for the degree of divergence of the dressing functions.

## C.4 Finite Temperature Calculations

### C.4.1 The Anomaly from an Analytic Derivative

We now show how the anomaly (5.3) can be obtained in the approach outlined in sec. 5.2 without the necessity for numerical differentiation. In the following, we always understand  $g^2 = g^2(\mu)$  and  $\mu = \mu(T)$ .

One-loop expansion of the gap equation gives for the rescaled pressure

$$\frac{p}{T^4} \equiv \frac{w}{T^3} = (N^2 - 1) \left[ \frac{3}{2N} \frac{m^{*4}}{g^2(\mu)} + \frac{1}{3\pi^2} K(m^*) \right] \quad (\text{C.50})$$

with  $K(m^*) = m^{*4} I(m^*)$  and

$$I(m^*) := \int_0^\infty \frac{dx}{u(x)} \frac{x^4 - 1}{e^{m^* u(x)} - 1}, \quad (\text{C.51})$$

using the reduced dispersion relation (5.24). From this, we obtain

$$\begin{aligned} A_r &= T \frac{d}{dT} \frac{p}{T^4} \\ &= (N^2 - 1) \left[ \frac{3}{2N} T \frac{d}{dT} \frac{m^{*4}}{g^2} + \frac{1}{3\pi^2} T \frac{\partial K(m^*)}{\partial T} \right] \\ &= 3 \frac{N^2 - 1}{2N} \left[ -\frac{m^{*4}}{g^4} T \frac{dg^2}{dT} + \frac{4m^{*3}}{g^2} T \frac{dm^*}{dT} \right] + \frac{N^2 - 1}{3\pi^2} T \frac{\partial K(m^*)}{\partial T}. \end{aligned} \quad (\text{C.52})$$

The derivative of  $g^2$  with respect to  $T$  be easily calculated using the  $\beta$ -function,

$$T \frac{d(g^2)}{d\mu} = \frac{T}{\mu} \mu \frac{d(g^2)}{d\mu} = \frac{T}{\mu} \beta(g^2). \quad (\text{C.53})$$

From this, we obtain

$$T \frac{dg^2(\mu)}{dT} = \frac{T}{\mu} \mu \frac{dg^2(\mu)}{d\mu} \frac{d\mu(T)}{dT} = \beta(g^2(\mu)) \frac{T}{\mu} \frac{d\mu(T)}{dT}. \quad (\text{C.54})$$

For the last term in (C.52) we have

$$T \frac{\partial K(m^*)}{\partial T} = T \frac{\partial m^*}{\partial T} \frac{\partial K(m^*)}{\partial m^*} \quad (\text{C.55})$$

$$\frac{\partial K(m^*)}{\partial m^*} = 4m^{*3} I(m^*) - m^{*4} L(m^*) \quad (\text{C.56})$$

$$L(m^*) = \int_0^\infty dx \frac{(x^4 - 1) e^{m^* u(x)}}{(e^{m^* u(x)} - 1)^2}. \quad (\text{C.57})$$

We obtain  $T \frac{\partial m^*}{\partial T}$  by differentiating the gap equation  $f(m^*) = y(T)$  with respect to  $T$ , where

$$f(m^*) = \frac{1}{2} \ln \frac{1}{m^*} + \int_0^\infty \frac{dx}{u(x)} \frac{1}{e^{m^* u(x)} - 1}, \quad (\text{C.58})$$

$$y(T) = \frac{3\pi^2}{N g^2(\mu)} - \frac{1}{4} \ln \frac{e\mu^2(T)}{2T^2}. \quad (\text{C.59})$$

Since the left-hand side depends on  $T$  only implicitly via  $m^*$ , we have

$$\frac{d}{dT} f(m^*) = \frac{df}{dm^*} \frac{dm^*}{dT} = \left[ -\frac{1}{2} \frac{1}{m^*} - J(m^*) \right] \frac{dm^*}{dT}, \quad (\text{C.60})$$

$$J(m^*) = \int_0^\infty dx \frac{e^{m^* u(x)}}{(e^{m^* u(x)} - 1)^2}. \quad (\text{C.61})$$

Differentiation of the right-hand side yields

$$\begin{aligned} \frac{dy(T)}{dT} &= \frac{d}{dT} \left[ \frac{3\pi^2}{N g^2(\mu)} - \frac{1}{4} \ln \frac{e\mu^2(T)}{2T^2} \right] \\ &= -\frac{3\pi^2}{N g^4(\mu(T))} \frac{dg^2(\mu)}{dT} - \frac{d}{dT} \frac{1}{2} \ln \left( \sqrt{\frac{e}{2}} \frac{\mu(T)}{T} \right) \\ &= -\frac{3\pi^2}{N g^4(\mu(T))} \frac{1}{\mu(T)} \mu(T) \frac{dg^2(\mu)}{dT} - \frac{1}{2} \frac{T}{\mu(T)} \left( \frac{\frac{d\mu}{dT}}{T} - \frac{\mu}{T^2} \right) \\ &= -\frac{1}{\mu(T)} \left\{ \frac{3\pi^2}{N} \frac{\beta(g^2)}{g^4(\mu)} \frac{d\mu}{dT} + \frac{1}{2} \left( \frac{d\mu}{dT} - \frac{\mu}{T} \right) \right\}. \end{aligned} \quad (\text{C.62})$$

The second term inside the curly brackets is a measure for the deviation from the asymptotic behaviour; in the asymptotic regime with  $\mu(T) = 2\pi T$ , the above expression simplifies to

$$\left. \frac{dy(T)}{dT} \right|_{\text{asympt}} = -\frac{3\pi^2}{N} \frac{1}{T} \frac{\beta(g^2(2\pi T))}{g^4(2\pi T)}. \quad (\text{C.63})$$

Collecting our results, we obtain

$$\begin{aligned} T \frac{dm^*}{dT} &= \frac{T \frac{dy}{dT}}{-\frac{1}{2m^*} - J(m^*)} \\ &= \frac{T}{\mu(T)} \frac{1}{\frac{1}{2m^*} + J(m^*)} \left\{ \frac{3\pi^2}{N} \frac{\beta(g^2)}{g^4} \frac{d\mu}{dT} + \frac{1}{2} \left( \frac{\partial \mu}{\partial T} - \frac{\mu}{T} \right) \right\}, \end{aligned} \quad (\text{C.64})$$

and the rescaled anomaly is given by

$$\begin{aligned} A_r &= 3 \frac{N^2 - 1}{2N} \left[ -\frac{m^{*4}}{g^4} \beta(g^2) \frac{T}{\mu} \frac{d\mu}{dT} + \frac{4m^{*3}}{g^2} T \frac{dm^*}{dT} \right] \\ &\quad + \frac{N^2 - 1}{3\pi^2} \left( 4m^{*3} I(m^*) - m^{*4} L(m^*) \right) T \frac{dm^*}{dT}. \end{aligned} \quad (\text{C.65})$$

### C.4.2 Evaluation of Power-Law Integrals

Determination of the infrared critical exponents requires evaluation of the integrals (5.84) to (5.87) which yields the results stated in (5.89) to (5.94). In order to illustrate the calculational scheme, we explicitly discuss the evaluation the integral (5.84). The evaluation of such integrals is also discussed for example in the appendix of [227] and in more detail in the appendix of [132].

First we check issues of convergence: We write

$$I_{S(V,S)}(\alpha_{\mathbf{A}}, \alpha_{\varphi}) = N k^{-s+2\alpha_{\mathbf{A}}+2\alpha_{\varphi}+2} \underbrace{\int \frac{d^s p}{(2\pi)^s} \frac{k^2 p^2 - (p \cdot k)^2}{(p^2)^{2+\alpha_{\mathbf{A}}} [(k-p)^2]^{1+\alpha_{\varphi}}}}_{:=I_1}. \quad (\text{C.66})$$

In this integral we obtain the power  $p^{s+2}$  from the numerator. In the infrared ( $p \rightarrow 0$ ) the term  $(k-p)^2$  is finite for  $k \neq 0$ , so we can neglect it for questions of convergence.<sup>5</sup> Thus the denominator contributes the power  $p^{2(2+\alpha_{\mathbf{A}})}$  and a necessary condition for infrared convergence is

$$s+2 > 4+2\alpha_{\mathbf{A}}, \quad \text{i.e.} \quad \alpha_{\mathbf{A}} < \frac{s}{2} - 1. \quad (\text{C.67})$$

(C.66) may also have a non-integrable singularity at  $p = k$ . By the substitution  $p \rightarrow p+k$  the integral takes the form

$$I_1 = \int \frac{d^s p}{(2\pi)^s} \frac{k^2 p^2 - (p \cdot k)^2}{[(p+k)^2]^{2+\alpha_{\mathbf{A}}} (p^2)^{1+\alpha_{\varphi}}}. \quad (\text{C.68})$$

The denominator now contributes the power  $p^{2(1+\alpha_{\varphi})}$  and we see that we also have to demand

$$s+2 > 2+2\alpha_{\varphi}, \quad \text{i.e.} \quad \alpha_{\varphi} < \frac{s}{2} \quad (\text{C.69})$$

in order to have infrared convergence. In the ultraviolet,  $k$  is negligible compared to  $p$  and the denominator in (C.66) contributes the power  $p^{2(2+\alpha_{\mathbf{A}}+2(1+\alpha_{\varphi}))}$ . To have ultraviolet convergence we have to demand

$$s+2 < 6+2\alpha_{\mathbf{A}}+2\alpha_{\varphi}, \quad \text{i.e.} \quad \alpha_{\mathbf{A}} + \alpha_{\varphi} > \frac{s}{2} - 1. \quad (\text{C.70})$$

These conditions are compatible; by combining them one can also deduce the conditions  $\alpha_{\varphi} > 0$  and  $\alpha_{\mathbf{A}} > -1$ .

Now we proceed with the evaluation of the integrals. In (C.66) we represent the powers of propagators by integrals over auxiliary variables. This employs the integral representation of the gamma function,

$$\int_0^\infty t^{x-1} e^{-kt} dt \stackrel{u=kt}{=} \frac{1}{k^x} \int_0^\infty u^{x-1} e^{-u} du = \frac{\Gamma(x)}{k^x}, \quad (\text{C.71})$$

( $k > 0$ ) which allows us to write

$$\frac{1}{(p^2)^{2+\alpha_{\mathbf{A}}}} = \int_0^\infty da \frac{a^{1+\alpha_{\mathbf{A}}}}{\Gamma(2+\alpha_{\mathbf{A}})} e^{-ap^2}, \quad (\text{C.72})$$

$$\frac{1}{[(k-p)^2]^{1+\alpha_{\varphi}}} = \int_0^\infty db \frac{b^{\alpha_{\varphi}}}{\Gamma(1+\alpha_{\varphi})} e^{-b(k-p)^2}. \quad (\text{C.73})$$

With these identities  $I_1$  takes the form

$$I_1 = \int_0^\infty da \frac{a^{1+\alpha_{\mathbf{A}}}}{\Gamma(2+\alpha_{\mathbf{A}})} \int_0^\infty db \frac{b^{\alpha_{\varphi}}}{\Gamma(1+\alpha_{\varphi})} I_2 \quad (\text{C.74})$$

---

<sup>5</sup>Note that for  $k = 0$  the numerator vanishes, so this case is not problematic; for all other cases the argument holds.

with

$$I_2 = \int \frac{d^s p}{(2\pi)^s} [k^2 p^2 - (p \cdot k)^2] e^{-\Phi}, \quad (\text{C.75})$$

$$\begin{aligned} \Phi &= ap^2 + b(k-p)^2 = (a+b)p^2 + bk^2 - 2b(k \cdot p) \\ &= (a+b) \left( p - \frac{b}{a+b} k \right)^2 - \frac{b^2}{a+b} k^2 + bk^2 =: (a+b)q^2 + \frac{ab}{a+b} k^2. \end{aligned} \quad (\text{C.76})$$

The substitution  $p \rightarrow q = p - \frac{b}{a+b} k$  yields

$$\begin{aligned} I_2 &= \int \frac{d^s q}{(2\pi)^s} (k^2 q^2 - (q \cdot k)^2) e^{-(a+b)q^2 - \frac{ab}{a+b} k^2} \\ &= e^{-\frac{ab}{a+b} k^2} k^2 \int \frac{d^s q}{(2\pi)^s} (1 - (\hat{q} \cdot \hat{k})^2) q^2 e^{-(a+b)q^2}. \end{aligned} \quad (\text{C.77})$$

One can rewrite an integral of the form

$$J = k^2 \int \frac{d^s q}{(2\pi)^s} (1 - (\hat{q} \cdot \hat{k})^2) f(q^2) \quad (\text{C.78})$$

as

$$J = k_i k_j \int \frac{d^s q}{(2\pi)^s} (\delta_{ij} - \hat{q}_i \hat{q}_j) f(q^2). \quad (\text{C.79})$$

Since  $J$  is a scalar which is quadratic in  $k$ , one has to find

$$\int \frac{d^s q}{(2\pi)^s} (\delta_{ij} - \hat{q}_i \hat{q}_j) f(q^2) = C \delta_{ij}. \quad (\text{C.80})$$

Taking the trace of this equation ( $\delta_{ii} = s$ ,  $\hat{q}_i \hat{q}_i = 1$ ) and a small rearrangement of factors yields

$$C = \frac{s-1}{s} \int \frac{d^s q}{(2\pi)^s} f(q^2). \quad (\text{C.81})$$

So we have

$$I_2 = e^{-\frac{ab}{a+b} k^2} k^2 \frac{s-1}{s} I_3 \quad (\text{C.82})$$

with

$$I_3 = \int \frac{d^s q}{(2\pi)^s} q^2 e^{-(a+b)q^2} = \frac{1}{(2\pi)^s} \int d\Omega_s \int_0^\infty q^{s+1} e^{-(a+b)q^2} \quad (\text{C.83})$$

The substitution  $x = (a+b)q^2$  yields

$$\begin{aligned} I_3 &= \frac{1}{(2\pi)^s} \int d\Omega_s \int_0^\infty \left( \frac{x}{a+b} \right)^{(s+1)/2} \frac{e^{-x} dx}{2x^{1/2}(a+b)^{1/2}} \\ &= \frac{1}{(2\pi)^s} \int d\Omega_s \frac{1}{2(a+b)^{1+s/2}} \int_0^\infty x^{(s/2+1)-1} e^{-x} dx \\ &= \frac{1}{(2\pi)^s} \frac{2\pi^{s/2}}{\Gamma(\frac{s}{2})} \frac{1}{2(a+b)^{1+s/2}} \Gamma\left(\frac{s}{2} + 1\right) \\ &= \frac{1}{(4\pi)^{s/2}} \frac{1}{(a+b)^{1+s/2}} \frac{\frac{s}{2} \Gamma(\frac{s}{2})}{\Gamma(\frac{s}{2})} \\ &= \frac{s}{2(4\pi)^{s/2} (a+b)^{1+s/2}} \end{aligned} \quad (\text{C.84})$$



Consequently we obtain (with slight rearrangements)

$$I_2 = \frac{(s-1)k^2}{2(4\pi)^{s/2}} \frac{e^{-\frac{ab}{a+b}k^2}}{(a+b)^{s/2+1}}. \quad (\text{C.85})$$

To proceed with the evaluation of

$$I_1 = \frac{(s-1)k^2}{2(4\pi)^{s/2}} \int_0^\infty da \frac{a^{1+\alpha_{\mathbf{A}}}}{\Gamma(2+\alpha_{\mathbf{A}})} \int_0^\infty db \frac{b^{\alpha_\varphi}}{\Gamma(1+\alpha_\varphi)} \frac{e^{-\frac{ab}{a+b}k^2}}{(a+b)^{s/2+1}}. \quad (\text{C.86})$$

we introduce another auxiliary variable  $\tau$  by integrating over  $\delta(a+b-\tau)$ ,

$$I_1 = \frac{(s-1)k^2}{2(4\pi)^{s/2}} \int_0^\infty d\tau \int_0^\infty da \frac{a^{1+\alpha_{\mathbf{A}}}}{\Gamma(2+\alpha_{\mathbf{A}})} \int_0^\infty db \frac{b^{\alpha_\varphi}}{\Gamma(1+\alpha_\varphi)} \frac{e^{-\frac{ab}{a+b}k^2}}{(a+b)^{s/2+1}} \delta(a+b-\tau). \quad (\text{C.87})$$

The substitution  $a = \tau\alpha$ ,  $b = \tau\beta$  yields

$$I_1 = \frac{(s-1)k^2}{2(4\pi)^{s/2}} \frac{1}{\Gamma(2+\alpha_{\mathbf{A}})\Gamma(1+\alpha_\varphi)} \int_0^\infty d\alpha \int_0^\infty d\beta \frac{\delta(\alpha+\beta-1)}{(\alpha+\beta)^{s/2+1}} \alpha^{1+\alpha_{\mathbf{A}}} \beta^{\alpha_\varphi} I_4 \quad (\text{C.88})$$

with

$$I_4 := \int_0^\infty d\tau \tau^{\alpha_{\mathbf{A}}+\alpha_\varphi+1-\frac{s}{2}} e^{-\alpha\beta\tau k^2}. \quad (\text{C.89})$$

(Note that  $\delta(\tau\alpha + \tau\beta - \tau) = \frac{1}{\tau}\delta(\alpha + \beta - 1)$ .) We now substitute  $t = \alpha\beta k^2 \tau$ ,

$$\begin{aligned} I_4 &:= \frac{1}{(\alpha\beta k^2)^{\alpha_{\mathbf{A}}+\alpha_\varphi+2-\frac{s}{2}}} \int_0^\infty dt t^{(\alpha_{\mathbf{A}}+\alpha_\varphi+2-\frac{s}{2})-1} e^{-t} \\ &= \frac{\Gamma(\alpha_{\mathbf{A}} + \alpha_\varphi + 2 - \frac{s}{2})}{(\alpha\beta)^{\alpha_{\mathbf{A}}+\alpha_\varphi+2-\frac{s}{2}} k^{2\alpha_{\mathbf{A}}+2\alpha_\varphi+4-s}}. \end{aligned} \quad (\text{C.90})$$

and obtain

$$I_{S(V,S)}(\alpha_{\mathbf{A}}, \alpha_\varphi) = \frac{N(s-1)}{2(4\pi)^{s/2}} \frac{\Gamma(\alpha_{\mathbf{A}} + \alpha_\varphi + 2 - \frac{s}{2})}{\Gamma(2+\alpha_{\mathbf{A}})\Gamma(1+\alpha_\varphi)} I_5 \quad (\text{C.91})$$

with

$$I_5 = \int_0^\infty d\alpha \int_0^\infty d\beta \frac{\delta(\alpha+\beta-1)}{(\alpha+\beta)^{s/2+1}} \alpha^{\frac{s}{2}-1-\alpha_\varphi} \beta^{\frac{s}{2}-2-\alpha_{\mathbf{A}}}. \quad (\text{C.92})$$

Because of the delta functional, one only has contributions from  $\alpha + \beta \leq 1$ , accordingly one can restrict the integrations in (C.92) to the interval  $[0, 1]$ . Performing one integration explicitly yields

$$\begin{aligned} I_5 &= \int_0^1 d\alpha \alpha^{(\frac{s}{2}-\alpha_\varphi)-1} (1-\alpha)^{(\frac{s}{2}-1-\alpha_{\mathbf{A}})-1} \\ &= B\left(\frac{s}{2} - \alpha_\varphi, \frac{s}{2} - 1 - \alpha_{\mathbf{A}}\right) = \frac{\Gamma(\frac{s}{2} - \alpha_\varphi) \Gamma(\frac{s}{2} - 1 - \alpha_{\mathbf{A}})}{\Gamma(s-1-\alpha_\varphi-\alpha_{\mathbf{A}})}. \end{aligned} \quad (\text{C.93})$$

Plugging this result into (C.91) yields

$$I_{S(V,S)}(\alpha_{\mathbf{A}}, \alpha_{\text{gh}}) = \frac{N(s-1)}{2(4\pi)^{s/2}} \frac{\Gamma(\alpha_{\mathbf{A}} + \alpha_\varphi + 2 - \frac{s}{2})}{\Gamma(2+\alpha_{\mathbf{A}})} \frac{\Gamma(\frac{s}{2} - \alpha_\varphi) \Gamma(\frac{s}{2} - 1 - \alpha_{\mathbf{A}})}{\Gamma(1+\alpha_{\text{gh}}) \Gamma(s-1-\alpha_{\text{gh}}-\alpha_{\mathbf{A}})}, \quad (\text{C.94})$$

which is the result stated in (5.89). The other power-law integrals are evaluated in a similar way. Note that the integrals  $I_{V(\cdot,\cdot)}$  contain a factor  $(s-1)^{-1}$  which stems from taking the trace of the projector on the lhs of the corresponding DS equation,

$$\text{tr} P_{ij}(p) = \text{tr} \left( \delta_{ij} - \frac{p_i p_j}{p^2} \right) = \delta_{ii} - \frac{p_i p_i}{p^2} = s-1, \quad (\text{C.95})$$

and is included for convenience in the definition of the integral.

# Bibliography

- [1] S. L. Adler and A. C. Davis. Chiral Symmetry Breaking in Coulomb Gauge QCD. *Nucl. Phys.*, B244:469, 1984.
- [2] O. Aharony, S. S. Gubser, J. M. Maldacena, H. Ooguri, and Y. Oz. Large N Field Theories, String Theory and Gravity. *Phys. Rept.*, 323:183–386, 2000.
- [3] I. J. R. Aitchison and A. J. G. Hey. *Gauge Theories in Particle Physics: A Practical Introduction. Vol. 1: From Relativistic Quantum Mechanics to QED*. Bristol, UK: IOP (2003) 406 p.
- [4] I. J. R. Aitchison and A. J. G. Hey. *Gauge Theories in Particle Physics: A Practical Introduction. Vol. 2: Non-Abelian Gauge Theories: QCD and the Electroweak Theory*. Bristol, UK: IOP (2004) 454 p.
- [5] R. Alkofer. *Chirale Symmetriebrechung und der chirale Phasenübergang in instantanen Näherungen zur Quantenchromodynamik in Coulombbeichung*. PhD thesis, Technische Universität München, 1988.
- [6] R. Alkofer and P. A. Amundsen. Chiral Symmetry Breaking in an Instantaneous Approximation to Coulomb Gauge QCD. *Nucl. Phys.*, B306:305–342, 1988.
- [7] R. Alkofer, C. S. Fischer, F. J. Llanes-Estrada, and K. Schwenzer. The Quark-Gluon Vertex in Landau Gauge QCD: Its Role in Dynamical Chiral Symmetry Breaking and Quark Confinement. *Annals Phys.*, 324:106–172, 2009.
- [8] R. Alkofer, C. S. Fischer, and R. Williams.  $U_A(1)$  Anomaly and  $\eta'$  Mass from an Infrared Singular Quark-Gluon Vertex. *Eur. Phys. J.*, A38:53–60, 2008.
- [9] R. Alkofer and J. Greensite. Quark Confinement: The Hard Problem of Hadron Physics. *J. Phys.*, G34:S3, 2007.
- [10] R. Alkofer, M. Q. Huber, and K. Schwenzer. Algorithmic Derivation of Dyson-Schwinger Equations. *Comput. Phys. Commun.*, 180:965–976, 2009.
- [11] R. Alkofer, M. Kloker, A. Krassnigg, and R. F. Wagenbrunn. Aspects of the confinement mechanism in Coulomb-gauge QCD. *Phys. Rev. Lett*, 96:022001, 2006.
- [12] R. Alkofer, A. Maas, and D. Zwanziger. Truncating First-Order Dyson-Schwinger Equations in Coulomb-Gauge Yang-Mills Theory. *Few Body Syst.*, 47:73–90, 2010.
- [13] R. Alkofer and L. von Smekal. The infrared behavior of QCD Green’s functions: Confinement, dynamical symmetry breaking, and hadrons as relativistic bound states. *Phys. Rept.*, 353:281, 2001.
- [14] C. Anastasiou, E. W. N. Glover, and C. Oleari. Application of the Negative-Dimension Approach to Massless Scalar Box Integrals. *Nucl. Phys.*, B565:445–467, 2000.

- [15] A. Andrasi and J. C. Taylor. Cancellation of Energy-Divergences in Coulomb Gauge QCD. *Eur. Phys. J.*, C41:377–380, 2005.
- [16] O. Andreev. Some Thermodynamic Aspects of Pure Glue, Fuzzy Bags and Gauge/String Duality. *Phys. Rev.*, D76:087702, 2007.
- [17] T. Appelquist and R. Pisarski. High-Temperature Yang-Mills Theories and Three-Dimensional Quantum Chromodynamics. *Phys. Rev.*, D23:2305, 1981.
- [18] T. Arens, F. Hettlich, C. Karpfinger, U. Kockelkorn, K. Lichtenegger, and H. Stachel. *Mathematik*. Spektrum Akademischer Verlag, 2008.
- [19] P. Arnold and C.-X. Zhai. The Three Loop Free Energy for Pure Gauge QCD. *Phys. Rev.*, D50:7603–7623, 1994.
- [20] P. Arnold and C.-X. Zhai. The Three Loop Free Energy for High Temperature QED and QCD with Fermions. *Phys. Rev.*, D51:1906–1918, 1995.
- [21] M. F. Atiyah and I. M. Singer. The Index of Elliptic Operators. 1. *Annals Math.*, 87:484–530, 1968.
- [22] M. F. Atiyah and I. M. Singer. The Index of Elliptic Operators. 3. *Annals Math.*, 87:546–604, 1968.
- [23] C. Bachas. Convexity of the Quarkonium Potential. *Phys. Rev.*, D33:2723, 1986.
- [24] G. S. Bali. QCD Forces and Heavy Quark Bound States. *Phys. Rept.*, 343:1–136, 2001.
- [25] J. S. Ball and T.-W. Chiu. Analytic Properties of the Vertex Function in Gauge Theories. 1. *Phys. Rev.*, D22:2542, 1980.
- [26] J. S. Ball and T.-W. Chiu. Analytic Properties of the Vertex Function in Gauge Theories. 2. *Phys. Rev.*, D22:2550, 1980.
- [27] V. M. Bannur. Quark Gluon Plasma as a Strongly Coupled Color-Coulombic Plasma. *Eur. Phys. J.*, C11:169–171, 1999.
- [28] I. Bars and M. B. Green. Poincare and Gauge Invariant Two-Dimensional QCD. *Phys. Rev.*, D17:537, 1978.
- [29] L. Baulieu, A. Rozenberg, and M. Schaden. Topological Aspects of Gauge Fixing Yang-Mills Theory on  $S_4$ . *Phys. Rev.*, D54:7825–7831, 1996.
- [30] L. Baulieu and M. Schaden. Gauge Group TQFT and Improved Perturbative Yang-Mills Theory. *Int. J. Mod. Phys.*, A13:985–1012, 1998.
- [31] L. Baulieu and D. Zwanziger. Renormalizable Non-Covariant Gauges and Coulomb Gauge Limit. *Nucl. Phys.*, B548:527–562, 1999.
- [32] L. Baulieu and D. Zwanziger. Regularized Coulomb Gauge. *Braz. J. Phys.*, 37:293–305, 2007.
- [33] C. Becchi. Nonstandard Gauges: A Personal Point of View. Presented at Workshop on Physical and Nonstandard Gauges, Vienna, Austria, Sep 19-23, 1989.
- [34] C. Becchi, A. Rouet, and R. Stora. Renormalization of Gauge Theories. *Annals Phys.*, 98:287–321, 1976.

- [35] J. P. Blaizot, E. Iancu, and A. Rebhan. On the Apparent Convergence of Perturbative QCD at High Temperature. *Phys. Rev.*, D68:025011, 2003.
- [36] C. G. Bollini and J. J. Giambiagi. Dimensional Renormalization: The Number of Dimensions as a Regularizing Parameter. *Nuovo Cim.*, B12:20–25, 1972.
- [37] G. Boyd, J. Engels, F. Karsch, E. Laermann, C. Legeland, M. Lutgemeier, and B. Petersson. Thermodynamics of SU(3) Lattice Gauge Theory. *Nucl. Phys.*, B469:419–444, 1996.
- [38] E. Braaten. Solution to the Perturbative Infrared Catastrophe of Hot Gauge Theories. *Phys. Rev. Lett.*, 74:2164–2167, 1995.
- [39] E. Braaten and A. Nieto. Effective Field Theory Approach to High Temperature Thermodynamics. *Phys. Rev.*, D51:6990–7006, 1995.
- [40] S. J. Brodsky and P. B. Lepage, G. P. and Mackenzie. On the Elimination of Scale Ambiguities in Perturbative Quantum Chromodynamics. *Phys. Rev.*, D28:228, 1983.
- [41] S. G. Brown. Dirac-Schwinger Covariance Condition in Canonical Theories. *Phys. Rev.*, 158, 5, 1967.
- [42] W. Bulla. Mathematische Behandlung der Wellenmechanik (lecture notes). URL <http://itp.tugraz.at/LV/bulla/MGQM/MWM.pdf>.
- [43] J. Callan, C. G., N. Coote, and D. J. Gross. Two-Dimensional Yang-Mills Theory: A Model of Quark Confinement. *Phys. Rev.*, D13:1649, 1976.
- [44] M. A. L. Capri, R. F. Sobreiro, and S. P. Sorella. Interpolating among the Landau, Coulomb and Maximal Abelian Gauges. *Phys. Rev.*, D73:041701, 2006.
- [45] M. A. L. Capri, R. F. Sobreiro, S. P. Sorella, and R. Thibes. Renormalizability of a Generalized Gauge Fixing Interpolating among the Coulomb, Landau and Maximal Abelian Gauges. *Annals Phys.*, 322:1776–1789, 2007.
- [46] A. Casher. Chiral Symmetry Breaking in Quark Confining Theories. *Phys. Lett.*, B83:395, 1979.
- [47] J. Cham. Piled Higher & Deeper. Life (or the Lack thereof) in Academia. URL [www.phdcomics.com](http://www.phdcomics.com).
- [48] H. Cheng and E.-C. Tsai. Inconsistency of Feynman Rules Derived via Path Integration. *Phys. Rev. Lett.*, 57:511, 1986.
- [49] H. Cheng and E.-C. Tsai. Gauge Invariance of the Quantum Wilson Loop. *Phys. Rev.*, D36:3196, 1987.
- [50] S. A. Chin. Transition to Hot Quark Matter in Relativistic Heavy Ion Collision. *Phys. Lett.*, B78:552–555, 1978.
- [51] N. H. Christ and T. D. Lee. Operator Ordering and Feynman Rules in Gauge Theories. *Phys. Rev.*, D22:939, 1980.
- [52] Clay-Math-Institute. Millenium Problems. URL <http://www.claymath.org/millennium>.
- [53] M. Creutz. So You Want to be a Lattice Theorist? 2006. URL [arXiv:hep-lat/0610067](http://arxiv.org/abs/hep-lat/0610067).

- [54] A. Cucchieri. Lattice Results in Coulomb Gauge. *AIP Conf. Proc.*, 892:22–28, 2007.
- [55] A. Cucchieri, A. Maas, and T. Mendes. Infrared-Suppressed Gluon Propagator in 4D Yang-Mills Theory in a Landau-like Gauge. *Mod. Phys. Lett.*, A22:2429–2438, 2007.
- [56] A. Cucchieri and T. Mendes. What’s up with IR Gluon and Ghost Propagators in Landau Gauge? A Puzzling Answer from Huge Lattices. *PoS, Lattice:297*, 2007.
- [57] A. Cucchieri and T. Mendes. Landau-Gauge Propagators in Yang-Mills Theories at  $\beta = 0$ : Massive Solution Versus Conformal Scaling. 2009.
- [58] A. Cucchieri, T. Mendes, and D. Zwanziger. SU(2) Running Coupling Constant and Confinement in Minimal Coulomb and Landau Gauges. *Nucl. Phys. Proc. Suppl.*, 106: 697–699, 2002.
- [59] A. Cucchieri and D. Zwanziger. Confinement Made Simple in the Coulomb Gauge. *Nucl. Phys. Proc. Suppl.*, 106:694–696, 2002.
- [60] A. Cucchieri and D. Zwanziger. Fit to Gluon Propagator and Gribov Formula. *Phys. Lett.*, B524:123–128, 2002.
- [61] A. Cucchieri and D. Zwanziger. Gluon Propagator and Confinement Scenario in Coulomb Gauge. *Nucl. Phys. Proc. Suppl.*, 119:727–729, 2003.
- [62] D. C. Curtis and M. R. Pennington. Truncating the Schwinger-Dyson equations: How multiplicative renormalizability and the Ward identity restrict the three point vertex in QED. *Phys. Rev.*, D42:4165–4169, 1990.
- [63] P. Cvitanovic. *Field Theory*. RX-1012 (Nordita), 1983.
- [64] T. DeGrand and C. E. Detar. Lattice Methods for Quantum Chromodynamics. New Jersey, USA: World Scientific (2006) 345 p.
- [65] G. Dell’Antonio and D. Zwanziger. All Gauge Orbits and some Gribov Copies Encompassed by the Gribov Horizon. In *Cargese 1989, Proceedings, Probabilistic methods in quantum field theory and quantum gravity* 107-130. (see High Energy Physics Index 29 (1991) No. 10571).
- [66] G. Dell’Antonio and D. Zwanziger. Ellipsoidal Bound on the Gribov Horizon Contradicts the Perturbative Renormalization Group. *Nucl. Phys.*, B326:333–350, 1989.
- [67] G. Dell’Antonio and D. Zwanziger. Every Gauge Orbit Passes Inside the Gribov Horizon. *Commun. Math. Phys.*, 138:291–299, 1991.
- [68] F. Di Renzo, M. Laine, V. Miccio, Y. Schroder, and C. Torrero. The Leading non-Perturbative Coefficient in the Weak-Coupling Expansion of Hot QCD Pressure. *JHEP*, 07:026, 2006.
- [69] L. Diósi. Feynman Path Integral and Weyl Ordering – One-Page-Tutorial. 2008. URL [www.rmki.kfki.hu/~diosi/pathinttutor.pdf](http://www.rmki.kfki.hu/~diosi/pathinttutor.pdf).
- [70] D. Dudal, J. Gracey, S. P. Sorella, N. Vandersickel, and H. Verschelde. A Refinement of the Gribov-Zwanziger Approach in the Landau Gauge: Infrared Propagators in Harmony with the Lattice Results. 2008.
- [71] D. Dudal, S. P. Sorella, N. Vandersickel, and H. Verschelde. New Features of the Gluon and Ghost Propagator in the Infrared Region from the Gribov-Zwanziger Approach. *Phys. Rev.*, D77:071501, 2008.

- [72] D. W. Duke and R. G. Roberts. Determinations of the QCD Strong Coupling  $\alpha_s$  and the Scale Lambda (QCD). *Phys. Rept.*, 120:275, 1985.
- [73] G. V. Dunne and I. G. Halliday. Negative Dimensional Integration. 2. Path Integrals and Fermionic Equivalence. *Phys. Lett.*, B193:247, 1987.
- [74] G. Eichmann. *Hadron Properties from QCD Bound-State Equations*. PhD thesis, Graz University, 2009.
- [75] G. Eichmann, A. Krassnigg, M. Schwinzerl, and R. Alkofer. A Covariant View on the Nucleons' Quark Core. *Annals Phys.*, 323:2505–2553, 2008.
- [76] M. B. Einhorn. Form-Factors And Deep Inelastic Scattering In Two-Dimensional Quantum Chromodynamics. *Phys. Rev.*, D14:3451, 1976.
- [77] L. D. Faddeev and V. N. Popov. Feynman Diagrams for the Yang-Mills field. *Phys. Lett.*, B25:29–30, 1967.
- [78] C. Feuchter and H. Reinhardt. Quark and Gluon Confinement in Coulomb Gauge. 2004. URL [arXiv:hep-th/0402106](https://arxiv.org/abs/hep-th/0402106).
- [79] C. Feuchter and H. Reinhardt. Variational Solution of the Yang-Mills Schrödinger Equation in Coulomb Gauge. *Phys. Rev.*, D70:105021, 2004.
- [80] C. S. Fischer. Infrared properties of QCD from Dyson-Schwinger equations. *J. Phys.*, G32:R253–R291, 2006.
- [81] C. S. Fischer and R. Alkofer. Non-perturbative propagators, running coupling and dynamical quark mass of Landau gauge QCD. *Phys. Rev.*, D67:094020, 2003.
- [82] C. S. Fischer, A. Maas, and J. M. Pawłowski. On the Infrared Behavior of Landau Gauge Yang-Mills Theory. *Annals Phys.*, 324:2408–2437, 2009.
- [83] C. S. Fischer, D. Nickel, and R. Williams. On Gribov's Supercriticality Picture of Quark Confinement. *Eur. Phys. J.*, C60:1434–6052, 2008.
- [84] C. S. Fischer and D. Zwanziger. Infrared Behaviour and Running Couplings in Interpolating Gauges in QCD. *Phys. Rev.*, D72:054005, 2005.
- [85] J. Frenkel. A Class of Ghost Free Nonabelian Gauge Theories. *Phys. Rev.*, D13:2325–2334, 1976.
- [86] R. Gilmore. *Lie Groups, Lie Algebras, and Some of Their Applications*. Dover, 2006.
- [87] L. Giusti, M. L. Paciello, C. Parrinello, S. Petrarca, and B. Taglienti. Problems on Lattice Gauge-Fixing. *Int. J. Mod. Phys.*, A16:3487–3534, 2001.
- [88] F. Gliozzi. The Stefan-Boltzmann Law in a Small Box and the Pressure Deficit in Hot SU(N) Lattice Gauge Theory. *J. Phys.*, A40:F375–4922, 2007.
- [89] L. Y. Glozman. Confined but Chirally Symmetric Hadrons at Large Density and the Casher's Argument. *Phys. Rev.*, D80:037701, 2009.
- [90] J. Greensite. The Gluon Chain Model Revisited. 2002. URL [arXiv:hep-lat/0204026](https://arxiv.org/abs/hep-lat/0204026).
- [91] J. Greensite. The Confinement Problem in Lattice Gauge Theory. *Prog. Part. Nucl. Phys.*, 51:1, 2003.



- [92] J. Greensite and S. Olejnik. Coulomb Energy, Vortices, and Confinement. *Phys. Rev.*, D67:094503, 2003.
- [93] J. Greensite, S. Olejnik, and D. Zwanziger. Coulomb Energy, Remnant Symmetry, and the Phases of non-Abelian Gauge Theories. *Phys. Rev.*, D69:074506, 2004.
- [94] J. Greensite, S. Olejnik, and D. Zwanziger. Center Vortices and the Gribov Horizon. *JHEP*, 05:070, 2005.
- [95] V. N. Gribov. Quantization of non-Abelian Gauge Theories. *Nucl. Phys.*, B139:1, 1978.
- [96] V. N. Gribov. QCD at Large and Short Distances (Annotated Version). *Eur. Phys. J.*, C10:71–90, 1999.
- [97] V. N. Gribov. The Theory of Quark Confinement. *Eur. Phys. J.*, C10:91–105, 1999.
- [98] D. J. Gross, R. D. Pisarski, and L. G. Yaffe. QCD and Instantons at Finite Temperature. *Rev. Mod. Phys.*, 53:43, 1981.
- [99] R. Haag. *Local Quantum Physics: Fields, Particles, Algebras*. Springer, Berlin, Germany, 1992. 356 pp. (Texts and monographs in physics).
- [100] R. Hagedorn. Statistical Thermodynamics of Strong Interactions at High-Energies. *Nuovo Cim. Suppl.*, 3:147–186, 1965.
- [101] I. G. Halliday and R. M. Ricotta. Negative Dimensional Integrals. 1. Feynman Graphs. *Phys. Lett.*, B193:241, 1987.
- [102] T. Heinzl, A. Ilderton, K. Langfeld, M. Lavelle, and D. McMullan. The Ice-Limit of Coulomb Gauge Yang-Mills Theory. *Phys. Rev.*, D78:074511, 2008.
- [103] H. Heuser. *Lehrbuch der Analysis, Teil II*. Teubner, 2002. 12. Auflage.
- [104] A. Hietanen, K. Kajantie, M. Laine, K. Rummukainen, and Y. Schroder. Plaquette Expectation Value and Gluon Condensate in Three Dimensions. *JHEP*, 01:013, 2005.
- [105] A. Hietanen and A. Kurkela. Plaquette Expectation Value and Lattice Free Energy of Three-Dimensional SU(N) Gauge Theory. *JHEP*, 11:060, 2006.
- [106] M. Q. Huber, R. Alkofer, C. S. Fischer, and K. Schwenzer. The Infrared Behavior of Landau Gauge Yang-Mills Theory in d=2, 3 and 4 Dimensions. *Phys. Lett.*, B659:434–440, 2008.
- [107] T. Huber and D. Maitre. HypExp 2, Expanding Hypergeometric Functions about Half-Integer Parameters. *Comput. Phys. Commun.*, 178:755–776, 2008.
- [108] M. Inui, A. Niegawa, and H. Ozaki. Improvement of the Hot QCD Pressure by the Minimal Sensitivity Criterion. *Prog. Theor. Phys.*, 115:411–424, 2006.
- [109] C. Itzykson and J. B. Zuber. *Quantum Field Theory*. New York, Usa: McGraw-Hill (1980) 705 p. (International Series In Pure and Applied Physics).
- [110] G. Jona-Lasinio. Relativistic Field Theories with Symmetry Breaking Solutions. *Nuovo Cim.*, 34:1790–1795, 1964.
- [111] K. Kajantie, M. Laine, K. Rummukainen, and Y. Schroder. How to Resum Long-Distance Contributions to the QCD Pressure? *Phys. Rev. Lett.*, 86:10–13, 2001.



- [112] K. Kajantie, M. Laine, K. Rummukainen, and Y. Schroder. The Pressure of Hot QCD up to  $g^{*6} \ln(1/g)$ . *Phys. Rev.*, D67:105008, 2003.
- [113] M. Y. Kalmykov, B. A. Kniehl, B. F. L. Ward, and S. A. Yost. Hypergeometric Functions, their epsilon Expansions and Feynman diagrams. 2008.
- [114] M. Y. Kalmykov, B. F. L. Ward, and S. Yost. All Order epsilon-Expansion of Gauss Hypergeometric Functions with Integer and Half-Integer Values of Parameters. *JHEP*, 02:040, 2007.
- [115] M. Y. Kalmykov, B. F. L. Ward, and S. A. Yost. Multiple (Inverse) Binomial Sums of Arbitrary Weight and Depth and the All-Order epsilon-Expansion of Generalized Hypergeometric Functions with one Half-Integer Value of Parameter. *JHEP*, 10:048, 2007.
- [116] M. Y. Kalmykov, B. F. L. Ward, and S. A. Yost. On the All-Order epsilon-Expansion of Generalized Hypergeometric Functions with Integer Values of Parameters. *JHEP*, 11:009, 2007.
- [117] J. I. Kapusta. Quantum Chromodynamics at High Temperature. *Nucl. Phys.*, B148:461–498, 1979.
- [118] J. I. Kapusta and C. Gale. *Finite-Temperature Field Theory: Principles and Applications*. Cambridge, UK: Univ. Pr. (2006) 428 p.
- [119] F. Karsch, D. Kharzeev, and K. Tuchin. Universal Properties of Bulk Viscosity near the QCD Phase Transition. *Phys. Lett.*, B663:217–221, 2008.
- [120] D. Kharzeev and K. Tuchin. Bulk Viscosity of QCD Matter near the Critical Temperature. *JHEP*, 09:093, 2008.
- [121] M. Klokner. *The QCD Quark Propagator in Coulomb Gauge and some Implications for Hadronic Physics*. PhD thesis, 2007. URL <http://tobias-lib.uni-tuebingen.de/volltexte/2007/2939/>.
- [122] J. B. Kogut. An Introduction to Lattice Gauge Theory and Spin Systems. *Rev. Mod. Phys.*, 51:659, 1979.
- [123] A. Krassnigg and C. D. Roberts. Dyson-Schwinger Equations: An Instrument for Hadron Physics. *Nucl. Phys.*, A737:7–15, 2004.
- [124] R. Krenn. Optimierung eines numerischen Lösungsverfahrens für ein nichtlineares Integralgleichungssystem. Master’s thesis, Karl-Franzens Universität Graz, 2007.
- [125] M. Laine. What is the Simplest Effective Approach to Hot QCD Thermodynamics? 2003. URL [arXiv:hep-ph/0301011](http://arxiv.org/abs/hep-ph/0301011).
- [126] M. Laine and Y. Schroder. Two-Loop QCD Gauge Coupling at High Temperatures. *JHEP*, 03:067, 2005.
- [127] K. Langfeld and L. Moyaerts. Propagators in Coulomb Gauge from SU(2) Lattice Gauge Theory. *Phys. Rev.*, D70:074507, 2004.
- [128] G. Lassnig. private communication. 2008-10.
- [129] G. Leibbrandt. *Noncovariant Gauges: Quantization of Yang-Mills and Chern-Simons Theory in Axial Type Gauges*. World Scientific, 1994. 212 p.

- [130] G. Leibbrandt and J. Williams. Split Dimensional Regularization for the Coulomb Gauge. *Nucl. Phys.*, B475:469–483, 1996.
- [131] K. Lichtenegger and D. Zwanziger. Nonperturbative Contributions to the QCD Pressure. *Phys. Rev.*, D78:034038, 2008.
- [132] K. Lichtenegger and D. Zwanziger. Infrared Critical Exponents in Finite-Temperature Coulomb Gauge QCD. 2009. URL [arXiv:0911.5435\[hep-ph\]](https://arxiv.org/abs/0911.5435). submitted to *Phys. Rev. D*.
- [133] A. D. Linde. Infrared Problem in Thermodynamics of the Yang-Mills Gas. *Phys. Lett.*, B96:289, 1980.
- [134] A. Maas. private communication. 2007-2010.
- [135] A. Maas, A. Cucchieri, and T. Mendes. Propagators in Yang-Mills Theory for Different Gauges. *PoS, Confinement* 8:181, 2008.
- [136] A. Maas, J. Wambach, and R. Alkofer. The High-Temperature Phase of Landau-Gauge Yang-Mills Theory. *Eur. Phys. J.*, C42:93–107, 2005.
- [137] A. Maas, J. Wambach, B. Gruter, and R. Alkofer. High-Temperature Limit of Landau-Gauge Yang-Mills Theory. *Eur. Phys. J.*, C37:335–357, 2004.
- [138] N. Maggiore and M. Schaden. Landau Gauge within the Gribov Horizon. *Phys. Rev.*, D50:6616–6625, 1994.
- [139] J. M. Maldacena. The Large N Limit of Superconformal Field Theories and Supergravity. *Adv. Theor. Math. Phys.*, 2:231–252, 1998.
- [140] W. J. Marciano and H. Pagels. Quantum Chromodynamics: A Review. *Phys. Rept.*, 36:137, 1978.
- [141] H. H. Matevosyan, A. W. Thomas, and P. C. Tandy. Quark-Gluon Vertex Dressing and Meson Masses Beyond Ladder-Rainbow Truncation. *Phys. Rev.*, C75:045201, 2007.
- [142] V. A. Miransky. *Dynamical Symmetry Breaking in Quantum Field Theories*. Singapore, Singapore: World Scientific, 1993. 533 p.
- [143] B. Muller and J. L. Nagle. Results from the Relativistic Heavy Ion Collider. *Ann. Rev. Nucl. Part. Sci.*, 56:93–135, 2006.
- [144] H. J. Munczek. Dynamical Chiral Symmetry Breaking, Goldstone’s Theorem and the Consistency of the Schwinger-Dyson and Bethe-Salpeter Equations. *Phys. Rev.*, D52:4736–4740, 1995.
- [145] Y. Nakagawa, A. Nakamura, T. Saito, H. Toki, and D. Zwanziger. Properties of Color-Coulomb String Tension. *Phys. Rev.*, D73:094504, 2006.
- [146] Y. Nakagawa, T. Saito, H. Toki, and A. Nakamura. Infrared Divergence of the Color-Coulomb Self-Energy in Coulomb Gauge QCD. *PoS, LAT2006*:071, 2006.
- [147] Y. Nakagawa, H. Toki, A. Nakamura, and T. Saito. Color Confinement and the Faddeev-Popov Ghosts in Coulomb Gauge QCD. *PoS, LAT2007*:319, 2007.
- [148] Y. Nakagawa, H. Toki, A. Nakamura, T. Saito, and H. Toki. Color-Singlet Instantaneous Potential in the Coulomb Gauge QCD. *Prog. Theor. Phys. Suppl.*, 168:381–384, 2007.

- [149] M. Nakahara. *Geometry, Topology and Physics*. Inst of Physics Pub., 2003 (2nd ed.).
- [150] A. Nakamura and T. Saito. Color Confinement in Coulomb Gauge QCD. *Prog. Theor. Phys.*, 115:189–200, 2006.
- [151] A. H. Nayfeh. *Perturbation Methods*. John Wiley & Sons Inc, 1973.
- [152] H. Neuberger. Nonperturbative BRS Invariance. *Phys. Lett.*, B175:69, 1986.
- [153] A. Niegawa. Renormalization in a Generic Coulomb-Gauge QCD within the Lagrangian Formalism. *Phys. Rev.*, D74:045021, 2006.
- [154] A. Niegawa, M. Inui, and H. Kohyama. Cancellation of Energy Divergences and Renormalizability in Coulomb Gauge QCD within the Lagrangian Formalism. *Phys. Rev.*, D74:105016, 2006.
- [155] M. Okamoto et al. Equation of State for Pure SU(3) Gauge Theory with Renormalization Group Improved Action. *Phys. Rev.*, D60:094510, 1999.
- [156] F. Palumbo. Exact Evaluation of the Faddeev-Popov Determinant in a Complete Axial Gauge on a Torus. *Phys. Lett.*, B243:109–115, 1990.
- [157] K. Peeters and M. Zamaklar. The String/Gauge Theory Correspondence in QCD. *Eur. Phys. J. ST*, 152:113–138, 2007.
- [158] M. E. Peskin and D. V. Schroeder. *An Introduction to Quantum Field Theory*. Reading, USA: Addison-Wesley (1995) 842 p.
- [159] R. D. Pisarski. Effective Theory of Wilson Lines and Deconfinement. *Phys. Rev.*, D74:121703, 2006.
- [160] C. Popovici, P. Watson, and H. Reinhardt. Quarks in Coulomb Gauge Perturbation Theory. *Phys. Rev.*, D79:045006, 2009.
- [161] E. Rebhan. *Theoretische Physik, Bd.1: Mechanik, Elektrodynamik, Relativitätstheorie, Kosmologie*. Spektrum Akademischer Verlag, 1999.
- [162] H. Reinhardt, D. Campagnari, D. Epple, M. Leder, M. Pak, and W. Schleifenbaum. Coulomb Gauge Yang-Mills Theory in the Hamiltonian Approach. 2008.
- [163] H. Reinhardt and C. Feuchter. On the Yang-Mills Wave Functional in Coulomb Gauge. *Phys. Rev.*, D71:105002, 2005.
- [164] H. Reinhardt and W. Schleifenbaum. Hamiltonian Approach to 1+1 dimensional Yang-Mills Theory in Coulomb Gauge. *Annals Phys.*, 324:735–786, 2009.
- [165] H. Ren. Path Integrals, BRST Identities and Regularization Schemes in Nonstandard Gauges. *Annals Phys.*, 283:57–93, 2000.
- [166] J. L. Richardson. The Heavy Quark Potential and the Upsilon, J/psi Systems. *Phys. Lett.*, B82:272, 1979.
- [167] R. J. Rivers. *Path Integral Methods in Quantum Field Theory*. Cambridge, UK: Univ. Pr., 1987. 339 p. (Cambridge monographs on math. physics).
- [168] C. D. Roberts and S. M. Schmidt. Dyson-Schwinger Equations: Density, Temperature and Continuum Strong QCD. *Prog. Part. Nucl. Phys.*, 45:S1–S103, 2000.

- [169] Rocchini. Wikimedia Commons – Hausdorff distance. URL [http://commons.wikimedia.org/wiki/File:Hausdorff\\_distance\\_sample.svg](http://commons.wikimedia.org/wiki/File:Hausdorff_distance_sample.svg).
- [170] H. J. Rothe. Lattice Gauge Theories: An Introduction. *World Sci. Lect. Notes Phys.*, 74: 1–605, 2005.
- [171] T. Saito, H. Toki, Y. Nakagawa, and A. Nakamura. Lattice Study of Color Confinement Mechanism in Coulomb Gauge. *PoS, LAT2005:303*, 2006.
- [172] E. E. Salpeter and H. A. Bethe. A Relativistic Equation for Bound State Problems. *Phys. Rev.*, 84:1232–1242, 1951.
- [173] Y. Schroder. Automatic Reduction of Four-Loop Bubbles. *Nucl. Phys. Proc. Suppl.*, 116: 402–406, 2003.
- [174] Y. Schroder. Evading the Infrared Problem of Thermal QCD. 2004. URL [arXiv:hep-ph/0410130](http://arxiv.org/abs/hep-ph/0410130).
- [175] Y. Schroder. Tackling the Infrared Problem of Thermal QCD. *Nucl. Phys. Proc. Suppl.*, 129:572–574, 2004.
- [176] M. Semenov-Tian-Shansky and V. Franke. *Report of the Steklov Institute (Leningrad)*, 1982. (in Russian).
- [177] E. V. Shuryak. Quark-Gluon Plasma and Hadronic Production of Leptons, Photons and Psions. *Phys. Lett.*, B78:150, 1978.
- [178] E. V. Shuryak. Theory of Hadronic Plasma. *Sov. Phys. JETP*, 47:212–219, 1978.
- [179] E. V. Shuryak. What RHIC Experiments and Theory Tell us about Properties of Quark-Gluon Plasma? *Nucl. Phys.*, A750:64–83, 2005.
- [180] E. V. Shuryak. Signatures for Strongly Coupled Quark-Gluon Plasma. *J. Phys. Conf. Ser.*, 50:62–69, 2006.
- [181] I. M. Singer. Some Remarks on the Gribov Ambiguity. *Commun. Math. Phys.*, 60:7–12, 1978.
- [182] P. M. Stevenson. Optimized Perturbation Theory. *Phys. Rev.*, D23:2916, 1981.
- [183] A. T. Suzuki and A. G. M. Schmidt. Negative Dimensional Integration: *Lab Testing* at Two Loops. *JHEP*, 09:002, 1997.
- [184] A. T. Suzuki and A. G. M. Schmidt. Negative-Dimensional Integration Revisited. *J. Phys.*, A31:8023–8039, 1998.
- [185] A. T. Suzuki and A. G. M. Schmidt. Two-Loop Self-Energy Diagrams Worked out with NDIM. *Eur. Phys. J.*, C5:175–179, 1998.
- [186] A. T. Suzuki and A. G. M. Schmidt. Feynman Integrals with Tensorial Structure in the Negative Dimensional Integration Scheme. *Eur. Phys. J.*, C10:357–362, 1999.
- [187] A. T. Suzuki and A. G. M. Schmidt. NDIM Achievements: Massive, Arbitrary Tensor Rank and N-Loop Insertions in Feynman Integrals. *J. Phys.*, A33:3713–3722, 2000.
- [188] A. T. Suzuki and A. G. M. Schmidt. Negative Dimensional Approach for Scalar Two-Loop Three-Point and Three-Loop Two-Point Integrals. *Can. J. Phys.*, 78:769–777, 2000.

- [189] A. T. Suzuki and A. G. M. Schmidt. First Results for the Coulomb Gauge Integrals using NDIM. *Eur. Phys. J.*, C19:391–396, 2001.
- [190] A. T. Suzuki, A. G. M. Schmidt, and R. Bentin. Probing Negative Dimensional Integration: Two-Loop Covariant Vertex and One-Loop Light-Cone Integrals. *Nucl. Phys.*, B537:549–560, 1999.
- [191] G. 't Hooft. A Two-Dimensional Model for Mesons. *Nucl. Phys.*, B75:461, 1974.
- [192] G. 't Hooft. Topology of the Gauge Condition and New Confinement Phases in Nonabelian Gauge Theories. *Nucl. Phys.*, B190:455, 1981.
- [193] G. 't Hooft and M. J. G. Veltman. Regularization and Renormalization of Gauge Fields. *Nucl. Phys.*, B44:189–213, 1972.
- [194] J. C. Taylor. Ward Identities and Charge Renormalization of the Yang-Mills Field. *Nucl. Phys.*, B33:436–444, 1971.
- [195] T. Toimela. The Next Term in the Thermodynamic Potential of QCD. *Phys. Lett.*, B124:407, 1983.
- [196] I. V. Tyutin. Gauge Invariance in Field Theory and Statistical Physics in Operator Formalism. 1975.
- [197] P. van Baal. More (Thoughts on) Gribov Copies. *Nucl. Phys.*, B369:259–275, 1992.
- [198] P. van Baal. Some Comments on Laplacian Gauge Fixing. *Nucl. Phys. Proc. Suppl.*, 42:843–845, 1995.
- [199] J. A. M. Vermaseren. New Features of FORM. 1000. URL [arXiv:math-ph/0010025](https://arxiv.org/abs/math-ph/0010025).
- [200] S. Villalba-Chavez, R. Alkofer, and K. Schwenzer. On the Connection between Hamilton and Lagrange Formalism in Quantum Field Theory. 2008. URL [arXiv:0807.2146](https://arxiv.org/abs/hep-th/0807.2146) [hep-th].
- [201] J. C. Vink and U.-J. Wiese. Gauge Fixing on the Lattice without Ambiguity. *Phys. Lett.*, B289:122–126, 1992.
- [202] A. Voigt, E.-M. Ilgenfritz, M. Muller-Preussker, and A. Sternbeck. Coulomb Gauge Studies of SU(3) Yang-Mills Theory on the Lattice. *PoS, LAT2007*:338, 2007.
- [203] A. Voigt, E. M. Ilgenfritz, M. Muller-Preussker, and A. Sternbeck. The Effective Coulomb Potential in SU(3) Lattice Yang-Mills Theory. *Phys. Rev.*, D78:014501, 2008.
- [204] L. von Smekal, R. Alkofer, and A. Hauck. The Infrared Behavior of Gluon and Ghost Propagators in Landau Gauge QCD. *Phys. Rev. Lett.*, 79:3591–3594, 1997.
- [205] L. von Smekal, A. Hauck, and R. Alkofer. A Solution to Coupled Dyson-Schwinger Equations for Gluons and Ghosts in Landau Gauge. *Ann. Phys.*, 267:1, 1998.
- [206] L. von Smekal, D. Mehta, A. Sternbeck, and A. G. Williams. Modified Lattice Landau Gauge. *PoS, Lattice*:382, 2007.
- [207] P. Watson. private communication. 2008.
- [208] P. Watson and H. Reinhardt. Completing Continuum Coulomb Gauge in the Functional Formalism. 2007.

- [209] P. Watson and H. Reinhardt. Perturbation Theory of Coulomb Gauge Yang-Mills Theory Within the First Order Formalism. *Phys. Rev.*, D76:125016, 2007.
- [210] P. Watson and H. Reinhardt. Propagator Dyson-Schwinger Equations of Coulomb Gauge Yang-Mills Theory within the First Order Formalism. *Phys. Rev.*, D75:045021, 2007.
- [211] P. Watson and H. Reinhardt. Two-Point Functions of Coulomb Gauge Yang-Mills Theory. *Phys. Rev.*, D77:025030, 2008.
- [212] P. Watson and H. Reinhardt. Slavnov-Taylor Identities in Coulomb Gauge Yang-Mills Theory. *Eur. Phys. J.*, C65:567–585, 2010.
- [213] S. Weinberg. The U(1) Problem. *Phys. Rev.*, D11:3583–3593, 1975.
- [214] S. Weinberg. A New Light Boson? *Phys. Rev. Lett.*, 40:223–226, 1978.
- [215] F. Wilczek. Problem of Strong P and T Invariance in the Presence of Instantons. *Phys. Rev. Lett.*, 40:279–282, 1978.
- [216] F. J. Yndurain. The Theory of Quark and Gluon Interactions. Berlin, Germany: Springer (1999) 413 p.
- [217] V. I. Yukalov and E. P. Yukalova. Thermodynamics of Strong Interactions. *Phys. Part. Nucl.*, 28:37–65, 1997.
- [218] I. Zahed and D. Zwanziger. Zero Color Magnetization in QCD Matter. *Phys. Rev.*, D61:037501, 2000.
- [219] C.-X. Zhai and B. M. Kastening. The Free Energy of Hot Gauge Theories with Fermions through  $g^{*5}$ . *Phys. Rev.*, D52:7232–7246, 1995.
- [220] D. Zwanziger. Nonperturbative Modification of the Faddeev-Popov Formula and Banishment of the Naive Vacuum. *Nucl. Phys.*, B209:336, 1982.
- [221] D. Zwanziger. Local and Renormalizable Action from the Gribov Horizon. *Nucl. Phys.*, B323:513–544, 1989.
- [222] D. Zwanziger. Vanishing of Zero Momentum Lattice Gluon Propagator and Color Confinement. *Nucl. Phys.*, B364:127–161, 1991.
- [223] D. Zwanziger. Critical Limit of Lattice Gauge Theory. *Nucl. Phys.*, B378:525–590, 1992.
- [224] D. Zwanziger. Renormalizability of the Critical Limit of Lattice Gauge Theory by BRS Invariance. *Nucl. Phys.*, B399:477–513, 1993.
- [225] D. Zwanziger. Continuum and Lattice Coulomb-Gauge Hamiltonian. 1997. URL [arXiv: hep-th/9710157](https://arxiv.org/abs/hep-th/9710157).
- [226] D. Zwanziger. Renormalization in the Coulomb Gauge and Order Parameter for Confinement in QCD. *Nucl. Phys.*, B518:237–272, 1998.
- [227] D. Zwanziger. Non-Perturbative Landau Gauge and Infrared Critical Exponents in QCD. *Phys. Rev.*, D65:094039, 2002.
- [228] D. Zwanziger. No Confinement without Coulomb Confinement. *Phys. Rev. Lett.*, 90:102001, 2003.
- [229] D. Zwanziger. Non-Perturbative Faddeev-Popov Formula and Infrared Limit of QCD. *Phys. Rev.*, D69:016002, 2004.

- [230] D. Zwanziger. Equation of State of Gluon Plasma and Renormalization of Local Action. *Braz. J. Phys.*, 37:127–143, 2007.
- [231] D. Zwanziger. Equation of State of Gluon Plasma from Local Action. *Phys. Rev.*, D76: 125014, 2007.
- [232] D. Zwanziger. On the Equation of State of the Gluon Plasma. *AIP Conf. Proc.*, 892: 121–127, 2007.
- [233] D. Zwanziger. private communication. 2007-10.